



**Identification of exosomal proteins in primary
human bronchial tracheal epithelial cell HBTE and
the H358, THP1 and MCF7 cell lines**

MD Faruk Abdullah Saurav

(BPharm, MSc)

*A thesis submitted in partial fulfilment of the
requirements of the University of Greenwich for
the Degree of Doctor of Philosophy.*

February 2018

Declaration

I certify that the work contained in this thesis, or any part of it, has not been accepted in substance for any previous degree awarded to me, and is not concurrently being submitted for any degree other than that of Doctor of Philosophy being studied at the University of Greenwich. I also declare that, this work is the result of my own investigations, except where otherwise identified by references and that the contents are not the outcome of any form of research misconduct.

Candidate:

MD Faruk A Saurav

Supervisor:

Dr Azizur Rahman

ACKNOWLEDGEMENT

First of all I would like to thank almighty Allah for providing me to chase my dream. I would like to thank my Supervisor Dr Azizur Rahman for supporting me in every step even if when I was down for providing me enough opportunity to expand my project beyond my initial plan and allowing me to learn new techniques. I would also like to thank my second supervisor Dr. Lauren Pecorino for showing me the right way.

I would also like to thank my colleagues who supported me by helping me throughout my project. It would also like to express gratitude to the entire technician team in the link lab, especially John and Cliff for supporting me all the time sometime even out of their way.

The best support is the support from family. I want to thank my family members, each one of them. My father, my first hero, who supported me when I fell down, encourages me to get up again. My mother, who prays for me all the time; my brother and sister and as well as my in-laws who always pray for my success.

Lastly, I want to thank my lovely wife, Tanzena Akter, without whom my study would not been finished. Her tiring effort to keep in my foot, continuous praying for my wellbeing and the support she gave me was the essential element of my path from beginning to the end.

MD Faruk Abdullah Saurav

Abstract

Background: Early detection of cancer is of paramount importance for successful treatment. Unfortunately, this is currently complex and time consuming. New sources of biomarkers are needed to improve. Exosomes are nano sized extracellular vesicles released by almost all cells have gained much interest as a cancer biomarker source due to their ability to transfer genetic materials, stability and ease of availability.

Aims: The aim of this study is to investigate the potentials of exosomes as a source of biomarkers of cancer in general and lung cancer in particular. To achieve this, exosomes from three difference cancer cell lines (lung cancer H358, leukaemia THP1 and breast cancer MCF7) and a primary lung cell HBTE were isolated and their protein contents were analysed to establish wheather cancer specific proteins are present.

Methods and Materials: Exosomes were isolated and characterized by scanning (SEM) and transmission electron microscopy (TEM), dynamic light scattering (DLS) and Western Blot analysis. The exosome number and protein profile were analysed at different cellular growth stages using Exo-Elisa based on exosomal marker CD63 and mass spectrometry (MS) respectively. LC-MS based proteomic approach has been used to compare the proteomic profile of exosomes from three cancer cells. Finally, comparative proteomic study and gene expression analysis were carried out between exosomes from lung cancer cell (H358) and its counterpart normal cell (HBTE)

Results and Discussions: Successful isolation of exosomes from H358, THP1 and MCF7 was confirmed based on their size distribution (ranging from 96.54 ± 28.53 nm to 128.06 ± 17.74 nm) and by the presence of exosomal markers (CD63, CD81, CD9 and Hsp70). The number of exosomes released/cell was shown to increase with time ranging from 14500 on day 1 to 18000 at day 15. Interestingly, MS analysis revealed that, alpha-2-macroglobulin (A2M) and pregnancy zone protein was present only in stationary phase indicative of the oxidative stress.

Comparative proteomic study by LC-MS identified a total of 613 proteins commonly found across three cell lines. A large proportion of membranous proteins were identified including integrins, catenins, cadherins, and cathepsins. Most of which are involved in molecular signalling, cellular growth and transport, supporting the role of exosomes in cellular communication. Several adhesion molecules such as integrins, laminlins, catenins as well as cadherins and cathepsins were also identified as differentially expressed between different types of cancer derived exosomes.

Proteomic profiling of HBTE cell derived exosomes revealed 1011 proteins which only partially overlapped with those identified in H358 exosomes. A total of 205 proteins were specific for the cancerous lung cell line derived exosomes. Of particular interest was the identification of CTNNB1, an adhesion molecule known to be present in several other lung cancers, making it an ideal candidate for biomarker for non-small cell lung cancer, bronchioalveolar carcinoma. Gene expression analysis revealed that this protein is expressed at cellular level in both cancerous and normal lung cells, albeit found in a significantly higher level in H358 ($p \leq 0.05$).

Conclusion: This is the first report to show successful isolation and characterization of exosomes from H358 and HBTE. Comparative proteomic analysis of the newly isolated exosomes not only revealed that exosomes are a good source of lung cancer biomarkers but identified a potential candidate. CTNNB1 was selectively found in lung cancer cell derived exosomes but not in the counterpart normal cell (HBTE) and was selected for further investigation.

Table of Contents

Declaration	i
Acknowledgements	ii
Abstract	iii
Table of Contents	iv
List of Tables	Xii
List of Figures	xiii
List of Abbreviations	xvi
Chapter 1:	1
Introduction:.....	1
1.1 Overview of the project:.....	1
1.2 Cancer:	1
1.3 Cancer Discussed in this study:.....	2
1.3.1 Lung Cancer:.....	3
1.3.2 Breast Cancer:.....	4
1.3.3 Leukaemia:.....	5
1.4 Mechanism of Metastasis:	7
1.5 Exosome:.....	10
1.5.1 Role of exosomes in metastasis:	11
1.6 Composition of Exosome:	14
1.6.1 Lipid Composition:	14
1.6.2 Exosomal Protein Composition:	15
1.6.3 Exosomal RNA composition:	18
1.6.4 Biogenesis of Exosomes:	19

1.7	Isolation of Exosomes:	21
1.7.1	Ultracentrifugation:	21
1.7.2	Density Gradient Ultracentrifugation:	23
1.7.3	Size exclusion chromatography:	23
1.7.4	Ultrafiltration:	24
1.7.5	Magnetic Beads:.....	24
1.7.6	Precipitation methods:	25
1.7.7	Isolation of exosomes by sieving:.....	25
1.8	Detection and characterisation of Exosomes:	26
1.8.1	Electron Microscopy:.....	26
1.8.2	Western Blot:	26
1.8.3	Flow Cytometry:	27
1.8.4	Atomic force microscopy:.....	27
1.8.5	Nano Particle Tracking Analysis (NTA):	28
1.8.6	Dynamic Light Scattering:.....	28
1.9	Functions of Exosome:.....	28
1.9.1	Exosome on Cell to Cell Communication:	29
1.9.2	Exosomes in Signalling Pathways:	29
1.9.3	Exosomes on Immune Response:	30
1.9.4	Exosomes in Elimination of Molecules:	30
1.9.5	Role of Exosomes on Cancer Progression:.....	31
1.9.6	Role of Exosomes on Cancer Biomarker Discovery:	32
1.9.7	Exosomes in therapeutic drug delivery:.....	32
1.9.8	Proteomic Analysis of Exosomes:	33
1.10	Aims and Objectives:	35

Chapter 2:	36
General methods and materials	36
2.1 Method and Materials:	36
2.2 Cell Culture:	36
2.2.1 Culture of Human Cell Lines:.....	36
2.2.2 Adherent Cell Culture:.....	36
2.2.3 Suspension Cell Culture:.....	37
2.2.4 Assessment of Cell Number, Viability and Growth Curve:	37
2.2.5 Cryopreservation of Cells:	37
2.2.6 Thawing of Cryopreserved Cells:	38
2.3 Isolation of Exosomes:	38
2.4 Protein extraction from Cell and Exosomes:.....	38
2.5 Determination of Protein Concentration (Bradford Assay):	39
2.6 Statistical analysis:	39
2.7 Software used:	39
Chapter 3:	40
Identification and characterisation of exosomes derived from three different types of cancer cells:	40
3.1 Introduction:	40
3.1.1 Exosomes:	40
3.1.2 Ectosomes:	41
3.1.3 Protasomes:	41
3.1.4 Identification of exosomes:.....	41
3.2 Methods and Materials:	43
3.2.1 Cell Culture and Isolation of Exosomes:	43
3.2.2 Isolation of Exosome by Ultracentrifugation:.....	43
3.2.3 Isolation of Exosome with Exosome Isolation Kit:	43

3.2.4	Isolation of Exosome with PEG Solution:	44
3.2.5	Electron Microscopy:	44
3.2.6	Dynamic Light Scattering and Zeta Potential:	45
3.2.7	Determination of Exosomal Protein Concentration:	45
3.2.8	Protein Separation by one dimensional gel Electrophoresis:	45
3.2.9	Developing the Gel:	46
3.2.10	Western Blot:	46
3.3	Results:	48
3.3.1	Analysis of Exosomes by Electron Microscopy:	48
3.3.2	Size Distribution Analysis by Dynamic Light Scattering:	52
3.3.3	Comparison exosome isolation by PEG:	54
3.3.4	One Dimensional Gel Electrophoresis and Western Blot:	57
3.4	Discussion:	59
3.5	Conclusion:	61
Chapter 4:	62
Dynamics of exosome release during cellular growth.	62
4.1	Introduction:	62
4.2	Methods and Materials:	64
4.2.1	Protein Extraction and Calibration Curve:	64
4.2.2	Quantification of Exosomes by ELISA Method:	64
4.2.3	Determination of Protein Concentration:	65
4.2.4	One Dimensional Gel Electrophoresis:	65
4.2.5	Protein Identification by LC-MS (University of York):	65
4.3	Results:	67
4.3.1	Quantification of Exosomes by ELISA:	67
4.3.2	Bradford Assay of Exosomal Protein:	70
4.3.3	Analysis of Exosomal Proteins by One Dimensional Gel Electrophoresis:	72

4.3.4	Dynamics of Protein Transportation by Exosomes Derived from H358 Cells:	72
4.3.5	Dynamics of Protein Transportation by Exosomes Derived from THP1 Cells:	73
4.3.6	Dynamics of Protein Transportation by Exosomes Derived from MCF7 Cells:	74
4.4	Discussion:	77
4.5	Conclusion:.....	80
Chapter 5:		81
Comparative proteomic study of different types of cancer cells and exosomes:		81
5.1	Introduction:	81
5.1.1	Biomarker Discovery:.....	82
5.1.2	Strategies in Proteome Research:.....	83
5.1.3	Methods Used in Proteomic Study:	84
5.2	Methods and Materials:	87
5.2.1	Preparation of Sample for 2D Gel:	87
5.2.2	Two Dimensional Gel Electrophoresis:	87
5.2.3	Sample Preparation for LC-MS (University of York):	88
5.3	Results:	91
5.3.1	Comparative Proteomic Study between Cancer Cells:	91
5.3.2	Comparative Proteomic Study of Exosomes by 2D Gel Electrophoresis:.....	92
5.3.3	Proteins Identified from exosomes by LC-MS:	93
5.3.4	Functional analysis of exosomal proteins:	94
5.3.5	Comparison between H358 and THP1:	98
5.3.6	Comparison between MCF7 and H358:	99
5.3.7	Comparison between MCF7 and THP1:.....	99
5.3.8	Protein network and KEGG pathway analysis:	100
5.3.9	Comparative proteomic analysis:.....	102

5.4	Discussion:	104
5.5	Conclusion:.....	109
Chapter 6:		110
Comparative proteomic study and gene expression analysis of exosomes from lung cancer cell line and normal cell line		110
6.1	Introduction:	110
6.2	Methods and Materials:	112
6.2.1	Cell Culture and Isolation of exosomes:	112
6.2.2	Proteomic Analysis by LC-MS:.....	112
6.2.3	Isolation of RNA from cells:.....	112
6.2.4	Sample preparation for RT-PCR:.....	113
6.3	Results:	115
6.3.1	Identification and characterisation of exosomes:.....	115
6.3.2	Proteomic analysis:	116
6.3.3	Functional analysis of exosome proteins:	116
6.3.4	Comparative proteomic analysis:.....	119
6.3.5	Protein network and KEGG pathway analysis:	123
6.3.6	Real time PCR analysis:.....	133
6.3.7	Relative gene expression analysis:.....	134
6.4	Discussion:	142
6.5	Conclusion:.....	145
Chapter 7:		146
General discussion and future prospects		146
7.1	General Discussion:.....	146
7.2	Conclusion:.....	149
7.3	Future prospects:	149

Chapter 8:	151
References:	151
Appendix	190
Chapter 9:	266
Poster Presentations	266
9.1 Poster presented on 28 th April 2016:	267
9.2 Poster presented on 23 th January 2017:	269

List of Tables

Tables	Titles	Pages
Table 3.1:	Dynamic Light scattering and zeta potential of exosomes from H358, THP1 and MCF7 cell lines	52
Table 4.1:	List of Proteins identified by Mass Spectrometry from day 3 to day 15 with their functions	75
Table 5.1:	Partial list of proteins with their functions with their relative expression in exosomes of the three cancer cell lines analysed.	96
Table 6.1:	List of primers designed for the RT-PCR analysis for the selected proteins.	113
Table 6.2:	Primers for the qRT-PCR analysis. Primers were acquired from literature search	113
Table 6.3:	Partial list of proteins with their functions and difference in their relative expressions. Na= not available in HBTE	120
Table 6.4:	Gene expression analysis by qPCR of six selected genes. The $\Delta\Delta Ct$ was calculated after the normalisation with beta tubulin. The threshold for the Ct value was considered 0.2.	134

List of Figures

Figures	Titles	Pages
Figure 1.1:	Structural Differences between Cancer Cells and Normal Cells	2
Figure 1.2:	Stages of Metastatic Process	7
Figure 1.3:	Biogenesis of exosomes.	11
Figure 1.4:	Role of exosomes in metastasis	13
Figure 1.5:	Protein composition of exosomes	18
Figure 1.6:	Biogenesis and secretion of exosome	20
Figure 1.7:	Isolation of exosomes by step wise centrifugation	22
Figure 3.1:	Scanning and Transmission of Electron Microscopic Images of Exosomes derived from H358 Cell Line	50
Figure 3.2:	Scanning and Transmission of Electron Microscopic Images of Exosomes derived from THP1 Cell Line	51
Figure 3.3:	Scanning and Transmission of Electron Microscopic Images of Exosomes derived from MCF7 Cell Line	52
Figure 3.4:	Comparison of exosome size obtained from EM and DLS analysis for H358, THP1 and MCF7	54
Figure 3.5:	Comparison of PEG solution of different molecular weight and different concentration	56
Figure 3.6:	Comparison of commercially available exosome isolation kit (TEI) and PEG solutions of different concentrations	56
Figure 3.7:	TEM images of exosomes isolated from H358 cell lines by PEG solution with different molecular weight and at different concentrations	57
Figure 3.8:	Comparison of proteins extracted by three methods	58
Figure 3.9	1D gel electrophoresis of cellular protein and exosomal proteins.	59
Figure 4.1:	Calibration curve of exosomes using exosome standard CD63 to count the exosomes by the ELISA method	68
Figure 4.2:	Number of H358 Cells ($\times 10^5$) vs Number of Exosomes Released ($\times 10^8$) from H358 Cells	70
Figure 4.3:	Number of THP1 Cells ($\times 10^5$) vs Number of Exosomes Released ($\times 10^8$) from THP1 Cells	70
Figure 4.4:	Number of MCF7 Cells ($\times 10^5$) vs Number of Exosomes Released ($\times 10^8$) from MCF7 Cells	70
Figure 4.5:	Average number of exosomes per cell by H358, THP1 and MCF7 cell lines	71

Figure 4.6:	Protein Concentration against the Number of Exosomes Released H358 Cells	72
Figure 4.7:	Average protein concentrations per day by exosomes from three cells.	72
Figure 4.8:	1D Gel Electrophoresis of Exosomal Protein Extracted from H358 Derived Exosomes from DAS3 to DAS15	74
Figure 4.9:	1D Gel Electrophoresis of Exosomal Protein Extracted from THP1	75
Figure 4.10:	1D Gel Electrophoresis of Exosomal Protein Extracted from MCF7	76
Figure 5.1:	Different strategies and methods used in proteomics.	85
Figure 5.2:	A complete work flow of gel electrophoresis based proteomic study.	87
Figure 5.3:	A complete work flow of LC-MS based proteomic study	87
Figure 5.4:	Two dimensional gel electrophoresis of cellular protein from H358, MCF7 and THP1.	92
Figure 5.5:	Two dimensional gel electrophoresis of exosomal protein derived from H358, MCF7 and THP1 cell lines.	94
Figure 5.6:	Venn Diagrams of common and uncommon proteins distribution between three cancer cell exosomes.	95
Figure 5.7:	Proteins involved in biological process.	96
Figure 5.8:	Function detailed in pie chart for the identified proteins for all the three exosomes.	97
Figure 5.9:	Association of the identified proteins in cellular compartments.	97
Figure 5.10:	Network analyses of the proteins with differential expression level ($p \leq 0.05$) within the exosomes from three cancer cells.	102
Figure 5.11:	KEGG Pathways detected by STING software. The FDR value is normalised by using $-\log_{10}$.	103
Figure 5.12:	Heat map of exosomal proteins from three cancer cells with different expression level	104
Figure 6.1:	TEM images of exosomes from H358 and HBTE showing round shaped morphology.	116
Figure 6.2:	A Venn diagram showing number of the shared proteins between HBTE and H358 as well as the unique proteins in H358 and HBTE.	117
Figure 6.3:	Doughnut chart showing the involvement of proteins H358 and HBTE in biological process.	118
Figure 6.4:	Doughnut chart showing the involvement of proteins H358 and HBTE in cellular compartments.	119
Figure 6.5:	Bar chart showing the involvement of proteins H358 and HBTE in	120

molecular functions.

Figure 6.6:	An unsupervised heat map of proteins among three biological replicates between the H358 exosomes and HBTE exosomes with different expression level	121
Figure 6.7:	The protein network analysis for the shared proteins between H358 and HBTE	125
Figure 6.8:	KEGG pathway analysis of shared proteins with $p < 0.05$.	126
Figure 6.9:	The protein network analysis for the proteins present only in H358 using STRING v10.0 with a confidence level of 0.4 revealed a complex protein network.	127
Figure 6.10:	KEGG pathway analyses of proteins only present in H358 exosomes.	128
Figure 6.11:	The protein network analysis for the proteins present only in HBTE using STRING v10.0 with a confidence level of 0.4 revealed a complex protein network.	129
Figure 6.12:	KEGG pathway analyses of proteins only present in HBTE with p value.	130
Figure 6.13:	The protein network analysis for the upregulated proteins in H358	131
Figure 6.14:	KEGG pathway analysis of up regulated proteins in H358 with $p < 0.05$	132
Figure 6.15:	The protein network analysis for the upregulated proteins in HBTE	133
Figure 6.16:	KEGG pathway analysis of up regulated proteins in HBTE exosomes	134
Figure 6.17:	Presence of RNA on agarose gel. The dark band of 00bp represents 28s RNA and the lighter one on 00bp represents 18s RNA.	134
Figure 6.18:	Bar graph qRT-PCR analysis data of six selected genes of H358 and HBTE.	136
Figure 6.19:	Amplification plot (Ct value) and melting curve of Integrin alpha 3 (ITGA3).	137
Figure 6.20:	Amplification plot (Ct value) and melting curve of Cadherin 1 (CDH1)	138
Figure 6.21:	Amplification plot (Ct value) and melting curve of Laminin gamma 1 (LAMC1)	139
Figure 6.22:	Amplification plot (Ct value) and melting curve of Catenin Beta 1 (CTNNB1)	140
Figure 6.23	Amplification plot (Ct value) and melting curve of Transforming growth factor beta 2 (TGFB2).	141
Figure 6.24:	Amplification plot (Ct value) and melting curve of Cathepsin D (CSTD)	142

List of Abbreviation:

2DE	Two-Dimensional Electrophoresis
A2M	Alpha-2-macroglobulin
AC	Adenocarcinoma
AFM	Atomic force microscopy
ALL	Acute Lymphocytic Leukaemia
AML	Acute Myeloid
APC	Antigen presenting cells
ATCC	American Type Culture Collection
BAC	Brocheoalvelar Carcinoma
BBB	Blood brain barrier
BMDC	Bone Marrow Derived Cells
BMP	Bone Morphogenetic Protein
BSA	Bovine Serum Albumin
CBE	Clinical Breast Examination
CCD	Charge Couple Device
CCM	Conditioned Cell Culture Medium
CCV	Clathrin-coated vesicles
CDH1	Cadherin-1
CLL	Chronic Lymphocytic
CM	Culture Medium
CML	Chronic Myeloid
CTNNB1	Catenin Beta-1
DEPC	Diethyl pyro-carbonate
DLS	Dynamic Light Scattering
DMSO	Dimethyl Sulfoxide
DTE	Dithioerythritol
DTT	Dithiothreitol
EGF	Epidermal Growth Factor
ELISA	Enzyme linked immunosorbant assay
EM	Electron Microscopy
EML4	Echinoderm microtubule-associated protein-like 4
EMT	Epithelial Mesenchymal Transition,
EpCAM	Epithelial Cell Adhesion Molecule
ERRB2	oestrogen-related receptor beta type 2
ESCC	Esophageal Squamous Cell Carcinoma
ESCRT	Endosomal Sorting Complex Required for Transport
FBS	Foetal Bovine Serum
FDR	False discovery rate
GO	Gene ontology
GSTM1	Glutathione S transferase mu 1

HBTE	Human bronchial tracheal epithelial cell line
HMDS	Hexamethyldisilazane
ILV	Intraluminal Vesicles
ITGA3	Integrin alpha-3
KASH	Klarsicht Homology
KEGG	Kyoto Encyclopedia of Genes and Genomes
LAMP	Lysosomal-Associated Membrane Protein
LCC	Large Cell Carcinoma
LCNEC	Large Cell Neuroendocrine Carcinoma
LINC	Linkers of the Nucleus and Cytoskeleton
MALDI	Matrix Assisted Laser Desorption/Ionization
MCS _c	Mesenchymal Stem Cells
MET	Mesenchymal-to-Epithelial Transition
MMP	Matrix Metalloproteinases
MP	Micro Particles
MS	Mass Spectrometry
MVBs	Microvesicular Bodies
MVEs	Multivesicular Endosomes
NSCLC	Non-small Cell Lung Cancer
NTA	Nano Particles Tracking Analysis
PDGF	Platelet Derived Growth Factors
PDI	Polydispersity Index
PEG	Polyethylene Glycol
PIK3CA	phosphatidylinositol-4,5-bisphosphate 3-kinase, catalytic subunit alpha
PMSF	Phenylmethylsulfonyl Fluoride
PS	Phosphatidylserine
PZP	Pregnancy zone protein
RIPA	Radio Immunoprecipitation Assay
RT-PCR	Real Time Polymerase Chain Reaction
SCC	Squamous Cell Carcinoma
SCLC	Small Cell Lung Cancer
SDS-PAGE	Sodium dodecyl sulfate polyacrylamide gel electrophoresis
SELDI	Surface-enhanced laser desorption/ionization
SEM	Scanning Electron Microscopy
STRING	Search Tool for the Retrieval of Interacting Genes/Proteins
SUN	Sad1 and UNC-84 Domain
TBS	Tris Buffer Saline
TDE	Tumour Derived Exosomes
TEI	Total Exosome Isolation Kit
TEM	Transmission Electron Microscopy
TfR	Transferrin Receptor
TGF β	Transforming Growth Factor Beta

TME	Tumour Micro-Environment
UC	Ultracentrifugation
UHP	Ultra high pressure
VEGF	Vascular Endothelial Growth Factor
VPS	Vacuolar protein sorting
WB	Western Blot
WHO	World Health Organization
ZEB	E-box Binding Home Box

Chapter 1:

Introduction:

1.1 Overview of the project:

Understanding any human disease needs comprehensive analysis of the biological systems involved in that disease. For example, recently, it has been reported that extracellular vesicles such as exosomes released by almost all cells play an important role in the biological function of cancer. Several studies have addressed the proteomic profiling of cell as well as exosomes to analyse the molecular characteristics of proteins involved in physiological and pathological state of the biological system. The purpose of the project is to investigate exosomes from lung cancer cell line H358, leukaemia cell line THP1, breast cancer cell line MCF7 and primary lung cell HBTE as a source for cancer biomarker in general and lung cancer in particular.

1.2 Cancer:

Cancer is usually results of a series of molecular events where the functional properties of normal cells are altered. The alteration of normal cells to abnormal ones happens due to mutations of protein encoding genes which maintain cell division (Pierotti, 2017). Due to the gene mutation, the proteins that normally counter the DNA damage by triggering cell death, fails to do the DNA maintenance, which in turns increases the number of mutated cells with more mutations (Vogelstein et al., 2013). These mutated abnormal cells has the capability to invade or spread into other normal cells in the body (Kalia, 2015). Malignant cancer is normally characterised by the presence of six hallmarks which include cell proliferation, escape cell death, introduce angiogenesis, evade growth suppressors, disseminate, invade and metastasize (Hanahan and Weinberg, 2000).

According to World Health Organisation (WHO), cancer is one of the leading cause of death accounting for 8.8 million deaths in 2017 (Global Burden of Disease Cancer Collaboration, 2017) and within 2018 over 1.7 million new cancer cases are expected to be diagnosed in United States alone (Siegel et al., 2018). The basic difference between normal cells and cancer cells is that a normal cell grows into very specific cell type with distinct function. Normal cells have a well-defined nucleus, shape and fine chromatin. On the contrary, cancer cells do not follow this pattern and have multiple nuclei, an unorganised shape and a coarse

chromatin (Figure 1.1) (Webster et al., 2009). Normal cells are regulated by the signals which control cell divisions. But cancer cells can avoid the signals and divide without pause as long as they receive oxygen and nutrients to grow (Hanahan and Weinberg, 2000). This unregulated proliferation of cell brings abnormalities to cellular behaviour. Normal cells produce some growth factors such as epidermal growth factor (EGF) (Janmaat and Giaccone, 2003) and platelet derived growth factors (PDGF) by which normal cell sends signal to other cells to proliferate (Ranza et al., 2007). But cancer cells, instead of responding to these signals, continue to grow in an uncontrolled manner, invade other surrounding tissues and eventually end up being spread throughout the body (Jiang et al., 2015). Because of these uncontrolled behaviour cancer cells become totally independent to these signals that control cell growth or death and start to act as an autonomous entity rather than a part of the body (Aktipis et al., 2015). Cancer can occur from abnormal proliferation from any kind of normal cells so there can be many types of cancer depending on their origin of cell types (Hanahan and Weinberg, 2000). Cancer can be divided into two types such as benign tumours which do not metastasize and have distinct shape, have very low rate of growth and since they do not go through metastasis, they expands within the originated tissue. The other type is malignant tumours which have the ability to metastasise and avoid cell death. They also have a fast growth rate and doubling time. Metastasis is the penetration of the basement tissue membrane and invading other potential tissue (Morrissey et al., 2013).

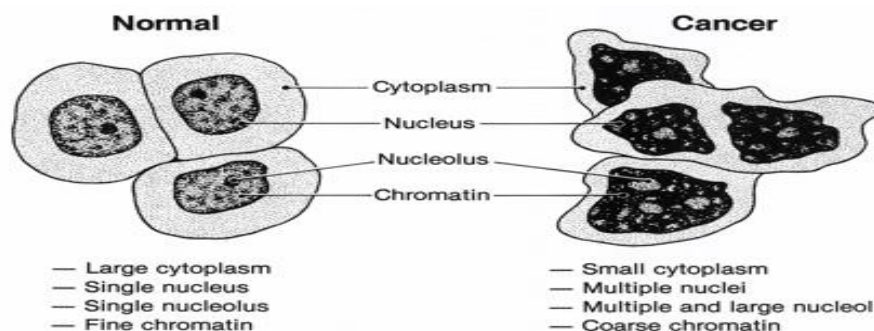


Figure 1.1: Structural differences between cancer cells and normal cells. On the left normal cell has a clear defined shape with distinct nucleus and nucleolus whease on the right, cancer cell does not have a distinct shape with multiple nuclei and coarse chromatin (Webster et al., 2009).

1.3 Cancer Discussed in this study:

Three cancers will be used in this study using representative cell lines. The first one is lung cancer. To study the exosomes of lung cancer, bronchoalveolar carcinoma, non-small cell lung cancer cell line H358 is used. The other two cancers are leukaemia and breast cancer. To

study the proteomics of exosomes from leukaemia, acute monocytic leukaemia cell line THP1 was used and breast adenocarcinoma cell line MCF7 was used to study breast cancer cell derived exosomes. These three cancers will be discussed individually in detail below.

1.3.1 Lung Cancer:

Among all cancers, lung cancer is the leading cause of death in both men and women followed by the prostate and breast cancer for men and women respectively (Siegel et al., 2016). Lung cancer is the main cause of one third of the total death from cancer in the world. Lung cancer can be divided into two major groups, non-small cell lung cancer (NSCLC) making up 80% of the total lung cancers and thought to be originated from epithelial cells from the lung and rest of the 20% are small cell lung cancer (SCLC) which is a tumour of neural crest origin (Sharma et al., 2007). SCLC consists of the major subtype of neuroendocrine tumours including typical carcinoid, atypical carcinoid, and large cell neuroendocrine carcinoma (LCNEC) (Chong et al., 2006). Smoking is one of the main causes for SCLC. Patients with SCLC are rarely operated due to the fast nature of spread and their aggressiveness (Rekhtman, 2010). NSCLC comprises the three major histotypes, including squamous cell carcinoma (SCC), large cell carcinoma (LCC) and adenocarcinoma (AC), the latter covers 30% of all lung cancers (Dela Cruz et al., 2011; Kayser et al., 2013) and reported as the most frequent histotypes in recent years replacing SCC (Devesa et al., 2005). AC consists of cells with secretory or glandular properties from the periphery of the lung (Sun et al., 2007). The recent changes in the histology is due to the increased rate of smoking in women and increased concentration of certain carcinogens in the modern cigarettes (Stellman et al., 1997). Interestingly, even though among all AC cases a total of 20% are associated with cigarette smoking, but the rest of the AC cases are non-smoker and women (Brambilla and Gazdar, 2009). On the other hand, SCC consists of multi-layered squamous cells usually not present in the respiratory epithelium but arises from the glandular or secretory cells due to the metaplastic changes as a result of smoking tobacco (Belinsky, 2004; Sun et al., 2007). The five-year survival rate after surgical treatment ranges from 80% for NSCLC in early stages (Uzel and Abacıoğlu, 2015). Smoking is one of the major risks for early onset of lung cancer. However, historical type, genetic susceptibility and gender distribution have also have impact on the early onset of lung cancer (Alexandrov et al., 2016; Kreuzer et al., 1998). However, mutation of *TP53*, Kirsten rat sarcoma virus (*KRAS*) and epidermal growth factor receptor (*EGFR*) genes are mostly altered in lung cancers. These genes are responsible for monitoring DNA damage and cell proliferation. Mutations of *TP53*

results altered p53 protein that fails to control cell proliferation and allows the damaged DNA to reside in cells (Collisson et al., 2014). Furthermore, altered *KRAS* and *EGRF* produces a GTP protein that fails to regulate cell division resulting tumour formation (Karachaliou et al., 2013). Risk factors of lung cancer include association of single nucleotide polymorphisms in matrix-metalloproteinase 1 (*MMP1*), Glutathione S transferase mu1 (*GSTM1*), and Cytochrome P 450 (*CYP450*) genes to the early onset of lung cancer (Sauter et al., 2008; Timofeeva et al., 2010). Additional risks include first degree relatives with cancer, even higher risk if the parent or siblings were affected with lung cancer (Bromen et al., 2000).

The cell line used in this study as lung cancer is H358 which is a bronchoalveolar carcinoma (BAC), which is a subset of lung adenocarcinoma arises from the distal bronchioles or alveoli and shows non invasive growth pattern (Van Schil et al., 2012). Due to the multicentric nature of BAC may arise from multiple lobes in the chest. The symptoms of BAC such as chest pain, cough and sputum production may mislead BAC with pneumonia or any other non-infectious diseases (Thompson, 2004). Clinical reports suggested that 62% BAC patients do not show any symptoms of BAC while 38% patients showed symptoms of chest pain, cough and sputum production (Dumont et al., 1998). H358 is a non small cell lung carcinoma which is different in clinical presentation, tumor biology and response to therapy compared to other non small cell lung carcinoma (Raz et al., 2006). Mutations in *EGFR* and *KRAS* genes are common with bronchioalveolar carcinoma (Garfield et al., 2006).

1.3.2 Breast Cancer:

The other two types of cancer cell investigated in this project are Breast cancer cell and acute monocytic leukaemia. Breast cancer is one of the leading public health issue worldwide (Stuckey, 2011). It is a heterogeneous disease for women with 252,710 new cases for invasive breast cancer were diagnosed in 2017 (American Cancer Society, 2017). The 5 year survival rate for breast cancer is 89% which goes down to 83% for 10 years and even lower at 78% for 15 years (Miller et al., 2016). Breast cancer starts from the parts of breast tissue that are meant to produce milk called lobules and ducts that linked with lobules with the nipples (Hansen and Bissell, 2000). *BRCA1*, *BRCA2*, *TP53* and *PTEN* are the most common genes that are found mutated in breast cancer (Filippini and Vega, 2013). However, genes involved in DNA repair such as *ATM*, *CHEK2*, *BRIP1*, *PALB2* and *RAD50* have been reported to be mutated in breast cancer (Ripperger et al., 2009). Apart from gender, factors considered as risk for breast cancer include age, family history, exposure to radiation, other carcinogens,

alcohol, ethnic groups, life styles such as diet and exercise (Stuckey, 2011). Other risk factors causes breast cancer include level of circulating oestrogen, events and choice of life, for example, giving birth for the first time, number of child she has, early menarche, late menopause, breastfeeding, the use of the contraceptive pill and hormone replacement therapy can all affect breast cancer risk (American Cancer Society, 2015). There are five subtypes of breast cancer which include Luminal A, Luminal B, Basal-like, Human Epidermal growth factor Receptor 2 (HER2) positive/Oestrogen Receptor (ER) negative, and normal breast-like (Polyak, 2007). Early detection of breast cancer is pivotal for improved diagnosis and treatments (Kösters and Gøtzsche, 2003).

The cell line used for the study of breast cancer is MCF7 cell line which is a breast adenocarcinoma derived from the metastatic site of pleural effusion. MCF7 is a ER-positive cell line (Lee et al., 2015). Mutations in *p53* gene (Balcer-Kubiczek et al., 1995) and *ESR1* have been reported MCF7 cell line.

1.3.3 Leukaemia:

Leukaemia is a disease of white blood cells circulating through the body. In a person with leukaemia, the bone marrow (BM) produces abnormal white blood cells that are called leukaemia cells and leukemic blast cells. Leukaemia is characterised by abnormal and uncontrolled proliferation of blood cells usually associated with mutated gene such as oncogenes, tumour suppressor genes (Crans and Sakamoto, 2001). Chimeric genes, one of the major contributor for the oncogenic abnormalities of normal cells which results due to the chromosomal translocation (Nambiar et al., 2008). Depending on the pathways of the stem cells leukaemia can be divided into two subtypes, myeloid or lymphoid. Moreover, based on the growth rate of either lymphoid or myeloid cells leukaemia is divided into two further subtypes including acute and chronic. In acute leukaemia, the BM produces vast amount of blood cells with impaired functionalities and very aggressive in nature with fast growing capability. So fast treatment is essential for the survival of the host (Blair et al., 1998). In contrast, chronic leukaemia cells have much slower growth rate and requires prolonged treatment and attention without any specific therapy (Rodrigues et al., 2016). In addition, depending on growth rate and type of cells leukaemia can be divided into four groups, acute lymphocytic (ALL), chronic lymphocytic (CLL), acute myeloid (AML), and chronic myeloid (CML). Although leukaemia is often thought of as a childhood cancer, the majority (91%) of cases are diagnosed in adults 20 years of age and older. Among adults, the most common

types are CLL (37%) and AML (31%), while ALL is most common in those 0 to 19 years, accounting for 75% of cases. There are no early screening tests recommended for leukaemia but diagnosis is done sometimes based on the irregular blood test results performed for other indications. AML is a heterogeneous disease with different immune phenotyping and cytogenic characteristics. The basic characteristics of AML are the production of extremely high number of abnormal cells without the capability to mature into functional cells, such as monocytes. The high number of abnormal cells with dysfunctional characteristics replaces the normal cells in the BM, which hampered the production of white blood cells, red blood cells and platelets. As a result, the whole immune systems suffer insufficiency. Several abnormalities in the chromosome have been detected which lead to AML and decides the outcome of the treatment (Döhner et al., 2010). *FLT3*, *NPM1* and *CEBPA* are reported as the most mutated genes in AML (Nardi and Hasserjian, 2016). Mutation analysis several other genes are also considered significantly important. For instance, in a study of 1185 AML patients, mutations in several other genes such as *KIT*, *N-RAS*, *MLL*, *WT1*, *IDH1/2*, *TET2*, *DNMT3A* and *ASXL1* were observed most frequently (Dombret, 2011). This irregularity and heterogeneity of genetic variations in AML make the improvement of individual treatments greatly difficult. A few works have demonstrated a high relationship between the level of heterogeneity, treatment result and the presence of remaining residues after treatment (Vo et al., 2012). This is because even a little subpopulation of cells with genetic abnormalities might be of significant reoccur the disease and should be considered in treatment plan (Saultz and Garzon, 2016).

THP1 cell line is used as a representative for leukaemia. THP1 is an acute monocytic leukaemia (AML-M5) and derived from peripheral blood which mainly consists of monocytes. It is considered as one of the sub type of AML and represents 3-6% of all AML and characterised by the symptoms such as fatigue, fever, bleeding disorders and gingival hyperplasia. The incidence of AML-M5 is higher in men than female with a ratio of 1.8 male to female (Khokhar et al., 2010). In AML-M5 around 20% of bone marrow cells are monocytes. AML-M5 is usually associated with abnormalities in the chromosomes normally chromosome 11 such as t(9:11) (Kollmannsberger et al., 1998). Genetic mutations of acute monocytic leukaemia include *MLL* and *DMNT3A* genes (Yan et al., 2011).

1.4 Mechanism of Metastasis:

Metastasis plays a vital role in cancer development. It is the main reason of death for 90% cancer patients. It is the end product of a very complex multistep biological process (Mehlen and Puisieux, 2006). Metastasis is the formation of progressive secondary tumour distant from their site of origin (Keller, 2002). During metastasis the tumour cells have to go through several discrete processes starting with tumour cells invading the surrounding tissues (local invasion). Then penetrating the blood and lymphatic vessels (intravasation), and being transported to distant sites (transport) only to escape the circulatory systems (extravasation) and form small nodules (micro metastases), which finally grows into fully developed macro metastases (metastatic colonization) (Nguyen et al., 2009). Figure 1.2 shows the schematic steps of metastasis.

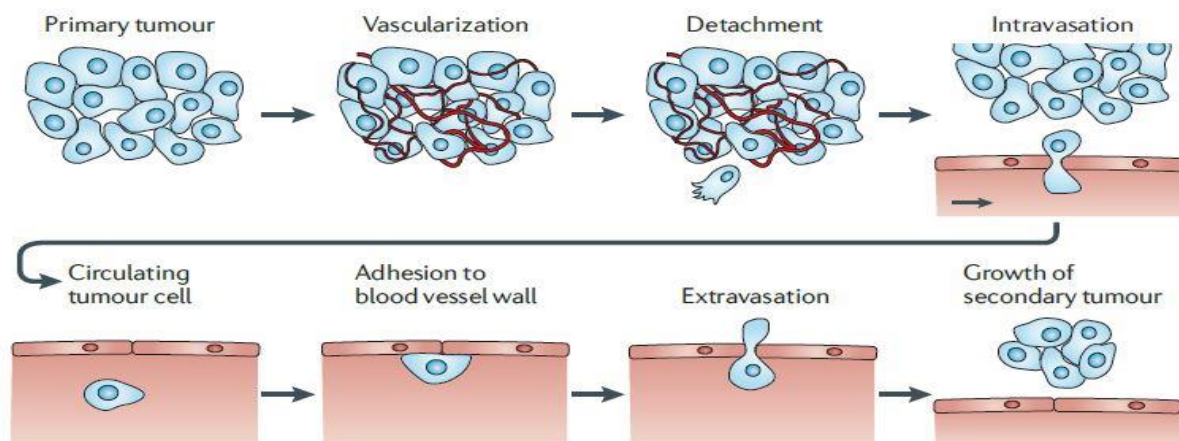


Figure 1.2: Stages of metastatic process, from primary tumour invasion to growth of secondary tumour. Cancer cells escape from the primary tumour site, pass through the membrane of the blood vessels or lymphatic vessels, travel through the vessels and finally escapes the vessels when they reach the secondary tumour site to metastasize (Wirtz et al., 2011).

Cancer progression and metastasis starts by invasion, where cancer cells overcome the extracellular barrier by their ability to attach, proteolyse the extracellular matrix components and then migrate into surrounding tissues either collectively or individually. Initiation of invasion occurs once tumour cells have the capability to pass through the membrane of the surrounding tissues and the extracellular matrix (Soung et al., 2015). During invasion, tumour cells adhere to the cellular components of the cell surface receptors called adhesion molecules or CAMs (cell to cell adhesion molecules) and glycoproteins of the cell surface. These proteins belong to the six proteins families such as cadherins, integrins, immunoglobulin superfamily, selectin and lymphocytes homing receptors (Bozzuto et al.,

2010). The successful completion of invasion of cancer cells will lead to intravasation of tumour cells by penetrating through the lymphatic or vascular circulation (Martin et al., 2000). Once in the circulatory system tumour cells have to face the fluid shear stress, hydrostatic pressure, and tension as well as compression forces of the soft tissues (Butcher et al., 2009). During intravasation and extravasation, tumour cells overcome severe cell deformation and squeeze through the endothelial junctions and show severe resistance against cell deformations (Mitchell and King, 2013). This requires increased elasticity of the cytoplasm and the interphase nucleus that is driven by cytoskeletal remodelling, chromatin organization and nuclear envelope interactions, via linkers of the nucleus and cytoskeleton (LINC) proteins, SUN domain containing proteins and Klarsicht homology (KASH) domain-containing proteins, with the cytoskeleton (Wirtz et al., 2011).

Once in the circulatory system, cancer cells must overcome the shear stress and collisions with other cell types and immunologic surveillance (Talmadge and Fidler, 2010; Wirtz et al., 2011). Activated platelets and leukocytes cluster with cancer cells and protect the cancer cells from shear stress and immunologic surveillance (Lou et al., 2015).

For extravasation to occur, circulating tumour cells have to be either trapped in small vessels, whose diameter is less than that of tumour cells, or adhere to the vessel walls. Adhesion of circulating tumour cells depends on shear flow and is mediated by receptor-ligand interactions between cancer cells and activated endothelium (Gay and Felding-Habermann, 2011; Wirtz et al., 2011). It is thought that activated platelets release a multitude of growth factors including VEGF (vascular endothelial growth factor), PDGF (platelet derived growth factor), TGF β and promote tumour cell extravasation and invasion into the new microenvironment (Roberts et al., 2013).

The location of metastatic sites has been a controversial topic in the field of cancer research (Talmadge and Fidler, 2010). In 1889, Stephen Paget recognized that cancer cells show a specific affinity or tropism for particular organs (Ribatti et al., 2006). For instance, breast cancer cells metastasize typically to lungs, bones, liver and less often brain tissue while prostate cancer cells almost exclusively metastasize to bone and liver but not lungs (Talmadge and Fidler, 2010). As a result, Paget first proposed the 'seed and soil' hypothesis, which upholds that organ specificity of metastasis corresponds to innate characteristics of the tumour cell, the 'seed' as well as a particular organ micro-environment; the 'soil' which has to fit the requirements of the cancer cells (Ribatti et al., 2006). This was later challenged by

an alternative hypothesis, which states that the location of a metastatic site depends on the pattern of blood flow. However, both the pattern of blood flow and the local microenvironment may have a complementary role in influencing the site at which secondary metastases grow (Talmadge and Fidler, 2010).

Once at the secondary organ, single tumour cells form micro-metastatic lesions that eventually grow into macro-metastatic tumours, in a process known as colonization (Talmadge and Fidler, 2010). However, colonization is thought to be a rate-limiting step in the metastatic cascade because many patients have a number of microscopic colonies that do not progress to macro-metastases (Bissell and Hines, 2011; Talmadge and Fidler, 2010). It has been suggested that EMT (epithelial mesenchymal transition), which is associated with cell cycle arrest in disseminating tumour cells, may prevent efficient growth of metastases (Brabletz, 2012). This was recently supported by the findings that in secondary tissues, cancer cells undergo a mesenchymal-to-epithelial transition (MET), which facilitates growth of metastases by promoting stem cell like properties (Ocaña et al., 2012), proliferation (Tsai et al., 2012) and alteration of the secretome (Korpál et al., 2011). Importantly, EMT and MET are regulated by reciprocal interactions between EMT-inducing transcription factors, such as the zinc finger E-box binding home box (ZEB) family members and Snail, and MET-inducing microRNAs, including miR-200 and miR-34 families (Brabletz, 2012; Théry et al., 2009). It is currently unknown what signalling molecules induce MET in metastatic cells, however, a TGF β –related protein, bone morphogenetic protein (BMP), stimulates expression of miR-200 family members to drive MET during somatic cell reprogramming (Samavarchi-Tehrani et al., 2010).

Recently it has been found that, nano sized vesicles released by cells called ‘exosomes’ play an important role in invasion and cancer progression by enhancing the interaction between the cells and their microenvironment (De Toro et al., 2015). Exosomes gained much attention recently because they contain biomolecules like protein, lipids, nucleic acids that can be transferred from primary tumour cells to various organs and tissues and help to create an ideal environment by transforming the neighbouring cells within the microenvironment so that the tumour cells can interact with neighbouring cell for successful growth and metastasis (Soung et al., 2015).

1.5 Exosome:

Exosome are a distinct type of vesicles secreted by almost all cells and differ from other released vesicles from the cell due to their size, shape and biogenesis (Pan et al., 1985). They are formed by the budding of the limiting membrane of the sorting vascular endosomes towards the lumen of these compartments thus forming intraluminal vesicles (ILVs). The endosomes are then termed as micro vesicular bodies (MVBs) or multivesicular endosomes (MVEs). Upon fusion of the MVEs to the plasma membrane the internal vesicles are released to the extracellular space and termed as exosomes (Figure 1.3).

Exosomes are extracellular vesicles enclosed by a lipid bilayer, released by almost all cells including normal and cancer cells. They have a round-cup shaped morphology with a size range of 30-150nm (Zerlinger et al., 2013; Sun et al., 2013; Yellon and Davidson, 2014). Exosomes have some defining characteristics such as their nano size morphology, a density gradient of 1.13-1.21g/ml and presence of several protein markers such as the tetraspanins, TSG101, Alix (Zhang et al., 2014). Previously, exosomes were thought to be involved in waste disposal mechanism to remove any unwanted materials from cells (Tickner et al., 2014) but recently they gained much interest because of their role in cancer development and other biological functions (Greening et al., 2015). Several studies show that exosomes from both normal and malignant cells play vital role in tumorigenesis, apoptosis, and chemotherapeutic resistance. They also works as important mediators in extracellular signalling of cellular materials to other cells through the membrane (Figure 1.3) (Azmi et al., 2013). Therefore, exosomes gained one of top priorities in cancer research because of the molecular constituents of their cell origin including protein, lipids, miRNAs which play important role tumorigenesis (Minciacchi et al., 2015).

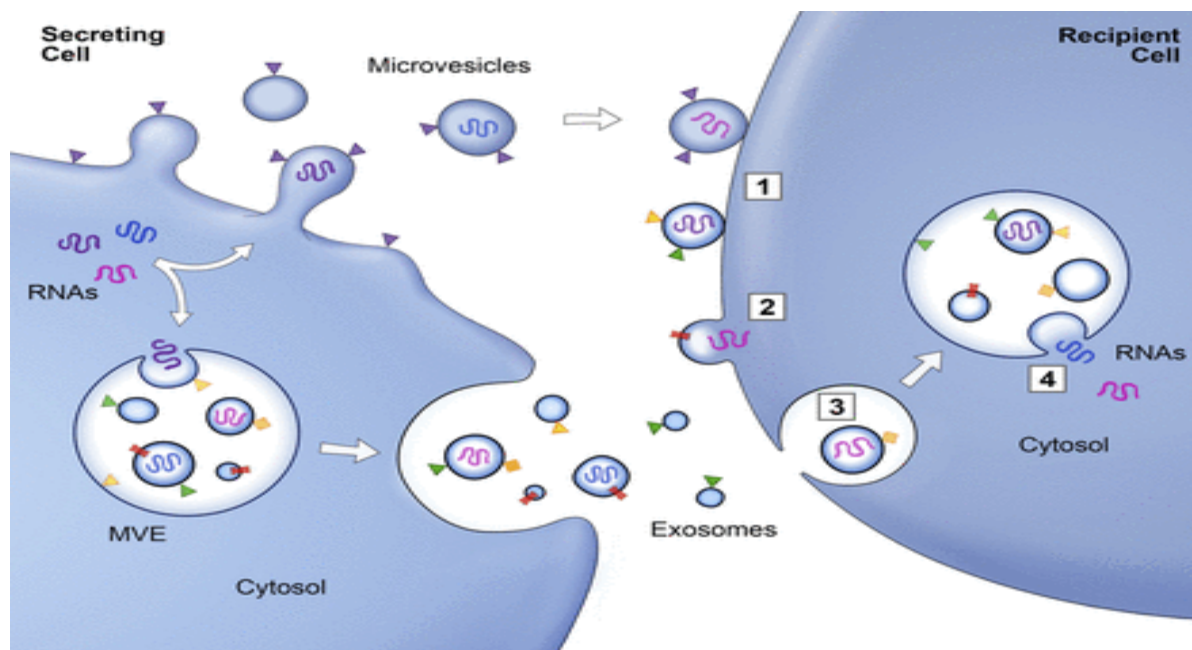


Figure 1.3: Biogenesis of exosomes. Exosomes are secreted by the exocytosis of the multivesicular endosomes and taken up by the recipient cells by endocytosis.

1.5.1 Role of exosomes in metastasis:

Tumour derived exosomes help in metastatic process in cancer cells, it has been reported that exosomes from tumour cells have the potential to assist the pre-metastatic niche, a chain of events that prepare for the metastatic sites for the incoming metastatic cells (Costa-Silva et al., 2015). In figure 1.4 a schematic diagram explains the role of exosomes in the process of metastasis. At first cancer exosomes initiate the epithelial mesenchymal transition in tumour epithelial cells by mediating autocrine and paracrine signals within the microenvironment. This transition allows exosomes to enter into the blood circulation by invading other surrounding tissues (Syn et al., 2016). The exosomes are then taken up by the distant tissues to form a premetastatic niche which facilitates the metastatic cells to attach and extravasate and eventually form colony of secondary tumour (Hood et al., 2011; Peinado et al., 2012). Cancer exosomes modulate the host immunity to allow uncontrolled disease progression, and even convert immune system into fostering a prometastatic microenvironment by activating inflammation response pathways (Costa-Silva et al., 2015).

Furthermore, it is reported that, the metastatic behaviour of bone marrow progenitor cells was increased by the introduction of exosomes derived from highly metastatic melanoma cells by increasing the expression of MET receptor and enhancing their colonization to new metastatic sites including the lungs and lymph nodes (Zhang and Wang, 2015). This behaviour was dependant on the inhibition of receptor tyrosine kinase, MET in exosome

derived from aggressive melanoma cells (Quail and Joyce, 2013a). Melanoma-derived exosomes were also capable of stimulating endothelial signalling that is important for endothelial angiogenesis. Recently it was also revealed that melanoma exosomes injected locally preferentially travelled to sentinel lymph nodes and that this homing caused molecular signals that provoked melanoma cell recruitment, extracellular matrix deposition, and vascular proliferation in the lymph nodes (Hood et al., 2011). Tetraspanins, (CD9, CD63, CD81 and CD82), which are enriched in exosomes, have been reported to contribute to exosome-mediated angiogenesis. In a study carried out by Gesierich et al., 2006, it was demonstrated that exosomes secreted from a pancreatic tumour cell lines that overexpress D6.1A (Human homologue CO-029, a tetraspanin associated with poor prognosis in patients with gastrointestinal cancer (Gesierich et al., 2006)), which enhanced tumour growth by its capacity to induce systematic angiogenesis in a rat model. Their results showed that D6.1A induces overexpression some proangiogenic factors and matrix metalloproteinase which are essential for the release of the angiogenic factors to induce the transcription of angiogenesis (Kräling et al., 1999).

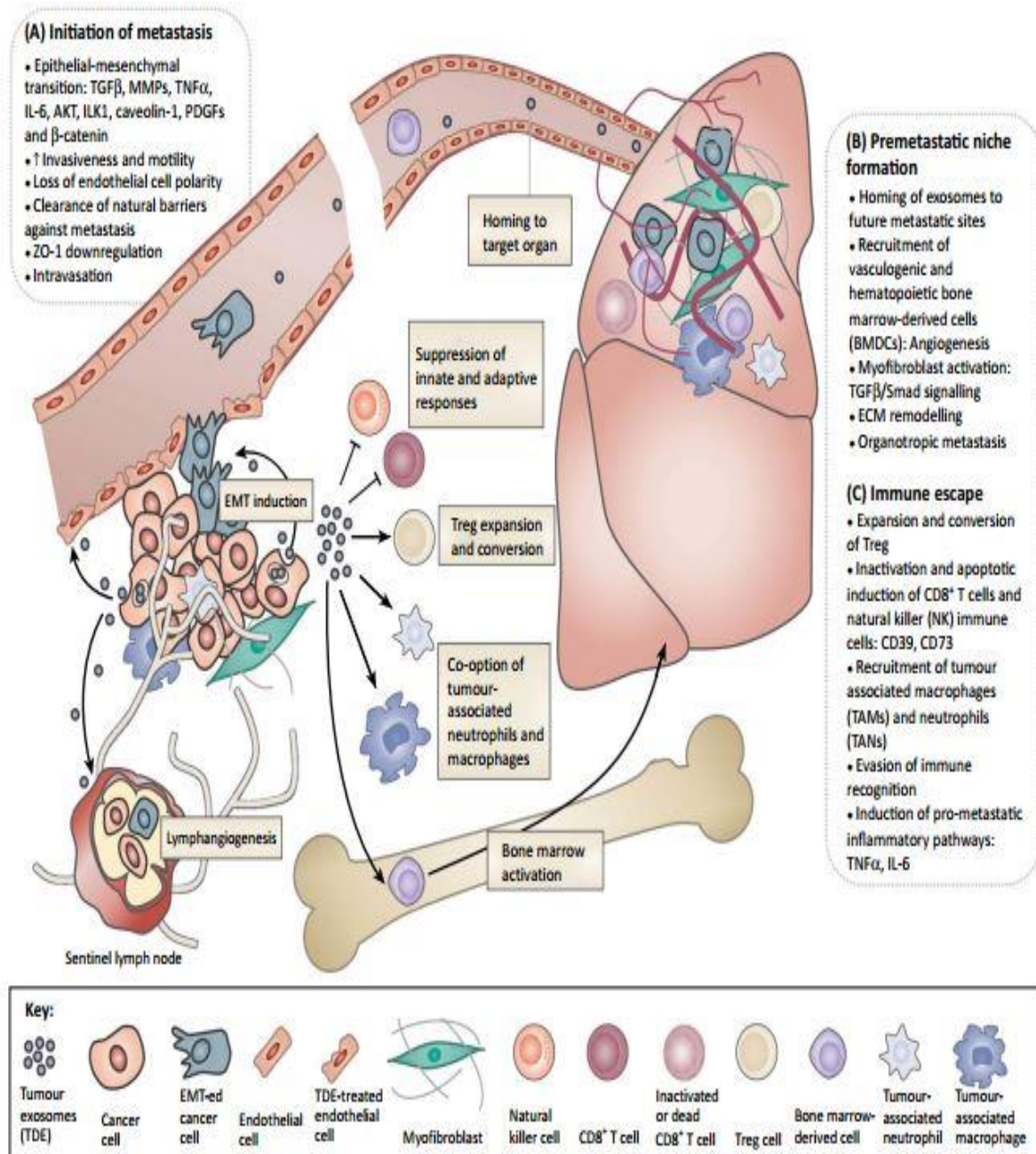


Figure 1.4: Role of exosomes in metastasis. (A) exosome initiate metastasis, by activating EMT pathways to enhance the invasiveness and motility of neoplastic cells and clearance of natural barriers against metastases; (B) the preparation of a premetastatic niche, via the recruitment of BMDCs, myofibroblast activation, and induction of ECM remodelling and angiogenic processes; and (C) the escape of tumour cells from immuno-surveillance, which may occur via the suppression of the innate and adaptive arms of the host immunity, and conversion of reactive tumour infiltrates into accomplices in malignancy. Abbreviations: Treg, regulatory T cell; TGF β , transforming growth factor beta; MMPs, matrix metalloproteinases; TNF α , tumour necrosis factor alpha; IL-6, interleukin-6; AKT, proto-oncogene Akt; ILK1, integrin-linked kinase 1; PDGF, platelet-derived growth factor; ZO-1, tight junction protein 1; ECM, extracellular matrix; EMT, epithelial–mesenchymal transition; BMDCs, bone marrow-derived cells; TDEs, tumour-derived exosomes. 608 Trends(Syn et al., 2016).

1.6 Composition of Exosome:

Exosomes are one of the most complex nano entities that are enriched in an arrays of proteins, lipids, nucleic acid and RNAs (Kalani and Tyagi, 2015). This kind of molecular arrangement is very versatile and depends on the specific cell type (Beach et al., 2014; Kooijmans et al., 2012). During the last decade or so, the composition of exosomes has been thoroughly investigated using various techniques including electrophoresis, mass spectrometry, western blotting, flow cytometry, immune-EM. Recent advances in the MS-based proteomic analysis, RNA analysis has been involved in a very crucial role to enhance the understanding of the composition of exosomes derived from various body fluids (Choi et al., 2013). All the proteins and RNA that are identified from exosomes so far are freely available to the scientific community in ExoCarta (<http://www.exocarta.org/>), a free compendium of proteins and RNA identified from exosomes (Mathivanan and Simpson, 2009).

1.6.1 Lipid Composition:

The first layer or the membrane of exosomes is composed of lipid bilayer which is partially resistant to detergent. Several studies have shown that, exosomal membrane from different cell types including B-cell has been found enriched of lipid rafts which includes cholesterol, shingomyelin and ganglioside GM3 (Miyaniishi et al., 2007; Smalheiser, 2007; Wubbolts et al., 2003). However, exosomes derived from mast cells and DCs showed decrease level of cholesterol and loss of phospholipid asymmetry but they did show increase in flip-flop of lipids between the two leaflets when compared with the plasma membrane (Laulagnier et al., 2004).

Exosome membrane has been reported to have phosphatidylserine (PS) which is distributed between inner and outer side equally whereas plasma membrane in normal cells contain phosphatidylserine to their inner side. At early stage of apoptosis, this phosphatidylserine becomes exposed to the cell surface and recognised by the macrophages to help mediate phagocytosis of apoptotic cells (Kooijmans et al., 2012; Miyaniishi et al., 2007). PS was also observed by flow cytometry analysis of Annexin-V stained exosome-bead complexes (Fomina et al., 2003; Heijnen et al., 1999).

1.6.2 Exosomal Protein Composition:

From the initial characterisation, a lot of efforts have been put on to identify and characterise good quality exosomes. The presence of TfR (Transferrin receptor) associated to exosomes released by reticulocytes was first identified by electron microscopy (EM) analysis (Pan et al., 1985). Later on western blot analysis was used coupled with EM showed the presence of exosomes in B lymphocytes enriched with MHC class II (Raposo et al., 1996) and subsequently identified MHC class I and II, as well as Tfr along with the tetraspanins (CD63 and CD82) were found in dendritic cells (Zitvogel et al., 1998). Exosomal protein composition has been one of the main focuses for the researcher in recent years. It has been found that, exosomes share some common proteins within all exosomes derived from all cell types and some with their parent cells. Even though exosomes share some common proteins regardless of the cell of origin, they do not cover the entire proteome of the parent cells (Mears et al., 2004). Exosomes also have some cell type specific proteins which perform specific function directed by the cells. Such as A33, cadherin-17, CEA, epithelial cell surface antigen (EpCAM) and mucin-13 were identified from colon tumour cells (Mathivanan and Simpson, 2009). The universal exosomal proteins include, the tetraspanins, (CD63, CD81, CD9, CD82), the heat shock proteins70 (Hsp70), Rab protein family, cytoskeletal components – actin, antigen presentation - MHC class I, lysosome markers - LAMP1, LAMP2, Alix, tumour suppressor gene101 (Tsg101) (Conde-Vancells et al., 2008; Yoshioka et al., 2013a) (Figure 1.5). A number of proteins common to almost all exosomes have been identified which includes membrane adhesion proteins such as integrins which are cell specific (Lamparski et al., 2002). Other examples are, α M from DCs, β 2 from DCs. Mast cells, T cells and α 4 β 1 from reticulocytes (Théry, Zitvogel, et al., 2002).

1.6.2.1 CD63:

CD63 belongs to the family of tetraspanins, whose gene is located on chromosome 12 in humans and is a transmembrane glycoprotein which interacts directly or indirectly with other molecules such as CD9, CD 81, CD 3, MHC II etc. CD63 is one of the most frequently used exosome marker protein expressed on the surface of late endosomes (exosomes) and lysosomes (Lin et al., 2015) found in various cancer cells *in vitro* and *in vivo*. For example high levels of CD63 expression was observed in exosomes derived from melanoma patients (Logozzi et al., 2009). Furthermore, immunoblotting analysis on three different prostate cell lines including normal and cancerous cell lines and five breast cancer cell line were found positive for the expression of CD63 (Yoshioka et al., 2013a). Alike LAMP 1 and LAMP2,

CD63 contain YXXØ motif at the carboxylic end which is important for endocytosis at the plasma membrane.

The formation of exosomal sorting complex plays an important role in incorporation of this protein on exosome surface. CD63 was first discovered to be expressed on the surface of early stage melanoma cells (Hotta et al., 1988). However the expression of CD63 decreases as cancer reaches to the late stage (Jang and Lee, 2003). As a result, this negative co-relation is very important as it helps to detect cancer at early stage. The CD 63 plays vital role in transporting protein which is specifically associated with tumour within the cell. In breast cancer the CD63 interact with TIMP1 which result in activation of integrin $\beta 1$ and thereby help in cell survival signalling and inhibition of apoptosis (Pols and Klumperman, 2009).

1.6.2.2 CD81:

CD81 is another member of the family of tetraspanin proteins which is expressed on the surface of the cell (Bartosch et al., 2003). The gene of CD81 is located on chromosome number 11 in humans. It is considered as surface protein whose molecular weight is 26 kDa. The gene of CD81 found to be expressed in haemopoietin, epithelial and endothelial cells. CD81 has been reported to be involved in various cellular function which includes adhesion, activation and differentiation of B, T and other cells (Levy et al., 1998). Evidence also suggests that CD81 like other tetraspanins are involved in tumour progression and metastasis. In a study on mice model it has been observed that lack of expression of CD81 in lung carcinoma cell line reduced tumour growth compared to the control. In the follow up study similar effect was also seen on breast cancer cells on the same mice model (Vences-Catalán et al., 2015). The main function of CD81 is in regulation of signal pathway, like the other members of tetraspanins family. CD81 helps in cell development, activation, growth and motility (Levy et al., 1998).

1.6.2.3 CD9:

According to ExoCarta (<http://www.exocarta.org/>) a CD9 is the most identified exosomal protein. CD 9 is the surface glycoprotein which interacts with integrins and other transmembrane 4 superfamily proteins. Similarly to its other tetraspanins family members CD9 plays an important role in cell adhesion and migration (Andreu and Yáñez-Mó, 2014). Furthermore, like other tetraspanins CD9 also plays a vital role in cancer cell motility, growth and proliferation (Kwon et al., 2014). Overexpression of CD9 in melanoma, lung, and breast cancer were found to be associated with the suppression of cell motility and metastasis of

these cancer cells (Wang et al., 2011). Evidence suggests that tumour stage and metastasis of the lymph node in esophageal squamous cell carcinoma (ESCC) have been found to be dependent on the expression of CD9. The expression level was found higher oesophageal squamous cell carcinoma (ESCC) when compared to normal Oesophageal cells (Jian et al., 2015).

1.6.2.4 Alix:

Alix is a well-known exosomal marker protein. It is a cytosolic protein found in mammalian cells. It was identified as the molecule which assists in pro apoptotic signalling. It plays a vital part in cell adhesion and endocytic membrane trafficking. Alix has been reported to play a vital role in apoptosis (Odorizzi, 2006). It binds with ALG-2, a member of the tetra-EEE hand protein family of Ca⁺ protein family (Maki et al., 2002). It has been shown that up regulation of endogenous Alix ends up with cell death (Blum et al., 2004). If the expression of Alix are overexpressed, it triggers the caspase activation and apoptosis in the absence of pro-apoptotic signals (Mahul-Mellier, 2006; Trioulier et al., 2004).

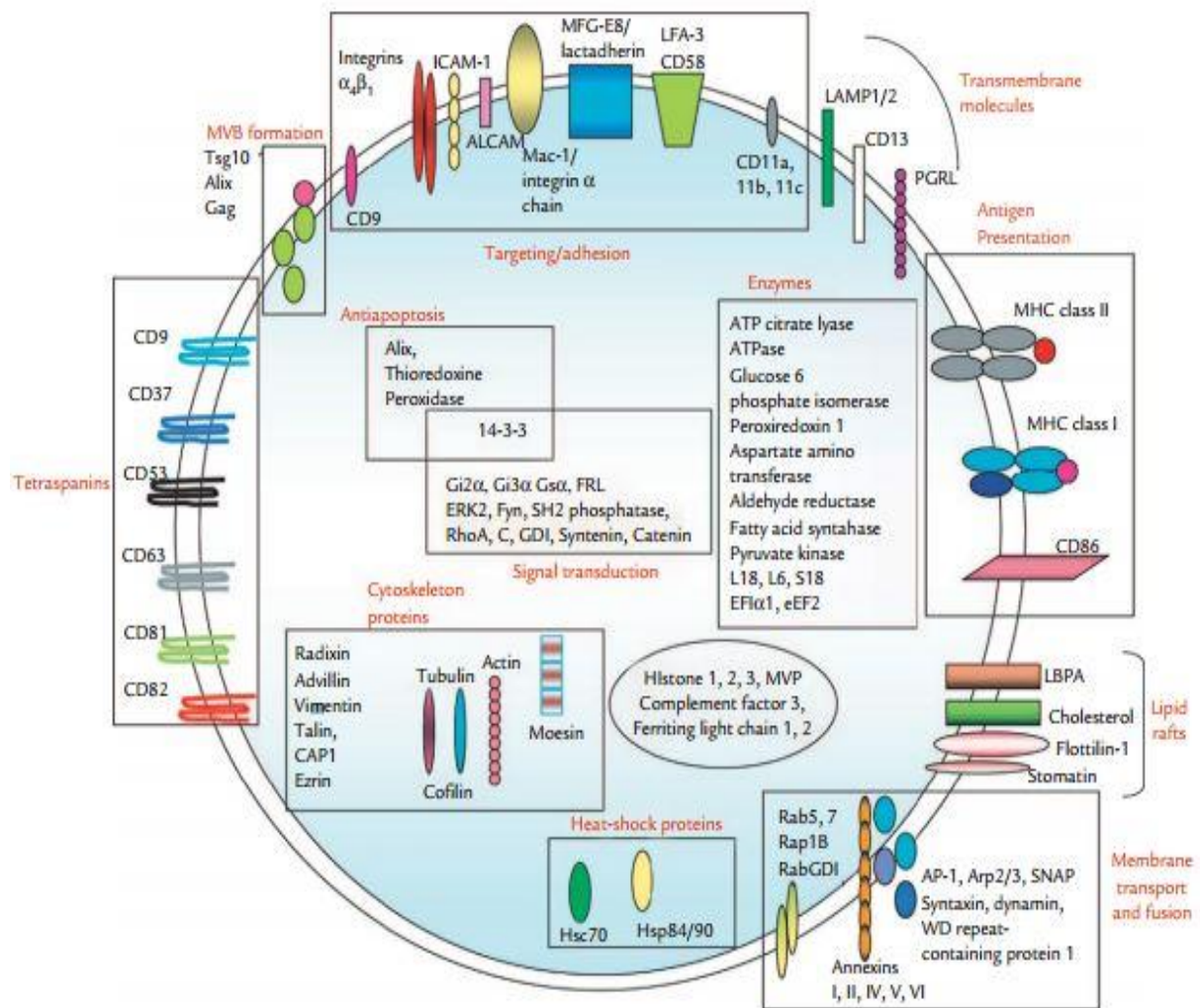


Figure 1.5: Protein composition of exosomes. Common exosomal protein with their location including tetraspanins (CD63, -81, -9, 82), multi-vesicular body (MVB) formation proteins, transmembrane proteins, antigen preparation proteins, enzymes (Natasha et al., 2014).

1.6.3 Exosomal RNA composition:

Recent studies have suggested that exosomes contain an array of RNAs. Their RNA content includes miRNA, some non-coding RNA, as well as mRNA (Melo et al., 2014). The presence of messenger RNA (mRNA) has been discovered by Valadi et al., 2007. They identified 1300 mRNA and 120 miRNA from Rat and human mast cells derived exosomes. They further demonstrated that the mRNA was transferable from one cell to another and the transferred mRNA can be functional in its new location leading to the translation of the acquired RNA (Valadi et al., 2007). Since then miRNAs from tumour derived exosomes have been identified from ovarian cancer patients and lung adenocarcinoma patients by using magnetic beads coated with anti-EpCam antibody. These studies enhanced the comparison of RNA profile of control and cancer patients (Rabinowits et al., 2009; Taylor and Gerchel-

Taylor, 2008). Recently it has been reported that exosomal regulatory RNAs are functional in their target cells. It was showed that exosomes from EBV-infected virus has successfully transfer miRNA to an uninfected cells. Once the miRNAs are inside the target cells they were capable of repress EBV target genes. This was demonstrated by new mouse proteins being transiently expressed in recipient cells (Pegtel et al., 2010).

1.6.4 Biogenesis of Exosomes:

The uptake of materials from the exterior of the cells is managed by the endocytosis. The endocytic vesicles are then delivered to late endosomes together with other proteins or transported back to the plasma membrane (Février and Raposo, 2004). In the late endosomes, proteins are accumulated inside the intraluminal vesicles by the inward budding of the limiting membrane into the endosomal lumen. However, proteins are incorporated into the invaginating membrane and maintains the symmetric properties compared to the plasma membrane while the cytosolic materials are being submerged and enclosed into the small vesicles (Pant et al., 2012).

The mechanisms by which proteins are sorted into the intraluminal vesicles at the endosomal limiting membrane are not fully understood. One mechanism demonstrated where the ubiquitinated proteins were recognised by the Endosomal Sorting Complex Required for Transport (ESCRT). The ESCRT machinery includes four heterogenic protein complexes. The ubiquitinated proteins were recognised and kept separated by the three ESCRT protein complexes such as they are the ESCRT-0, I and II. But not all the proteins in the exosomes are ubiquitinated. So the idea of other mechanism was taken into consideration by which proteins are sorted into the exosomes such as oligomerization or partition of proteins in the lipid raft domain was thought to be involved (Gassart et al., 2003; Simons and Raposo, 2009). Furthermore, in a study carried on melanocytes, it was observed that the tetraspanins CD63 was involved in an ESCRT independent mechanism and also showed the involvement of different sorting complexes for the decider of protein secretion or degradation (van Niel et al., 2011).

In the final step, lipid components have been implicated in the process. As mentioned before exosomes have lipid-raft micro domains on their surface which are enriched with sphingolipids which might concentrate the protein cargo and play a role in initiating the secretion of exosomes (Gassart et al., 2003; Trajkovic et al., 2008).

Taking both the methods in consideration, they are not actually opposed to each other; it rather shows the presence of heterogeneous populations of MVEs and exosomes (Figure 1.6). Accordingly it has been demonstrated in many studies that exosomes from different cancer cells differ in their types but they share morphological characteristics and some stereo-typical exosome markers such as Alix, TSG101, Hsp70 but have differences in their miRNA composition and also they are enriched in specific marker such as CD63 (Villarroya-Beltri et al., 2014).

After the sorting out of materials by either method, the ILVs are released in the extracellular space by the fusion of the MVEs with the plasma membrane and from this point on these ILVs are termed as exosomes. This transport process is dependent on several components of the endocytic machinery such as Rab, GTPase, Rab11, Rab27a and Rab27b, cytoskeleton regulatory proteins, molecular motor such as myosin and SNAREs for targeted fusion (Ostrowski et al., 2010; Pant et al., 2012).

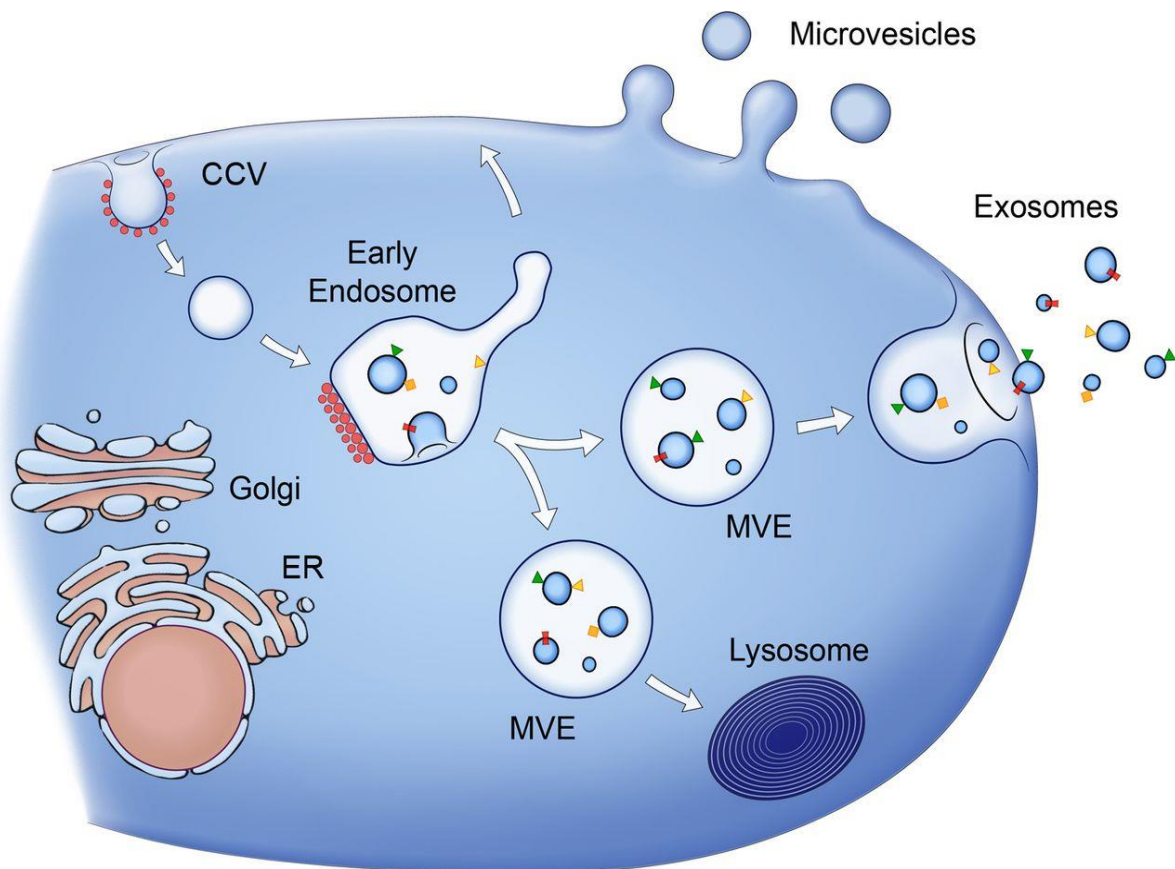


Figure 1.6: Biogenesis and secretion of exosome. Exosomes are secreted by the fusion of the MVEs with plasma membrane. MVEs are formed by the inclusion of late endosomes with the Golgi such as MHC class II molecules or the cell surface such as growth factor receptor. Source : (Raposo and Stoorvogel, 2013).

1.7 Isolation of Exosomes:

Before any kind of analysis with exosomes, it needs to be purified or isolated, identified and characterised to differentiate from other vesicles secreted by cells. There are many methods to isolate exosomes from biological fluids or cell culture medium. The main methods published in the literatures include differential ultracentrifugation, continuous sucrose gradient, preparation on a 30% sucrose cushion or another dense medium, and immune-isolation. Using polymer based isolation of exosomes by commercially available exosome isolation kit or PEG (Polyethelyn Glycol) based isolation have recently been employed in exosomal isolation (Helwa et al., 2017). The choice of method for exosomes isolation is really important because the smallest components of exosomes can now be detected and identified due to the high sensitivity of recent molecular technologies. So, isolated exosomes with contaminating aggregates would create false interpretation. Similarly, fractionated exosome isolation or exosomes with disrupted membrane can alter the protein or RNA profile. So, deciding the right method for exosome isolation depending on the downstream analysis is very crucial (Taylor and Shah, 2015). According to the International Society of Extracellular Vesicles (ISEV), to determine the purity of exosomes, several recommendations are made such as the morphology needs to be checked by electron microscopy as well as the presence of exosomes. To quantify the isolation efficacy, the number of exosomes should be 3×10^{10} per μg of protein (Coumans et al., 2017).

1.7.1 Ultracentrifugation:

For many years, isolation of exosomes by ultracentrifugation is a traditional and most widely used method (Witwer et al., 2013). This is the first and most common method to purify exosomes from culture medium (CM) or biological fluids either coupled with density gradient ultracentrifugation or alone. The size filtration can also be added in this method to separate vesicles bigger than the expected exosome size (Peterson et al., 2015). In this method the CM or biological fluid is subjected to increasing centrifugal forces over several steps. Subsequent washing step is performed at the same speed as the drawbacks of this method is it enriches exosomes and any other vesicles in the same size range with contaminating proteins (Figure 1.7) (Théry et al., 2006). Even though isolation of exosomes by this method was considered to be the gold standard method for several years, this method is not capable to isolate exosomes completely based on particle size. Furthermore, due to the high g-force extra vesicular protein aggregates, lipoproteins, other contaminants may also be

pelleted down with the exosomes where density gradient method can be used to resolve the issue (Caradec et al., 2014). While this may be the widely used method, the method may have limited uses in proteomic study for biomarker research as it pellets down exosome as well as contaminating proteins. To add to its drawbacks, this methods is very time consuming and requires access of a ultracentrifuge with large capacity and the high g-force can also rapture the exosomes (Peterson et al., 2015). The advantages of ultracentrifugation is that it does not require any chemical addition (Abramowicz et al., 2016). Exosome isolation by ultracentrifugation is considered to be the method of choice covering more than 50% of exosome preparation (Li et al., 2017). However, carefull considerations should be taken about the soluble proteins that aggregate with the islolated exsomes and a further washing step should be added to avoid these protein contaminations (Coumans et al., 2017).

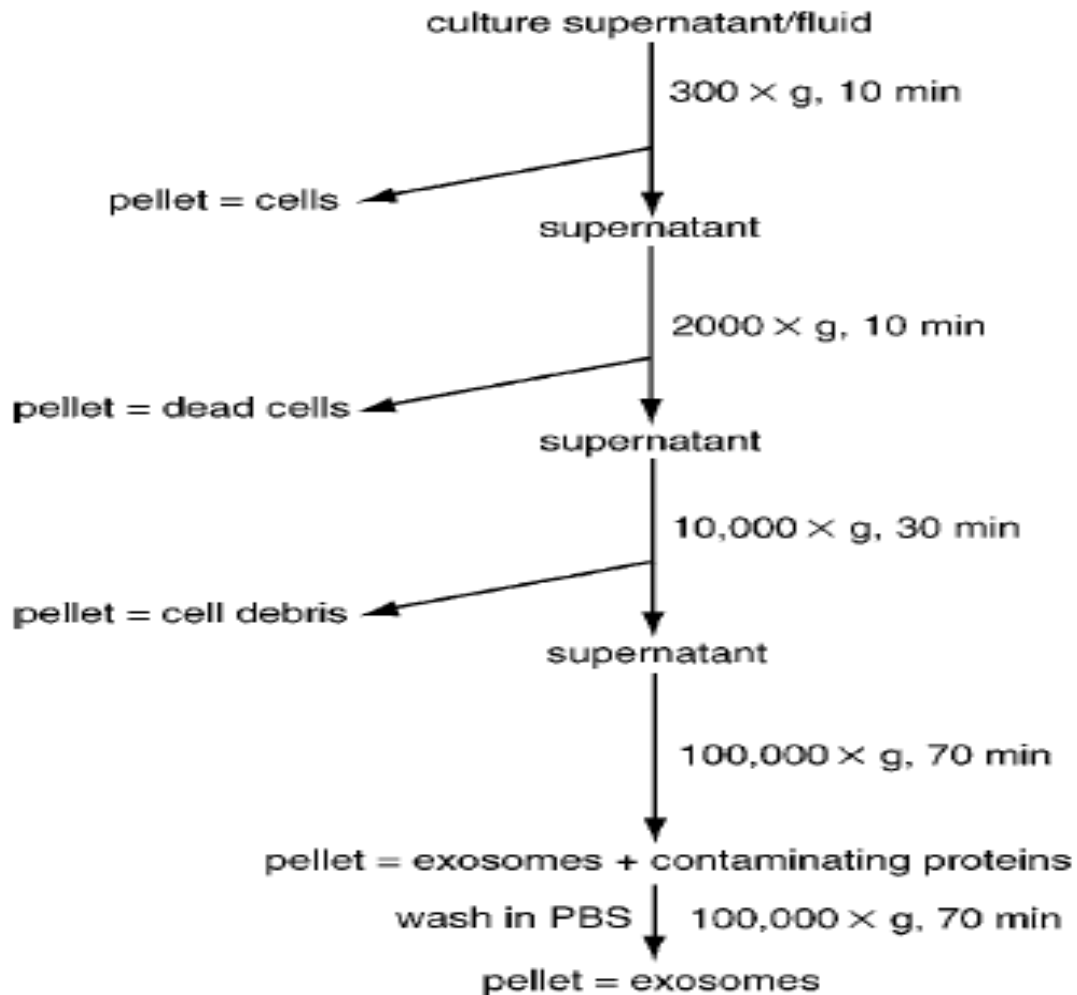


Figure 1.7: Isolation of exosomes by step wise centrifugation. The process starts with a low speed centrifuge to remove any dead cells and debris, then gradually speeding up to ultracentrifuge to separate exosomes from the supernatant. The final centrifuge is in PBS to avoid contamination of aggregating proteins (Théry et al., 2006).

1.7.2 Density Gradient Ultracentrifugation:

Another improved method for purifying exosomes using a sucrose density gradient. This method is based on the density gradient of exosomes and works in combination with ultracentrifugation and sucrose density gradients or sucrose cushion to float exosomes with low density gradient (Witwer et al., 2013). After the ultracentrifugation at 100000 x g, the pellet of exosomes is placed in a sucrose gradient using the theory that exosomes float on a sucrose gradient between 1.13 to 1.19 gm/ml (Witwer et al., 2013). This method helps to remove the contaminants like protein aggregates and soluble proteins. The enriched exosomes stay in different gradient which then can be pooled down for further analysis. The advantage of this method is it ensures less amount of contaminating proteins and debris (Lane et al., 2015; Théry et al., 2006). This method can be used to separate exosomes from mixture of particles such as proteins and proteins/RNA aggregates. The optimum centrifugation time is essential due to the risk of vesicles with similar density may still be present in the preparation. The disadvantage of this method is the long continuous centrifugation time (Keller et al., 2011). Factors need to be considered before applying density gradient method includes the choice of density medium and the sample loading approach due to the different viscosity of different biofluids (Coumans et al., 2017).

1.7.3 Size exclusion chromatography:

Size exclusion chromatography (SEC) is another method used to separate exosomes based on their size mostly from biological fluid such as urine or blood (Taylor et al., 2002). The method consists of a specialised column with porous polymeric beads. The polymeric beads contain multiple pores and tunnels. The extracellular particles pass through the column based on their diameter. Naturally the smaller particles take longer time than the larger particles due to their smaller size they had to cover more surface area. The size exclusion chromatography can be useful to separate nano and macro molecules from the sample based on their size. The advantage of this method over centrifugation methods is that it is not affected by the shearing force generated by the centrifuge which may affectively alter the structure of the particles (Taylor et al., 2011). The risk on this method was to lose any aggregated small particles (Thery et al., 2001; Valadi et al., 2007). According to ISEV, several factors need to assess before SEC such as the column height, pore size, quality of column stacking. In addition, to achieve the purest quality exosomes by SEC the fractions with the most concentrated exosomes need to be determined carefully. Furthermore, careful considerations should be

given as SEC includes the risk of eluting non-EV components such as cells, cellular debris and high molecular weight proteins. A second SEC steps using a new column and the separated fractions might remove the non-EV components (Böing et al., 2014).

1.7.4 Ultrafiltration:

Ultrafiltration method of exosome isolation is one of the size based isolation. The basic theory behind ultrafiltration is similar to conventional filtration technique where separation of suspended particles is carried out based on their size. So, exosomes can be isolated based on their size using membrane filter with designated size cut off (Quintana et al., 2015). It is less time consumable than ultracentrifugation and isolates better quality exosomes than other methods because the amount of pressure applied in this method is less than the centrifugal force applied in ultracentrifugation so there is less chance of disruption of exosomes (Li et al., 2017). However, the use of force could break up the large vesicles and may end up contaminating the exosome preparation (Batrakova and Kim, 2015). The advantages of this method are the separation of small particles and soluble contaminants from the exosome preparation and also the exosome preparation is concentrated during the filtration process. However, the drawbacks of this method is that, exosomes may attach with the membrane during filtration which (Benedikter et al., 2017) may lead to block the membrane and reduce the life time which is leads to low exosome yield (Liga et al., 2015; Xin et al., 2012).

1.7.5 Magnetic Beads:

Affinity based methods are based on the presence of the surface proteins of exosomes, where antibody coated magnetic beads or latex beads specific to those surface proteins were used to enrich exosomes. This method relies on the enrichment of surface proteins, trapping them on the magnetic beads and analyse them by flow cytometry. One example utilises magnetic beads coated with a particular antibody against a known exosomal membrane protein. For example when isolating exosomes from antigen-presenting cells an anti-MHC class II antibody may be used. The cell culture media or biological fluid is incubated with the beads for 24 h ensuring bead saturation. The bead exosome complexes are then thoroughly washed leaving just the exosome coated beads which can be subsequently analysed. The advantage of this method is that it separates exosomes from other particles based on the presence of the surface proteins. The limitation of this method is it is very difficult to extract the exosomes from the magnetic beads and narrows down the uses to a particular molecular signature.

Furthermore, the method is not suitable for large volume of samples (Clayton et al., 2001; Wubbolts et al., 2003).

1.7.6 Precipitation methods:

Another well-established method of exosome isolation is the precipitation method based on the similar method used in viral studies to isolate virus from culture medium (Taylor and Shah, 2015). It is a polymer based method which works by forming a network under optimal condition such as salt concentration and low temperature. By achieving this condition the polymer network traps the entire component in the sample medium and decreases their solubility. The popularity of this method increased after the use of two commonly used commercial product for exosome isolation. One of them is the ExoQuick from System Bioscience and the other one is Total Exosome Isolation kit by Invitrogen. Other products are also available in the market (Abramowicz et al., 2016). Instead of using commercially available polymer solution Polyethylene Glycol of various molecular weights have been used to isolate exosomes from culture supernatant (Rider et al., 2016). The advantages of polymer based isolation include less effects of shearing force on the isolated exosomes and precipitate exosomes in a neutral pH environment (Colombet et al., 2009; Inamdar et al., 2017). The method even after being a useful method for isolation of exosomes is not free from its drawbacks. The major drawbacks of this method are contamination of protein aggregates which affects the purity of the isolated exosomes. Washing the pelleted exosomes with PBS and ultracentrifuge for an hour can resolve the problem (Rider et al., 2016). The excessive PEG that aggregates with the exosomes is another limitation of this method, which can affect in any proteomic analysis (YAMADA et al., 2012). Several commercial products have been developed for the PEG based isolation. Amongst them, Exo-Quick from System Bioscience and Total Exosome Isolation Kit from Invitrogen are the two products most commonly used. The PEG based isolation is relatively easy and does not require any special equipment or person. For isolation of exosomes, the PEG is often dissolved in PBS due to their isotonic nature and also to main the neutral pH and osmolality near to normal physiology. The concentration of PEG can vary from 30% to 50% by weight (Taylor et al., 2011).

1.7.7 Isolation of exosomes by sieving:

This method is non selective to the specificity of exosomes. Here exosome is isolated from bio fluids using a nano membrane and passing through a nano filter either by pressure or electrophoresis (Davies et al., 2012). The advantage of this method is it requires less times

compared to other methods and yields high purity exosomes. The only disadvantage of this method is the low recovery of exosomes (Sparks and Phillips, 1992).

1.8 Detection and characterisation of Exosomes:

The analysis of exosomal sub population is highly challenging due to their nano sized characteristics and similarities between other vesicles. Even after the advances of the molecular technologies, no single method is suitable to distinguish exosomes from other extracellular particles. So it is very important to distinguish exosomes from other vesicles using a combination of two or more techniques.

1.8.1 Electron Microscopy:

Due to the nano meter size range, the one of the most suitable and common way to visualise the size and morphology of exosomes is electron microscopy (EM). Pelleted exosomes, resuspended in small volume of buffer and fixed on a grid using any fixing chemical like paraformaldehyde or glutaraldehyde or mixture of both, contrasted using a mixture of methyl cellulose and a heavy metal and uranyl acetate before the analysis. Electron microscopy is widely used to differentiate the cup-shaped exosomes from other extracellular vesicles (Conde-Vancells et al., 2008). Both transmission (TEM) and scanning electron microscopy (SEM) can be used to visualise exosomes. TEM is the most widely used technique due to the high resolution images it produces while SEM produce a detail three dimensional image which gives more precise morphological information (Pisitkun et al., 2004; Van Der Pol et al., 2012). Another EM method is the Cryo-electron microscopy where the particles are visualised at very low temperature, approximately -100°C or below (Conde-Vancells et al., 2010). The advantage of this method is that the sample does not need to be fixed with any fixing chemicals and hence produces a more detailed three dimensional images (Liu and Wang, 2011).

1.8.2 Western Blot:

Western blot is one of the most widely used technique to characterise exosomes based on their protein contents (Lässer et al., 2012). Several proteins were regularly found in exosomes. Exosomes can be characterised based on the information of their protein contents by using the classical protein separation methods such as gel electrophoresis and western blot. Gel electrophoresis is used to compare the pattern of bands between the whole cell lysate and the exosomes. A different band pattern indicates the purity of exosomes since it

rules out the possibility of cell debris (Théry et al., 2006). Western blotting is also a method of choice for the researcher to characterise exosomes, based on some particular protein marker in exosome and compare that with the cell lysate. Exosomes are enriched in some proteins like the tetraspanins (CD63, CD81, CD9), MHC class II and TfR depending on cell type (Raposo., et al., 1996; Théry et al., 1999).

1.8.3 Flow Cytometry:

Another powerful method has been used to detect exosome quantitatively based on their protein content is flow cytometry (Théry et al., 2006). However a typical flow cytometer has a detection limit of 200nm but as mentioned before the size of exosomes is about 150nm therefore, the chances are exosomes would be detected as background noise (Pospichalova et al., 2015). The use of magnetic beads has been used to detect different exosomal proteins with the aid of fluorescently labelled specific antibodies. To achieve good detection of exosome the sample preparation has to be pure. Methods have been developed to use beads coated with antibodies against well-established exosomal marker proteins (Clayton et al., 2001; Ostrowski et al., 2010). An alternative method has been developed involving the use of high resolution flow cytometry. This method uses a combination of influx flow cytometer and fluorescently labelled vesicles. Advantages of this method are particles less than 100nm and heterogeneous particles can be detected with this method (Hoen et al., 2012).

1.8.4 Atomic force microscopy:

Atomic force microscopy (AFM) is another technique that has been used to detect exosome like membrane vesicles to a level of single particle. This method can be used to understand the structural information as well as a specific protein marker (Sharma et al., 2010). It is another type of scanning microscopy which yields high resolution images. Here, a mechanical probe scans the surface of the sample without actual contact. The movement of the probe in height, width and length are measured along with the resolution and sensitivity at nano scale level. Due to the high resolution of the AFM, the actual morphological characteristics of the extracellular vesicles can be visualised in their original physical state. Antibody can also be bound to the surface of the extracellular vesicles to analyse the biochemical properties of the vesicles (Erdbrügger and Lannigan, 2016).

1.8.5 Nano Particle Tracking Analysis (NTA):

A new instrument has been introduced recently to determine the size distribution and concentration of nanoparticles called Nanosight (Dragovic et al., 2011a). It works based on the Brownian motion that, particles in suspension move under Brownian motion and when they scatter light their movements can be detected by technology called Nano particles Tracking Analysis (NTA). Both size and number of exosomes can be measured by NTA using light microscopy and a software that measures Brownian motion of the particles. The software simultaneously records the Brownian motion of the diffuse particles and calculates the size based on these motions (Ko et al., 2016). In this technique, the light scattering microscopy is equipped with a CCD (Charge Couple Device) camera which allows the visualisation and analyse the size of the suspended particles (Erdbrügger and Lannigan, 2016). Both light scattering and fluorescence methods have been extensively used to measure size and detect molecular marker. NTA, now a days has become the method of choice and standard for exosome research (Dragovic et al., 2011b).

1.8.6 Dynamic Light Scattering:

The basic principle of DLS is similar to NTA as it also uses Brownian motion theory to measure the size distribution of nano particles in suspension (Palmieri et al., 2014). The velocity distribution of particles depends on the temperature at which they are moving, viscosity and hydrodynamic particle diameter. The smaller the particles, the faster the Brownian motion. The movement causes the particles to scatter light which is similarly detected and calculated by the software (Van Der Pol et al., 2010). The relative size of the particles sizing from 10nm to 6µm can be measured by this technique (Clark, 1970). The limitation of DLS is it shows relatively accurate result for particles with mono dispersed size but with polydispersed particles is less accurate (Filipe et al., 2010).

1.9 Functions of Exosome:

The exact functions of exosomes are still remains in doubt. Previously exosome was thought to be the means of release of unwanted or excess or non-functional materials from the cells (Oshikawa et al., 2016) but recent studies have shown that exosomes play a vital role in normal and assorted physiological conditions. Mechanisms for these functions are very complex including a set of ligands which have the ability to bind with different cell surface receptor on the target cells stimulating a response. Cells release exosomes for transferring

surface molecules, cytosolic contents, RNAs to other potential recipient cells (Clayton et al., 2007, 2008). Several functions of exosomes are described below.

1.9.1 Exosome on Cell to Cell Communication:

Exosomes are now a days considered to be an important part of intercellular microenvironment and have been reported to play an integral part in cell to cell communication. It is worth mentioning that exosomes influence the behaviour of local cells as well as the distant cells by entering into the body fluids (Wang et al., 2017). In a study, Valadi et al., 2007 showed that, the presence of mRNA and miRNA in exosomes secreted by mast cells ensures that exosomes play a part in cell to cell communication. Exosomes secreted from these cells transfer mRNA to the recipient cells which in turn translated into proteins. It also shows that exosomes carry genetic materials from one cell to another. Not all the mRNA from the parent cells was transferred to exosomes which suggest that there is targeting machinery for mRNA into exosomes. In one more study it was revealed that exosomes released from Epstein Barr virus infected B cells containing miRNA from viral origin could be transported to the uninfected cells into the surrounding influencing viral miRNA targeted gene (Bang and Thum, 2012; Valadi et al., 2007). In another study it was observed that exosomes from the intestinal epithelial cells on immune system interacted with the immature DCs rather than B or T lymphocytes. So, it is clear that some specific receptor interacts with exosome for a particular type of recipient cells (Mallegol et al., 2007). In addition, there are some proteins found active in cellular signalling pathways such as like β -catenin, Wnt 5B or the Notch ligand Delta-like 4. When it comes to cellular communication, it has been reported that exosomes play a novel role in mediating intercellular signalling where they act independently but uniting with soluble growth factors (Ludwig and Giebel, 2012). The exosomal association TGF- β depends on the expression level of transmembrane proteoglycan beta glycan which is a relevant factor in tethering TGF- to the exosomal surface (Webber et al., 2010).

1.9.2 Exosomes in Signalling Pathways:

Proteomic studies have revealed that proteins from exosome are involved in cellular signalling pathways (Urbanelli et al., 2013). The impact of these exosome derived proteins on cellular signalling is not completely understood but recent studies have shed light on it, especially when the involvement of exosome in Wnt signalling has been revealed by proteomic investigation. Wnt which plays crucial role during embryo development and tissue

regeneration and also cancer progression (Simpson et al., 2009). Exosomes derived from MSCs promoted migration and proliferation of breast cancer cells by the activation of Wnt signalling pathway (Lin et al., 2013). In another study carried out by Cai et al, exosomes were found to elevate tumour invasion via Fas signalling which subsequently induced up regulation of MMP8 expression in melanoma cells (Cai et al., 2012). Similar tumour progression was also observed in Gastric cells, where exosomes from gastric cells up regulated the expression of Akt and ERK signalling pathways to enhance the growth and proliferation of tumour cells (Qu et al., 2009).

1.9.3 Exosomes on Immune Response:

There are several reports have been found regarding the involvement of exosome in the immune systems (Bobrie et al., 2011; Chaput and Théry, 2011). The first report regarding the active involvement was of the direct presentation of antigens by exosomes to T-cells. It demonstrated that multivesicular MHC class II-enriched compartments (MIIC) of B cells are exocytic. When the MIICs fused with the plasma membrane they released exosomes into the culture media. The MHC class II molecules on the surface of these exosomes were recognisable by helper T lymphocytes (CD4+ T cells). The interaction of these exosomes with CD4+ T cells stimulated T cell proliferation in a peptide specific, MHC restricted manner (Raposo et al., 1996). It is thought that exosomes from antigen presenting cells (APC) like B cells and particularly dendritic cells may function as carriers of MHC class II complexes for amplifying the immune response. There is also evidence that tumour exosomes may in fact exhibit immune evasive functions. Tumour exosomes have been shown to selectively impair lymphocyte responses to interleukin-2 (IL-2). Strong inhibition of IL-2-driven lymphocyte proliferation has been observed in the presence of tumour exosomes. The lymphocyte subsets were also examined individually showing the main anti-proliferative effect was through CD4+ T-cells implicating an influence on regulatory T cells. In fact exosomes can support inducible T regulatory cells (T-reg), defined by FOXP3 expression, and enhance their suppressive functions (Clayton et al., 2007).

1.9.4 Exosomes in Elimination of Molecules:

Exosomes have been reported to take part in the elimination of unnecessary molecules from the cells. Studies suggested that exosome have been used by the cell to eliminate TfR during reticulocyte maturation into erythrocytes (Johnstone et al., 1989). Not only TfR, exosomes

from ovarian carcinoma cells have also been reported to dispose the cytotoxic drugs such as the release of the DNA binding anti-cancer drug doxorubicin (Iero et al., 2008).

Further study showed that, exosomes secreted from B cells can induce immune response (Raposo et al., 1996) and exosomes from B lymphocytes could be targeted to the surface follicular dendritic cells in germinal centre in the tonsil to transfer MHC class II to class II negative cells (Denzer, van Eijk, et al., 2000).

1.9.5 Role of Exosomes on Cancer Progression:

Cancer retain their originality by continuous interaction between surroundings and monitored by complex signalling and constant mobilization of biological components across membranes of surrounding cells (Quail and Joyce, 2013b). Tumour cells continuously release exosomes in the peripheral fluid or other biological fluids and play a vital role in the tumour micro-environment (TME). Researchers are trying to explain the role of exosomes mediated signalling pathways to promote TME. Exosomes can alter the systemic environment to assist cancer growth and control the immune system to escape the anti-tumour response (Kahlert and Kalluri, 2013). Exosomes from neoplastic cells contain a vast group of oncogenic molecules including proteins and microRNAs that could pass the phenotype transforming signals to normal cells which leads to tumour progression and metastasis (Valadi et al., 2007). Evidence was found of the communication of cancer cells and mesenchymal stem cells (MSCs) and in the transformation or recruitment of MSCs to tumour sites and this neoplastic reprogramming was conducted by exosomal trafficking of oncogenic microRNAs (miR-125b, miR-130b and miR-155), K-ras and H-ras mRNAs and also oncoproteins, such as Ras superfamily of GTPases Rab1a, Rab1b, and Rab11a. The reformed MSCs thus undergo mesenchymal to epithelial transition shows neoplastic and vasculogenic effect and also express epithelial markers similar to the molecular combinations of prostate cancer *in vivo* (Saleem and Abdel-Mageed, 2015). Similar changes have been reported where breast and ovarian cancer cell exosomes changes the functional properties of tumour associated myco fibroblast. In study it was shown that the transformed myco-fibroblast from MSCs showed enriched expression of α -SMA and tumour promoting factors such as SDF-1, VEGF, CCL5 and TGF β when treated with exosomes derived from breast cancer and also from ovarian cancer cells (Cho et al., 2011, 2012).

1.9.6 Role of Exosomes on Cancer Biomarker Discovery:

The dynamic and emerging role of exosomal involvement in cancer progression, metastasis, angiogenesis, extracellular matrix remodelling, immune evasion, chemo resistance and in the preparation of premetastatic niche has been the centre of exosomal research in the recent years (EL Andaloussi et al., 2013). The ability of exosomes to exchange information between surrounding cells, communicate with cells at distal sites to induce cellular responses for tumorigenesis make them a key element in biomarker discovery for early detection and therapy of cancer (Munson and Shukla, 2015). In broad scenario, there are two basic reasons for the wide acceptance of exosomes as a biomarker tool. Firstly, sustainable and mounting evidence has proven that tumour derived exosomes contain protein and nucleic acids that can be used as diagnostic tools for cancer and secondly exosomes can easily be isolated from biological sample such as blood, urine, milk and saliva (Lin et al., 2015).

Now a days finding new biomarkers from the body fluids is a challenge since the high abundance of proteins make up about 97% of the total proteins and they hinder the presence of low abundance proteins which are generally most promising candidates for biomarker discovery (Duijvesz et al., 2013). As mentioned earlier, exosomes are an extra ordinary group of vesicles containing diverse types of proteins including some common ones and some are cell specific released depending on the cellular functions and conditions, which emerged as next generation biomarkers (Iraci et al., 2016). For instance, in a proteomic study demonstrated that the tetraspanin protein CD63, one of the most common exosomal marker protein and a member of the family of scaffolding proteins, has a higher level of expression in different types of tumour cell derived exosomes compared to their counterpart exosome from non-malignant cells which signifies CD63 as a potential biomarker for cancer (Yoshioka et al., 2013b). Since exosome represents the sub-proteome of the whole cell, it gives an advantage on identifying those low abundance proteins specially membrane proteins. Exosomes are also rich in tumour associated antigens which can reflects the stress situation of the parent cells (Clayton and Mason, 2009; Yang and Robbins, 2011).

1.9.7 Exosomes in therapeutic drug delivery:

Recently exosomes have been exploited as a drug delivery system for various diseases (Ha et al., 2016). The reason for their acceptance as a drug delivery vehicles include the nano size morphology, stability and availability in biological systems along with their ability to pass the blood brain barrier (BBB) if necessary (Yang, Martin, et al., 2015). Their ability to travel to

distance cells though both physiological and pathological conditions make them a better choice over the conventional nano carrier based drug delivery (Jiang and Gao, 2017). Furthermore, the presence of the hydrophilic core in exosomes are suitable to load soluble drugs to be delivered (Yousefpour and Chilkoti, 2014). In addition, the patients can be used as the source for the exosomes to be used as carrier. The exosomes can be isolated from the patients and then engineered with the drug *in vitro* and transferred back to the patients (Wahlgren et al., 2012). However, even with the enormous potential of exosomes as drug delivery system, still there some limitations that need to be addressed. For instance, the mechanism by which exosomes cross the BBB is still not fully understood which limits the targeting of tissue specific peptides. Moreover, the complete proteomic study of exosome is yet to be established, which is very crucial to characterise exosome for any endogenous proteins which might lead any adverse effects (Lakhal and Wood, 2011). Finally, the current protocols for purification of exosomes do not yield pure exosomes rather the final products are always a heterogeneous mixture which hampers the clinical translation of exosomes as drug delivery vehicles. So, although exosomes has a huge prospects as a drug delivery vehicle, the better understanding of the biology, function of exosomes as well as a complete workflow of exosome as a drug delivery system from purification to loading the drug is yet to be need to be established (Alvarez-Erviti et al., 2011).

1.9.8 Proteomic Analysis of Exosomes:

The use of proteomics technologies to examine the proteome of exosomes may offer a portal to distinguish potential biomarkers for cancer and different kinds of diseases. It might likewise offer bits of knowledge about exosome biogenesis and functionality. In recent years there has been expanding interest for the exosome proteome and its potential as a biomarker source. Up until the recent years proteomic analysis of exosomes has been depended on two-dimensional electrophoresis (2DE) and western blotting (WB). The depth of scope of these systems is confined to the all the more abundant proteins which restricts the information that can be gathered (Rabilloud and Lelong, 2011). Significant improvement has been achieved over the last few years in all sectors of proteomics from sample preparations to data analysing, from hardware to software (Cox and Mann, 2007; Domon and Aebersold, 2006). Furthermore, the advances in the isolation and purification of exosomes together with the improvements of mass spectrometry instrumentation with more accuracy in sensitivity and mass calculation have enabled a vast improvement on the proteomic composition of exosomes (Thomas et al., 2013). These improvements have led to a substantial number of

identified proteins from exosomes (Théry et al., 2009). Proteomic studies have been used to characterise exosomes derived from urine (Gonzales et al., 2009), blood (Caby et al., 2005), saliva (Gonzalez-Begne et al., 2009), pleural effusion (Andre et al., 2002) and breast milk (Admyre et al., 2007). Now a days there is also a database for exosomal proteome called ExoCarta (<http://www.exocarta.org/>) which allows the researcher who works with exosomes to compare their data with the data stored there (Mathivanan and Simpson, 2009).

1.10 Aims and Objectives:

The aim of this study is to investigate the potentials of exosomes as source of biomarkers of cancer in general and lung cancer in particular. To achieve this, exosomes from three different cancer cell lines: a lung cancer cell line (H358), a breast cancer cell line (MCF7) and leukaemia cell line (THP1) as well as a normal lung cell line (HBTE); were isolated and their protein content analysed. In order to establish whether exosomes are a suitable source of biomarkers the presence of cancer-specific protein was established following the below steps:

- Optimisation of exosome isolation method for proteomic study to minimise the time and cost.
- Exosomes isolation from four different cell lines including lung cancer cell line H358, leukemic cell line THP1 and breast cancer cell line MCF7....
- Characterization of exosomes via detection of size by TEM, SEM and DLS as well as presence of marker proteins (CD63, CD81, CD9 and Hsp70) by western blot analysis.
- Investigation of Exosome release dynamic during cellular growth.
- Comparative proteomic analysis of three cancer cell lines.
- Identification of lung cancer specific biomarker by comparative proteomic study of exosomes from lung cancer cell line H358 and its normal counterpart HBTE.
- Gene expression analysis selected proteins from H358 and HBTE cell to confirm the suitability of lung cancer biomarker.

Chapter 2:

General methods and materials

2.1 Method and Materials:

All general reagents, unless otherwise stated were molecular biology grade. All water used in this project were pure deionised water (18.2mΩ) purified by Purite water dispenser. All wastage was disposed after autoclave.

2.2 Cell Culture:

2.2.1 Culture of Human Cell Lines:

Three cancer cell lines were used in all experiments. They are H358 (non-small cell lung cancer) purchased from ATCC (CRL-5807), THP1 (acute monocytic leukaemia) and MCF7 (breast cancer) were obtained from University of Greenwich. All cells were maintained at 37°C in 5% CO₂. For H358 and THP1 cell lines RPMI-1640 from Fisher Scientific UK and for MCF7, DEMEM also from Fisher Scientific UK were used with the addition of 10% FBS (Foetal Bovine Serum) and 1% antibiotic-antimycotic (100X) from Fisher Scientific UK (10,000µg/ml of Streptomycin, 25µg/ml of Amphotericin B, and 10,000 units/ml of Penicillin). Among the three cell lines, H358 and MCF7 are adherent cells and THP1 is suspension cell. Cell culture was carried out in a laminar air flow hood with UV sterilisation system. Culture media were kept in 37°C to equilibrate with the cell culture flask. Cells were grown in T75, T25 flasks and 6 well plates depending on the experiments. The culture medium was changed with serum free conditioned cell culture medium (CCM) for all cells after they reached 80-90% confluency and incubated as required for exosome isolation.

2.2.2 Adherent Cell Culture:

Both the cells were sub-cultured after 80-90% confluency. The flask was then rinsed out with equal volume of PBS to ensure the removal of any residual media. Depending on the size of the flask, 1-2ml of Trypsin EDTA solution (TrypLE™ Express from Fisher Scientific UK) was added to the flask and incubated at 37°C for approximately 5-7 minutes, until all of the cells were detached from the inside surface of the flask, monitored by microscopic observation. After that an equal volume of complete media was added to the flask to deactivate the enzymatic activity of the trypsin solution. The cell suspension was removed

from the flask and placed in a sterile centrifuge tube and centrifuged at 500g for 5 minutes. The supernatant was then discarded from the centrifuge tube and the pellet was resuspended gently in complete medium. A cell count was performed using Haemocytometer and an aliquot of cells was used to seed a flask at the required density. All cell waste exposed to cells was autoclaved before disposal.

2.2.3 Suspension Cell Culture:

THP1 was sub-cultured in a ratio of 1:3 and when it reaches 80-90% confluency, like adherent cells. Unlike adherent cells, suspension cell floats in the medium so after removing the spent medium from the flasks, it was centrifuged at 500g for 5min at room temperature. Then the spent medium was kept separately for exosome isolation and the pellet of cells were resuspended in new fresh medium. The cells were then counted in the same way as described before and an aliquot was used to seed the flask at required density.

2.2.4 Assessment of Cell Number, Viability and Growth Curve:

Prior to cell counts, cells were prepared for sub-culturing as detailed in 2.1.3 or 2.1.4 depending on adherent or floating aggregates. An aliquot of the cell suspension was then added with equal volume of trypan blue (Gibco, 525). The mixture was incubated for 3 minutes at room temperature. An aliquot (10 μ l) was then applied to the chamber of a glass coverslip-enclosed Haemocytometer. Four squares in four sides along with the centre square were counted to determine the total cell number per ml. The average of five grids were multiplied by a factor of 10⁴, volume of the grid and the relevant dilution factor to determine the average cell number per ml in the original cell suspension. Non-viable cells stained blue, while viable cells excluded the trypan blue dye as their membrane remained intact and unstained. On this basis, percentage viability could be calculated.

2.2.5 Cryopreservation of Cells:

Cells for cryopreservation were harvested from the log phase of growth and counted as described before. Cell pellets were resuspended in a suitable volume of complete culture medium supplemented with 10% DMSO. The cell suspension was then aliquoted in 1 ml volumes containing one million cells to cryo-vials (Nalgene Cryoware Cryogenic Vials) and kept in -20°C overnight followed by incubation in -80°C. On the next day vials were transferred to the liquid nitrogen phase for long term storage (-196°C) and some were kept in -80°C freezer for short time use.

2.2.6 Thawing of Cryopreserved Cells:

A volume of 9.0ml of fresh growth medium was added to a sterile universal tube. The cryopreserved cells were removed from the liquid nitrogen and thawed at 37°C quickly. The cells were removed from the vials and transferred to the aliquoted media. The resulting cell suspension was centrifuged at 350g for 5 minutes. The supernatant was removed and the pellet was resuspended in fresh culture medium. An assessment of cell viability on thawing was then carried out. Thawed cells were then added to an appropriately sized tissue culture flask with a suitable volume of growth medium and allowed to attach overnight. The following day, flasks were re-fed with fresh media to remove any non-viable cells.

2.3 Isolation of Exosomes:

Exosomes were isolated by two different methods including ultracentrifugation and precipitation method. Centrifugation steps were performed using Mikro 200R for the lower speed centrifugation and Sorval Discovery 150 Micro-ultracentrifuge for the ultracentrifugation. For precipitation method, either commercially available exosomes isolation reagent or in house polyethylene (PEG) solution was used. In all methods, the supernatant collected from the cell culture step was centrifuged at 2000g for 30mins at room temperature to remove all the dead cells and debris. Then the supernatant was passed through a 0.22µm sterile membrane filter and passed to a new tube. The supernatant was then subjected to either ultracentrifugation or precipitation steps.

2.4 Protein extraction from Cell and Exosomes:

For protein extraction from cells or exosomes, RIPA (Radio immunoprecipitation assay) lysis buffer was used. The cell pellet was incubated on ice with 1ml of RIPA buffer (50mM Tris pH 7.4, 1% NP-40, 0.5% Na-deoxycholate, 0.1% SDS, 150mM NaCl, and 2mM EDTA) with 1mM of PMSF (phenylmethylsulfonyl fluoride) for 30 minutes with occasional vortex for 30 sec every 10 minutes. Then the cell lysate was centrifuge at 14000g on a bench top centrifuge (Hettich Mikro 200R) for 30 minutes to remove dead cells and cellular debris. The exosome pellet obtained from the isolation step was also subjected to RIPA lysis buffer and followed the same protocol except samples were sonicated at 4°C for 10s every 10min interval and centrifuged as before. Then both cellular lysate and exosomal lysate were transferred to a new Eppendorf tube. Both the cellular proteins and the exosomal proteins were subjected to a Bradford assay for protein quantification.

2.5 Determination of Protein Concentration (Bradford Assay):

Protein concentration was determined by using the Bio-Rad protein assay kit (Bio-Rad, Quick Start™ Protein Assay Kit) following the manufacturer's instructions. A 1mg/ml bovine serum albumin (BSA) solution (Sigma, A9543) was prepared freshly in dH₂O. A protein standard curve (0, 20, 40, 60, 80 and 100µg/ml) was prepared (Figure: 6) from the BSA stock with dilutions made in lysis buffer. The Bio-Rad reagent was diluted 1:5 in UHP (Ultra high pressure) water. A 20µl volume of protein standard dilution or sample (diluted 1:10) was added to 980 µl of diluted dye reagent and the mixture was vortexed. All samples were assayed in triplicate. After 5 minutes incubation, 300µl of the solution was taken into a 96 well plate and the absorbance was assessed at 595nm using a Spectra Max M5 multi-scanner. The concentration of the protein samples was determined from the plot of the absorbance at 595nm versus the concentration of the protein standard.

2.6 Statistical analysis:

Statistical analyses were carried out using Microsoft Excel 2010 to define the significant differences or similarities between samples. Student t-test was used to evaluate the statistical differences and any statistical significance was determined by $p \leq 0.05$ as significant, $p \leq 0.01$ highly significant and $p \geq 0.05$ not significant.

2.7 Software used:

Several softwares were used in this study for different purpose. To analyse the 1D gel, CLIQS gele analysis software were used (<http://totallab.com/home/cliqs/>). Scaffold sotware (<http://www.proteomesoftware.com/products/scaffold/>) was used for the gene ontology analysis after protein identification. Online based softare STRING (Search Tool for the Retrieval of Interacting Genes/Proteins) version 10.5 (www.string-db.org) was used for the protein network and pathway analysis. To generate the heat map, a free version of RStudio (<https://www.rstudio.com/>) was used. All the images were processed with image processing softwere ImageJ (<https://imagej.nih.gov/ij/download.html>).

Chapter 3:

Identification and characterisation of exosomes derived from three different types of cancer cells:

3.1 Introduction:

Cells from prokaryotes to eukaryotes release several types membrane enclosed vesicles in their microenvironment to maintain the biological process (Yáñez-Mó et al., 2015). In 1987 Johnstone et al termed these vesicles as exosomes when they isolated exosomes from culture supernatant of reticulocytes (Johnstone et al., 1987). In 1996, Raposo et al also used the term exosome and gave a modified definition as nano-sized vesicle which was isolated from B cells (Raposo et al., 1996). After that, exosome gained much interest for the first time when it was observed that exosomes participated in the T-cell responses (Théry et al., 2002). Recently, exosomes gained much interest in cancer research due to their ability to carry genetic material across neighbouring cells, their stability in biological fluids and their acceptance to the host cells because of their composition which is similar to their originated cells (Edgar et al., 2016).

The goals of this chapter are to optimise the method to isolate exosomes from cell culture media and characterise exosomes, to optimise precipitation based method using polyethylene glycol (PEG) with different molecular weight at different concentrations and compare the optimised method with ultracentrifugation and commercial exosome isolation kit. The best polyethylene glycol with the best concentration will subsequently be used in this project for further exosome analysis. The PEG based exosome isolation method was optimised due to the excessive cost of the commercially available exosome isolation kit and unavailability of large scale exosome isolation equipments by ultracentrifuge method.

3.1.1 Exosomes:

Exosomes are extracellular vesicles released by almost all type of cells including B-cells (Johnstone et al., 1987), dendritic cells (Denzer, Kleijmeer, et al., 2000), macrophages (Nguyen and Hildreth, 2000), mast cells (Skokos et al., 2001), T-cells (Blanchard et al., 2002), epithelial cells (Karlsson et al., 2001). Exosomes are not the only extracellular vesicles released by the cell, there are other vesicles released into the body fluids which differ in

structure, size, biogenesis and composition. These vesicles are ectosomes, micro vesicles, prostasomes (Aalberts et al., 2014; Ciardiello et al., 2016; Yáñez-Mó et al., 2015).

3.1.2 Ectosomes:

Ectosomes, also known as micro particles (MP) are released from a cell by exocytic budding of the plasma membrane and typically larger than exosomes (100 to 1000 nm in size) and shed by cells *in vitro* and *in vivo* (Ciardiello et al., 2016). They are defined as lacking a nucleus, containing a membrane cytoskeleton, containing variable amounts of surface phosphatidylserine, and can be pro- or anti-coagulant. They are released under various stimuli such as shear stress, activation, or pro-apoptotic stimulation. MPs may be involved in numerous processes including vascular function, tumour metastasis and angiogenesis (Nomura et al., 2008). The term MPs has also been used to describe membrane vesicles purified from urine. However, these membrane vesicles may also include exosomes (Smalley et al., 2008). Apart from the size differences, the basic differences between exosomes and ectosomes are in their biogenesis and marker specificity. Exosomes are produced by the inward budding of the plasma membrane, while ectosome production occurs during the outward budding of the plasma membrane. Biogenesis of exosome is much slower than ectosomes. Several reports have also suggested that, the exosome marker proteins CD63 and CD61 were present in exosomes only. However, two other proteins, TyA and C1a are considered as ectosomal protein markers (Meldolesi, 2016).

3.1.3 Prostrasomes:

Prostrasomes (aposomes or seminosomes) are 50-500 nm vesicles secreted from the apical region of prostatic luminal epithelial cells (Luchter-Wasylewska and Wasylewski, 2007). Prostrasomes are enveloped in a storage vesicle and are released into the seminal fluid by diacytosis or exocytosis (Stewart et al., 2004). Diacytosis is a mechanism by which the storage vesicles tear a repairable hole in the plasma membrane to release the prostrasomes (Simpson et al., 2008). Prostrasomes have high cholesterol to phospholipid ratio as well as high sphingomyelin and monounsaturated fatty acid content, giving the membrane a highly ordered structure (Luchter-Wasylewska and Wasylewski, 2007).

3.1.4 Identification of exosomes:

Because of the varieties of vesicles secreted by the cells, it is crucial to identify and characterise exosomes prior to any investigation. Otherwise, there is always a risk of carrying

contamination of unexpected particles in any exosome research (Théry et al., 2006). There are several reports, suggesting that the size of exosomes varies according to the cell of origin for example, the size of exosomes derived from T cell was found less than 50nm (Muller et al., 2016), exosomes derived from four different types of B- cell was found to have a size distribution of approximately 100nm (Oksvold et al., 2014), dendritic cells showed a size distribution of 40-90nm (Théry et al., 1999). In general, the size distribution of exosomes were reported in several reports between 30-150nm (Li et al., 2014). Exosomes are found in various body fluids including, plasma, urine, saliva, cerebral spinal fluid, breast milk and act as a vital tool for cellular communication (Keller et al., 2011).

In this chapter, all three cell lines were established and exosomes were isolated initially by using Total exosome isolation kit (TEI). The exosomes were identified by electron microscopy, both scanning and transmission. Then western blot and DLS analysis were used to characterise exosomes. Due to the cost of the exosome isolation kit, alternative exosome isolation methods were optimised by using TEM, DLS and measuring the protein concentration. The idea was to isolate large quantities of exosomes for proteomic study.

There are several methods have been established to isolate, detect and characterise exosomes from various body fluids. In this chapter, exosomes were isolated from conditioned cell culture medium by two different methods, number one, differential ultra-centrifugation and Polyethylene glycol (PEG) precipitation. For PEG precipitation method, a commercial exosome isolation kit from Fisher UK and an in house PEG polymer was made as an alternative to the commercial product which is very expensive. The isolated exosomes were then visualised by using electron microscopy. The western blot analysis was carried out to characterise exosomes by using exosomal protein markers, the size distribution was analysed by using dynamic light scattering and finally a one dimensional gel electrophoresis was carried out to visualise the pattern of protein bands between cell and exosomes.

3.2 Methods and Materials:

3.2.1 Cell Culture and Isolation of Exosomes:

For exosome isolation and characterisation, 2.5×10^5 cells were seeded in a T75 culture flask with fresh culture medium. After reaching confluency the spent culture medium was discarded and the cells were washed with PBS (Phosphate Buffer Saline). CCM supplemented with 1% antibiotic-antimycotic was added to the culture flask and incubated for 24hrs in 5% CO₂ humidified incubator. The supernatant was then collected and subjected to exosome isolation.

3.2.2 Isolation of Exosome by Ultracentrifugation:

Isolation of exosomes by ultra-centrifugation method involves variable low speeds (2000×g to 10,000×g) centrifugation to remove all dead cells and cellular debris, then centrifuge at high speed to pellet the exosomes as previously described in They et al., 2006 with the filtration of supernatant described in chapter 2.3. After the filtration, the supernatant was then centrifuged at 10,000×g for 30mins at 4°C to remove any remaining large particles. The pellet was discarded and the collected supernatant was subjected to ultracentrifuge at 100,000×g for 70 mins at 4°C to pellet the exosomes. The exosome pellet was resuspended in PBS and centrifuged again at 100,000×g for one hour at 4°C again to remove all the contaminating proteins. The pelleted exosomes were resuspended in PBS or buffer of choice depending on the experiments.

3.2.3 Isolation of Exosome with Exosome Isolation Kit:

Exosomes from three cancer cells used were isolated using the Total Exosome Isolation Kit by Fisher Scientific following the manufacturer's protocol with slight modification of filtration described in chapter 2.3. Half the volume of exosome isolation reagent was added to the supernatant and vortexed briefly for 10sec and incubated overnight at 4°C. On the next day all tubes were centrifuged at 10,000g on 4°C. The supernatant was then discarded leaving the exosome pellet on the bottom of the centrifuged tube. The pelleted samples were resuspended in appropriate amount of PBS or protein lysis buffer depending on the experiment.

3.2.4 Isolation of Exosome with PEG Solution:

For PEG based exosome isolation, exosomes were isolated from cell culture supernatant using a PEG solution following the method as described in Rider et al., 2016 with slight modification added from Weng et al., 2016. To compare the best fit PEG solution, 10%, 20%, 30% and 40% (w/v). PEG solution was made by using of PEG Mw 4000Da, 6000Da and 8000Da with 50ml sterile deionized water (Rider et al., 2016; Weng et al., 2016). The solution was vortexed for 10mins and then sonicated at 4°C until a clear solution was achieved. The supernatant resulting from the filtration step was then mixed with the 0.5 volume of each PEG solutions and vortexed for 15sec to mix the PEG with the culture supernatant and incubated overnight at 4°C. The supernatant was then centrifuged at 10,000×g for 1hour in 4°C in Mikro 200R centrifuge. The exosome pellet was then resuspended in either PBS or RIPA buffer depending on the experiments.

3.2.5 Electron Microscopy:

Exosome from all three cell lines were visualized by scanning electron microscopy (SEM) and transmission electron microscopy (TEM) by following a modified version of the method used by Thery et al., 2006 and Sokolova et al., 2011. First the formvar coated electron microscopy grid was placed on a piece of parafilm. Then 50µl of exosomes in PBS was placed on top of the EM grid and allowed to settle down for 30-45 minutes at room temperature. After that the excess PBS was sucked out by a filter paper. Then 20µl of 2.5% glutaraldehyde was added to the EM grid and left at room temperature for 20 minutes. After 20 minutes the glutaraldehyde was taken out by filter paper. The EM grid was wash three times with cold PBS, each time for 15 minutes and after every wash the PBS was removed by filter paper. The EM grid was then subjected to a series of dehydration steps with gradient percentage (30%, 40%, 50%, 60%, 70%, 90% and 100%) of ethanol, for 15 minutes each time. The excess ethanol was sucked out by filter paper. After that 20µl of HMDS (Hexamethyldisilazane) solution and incubated for 15min. Then the grid was left to dry overnight at room temperature (Sokolova et al., 2011; Thery et al., 2006). The next day all the grids were subjected to electron microscopy. All the samples were then visualised within 50K to 100K magnifications using a Hitachi SU-8030 electron microscopy.

3.2.6 Dynamic Light Scattering and Zeta Potential:

To determine the size of the exosome, dynamic light scattering was performed using Zetasizer Nano ZS system (Malvern Instruments, Malvern, U.K.). The dynamic light scattering uses the velocity distribution of particles movement by analysing the fluctuations of light intensity exerted by the particles at a fixed angle of 173° caused by the Brownian motion. The particles are assessed at the perpendicular angle of the light source at that moment resulting in the particles hydrodynamic radius (Rh) or diameter calculated with the aid of the Stokes–Einstein equation (Kesimer and Gupta, 2015). Exosome pellet previously re-suspended in PBS was diluted in 1:1000 ratios with PBS, filtered through $0.22\mu\text{m}$ filter, sonicated for 5 min just before the measurement was taken. All samples were done in triplicates. The parameter was set as density gradient of exosome 1.13-1.19g/ml, the viscosity was set as 0.89 and the temperature was kept constant at 25°C . All the samples were sonicated for 5min prior to measurement. All samples were performed in triplicate. The size was expressed as diameter (d.nm) and was recorded by the Malvern Zetasizer software. With the same parameters and protocol, zeta potential of the exosomes were analysed to check the charge of the nano sized vesicles. Zeta potential was measured to determine the charge of the particles present in the samples. Exosomes are negatively charged due to the presence of negatively charged phospholipid membrane, therefore, any negative values in the zeta potential confirms the presence of exosomes (Sokolova et al., 2011).

3.2.7 Determination of Exosomal Protein Concentration:

The exosomal protein was extracted with RIPA buffer following the same method for cell lysate as described in general methods and materials in section 2.4 in chapter 2. To compare the protein concentration achieved from three methods of exosome isolation, a Bradford assay was performed in a 96 well plate and the absorbance was measured with multi-scanner SpectraMax M5 at a wavelength of 595nm.

3.2.8 Protein Separation by one dimensional gel Electrophoresis:

One dimensional gel electrophoresis was performed to separate the proteins from exosomes released by the cancer cells by their molecular weight. This was done to analyse the protein patterns of exosome. The electrophoresis gel (12%-4%) was made using the method described by Thery et al. 2006 in the study of exosomes and cellular proteins (Théry et al., 2006). A separating gel (3.4ml dH_2O , 2.4ml of 30% poly acrylamide, 2ml of 1.5M Tris-HCl

pH 8.8, 100µl of 10% SDS, 100µl of 10% APS and 10 µl of TEMED) was pour into the gel cassette (Bio-Rad) assembled by the Bio-Rad frame and gel cassette holder. The gel was then allowed to solidify for 15-20mins. Once the gel was solidified the stacking gel (3.1ml of dH₂O, 0.5ml of 30% poly acrylamide, 1.25 ml of 0.5M Tris-HCl pH 6.8, 50µl of 10% SDS, 50µl of 10% APS and 5µl of TEMED) was pour on top of the separating gel and a 10lane comb was added. The gel was then allowed to solidify for 30mins. Samples were prepared by mixing 25µg of protein from each sample with 10µl of sample buffer (0.5 M Tris pH 6.8, 25% Glycerol, 1% SDS, Bromophenol blue). All the samples were heated at 95°C for 10 min in DIGI-BLOCK™ heating block to denature the disulfied bonds. The gel was placed in a Bio-Rad mini gel tank and both the upper and lower chamber was filled with SDS-running buffer (14.4gm glycine, 3.03gm Tris Base and 1.0gm of SDS and made up to 1L). in each well 20µl of each sample was then added along with a molecular weight ladder (Precision Plus Protein™ Standards, Invitrogen). The gel run was performed at a constant voltage of 200V and 100mA current for 1 hour. Once the gel run was completed the gel was separated immediately and washed with dH₂O for 10mins with gentle shaking to remove all the residual SDS. After that the gel was subjected to fixing and development.

3.2.9 Developing the Gel:

Developing the gel involves three steps including fixing the gel, staining and developing or detaining the gel. When the gel run was complete, the gel was washed with deionized water for 10mins to remove any residual SDS. Then the gel was fixed with the fixing solution (50% ethanol in deionized water with 10% acetic acid) for 20mins. Then the gel was poured into the staining solution (0.1% (w/v) Coomassie blue R350, 20% (v/v) methanol, and 10% (v/v) acetic acid) and heated in a microwave for 1min. The gel was then incubated at room temperature with gentle shaking for one hour. After that the gel was destained with (30% methanol in deionized water with 10% acetic acid) until the bands were visible with clear background. The developed gel was analysed with gel analysing software. The gel was stored at storage solution of 5% acetic acid in deionized water.

3.2.10 Western Blot:

Exosome pellet from all three cells were re-suspended in 50µl of RIPA buffer and protein was extracted as described in section 2.4 in chapter 2. To run the gel for western blot, 20µg of protein was diluted with 10µl laemmli sample buffer and the gel was run by Bio-Rad mini gel system. Gel was run at a constant voltage of 200V and current of 100mA for 1.5 hours.

Immediately after the run the gel was separated from the cassette and washed with towbin buffer and the protein was transferred on a nitrocellulose membrane using Bio-Rad protein transfer system at 200V and 100mA for 2 hours. The protein transfer was carried out using towbin transfer buffer. After the transfer the membrane was briefly stained with Ponceau S solution and wash three times using Tris Buffer Saline (TBS), each time for 5 minutes. Then the membrane was blocked for one hour at 37° C with gentle shaking using 5% non-fat dry milk in TBS solution containing 0.1% Tween 20. Then the membrane was incubated overnight with primary antibodies specific for exosomes, CD63, CD81, CD9, Hsp70 (System Bioscience). The primary antibody was diluted to 1:1000 with blocking buffer. After that the primary antibody solution was discarded and the membrane was washed three times with TBS, each time for 5 minutes. After the final wash the membrane was incubated at room temperature for one hour with secondary antibody horseradish peroxidase (HRP) diluted to 1:20000 with blocking buffer. The membrane was washed again for three times, each time 5 minutes. After washing the membrane was exposed to X-ray film with Pierce ECL Western Blotting Substrate. From this point on everything was done under dark condition using red light. The film was then placed in a film cassette and hold for 1min, 10min and 1 hour to optimise the exposure of the protein to the film.

3.3 Results:

3.3.1 Analysis of Exosomes by Electron Microscopy:

Since exosomes are nano sized particles, the best way to visualise them is electron microscopy (Peterson et al., 2015). In this study both scanning (SEM) and transmission (TEM) electron microscopy were used to examine the morphology and size of exosomes released from the three chosen cancer cell lines. Formvar coated grid was chosen as a suitable way to analyse exosome samples on both SEM and TEM due to their different working conditions. SEM was used to visualise the 3D structure of the exosomes and TEM was used to measure the size distribution of the exosomes in the preparations. In figure 3.1-3.3 (A, B, C, D, E and F) electron microscopic images from SEM as well as TEM represent round cup shaped like vesicles with heterogeneous size distribution (n= 100) with highest three being 144nm, 170nm and 146 nm for THP1, H358 and MCF7 respectively. The images of the electron microscopy were taken with 50K to 100K magnifications. The average size of the vesicles from H358 was 128.06 ± 17.74 nm while the average size resulted from THP1 and MCF7 derived vesicles were 111.52 ± 13.95 nm and 88.39 ± 19.53 nm respectively. It is clear that these vesicles demonstrate a heterogeneous size distribution indicating a non-uniform morphology and size which is visible in all the exosomes released by these cell lines.

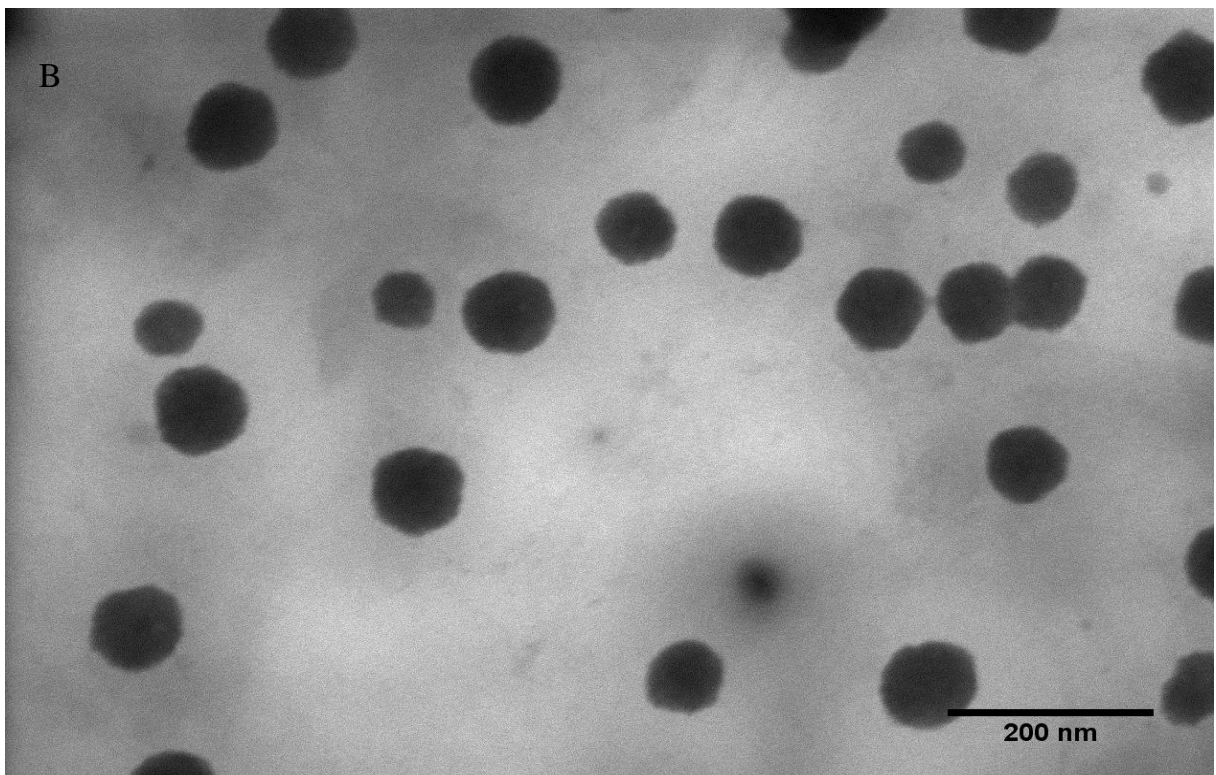
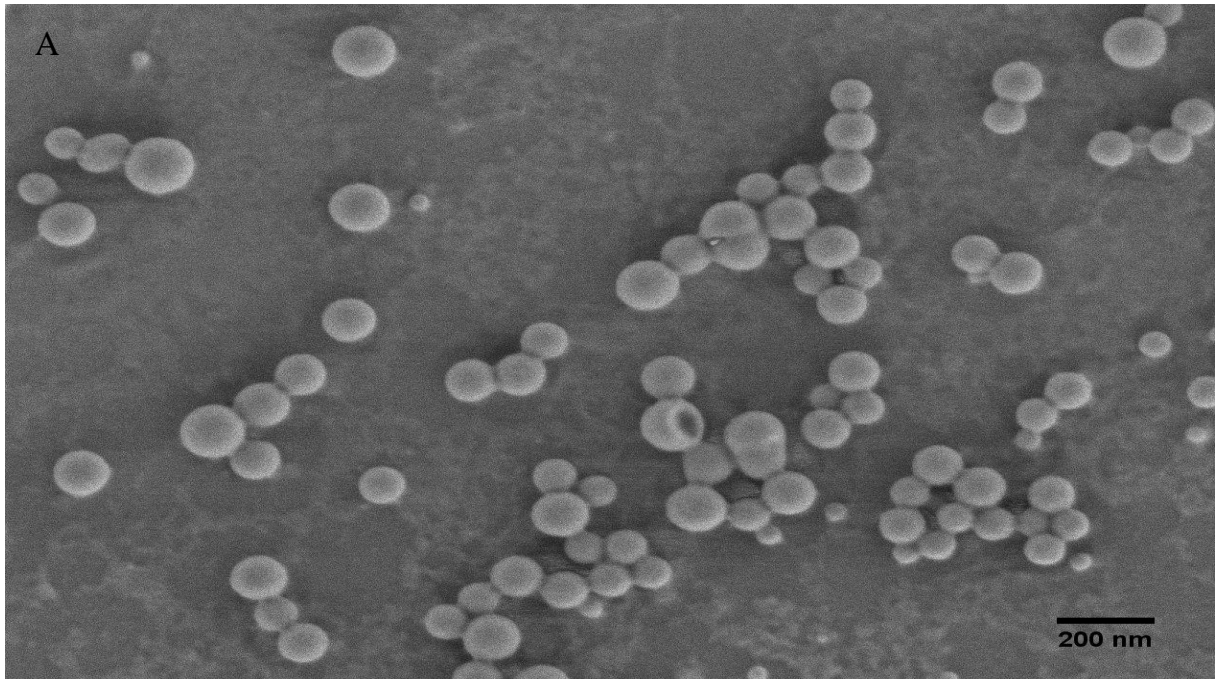


Figure 3.1: A and B represents scanning and transmission electron microscopic images of exosomes derived from H358 cell line respectively at different magnifications.

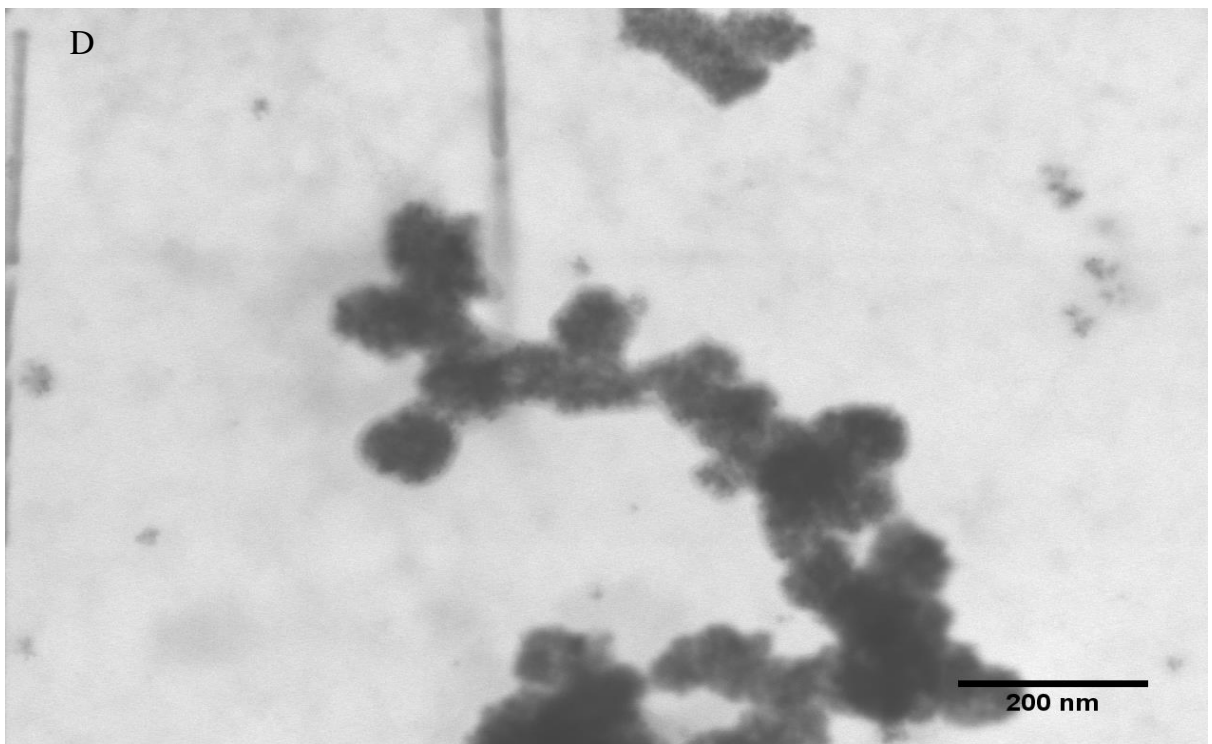
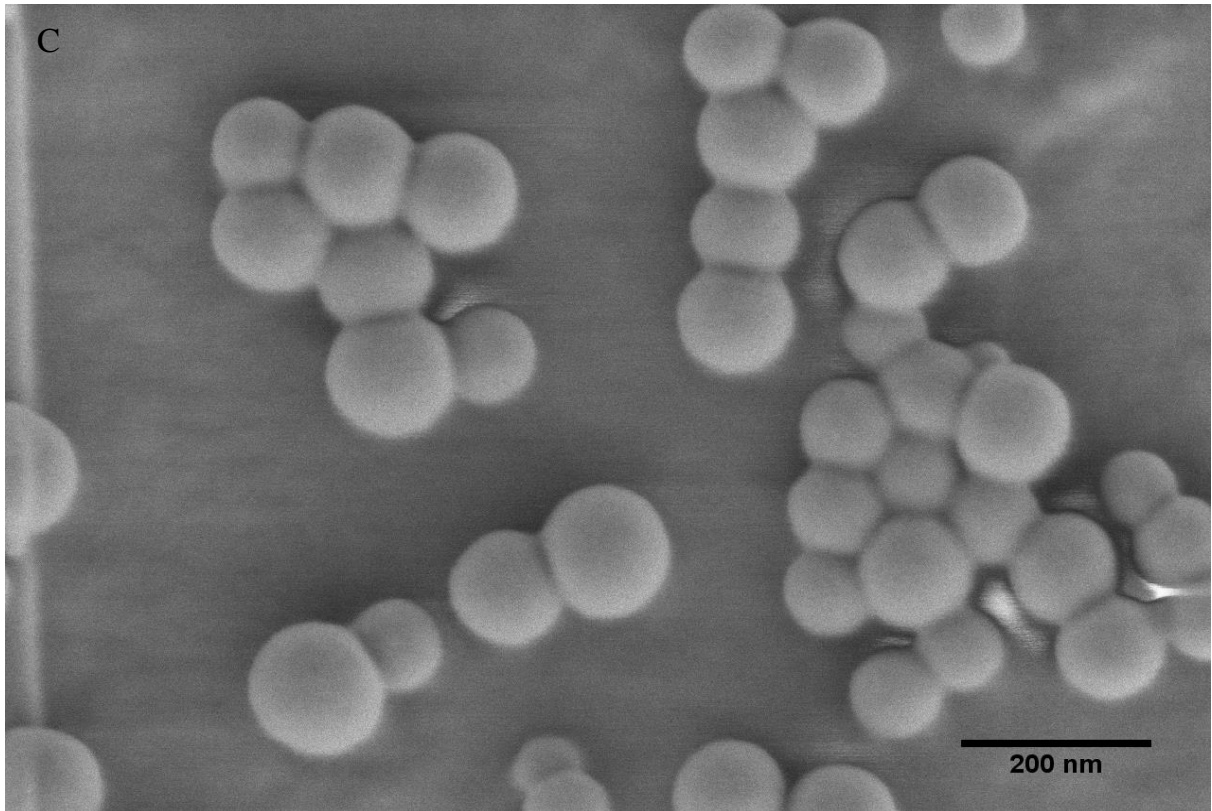


Figure 3.2: C and D represents scanning and transmission electron microscopic images of exosomes derived from THP1 cell line respectively.

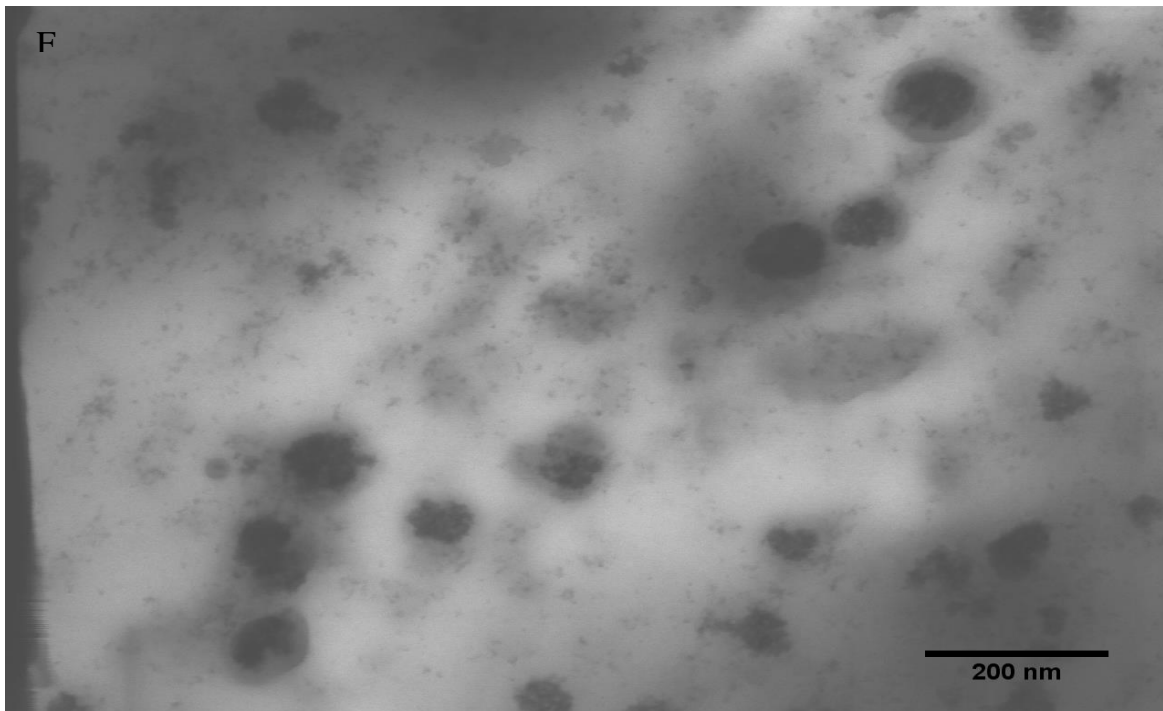
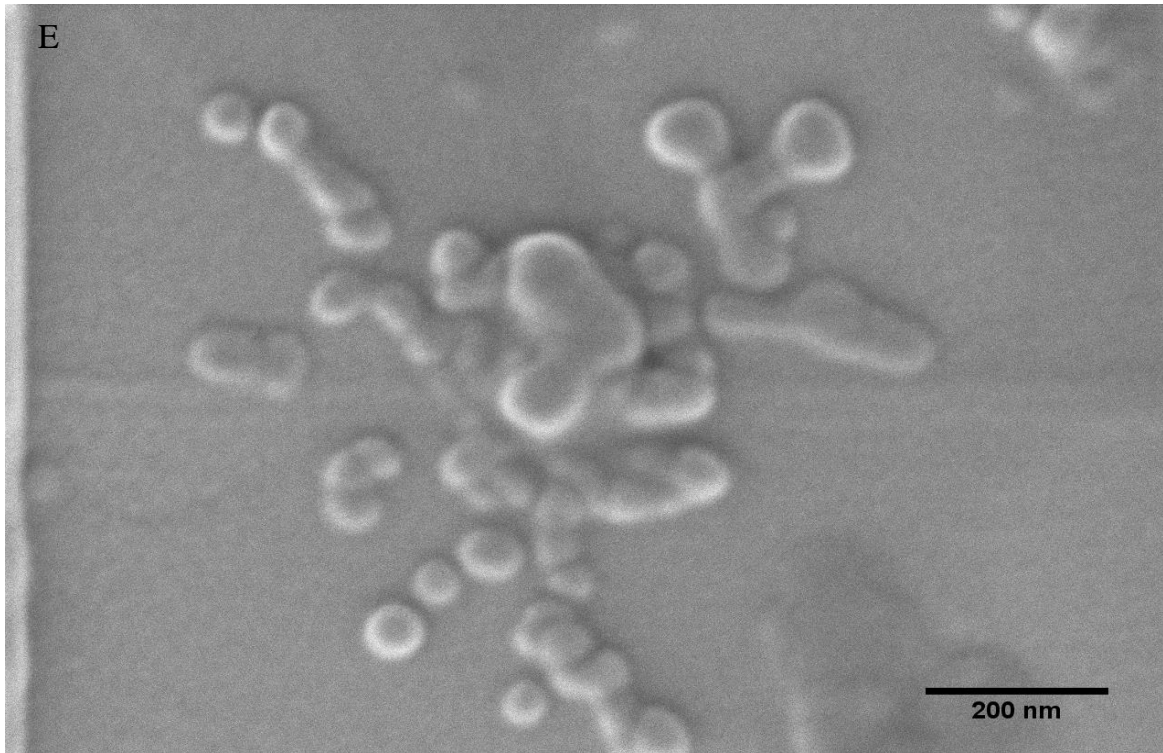


Figure 3.3: E and F represents scanning and transmission electron microscopic images of exosomes derived from MCF7 cell line respectively.

3.3.2 Size Distribution Analysis by Dynamic Light Scattering:

The differential size distribution of nano sized particles was determined by using dynamic light scattering (DLS) or also known as photon correlation spectroscopy. All vesicles scatter light when they are illuminated with a laser beam. The size distribution of these vesicles was calculated (n=10 with triplicates) as described earlier by measuring the intensity fluctuation of the scattered lights and applying the Brownian motion and light scattering theory. DLS is used to measure the size distribution of exosomes secreted by the cancer cell lines used. The average size analysed by DLS for the exosomes from H358 is (165.96±40.26) nm (Table 3.1) with PDI (Polydispersity Index): 0.513. For THP1 the average size is (146.23±38.18) nm (Table 3.1) with PDI: 0.412. For MCF7 the average size is (137.49±26.75) nm (Table 3.1) with PDI: 0.397. The results from EM and DLS showed significant statistical difference ($p < 0.05$, Figure 3.4). However, the results from DLS were comparable with the results from EM (Figure 3.4) as both the results were within the expected exosomal size range. The DLS analysis also showed a strong negative zeta potential (Table 3.1) of (-46.32±7.80) mV for H358 exosomes, (-43.34±6.17) mV for THP1 exosomes and (-51.21±5.23) mV for MCF7 exosomes. The highly negative charge of exosome was due to the presence of phospholipid membrane.

Table 3.1: Dynamic Light scattering and zeta potential of exosomes from H358, THP1 and MCF7 cell lines are shown in the table below. Here, n=10 each with triplicates.

Samples	H358			THP1			MCF7		
	Size (nm)	PDI	Z-potential (mV)	Size (nm)	PDI	Z-potential (mV)	Size (nm)	PDI	Z-potential (mV)
Sample 1	171.83	0.465	-48.12	192.94	0.455	-37.23	118.33	0.461	-56.31
Sample 2	136.12	0.552	-52.56	219.03	0.369	-41.26	106.87	0.423	-49.88
Sample 3	216.25	0.663	-49.43	128.24	0.422	-52.14	177.32	0.289	-52.05
Sample 4	111.28	0.611	-33.11	93.12	0.613	-51.8	159.33	0.603	-41.11
Sample 5	165.69	0.418	-36.17	171.6	0.211	-48.79	179.21	0.326	-54.39
Sample 6	111.7	0.289	-40.25	120.6	0.563	-41.03	110.12	0.416	-46.27
Sample 7	235.31	0.509	-58.13	151.6	0.383	-39.54	139.36	0.397	-47.51
Sample 8	179.24	0.572	-49.87	119.36	0.474	-46.19	128.39	0.365	-52.37
Sample 9	155.78	0.533	-44.26	139.33	0.417	-41.66	115.45	0.317	-59.09
Sample 10	176.4	0.516	-51.34	126.44	0.217	-33.8	140.54	0.366	-53.14
Average	165.96	0.513	-46.32	146.23	0.412	-43.34	137.49	0.397	-51.21
STD	40.26	0.11	7.80	38.18	0.13	6.17	26.75	0.09	5.23

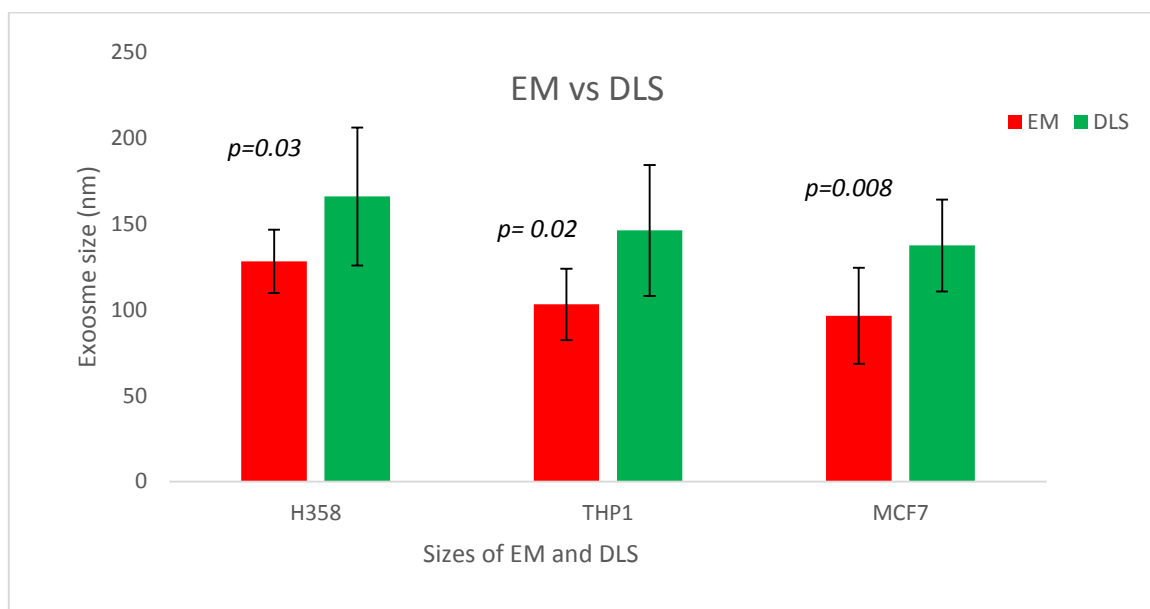


Figure 3.4: Comparison of exosome size obtained from EM and DLS analysis for H358, THP1 and MCF7. A t-test on the size distribution showed significant differences ($p \leq 0.05$) between the results of EM and DLS.

3.3.3 Comparison exosome isolation by PEG:

To identify the best PEG and their concentration, three PEG polymers with different molecular weight (4000Da, 6000Da and 8000Da) were used and exosomes from lung cancer cell lines were used as reference. Exosomes were isolated by 10%, 20%, 30% and 40% (w/v) of each of the molecular weight. To compare the best polymer and concentration to be used, the protein concentration (Figure 3.5) of the isolated exosomes were measured by Bradford assay method using BSA as standard. Although protein concentrations did not show much difference ($p \geq 0.05$) between the polymers and their working concentration, it was observed that 30% PEG with 8000KDa molecular weight yielded the highest protein concentration (Figure 3.5). However, DLS analysis showed that the average size of exosomes from 30% was higher than the commercial kit as well as other PEGs (Figure 3.6). To further identify the best suit PRG concentration, TEM analysis was perform with all working concentrations (10%, 20%, 30% and 40%) from each different molecular weight. Images from the TEM analysis (Figure 3.7) showed that, irrespective of concentrations, all PEG solutions were able to isolate exosomes like vesicles. However, images acquired from 8000Da solutions were better than other two PEGs. Images from 10% solution of all PEGs with different molecular weight showed the presence of some other particles or leftover cellular debris. Image from 40% solution of 4000Da showed very little to no exosome like particles. Average particle size measured by DLS showed very little difference between 30% and 40% of 8000Da PEG solution. Due to the higher protein concentration and from the images of TEM, 30% solution of 8000Da was chosen for exosome isolation for later part of the thesis.

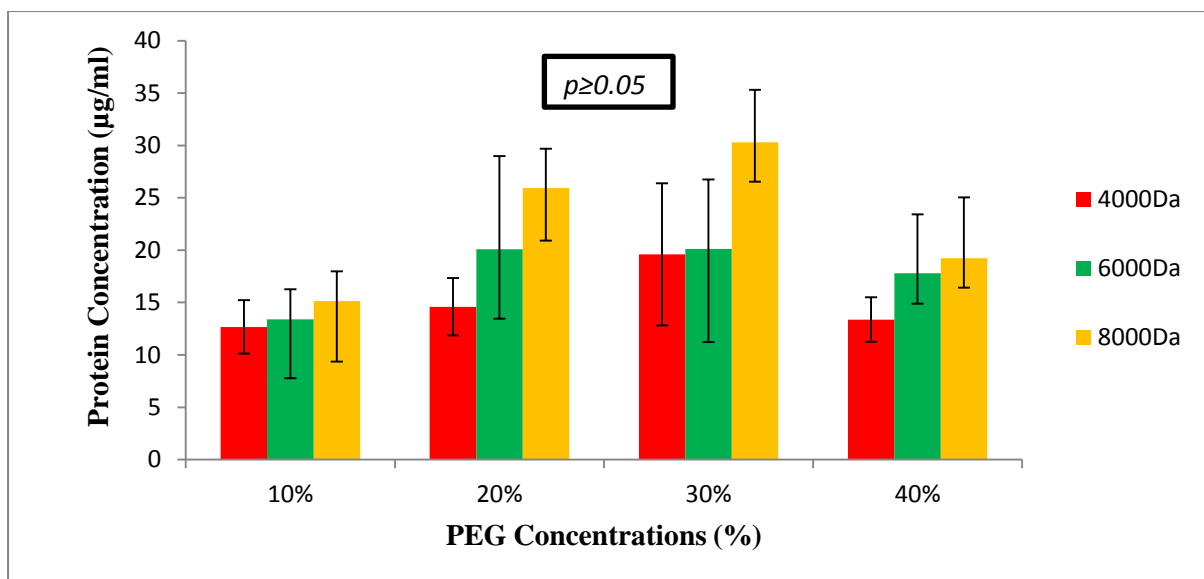


Figure 3.5: Comparison of PEG solutions of different molecular weight and different concentration. As a reference sample, only exosomes from H358 was used. A t-test was carried out to analyse the differences within each concentrations which did not show any significant differences ($p \geq 0.05$).

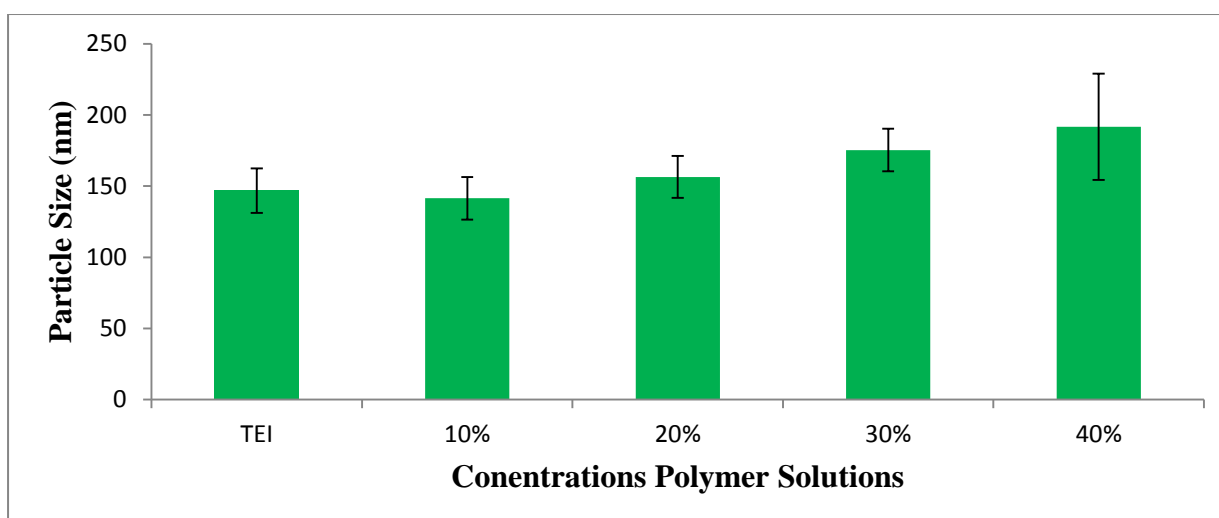


Figure 3.6: Comparison of commercially available exosome isolation kit (TEI) and PEG solutions of different concentrations. DLS analysis was performed to analyse the particle size distribution.

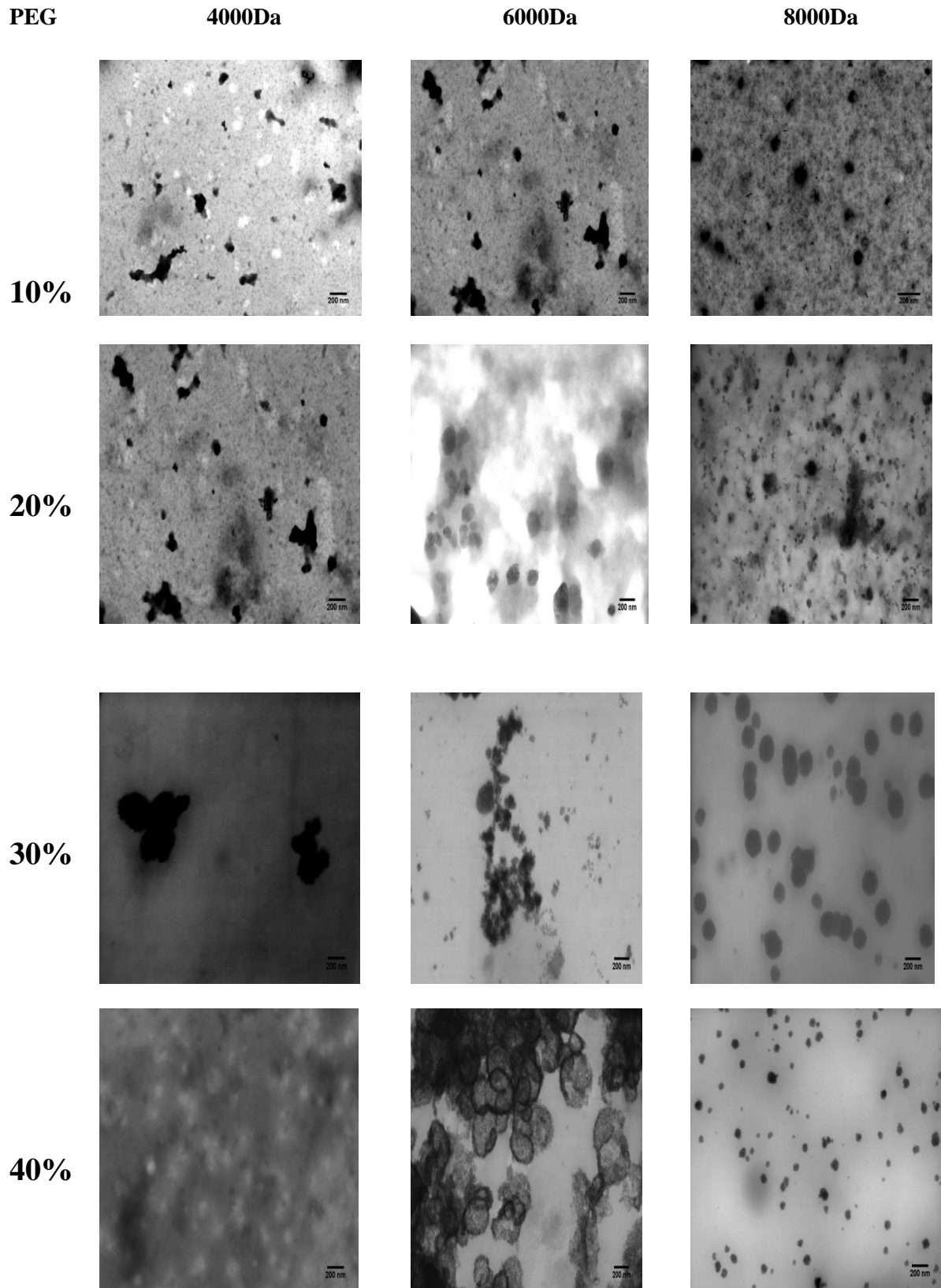


Figure 3.7: TEM images of exosomes isolated from H358 cell lines by PEG solution with different molecular weight and at different concentrations. All the images are taken within 50K to 100K magnification.

Then comparison was made between ultracentrifugation method, precipitation method with commercial kit and in-house PEG 8000Da polymer based solution. Equal amount of cell culture supernatant (2ml) was taken from all three cell lines. After isolation of exosome by three methods exosomes were lysed with RIPA buffer and protein concentration was determined by Bradford assay. In figure 3.8 it is clearly visible that, the protein concentration from UC is lower than both the precipitation solution while the protein concentration from TEI and EXPEG is very similar in three cell lines. Although the difference in protein concentration is not significant but as the in house PEG solution yielded the highest concentration, the 8000Da has been chosen for subsequent proteomic studies.

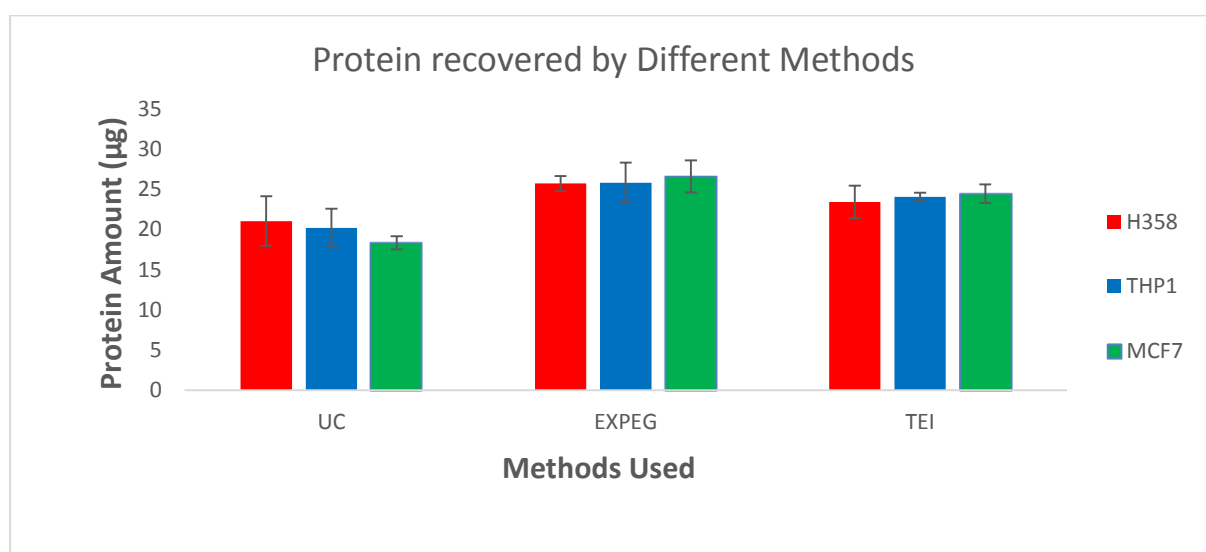


Figure 3.8: Comparison of proteins extracted by three methods, ultracentrifugation (UC), polyethelyn glycol solution (EXPEG) and total exosome isolation kit (TEI) for three cancer cell derived exosomes.

3.3.4 One Dimensional Gel Electrophoresis and Western Blot:

A simple 1D gel technique was applied to see the protein patterns of three cancer cells and their corresponding exosome (Figure 3.9A). Ideally exosomes shares similar protein bands with their cell of origin. On 1D PAGE more distinct protein bands were detected on the cell lysates, compared to exosome protein bands. Apart from some common bands, there were more than 25 protein bands of the cellular samples were absent or present in very low level in example while the intensity of some bands much clear in the exosome sample. Furthermore approximately 10 distinct bands on the exosome samples were variably present on the cellular lanes.

There are several differences in the band patterns between the cell lysates and the exosomal proteins. Several protein bands are not present in the exosome but there are three bands marked red arrow in (Figure 3.9A) with the molecular weight of just around 250kDa, between 250kDa -100kDa and the last one very close to 10kDa, are not present in the cell lysate. There are two bands very close to each other (Yellow boxed) are either not present in the cell lysates or present in lower abundance compared to the exosomes along with the bands marked with red arrows around 25kDa to 15kDa in the exosome samples which are not present in cellular samples. Furthermore, there are one band in each cell lysate (White box) which are not seen in exosome samples around 15kDa (Figure 3.9A).

Exosomes from three cancer cell lines were characterised by western blot analysis using most commonly used exosomal protein marker CD63, CD81, CD9 and Hsp70 to establish whether the exosomes from these three cancer cell lines express these exosomal proteins (Figure 3.7 B). The presence of CD63 in 53kDa, CD9 in 28kDa, CD81 in 26kDa and Hsp70 in 70kDa in all three exosomes suggests the presence of exosomes in the preparation. The observation of SEM, DLS along with the presence of exosomal marker proteins in the preparation confirms the presence of exosomes in the preparation.

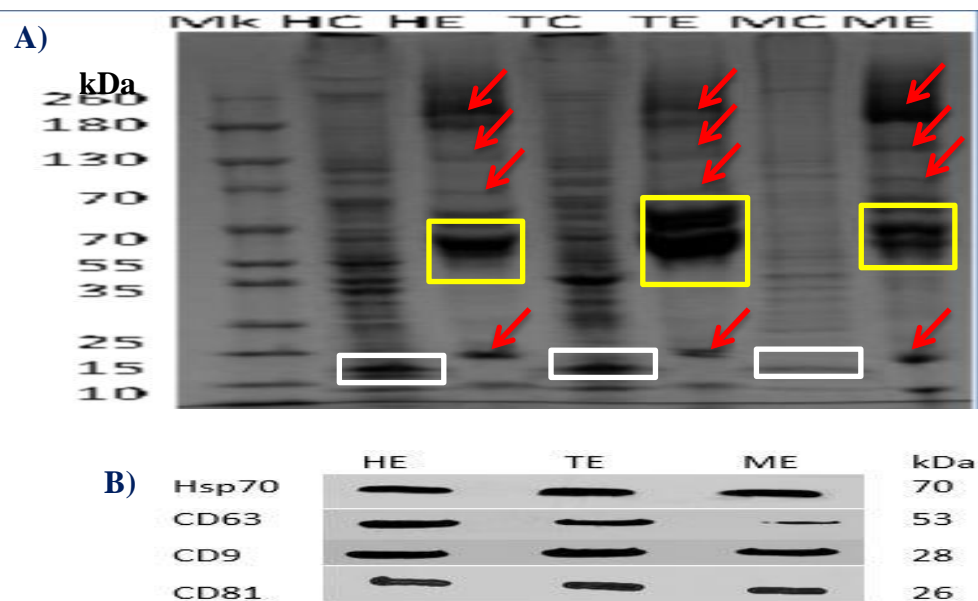


Figure 3.9: A) 1D gel electrophoresis of cellular protein and exosomal protein where H and HE represent H358 and exosomes from H358, similarly for T and TE are THP1 and exosomes from THP1 and M and ME stand for MCF7 and exosomes from MCF7 respectively. Bands with red arrow and yellow box in exosome sample are either absent or present in low abundance in cell lysates. Bands in white box are not present in exosome sample but present in cell lysates. B) Western blot analysis of exosomes using exosome marker CD63, CD81, CD9 and Hsp70 from lung cancer cell line H358 (HE), leukaemia cell line THP1 (TE), breast cancer cell line MCF7 (ME).

3.4 Discussion:

Over the last few years, focus on exosome research has gained huge attention (Lane et al., 2015) due to its versatile application in drug delivery systems (Haney et al., 2015) and cancer biomarkers (Sandfeld-Paulsen et al., 2016). Isolation of exosomes from various complex body fluids with their inherent intact properties is one of the fundamental parts in any downstream analysis of exosomes (Li et al., 2017). The main goals for this chapter were to identify and characterise exosomes and establish a method for the purification, identification and characterization of exosomes from cell culture supernatant, derived from the three cancer cell lines which are time and cost effective. Several experiments have been performed and optimised to establish the methodologies. The culture conditions were optimised in order to obtain good quality exosomes from each cell lines.

To choose the method that best suits with the availability of instruments, broadly two methods of exosome isolation have been experimented including ultracentrifugation and polymer based precipitation. PEG with three different molecular weights and at different concentrations was used to find out the most suitable methods to isolate exosomes. Although, the results do not suggest any significant difference between 4000Da, 6000Da and 8000Da, however 30% PEG 8000Da shows higher protein concentration any others (Figure 3.5). The average size distributions were relatively comparative amongst 10%, 20% and 30% where 30% being the top ranked. The average size distribution for 40% PEG 8000Da was even higher but 30% was chosen over it due to higher protein concentration and lower size distribution ($175.29 \pm 15\text{nm}$ for 30% and $191.67 \pm 37.26\text{nm}$ for 40% PEG). The results between TEI, UC and EXPEG does not suggest a significant differences however the result from the Bradford assay shows that the protein concentration from both the polymer was higher than the UC (Figure 3.6). The advantages of ultracentrifuge method include low or no chemical cost and lower risk of having contaminating proteins with large scale capacity. However, the limitations of the ultracentrifuge technique includes requirement of special equipment and tubes with careful balancing (Li et al., 2017). Other limitations includes relatively low recovery of exosomes has been reported for ultracentrifuge method (Sunkara et al., 2016). However, the PEG based precipitation method also has some pros and cons. The advantages of the precipitation method include better yield, easy to use, does not require any specialised equipment and easily scalable for large samples. On the contrary, the limitations of precipitation method are risk of getting contaminating proteins and other extracellular vesicles as the polymer reduces the solubility of all vesicles including exosomes which aids

to the total protein concentration, longer run time for exosome isolation and finally this method requires pre and post clean up steps to remove the contaminating proteins (Li et al., 2017). Furthermore, the commercial kits available in the market are very expensive to use widely in laboratory experiment but PEG based method is very easy to isolate exosome from the culture medium even with the risk of isolating exosomes with contaminating proteins if the post clean up steps are applied (Atha and Ingham, 1981). Several studies have successfully isolated exosomes using PEG. For example, PEG 10,000Da was used to isolate exosomes from HeLa cells which showed an average particle size of 100nm and western blot analysis confirmed the presence of exosomal marker proteins CD81, CD9 and ALIX (Weng et al., 2016).

Two cell lines used in this study out of the three cancer cell lines were epithelial adherent cells. They were lung cancer cell line (H358) and breast cancer cell line (MCF7). The other cell line was a monocyte suspension cell line from leukaemia (THP1). Exosomes from each cell line were characterised by exosomal protein markers CD63, CD81, CD9 and Hsp70 (Figure 3.8). Exosomes from all the cell lines expressing these well-known exosomal markers confirms the presence of exosomes in the culture media. The results of EM also showed the presence of a heterogeneous population of vesicles within the accepted size range (30nm-150nm) of exosomes. The size and morphology of exosomes from THP1 (30-100nm) and MCF7 (20-300nm) cell lines were comparable to previously reported sizes of these two cell lines (Redzic et al., 2013; Wang et al., 2015). Due to the hydrophobic surface of exosomes drying steps in the sample preparation for electron microscopy causes the agglomeration, which is also visible in the images (Mizutani et al., 2014; Sokolova et al., 2011). All the images taken by the electron microscopy showed the presence of exosomes with a heterogeneous size distribution which indicates that the populations of exosomes produced by the cell lines are not uniform which is an accepted characteristics described in published works (Bobrie et al., 2011; Palmieri et al., 2014). However some vesicles were damaged due to the techniques used to fix and dry the exosomes onto the EM grid. Although no presence of micro vesicles/apoptotic bodies were seen on the images, there was some non-exosomal materials seen on the images which could be some cell debris or protein aggregates. In EM images exosomes are distinct and clear in SEM which is shown in figure 3.2.

The presence of exosomes was established by DLS. DLS is a much more simple method than EM. DLS method is suitable to determine the average size of mono dispersed particles but for highly poly disperse particles accurate sizing is very difficult (Sunkara et al., 2016) which

complied with the result as it showed a polydispersity index of over 0.2. However, DLS has been previously used to detect exosomes three human colon cancer cell lines (Palmieri et al., 2014). Furthermore, the PEG polymer also isolates some larger extracellular vesicles which DLS method cannot distinguish and hence those larger particles contribute to the average size which also supported by previous published paper (Lane et al., 2015).

3.5 Conclusion:

The proper isolation, identification and characterisation of exosomes are crucial for the subsequent exosome analysis. Methods to isolate exosomes from different source such as blood or cell culture media have been reported to suffer several issues which question their acceptability. In this chapter, it was shown that exosomes from cell culture media was successfully isolated by using polyethylene glycol based precipitation method and the presence of exosomes were confirmed by TEM and the size distribution was evaluated by DLS.

Chapter 4:

Dynamics of exosome release during cellular growth.

4.1 Introduction:

Exosomes are extracellular vesicles released by cells to their microenvironment to maintain intracellular communication by transferring biological contents such as proteins, lipids, nucleic acid to the neighbouring cells. Recently it was revealed that cells release different subpopulation of exosomes with distinct composition and biological information that have different effect on the recipient cells (Corrado et al., 2013; Willms et al., 2016). In recent years exosomes studies have taken a huge dive to find out the total protein content of tumour derived exosomes by mass spectrometry based proteomics to look for potential biomarker for disease (Fontana et al., 2013). In any proteomic study the protein concentration of the sample is crucial especially if the experiment is based on gel electrophoresis. The total protein concentration of cell lysate is dependent on the total cell number; likewise the total protein concentration of exosomal protein is dependent on the number of exosomes secreted by the cells. All cells release exosomes in their biological fluids during their growth phases to perform several biological functions such as immune response, communicate with neighbouring cells, removing waste materials. These exosomes are taken up by other cells from the extracellular matrix. The time exosomes stays in the biological fluids vary between cell types. It has been reported that the half-life of the exosomes from B16 melanoma cells is 30mins and this was observed when exosomes were labelled with fluorescent dye to check their stability (Takahashi et al., 2013). In another report, exosomes from human platelet concentrate showed a half-life of 5.5hours (Yáñez-Mó et al., 2015). Several reports revealed that within these short period of times, exosomes carries various proteins and RNAs depending on the cell of origin and also on condition of the environment such as hypoxia or inflammation (de Jong et al., 2012; Théry, Zitvogel, et al., 2002). It has been reported that tumour derived exosomes elevated the expression level of luciferase receptor by 60-fold in breast cancer cells (Chow et al., 2014). It was observed that CD53 and CD63, two members of the tetraspanins, showed increased expression during apoptosis. In this report spontaneous apoptosis of human neutrophil cells was achieved by aging which resulted the increased level of expression of the tetraspanins CD53 and CD63, and down regulated the expression of CD62L, a surface adhesion receptor (Beinert et al., 2000).

In this chapter, the total number of exosomes released by the cell was examined in relation to culture time/growth phases by applying ELISA based exosome quantification method. Total protein concentration was measured by Bradford assay and the proteins from exosomes of different growth stages were separated by 1D gel electrophoresis and identified by mass spectrometry. The goal of this chapter is to quantify exosomes in different growth phases. The protein concentration will also be measured to justify the exact time and number of exosomes required for any specific amount of protein needed for any subsequent exosome analysis for example, exosomal protein concentration required for 2D gel based proteomics. For any 2D gel based proteomics, 100 μ g to 200 μ g of protein required. So to determine the accurate time and cell number required for that amount of protein the number of exosomes needed to be quantified. The result of this chapter will be used in the following chapter to collect exosomes.

4.2 Methods and Materials:

4.2.1 Protein Extraction and Calibration Curve:

Protein extraction was performed by following the manufacturer's protocol with slight modification. Exosome pellet isolated from culture medium as described in previous chapter using Total Exosome Isolation Kit from Invitrogen (Fisher Scientific UK) was suspended in 100µl of exosome binding buffer. The sample was vortexed for 15 seconds to resuspend the exosome particles. Then the samples were incubated at 37°C for 30min to liberate all the exosomal proteins with occasional vortex every 10min. After the incubation steps the samples were centrifuged on a bench top centrifuge at 1500g for 30mins to pellet down any residual debris. The temperature was kept at 4°C during the centrifugation. The supernatant containing protein was collected in a sterile eppendorf tube and kept on -80°C for future analysis. The calibration curve was obtained by serial dilution of the ExoElisa protein standard (CD63). Absorbance was taken by a multi plate reader SpectraMax M5 at 450nm.

4.2.2 Quantification of Exosomes by ELISA Method:

To count the number of exosomes, equal number of cells (0.5×10^5) from H358, THP1 and MCF7 cell lines was seeded in a six well plate. The experiment was done in triplicate. Samples were collected every three days interval up to five collection. An enzyme linked immunosorbant assay (ELISA) method was applied to count the exosomes secreted by the cells. The Exo-ELISA method works based on the exosomal marker protein CD63. The exosomal proteins were directly immobilised into the well and coated to a blocking buffer to prevent non-specific binding. The detection (primary) antibody which is specific to antigen protein CD63 was added and a secondary antibody HRP (Horseradish peroxidase) was used to detect the primary antibody.

Exosome was counted using the manufacturer's protocol. Briefly, 50 µl of prepared protein standards and exosome protein sample (10µg) were added to the appropriate well of the micro-titer plate. The plate with sealed with film/cover. The plate was then incubated at 37°C overnight. After incubation step, the plate was inverted to empty all contents. Then the plate was washed 3 times for 5 minutes each with 100 µl 1X Wash buffer. A shaker was used for all subsequent washing and incubation steps. Residual liquid was removed by hard-tapping the plate on fresh paper towels, while taking care not to let the wells dry out completely. Exosome specific primary antibody was (CD63) to 1:100 with 1X blocking buffer and was added 50 µl of to each well and incubated at room temperature for 1 hour with shaking. Then

the plate was washed 3 times for 5 minutes each with 100 μ l 1X Wash buffer. Exosome validated secondary antibody (HRP) was diluted to 1:5,000 with 1X blocking buffer and 50 μ l was added to each well and incubated at room temperature for 1 hour with shaking. The plate was washed 3 times for 5 minutes each with 100 μ l 1X Wash buffer. Then 50 μ l of Super-sensitive TMB ELISA substrate was added and incubated at room temperature for 45 minutes with shaking. Then the absorbance was taken using a micro plate reader at 450nm.

4.2.3 Determination of Protein Concentration:

The protein concentration was determined by using a modified Bradford assay method. A standard curve was made by diluting 0, 2, 4, 6, 10, 15 and 20 μ g of BSA standard solution (1.0g/ml) into assigned wells of a 96-well plate. The volume was made up to 100 μ l with deionised water. 20 μ l from each sample was taken in separate wells. 200 μ l of Bradford reagent was added to each well including standards and samples. The plate was then incubated for 5min and the absorbance was taken by the multi plate reader Spectra Max M5 at 595nm with a constant temperature of 25°C.

4.2.4 One Dimensional Gel Electrophoresis:

In this chapter, for 1D gel, the running condition was same with the previous chapter but instead of handmade gel, NuPage 12%-4% gels from Invitrogen (Fisher UK) and SureLock mini gel tank were used. For the running buffer MOPS running buffer also from Invitrogen was used. 25 μ g from each sample were diluted with sample buffer (0.5 M Tris pH 6.8, 25% Glycerol, 1% SDS, Bromophenol blue) and heated at 70°C for 10min. 15 μ l of sample were loaded in each lane. The gel was run under denaturing condition at a constant voltage of 200V and current of 100mA for 45min. Gel bands were cut into pieces and sent to University of York for protein identification by mass spectrometry. The protocols used for LC/MS are described below.

4.2.5 Protein Identification by LC-MS (University of York):

In-gel tryptic digestion was performed after reduction with DTE and S-carbamidomethylation with iodoacetamide. Gel pieces were washed two times with 50% (v/v) aqueous acetonitrile containing 25mM ammonium bicarbonate, then once with acetonitrile and dried in a vacuum concentrator for 20 min. Sequencing-grade, modified porcine trypsin (Promega) was dissolved in the 50mM acetic acid supplied by the manufacturer, then diluted 5-fold by adding 25mM ammonium bicarbonate to give a final trypsin concentration of 0.02 μ g/ μ L.

Gel pieces were rehydrated by adding 10 μ l of trypsin solution, and after 5 min enough 25mM ammonium bicarbonate solution was added to cover the gel pieces. Digests were incubated overnight at 37°C. A 1 μ l aliquot of each peptide mixture was applied directly to the ground steel MALDI target plate, followed immediately by an equal volume of a freshly-prepared 5 mg/mL solution of 4-hydroxy- α -cyano-cinnamic acid (Sigma) in 50% aqueous (v/v) acetonitrile containing 0.1% , trifluoroacetic acid (v/v).

Positive-ion MALDI mass spectra were obtained using a Bruker ultraflex III in reflectron mode, equipped with a Nd:YAG smart beam laser. MS spectra were acquired over a mass range of m/z 800-4000. Final mass spectra were externally calibrated against an adjacent spot containing 6 peptides (des-Arg1-Bradykinin, 904.681; Angiotensin I, 1296.685; Glu1-Fibrinopeptide B, 1750.677; ACTH (1-17 clip), 2093.086; ACTH (18-39 clip), 2465.198; ACTH (7-38 clip), 3657.929.). Monoisotopic masses were obtained using a SNAP averaging algorithm (C 4.9384, N 1.3577, O 1.4773, S 0.0417, H 7.7583) and a S/N (Signal to noise) threshold of 2.

For each spot the ten strongest peaks of interest, with a S/N greater than 30, were selected for MS/MS fragmentation. Fragmentation was performed in LIFT mode without the introduction of a collision gas. The default calibration was used for MS/MS spectra, which were baseline-subtracted and smoothed (Savitsky-Golay, width 0.15 m/z, cycles 4); monoisotopic peak detection used a SNAP averaging algorithm (C 4.9384, N 1.3577, O 1.4773, S 0.0417, H 7.7583) with a minimum S/N of 6. Bruker flexAnalysis software (version 3.3) was used to perform the spectral processing and peak list generation for both the MS and MS/MS spectra. Tandem mass spectral data were submitted to database searching using a locally-running copy of the Mascot program (Matrix Science Ltd., version 2.5.1), through the Bruker BioTools interface (version 3.2). Search criteria included: Enzyme, Trypsin; Fixed modifications, Carbamidomethyl (C); Variable modifications, Oxidation (M); Peptide tolerance, 100 ppm; MS/MS tolerance, 0.5 Da; Instrument, MALDI-TOF-TOF; Database, Uniprot (552259 sequences; 197423140 residues).

4.3 Results:

4.3.1 Quantification of Exosomes by ELISA:

To count the exosome from the samples, a calibration curve (Figure 4.1) was drawn using CD63 standard. Exosomes were calculated with the equation ($y = 3E-11x + 0.0425$) generated by the calibration curve. Absorbance was taken 450nm with triplicates.

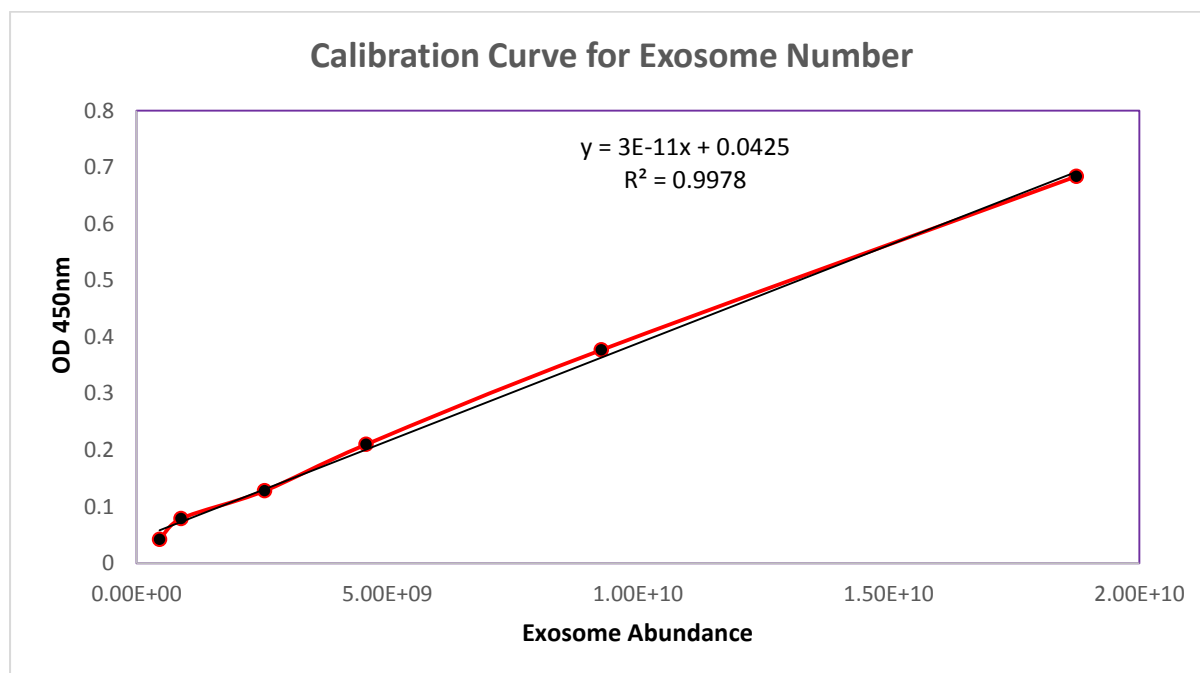


Figure 4.1: Calibration curve of exosomes using exosome standard CD63 to count the exosomes by the ELISA method. Absorbance was taken at 450nm using SpectraMax 5.

Exosomes were counted to determine the relationship between the number of cells and exosomes. Sampling was carried out every three days for up to 15 days. In Figure 4.2 for H358 cell line, it is clearly visible that the number of exosomes increased proportionately from 0.518×10^9 to 13.66×10^9 with increasing number of cells up to day 15. However, after confluency, the number of exosomes increased very sharply and reached to 13.66×10^9 . The number of exosomes released per cell was $\sim 6000/\text{cell}$ on day 3 to $\sim 30,000/\text{cell}$ at day 15. However, the number of exosomes/cell up to confluency stage (on 9th day) was ($\sim 9000/\text{cell}$) but it rose up to $\sim 31600/\text{cell}$ after confluency till the end on 15th day. The overall average exosomes released from day 3 to Day 15 was $\sim 18000/\text{cell}$ (Figure 4.5), the most found in this study.

The THP1 cell line (Figure 4.3) showed a similar trend as the H358 cell line. The exosome number increased consistently from day 3 until day 15 (From 0.335×10^9 to 17.7×10^9) with a slow increase up to day 6 compared to H358 cell line. The THP1 cell reached stationary

phase at day 6 and which is 3 days and 9 days earlier than H358 and MCF7 respectively. Like H358 cells the exosome number from THP1 increased sharply from day 9 (3.34×10^9) to day 12 (17.7×10^9). The average number of exosomes/cell from THP1, on the first collection on day 3 was ~ 14000 and on the last day at day 15 it reached to ~ 32000 . Furthermore, the number of exosomes/cell up to confluency was ~ 2350 /cell but after confluency the number of exosomes/cell was ~ 32600 /cell. However, the overall average exosomes released per cell for THP1 was almost similar (~ 15500 /cell) to H358 (Figure 4.5).

In case of MCF7 cells, (Figure 4.4) the increase of exosome number followed the similar trend of H358. Here, the number of exosomes started to increase slowly from day 3 to day 15 (from 1.62×10^9 to 16.02×10^9). Unlike H358 cell line, the exosome number of MCF7 cell lines increased consistently till day 15. The number of exosomes/cell on day 3 was ~ 1800 /cell, but at day 15 the number of exosomes/cell reached to ~ 45000 . However, up to the confluency stage on 12th day the average number of exosomes released per cell ~ 9650 /cell and after confluency the number of exosomes/cell raised to ~ 17400 /cell. Finally the overall average from day 3 to day 15 the number of exosomes/cell was steady throughout the experiment (~ 14500 /cell) (Figure 4.5).

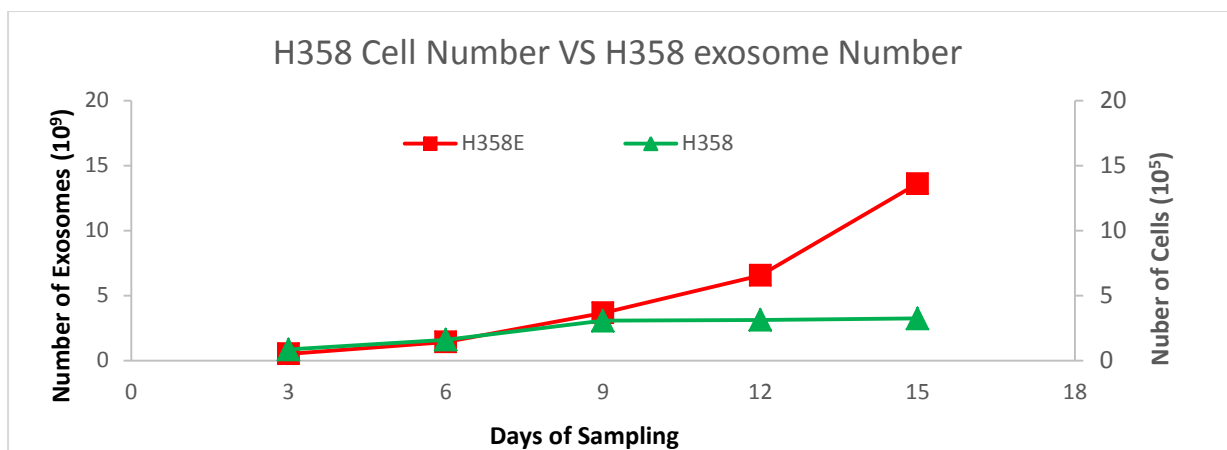


Figure 4.2: Number of H358 cells ($\times 10^5$) vs number of exosomes released ($\times 10^9$) from H358 cells. The number of exosomes was quantified using the ExoElisa method and cells were counted by haemocytometer with every three days interval.

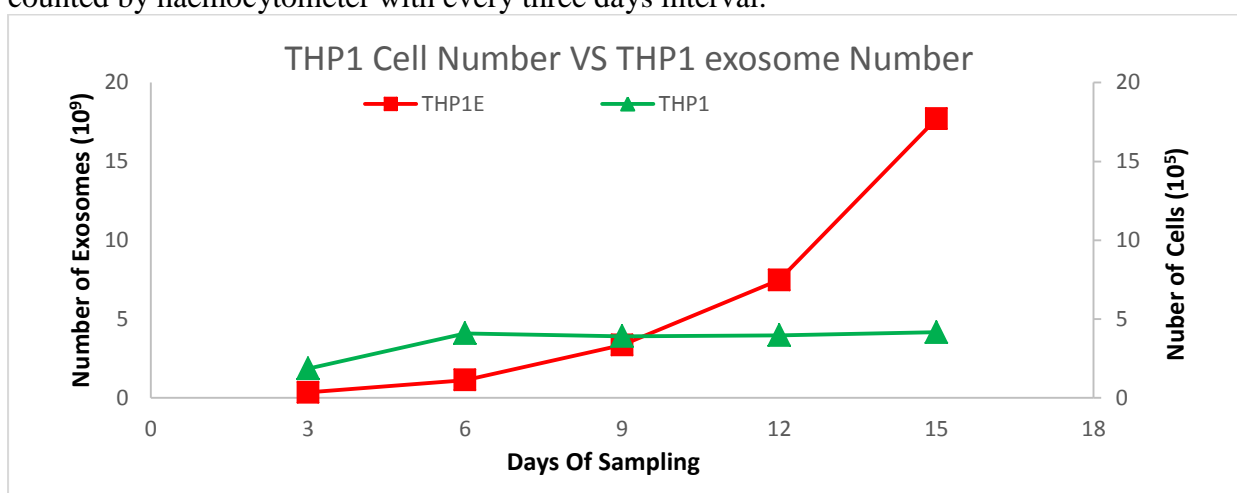


Figure 4.3: Number of THP1 cell ($\times 10^5$) vs number of exosomes released ($\times 10^9$) from THP1 cells. The number of exosomes was quantified using the ExoElisa method and cells were counted by haemocytometer with every three days interval.

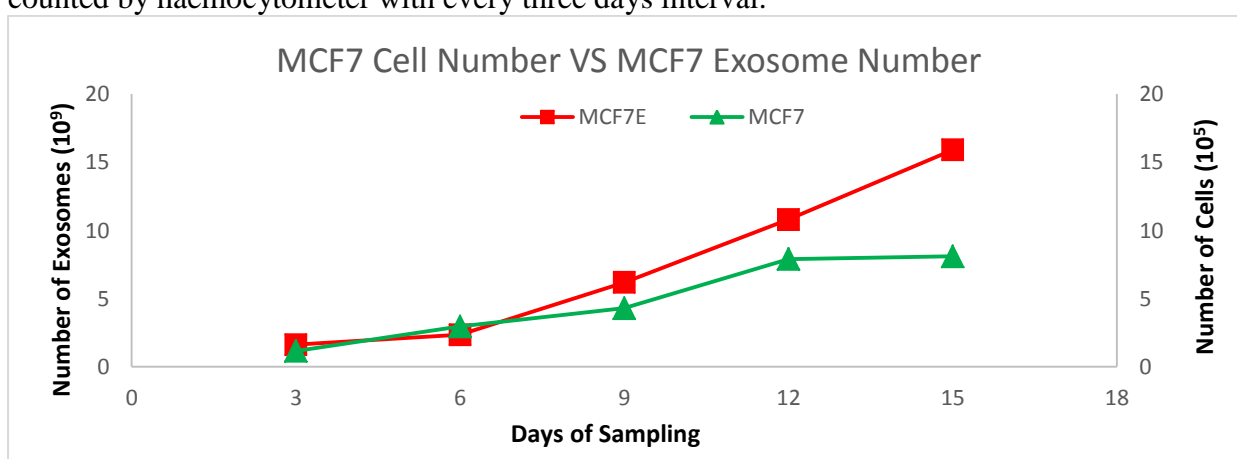


Figure 4.4: Number of MCF7 cell ($\times 10^5$) vs number of exosomes released ($\times 10^9$) from MCF7 cells. The number of exosomes was quantified using the ExoElisa method and cells were counted by haemocytometer with every three days interval.

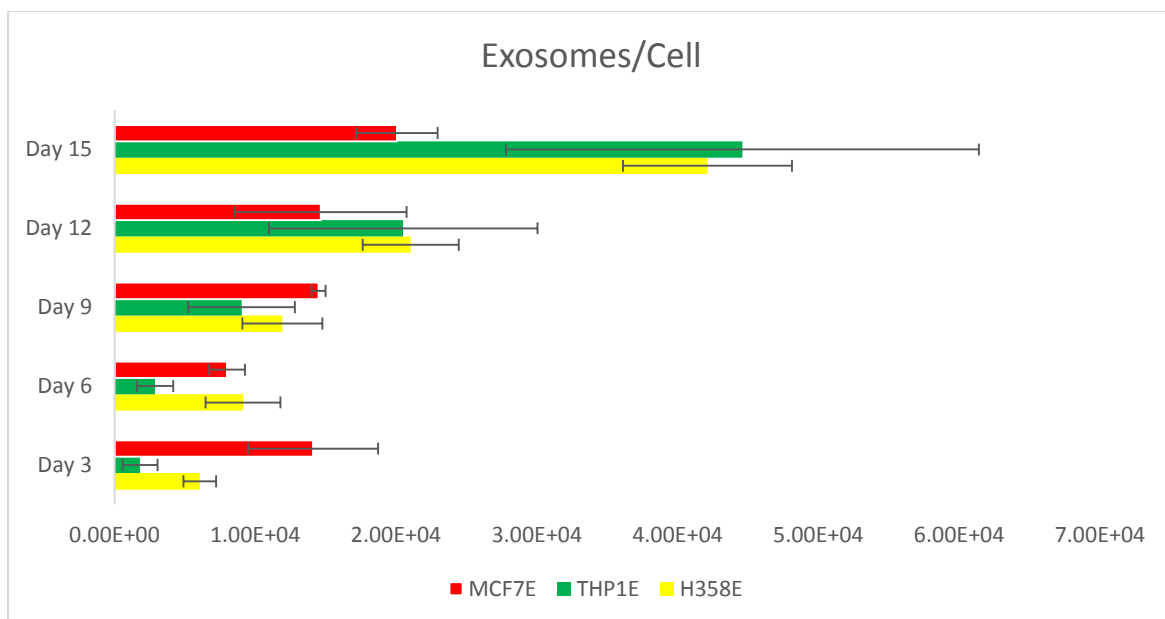


Figure 4.5: Average number of exosomes per cell by H358, THP1 and MCF7 cell lines from day 3 till day 15 on different cellular growth stages.

4.3.2 Bradford Assay of Exosomal Protein:

The protein concentration of the exosome samples collected at different stages of cellular growth was done by Bradford assay. In all three cell lines increasing amount of protein was obtained with increasing number of exosomes, except for THP1 cells where the amount of protein found to be similar between sampling two and three. The rate of increase of protein concentration was faster between the first two sampling in all 3 cell lines. In the figure 4.6 it is clearly visible that with the increase of exosome number the concentration of protein is increasing but it is observed that on 3rd sample collection which is after 9 days the rate of increase slows down. However the overall average rate of protein increase did not show any significant difference. Despite showing a static phase in the protein concentration by both THP1 and H358, the overall protein secretion by the exosomes per day on an average is very similar with H358 showing the highest amount of protein per day (25.476µg/ml) and MCF7 being the lowest (21.736µg/ml) and THP1 (22.6µg/ml) is very similar to MCF7 (Figure 4.7).

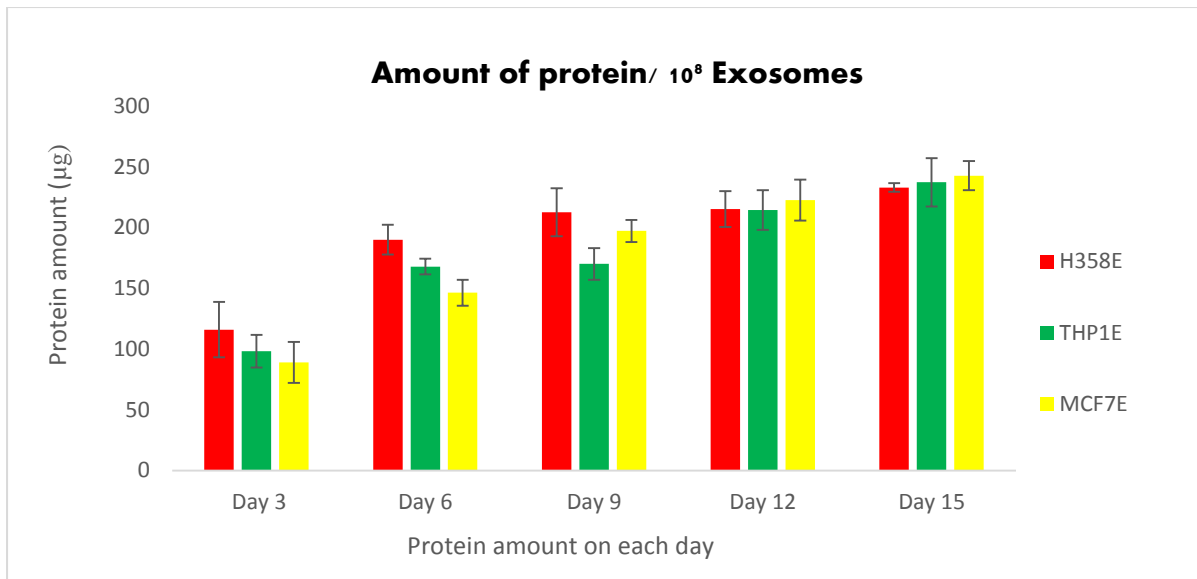


Figure 4.6: Protein concentration against the number of exosomes released by 3 different cell lines at different growth stages. Protein concentration was calculated against per 10⁸ exosomes.

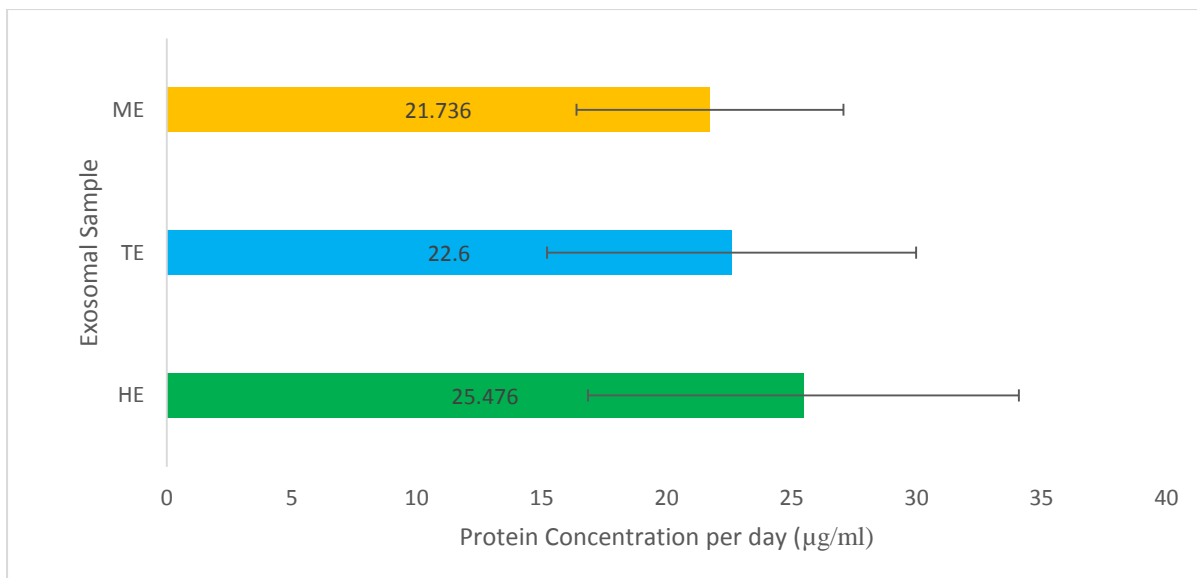


Figure 4.7: Average protein concentration per day by exosomes from three cells. Here, HE, TE and ME represents protein concentrations from H358, THP1 and MCF7 cell derived exosomes.

4.3.3 Analysis of Exosomal Proteins by One Dimensional Gel Electrophoresis:

One dimensional gel electrophoresis was performed on exosomes released by 3 different cell lines which were collected in different cellular growth phases. The results showed variable number of protein bands in different growth phases in 3 different cell lines (Table 4.1). An intense band of approximately 60KDa was observed in each lane (Appnedix Figure 1).

The protein bands on each lane was analysed by using 1D gel electrophoresis analysing software CLIQS (Total lab). The first lane on each gel contains the molecular standard marker and on the basis of molecular marker sizes the approximate molecular weight of each band was measured (Appnedix Figure 1). The similar number of protein bands were observed in all 3 cell lines at sampling 1 on day 3 (4-5 bands) then declined in case of H358 and MCF7 cell lines until sampling 3 on day 9 which is cell confluency stage for these 2 cell lines (Fig. 4.8; 4.10). From sampling 3 the number of protein bands increased until sampling 5 in all 3 cell lines. In case of THP1 cell line protein bands increased from sampling 1 and sampling 2 (confluence stage) then dropped in sampling 3 (Table 4.1).

4.3.4 Dynamics of Protein Transportation by Exosomes Derived from H358 Cells:

There are clear differences in protein band profile in different growth phases (Figure 4.8). The most prominent band observed in each line lies around 60kDa. Apart from the dark band there very faint protein bands (approximately 4KDa to 22KDa) present in sampling 2 and 3 (confluency stage) but these bands found to be absent in sampling 1. However, these proteins band became more prominent in sampling 4 and sampling 5. Moreover, there are few protein bands appeared around 160kDa and above in sampling 4 and Sampling 5. Due the differential presence of the protein bands at later stages, these bands were subjected to Mass spectrometry analysis for protein identification. Four bands (HS4.1, HS4.2, HS4.3 and HS4.4) were isolated and analysed for protein identification. The result showed that HS4.1 and HS 4.2 represent alpha-2- macroglobulin (A2M) and Pregnancy zone protein (PZP) respectively. These stress regulator proteins. The HS4.3 band (due to presence of other bands in this area) analysis identified many proteins which are serum albumin, alpha-2-HS-glycoprotein and alpha -1-antiproteinase and HS4.4 band identified as Apolipoprotein A-1. The functions of these proteins are given in Table 4.1

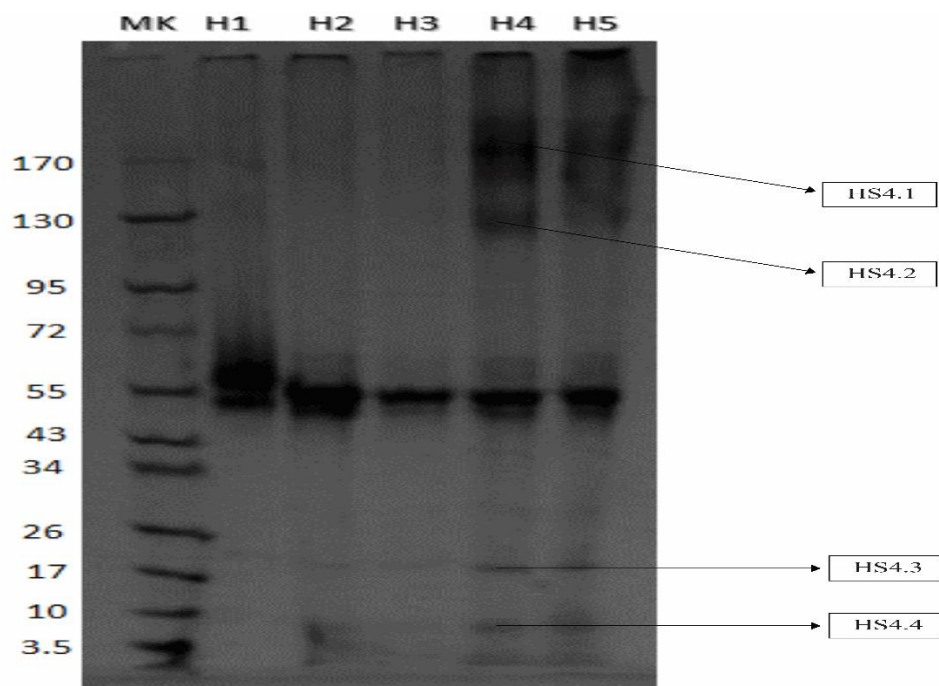


Figure 4.8: 1D gel electrophoresis of exosomal protein extracted from H358 derived exosomes from day 3 till the end on day 15. Here H1 to H5 represent the samples from day 3 to day 15 where H1 represents day 3 or sampling one H5 is sampling five on day 15. The band number is denoted by HS4.1, HS4.2, HS4.3 and HS4.4 represent first, second, third and fourth band from sampling four or day 12 from H358 cell derived exosomes respectively.

4.3.5 Dynamics of Protein Transportation by Exosomes Derived from THP1 Cells:

The protein profile in THP cell line was found to be similar to H358 cell line with exception that the presence of higher molecular weight bands around 160KDa appeared at sampling 2 and then disappeared at sampling 3 and reappeared again at Sampling 4 and sampling 5 (Figure 4.9). Four protein bands from earlier stage (TS2.1 and TS2.2) and later stages (TS4.1 and TS4.2) were isolated and subjected to protein identification. The results showed that TS2.1 and TS 2.2 band was identified as Alpha-macroglobulin (A2M) and Pregnancy Zone Protein (PZP) respectively. The bands TS4.1 and TS4.2 were identified as A2M and PZP again on the later stage of the growth curve.

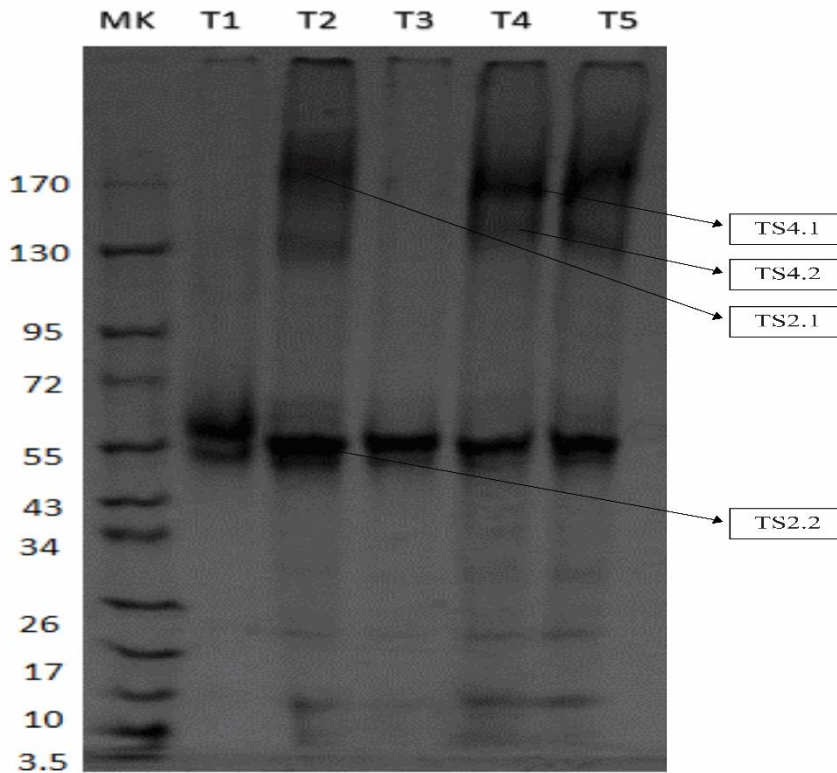


Figure 4.9: 1D gel electrophoresis of exosomal protein extracted from THP1 derived exosomes from day 3 till the end on day 15. Here T1 to T5 represent the samples from day 3 to day 15 where T1 represents day 3 or sampling one T5 is sampling five on day 15. TS2.1 and TS2.2 represent the first and second band from sampling two or day 6 and TS4.1, TS4.2 represent first and second band from sampling four or day 12.

4.3.6 Dynamics of Protein Transportation by Exosomes Derived from MCF7 Cells:

In case of MCF7 cell line similar profile band was observed as H358 cell line (Figure 4.10) but the lower molecular weight bands (approx.4KDa to 22KDa) found to be more prominent from sampling 2 whereas these bands were prominent at sampling 4 and sampling 5 stages in H358 cells. Similar to the H358 cell the higher molecular bands around 160KDa above were observed at sampling 4 and sampling 5 and one band (MS 4.1) was subjected to mass spectrometry analysis for protein identification. The result showed that this band was identified as alpha -2-marcoglobulin and Pregnancy zone proteins (Table 4.1).

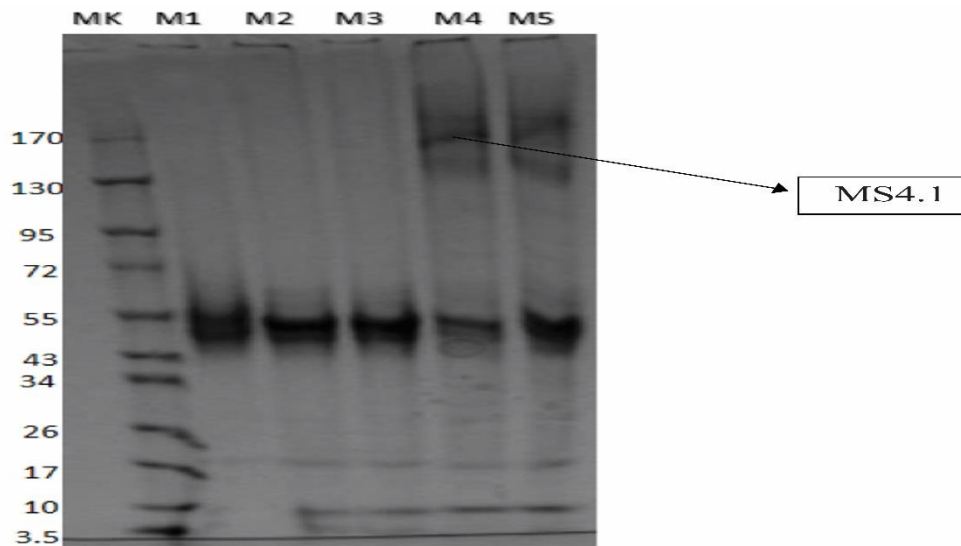


Figure 4.10: 1D gel electrophoresis of exosomal protein extracted from THP1 derived exosomes from day 3 till the end on day 15. Here M1 to M5 represent the samples from day 3 to day 15 where M1 represents day 3 or sampling one M5 is sampling five on day 15. Here, MS4.1 represents the first band on lane 4 which is on day 12.

Table 4.1: List of Proteins identified by Mass Spectrometry from from day 3 to day 15 with their functions.

Band ID	Protein	Accession Number	Cell	Origin	Mol. Wt (Da)	MASCOT Score	pI	Functions
HS 4.1; TS 2.1; TS 4.1 MS 4.1	Alpha-2-macroglobulin	P01023	H358 THP1 MCF7	Human	164613	89	6.03	Vesicle mediated transport Cell differentiation Localization Response to stress Protein binding Protease inhibitor
HS 4.2; TS 2.2; MS4.1	Pregnancy zone protein	P20742	H358 THP1 MCF7	Human	165242	101	5.97	Response to stress Cell differentiation Protein binding Protease inhibitor
HS 4.3; T 4.3	Serum albumin	P02768	H358 THP1	Bos Taurus	71317	137	5.92	Cellular growth Cell Communication Biological regulation
HS 4.3; T 4.3	Alpha-2-HS-glycoprotein	P12763	H358 THP1	Bos Taurus	39193	102	5.26	Membrane invagination Localization Response to stress Kinase inhibitor
HS 4.3; T 4.3	Alpha-1-antiproteinase	P34955	H358 THP1	Bos Taurus	46417	177	6.05	Protease inhibitor Biological adhesion Biological regulation Protein binding
TS 4.1	Haemoglobin subunit delta	P02042	THP1	Human	16159	122	7.85	Cellular growth Transport Localization Biological adhesion Biological regulation
H.S.4.4	Apolipoprotein A-I	P15497	H358	Bos Taurus	30258	264	5.71	Transport Localization Biological adhesion Biological regulation

4.4 Discussion:

Cells were cultured in exosome depleted FBS medium to avoid contamination of bovine exosomes which interferes exosomal function and determination (Shelke et al., 2014). On day 6 serum free medium was added to maintain the volume in the culture flask. The slow cellular growth of the cell lines was due to the exosome depleted FBS as it has been suggested that exosome depleted FBS shows better survival and slow growth rate (Eitan et al., 2015). In this study, the number of exosomes found to be increased with the number of cells during log phase. The stationary/confluency phase occurred in these cell lines varied after seeding. THP1 cell grew faster and reached stationary phase on 6 days due its suspension nature. Whereas, MCF7 reached stationary phase on 12 days after seeding, and H358 on 9 days after seeding. The exosomes per cell increased consistently but the number of exosomes per cell increased sharply after the cells had reached confluency (Figure 4.2; 4.3 and 4.4). There can be several reasons for that, such as the cells were in stationary phase which meant, the number of donor cells and recipient cells were almost even and hence the number of exosome uptake was less than the number of exosome released. In addition, the pH of the culture medium is an important factor for increased exosomes. The pH of the culture medium decreases with the increase number of cells and the low pH increases the secretion of exosomes (Parolini et al., 2009). Furthermore, as the cells reached the stationary phase which resulted high demands of oxygen and led to possible hypoxic condition in the culture medium (Zeitouni et al., 2016). Hypoxic condition have been identified as one of the reasons for increased exosome secretion (King et al., 2012; Umezu et al., 2014). The average number of exosomes per cells (4570~12200)/cell, before the cell reached confluency which is similar results (6500/cell) compared to other published reports (Agarwal et al., 2015). Nevertheless, the number of exosomes per cells throughout the whole experiment supports previously reported data for other published data. For example, in human thyroid cancer cell, the average number was reported between 8700 and 15900 per cell (Agarwal et al., 2015; El-Andalousi et al., 2012). Interestingly, the number of exosomes per cells from the highly metastatic cell line H358 was higher than the less metastatic breast cancer cell line MCF7. However, because of the non-adherent nature of THP1 cells, the secretion of exosome was higher than other two adherent cell lines H358 and MCF. It has been reported that the suspension cells tends to release more intracellular calcium which in turns increase the secretion of exosomes (Koumangoye et al., 2011).

The exosomal protein profiles were similar in all three cells, but their abundance varied in different cell growth stages. An intense band was observed in all lanes around 60kDa and MS analysis revealed that this band represents serum albumin. Presence of serum albumin has been reported in almost all exosomal protein analysis and can be used as a control for 1D gel analysis for exosomal protein (Balaj et al., 2015). The two proteins appeared between 160kDa to 260kDa in H358, THP1 and MCF7 was found in sampling four and five which is after confluency, they were not detected or visible from day 3 till day 9. However, the same band was observed in case of THP1 on sampling two. The MS based identification revealed that one of the proteins were Alpha-2macroglobulin (A2M) (HS 4.1; TS 2.1; MS 4.1; Table 4.1) with a molecular weight of ~164kDa and the other one is pregnancy zone protein (PZP) (HS 4.2; TS 2.2; MS4.1, Table 4.1) with a molecular weight of ~165kDa. The detectable level of A2M and PZP were found invariably at stationary phases of these three cell lines. A2M and PZP are reported to be related with cellular stress (Sottrup-Jensen et al., 1984). Now, here A2M was observed on the day 6 (THP1) and day 9 (H358 and MCF7) and as mentioned before due to the suspension nature the THP1 cell line reached confluency faster than lung cancer cell line H358 and breast cancer cell line MCF7. The reason behind this phenomenon was not investigated in this study. A2M, along with other macroglobulin belongs to the macroglobulin super family. Their basic function is to inhibit proteinase activity by preventing large molecular weight substance to access the active proteinase site. Nevertheless, its other function has been reported to eliminate proteinase out of the cells (Rehman et al., 2013). Previous proteomic study has also revealed that exosomes release Alpha-2-macroglobulin in hypoxic condition as seen when the oxygen level was reduced down to 1% to find out the effects of oxygen on the release of exosome from placental mesenchymal stem cells. Alpha-2-macroglobulin is a transporter protein which is involved in biogenesis and secretion of exosomes (Salomon et al., 2013) which could have enhanced the number of exosome secretion in the later part of cellular growth. As previously mentioned, exosomes have the capability to secrete different proteins or show different expression level in hypoxic conditions to protect their target cells from hypoxic stress (de Jong et al., 2012). The data presented here demonstrates that exosomal protein levels changes depending on the cell culture condition and stress situation and cells utilize exosome mediate cellular communication to cope up with the stress condition they were. The pregnancy zone protein which is actually a homolog of alpha-2-macroglobulin (Petersen, 1994) has been reported to be involved in proteolipid sorting of exosomes to eliminate unwanted materials from cells (Carayon et al., 2011). Recent report suggests that A2M increased the survival rate of septic

cells in a mouse where A2M enriched extracellular vesicles were administered in a mouse model with sepsis increased the survival rate (Dalli et al., 2014). However, after day 6 to day 9, the doubling of cells were reduced or did not double till the end on day 15 which could result the cells to rapture and elevated the abundance of the stress proteins as well as the abundance of CD63 to some extent. Furthermore, from day 6 and onward cell doubling was affected due to several reasons such as shortage of nutrient as no further nutrient was added, the cells exhausted and the space for their growth was reduced. The other proteins identified were Alpha-2-HS-glycoprotein with the molecular weight of ~39kDa, Alpha-1-antitrypsin, (46kDa), Apolipoprotein A-I (~30kDa) and Haemoglobin subunit delta (~16kDa). Except for serum albumin which was either acquired from the culture medium (Théry et al., 2001) or it was eliminated from the cells through the exosome as it is documented that exosomes are used as a vehicle to remove unwanted material out of the cells by endocytosis (Francis, 2010). Alpha 1 antitrypsin, also known as anti-trypsin is reported to be a biomarker for urethral cancer detected in exosomes from diseased patients. The expression level of alpha 1 antitrypsin in cancer patients were high compared to normal exosomal protein expression of alpha 1 antitrypsin.

Further study needs to be done on whether alpha 1 antitrypsin can be remark as a potential biomarker for other cancer such as lung cancer or breast cancer. All the protein identified by MS analysis scored more than 90 as a score of 70 or more in MASCOT, considered as reliable (Hossain et al., 2014). The source of the protein was identified by MASCOT, a protein data base which uses MS data to identify protein from peptide sequence, (Table 4.1) is either from Human or *Bos Taurus* which suggests that, the proteins were taken by the cells from the medium were transported to the exosomes and recycled during cellular growth. Most of the lower molecular weight proteins found to be from *Bos Taurus* and with increased abundance during later stages of cell culture phases (grown in serum free medium) therefore it is unlikely that these proteins were derived from the culture supernatant rather taken from medium by the cells and released when they were in excess which also justifies the role of exosomes as a waste removal mechanism (Kalluri, 2016). In exosomal proteomics, some proteins may derived from the medium itself since it very difficult to avoid serum contaminating proteins (Théry, Zitvogel, et al., 2002). The proper reason for the secretion of these proteins after so long period of time were not properly understood and there are no supporting data that shows the result of these prolonged cell culture and isolation of

exosomes. More extensive research needs to be done to understand the different protein patterns and exosomal behaviour.

Finally, the number of exosomes from lung cancer cell lines H358, leukemic cell lines THP1 and breast cancer cell lines MCF7 were quantified and compared at different stages of cellular growth which suggested that the number of exosomes varies in different cellular growth stages and it is comparable to three cell lines. In addition, it was also found out that A2M was found out only when the cells were at confluency state. Further work needs to be done to the exact function of A2M regarding their involvement in cellular growth stages. Since the cells did not double their after the confluency state, there is a possibility that cells were dead by then due to shortage of nutrients in the media, lack of space and oxygen. The presence of stress proteins could be the reflection of these dead cells and the ruptured dead cells could have raised the level of CD63 to some extent. Although several studies have shown that exosomes can be collected as long as after 15days of seeding. For example, to investigate the interaction of exosomes between mesenchymal stromal cells (MSCs) and two breast cancer cell lines MCF7 and MDA-MB231, the MSCs were co-cultured with MCF7 and MDA-MB231. Exosomes were collected at day 7 and day 15 which showed MSCs interacted with both the cancer cell lines and inherited the marker proteins of MCF7 and MDA-MB231 through exosome interaction. The presence of the marker proteins were investigated by western blot analysis as well as 2D gel electrophoresis (Yang et al., 2015). In another study MSCs was co-cultured with MCF7 in a 3D *in vitro* model cell culture system which suggested some minor aggregation at day 15 in the cellular polarity of MCF7 cells (Estrada et al., 2016).

4.5 Conclusion:

The quantification of exosome number is vital for exosome based biomarker research and drug delivery application. For proteomic study based on exosomes, amount of protein concentration is crucial. This chapter provided the information about the approximate number of exosome and at which stage of cellular growth should be focused on for a given amount of protein concentration or number of exosomes. The protein identification also provided information about the stress related proteins that are secreted during different growth stages from different cell line which suggested that regardless of cancer cell lines exosomal protein secretion in stress showed good resemblance.

Chapter 5:

Comparative proteomic study of different types of cancer cells and exosomes:

5.1 Introduction:

In general, proteomics is the study of total proteins in a cell or tissue or even in a whole organism (Blackstock and Weir, 1999). The term proteome was first used by Wasinger et al., 1995 to describe the proteins identified from *M. genitalium* on a large scale, meaning to define the entire proteome (Wasinger et al., 1995). The goal of proteomic study is gain a more integrated and comprehensive view of funtinal biology (Graves and Haystead, 2002). Proteomics has evolved since the post genomic era (Gupta et al., 2016). Since the establishment of human genome, around 20,000 to 25,000 genes have been recorded (Naidoo et al., 2011). Various genes encode different proteins which lead to many different combinations of proteins in the human body. So, in addition to protein studies complement studies of genes together allows a better understanding about the construction, function and characteristic of many diseases including cancer (Pandey and Mann, 2000). Proteomics is a versatile field evolved by the outcome of the changes in the genomics due to the changes in cellular micro environment such as stress or disease (Doytchinova et al., 2003). Understanding these dynamic processes will be important in understanding the mechanisms of disease. One of the most important applications of proteomics is the discovery and identification of biomarkers for disease (Jones et al., 2002). Proteomics discusses the expression of proteins, interaction and functional state of proteins in cell, organism or organ (Graves and Haystead, 2002). The one setback of proteomics is the lack of improved analytical tools compared to genomics (Elrick et al., 2006). But since the human genome is complete, the researcher are leaning towards proteomics to find out the best use of available technologies to search for new protein based drug targets for cancer therapy. Proteomics allowed the researcher to search for new biomarker or tumour markers to be used as therapeutic or diagnostic tools (Wu et al., 2002). Several studies have suggested that, tumour derived exosomes have the potential to be considered as cancer biomarker as they represent part of the whole cellular proteome and their ability to carry out cancer promoting genetic or signalling material that promote cancer progression (Turay et al., 2016). The advantages of exosomes as biomarker are their stability and availability in most body fluids (Li et al., 2017).

Tumour cells release exosomes in their extracellular spaces containing genetic materials like miRNA, proteins, nucleic acids and lipids which are sorted into them by the cells to communicate with neighbouring cells (Tkach and Théry, 2016). Exosomes from neoplastic cells contain a vast group of oncogenic molecules including proteins and microRNAs that could pass the phenotype transforming signals to normal cells which leads to tumour progression and metastasis (Valadi et al., 2007). For example, invasion and cell migration were analysed within breast cancer cell lines with different metastatic potentials. Results suggested that exosomes from MCF7 transfected with GFP-tagged Rab27b showed more invasive properties than less metastatic MCF7 cells. The expression of Rab27b from transfected MCF7 and highly metastatic breast cancer cell line MDA-MB-231 was compared and the result showed in both cells the expression of Rab27b was similar and up regulated than the less metastatic MCF7 cell lines (Harris et al., 2015). In another study, it was found out that MDAMB231 breast carcinoma cells and U87 glioma cells have the ability to induce cancer characteristics in normal fibroblasts by a protein enzyme cross link between fibronectin and tissue transglutaminase (Antonyak et al., 2011). In addition, exosomes preserve and protect the genetic materials inside them from enzymatic degradation and function as a stable cargo for transferring genetic materials across cells which is very suitable for biomarker research due to the ease of availability with compact physiological or pathological information supplied by exosomes.

The goal of the chapter is to generalise a platform for exosomal proteomics from different cancer cell lines. Several proteomics studies have been documented the similarities and differences of proteomics based on different cellular proteins. But a comparative and generalised platform for exosomal proteomics from different cancer cell lines has yet to be done. The basic aim of this chapter is to identify how similar or different are exosomes from different sources, in this case different cancer cell lines which can be useful for biomarker search in the long run.

5.1.1 Biomarker Discovery:

According to Biomarker Definition Working Group, biomarker is a characteristic that is measured objectively as an indicator of normal biological processes, pathogenic process, pharmacological responses to therapeutics (Atkinson et al., 2001). Body fluids pass through tissues, containing proteins and peptides that indicate the status of the health. The ideal biomarkers are those that are present in a diseased state and absent in healthy controls or vice versa. In reality these biomolecules can be more than one or even a change in abundance of

the marker or relative abundance between markers (Wu et al., 2002). Biological fluids such as blood, urine, saliva etc. are considered as the better source of possible biomarkers compared to tissues due to several factors which include ease of accessibility, avoiding risks of invasive tissue sampling through biopsies, relatively cheap to obtain sample, availability of monitoring based on multiple sampling, and the potential for large-scale, valuable prognostic/diagnostic tests (Good et al., 2007). However, the detection of tissue-specific biomarkers in body fluids requires identification of disease tissue-specific biomarker from thousands of other proteins in circulation and also requires it to be secreted in the first place, whereas tissue can be used to find tumour specific protein biomarkers directly from the source (Shiwa et al., 2003).

5.1.2 Strategies in Proteome Research:

The qualitative and quantitative analysis of complex protein mixtures has become one of the main topics in many laboratories worldwide. Several strategies have been employed for protein analysis in proteomic studies; including bottom-up, top-down and more recently appeared middle-down proteomics (Figure 5.1). “Bottom-up” proteomics is a method of protein identification by characterization of amino acid sequences through proteolytic digestion using mass spectrometry. When a bottom-up analysis is performed on a mixture of proteins, it is called shotgun proteomics (Wolters et al., 2001; Yates, 2004), where the biological sample is, firstly, digested by proteolytic enzyme (e.g. trypsin) that cleaves peptide bonds of proteins at well-defined sites (lysine or arginine) to create peptide mixtures. The generated mixture is separated by liquid chromatography (LC) and characterized by tandem mass spectrometry (LC-MS/MS) (Link et al., 1999).

When the large peptide fragments in the range between 5-15kDa are produced by the cleavage of rarely expressed amino acids or combinations of amino acid residues for MS analysis such approach is called “middle-down” proteomics (Sidoli et al., 2015). Studies of such large peptide fragments may give advantages, such as information about post-translational modifications (PTMs) and high sequence coverage, and relatively short peptide chain can be easily separated and ionized compared to the intact protein analysis.

Another strategy called “top-down” proteomics uses mass spectrometric analysis in order to characterize intact proteins from complex biological mixtures without any digestion to peptides. Analysis by two-dimensional (2D) gel electrophoresis is one of the examples of top-down proteomics (Tran et al., 2011).

Proteomics Approaches

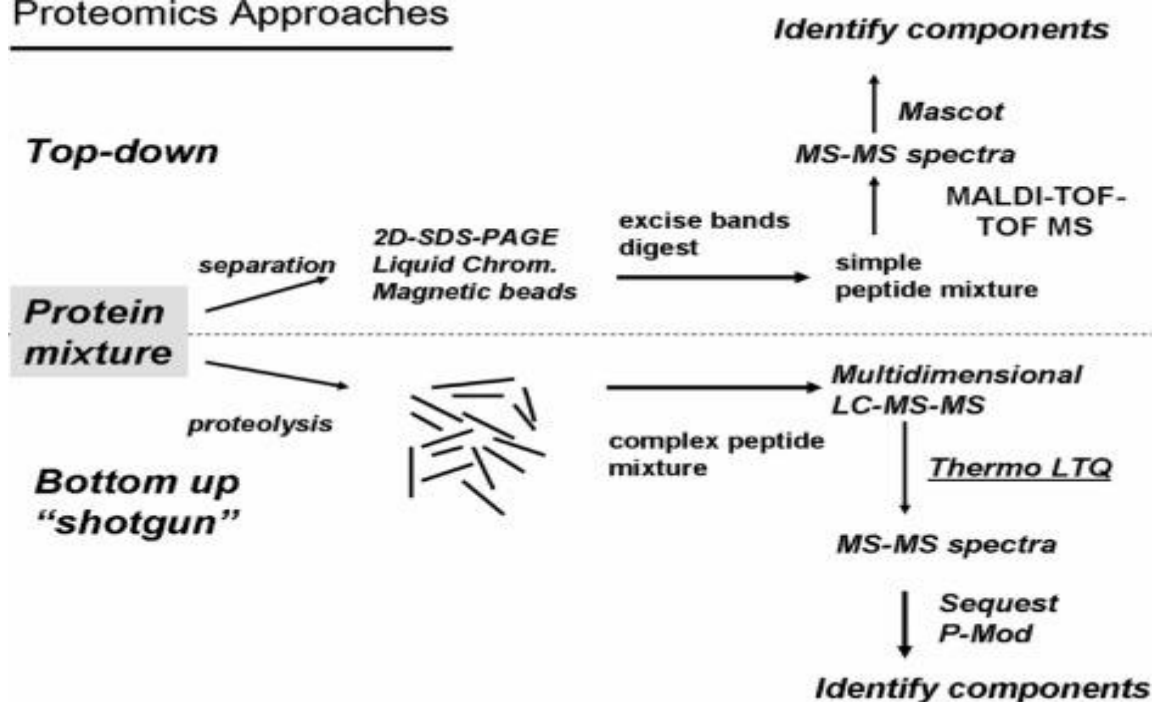


Figure 5.1: Different strategies and methods used in proteomics (Massion and Caprioli, 2006).

5.1.3 Methods Used in Proteomic Study:

In cancer research there are two techniques have been used frequently in expression proteomics such as two dimensional gel electrophoresis (2D) based multidimensional chromatography and other one is protein chips such as SELDI (Surface-enhanced laser desorption/ionization) protein chips systems (Wu et al., 2002).

In this chapter, a comprehensive proteomic study of exosomes from lung cancer cells H358, breast cancer cells MCF7 and leukemic cells THP1 has been carried out in two different ways. Firstly, a proteomic study was carried out between exosomes derived from three cancer cells by 2D gel electrophoresis and secondly, due to the low abundance of proteins in 2D gel, comprehensive and comparative proteomic study of exosomes derived from three cancer cells was carried out by LC-MS. A complete workflow of gel based proteomics is described in figure 5.1. In proteomics, proteins can be separated based on their pI, the pH and molecular weight by processes such as 2D gel electrophoresis and chromatography. The experimental design in proteomics often involves separating protein using 2D gel electrophoresis in a comparable system and quantifies the amount of protein in each sample by the density of staining of each respective protein bands. The 2D gel electrophoresis has a high resolving capacity of separating protein from mixture of protein samples (You and Wang, 2006). It

separates proteins in two steps. In the first step, the proteins are separated by their pI, the pH at which the proteins carry no net charge and will not migrate in the electrical field anymore. This process is called the isoelectric focussing (IEF) (Rabilloud and Lelong, 2011). In the next step, proteins separated in the IEF step are further resolved by their molecular weight in SDS-PAGE gels. The gel from the second step can be stained by using coomassie or silver staining and the protein spots of interest can be excised from the gel and further proceed by mass spectrometry analysis (You and Wang, 2006).

In 2D gel electrophoresis, the success of protein separation largely depends on the balanced sample preparation (Rabilloud, 2009). Proteins can be extracted from various biological fluids including urine, saliva, milk or either from tissue or cells using lysis buffer (Wu et al., 2002). In proteomic analysis solubilisation of the whole protein is a challenge itself. It must solubilise quantitatively whole protein without any modification in the whole process. It should also be compatible with the first separation and must eliminate all contaminating factors which could affect the IEF run and most importantly must not alter the net charge of the proteins (Rabilloud and Lelong, 2011). The choice of a lysis buffer which would extract total protein from tissue or cells without any modification to the protein is very difficult. There are various factors should be considered before choosing the lysis buffer which includes pH, ionic strength, detergents and denaturants and constituents to be added to prevent proteolysis of proteins (Peach et al., 2012). For extraction of proteins the chosen buffer must disrupts hydrophobic interaction, break the hydrogen as well as disulphide bonds, avoid unwanted aggregation and formation of secondary structures which would hamper the movement in the IEF (Harry et al., 2000; Lisacek et al., 2001). After preparation of the sample, next step is the protein separation. Proteins are separated by isoelectric focusing (IEF) with different pH gradient for the first dimension and then sodium dodecyl sulphate poly-acrylamide gel electrophoresis (SDS-PAGE) for the second dimension. The IEF is performed using a pH gradient strip with narrow or broad pH range containing urea, CHAPS, acrylamide, NP-40 and ampholytes. During the IEF process, protein migrates up to its pI in the gradient strip. After the IEF, the strips needs to be equilibrated immediately with buffer containing SDS, glycerol and DTT for the first equilibration and similar buffer with iodoacetamide for the second equilibration. After the equilibration the pH gradient strips are loaded on to a poly-acrylamide gel and proteins are then separated based on their molecular weights (Wu et al., 2002).

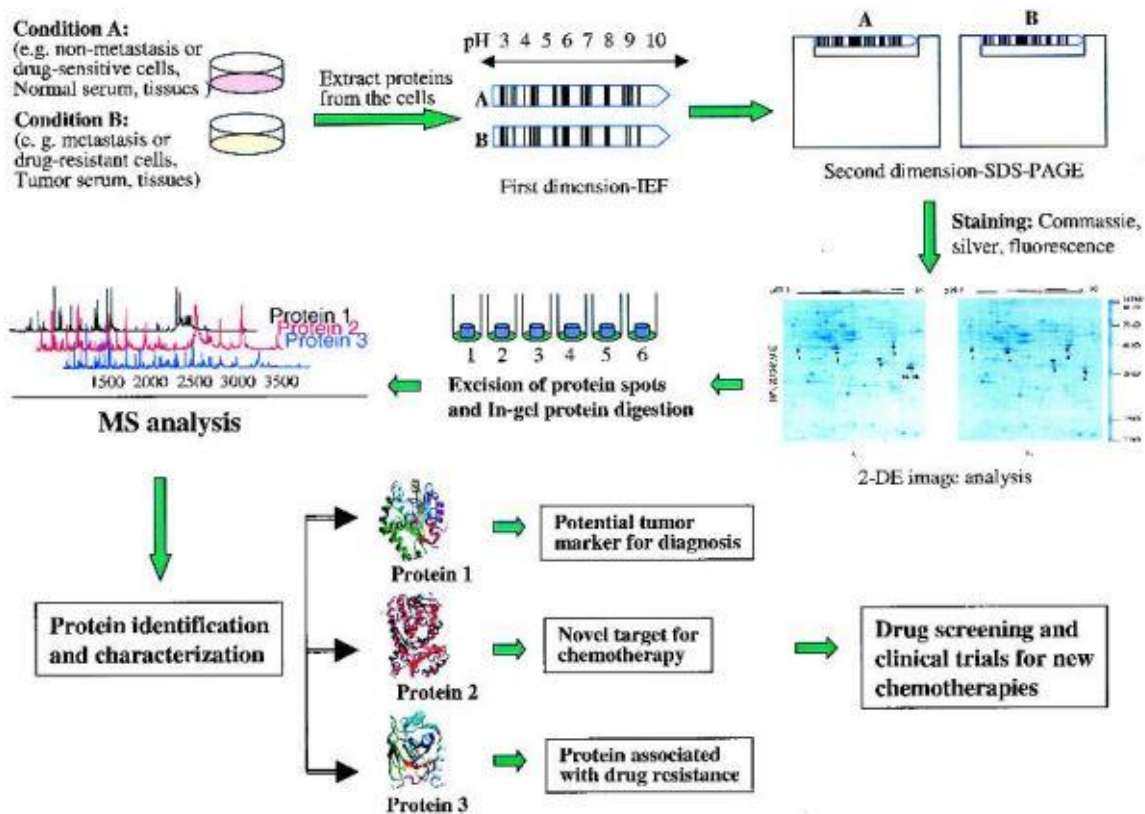


Figure 5.2: A complete work flow of gel electrophoresis based proteomic study (Wu et al., 2002).

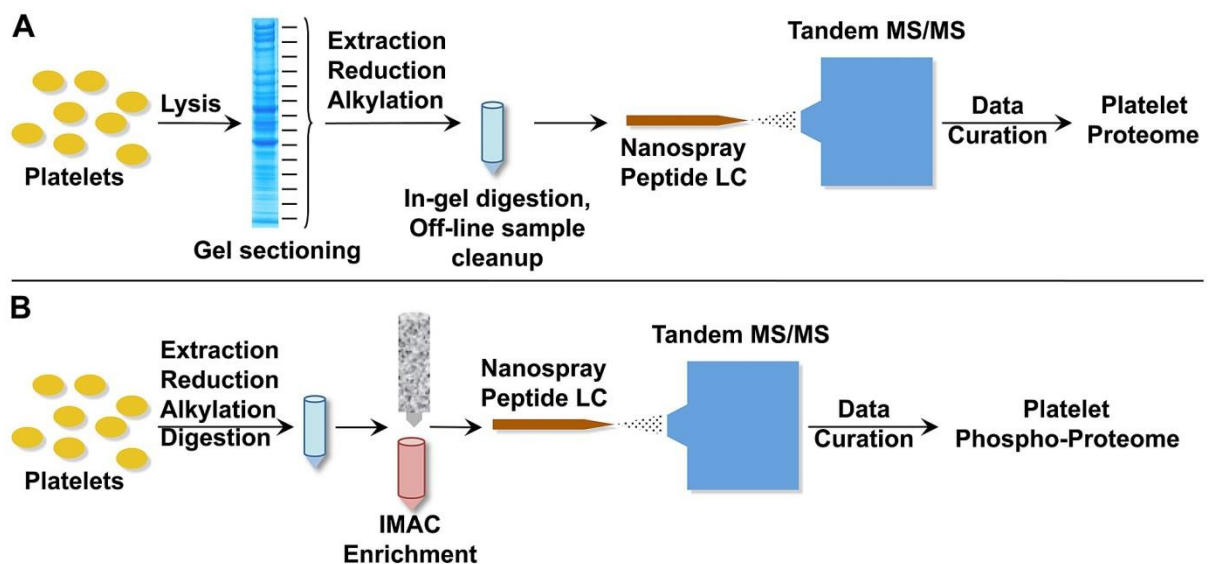


Figure 5.3: A complete work flow of LC-MS based proteomic study (Qureshi et al., 2009).

5.2 Methods and Materials:

5.2.1 Preparation of Sample for 2D Gel:

As described before sample preparation is the key step which is related to successful 2D gel analysis. Protein was extracted using RIPA buffer as described previously in section 2.4 in chapter 2. The protein concentration was determined by using Bradford assay also described in chapter 3. Then 250µg of protein was diluted with 150µl of rehydration buffer (8M Urea, 2% CHAPS, 0.5% Ampholytes, 0.002% Bromophenol blue) and sonicate for 5 minutes prior to load in gel.

5.2.2 Two Dimensional Gel Electrophoresis:

5.2.2.1 First Dimensional Separation:

The technique of 2D gel electrophoresis involves several steps starting with isoelectric focussing. 150µl (250µg protein) of the sample was loaded gently into the ZOOM focussing tray without introducing any air bubbles. The IPG strip from Invitrogen (Fisher Scientific) was taken out of the freezer 15mins prior to use just to equilibrate the temperature. Strips were peeled off from its plastic covering and held the negative side of the strips and pointed the printed side down; the gel was carefully slide inside the focussing tray. At this moment the gel side was faced up. Then the two openings of the focussing tray were sealed with coverings provided by the manufacturer. The focussing tray was then incubated for one hour at room temperature.

After the incubation, the protector of the focussing tray was peeled off and two electrode wicks were placed in both positive and negative side. The tray was then placed inside the SureLock mini cell (Invitrogen) with 600ml pure deionised water. The water was pour down into the outer chamber carefully without allowing any water to go into the inner chamber. The IEF was performed by gradient voltage as described by the manufacturer with slight optimisation. The voltage was started with 200V for the first 30 minutes then gradually increased to 3000V with 250V every 20 minutes for up to three hours with a constant current of 150mA.

5.2.2.2 Second Dimensional Separation:

On completion of the IEF, the sample was taken to the equilibration steps immediately. In the first equilibration samples were incubated with equilibration buffer 1 (50 mM Tris-HCl (pH 8.8), 6 M urea, 30% glycerol, 2% SDS, 0.002% Bromophenol blue, 1% DTT), for 15mins

with gentle shaking. After 15mins the spent buffer was discarded and the equilibration buffer 2 (50 mM Tris-HCl pH 8.8; 6 M urea, 30% glycerol, 2% SDS, 0.002% Bromophenol blue) was added and again incubated for 15mins. At this point the SDS gel was taken out of the fridge to equilibrate with the room temperature. After the incubation, the IPG strips were washed in the running buffer just to remove any residual SDS and immediately slide into the SDS gel for the second dimension separation. The gel was then put inside the SureLock mini gel tank and the gel run was performed at constant voltage of 200V for 45min.

5.2.3 Sample Preparation for LC-MS (University of York):

For LC-MS, exosomes were isolated from 200ml of cell culture supernatant by using in-house polymer solution (40% PEG-8000 solution) described in chapter 3, section 3.2.4. The resulting pellet was then lysed by using 0.5ml RIPA buffer with 1mM of PMSF by incubating 30mins on ice with occasional vortex and sonication (Thermo Fisher) of 10 sec pulse 2/3 times, every 10 minutes. After that the lysate was collected in a sterile Eppendorf tube by centrifugation at 14000g for 15mins at 4^oC using Mikro 200R centrifuge. The lysate was then concentrated by amicon ultrafiltration tubes with a 0.5kDa molecular cut off following the manufacturer's protocol. Protein concentration was measured by Bradford assay method. The protein samples were then prepared for protein identification by MS in University of York.

100µg of protein from each exosome sample of three cancer cells were diluted with sample buffer and heated at 95^oC for 5 minutes in DiziBlock heating system and run on a 12%-4% poly acrylamide gel for 6 minutes. After that the gel is washed with deionized water for 5mins to remove any residual SDS, fixed for 10mins with fixing solution, stained with coomassie blue and destained. The bands from the gel were then cut into pieces and put into sterile Eppendorf tube and sent to University of York for protein identification. Protein samples were digested by trypsin and analysed by LC-MS system in university of York. The protocol they followed is given below:

5.2.3.1 Digestion (University of York):

The digestion step was carried out at the University of York. In-gel tryptic digestion was performed after reduction with dithioerythritol and S-carbamidomethylation with iodoacetamide. Gel pieces were washed two times with aqueous 50% (v/v) acetonitrile containing 25 mM ammonium bicarbonate, then once with acetonitrile and dried in a vacuum concentrator for 20 min. Sequencing-grade, modified porcine trypsin (Promega) was

dissolved in 50 mM acetic acid, then diluted 5-fold with 25 mM ammonium bicarbonate to give a final trypsin concentration of 0.02 µg/µL. Gel pieces were rehydrated by adding 25 µL of trypsin solution, and after 10 min enough 25 mM ammonium bicarbonate solution was added to cover the gel pieces. Digests were incubated overnight at 37°C. Peptides were extracted by washing three times with aqueous 50% (v/v) acetonitrile containing 0.1% (v/v) trifluoroacetic acid, before drying in a vacuum concentrator and reconstituting in aqueous 0.1% (v/v) trifluoroacetic acid. A common sample pool was created by taking equal aliquots of all samples.

5.2.3.2 LC-MS/MS analysis at University of York:

Samples were loaded onto an UltiMate 3000 RSLCnano HPLC system (Thermo) equipped with a PepMap 100 Å C18, 5 µm trap column (300 µm x 5 mm Thermo) and a PepMap, 2 µm, 100 Å, C18 EasyNano nano-capillary column (75 µm x 150 mm, Thermo). The trap wash solvent was aqueous 0.05% (v/v) trifluoroacetic acid and the trapping flow rate was 15 µL/min. The trap was washed for 3 min before switching flow to the capillary column. Separation used gradient elution of two solvents: solvent A, aqueous 1% (v/v) formic acid; solvent B, aqueous 80% (v/v) acetonitrile containing 1% (v/v) formic acid. The flow rate for the capillary column was 300 nL/min and the column temperature was 40°C. The linear multi-step gradient profile was: 3-10% B over 7 mins, 10-35% B over 30 mins, 35-99% B over 5 mins and then proceeded to wash with 99% solvent B for 4 min. The column was returned to initial conditions and re-equilibrated for 15 min before subsequent injections.

The nanoLC system was interfaced with an Orbitrap Fusion hybrid mass spectrometer (Thermo) with an EasyNano ionisation source (Thermo). Positive ESI-MS and MS² spectra were acquired using Xcalibur software (version 4.0, Thermo). Instrument source settings were: ion spray voltage, 1,900 V; sweep gas, 0 Arb; ion transfer tube temperature; 275°C. MS¹ spectra were acquired in the Orbitrap with: 120,000 resolution, scan range: m/z 375-1,500; AGC target, 4e5; max fill time, 100 ms. Data dependent acquisition was performed in top speed mode using a 1 s cycle, selecting the most intense precursors with charge states >1. Easy-IC was used for internal calibration. Dynamic exclusion was performed for 50 s post precursor selection and a minimum threshold for fragmentation was set at 5e3. MS² spectra were acquired in the linear ion trap with: scan rate, turbo; quadrupole isolation, 1.6 m/z; activation type, HCD; activation energy: 32%; AGC target, 5e3; first mass, 110 m/z; max fill

time, 100 ms. Acquisitions were arranged by Xcalibur to inject ions for all available parallelizable time.

5.2.3.3 Data Analysis at University of York:

Peak lists were converted from centroided .raw to .mgf format using MSConvert (ProteoWizard 3.0.9967). Mascot Daemon (version 2.5.1, Matrix Science) was used to search against the human subsets of the UniProt database (20,261 sequences; 11,330,198 residues) using a locally-running copy of the Mascot program (Matrix Science Ltd., version 2.5.1). Search criteria specified: Enzyme, trypsin; Fixed modifications, Carbamidomethyl (C); Variable modifications, Oxidation (M), Deamidation (N,Q), Gln->pyroGlu (N-term Q), Glu->pyro-Glu (N-term E); Peptide tolerance, 3 ppm; MS/MS tolerance, 0.5 Da; Instrument, ESI-TRAP. The Mascot .dat result file was imported into Scaffold (version 4.7.5, Proteome Software) and a second search run against the same databases using X!Tandem.

Peptide identifications were accepted if they could be established at greater than 5.0% probability to achieve an false discovery rate (FDR) less than 1.0% by the Scaffold Local FDR algorithm. Protein identifications were accepted if they could be established at greater than 96.0% probability to achieve an FDR less than 1.0% and contained at least 2 identified peptides. Protein probabilities were assigned by the Protein Prophet algorithm (Nesvizhskii et al., 2003). Proteins that contained similar peptides and could not be differentiated based on MS/MS analysis alone were grouped to satisfy the principles of parsimony. Proteins sharing significant peptide evidence were grouped into clusters.

Spectral counting-based relative quantification and statistical testing were performed in Scaffold. Pair-wise comparisons were made using total spectral counts with the probability of difference calculated using Fisher's exact test. A multi-way comparison of all sample groups was performed by ANOVA of normalised spectral counts. In both cases a Hochberg and Benjamini multiple-test corrected p-value threshold of <0.05 was applied for acceptance of significant difference.

5.3 Results:

5.3.1 Comparative Proteomic Study between Cancer Cells:

The 2D gel electrophoresis was developed to optimise the methodology for comparative proteomic study of exosomal proteins. Since this was a development stage no biological replicates were performed. Initially cellular proteins were used to carry out 2D gel electrophoresis due to the high number and abundance of proteins. Results showed that high numbers of protein spots are visible in MCF7 cell followed by THP1 cell and least protein spots are visible in H358 cell. In THP1 cell (Figure 5.4) most protein spots and highly abundant proteins are clustered in the lower pI ranges between 3-6 and molecular weights ranges from 10kDa and 55kDa. In case of MCF7 most protein spots are found to be in lower to mid pI range (3-7) and aggregated near approximately pI 6 and molecular weight of proteins lies between 15KDa and 100KDa. In case of H358 cell protein spots are less than other two cells and most proteins are observed in higher pI (7-10) and molecular weight ranges from 35KDa to 30KDa.

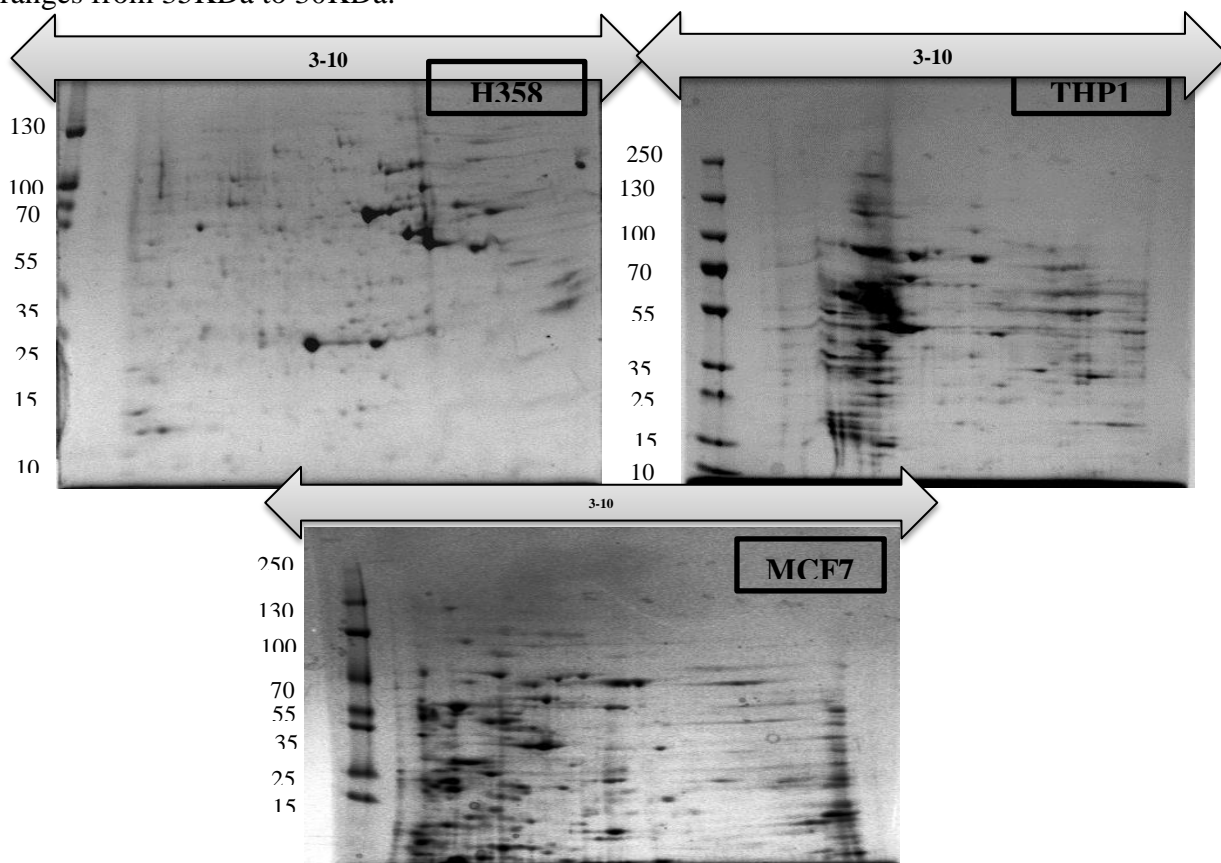


Figure 5.4: Two dimensional gel electrophoresis of cellular protein from H358, MCF and THP1 cell lines. The arrows on top of the gels represent the pI range from 3 to 10.

5.3.2 Comparative Proteomic Study of Exosomes by 2D Gel Electrophoresis:

The exosomal proteins derived from three cell lines did not show much difference than the 2D gel from cellular proteins however the spot density was much less due their low abundance of proteins compared to cell lines. However, the 2D gel from exosomes were resembling in appearance with the cellular 2D gel where, visually, THP1 and MCF7 cell derived exosome contain the highest number of protein spots followed by the least in exosome derived from H358 cell. The molecular weight of protein spots and the pI are also in line with cellular proteomics. In THP1 more protein spots can be seen within the range of 15kDa to 70kDa and mostly found in lower pI (Figure 5.5) whereas in MCF7 more protein spots densely reside around pI 6 and the molecular weight ranges from 35KDa to 100KDa (Figure 5.5). In case of H358 cell few highly abundant proteins spots are present in higher pI and higher molecular weight above 70kDa (Figure 5.5). Some protein spots can be seen as differential abundance such as in case of MCF7, only 3 spots were visible between 25kDa and 35KDa (Figure 5.5 spots M1, M2 and M3) are more abundant than THP1 (Figure 5.5 and spots T1, T2, T3) and large protein spot in H358 around 80KDa which is absent in THP1 and MCF7 derived exosomes. Due to the low number of visible protein spots in 2D gel analysis as well as the clustering of spots which made it even more difficult to isolate protein spots, LC-MS approach was taken to study comparative proteomic studies between these cells derived exosomes. Since 2D gel method was aborted and moved to LC-MS based proteomics, no biological or technical replicated were carried out.

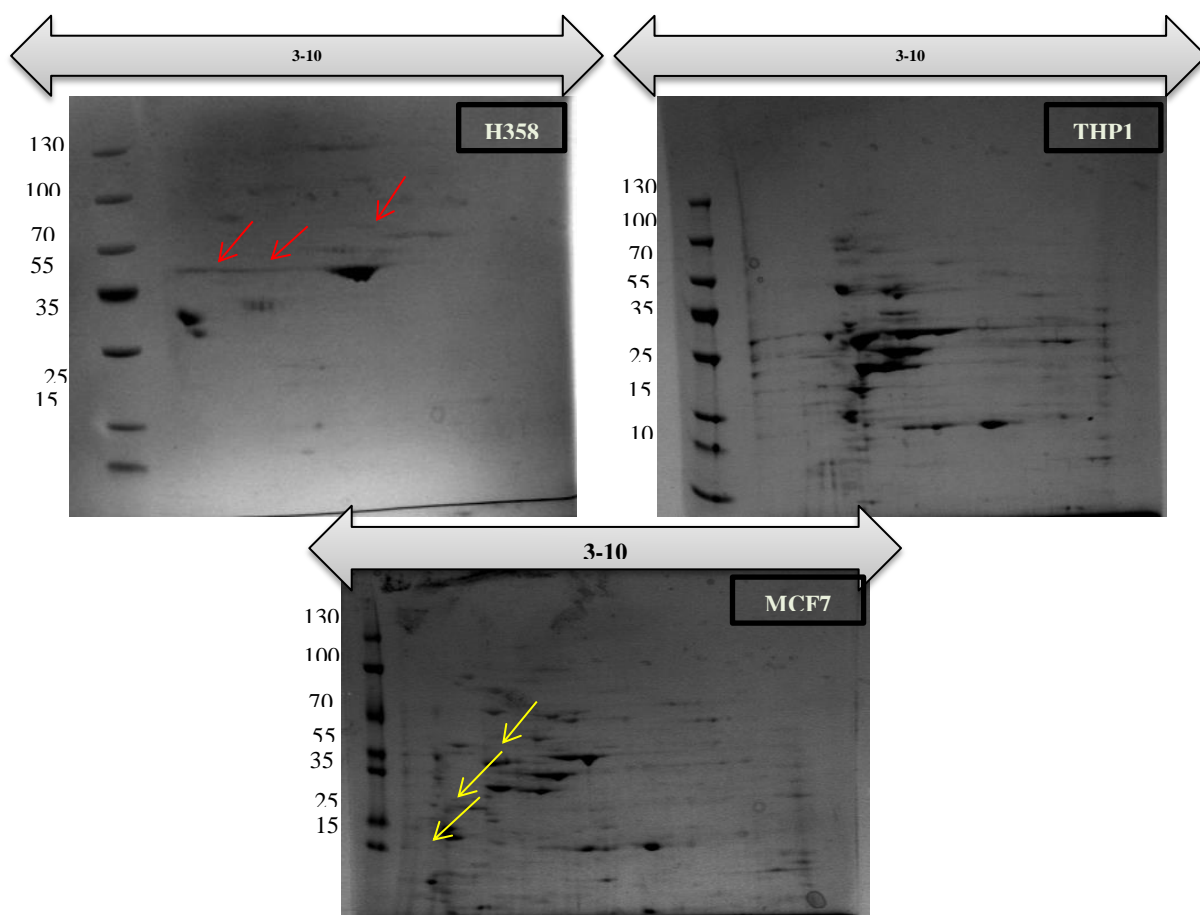


Figure 5.5: Two dimensional gel electrophoresis of exosomal proteins derived from H358 MCF7 and THP1 cell lines. The arrows (Red and yellow) represent the spots present in H358 and MCF7 cell derived exosomes respectively which are not in THP1 cell derived exosomes.

5.3.3 Proteins Identified from exosomes by LC-MS:

Proteins were identified by the shotgun service in University of York. Scaffold (version Scaffold_4.7.2, Proteome Software Inc., Portland, OR) was used to validate MS/MS based peptide and protein identifications. Peptide identifications were accepted if they could be established at greater than 25.0% probability to achieve an FDR (False Discovery Rate) less than 1.0% by the Scaffold Local FDR algorithm followed by protein identifications where they could be established at greater than 99.0% probability to achieve an FDR less than 1.0% and contained at least 2 identified peptides. Protein probabilities were assigned by the Protein Prophet algorithm. Proteins that contained similar peptides and could not be differentiated based on MS/MS analysis alone were grouped to satisfy the principles of parsimony. Proteins sharing significant peptide evidence were grouped into clusters. Proteins were annotated with Gene ontology. A total of 1596 proteins were identified (Appendix; Table 1) with a 0.9% FDR for peptide and 99% of at least 2 peptide match threshold. A total of 889 proteins were identified from H358 exosomes, 1175 were identified from THP1

exosomes and 1281 proteins were identified from MCF7 exosomes. Among all the proteins, 613 are shared by all exosomes from all three cells shown in the Venn diagrams (Figure 5.6). However, exosomes from MCF7 cell lines have the highest number of proteins (210 proteins) that are not shared by other two exosomes. In addition, H358 shared 75 and 65 proteins with MCF7 and THP1 respectively with a total of 136 exclusive proteins. MCF7 and THP1, on the other hand shared a total of 313 proteins between them and has 210 and 114 number of proteins respectively exclusively in MCF7 and THP1. Detail lists of all the proteins that are individually present in H358, MCF7 and THP1 respectively are listed in table 2, 3 and 4 in appendix.

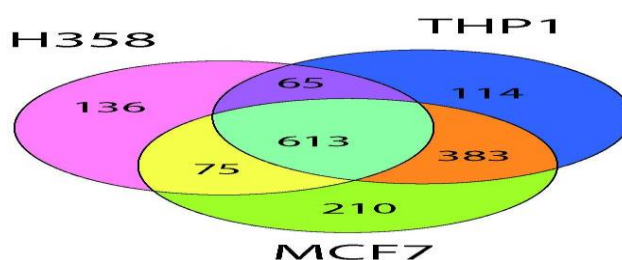


Figure 5.6: Venn Diagrams of common and uncommon proteins distribution between three cancer cell exosomes. The pink circle represents the proteins identified in exosomes from H358 cell line, blue circle is for THP1 cell and green circle represent proteins identified from MCF7 cell derived exosomes.

5.3.4 Functional analysis of exosomal proteins:

All the identified proteins were subjected to gene ontology (GO) by Scaffold software to obtain the information about the functions and origin of the proteins. All the identified proteins across three exosomal samples were categorised in three different groups depending on their nature and function: biological process (Figure 5.7), cellular compartment (Figure 5.8) and molecular function (Figure 5.9). It should be noted that, each single protein was assigned in multiple functions. For example, laminins, integrins, catenins were grouped in biological regulations, cellular process, growth and developments as well as localisation. In biological regulation, more than 93% are involved in cellular process such as cellular compartment organization, macromolecular complex assembly protein complex assembly etc., an average of 76.42% were found to be involved in biological regulation including cellular adhesion, positive and negative regulation of cytokine production etc., around 57% were involved in response to stimuli and only 9.7% were involved in cellular adhesion. At least two proteins shared by all three exosomes were found to be involved in cellular killing. Most of the proteins identified from exosomes were cytoplasmic proteins and intracellular

organelle proteins (76%), whereas extracellular (31%) and intracellular organelle (38%) proteins were evenly distributed. However, despite identifying such a high percentage cytoplasmic, intracellular and extracellular matrix proteins, the analysis also identified proteins associate with ribosome, Golgi apparatus, mitochondria, endoplasmic reticulum. Proteins from various functional categories were also identifies in the LC-MS analysis. An average of 88% of the identified proteins was found having various molecular functions and within these, a total of 72 proteins were found involved in transport activity (Figure 5.7).

The proteomic analysis also identified some renowned exosomal marker proteins listed in ExoCarta (<http://www.exocarta.org/>) which include CD81, CD9, CD82, Actin, beta Actin, Annexin A1, A5 etc. 10 members of the tumour associated protein integrins were identified across three cancer cell derived exosomes where only integrin beta-1 is present in all three exosomes however, integrin alpha-3 is only present in H358 and integrin alpha-5 is only present in THP1. Several tumour marker proteins were also identified such as B2M which is declared as a marker protein for leukaemia by the national cancer institute was only present in THP1 cell derived exosomes, BRCA1 was only present in exosome released by in MCF7 cells which is a marker protein for breast cancer and laminin for lung cancer which is present in exosome derived from H358. Among the shared proteins between all three exosomes (613 proteins) there were some tumour associated proteins like integrins, actin, galectin, cluster of talin, tsg101 (Table 5.1).

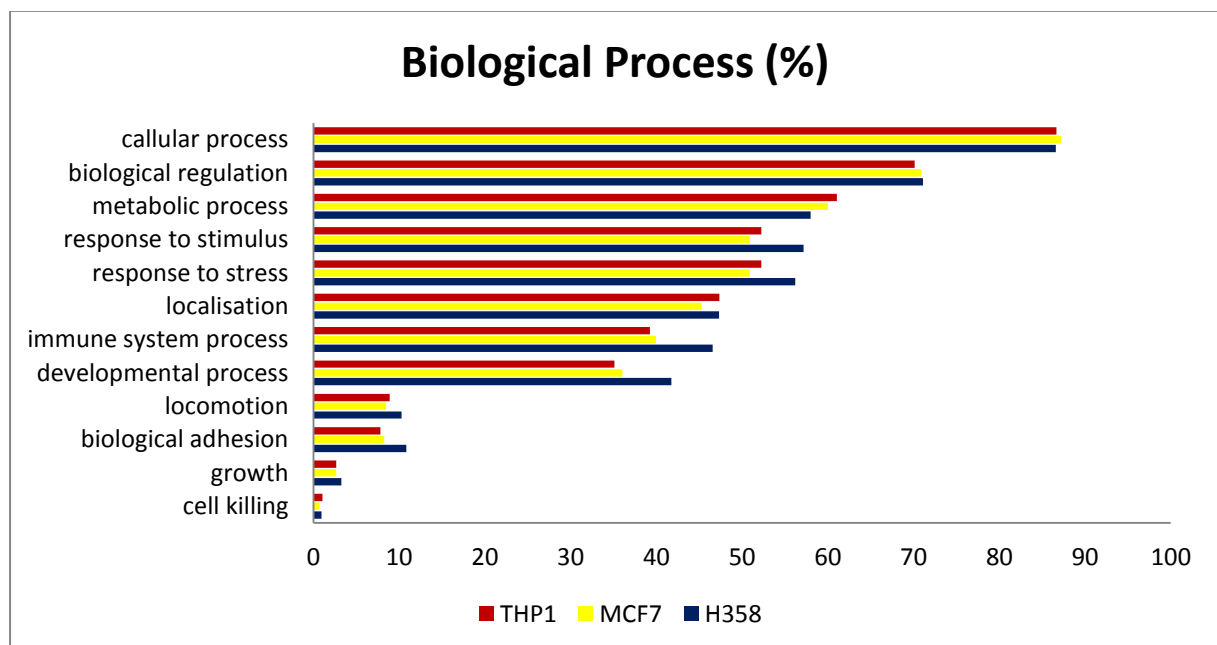


Figure 5.7: Proteins involved in biological process. Gene ontology of biological process was assigned by Scaffold software.

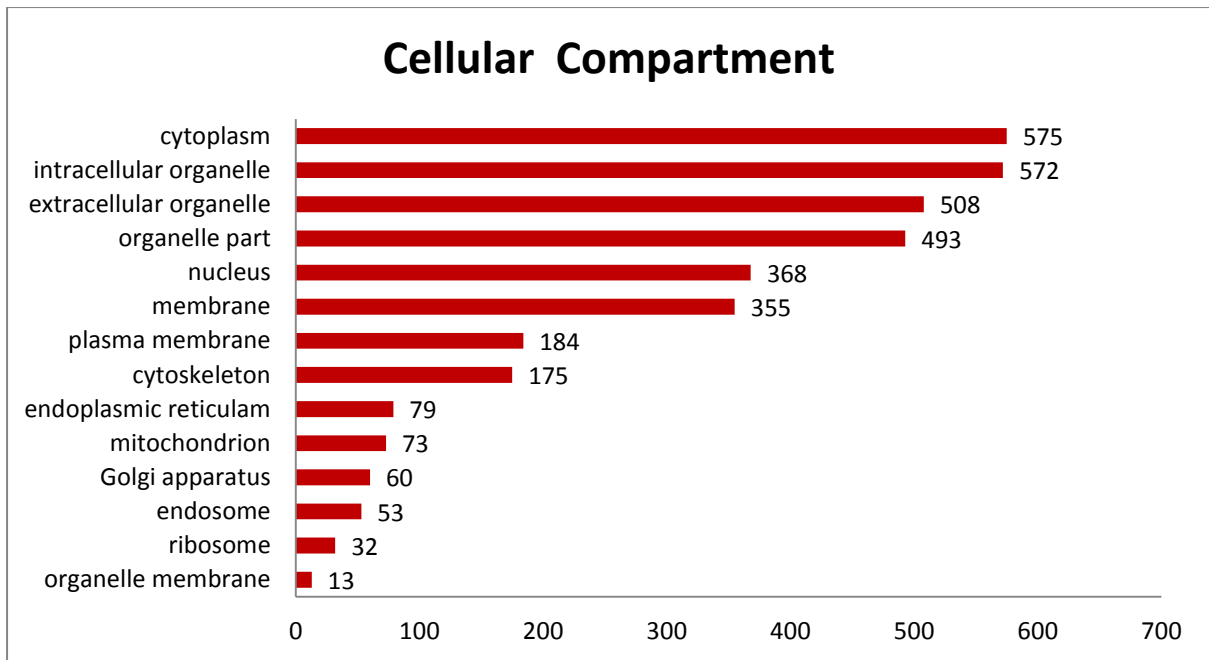


Figure 5.8: Function detailed in pie chart for the identified proteins for all the three exosomes. Gene ontology of cellular component was assigned by Scaffold software.

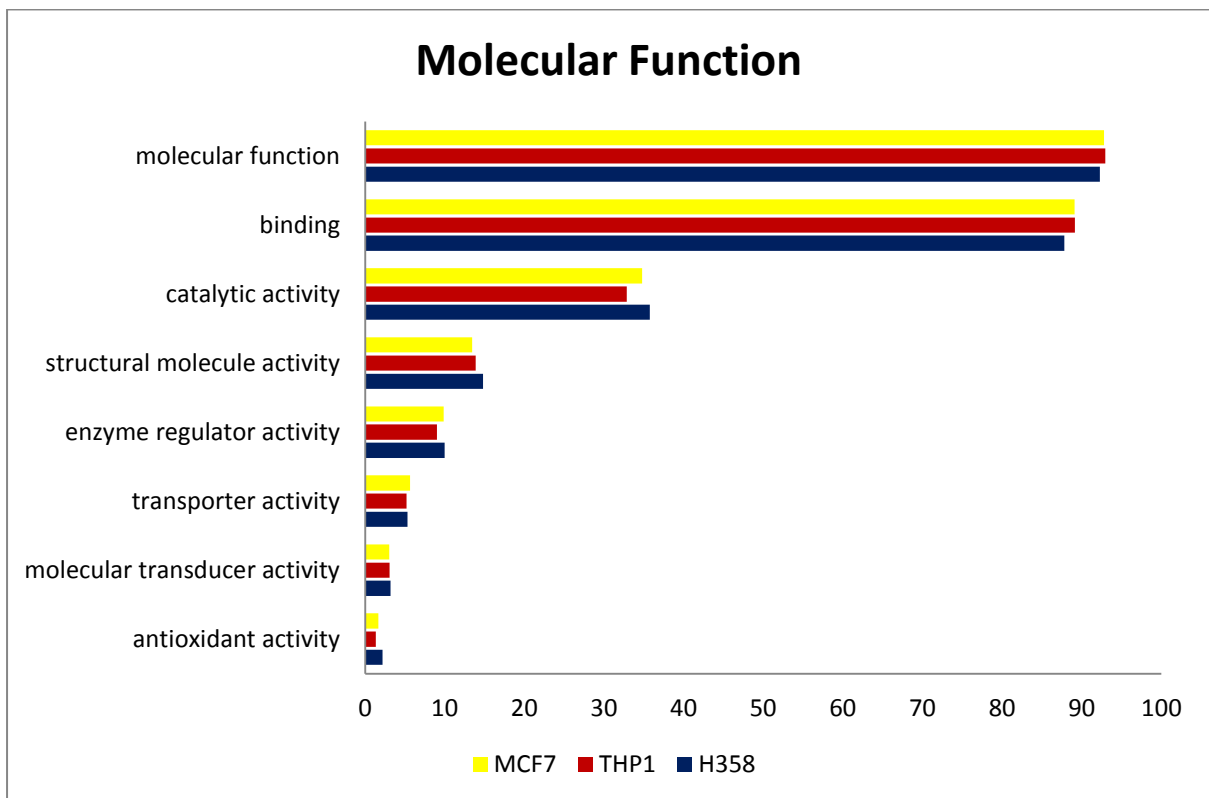


Figure 5.9: Association of the identified proteins in cellular compartments. . Gene ontology of molecular function was assigned by Scaffold software.

Table 5.1: Partial list of proteins with their functions relative expression with each other in exosomes from three cancer cell lines is shown in table below.

Functions	Proteins	Accession number	Relative Fold Changes		
			H358/THP1	H358/MCF7	THP1/MCF7
Cellular Adhesion	Cadherin-1	CDH1_HUMAN	12.0	-1.2	-15
	Catenin beta-1	CTNNB1_HUMAN	2.5	3.2	-8.0
	Vinculin	VINC_HUMAN	5.8	5.9	0
	Firbonectin	FINC_HUMAN	6.2	15.2	5.5
	Cathepsin D	CATD_HUMAN	2.2	1.4	-1.6
	Calsyntenin-1	CSTN1_HUMAN	1.41	2.2	1.6
	Plasminogen	PLMN_HUMAN	3	1.3	-2.2
	Integrin beta-1	ITB1_HUMAN	1.2	1.7	1.7
	Talin	TLN1_HUMAN	6.1	-3.3	-1.8
Cellular Transport	T-complex protein 1 subunit zeta	TCPZ_HUMAN	-17	-23	1.4
	Importin subunit beta 1	IMB1_HUMAN	-4.3	-7.1	1.64
	Hemoglobin subunit alpha	HBA_HUMAN	1.2	1.09	-1.3
	4F2 cell-surface antigen heavy chain	4F2_HUMAN	1.12	1.9	*4.0
	Protein S100-A6	S10A6_HUMAN	1.67	1.15	1.44
	Desmoplakin	DESP_HUMAN	1.27	3.1	3.9
Apoptosis	Ras-related protein Rab-11B	RAB11B_HUMAN	-4.0	-8.0	-2.0
	Tubulin beta chain	TBB5_HUMAN	-3.0	-3.5	1.18
	Glyceraldehyde-3-phosphate dehydrogenase	G3P_HUMAN	-1.2	-2.0	1.6
	Pyruvate Kinase PKM	KPYM_HUMAN	-1.2	-1.7	1.4
Cellular growth	Annexin A1	ANXA1_HUMAN	3.63	0	0
	Transketolase	TKT_HUMAN	-1.3	-1.2	-1.0
	Apolipoprotein E	APOE_HUMAN	2.9	3.22	-1.1
	Histone H4	H15_HUMAN	1.17	1	1.15
Cellular Signalling	Glucose-6-phosphate isomerase	G6PI_HUMAN	-2.6	-3.4	1.4
	Agrin	AGRIN_HUMAN	1.3	3.0	2.0

	Transitional endoplasmic reticulum ATPase	SFXN1_HUMAN	-2.4	-3.4	1.38
	Gelsolin	GELS_HUMAN	-2.4	1.09	-2.7
Cellular Communication	Annexin A5	ANXA5_HUMAN	-1.8	1.32	2.4
	60kDa Heat Shock protein	CH60_HUMAN	-1.8	-2.2	-2.0
Tumour associated proteins	Tumour protein D52	TACD2_HUMAN	-1.9	-3.5	3.5
	Tumour protein D54	TPD54_HUMAN	-2.0	-2.7	1.33
	Heat Shock Cognate 70	HSP70C_HUMAN	-2.0	-2.4	1.2
Response to stimulus	Tetranectin	TETN_HUMAN	-1.6	1.74	-2.7
	Elongation factor 2	STMN1_HUMAN	-2.1	-2.3	-1.2
	Complement C3	CO3_HUMAN	-1.1	1.4	-1.6
Exosomal marker proteins	CD81	CD82_HUMAN	-4.0	-4.0	1.0
	CD9	CD9_HUMAN	3.00	-2.1	6.33

5.3.5 Comparison between H358 and THP1:

Proteomic profile of exosomes derived from lung cancer cell line H358 was then compared with exosomes derived from leukemic cell line THP1. Amongst 889 proteins from H358 and 1175 proteins from THP1 which resulted from the database searching with MS/MS data, 678 proteins were common between them. However, only 65 proteins were exclusively shared by H358 and THP1. Apart from the shared proteins, 136 and 114 proteins were exclusively identified from H358 and THP1 cell derived exosomes respectively. Interestingly, the results from these two exosomes are enriched with many proteins common to exosome studies up to date. For example, the tetraspanins (CD9, CD81, CD44), proteins involved in the ESCRT machinery such as TSG101, vacuolar protein sorting-associated proteins (VPS25, VPS26A, VPS29 and VPS35). Other common exosomal proteins such as Rabs, Raps, annexin, cytoskeletal proteins, were also identified. Among them shared protein only in H358 and THP1, there were two exosomal marker proteins annexin (A1 and A4) and one member of the tetraspanin (CD44) family proteins was identified. Eight proteins has been found to be involved in biological adhesion, 47 proteins are involved in biological regulation. Two proteins were identified showing cellular killing. A total of 26 proteins were found to be involved in immune response. Several cellular adhesion proteins are up regulated in H358

exosomes compared to THP1. For example, catenin beta-1, cadherin-1 was upregulated in H358 by 2.5 and 12 fold higher respectively in H358. In addition, several proteins involved in cellular transport are down regulated. For example, Importin subunit beta 1 was downregulated in H358 by 4.3 fold. On the other hand, 4F2 cell-surface antigen heavy chain, protein S100-A6 were up regulated in H358 by 1.12 and 1.67 fold respectively. Four proteins function as apoptosis proteins identified between H358 and THP1 exosomes were up regulated in THP1. In addition, two exosomal marker was shared between THP1 and H358 including CD9 and CD81. CD9 was 3 fold up regulated in H358 while CD81 was 4 fold up regulated in THP1 (Table 5.1).

5.3.6 Comparison between MCF7 and H358:

Next, the comparison was carried out between the lung cancer cell H358 and Breast cancer cell MCF7. Investigation on the proteomic profile of H358 and MCF7 yielded a total of 688 proteins shared between them, which also include the similar common exosomal proteins. However, 75 proteins were exclusively shared between H358 and MCF7. No exosomal markers were shared exclusively in H358 and MCF7. But 15 proteins exclusively present in H358 and MCF7 has been identified with cellular adhesion function while 55 of them are involved in biological regulations. No proteins were found exclusively, involved in cellular killing. Proteins involved in cellular adhesion such as catenin beta 1, integrin beta 1, cathepsin D were up regulated in H358. However, cadherin 1 was upregulated in MCF7. 4F2 cell surface antigen, a transport protein which is also involve in cellular communication was up regulated more than 1 fold in H358 importin alpha 1, another protein involved in cellular transport as well as cell communication was up regulated in MCF7. Protein related to apoptosis such as Rab-11B was up regulated by 8 fold in MCF7. Nonetheless, proteins involved in cellular growth such as apolipoprotein E, histone H4 was up regulated in H358. Exosomal marker proteins CD9 and CD81 were both up regulated in exosomes derived from H358 (Table 5.1).

5.3.7 Comparison between MCF7 and THP1:

In case of the leukemic cell THP1 and Breast cancer cell MCF7, a total of 383 proteins were shared. Furthermore, expression of proteins associated with metastasis e.g. cadherin, intergrin β 1, histocompatibility, ecto-neucleotidase were lower compared to THP1. Proteins involved in cellular response for example, tetranectin, complement C3 was down regulated in MCF7. Exosomal marker proteins CD9, CD81 as well as annexin A5 was higher in MCF7 compared

to THP1. Proteins involved in cellular signalling, for example, agrin was up regulated in MCF7 while gelsolin was up regulated in THP1.

5.3.8 Protein network and KEGG pathway analysis:

STRING online database was used to analyse the protein network and KEGG pathway analysis was also performed to evaluate the significant pathways involved in the overlapped exosomal proteins. Figure 5.10 showing the cross networking of overlapped proteins between all exosomal samples. The nodes denote each protein, involved in the network and the thickness of the edge indicates the confidence of the protein-protein interaction the thickness of the line indicates the confidence of the protein-protein interaction. To understand the protein-protein interaction network, the overlapped proteins were subjected to STRING for network analysis (Figure 5.10). The thicker the edge the more interactive the proteins are. Proteins from the heat shock family (HSPA1A, HSPA4, and HSPA5), phosphoglycerate kinase 1, plastin 2, members of the Ras family proteins, actin family proteins, methionine aminopeptidase, catenins, cadherins are involved in most protein linkage. The KEGG pathway analysis was performed on the exosomal proteins from three cancer cells showing a *p*-value less than 0.05 resulting 58 pathways. The most number of proteins involved a pathway is the focal adhesion (29 proteins), followed by spliceosome (28 proteins) and proteasome (27 proteins). Proteins were also enriched in pathways such as ECM-receptor interaction (23 proteins), proteoglycans in cancer (20 proteins) etc. 16 proteins were involved in pathways in cancer including fibronectin 1, catenin alpha 1 and 2, beta 1, fumarate hydratase, cadherin etc. Signalling pathways reported to be involved in cancer has also been detected by the KEGG analysis. For example Akt-signalling pathways (15 proteins), Rap1 signalling pathways (7 proteins), HIF-1 signalling pathways (13 proteins). Several proteins identified in this study were involved in more than one pathway. For instance, CDH1, CTNNA1, TGFB2, several family members of laminin (alpha 3,5; beta 1,2,3, gamma 1,2,3), integrin alpha 5 and 6, family members of the histone family proteins, cathepsin D and cathepsin G are involved in several pathway including Akt signalling, focal adhesion, Rap1 signalling, HIF-1 signalling, pathways in cancer, endometrial cancer, thyroid cancer. A list of the pathways involved is shown in figure 5.11.

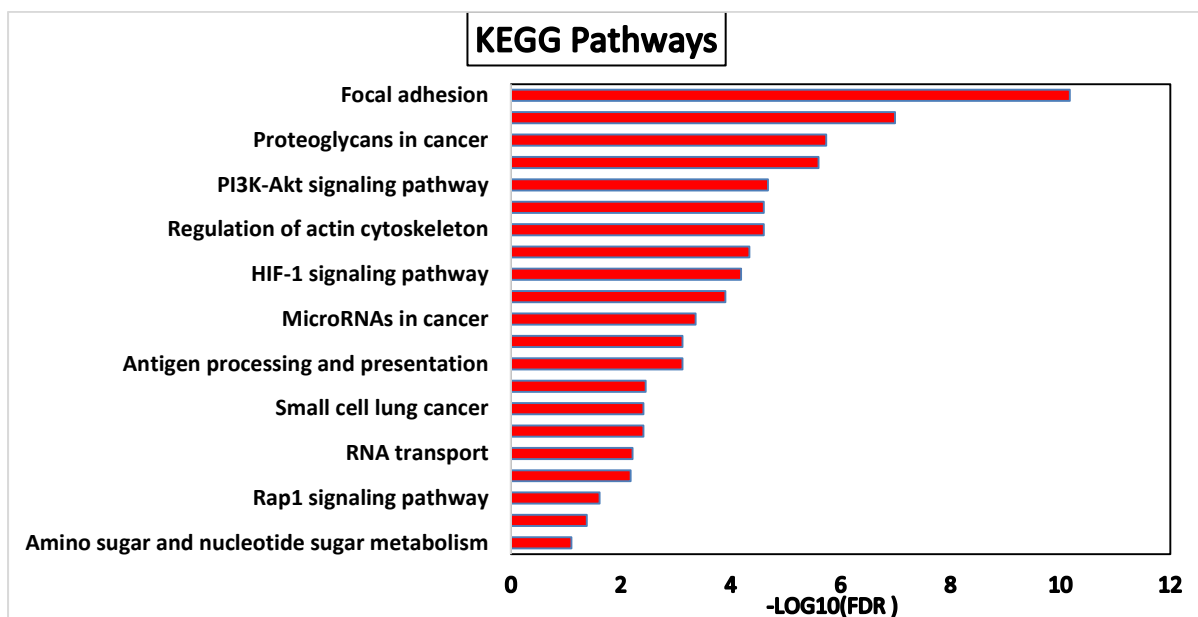


Figure 5.11: KEGG Pathways detected by STING software. The FDR value is normalised by using $-\log_{10}$. The pathway was generated using the shared proteins of exosomes from three cancer cell lines used with a p value of less than 0.05. Pathways shown in the figure are with the lowest FDR for each pathway.

5.3.9 Comparative proteomic analysis:

In this proteomic study, exosomal proteins from three different cells showed different expression level. Within the 613 shared proteins, 11 proteins from H358 exosomes including exosomal marker protein Annexin A1, tumour marker protein Laminin subunit beta-3, gamma-1 showed higher expression than other two samples while 67 number of proteins from H358 showed lower expression than THP1 and MCF7 cell derived exosomes. Similarly, a total of 32 and 49 number of proteins showed higher expression originated from THP1 and MCF7 exosomes respectively. Interestingly, some cancer marker proteins showed different expression in exosomes from three cancer cells. For example, proteins like interstitial collagenase (MMP1), cartilage oligomeric matrix protein (COMP), complement component (C9) are biomarkers for lung cancer cell are only present in lung cancer cell H358 and not in THP1 and MCF7. Regulation of metastatic cancer proteins like CD44, ezrin were higher in H358 and THP1 than MCF7. Interestingly, another metastatic protein cortactin was only present in MCF7. Furthermore only 3 and 5 proteins were under expressed in THP1 and MCF7 exosomes respectively. The expression level of all the shared protein with a fold change of minimum 2.0 and p value of less than 0.05 were included in the heat map using RStudio (Figure 5.12). As all experiments were carried out in triplicates, average of independent results were included in the heat map.

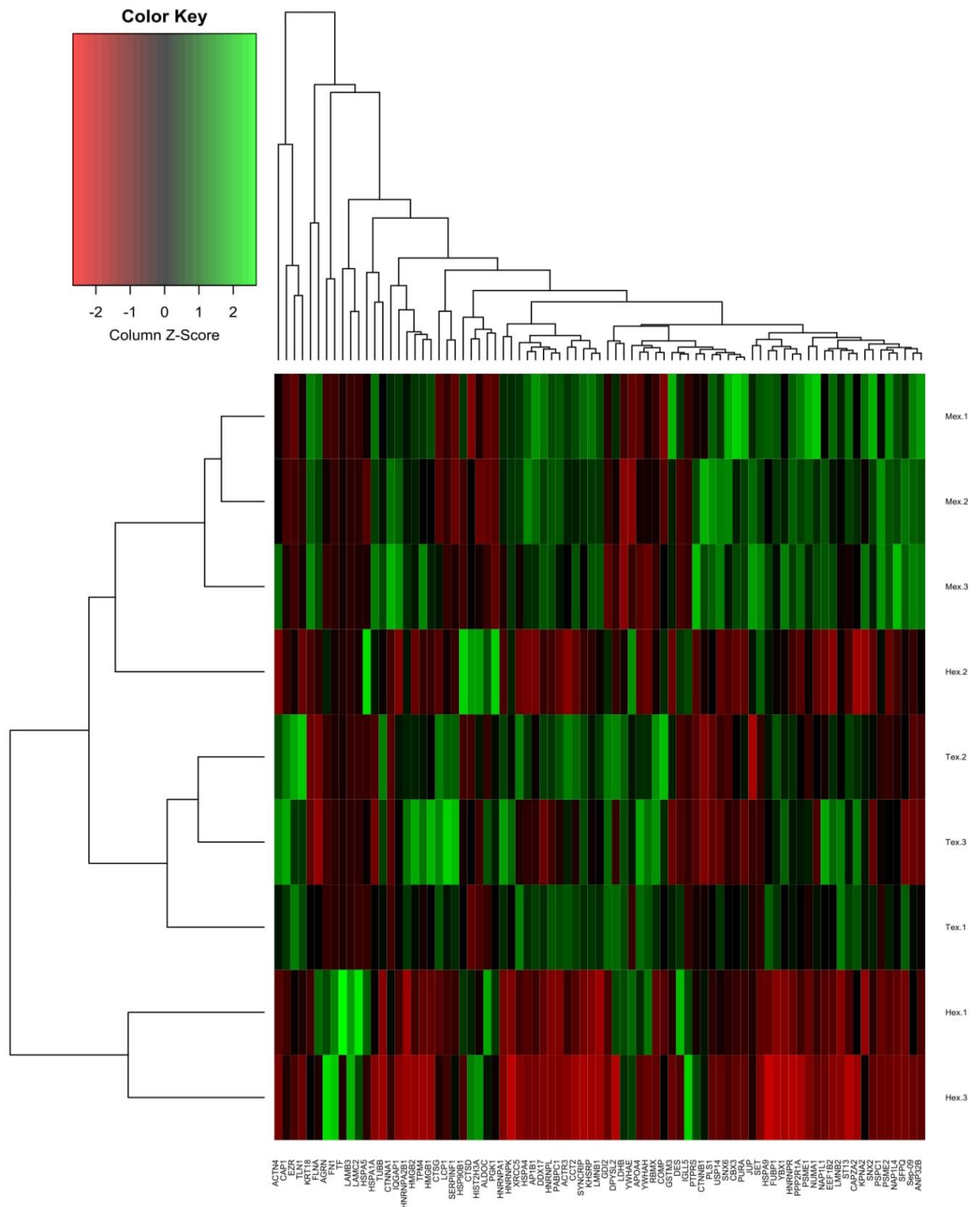


Figure 5.12: Heat map of exosomal proteins from three cancer cells with different expression level was generated by using R. Hierarchical clustering was also plotted showing the expression difference of exosomal proteins. In both cases triplicates with $p \leq 0.05$ were used for the protein clustering. The column Z score represents the expression from green to red (-2 to 2). Expression is higher from black to green and expression is lower from black to red. Here, HEX, TEX and MEX represent protein expression from exosomes of H358, MCF7 and THP1 cell lines. The heatmap is generated using RStudio.

5.4 Discussion:

Comparative proteomics of exosomal proteins coupled with LC-MS from cancer cells, enables to isolate and identify novel low abundant biomarkers for cancer (Duijvesz et al., 2013). Exosomes are very small, nano sized diameter vesicles originating from the late endosome (Jiang, Wang, et al., 2015), which gained much interest in the proteomic field due to the presence of tumour specific antigens which can be used as a diagnostic or therapeutic tools (Lin et al., 2015). Exosomes have been exploited as a good source in biomarker discovery because of the availability in different body fluids and also the difference in their proteomic profile from their counterpart normal cells (De Bock et al., 2010).

In this study, exosomes were isolated from conditioned cell culture medium using PEG based polymer (described in chapter 3.2.4). Both gel electrophoresis and liquid chromatography based approach have been applied to perform exosomal proteomics from three different cancer cell lines including highly metastatic cell lung cancer cell line H358, leukaemia cell line which is a suspension cell line and less metastatic breast cancer cell line MCF7. To optimise the 2D gel electrophoresis methodology cellular proteins were used because of the high abundance of proteins in cell and protein spots obtained in these three cell lines (Figure 5.4 and 5.5) are visually comparable to results obtained by other researchers (Mears et al., 2004; Zhou et al., 2006).

For exosomal proteomics, 2D gel electrophoresis method was applied which resulted few protein spots due to the low of protein abundance in exosomal samples (Abramowicz et al., 2016). Similar approaches have been seen in a study carried out by Bosque, A. et al, 2016 where comparative proteomic study between tumour Jurkat T cells and normal human T cell blasts resulted few proteins in their 2D approach for exosomal proteins while a much more complex proteome for cellular proteins. Furthermore, the difficulty of performing traditional 2D gel based proteomics on exosomal proteomics has been reported in several exosomal studies (Bosque et al., 2016). Due to the restricted use of ionic detergent which makes lysis of exosome samples very hard, extensive time consuming and requirement of expensive equipment for greater resolution and detection (Granvogl et al., 2007). However, gel analysis showed some differential protein spots in the exosomes of these three cell lines. Although the number of spots obtained in 2D gel electrophoresis from exosomal proteins were low but comparable with the results from LC-MS of exosomal proteins. For example, the number of spots detected by 2D gel electrophoresis was THP1, MCF7 and lastly H358. Similarly in LC-

MS, the most number of proteins were identified from MCF7 and THP1 followed by the lowest one H358.

For many years, mammalian cell lines isolated from various origin have been used extensively *in vitro* to identify the similarities and differences between various cancers which revealed vital information about the origin of the tumour as well as the biological functions of those proteins involved in cancer (Geiger et al., 2012). Since exosomes represents portion of the parent cell proteome, comparative proteomics of exosomes from different cancer cell lines will shed light into shared and unique features of different cancers (Mathivanan et al., 2010). In this study, exosomes were isolated from conditioned cell culture medium using PEG based polymer. In addition, it was further supported by the guidelines of International Society for Extracellular Vesicles (ISEV). According to ISEV, the exosomes preparation should contain at least one or more protein from transmembrane or lipid bound extracellular proteins, cytosolic proteins and absence of the proteins from endoplasm origin (Lötvald et al., 2014). More than three proteins from the guidance of the ISEV were identified in this proteomic study. Here, LC-MS based proteomic approach has been applied to perform exosomal proteomics from three different cancer cell line including highly metastatic cell lung cancer cell line H358, a metastatic acute monocytic leukaemia cell line THP1 and a less metastatic breast cancer cell line MCF7. The goal of this study was to evaluate the differences between the exosomes secreted from three different cancer cell lines by analysing their proteomic contents which play an important part in the cellular communication.

LC-MS based proteomic was successfully performed on three exosome samples derived from three different cancer cell lines, yielded over 1596 proteins (Appendix; Table 1). Among these, 889 proteins were detected in H358 derived exosomes, 1281 proteins were present in the exosomes derived from MCF7 cell line, THP1 cell derived exosomes resulted 1175 proteins. Protein yield was a little higher than previously published papers, for example 591 proteins were identified from the exosomes of human embryonic kidney cells by using PEG based solution for exosome isolation (Rider et al., 2016). In another proteomic study carried on two prostate cancer cell lines a total of 385 number of proteins were identified (Duijvesz et al., 2013). Among all the identified proteins in this study, presence of some exosomal marker proteins like CD81, CD82, CD9, Hsp70, Tsg101, Programmed cell death 6-interacting protein (ALIX), Annexin were identified. Interestingly, one of the most commonly used exosomal marker protein CD63 was only detected by western blot analysis (Chapter 3.3.4). Even though CD63 is considered as one of the most commonly used

exosome marker along with CD81 and CD9, several studies have had difficulties identifying CD63 from exosomal protein by LC-MS based proteomics but it was detected by western blot analysis. For example, proteomic study between tumoral Jurkat cell derived exosomes and normal human T cell blasts CD63 was only detected by western blot analysis (Bosque et al., 2016). In another study on B-cell exosomes, CD63 was not detected by the LC-MS method but was detected by western blot (Buschow et al., 2010). The absence of an individual protein can occur due the difference in protein purification from exosomes, methodology used in LC-MS analysis and also principal used in data processing (Duijvesz et al., 2013). In addition, due to the high glycosylated nature of CD63 it is difficult to detect any identifiable peptide. Furthermore, the high threshold set for this proteomic study (96% for peptide 1.0% FDR and at least 2 peptide match) a peptide from a highly glycosylated protein is very difficult to detect (Chertova et al., 2006).

Tumour protein such as tumour associated calcium transducer, tumour protein D54 and D52 were also identified from the exosomes from all three cells where D52 was over expressed by at least 3 fold in MCF7 exosomes (Table 5.1) several reports have suggested the involvement of D52 in tumour progression (Li et al., 2006; Xia et al., 2014). D52 is a protein involved in regulation of cellular growth and proliferation. Over expression of D52 has been observed in several reports. For example, up regulation of D52 was observed in prostate cancer where it worked in cellular proliferation and promoted tumour progression via integrin mediated B/Akt signalling pathway (Ummanni et al., 2008). Several proteins found to be involved in invasion and angiogenesis were also identified which includes, catenin beta-1 (Easwaran et al., 2003), EGF-like repeat and discoidin I-like domain-containing protein 3 (Zhong et al., 2003), and lactadherin (Table 5.1). For example, lactadherin was found to enhance angiogenesis in a transgenic rat model (Neutzner et al., 2007) and EDIL3 have a well-established role in angiogenesis and tumour growth. The expression level of EDIL3 was found higher in pancreatic ductal adenocarcinoma compared to its normal counterpart cells and this higher expression was also found to promote tumour growth (Aoka et al., 2002; Jiang, Wang, et al., 2015). In addition, within the 613 shared proteins, there were several proteins were reported to be involved in metastasis which include 10 members of the integrin family (In MCF7 only integrin beta-1) which are involved in cellular adhesion, the primary steps of metastasis (Bozzuto et al., 2010). Interestingly, only one member of the transmembrane glycoprotein family protein, integrin beta-1 showed down regulation in MCF7 which is a less metastatic cell line compared to the lung cancer cell line H358 and

leukaemia cell line THP1. Many studies have documented that altered expression of integrin was observed in metastatic tumour cell compared with the normal counterpart cell (Hood and Cheresh, 2002). For example, overexpression of integrin $\alpha 5$ and $\beta 3$ was observed at the invasive site of malignant tumour melanoma cells and angiogenic blood vessels (Brooks et al., 1994) but expression was found less in pre-metastatic melanoma and normal blood vessel (Felding-Habermann et al., 2002).

All the proteins identified were subjected to GO ontology for their functional characterisation which is shown in the bar chart in figure 5.7. Irrespective of the cell lines, all three exosomes from three cancer cell lines were enriched in membranous proteins. Although, within three cancer cell derived exosomes, there were adhesion, protease, extracellular proteins as well as signalling proteins identified (Table 5.1) but most of the proteins enriched in exosomes found to be involved in binding, catalytic, transport and most of them are evenly distributed in intracellular and extracellular matrix according to the GO analysis. Exosomes from all three cancer cells have shared and unique proteins. For example, cartilage oligomeric matrix protein which shows cellular adhesion properties found in the extra cellular matrix of all three cancer cell derived exosomes. On the other hand, extracellular protein fermitin showed adhesion properties was only found in THP1 cell line. Similar type protein such as desmoplakin was up regulated in MCF7 compared to the other two samples. Several cell signalling molecules which acts on cell proliferation were also identified in shared and as well as exclusive manner. For example, inhibin beta B chain which is a cytoplasmic protein and helps in cellular proliferation and cellular signalling was only present in H358, treacle protein found only in MCF7 derived exosomes shows similar properties of cell proliferation and cellular signalling and CTP synthase 1 found with similar functionality showed up regulation in THP1 cell derived exosomes than H358 and absent in MCF7. However, proteins like Apolipoprotein, exosomal marker annexin A1, spectrin beta, cell division control protein 42 homolog, and 4F2 cell surface protein were also identified from all three exosomes which were involved in cellular signalling and cell proliferation process (MacHnicka et al., 2012).

The KEGG pathway analysis has identified several key pathways includes renal cancer pathways, bladder cancer pathways, and thyroid cancer pathways focal adhesion, Akt signalling pathways. Proteins with the most linkage in the protein interaction network, such as the heat shock family proteins, the Ras family proteins, plastin 2, phosphoglycerate kinase 1, actin family proteins, cadherins, integrins, laminins and catenin have been previously found to be involved in cancer metastasis. For example, it has been reported that

phosphoglycerate kinase 1 has the ability to promote invasion and metastasis, when the expression of phosphoglycerate kinase 1 of metastatic colon cancer was compared with its non-metastatic counter-part (Ahmad et al., 2013). The Ras family proteins the modulator of several signalling pathways that regulate cell proliferation, differentiation, apoptosis as well as phagocytosis (Giehl, 2005). Heat shock proteins on the other hand, are molecular chaperones required protein synthesis and folding in response to cellular stress. They also play vital role in protein assembly, secretion, trafficking, degradation and regulation of transcription factors (Seiwert et al., 2005). Their ability to promote cancer and metastasis is well established. For example, heat shock proteins are required for the EMT formation via modulation of catenin beta/slug signalling pathways, plus they have the ability to avoid apoptosis by forming Hsp70 complex with dependent kinase protein and fanconi anemia group C proteins (Lianos et al., 2015). Catenin, cadherin, actin also play important role tumour progression and metastasis (Chairoungdua et al., 2010). Several reports have documented the involvement of cadherins, catenin and integrins in the initial steps of metastasis, invasion (Miroshnikova et al., 2017; Yang et al., 2017).

The proteomic profiling of exosomes by LC-MS showed resemblance with several previous studies as mentioned before, but the presence of endoplasmic reticulum (ER) protein in the preparations shows the unwanted contaminations in the exosome preparations. So even though the data presented here follows most of the guidelines provided by the ISEV about the purity of exosome preparation, presence ER proteins suggest that the exosome preparations may not be entirely pure.

Although, new discoveries are published on a regular basis, but exosome biology is still in its early stage, so further research needs to be done on the methods of identification and analysing their protein cargo to understand their biogenesis, secretion and function of exosomes. In summary, this study represents the first comparative proteomics of the cancer cell lines mentioned before and will be a step forward in understanding the relation within different cancer and with further work might improve the chances to find potential biomarkers for early detection and new therapeutic strategies.

5.5 Conclusion:

The goal of this chapter was to find out the differences and similarities of exosomal proteins from different cancer cell lines. The idea is to find out the proteomic profile of different cancer cell line derived exosomes. Exosomes are one of the newest inclusions of biomarker research. While the exact biological functions of exosomes are yet to be established, several studies have suggested their role in cellular communication as well as cancer progression. Proteomic studies of exosomes have greatly influenced the understanding molecular compositions of exosomes. Furthermore, increasing studies have proved that apart from the membranous and cytosolic proteins. Exosomes contain subsets of proteins that are cell specific functions. In this study, proteins from exosome derived from three different cancer cell lines have been successfully identified which showed several similarities and differences. This comparative proteomic study of exosomes from different cancer cell lines can be used as a start point for the future biomarker development by comparing through the versatilities of proteins secreted by exosomes from these three cancer cell lines.

Chapter 6:

Comparative proteomic study and gene expression analysis of exosomes from lung cancer cell line and normal cell line

6.1 Introduction:

Being one of the major causes of cancer related deaths worldwide, with non-small lung cancer (NSCLC) covering majority of lung cancer deaths, it still lacks the tool for early detection of lung cancer (Bharti et al., 2013). Due to the absence or lack of specified therapeutic options, late diagnostics and poor efficiency in preventing metastasis, NSCLC has a very poor survival rate combining all stages. NSCLC is a molecularly heterogeneous disease with ever changing genetic alterations (Pomplun, 2006). Other than the most common genetic alteration of EGFR and KRAS, several reports have suggested the alterations in Echinoderm microtubule-associated protein-like 4 (EML4) and anaplastic lymphoma kinase (ALK) fusion gene, oestrogen-related receptor beta type 2 (ERRB2), NRAS, v-raf murine sarcoma viral oncogene homolog B1 (BRAF), phosphatidylinositol-4,5-bisphosphate 3-kinase, catalytic subunit alpha (PIK3CA), met proto-oncogene (MET) and cadherin-associated protein beta 1 (CTNNB1) mutations (Pao and Girard, 2011; Seo et al., 2012). Furthermore, the present biomarkers for lung cancers such as CEA, NSE, TPA, CA125 and ProGRP have been reported to have limited sensitivity for early detection and diagnosis (Pan et al., 2008). Therefore, better understanding of the mechanisms of lung cancer progression and its early detection tools is vital (Cho, 2016). In recent years, quantitative and comparative proteomics have been used extensively to search for cancer biomarkers for early detection and diagnostics. The survival rate of lung cancer patients depend on the stage of detection, so to increase the survival rate of lung cancer patients, concentration must be given to the early detection strategies (Cheung and Juan, 2017). Quantitative proteomics between normal and lung cancer patients differentiate the relative protein abundance, reveal insights on molecular mechanism, interaction of signalling pathways and employed as a biomarkers tools for early detection prognosis (Cifani and Kentsis, 2016). Exosomes are the newest inclusion for the biomarker discovery for lung cancer due their similarities with the parent cells (Henderson and Azorsa, 2012) and reported to contain tumour associated proteins such as EGFR, KRAS,

Rab family, CD91, CD137 (Reclusa et al., 2017). So far, 9769 proteins have been identified from exosomes according to ExoCarta (<http://www.exocarta.org/>) database some of which reflects pathological disease states (Zhou et al., 2017). Cell releases exosomes in both diseased and healthy state. The content and number of exosomes varies between normal healthy exosomes and tumour exosomes. Recently it was shown that, the number of exosomes from clone of a breast cancer cell line was more than ten times higher than its normal counterpart exosomes per million cells (Riches et al., 2014). In another study, it was also shown that the mRNA content of normal cell was different to tumour derived exosomes (Melo et al., 2014). Because of these distinct nature and ability to carry specific genetic cargo, exosomes has become one of the major success in cancer research (Whiteside, 2016). Recently comparative proteomic study between lung cancer cell lines and their counterpart normal cell lines revealed differential protein expressions of proteins involved in signal transduction, cellular signalling, cell adhesion, extracellular remodelling. It was demonstrated in the same study that, the lung cancer exosomes enriched in proteins involved in signal transduction such as EGFR, SRC, MET receptor protein KRAS, RAC1 were overexpressed compared to the normal healthy lung cells (Clark et al., 2016).

In this chapter, proteomic profile of exosomes from normal human bronchial tracheal epithelial cell line (HBTE) was studied by using LC-MS based proteomic approach as described before and the proteomic data was compared with the proteomics of exosomes from non-small cell lung cancer cell line H358 originated from a metastatic alveolar site of the lung. Selected proteins with different expression were subjected to gene expression analysis by qPCR in cellular level to compare the protein expression levels of exosomes relate to cellular gene expression.

6.2 Methods and Materials:

6.2.1 Cell Culture and Isolation of exosomes:

Lung cancer cell line (H358) was cultured in the similar way as described in chapter 3. The primary immortal cell line, human bronchial tracheal epithelial cell (ATCC[®]PCS-300-010) was cultured in basal airway growth medium (ATCC[®]PCS-300-030). The growth medium was prepared by adding the airway epithelial growth kit (ATCC[®]PCS-300-040) and 1% antibiotic (ATCC[®]PCS-999-002) containing Penicillin 10,000 Units/mL, Streptomycin 10 mg/mL, Amphotericin B 25 µg/ml. Both the cells were maintained in 5% CO₂ and 37°C.

6.2.2 Proteomic Analysis by LC-MS:

Protein separation and proteomic profiling was carried out following similar protocol described in chapter 5.5.3.

6.2.3 Isolation of RNA from cells:

Total RNA from both H358 and HBTE cell lines were extracted using RNeasy Mini Kit from QIAGEN following manufacturer's protocol with slight modifications of 15sec to 30sec. Briefly, all cells were pelleted by centrifuging at low speed (500×g) for 5 min at 4°C, washed twice with cold PBS in DEPC (Diethyl pyro-carbonate) treated water and transferred in a RNase free Eppendorf tube to avoid contamination and kept on ice. The RLT buffer from the kit was heated at 60°C for 15 mins prior to use. β mercaptoethanol (β-ME) was added with RLT buffer in 1:100 ratio just before starting the RNA extraction to reduce the disulphide bonds of proteins which hampers the RNA extraction. 350µl of RLT+ β-ME buffer was added to the cell and incubated 10mins to break the cell membrane. Then the lysate was transferred immediately into QIAshredder spin column and centrifuged at 10000×g for 2 min to isolate the cellular debris from the lysate. The flow through lysate was collected and the column was discarded. After that 350 µl of 70% molecular grade ethanol was added to the lysate and immediately transferred into a RNeasy mini spin column and centrifuged for 30 sec at 8000×g. Ethanol helps to precipitate the RNA and removes the salt from the lysate. The column was then retained discarding the flow through. 700µl pf RW1 buffer was added to the column and centrifuge for 30 secs at 8000×g. Similarly the flow through was discarded leaving the column. After that the column was washed twice with 500µl of RPE buffer at 8000×g for 30sec and 1 min. The RNA was eluted from the spin column by solubilizing the RNA in RNase free water in 1min centrifuge at 10000×g. The concentration, purity and

integrity of extracted RNA were evaluated by using Nano-Drop analyser (Thermo Fisher) and in a 1.2% agarose gel respectively. The quality of RNA depends on the ratio of the 28s and 18s ribosomal RNA as more than 80% of the total RNA of the mammalian cell comprises of ribosomal RNA with majority of them being 28s and 18s rRNA. Due to the abundance of these two rRNA two distinct bands will be observed in the agarose gel. So to achieve a good quality RNA there should be two distinct bands of 28s and 18s. The RNA samples were stored at -80°C freezer for future analysis.

6.2.4 Sample preparation for RT-PCR:

6.2.4.1 Synthesis of cDNA:

To synthesise cDNA from the extracted RNA Promega GoStrip Reverse Transcriptase kit was used following the manufacturers protocol. Briefly, 600ng of RNA sample was mixed with 0.5µg Oligo (dT) primer and made the volume up to 5µl with nuclease free water. The mixture was heated at 70°C for 5mins and kept on ice immediately afterwards. The reverse transcription (RT) reaction mix was made by mixing the following components. GoStrip 5X reaction buffer 4µl, 1.2 µl of 25mM MgCl₂, 1µl of PCR nucleotide mix, 20units of RNasin and finally 1µl of GoStrip RT was added. The volume was made up to 15µl with nuclease free water. The RT reaction mix was combined together with the reaction mix previously kept on ice and heated for 5 min at 25°C for annealing and incubated at 42°C for one hour. To inactivate the RT the sample was heated to 70°C for 15 mins before proceeding to RT-PCR analysis.

6.2.4.2 Gene expression analysis by Real time PCR:

To compare the relative gene expression qPCR analysis was performed for the selected genes (Table 6.2). The qPCR was run with the following thermal cycle in table 6.1. Primers used in this study were obtained from Eurofins Genomics (Table 6.2). To run the qPCR, the cDNA (2µl) was mixed with 1µl of primers, both forward and reverse, along with 1µl of Go Taq qPCR master mix and 0.3µl of C×R fluorescence dye. The samples were then pipette into the assigned well and the PCR plate was centrifuged at 500×g for 1 min to pull down the reaction mix to the bottom of the wells. Primers were acquired from literature search and designed by Primer 3 web designing tool. A melting curve analysis was set to carry out by the instrument to check the specificity of the PCR product and any possible non specific amplification.

Table 6.1: Number of cycles at each stages and temperature are shown in the table below.

Stages	Cycles	Cycling programme
Hot-Start Activation	1	95°C for 2 minutes
Denaturation	40	95°C for 15 seconds
Annealing/Extension		60°C for 60 seconds
Dissociation	1	60°C- 95°C

Table 6.2: Primers for the qPCR analysis are shown below. Primers were acquired from literature search.

Names	Gene ID	Forward Primer	References	Product size
Cadherin-1	CDH1	AGAAAGTTTTCCACCAAAG	(Goyal et al., 2008)	213
		AAATGTGAGCAATTCTGCTT		
Transforming growth factor beta 2	TGFB2	ATCGATGGCACCTCCACATATG	Designed by Primer 3	193
		GCGAAGGCAGCAATTATGCTG		
Laminin gamma 1	LAMC1	ATGATGGTCGCTGTGAATGC	Designed by Primer 3	203
		CTCATCCCCAGTTCCAAGGT		
Integrin alpha-3	ITGA3	AAGGGACCTTCAGGTGCA	(Dingemans et al., 2010)	244
		TGTAGCCGGTGATTTACCAT		
Cathepsin D	CTSD	CAAGTTCGATGGCATCCTGG	Designed by Primer 3	219
		CGGGTGACATTCAGGTAGGA		
Catenin beta-1	CTNNB1	AGGGATTTTCAGTCCTTA	(Goyal et al., 2008)	197
		CATGCCCTCATCTAATGTCT		

6.3 Results:

6.3.1 Identification and characterisation of exosomes:

Exosomes from lung cancer cell line H358 and its counterpart normal cell HBTE were isolated from cell culture supernatant by using PEG based isolation method. To identify the presence of exosomes, purified exosomes from both cell lines were observed by TEM. Figure 6.1 shows the presence of exosome like vesicles with a round shaped morphology showing heterogeneous size population. Quantitative analysis revealed that, the average size of exosomes from both H358 as well as HBTE showed significant differences ($p= 0.003$, $n= 100$) between them. However, the average size of H358 and HBTE exosomes were $98.8\pm 11.8\text{nm}$ and $85.7\pm 17.4\text{nm}$ respectively which was within the expected exosome size (30-150nm as mentioned previously).

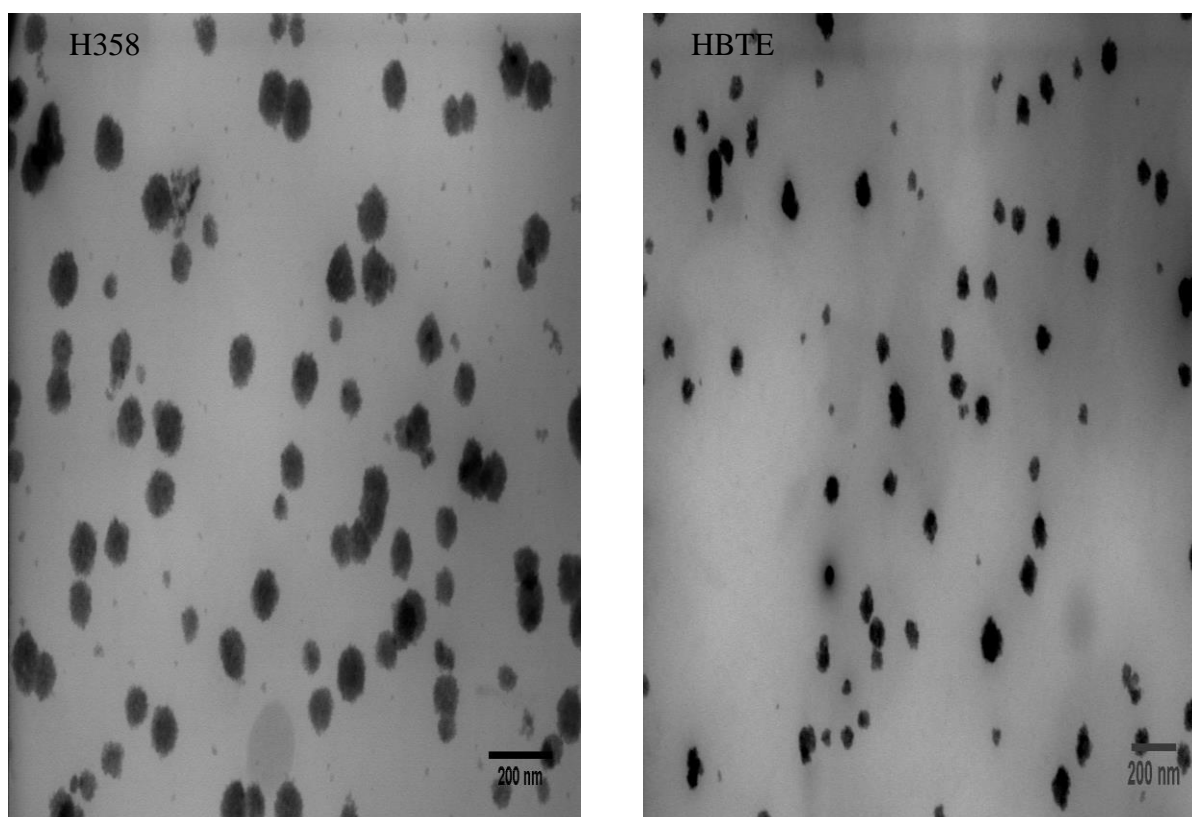


Figure 6.1: TEM images of exosomes from H358 and HBTE showing round shaped morphology with different magnifications.

6.3.2 Proteomic analysis:

Protein identification was carried out following similar methods described in previous chapter (Chapter 5; Section 5.3.2). Protein and peptide identification threshold were kept similar in this chapter too. Peptide identification was accepted with more than 25% probability and a FDR rate of less than 1.0%. Similarly, protein identification was also accepted with a probability of more than 99.0% to achieve a FDR of less than 1.0%. In this study, a total of 1011 proteins were identified from HBTE cell derived exosomes. As mentioned before a total of 889 proteins were identified from H358 cell derived exosomes. A total of 627 proteins (67.66%) were shared between exosomes from H358 and HBTE cell lines. Apart from the shared proteins, 205 (20.28%) and 327 (32.34%) proteins were unique in H358 and HBTE exosomes respectively (Figure 6.2).

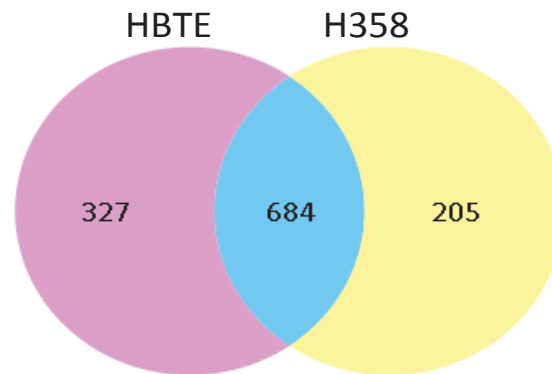


Figure 6.2: A Venn diagram showing number of the shared proteins between HBTE and H358 as well as the unique proteins in H358 and HBTE.

6.3.3 Functional analysis of exosome proteins:

To compare functional categories of exosomal proteins from both H358 and HBTE, GO analysis was performed using the Scaffold online software v10.5 as previously described (Chapter 5.6.2). Proteins were separated in three categories including biological process, cellular compartment and molecular functions. Proteins were grouped in 15 classes according to their biological process (Figure 6.3) including cellular adhesion, biological regulation, localization and responses to stimulus. Distribution of annotated proteins within this category was relatively uniform suggesting similar functionalities of exosomes across both cell lines. The highest ranked annotated proteins were from cellular process (86.6% for H358 and 87.74% for HBTE) and biological regulation (71.1% for H358 and 70.86%). Other than that, exosomes from both cell lines were enriched with proteins involved in metabolic process and response to stimulus. Each protein was found to be involved in multiple gene ontology

classes. For example, fibronectin, integrins, tenascin were found to be associated with cellular adhesion, biological regulation, cellular process as well as growth, localisation, immune system and metabolic process also. However, the lung cancer cell line H358 was more enriched with proteins involved in response to stimulus, multicellular organelle process, development process and biological adhesion. Nevertheless, the normal cell line HBTE was enriched with proteins involved in cellular process, metabolic process, viral process and localisation.

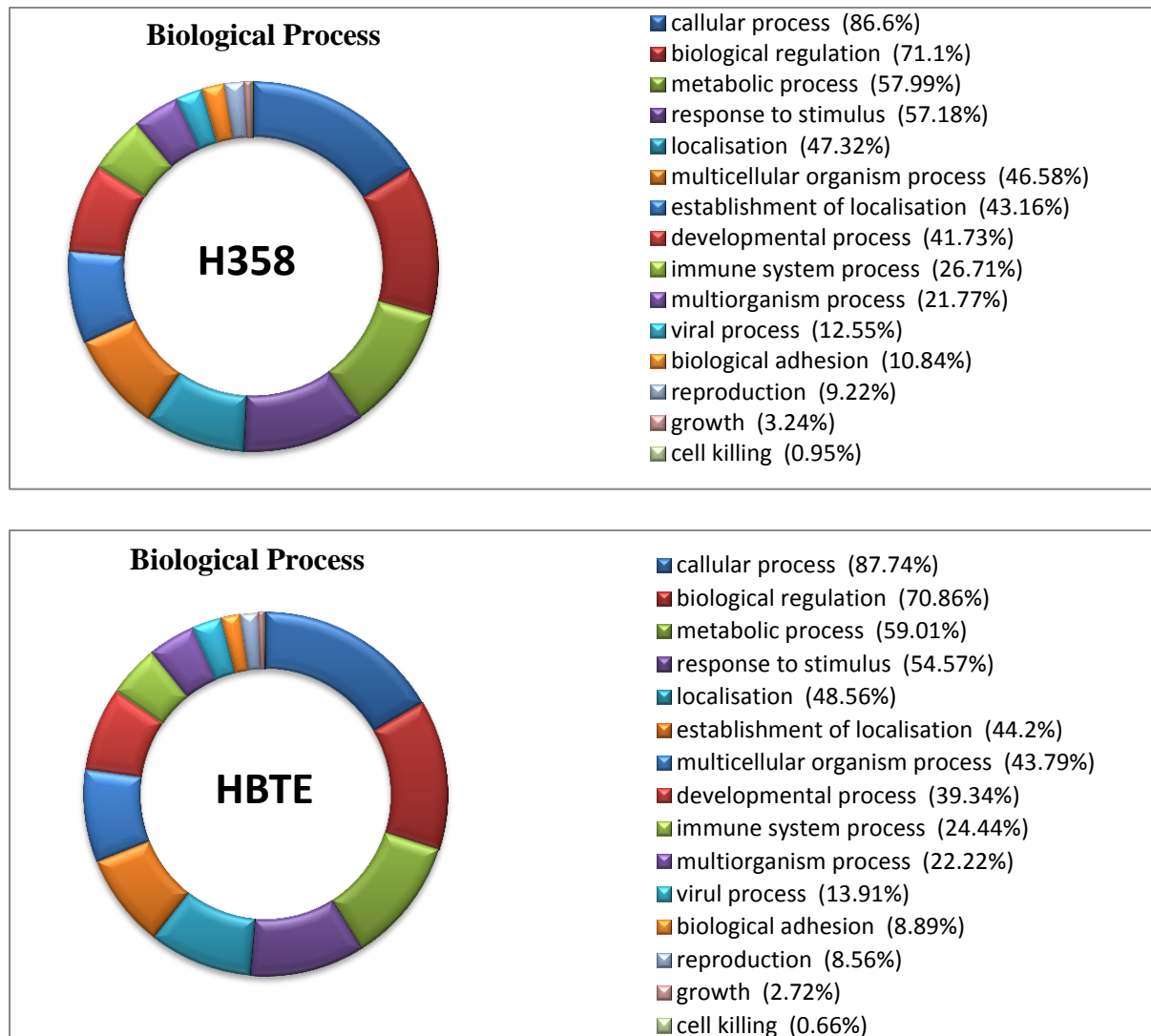


Figure 6.3: Doughnut chart showing the involvement of proteins H358 and HBTE in biological process.

Considering the enrichment of cellular component (Figure 6.4), exosomes from both cell lines were enriched with cytoplasmic and membranous proteins. 79.18% proteins from the cancer cell line H358 were cytoplasmic proteins while 82.14% proteins from normal cell were from the same group. Proteins from intracellular organelle were very similar where 77.28% proteins from H358 and 79.01% from HBTE. Distributions of annotation of cellular

component were generally similar. The highest gap between two exosomes was the extracellular organelle proteins. 70.34% proteins were identified from extracellular organelle from the cancer exosomes compared to 66.83% from the counterpart normal cell exosomes.

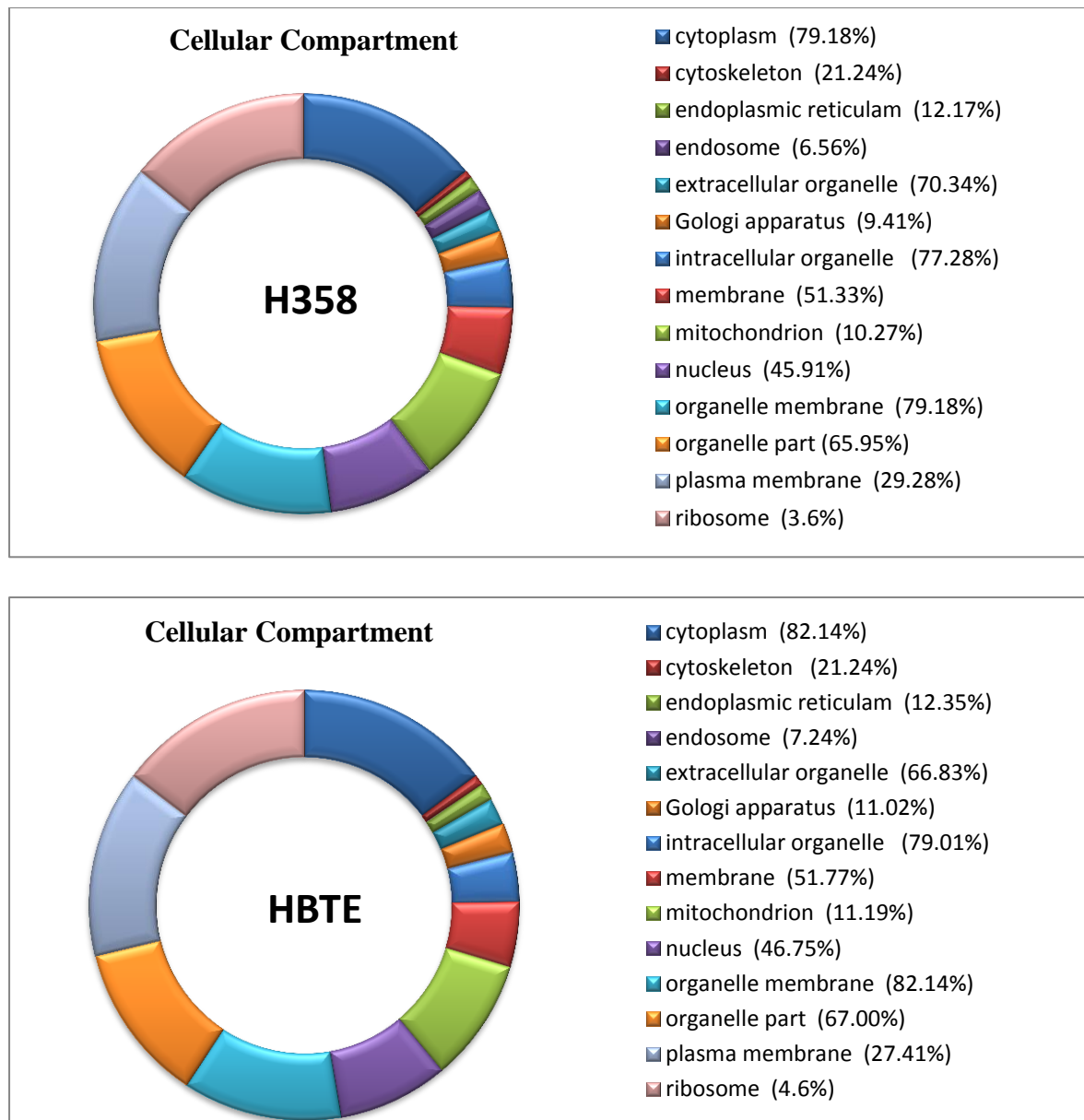


Figure 6.4: Doughnut chart showing the involvement of proteins H358 and HBTE in cellular compartments.

Finally, considering the last category of GO terms, molecular function, most of the proteins from both exosomes were enriched with binding activity where 87.83% proteins were grouped in this category for H358 and 88.31% proteins from HBTE with very low percentage of catalytic activity, enzyme regulator activity, and transport. A bar chart representing the molecular function of the shared proteins from H358 and HBTE are shown in figure 6.5.

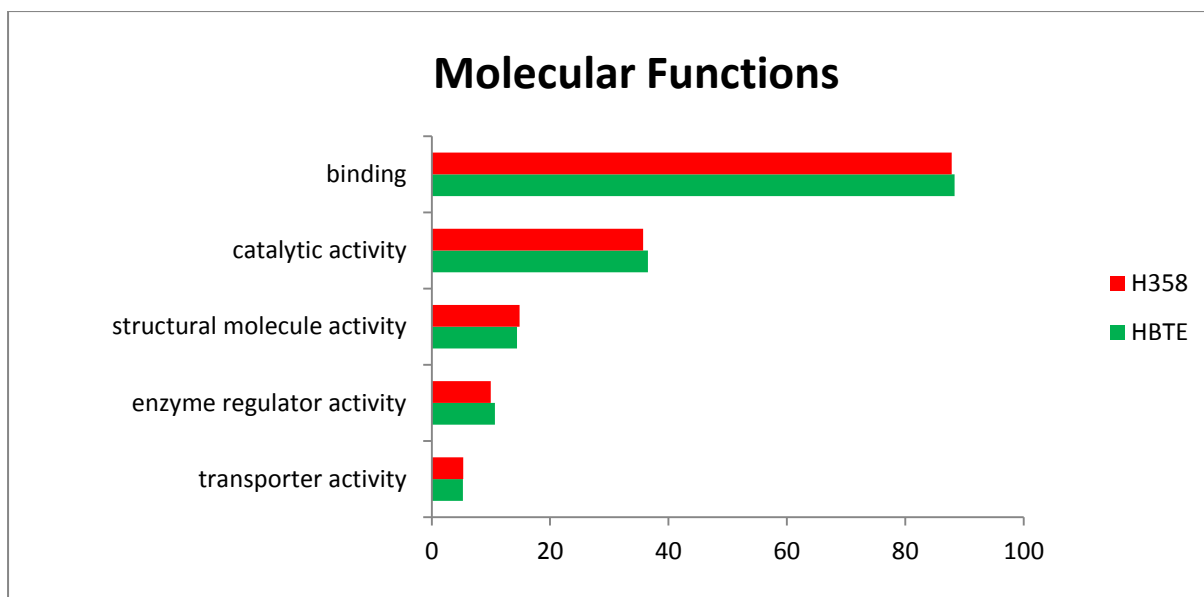


Figure 6.5: Bar chart showing the top five involvements of proteins from H358 and HBTE in molecular functions.

6.3.4 Comparative proteomic analysis:

Protein expression of HBTE exosomes were compared with proteins previously identified from H358 exosomes. The expression level of the 684 shared proteins between the lung cancer exosomes and normal exosomes were compared here. A total of 97 shared proteins were up regulated in HBTE by at least 2.0 fold compared to the lung cancer cell line H358 which includes programmed cell death 6-interacting protein which regulates cell death, 3 proteins from the heat shock family including heat shock protein 71kDa, 60kDa, 10kDa. Most of the up regulated proteins from HBTE were either from extracellular region or from membrane bound cytoplasmic proteins with various binding activity e.g. protein binding, RNA binding, ion binding and macromolecule complex binding. On the other hand, a total of 89 proteins were up regulated in H358 which includes exosomal marker proteins annexin A5, proteins from the histone family, 2 members of the laminin family proteins ($\beta 2$, $\alpha 5$). Similarly like HBTE, most of the proteins up regulated in H358 were also from either membrane bound cytoplasmic or extracellular region proteins most of which have the molecular function of binding and transport. In addition, the biological process of most of the up regulated proteins in H358 involve response to stress, response to wounding, response to stimulus, cell differentiation, cellular adhesion, response to drug, immune system. Furthermore, Proteins like integrin ($\alpha 3$ and $\beta 1$), laminin ($\beta 1$ and $\gamma 1$) and tenascin C involved in focal adhesion, small cell lung cancer and PI3K-Akt signalling pathways which leads to cancer were up regulated in H358 exosome. An unsupervised heat map of the proteins with up regulated or

down regulated proteins ($p < 0.05$) shows the different expression of proteins within H358 exosomes and HBTE exosomes (Figure 6.6).

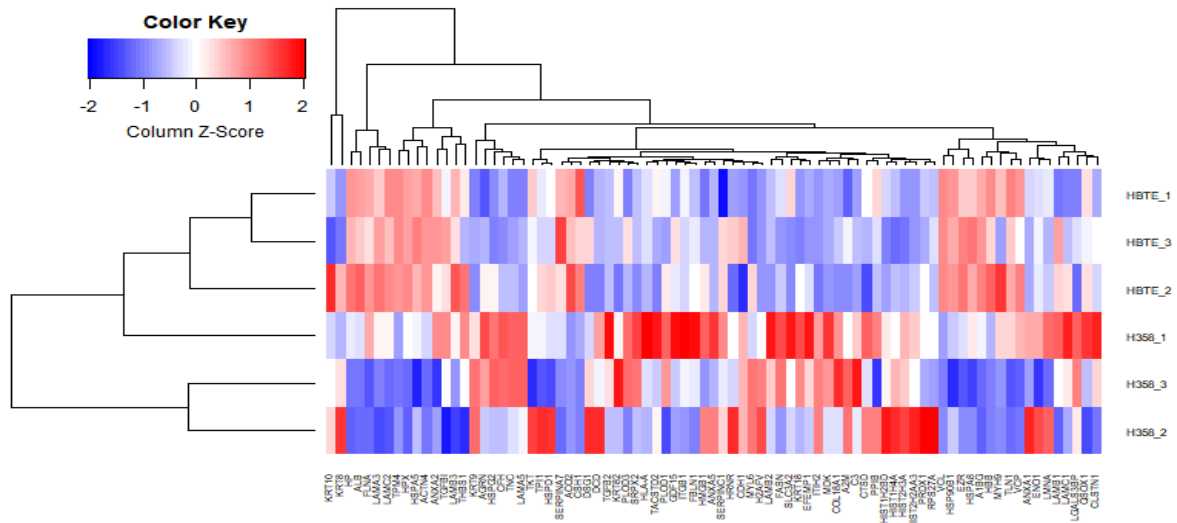


Figure 6.6: An unsupervised heat map of proteins among three biological replicates between the H358 exosomes and HBTE exosomes with different expression level ($p < 0.05$). The column represents each protein expression and the row represents each sample with their triplicates. The column Z score represents the relative abundance, from red higher expression to blue represents low expression and white being not expressed.

Table 6.3: Partial list of proteins with their functions and difference in their relative expressions. Na= not available in HBTE

Functions	Proteins	Accession number	Gene Symbol	Fold change
<i>Cellular Adhesion</i>	Epithelial cell adhesion molecule	EPCAM_HUMAN	EPCAM	na
	Cadherin-1*	CADH1_HUMAN	CDH1	1.7
	Desmoplakin-1	DESP_HUMAN	DSP	-1.3
	Cystatin-C	CYTC_HUMAN	CSTC	1.5
	Tenascin	TENA_HUMAN	TNC	6.25
	Laminin subunit gamma-1*	LAMC1_HUMAN	LAMC1	1.61
	Laminin subunit beta-1	LAMB1_HUMAN	LAMB1	1.00
	Integrin alpha-3	ITA3_HUMAN	ITGA3	1.62
	Calsyntenin-1	CSTN1_HUMAN	CLSTN1	1.33
<i>Cellular Transport</i>	T-complex protein 1 subunit zeta	TCPZ_HUMAN	TCPZ	-3.0
	Serotransferrin	TRFE_HUMAN	TF	-4.5
	Laminin subunit beta-1	LAMA5_HUMAN	LAMA5	5.43
	Protein S100-A6	S10A6_HUMAN	S100A6	1.28
<i>Receptor and Signalling</i>	Lactadherin	MFGM_HUMAN	MFGE8	10
	Transforming growth factor beta-2	TGFB2_HUMAN	TGFB2	2.33
	Annexin A1	ANXA1_HUMAN	ANXA1	1.53
	Antithrombin-III	ANT3_HUMAN	SERPINC1	1.24
	Proteasome activator complex subunit 1	SFXN1_HUMAN	36kDa	1.28
	Transforming growth factor-beta-induced protein ig	BGH3_HUMAN	TGFBI	1.42
<i>Tumour associated proteins.</i>	Guanine nucleotide-binding protein G(I)/G(S)/G(T) subunit beta-2	LTBP1_HUMAN	GNB2	1.29
	Annexin A5	ANXA5_HUMAN	36kDa	1.15
	CD44 antigen	CD44_HUMAN	CD44	2.00

	Ras-related C3 botulinum toxin substrate 1	RAC1_HUMAN	RAC1	1.14
	Tumour protein D54	TPD54_HUMAN	TPD52L2	1.5
	Heat Shock Cognate	HSP70C_HUMAN	HSPA8	2.4
	Cathepsin D	CATD_HUMAN	CSTD	1.75
Cellular Communication	Fibronectin	FINC_HUMAN	FN1	-1.5
	Basement membrane-specific heparan sulfate proteoglycan core protein	PGBM_HUMAN	HSPG2	3.88
	COP9 signalosome complex subunit 8	CSN8_HUMAN	CSN8	-2.5
Response to stimulus	Integrin beta-4	ITB4_HUMAN	ITB4	1.33
	Prelamin	LMNA_HUMAN	LMNA	1.42
	Histone H2A	H2AV_HUMAN	H2AV	2.83
Exosomal Markers	Programmed cell death 6-interacting protein (ALIX)	PDC6I_HUMAN	PDCD6IP	-1.0
	Glyceraldehyde-3-phosphate dehydrogenase	G3P_HUMAN	GAPDH	-1.3
	Annexin A2	ANXA2_HUMAN	ANXA2	-1.2
	Annexin A1	ANX1_HUMAN	ANX1	1.53
	Syntenin-1	SDCB1_HUMAN	SDCBP	1.5
	CD81 antigen	CD81_HUMAN	CD81	1.62
	CD9 antigen	CD9_HUMAN	CD9	1.29
NSCLC-related proteins	4F2 cell-surface antigen heavy chain	4F2_HUMAN	4F2	2.23
	Basigin	BASI_HUMAN	BSG	8.0
	Integrin beta -1	ITB1_HUMAN	ITGB1	1.68
	Heat shock protein 90	HS90A_HUMAN	HS90	-2.0
	Catenin beta -1*	CTNB1_HUMAN	CTNB1	na

6.3.5 Protein network and KEGG pathway analysis:

Proteins identified here were analysed for their protein-protein interaction network and KEGG pathways by using the string online tool v10.5. All the proteins including shared and exclusive to H358 and HBTE were analysed for their network. In the protein network the coloured nodes represent the protein involvement and the connecting lines represent the interaction amongst proteins. The thickness of the line represents the confidence level of the interaction. 195 of the shared protein with different expression level (more than one fold and $p < 0.05$) were subjected to network analysis (Figure 6.7) which showed a complex protein-protein interaction network. 184 proteins out of the 195 were connected with each other in a complex network with various confidence levels (thickness of the connecting lines). 11 proteins did not participate in any interaction at the minimum confidence level (STRING score = 0.400).

The KEGG pathway analysis revealed 37 pathways which include several pathways involved in cancer such as focal adhesion, PI3-Akt signalling pathways, small cell lung cancer and microRNAs in cancer. The pathway with the highest enrichment and important in cancer was focal adhesion. The top ten ranked pathways with the most enriched are shown in Figure 6.8. Proteins that are mostly involved in various pathways include CDH1, laminin family proteins ($\alpha 3$, $\alpha 5$, $\beta 1$, $\beta 2$, $\beta 3$, $\gamma 1$, $\gamma 2$), proteins from the integrin family ($\alpha 3$ and $\beta 1$) proteins from heat shock protein family such as Hsp ($\alpha 4$, 5 and 8).

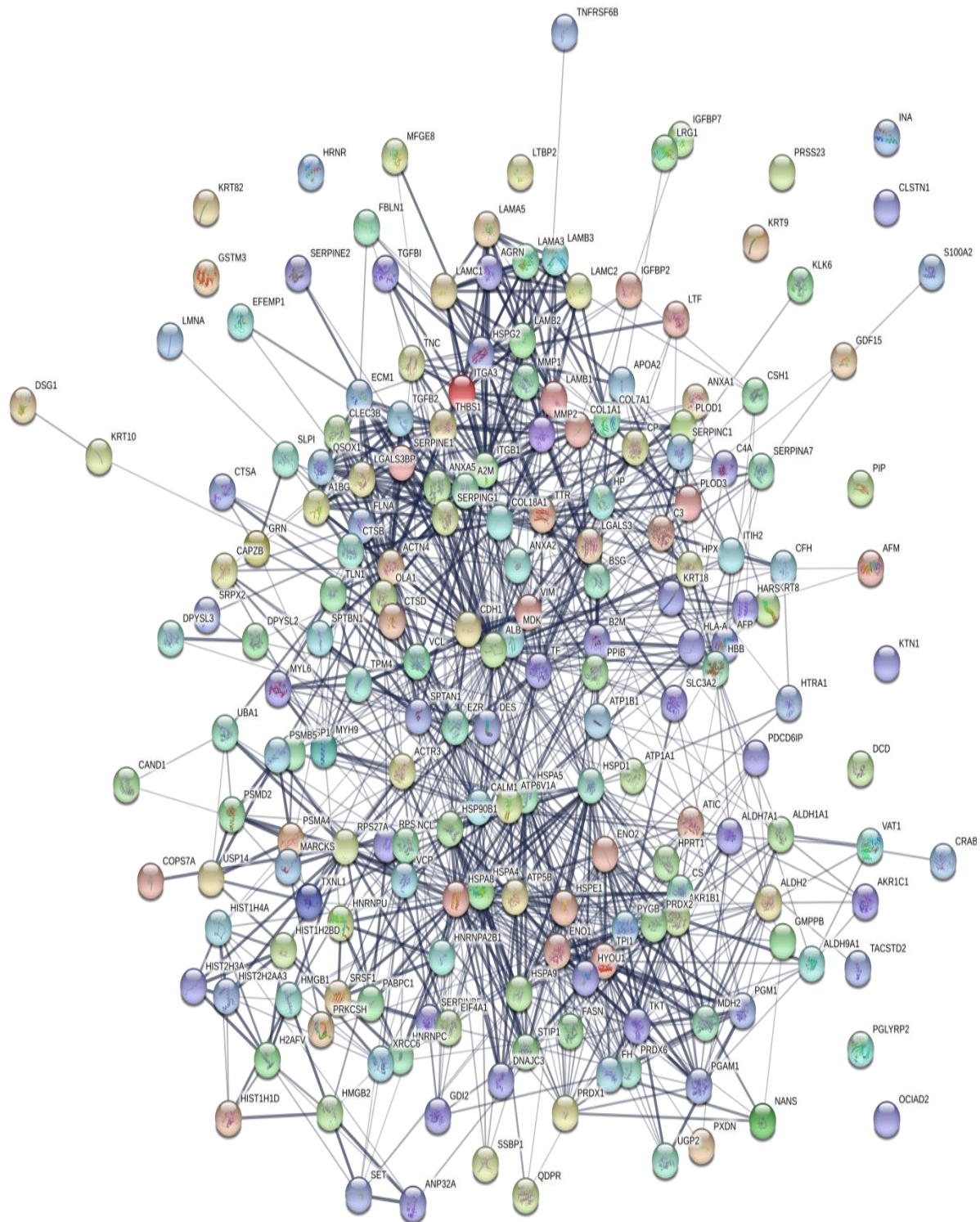


Figure 6.7: The protein network analysis for the shared proteins between H358 and HBTE, using STRING v10.0 with a confidence level of 0.4 revealed a complex protein network. The thickness of the connecting line represents the strength of the associations. Here, each node represents a protein and the line represents the interaction between the proteins. A thicker or darker line between nodes indicates stronger interaction and vice versa.

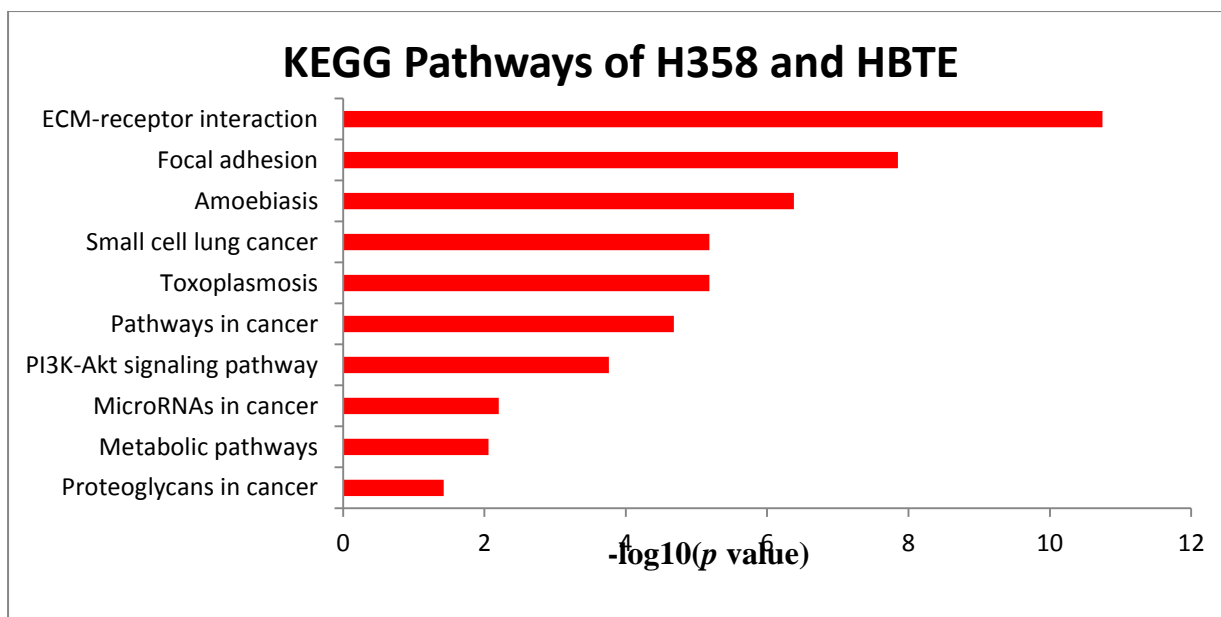


Figure 6.8: KEGG pathway analysis of shared proteins with $p < 0.05$. The number of the horizontal axis represents the $-\log_{10}$ of p value for the enrichment of genes with each pathway.

Proteins exclusively identified from both H358 and HBTE were also subjected to network and KEGG analysis. In figure 6.9 out of 226 proteins from H358 exosomes, 170 proteins were interconnected while 10 proteins were connected in three groups of two, three and five proteins separate from the large network while 46 proteins did not show any interlink within the similar confidence level used previously (STRING score: 0.400). The most significant GO terms detected were Rab protein signal transduction, DNA conformation change, response to stimulus, biological regulation, transport, cellular component organisation. Significant molecular functions include binding of proteins, RNA, GDP, GTP and enzyme. 6 signalling pathways were found to be significantly enriched which includes cellular adhesion molecules (CAMs), spliceosome and antigen processing and presentation. Identified members of the catenin, cadherins, annexin, Rab, laminin, histone family proteins were frequently found to be involved in these pathways.

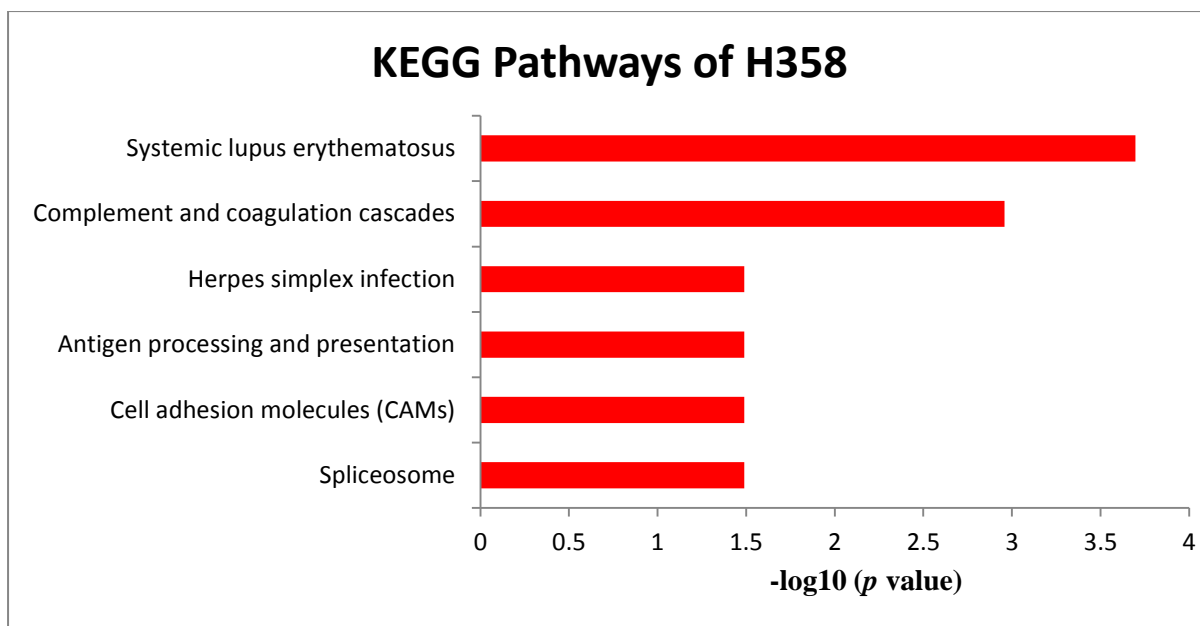


Figure 6.10: KEGG pathway analysis of proteins only present in H358 exosomes. The number of the horizontal axis represents the $-\log_{10}$ of p value for the enrichment of genes with each pathway.

The KEGG pathway analysis showed the enrichment of six pathways (Figure 6.10) which include spliceosome, cellular adhesion, antigen processing and presentation, herpes simplex infection and complement and coagulation cascades. The most prominent proteins in these six pathways were proteins from the histone family, HLA, ITG α 5, proteins from serine/arginine group.

On the other hand, all the proteins solely identified from HBTE were introduced to the network and pathway analysis which created a very complex network involving 295 proteins interlinked in a single network. With the same acceptable confidence threshold, 32 proteins did not show any interconnection. The clustering of these proteins showed one defined and major interaction nodes which represents ribosomal proteins (Figure 6.11) such as 40S ribosomal protein S6, S8, S9, S11, 60S ribosomal protein L3, L5, L8. The KEGG pathway analysis revealed enrichment of 24 pathways. The top ten enriched pathways are shown in figure 6.12. The highest ranked pathways identified by KEGG analysis were Ribosome and carbon metabolism pathways. The top ranked GO terms for the exclusive proteins involve cellular organisation, transport, localisation and metabolic process. Most of the unique proteins from HBTE were membrane bound or extracellular vesicles proteins.

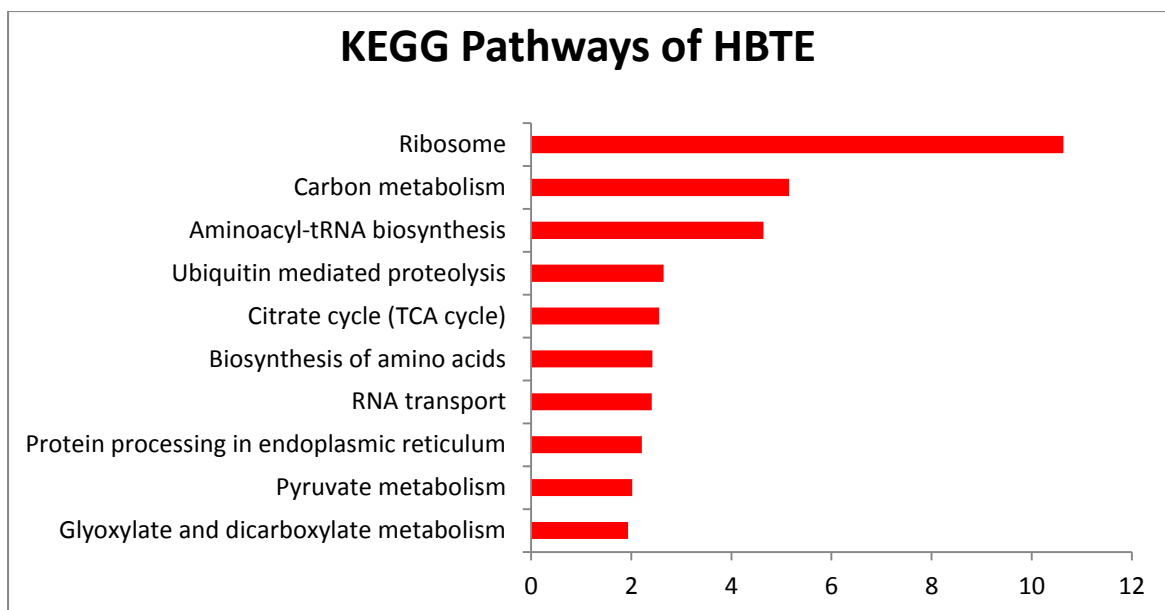


Figure 6.12: KEGG pathway analysis of proteins only present in HBTE with p value. To normalise the FDR value, negative \log_{10} was used. The number of the horizontal axis represents the $-\log_{10}$ of p value for the enrichment of genes with each pathway.

Next, 40 of the up regulated proteins from cancer cell H358 derived exosomes were subjected to the protein network analysis which yielded 33 interactions among proteins where 23 proteins interacted with each other while 17 proteins did not show any interaction (Figure 6.13). Within the protein network two clusters of five proteins were visible. The cluster on the upper left side consists of five of the histone family proteins while the lower right cluster is composed of laminin gamma 1, alpha 5, integrin beta 1, Heparan sulfate proteoglycan 2 and arginine. Apart from the clusters Cell division cycle 42 and laminin gamma 1 showed the most number of interaction (six edges each)

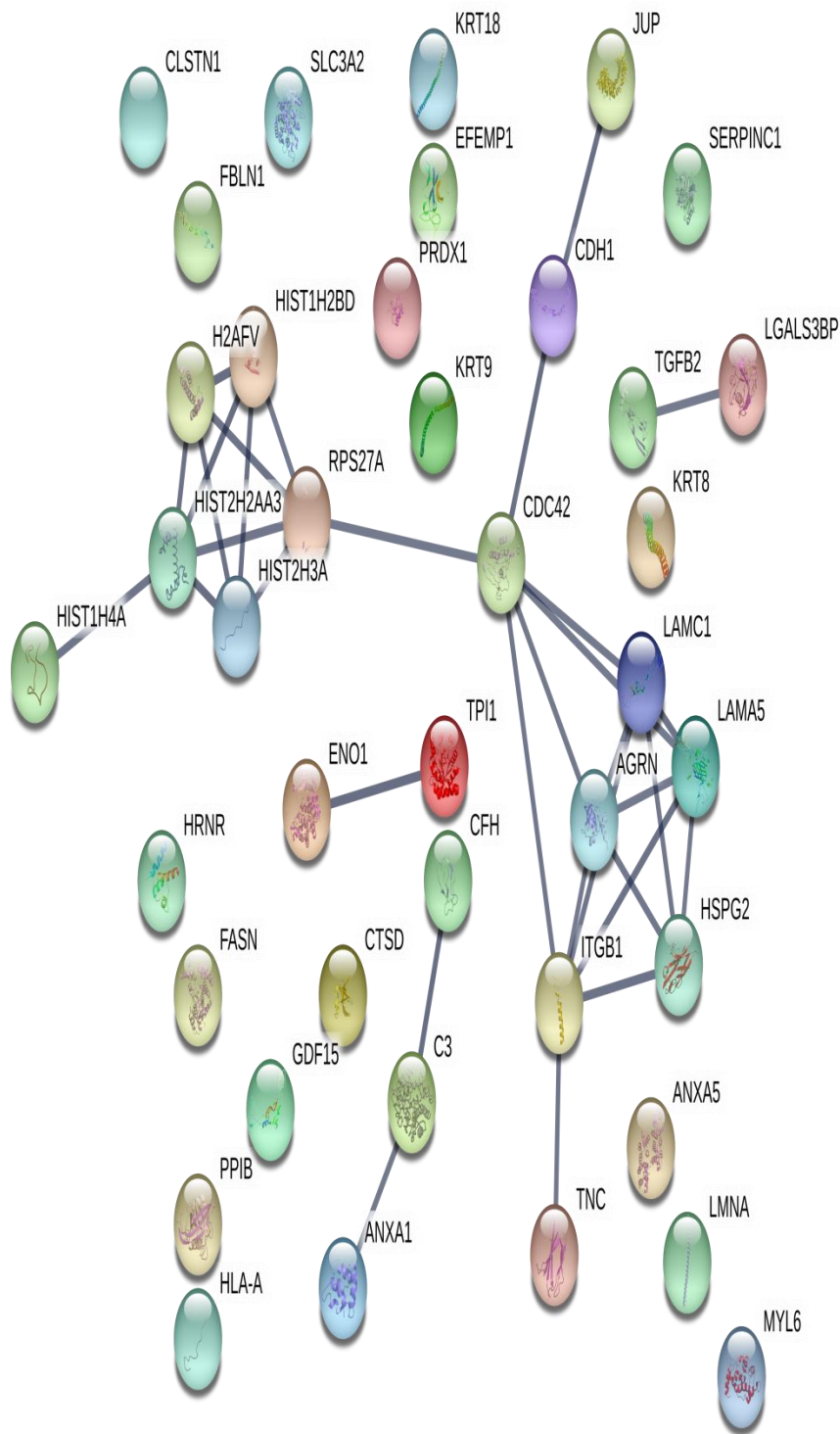


Figure 6.13: The protein network analysis for the upregulated proteins in H358 using STRING v10.0 with a confidence level of 0.4 revealed a complex protein network. The thickness of the connecting line represents the strength of the associations. Here, each node represents a protein and the line represents the interaction between the proteins. A thicker or darker line between nodes indicates stronger interaction and vice versa.

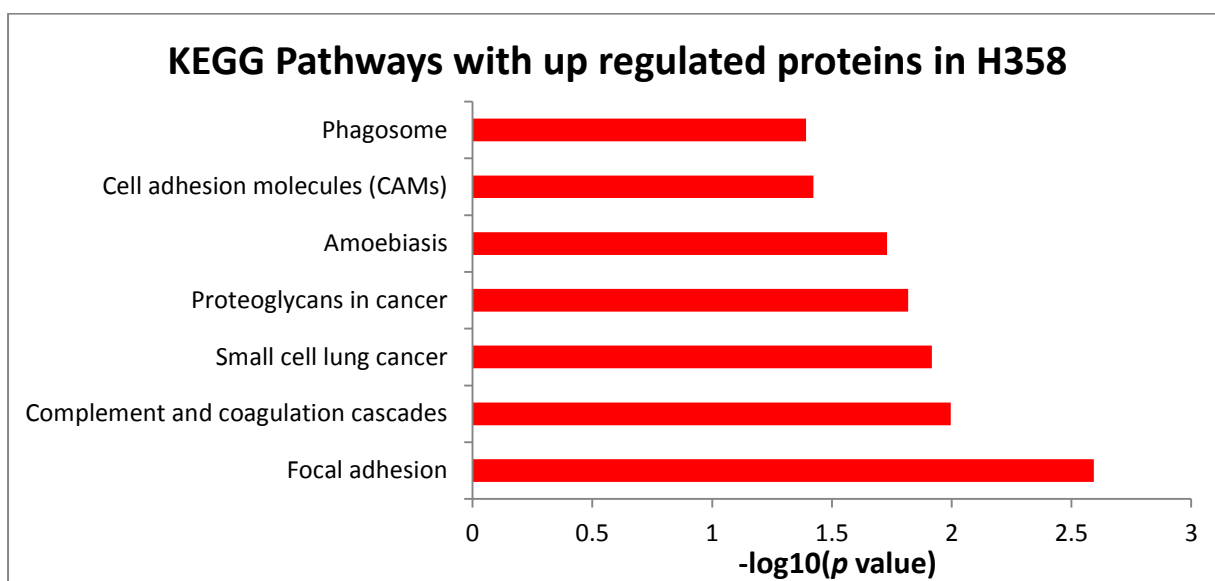


Figure 6.14: KEGG pathway analysis of up regulated proteins in H358 with $p < 0.05$. Proteins identified in all three triplicates were subjected to this pathway analysis. The number of the horizontal axis represents the $-\log_{10}$ of p value for the enrichment of genes with each pathway.

After the network analysis, KEGG pathway analysis was applied to the upregulated proteins from H358 which resulted six pathways (Figure 6.14) which include focal adhesion, small cell lung cancer, cellular adhesion molecules (CAMs). Proteins involved in multiple pathways are C3, CDH1, CDC42, integrin beta 1 and beta 2, laminin alpha 5 and gamma 1. These proteins are involved in focal adhesion, CAMs, small cell lung cancer, proteoglycans in cancer.

Network analysis with upregulated proteins from HBTE yielded a much more complex network than the upregulated proteins from H358. A total of 34 proteins (2.0 fold upregulated) were applied to the network analysis. The network was interconnected with 90 edges and only a single protein (AHCY) was not involved in any interaction (Figure 6.15). Although the protein network with the upregulated proteins from HBTE was much complex than the network of H358, it did not show any cluster of proteins. The KEGG pathway analysis resulted with 7 pathways which include P13K-Akt signaling pathway, focal adhesion, ECM receptor interaction (Figure 6.16). Two proteins are involved in multiple pathways such as ACTN4 and HSP90AA1. They are involved in focal adhesion, Antigen processing and presentation and P13K-Akt signaling pathway.

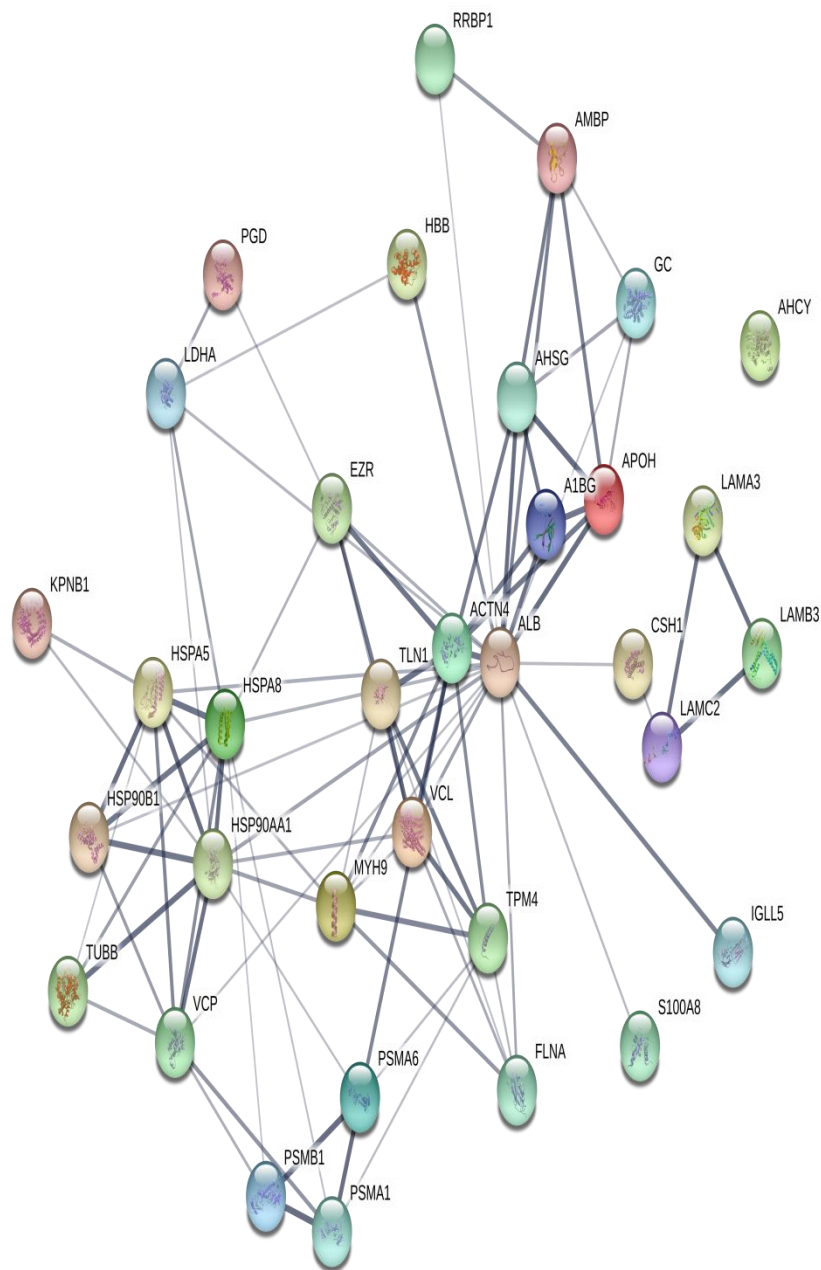


Figure 6.15: The protein network analysis for the upregulated proteins in HBTE using STRING v10.0 with a confidence level of 0.4 revealed a complex protein network. The thickness of the connecting line represents the strength of the associations. Here, each node represents a protein and the line represents the interaction between the proteins. A thicker or darker line between nodes indicates stronger interaction and vice versa.

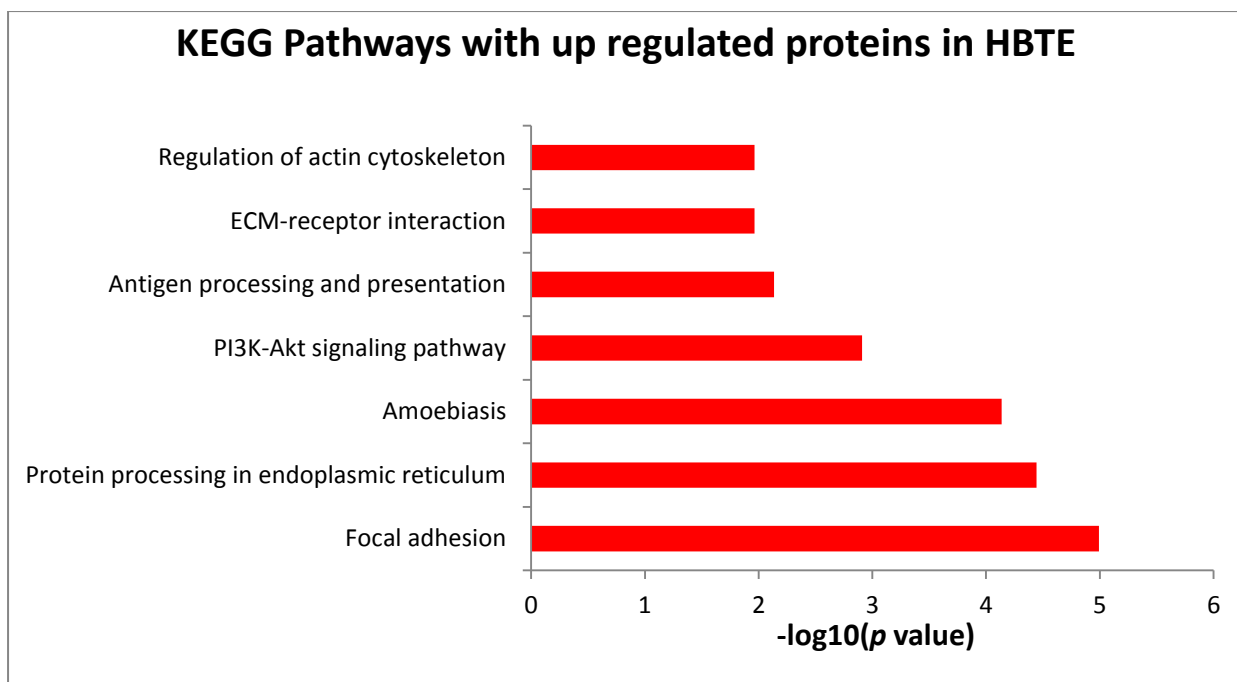


Figure 6.16: KEGG pathway analysis of up regulated proteins in HBTE exosomes. The number of the horizontal axis represents the $-\log_{10}$ of p value for the enrichment of genes with each pathway.

6.3.6 Real time PCR analysis:

The quality of the RNA was analysed by running the RNA sample on a 1.2% agarose gel for 45min. the two prominent bands represents 28S and 18S RNA around 700bp and 1100bp to 1200bp (Figure 6.17). The concentration was measured by nano drop which resulted good quality RNA from both cancer and normal cells.

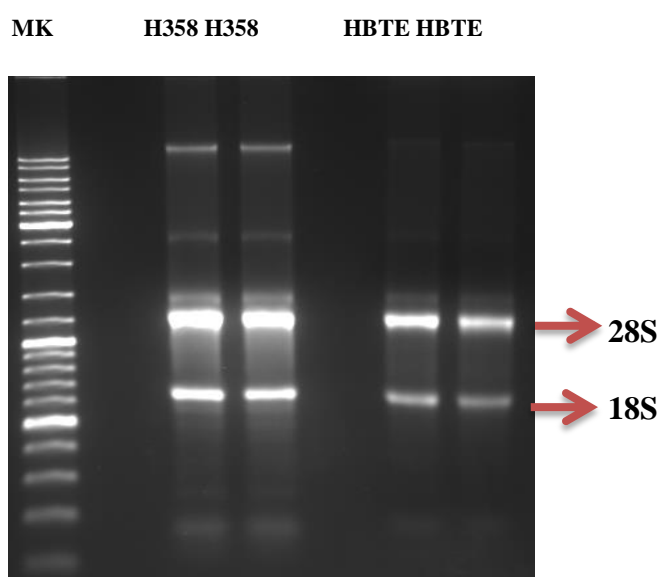


Figure 6.17: Presence of RNA on agarose gel. The dark band of 1100bp represents 28s RNA and the lighter one on 700bp represents 18s RNA.

6.3.7 Relative gene expression analysis:

Relative gene expression analysis was performed to compare the relative expression difference of RNA of the cell due to their differential regulation in exosomes. All six genes were accounted for the experiment and were done in triplicates. Beta-tubulin was used as the internal standard to normalise the values. Six different proteins were selected based on their expression on exosomes and function. Five proteins were selected after comparing literature search and upregulation in exosomes in H3588 compared to HBTE. To evaluate significance in expression t-test was carried out. All the genes from cancer cell H358 showed significant difference ($p < 0.05$) compared to the gene expression of normal cell (Figure 6.18). One protein was not (CTNNB1) present in HBTE exosome but present in H358 exosomes. The experiment was done in triplicates. Gene expression of the proteins that are upregulated in exosomes from H358 showed higher expression in their cellular level (Figure 6.18). For example, the proteomic study reveals that, TGFB2 was 2.33 fold up-regulated in H358 compared to HBTE, the highest within the six selected genes. The highest fold change was observed in their mRNA level was in ITGA3, followed by CDH1, LAMC1, TGFB2 and lastly CSTD (Table 6.4). Interestingly, the mRNA level of CTNNB1 was 2.67 fold higher in H358 cell compared HBTE even though the protein was only present in H358. The difference in their gene expression of mRNA between cancer cell (H358) and normal cell are (HBTE) shown in figure 6.18. To calculate the difference in expression, $\Delta\Delta C_t$ value was calculated using the equation from Schmittgen et al., 2008, where it was described that fold change between to samples can be calculated by using the formula of $2^{-\Delta\Delta C_t}$ (Schmittgen and Livak, 2008). The calculation was carried out using three triplicates of three independent samples from both H358 and HBTE cell lines.

Melting curve analysis was performed at the end of each cycle to test the primer pair specificity (Figure 6.19 to 6.23) at the end of each experiment. Single peak with no shouldering suggested the specificity of primer annealing. Melting curve with multiple peaks (Appendix Figure 2-19) could be due to the presence of genomic DNA or fragment of DNA which hampered the melting of the target genes. Results of melting curve analysis along with their amplification curve (Ct plots) were shown in figure 6.19 to 6.24.

Table 6.4: Gene expression analyses by qPCR of selected genes are shown in the table. The $\Delta\Delta C_t$ was calculated after the normalisation with beta tubulin. The threshold for the C_t value was considered 0.2.

Genes	Average Ct H358	Average Ct HBTE	Relative Fold Change ($2^{\Delta\Delta C_t}$)	T test (p value)
CDH1	19.3±1.19	21.74±1.19	7.12	0.004
CTNNB1	18.71±0.54	20.13±0.84	2.67	0.016
ITGA3	17.63±0.7	20.94±0.93	10.58	3.87×10^{-6}
TGFB2	7.73±0.71	9.29±0.88	2.98	0.007
CSTD	17.82±0.85	19.82±0.86	3.78	0.00073
LAMC1	19.68±0.57	21.35±1.24	2.76	0.011

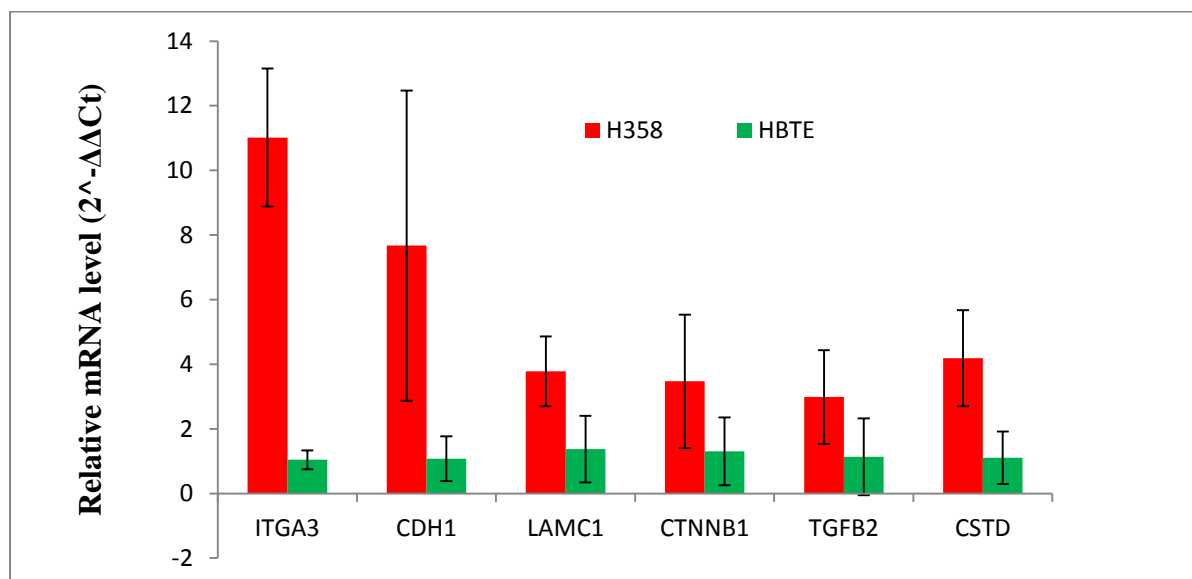


Figure 6.18: Bar graph for qRT-PCR analysis data of six selected genes of H358 and HBTE. Bar graph data are normalised with β -tubulin mRNA levels and is relative to β -tubulin mRNA levels of H358 and HBTE respectively. Significant differences ($p \leq 0.05$) have been observed in each gene.

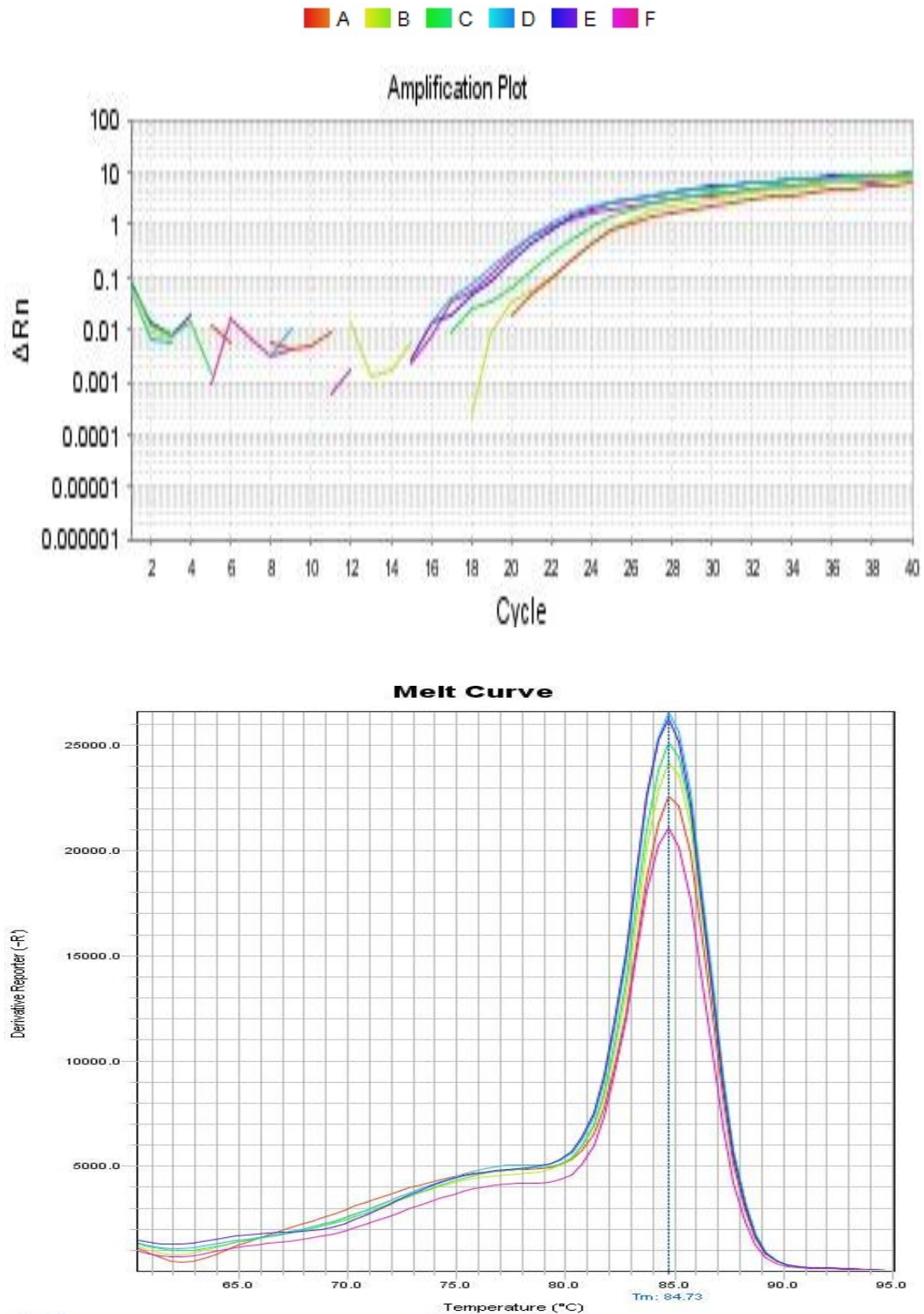


Figure 6.19: Amplification plot (Ct value) and melting curve of Integrin alpha 3 (ITGA3). The color indicates different samples. A,B and C represents triplicates of normal cell and E, F and G represents ct value and melting curve of cancer cell.

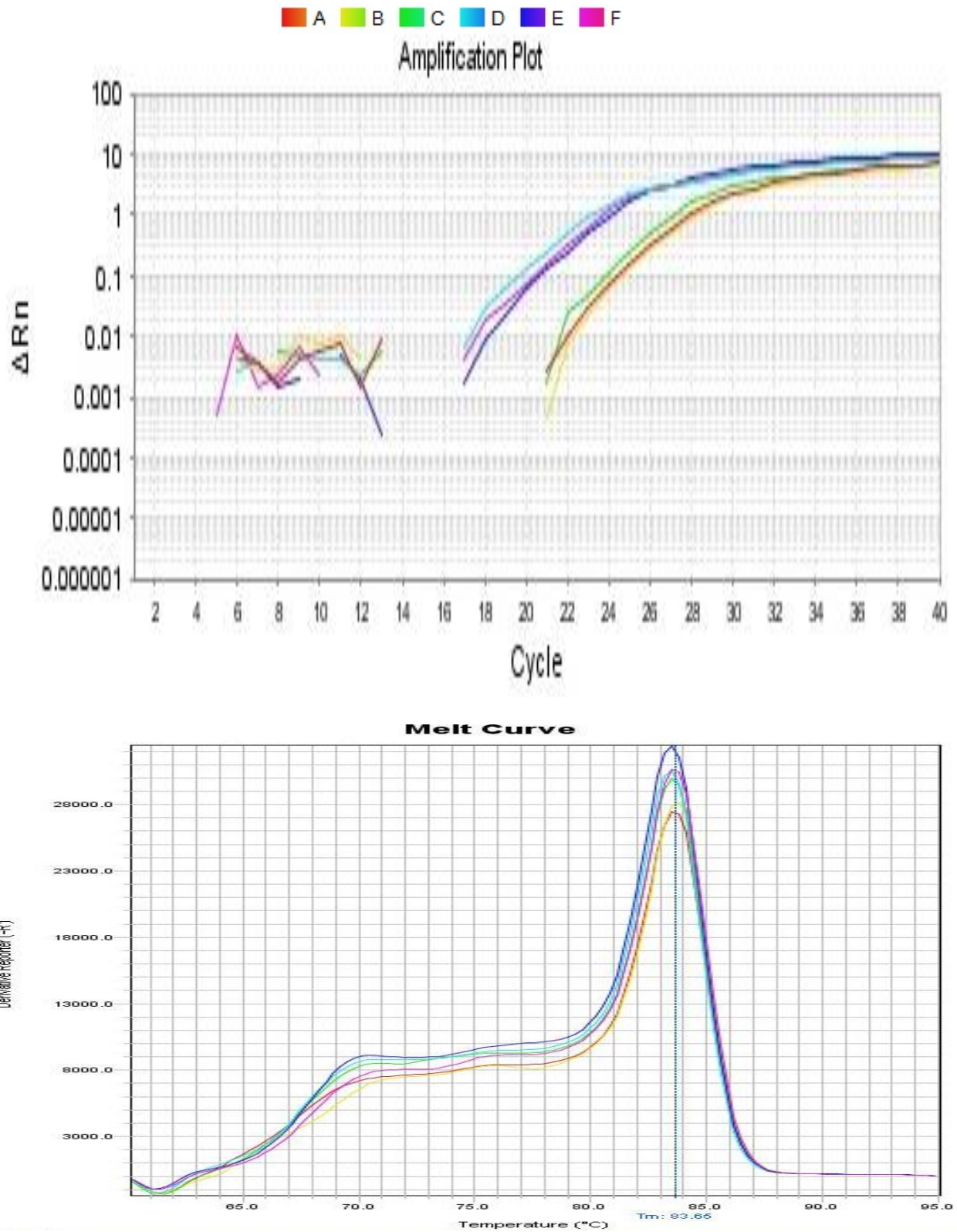


Figure 6.20: Amplification plot (Ct value) and melting curve of Cadherin 1 (CDH1). The color indicates different samples. A,B and C represents triplicates of normal cell and E, F and G represents ct value and melting curve of cancer cell.

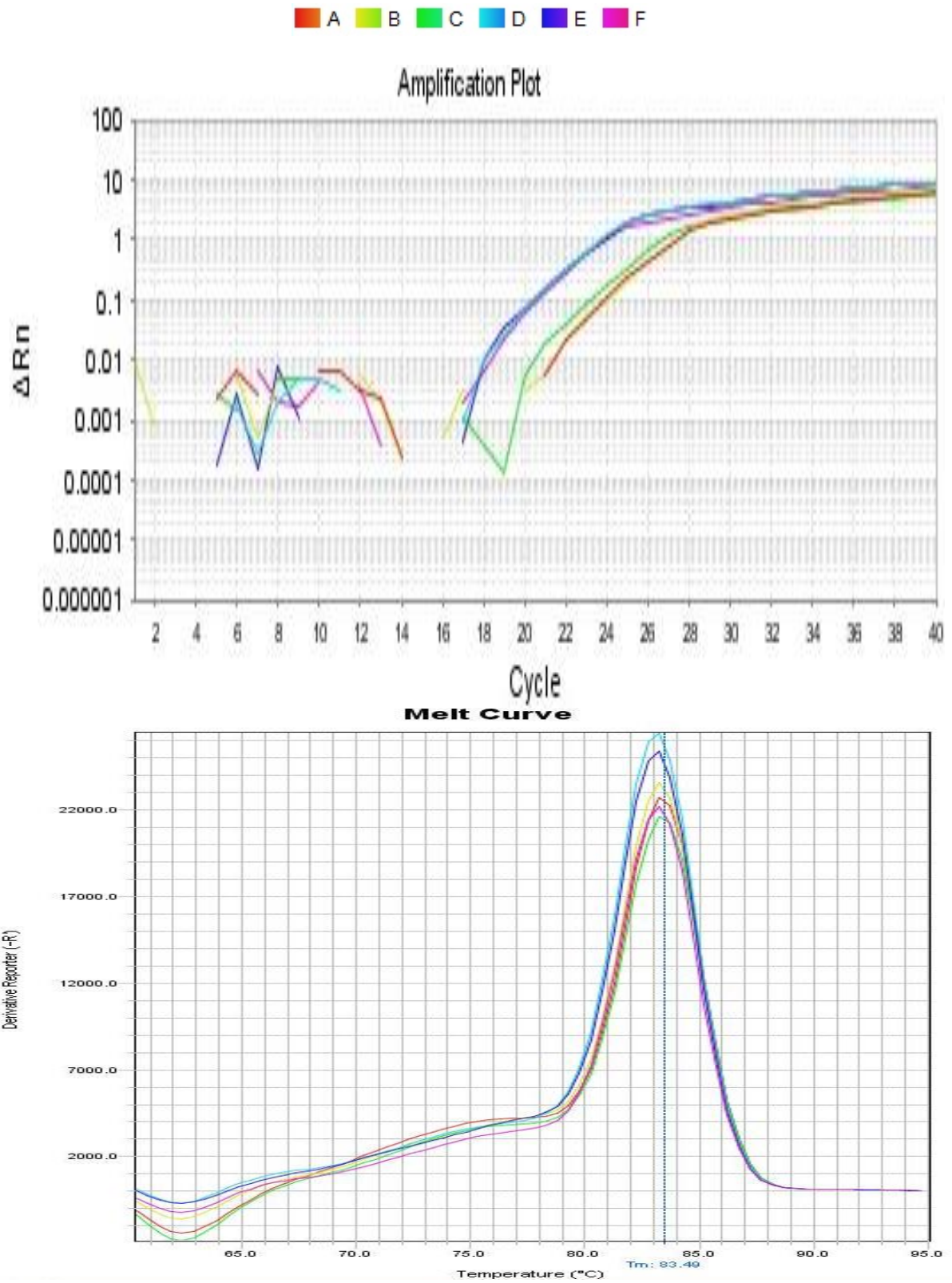


Figure 6.21: Amplification plot (Ct value) and melting curve of Laminin gamma 1 (LAMC1). The color indicates different samples. A,B and C represents triplicates of normal cell and E, F and G represents ct value and melting curve of cancer cell.

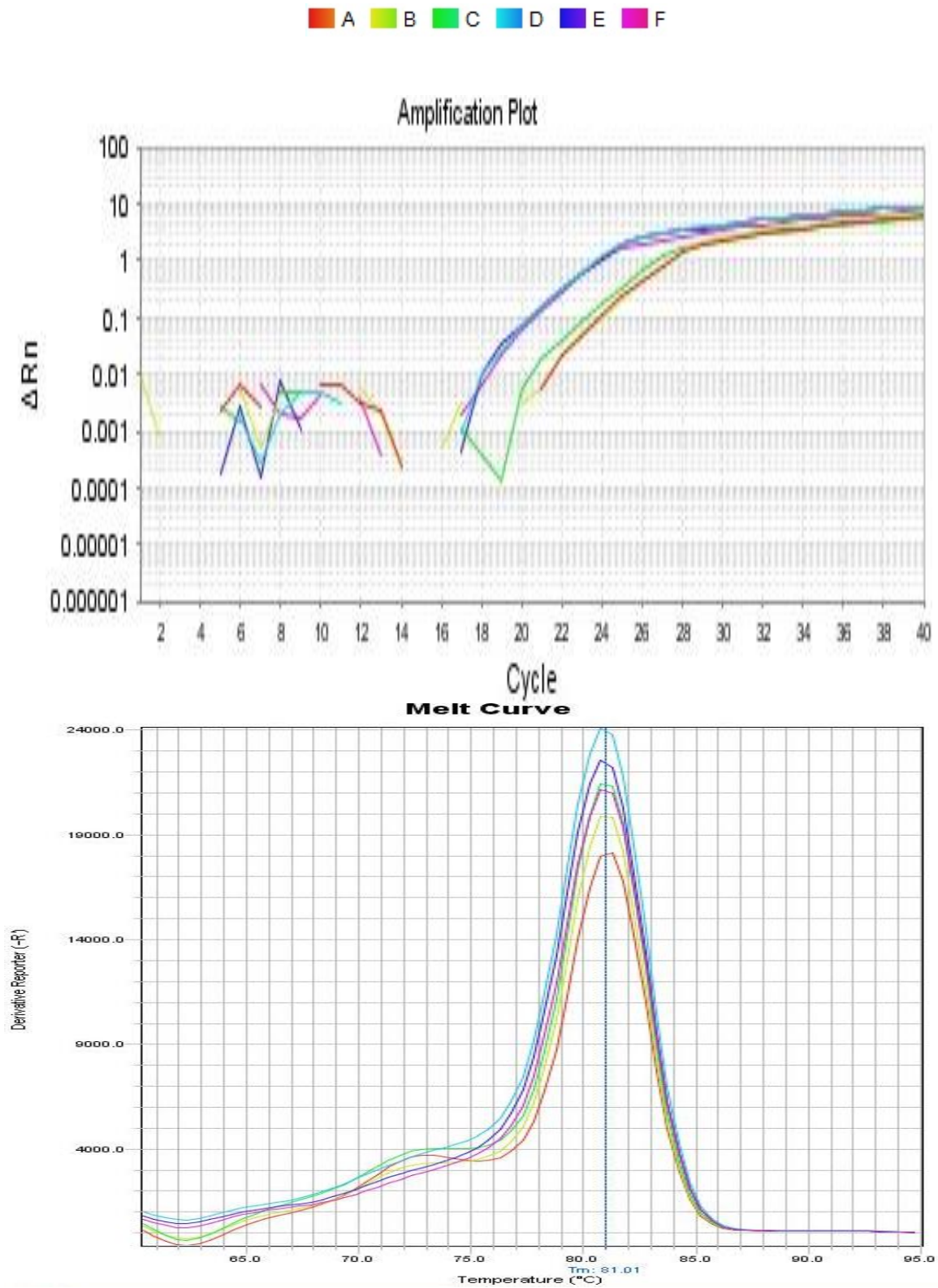


Figure 6.22: Amplification plot (Ct value) and melting curve of Catenin Beta 1 (CTNNB1). The color indicates different samples. A,B and C represents triplicates of normal cell and E, F and G represents ct value and melting curve of cancer cell.

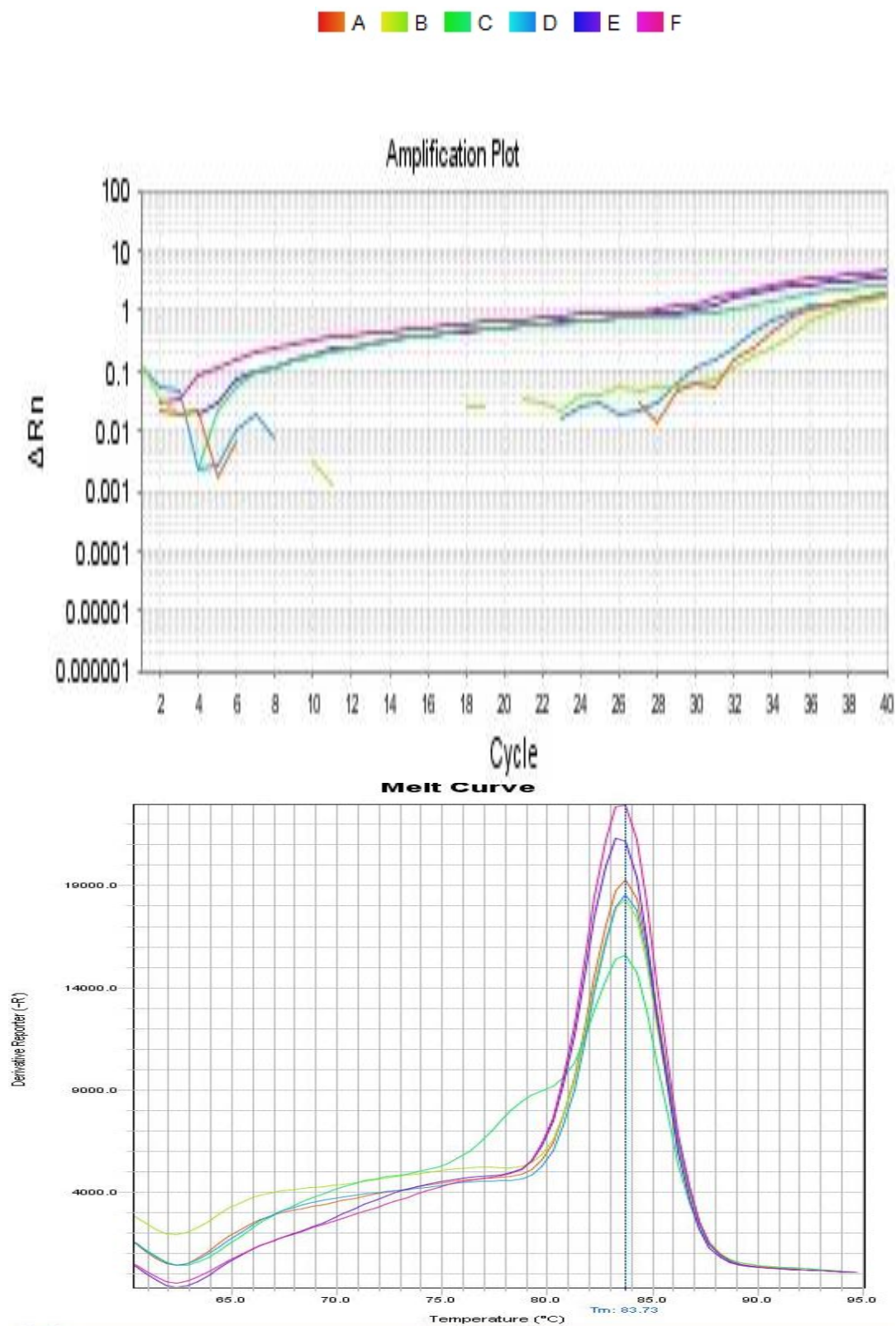


Figure 6.23: Amplification plot (Ct value) and melting curve of Transforming growth factor beta 2 (TGFB2). The color indicates different samples. A,B and C represents triplicates of normal cell and E, F and G represents ct value and melting curve of cancer cell.

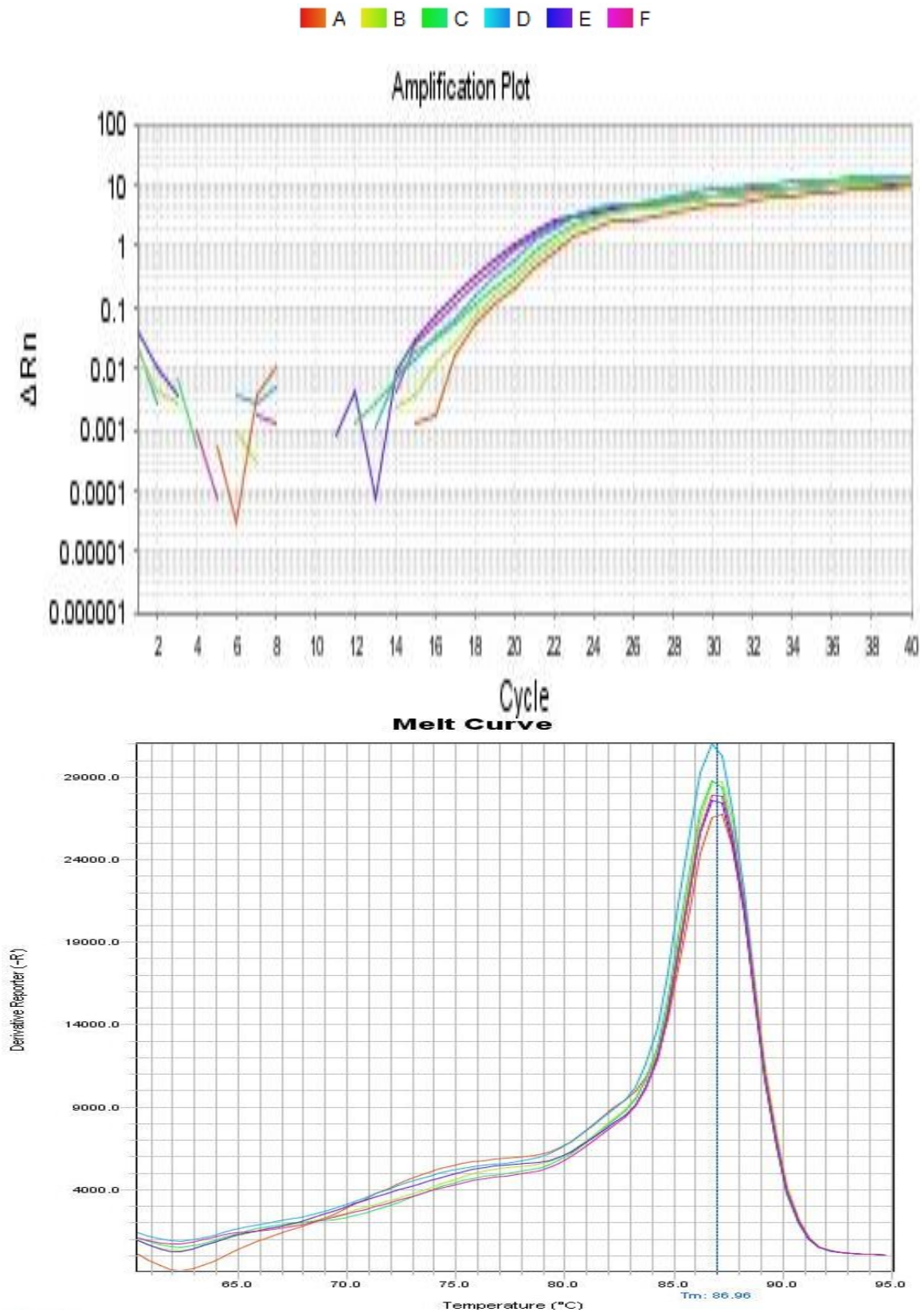


Figure 6.24: Amplification plot (Ct value) and melting curve of Cathepsin D (CSTD). The color indicates different samples. A,B and C represents triplicates of normal cell and E, F and G represents ct value and melting curve of cancer cell.

6.4 Discussion:

Comparative study of exosomes between normal and pathological conditions have been used extensively in recent years to investigate the differences in their proteomic signatures due to their stability in biological fluids and their ability to carry genetic information across cells (Henderson and Azorsa, 2012). To investigate the proteomic differences it is very important to characterise exosomes because the unique proteomic signature can indicate biological information about the state of the diseases (Hegmans et al., 2004). To compare the proteomic differences between lung cancer cell and normal cell derived exosomes, non-small cell lung cancer cell line H358 and primary cell line HBTE was used. Identification of exosomes from H358 was previously described in chapter 3. However to compare the morphological characteristics of H358 and HBTE exosomes from both the cell lines were isolated using the PEG method described in chapter 4. TEM analysis was performed to compare the morphology of the exosomes from lung cancer cell line with its normal counterpart HBTE. The size of the exosomes from primary lung cell HBTE was $85.7 \pm 17 \text{ nm}$, which is just a little on average smaller than its counterpart H358 exosomes but was comparable with previously studied non cancerous cell derived exosomes. For example, exosomes were isolated from primary thymic epithelial cell derived exosomes showed a size of 136nm (Skogberg et al., 2015).

In this chapter, comparative proteomic study was carried out between H358 and HBTE cell derived exosomes following the similar LC-MS approach described in previous chapter (Chapter 5.5.3). A total of 1011 proteins were identified which is a little higher than previously published proteomic studies. For example, in a quantitative proteomic study on exosomes from differentiated and differentiated primary calvarial osteoblasts of a mouse model, a total of 336 proteins were identified, while 770 proteins were identified from HIV-1 infected and uninfected exosomes from lymphocytic H9 cells in another study (Bilen et al., 2017; Li et al., 2012).

GO analysis revealed in this study that, proteins involved in response to stimulus, biological adhesion were comparatively higher in exosome from H358 than exosomes from HBTE (Figure 6.3). In contrast, number of proteins involved in metabolic process, localisation and cellular process was higher in HBTE exosomes. Exosomes from both cell lines were almost equally enriched with membrane proteins (Figure 6.4). Several studies have suggested that exosomes are enriched with membranous protein as they are present in the exosomal

membrane as they are essential for exosome release. For example, vesicle-associated membrane protein 7 was found to be essential in the formation of multivesicular bodies as well as release of exosomes from the cells in a study carried on human leukemic cell line K562 (Fader et al., 2009).

The current comparative proteomics also identified several extracellular matrix (ECM) proteins. It has been reported previously that, ECM proteins not only aid in the mechanical and structural supports but also plays a vital role in cancer progression via cellular signalling (Kim et al., 2011). In this study 66.84% and 70.34% of total proteins were from extracellular region from HBTE and H358 exosomes respectively. Several ECM proteins were identified in this study which includes fibronectin, prelamin, and integrins. Several integrin molecules have been reported to enhance cancer progression by binding with several ECM molecules with different affinity and regulate the fate of the cellular behaviour and cell signalling (Alam et al., 2007). Several ECM molecules with up regulation were observed in this study. For example, fibronectin, prelamin, agrin were all up regulated in H358 exosome, compared to HBTE exosomes. Fibronectin along with its integrin receptor adheres to the cell surface due to the low adhesiveness of tumour cells compared to normal cells (Ruoslahti, 1999).

In this study, cellular adhesion molecules, extracellular matrix proteins, cell signalling molecule were enriched in both exosomes. Several signalling proteins involved in cellular proliferation and biological regulation such as CDH1, CNTNB1, MFGE8, TGFB2, LAMC1, and ITGA3 were upregulated in H358 exosomes compared to HBTE exosomes (Table 6.3). Several studies have the similar results exosomes. For example, proteomic study between NCSLC pleural effusion and its counter-part revealed the similar overlap of protein profiling with (Clark et al., 2016). Several heat shock proteins showed higher expression in H358 exosomes which includes Hsp60, stress protein-70. Heat shock proteins are molecular chaperones and important for protein folding, transport, and mediating the formation of protein structures which is vital for the survival of cells from stress. The heat shock protein family is considered as a potential molecular biomarker and therapeutic target as they are reported to be over expressed in most of the tumorous lung cells compared to their adjacent normal cells (Seiwert et al., 2005) and aid in the development of several cancer progression. For example, overexpression of Hsp70 was reported in lung, liver, colorectal and cervical cancers while their downregulation was observed in renal cancer (Wu et al., 2017).

Proteins mostly involved in cancer pathways such as PI3K-Akt signalling pathways, focal adhesion are family members of integrin and laminin were either absent or down regulated in HBTE. For example, integrin alpha 3, 5, beta 4 and 6 were down regulated by at least 1.5 fold (Table 6.3). Both integrin and laminin play vital role in cell proliferation and metastasis. Their cellular adhesion properties are reported to play vital role in metastasis and tumour growth (Ganguly et al., 2013). Integrin and laminins are two of the most vital cell surface receptors (Zaidel-Bar et al., 2007) that localizes on the epithelial cell surface and binds with filaments to form a multiprotein adhesion complex called hemidesmosomes (Caccavari et al., 2009). The expression of integrin alpha 4 and 6 were analysed on a biopsy samples from tumours from head and neck which suggested that upregulation of hemidesmosomes components such as integrin alpha 4 and 6 was directly correlated with metastasis and tumour growth (Herold-Mende et al., 2001). Furthermore, cell adhesion molecule catenin beta and delta 1 were absent in HBTE and cadherin 1, another cellular adhesion molecule is upregulated in H358. Catenin family proteins are vital components of cell adhesion complex. Catenin beta is an important component of Wnt signalling which is associated with cancer progression and metastasis (Park et al., 2017). Although, several reports have demonstrated that downregulation of CDH1 promotes cancer metastasis, however few reports have also demonstrated the up regulation of CDH1 in non-small lung cancers specially bronchial alveolar carcinomas or adenocarcinomas (Clark et al., 2016; Lee et al., 2002). In addition, BCA-1, fibronectin, are considered as biomarker for lung cancer were up regulated in H358 exosomes (Mehan et al., 2012).

CDH1, CTNNB1, ITGA3, CTSD, LAMC1 and TGFB2 were selected for their gene expression analysis from the comparative proteomics on exosomes from H358 and HBTE which showed significant difference between H358 and HBTE ($p < 0.05$). Apart from CTNNB1, five of the six selected proteins were upregulated in H358 exosomes compared to HBTE exosomes (Table 6.4), while CTNNB1 was only present in H358 exosomes and did not show any expression in the three triplicates of HBTE exosomes. The gene expression analysis was carried out on cellular level. The qualitative RT-PCR analysis of relative gene expression levels in the cell revealed that, the mRNA levels in the cell of five of the selected up regulated proteins in exosomes were higher compared to the HBTE exosomes (Figure 6.18). Surprisingly, the mRNA of CTNNB1 was positive in both cells, even though the protein was only present in H358 exosomes. The mechanism behind the differential protein recruitment of exosomes is not properly established (Zhang et al., 2015). Nevertheless, it has

been suggest that the protein sorting in to exosomes partially depend on the parent cells to some extent (Schorey et al., 2015) although the relative mRNA levels and their subsequent protein expression remains still unclear (Pascal et al., 2008), but the mRNA level of CTNNB1 was found higher in cancer cells compared to its subsequent normal cells in several reports. For instance, previously it was demonstrated by RT-PCR and western blot analysis, overexpression of CTNNB1 was observed with cell proliferation, migration, invasion and inhibition of apoptosis on renal cell carcinoma and inhibition of CTNNB1 resulted with poor cell proliferation, migration and induction of apoptosis (Yang et al., 2017).

6.5 Conclusion:

Lung cancer being the second most cause of death worldwide there is still not enough resources to enhance the diagnosis and treatment. The study presented in this chapter shows valuable insights about the similarities and differences of exosomes between lung cancer cell line and its counterpart normal cell line. The comarasion between exosomes from lung cancer cell line H358 and normal lung cell HBTE showed distinct differences in their proteomic profiling. Integrin alpha-3, cadherin-1, transforming growth factor beta-2, cathepsin D, lamimin gamma-1 can be considered as potential biomarkers for non-small cell lung cancer as these proteins were over expressed in exosomes from lung cancer cell line H358. Their gene expression in cellular level was also significantly higher in lung cancer cell line compared to normal cell line. Catenin beta-1 can aslo been used as potential biomarker for non-small cell lung cancer as the gene expression of catenin beta-1 shown higher expression in cancer cell than normal cell and the protein was absent in all three replicates. The mRNA level of catenin beta 1 in H358 and HBTE exosomes illustrate the selective recruitment of proteins into exosomes which can be useful for future biomarker research with further clinical research. The relative gene expression data is the first to this lung cancer cell line and its counterpart which can be useful for future biomarker search NSCLC with further clinical research.

Chapter 7:

General discussion and future prospects

7.1 General Discussion:

Cancer is the one of the leading cause of death all around the world including United States. According to the American Society of Cancer Report 2018, lung cancer is one of the major causes of cancer related deaths in the US where more than 234 thousand new cancer patients are expected in 2018. The expected new breast cancer numbers are even more than lung cancer for women. Within 2018, around 266 thousand patients are expected to be diagnosed with breast cancer in US alone (Siegel et al., 2018). The management of cancer involves careful staging and interpretation of clinical information (Mariotto et al., 2014). The major challenge with cancer is their diagnosis and proper treatment at early stages (Halvaei et al., 2018). The major advantages of exosomes as a biomarker in clinical studies include their ease of availability, cost effectiveness and easy to analyse compare to the genetic testing which is expensive and requires trained personnel to analyse the samples (Sharma et al., 2017). The traditional tissue biopsy tests for cancer screening are not sufficient enough to diagnosis cancer properly. Furthermore, no diagnosis method available today detects cancer without hurting physical condition of the patients. For example, radiology is one of the most used methods of cancer detection but too excessive ionising radiation could cause serious health risks (Han et al., 2017), non-radiation methods such as ultrasound scan and magnetic resonance imaging are not fully capable to detect minimal residual diseases (Chaudhuri et al., 2015). In addition, the solid or tissue biopsy method has been reported to lack the ability to detect dynamic changes in tumor due to the tumour heterogeneity and can not detect cancer accurately (Hiley et al., 2014; Ignatiadis et al., 2015). This highlights for new and improved tools that can reduce the amount of clinical work needed to diagnose and manage cancer (Liu et al., 2015) for example, liquid biopsy which relies on extracellular particles and their cargo such as exosomes. Exosome based liquid biopsy is far more superior to other sources of liquid biopsy such as microvesicles, apoptotic bodies because unlike other subcellular vesicles exosomes are more heterogeneous in nature (Halvaei et al., 2018). However, there are no set up method to isolate exosomes and every methods available to isolate exosomes such as ultracentrifugation or precipitation method have its own advantages

and disadvantages which hampers the purity of exosomes and hence limited the use of exosomes as biomarkers in clinical study (Thind and Wilson, 2016).

The research presented within this thesis has focussed on the identification and characterisation of purified exosomes and their protein content, secretion pattern and number of exosomes in relation to the cellular growth. Several studies have documented proteomic studies to create a central proteomics based on common cell lines used in cancer study (Geiger et al., 2012). However, such a platform for exosomal proteins has not been done yet. The work presented here is a start for such a platform based on exosomal proteins. In addition, the comparative proteomics between the lung cancer cell line H358 and its counterpart HBTE is the first to the best of my knowledge which provides valuable information about future development of lung cancer biomarkers.

It has been proposed that molecular profiling or combining currently available diagnostic tests may improve the diagnosis and monitoring of cancer as compared to using a single marker test (Goodison et al., 2013; Hassanein et al., 2012). Whether single or multiple markers to be used for the diagnostic tests, it is clear that exosomes can be an ideal source for the hunt for these biomarkers due to their availability and biological properties (Fliser et al., 2007). Exosomes are a subcellular fraction of the whole cell and reported to be enriched in tumour antigens and membrane proteins. These enriched proteins are thought to be specifically incorporated in to exosomes during their biogenesis in the endocytic tract (They et al., 2001). As well as membrane proteins, several stress-related proteins can also be elevated in exosomes from cells undergoing forms of stress such as hypoxia, heat or radiation. In this situation exosomes can represent the stress states of the parent cell. Overall, cancer derived exosomes may provide a complex panel of cancer associated protein markers that could be detected using an exosome based multiple biomarker assay (Seo et al., 2012).

There is no set up method to isolate and purify exosomes from variable source which led to the use of variety of methods each one of them with varying degrees of purity and comparable results (Lobb et al., 2015). And sometimes the choice is between availability of equipment, time and cost effectiveness. As this is a proteomic study, methods were chosen based on the capability to isolate more exosomal proteins from the cell culture supernatant since protein concentration plays a vital part in any proteomic studies. In this study both ultra-centrifugation and polymer based isolation were compared and polymer based method was chosen because of its ability to yield more protein than ultra-centrifugation (Rider et al., 2016). Although more elaborate improvement could enhance the purity of exosome isolation, the in-house PEG based isolation can be used a starting method which yielded comparable

quality with the commercial product while saving time and cost. The issues concerning the quality of exosome samples are something that needs to be addressed. In this study, exosomes were isolated using PEG based in-house polymer consistently from conditioned cell culture medium of three cancer cell lines. However, at first exosomes were isolated by ultracentrifugation technique and commercial kit for the identification and characterisation of exosomes but the protein concentration of the resulted exosomes were very low for any kind of proteomic study. So, in order to optimise the protein concentration and the number of exosomes needs to reach that concentration, the dynamics of exosome release in relation to cellular growth was carried out without altering any of the cell culture conditions like level of oxygen, temperature and carbon dioxide. This study resulted with valuable information about the number of exosomes with relation to the growth time and the number of cells. It also provided the information about the approximate time to collect exosomes to achieve peak concentration of exosomal protein.

Proteomics study on exosomes has previously identified proteins of importance in exosome biology and also potentially significant proteins in disease (Liu et al., 2015). The issues that hampered the 2D gel electrophoresis were the methods of preparing exosomes for 2D gel electrophoresis, concentration and low abundance of proteins in exosome samples. The 2D gel method was developed using the cellular proteins due to the number and higher abundance of proteins in the cell. But due to the possibilities of lower abundant proteins to be potential biomarker, LC-MS was chosen over 2D gel electrophoresis to detect the lower abundance proteins. Because the detection limit of LC-MS is higher than gel electrophoresis. In this proteomic study, highly purified exosomes were used which were characterised by various techniques including western blot, DLS and also electron microscopy. The exosomes were derived from three cancer cell lines including lung cancer cell line H358, leukemic cell line THP1 and breast cancer cell line MCF7, resulted with a total of 1596 proteins using LC-MS with only good quality MS data and two or more peptides were reported in the final result giving a false discovery rate of 1.0. The number of proteins identified in this study is very comparable to other exosomal study and one of the very few as a comprehensive comparative proteomic study as well as the first to do a comprehensive proteomic study on Broncho alveolar lung cancer cell line H358 derived exosomes and its counterpart.

Proteomic study of exosomes irrespective of cell lines revealed that exosomes are enriched in membrane proteins. Several reports suggest that membrane proteins are involved in cellular signalling. For example, extracellular matrix proteins integrins, laminins, catenins, tenascin, heat shock proteins as well as several growth factor receptors such as transforming growth

factor receptors, platelet derived growth factor receptors are constantly reported for their role in the cellular signalling.

7.2 Conclusion:

The studies presented in this thesis aimed to enhance the understanding of the role of exosomes play in intercellular signalling in different cancer cells with different metastatic potentials including lung cancer, breast cancer and leukaemia. To achieve that, the proteome of exosome from three different cancer cell lines were compared with each other showing several similarities with some difference which suggest that regardless of the source of exosomes, their composition is very comparable to each other with distinct difference which separates them from each other. Then the proteome of lung cancer cell was compared in both normal lung cell lines. The results of the comparative proteomics of lung cancer and its counterpart opened up possibilities not only for new biomarker targets as well as possible new therapeutic targets. Further research needed on the gene expression on several proteins to further characterise them as cancer biomarker.

7.3 Future prospects:

Exosome is a promising field for future cancer research. It opens up opportunities in search for new biomarker tool for diagnosis and therapeutic drug delivery. However, several lacking still needs to be addressed. For example, an exosome isolation method which is not only time efficient but also would now require any special equipment such as ultracentrifugation, a method where the exosomes would be free from contaminating proteins and other extracellular vesicles. Such method is urgently needed for future exosomes research where the final product of the preparation will not have the above mentioned issues.

Several similarities and difference have been reported in the comparative proteomic study of three different cancer cell lines. The result presented within the comparative study of three different cancer cell lines can be useful for characterising exosome biology in different cancers.

The results of any comparative proteomic study offer opportunities of endless possibilities, for example, it defines the similarities and differences within the experimented samples. Several key findings are beneficial for future exosomal work. For example, the relative mRNA level of CTNNA1 was positive on both cell lines including H358 and HBTE on cellular level. Although the mRNA level CTNNA1 was more than 3 fold higher in H358 cell

line however the protein was present in any of the triplicates of exosomes from HBTE which could suggest the protein CTNNB1 was not transferred into the exosomes. Extensive research needs to be carried out on the protein expression of CTNNB1 on cellular level including cancer and normal exosomes. The results presented here were based on *in vitro* study on established cell lines. Similar proteomic approach needs to be taken from clinical samples thus finding much more information which will be helpful for future biomarker research. Nonetheless, further research needs to be addressed to establish to further characterise CTNNB1, CDH1, ITGA3, and LAMC1 as a general biomarker signature for cancer including lung cancer.

Chapter 8:

References:

- Aalberts, M., Stout, T.A.E. and Stoorvogel, W. (2014), “Prostasomes: Extracellular vesicles from the prostate”, *Reproduction*, Vol. 147 No. 1, available at:<https://doi.org/10.1530/REP-13-0358>.
- Abramowicz, A., Widlak, P. and Pietrowska, M. (2016), “Proteomic analysis of exosomal cargo: the challenge of high purity vesicle isolation”, *Mol. BioSyst.*, Vol. 12 No. 5, pp. 1407–1419.
- Admyre, C., Johansson, S.M., Qazi, K.R., Filen, J.-J., Lahesmaa, R., Norman, M., Neve, E.P.A., et al. (2007), “Exosomes with Immune Modulatory Features Are Present in Human Breast Milk”, *The Journal of Immunology*, Vol. 179 No. 3, pp. 1969–1978.
- Agarwal, K., Saji, M., Lazaroff, S.M., Palmer, A.F., Ringel, M.D. and Paulaitis, M.E. (2015), “Analysis of exosome release as a cellular response to MAPK pathway inhibition”, *Langmuir*, Vol. 31 No. 19, pp. 5440–5448.
- Ahmad, S.S., Glatzle, J., Bajaeifer, K., Buhler, S., Lehmann, T., Konigsrainer, I., Vollmer, J.-P., et al. (2013), “Phosphoglycerate kinase 1 as a promoter of metastasis in colon cancer.”, *International Journal of Oncology*, Vol. 43 No. 2, pp. 586–590.
- Aktipis, C.A., Boddy, A.M., Jansen, G., Hibner, U., Hochberg, M.E., Maley, C.C. and Wilkinson, G.S. (2015), “Cancer across the tree of life: cooperation and cheating in multicellularity”, *Philosophical Transactions of the Royal Society B: Biological Sciences*, Vol. 370 No. 1673, pp. 20140219–20140219.
- Alam, N., Goel, H.L., Zarif, M.J., Butterfield, J.E., Perkins, H.M., Sansoucy, B.G., Sawyer, T.K., et al. (2007), “The integrin—growth factor receptor duet”, *Journal of Cellular Physiology*, Vol. 213 No. 3, pp. 649–653.
- Alexandrov, L.B., Ju, Y.S., Haase, K., Van Loo, P., Martincorena, I., Nik-Zainal, S., Totoki, Y., et al. (2016), “Mutational signatures associated with tobacco smoking in human cancer”, *Science*, Vol. 354 No. 6312, pp. 618–622.
- Alvarez-Erviti, L., Seow, Y., Schapira, A.H., Gardiner, C., Sargent, I.L., Wood, M.J.A. and Cooper, J.M. (2011), “Lysosomal dysfunction increases exosome-mediated alpha-

- synuclein release and transmission”, *Neurobiology of Disease*, Vol. 42 No. 3, pp. 360–367.
- American Cancer Society. (2015), “Breast Cancer Facts & Figures 2015-2016.”, *American Cancer Society*, pp. 1–44.
- American Cancer Society. (2017), “Cancer Facts & Figures 2017”, *Cancer Facts & Figures 2017*, p. 1.
- EL Andaloussi, S., Mäger, I., Breakefield, X.O. and Wood, M.J.A. (2013), “Extracellular vesicles: biology and emerging therapeutic opportunities”, *Nature Reviews Drug Discovery*, Vol. 12 No. 5, pp. 347–357.
- Andre, F., Scharz, N.E.C., Movassagh, M., Flament, C., Pautier, P., Morice, P., Pomel, C., et al. (2002), “Malignant effusions and immunogenic tumour-derived exosomes”, *Lancet*, Vol. 360 No. 9329, pp. 295–305.
- Andreu, Z. and Yáñez-Mó, M. (2014), “Tetraspanins in extracellular vesicle formation and function.”, *Frontiers in Immunology*, Frontiers Media SA, Vol. 5, p. 442.
- Antonyak, M.A., Li, B., Boroughs, L.K., Johnson, J.L., Druso, J.E., Bryant, K.L., Holowka, D.A., et al. (2011), “Cancer cell-derived microvesicles induce transformation by transferring tissue transglutaminase and fibronectin to recipient cells”, *Proceedings of the National Academy of Sciences*, Vol. 108 No. 12, pp. 4852–4857.
- Aoka, Y., Johnson, F.L., Penta, K., Hirata, K.I., Hidai, C., Schatzman, R., Varner, J.A., et al. (2002), “The embryonic angiogenic factor Dell1 accelerates tumor growth by enhancing vascular formation”, *Microvascular Research*, Vol. 64 No. 1, pp. 148–161.
- Atha, D.H. and Ingham, K.C. (1981), “Mechanism of precipitation of proteins by polyethylene glycols. Analysis in terms of excluded volume.”, *Journal of Biological Chemistry*, Vol. 256 No. 23, pp. 12108–12117.
- Atkinson, A.J., Colburn, W.A., DeGruttola, V.G., DeMets, D.L., Downing, G.J., Hoth, D.F., Oates, J.A., et al. (2001), “Biomarkers and surrogate endpoints: Preferred definitions and conceptual framework”, *Clinical Pharmacology and Therapeutics*.
- Azmi, A.S., Bao, B. and Sarkar, F.H. (2013), “Exosomes in cancer development, metastasis, and drug resistance: A comprehensive review”, *Cancer and Metastasis Reviews*, December.

- Balaj, L., Atai, N.A., Chen, W., Mu, D., Tannous, B.A., Breakefield, X.O., Skog, J., et al. (2015), “Heparin affinity purification of extracellular vesicles”, *Scientific Reports*, Vol. 5 No. 1, p. 10266.
- Balcer-Kubiczek, E.K., Yin, J., Lin, K., Harrison, G.H., Abraham, J.M. and Meltzer, S.J. (1995), “p53 mutational status and survival of human breast cancer MCF-7 cell variants after exposure to X rays or fission neutrons.”, *Radiation Research*, Vol. 142 No. 3, pp. 256–262.
- Bang, C. and Thum, T. (2012), “Exosomes: New players in cell-cell communication”, *International Journal of Biochemistry and Cell Biology*.
- Bartosch, B., Dubuisson, J. and Cosset, F.-L. (2003), “Infectious Hepatitis C Virus Pseudo-particles Containing Functional E1–E2 Envelope Protein Complexes”, *The Journal of Experimental Medicine*, Vol. 197 No. 5, pp. 633–642.
- Batrakova, E. V. and Kim, M.S. (2015), “Using exosomes, naturally-equipped nanocarriers, for drug delivery”, *Journal of Controlled Release*, Vol. 219, pp. 396–405.
- Beach, A., Zhang, H.G., Ratajczak, M.Z. and Kakar, S.S. (2014), “Exosomes: An overview of biogenesis, composition and role in ovarian cancer”, *Journal of Ovarian Research*, available at:<https://doi.org/10.1186/1757-2215-7-14>.
- Beinert, T., Munzing, S., Possinger, K. and Krombach, F. (2000), “Increased expression of the tetraspanins CD53 and CD63 on apoptotic human neutrophils”, *J. Leukoc. Biol.*, Vol. 67 No. 3, pp. 369–373.
- Belinsky, S.A. (2004), “Gene-promoter hypermethylation as a biomarker in lung cancer”, *Nature Reviews Cancer*.
- Benedikter, B.J., Bouwman, F.G., Vajen, T., Heinzmann, A.C.A., Grauls, G., Mariman, E.C., Wouters, E.F.M., et al. (2017), “Ultrafiltration combined with size exclusion chromatography efficiently isolates extracellular vesicles from cell culture media for compositional and functional studies”, *Scientific Reports*, Vol. 7 No. 1.
- Bharti, A., Ma, P.C. and Salgia, R. (2013), “Biomarker discovery in lung cancer--promises and challenges of clinical proteomics.”, *Mass Spectrometry Reviews*, Vol. 26 No. 3, pp. 451–466.
- Bilen, M.A., Pan, T., Lee, Y.C., Lin, S.C., Yu, G., et al. (2017), “Proteomics Profiling of

- Exosomes from Primary Mouse Osteoblasts under Proliferation versus Mineralization Conditions and Characterization of Their Uptake into Prostate Cancer Cells”, *Journal of Proteome Research*, Vol. 16 No. 8, pp. 2709–2728.
- Bissell, M.J. and Hines, W.C. (2011), “Why don’t we get more cancer? A proposed role of the microenvironment in restraining cancer progression”, *Nature Medicine*. Vol. 17(3). pp. 320-329.
- Blackstock, W.P. and Weir, M.P. (1999), “Proteomics: Quantitative and physical mapping of cellular proteins”, *Trends in Biotechnology*, 1 March. Vol. 17(3). pp. 121-127.
- Blair, A., Hogge, D.E. and Sutherland, H.J. (1998), “Most acute myeloid leukemia progenitor cells with long-term proliferative ability in vitro and in vivo have the phenotype CD34(+)/CD71(-)/HLA-DR-.”, *Blood*, Vol. 92 No. 11, pp. 4325–35.
- Blanchard, N., Lankar, D., Faure, F., Regnault, A., Dumont, C., Raposo, G. and Hivroz, C. (2002), “TCR Activation of Human T Cells Induces the Production of Exosomes Bearing the TCR/CD3/ Complex”, *The Journal of Immunology*, Vol. 168 No. 7, pp. 3235–3241.
- Blum, D., Hemming, F.J., Galas, M.C., Torch, S., Cuvelier, L., Schiffmann, S.N. and Sadoul, R. (2004), “Increased Alix (apoptosis-linked gene-2 interacting protein X) immunoreactivity in the degenerating striatum of rats chronically treated by 3-nitropropionic acid”, *Neuroscience Letters*, Vol. 368 No. 3, pp. 309–313.
- Bobrie, A., Colombo, M., Raposo, G. and Théry, C. (2011), “Exosome Secretion: Molecular Mechanisms and Roles in Immune Responses”, *Traffic*. Vol. 12(12), pp. 1259-1268.
- De Bock, M., De Seny, D., Meuwis, M.A., Chapelle, J.P., Louis, E., Malaise, M., Merville, M.P., et al. (2010), “Challenges for biomarker discovery in body fluids using SELDI-TOF-MS”, *Journal of Biomedicine and Biotechnology*, Vol. 2010.
- Böing, A.N., van der Pol, E., Grootemaat, A.E., Coumans, F.A.W., Sturk, A. and Nieuwland, R. (2014), “Single-step isolation of extracellular vesicles by size-exclusion chromatography”, *Journal of Extracellular Vesicles*, Vol. 3 No. 1.
- Bosque, A., Dietz, L., Gallego-Lleyda, A., Sanclemente, M., Iturralde, M., Naval, J., Alava, M.A., et al. (2016), “Comparative proteomics of exosomes secreted by tumoral Jurkat T cells and normal human T cell blasts unravels a potential tumorigenic role for valosin-

- containing protein.”, *Oncotarget*, Vol. 7 No. 20, pp. 29287–29305.
- Bozzuto, G., Ruggieri, P. and Molinari, A. (2010), “Molecular aspects of tumor cell migration and invasion”, *Annali dell’Istituto Superiore Di Sanita*, Vol. 46 No. 1, pp. 66–80.
- Brabletz, T. (2012), “To differentiate or not — routes towards metastasis”, *Nature Reviews Cancer*, Vol. 12 No. 6, pp. 425–436.
- Brambilla, E. and Gazdar, A. (2009), “Pathogenesis of lung cancer signalling pathways: Roadmap for therapies”, *European Respiratory Journal*.
- Bromen, K., Pohlabeln, H., Jahn, I., Ahrens, W. and Jöckel, K.H. (2000), “Aggregation of lung cancer in families: results from a population-based case-control study in Germany.”, *American Journal of Epidemiology*, Vol. 152 No. 6, pp. 497–505.
- Brooks, P.C., Montgomery, A.M., Rosenfeld, M., Reisfeld, R.A., Hu, T., Klier, G. and Cheresch, D.A. (1994), “Integrin alpha v beta 3 antagonists promote tumor regression by inducing apoptosis of angiogenic blood vessels”, *Cell*, Vol. 79 No. 7, pp. 1157–1164.
- Buschow, S.I., Van Balkom, B.W.M., Aalberts, M., Heck, A.J.R., Wauben, M. and Stoorvogel, W. (2010), “MHC class II-associated proteins in B-cell exosomes and potential functional implications for exosome biogenesis”, *Immunology and Cell Biology*, Vol. 88 No. 8, pp. 851–856.
- Butcher, D.T., Alliston, T. and Weaver, V.M. (2009), “A tense situation: Forcing tumour progression”, *Nature Reviews Cancer*.
- Caby, M.-P., Lankar, D., Vincendeau-Scherrer, C., Raposo, G. and Bonnerot, C. (2005), “Exosomal-like Vesicles are present in Human Blood Plasma”, *International Immunology*, Vol. 17 No. 7, pp. 879–887.
- Caccavari, F., Valdembri, D., Sandri, C., Bussolino, F. and Serini, G. (2009), “Integrin signaling and lung cancer.”, *Cell Adhesion & Migration*, Vol. 4 No. 1, pp. 124–9.
- Cai, Z., Yang, F., Yu, L., Yu, Z., Jiang, L., Wang, Q., Yang, Y., et al. (2012), “Activated T cell exosomes promote tumor invasion via Fas signaling pathway.”, *Journal of Immunology (Baltimore, Md. : 1950)*, Vol. 188 No. 12, pp. 5954–61.
- Caradec, J., Kharmate, G., Hosseini-Beheshti, E., Adomat, H., Gleave, M. and Guns, E.

- (2014), “Reproducibility and efficiency of serum-derived exosome extraction methods”, *Clinical Biochemistry*, Vol. 47 No. 13–14, pp. 1286–1292.
- Carayon, K., Chaoui, K., Ronzier, E., Lazar, I., Bertrand-Michel, J., et al. (2011), “Proteolipidic composition of exosomes changes during reticulocyte maturation”, *Journal of Biological Chemistry*, Vol. 286 No. 39, pp. 34426–34439.
- Chairoungdua, A., Smith, D.L., Pochard, P., Hull, M. and Caplan, M.J. (2010), “Exosome release of β -catenin: A novel mechanism that antagonizes Wnt signaling”, *Journal of Cell Biology*, Vol. 190 No. 6, pp. 1079–1091.
- Chaput, N. and Théry, C. (2011), “Exosomes: immune properties and potential clinical implementations”, *Seminars in Immunopathology*, Vol. 33 No. 5, pp. 419–440.
- Chaudhuri, A.A., Binkley, M.S., Osmundson, E.C., Alizadeh, A.A. and Diehn, M. (2015), “Predicting Radiotherapy Responses and Treatment Outcomes Through Analysis of Circulating Tumor DNA”, *Seminars in Radiation Oncology*.
- Chertova, E., Chertov, O., Coren, L. V, Roser, J.D., Trubey, C.M., Bess, J.W., Sowder, R.C., et al. (2006), “Proteomic and biochemical analysis of purified human immunodeficiency virus type 1 produced from infected monocyte-derived macrophages.”, *Journal of Virology*, Vol. 80 No. 18, pp. 9039–9052.
- Cheung, C.H.Y. and Juan, H.-F. (2017), “Quantitative proteomics in lung cancer”, *Journal of Biomedical Science*, Vol. 24 No. 1, p. 37.
- Cho, J.A., Park, H., Lim, E.H., Kim, K.H., Choi, J.S., Lee, J.H., Shin, J.W., et al. (2011), “Exosomes from ovarian cancer cells induce adipose tissue-derived mesenchymal stem cells to acquire the physical and functional characteristics of tumor-supporting myofibroblasts”, *Gynecologic Oncology*, Elsevier Inc., Vol. 123 No. 2, pp. 379–386.
- Cho, J.A., Park, H., Lim, E.H. and Lee, K.W. (2012), “Exosomes from breast cancer cells can convert adipose tissue-derived mesenchymal stem cells into myofibroblast-like cells”, *International Journal of Oncology*, Vol. 40 No. 1, pp. 130–138.
- Cho, W.C.S. (2016), “Application of proteomics in non-small-cell lung cancer”, *Expert Review of Proteomics*.
- Choi, D.S., Kim, D.K., Kim, Y.K. and Gho, Y.S. (2013), “Proteomics, transcriptomics and lipidomics of exosomes and ectosomes”, *Proteomics*, Vol. 13 No. 10–11, pp. 1554–

1571.

- Chow, A., Zhou, W., Liu, L., Fong, M.Y., Champer, J., et al. (2014), “Macrophage immunomodulation by breast cancer-derived exosomes requires Toll-like receptor 2-mediated activation of NF- κ B.”, *Scientific Reports*, Vol. 4, p. 5750.
- Ciardello, C., Cavallini, L., Spinelli, C., Yang, J., Reis-Sobreiro, M., et al. (2016), “Focus on extracellular vesicles: New frontiers of cell-to-cell communication in cancer”, *International Journal of Molecular Sciences*, Vol. 17 No. 2, pp. 1–17.
- Cifani, P. and Kentsis, A. (2016), “Towards comprehensive and quantitative proteomics for diagnosis and therapy of human disease”, *PROTEOMICS*, p. n/a-n/a.
- Clark, D.J., Fondrie, W.E., Yang, A. and Mao, L. (2016), “Triple SILAC quantitative proteomic analysis reveals differential abundance of cell signaling proteins between normal and lung cancer-derived exosomes”, *Journal of Proteomics*, Vol. 133, pp. 161–169.
- Clark, N. a. (1970), “A Study of Brownian Motion Using Light Scattering”, *American Journal of Physics*, Vol. 38 No. 1970, p. 575.
- Clayton, A., Court, J., Navabi, H., Adams, M., Mason, M.D., et al. (2001), “Analysis of antigen presenting cell derived exosomes, based on immuno-magnetic isolation and flow cytometry”, *Journal of Immunological Methods*, Vol. 247 No. 1–2, pp. 163–174.
- Clayton, A. and Mason, M.D. (2009), “Exosomes in tumour immunity”, *Current Oncology*.
- Clayton, A., Mitchell, J.P., Court, J., Linnane, S., Mason, M.D., et al. (2008), “Human Tumor-Derived Exosomes Down-Modulate NKG2D Expression”, *The Journal of Immunology*, Vol. 180 No. 11, pp. 7249–7258.
- Clayton, A., Mitchell, J.P., Court, J., Mason, M.D. and Tabi, Z. (2007), “Human tumor-derived exosomes selectively impair lymphocyte responses to interleukin-2”, *Cancer Research*, Vol. 67 No. 15, pp. 7458–7466.
- Collisson, E.A., Campbell, J.D., Brooks, A.N., Berger, A.H., Lee, W., et al. (2014), “Comprehensive molecular profiling of lung adenocarcinoma”, *Nature*, Vol. 511 No. 7511, pp. 543–550.
- Colombet, J., Charpin, M., Robin, A., Portelli, C., Amblard, C., et a. (2009), “Seasonal depth-

- related gradients in virioplankton: Standing stock and relationships with microbial communities in Lake Pavin (France)", *Microbial Ecology*, Vol. 58 No. 4, pp. 728–736.
- Conde-Vancells, J., Rodriguez-Suarez, E., Embade, N., Gil, D., Matthiesen, R., Valle, M., et al. (2008), "Characterization and comprehensive proteome profiling of exosomes secreted by hepatocytes", *Journal of Proteome Research*, Vol. 7 No. 12, pp. 5157–5166.
- Conde-Vancells, J., Rodriguez-Suarez, E., Gonzalez, E., Berisa, A., Gil, D., et al. (2010), "Candidate biomarkers in exosome-like vesicles purified from rat and mouse urine samples", *PROTEOMICS - CLINICAL APPLICATIONS*, Vol. 4 No. 4, pp. 416–425.
- Corrado, C., Raimondo, S., Chiesi, A., Ciccia, F., De Leo, G. et al. (2013), "Exosomes as intercellular signaling organelles involved in health and disease: Basic science and clinical applications", *International Journal of Molecular Sciences*, Vol. 14 No. 3, pp. 5338–5366.
- Costa-Silva, B., Aiello, N.M., Ocean, A.J., Singh, S., Zhang, H., et al. (2015), "Pancreatic cancer exosomes initiate pre-metastatic niche formation in the liver", *Nat Cell Biol*, Vol. 17 No. 6, pp. 816–826.
- Coumans, F.A.W., Brisson, A.R., Buzas, E.I., Dignat-George, F., Drees, E.E.E., et al. (2017), "Methodological guidelines to study extracellular vesicles", *Circulation Research*.
- Cox, J. and Mann, M. (2007), "Is Proteomics the New Genomics?", *Cell*, Vol. 130 No. 3, pp. 395–398.
- Crans, H.N. and Sakamoto, K.M. (2001), "Transcription factors and translocations in lymphoid and myeloid leukemia.", *Leukemia : Official Journal of the Leukemia Society of America, Leukemia Research Fund, U.K.*, Vol. 15 No. August 2000, pp. 313–331.
- Dela Cruz, C.S., Tanoue, L.T. and Matthay, R.A. (2011), "Lung Cancer: Epidemiology, Etiology, and Prevention", *Clinics in Chest Medicine*, December.
- Dalli, J., Norling, L. V., Montero-Melendez, T., Canova, D.F., Lashin, H., et al. (2014), "Microparticle alpha-2-macroglobulin enhances pro-resolving responses and promotes survival in sepsis", *EMBO Molecular Medicine*, Vol. 6 No. 1, pp. 27–42.
- Davies, R.T., Kim, J., Jang, S.C., Choi, E.-J., Gho, Y.S. et al. (2012), "Microfluidic filtration system to isolate extracellular vesicles from blood", *Lab on a Chip*, Vol. 12 No. 24, p. 5202.

- Denzer, K., van Eijk, M., Kleijmeer, M.J., Jakobson, E., de Groot, C. et al. (2000), “Follicular dendritic cells carry MHC class II-expressing microvesicles at their surface.”, *The Journal of Immunology*, Vol. 165, pp. 1259–1265.
- Denzer, K., Kleijmeer, M.J., Heijnen, H.F., Stoorvogel, W., Geuze, H.J., et al. (2000), “Exosome: from internal vesicle of the multivesicular body to intercellular signaling device.”, *Journal of Cell Science*, Vol. 113 Pt 19 No. 19, pp. 3365–74.
- Devesa, S.S., Bray, F., Vizcaino, A.P. and Parkin, D.M. (2005), “International lung cancer trends by histologic type: Male:female differences diminishing and adenocarcinoma rates rising”, *International Journal of Cancer*, available at:<https://doi.org/10.1002/ijc.21183>.
- Dingemans, A.-M.C., van den Boogaart, V., Vosse, B.A., van Suylen, R.-J., Griffioen, A.W. and Thijssen, V.L. (2010), “Integrin expression profiling identifies integrin alpha5 and beta1 as prognostic factors in early stage non-small cell lung cancer.”, *Molecular Cancer*, Vol. 9, p. 152.
- Döhner, H., Estey, E.H., Amadori, S., Appelbaum, F.R., Büchner, T., et al. (2010), “Diagnosis and management of acute myeloid leukemia in adults: Recommendations from an international expert panel, on behalf of the European LeukemiaNet”, *Blood*.
- Dombret, H. (2011), “Gene mutation and AML pathogenesis”, *Blood*.
- Domon, B. and Aebersold, R. (2006), “Mass spectrometry and protein analysis.”, *Science (New York, N.Y.)*, American Association for the Advancement of Science, Vol. 312 No. 5771, pp. 212–7.
- Doytchinova, I.A., Taylor, P. and Flower, D.R. (2003), “Proteomics in Vaccinology and Immunobiology: An Informatics Perspective of the Immunone”, *Journal of Biomedicine and Biotechnology*.
- Dragovic, R.A., Gardiner, C., Brooks, A.S., Tannetta, D.S., Ferguson, D.J.P., et al. (2011), “Sizing and phenotyping of cellular vesicles using Nanoparticle Tracking Analysis”, *Nanomedicine: Nanotechnology, Biology, and Medicine*, Vol. 7 No. 6, pp. 780–788.
- Duijvesz, D., Burnum-Johnson, K.E., Gritsenko, M.A., Hoogland, A.M., Vredenburg-van den Berg, M.S., et al. (2013), “Proteomic profiling of exosomes leads to the identification of novel biomarkers for prostate cancer”, *PLoS ONE*, Vol. 8 No. 12, p.

e82589.

- Dumont, P., Gasser, B., Rougé, C., Massard, G. and Wihlm, J.M. (1998), “Bronchoalveolar carcinoma: Histopathologic study of evolution in a series of 105 surgically treated patients”, *Chest*, Vol. 113 No. 2, pp. 391–395.
- Easwaran, V., Lee, S.H., Inge, L., Guo, L., Goldbeck, C., et al. (2003), “Beta-Catenin regulates vascular endothelial growth factor expression in colon cancer.”, *Cancer Research*, Vol. 63 No. 12, pp. 3145–3153.
- Edgar, J.R., Harding, C., Heuser, J., Stahl, P., Pan, B., et al. (2016), “Q&A: What are exosomes, exactly?”, *BMC Biology*, Vol. 14 No. 1, p. 46.
- Eitan, E., Zhang, S., Witwer, K.W. and Mattson, M.P. (2015), “Extracellular vesicle–depleted fetal bovine and human sera have reduced capacity to support cell growth”, *Journal of Extracellular Vesicles*, Vol. 4, pp. 1–10.
- El-Andaloussi, S., Lee, Y., Lakhali-Littleton, S., Li, J., Seow, Y., et al. (2012), “Exosome-mediated delivery of siRNA in vitro and in vivo”, *Nature Protocols*, Vol. 7 No. 12, pp. 2112–2126.
- Elrick, M.M., Walgren, J.L., Mitchell, M.D. and Thompson, D.C. (2006), “Proteomics: recent applications and new technologies.”, *Basic & Clinical Pharmacology & Toxicology*, Vol. 98 No. 5, pp. 432–441.
- Emily Zerlinger., Mu Li., Tim Barta., Jeffrey Schageman., Ketil Winther Pedersen., et al. (2013), “Methods for the extraction and RNA profiling of exosomes”, *World J of Methodology*, Vol. 3 No. 1, pp. 11–18.
- Erdbrügger, U. and Lannigan, J. (2016), “Analytical challenges of extracellular vesicle detection: A comparison of different techniques”, *Cytometry Part A*.
- Estrada, M.F., Rebelo, S.P., Davies, E.J., Pinto, M.T., Pereira, H., et al. (2016), “Modelling the tumour microenvironment in long-term microencapsulated 3D co-cultures recapitulates phenotypic features of disease progression”, *Biomaterials*, Vol. 78, pp. 50–61.
- Fader, C.M., Sánchez, D.G., Mestre, M.B. and Colombo, M.I. (2009), “TI-VAMP/VAMP7 and VAMP3/cellubrevin: two v-SNARE proteins involved in specific steps of the autophagy/multivesicular body pathways”, *Biochimica et Biophysica Acta - Molecular*

Cell Research, Vol. 1793 No. 12, pp. 1901–1916.

- Felding-Habermann, B., Fransvea, E., O’Toole, T.E., Manzuk, L., Faha, B. and Hensler, M. (2002), “Involvement of tumor cell integrin alpha v beta 3 in hematogenous metastasis of human melanoma cells.”, *Clinical & Experimental Metastasis*, Vol. 19 No. 5, pp. 427–436.
- Février, B. and Raposo, G. (2004), “Exosomes: Endosomal-derived vesicles shipping extracellular messages”, *Current Opinion in Cell Biology*, August.
- Filipe, V., Hawe, A. and Jiskoot, W. (2010), “Critical evaluation of nanoparticle tracking analysis (NTA) by NanoSight for the measurement of nanoparticles and protein aggregates”, *Pharmaceutical Research*, Vol. 27 No. 5, pp. 796–810.
- Filippini, S.E. and Vega, A. (2013), “Breast cancer genes: beyond BRCA1 and BRCA2.”, *Frontiers in Bioscience (Landmark Edition)*, Vol. 18, pp. 1358–72.
- Fliser, D., Fliser, D., Novak, J., Novak, J., Thongboonkerd, V., et al. (2007), “Advances in urinary proteome analysis and biomarker discovery.”, *Journal of the American Society of Nephrology*, Vol. 18, pp. 1057–71.
- Fomina, A.F., Deerinck, T.J., Ellisman, M.H. and Cahalan, M.D. (2003), “Regulation of membrane trafficking and subcellular organization of endocytic compartments revealed with FM1-43 in resting and activated human T cells”, *Experimental Cell Research*, Vol. 291 No. 1, pp. 150–166.
- Fontana, S., Saieva, L., Taverna, S. and Alessandro, R. (2013), “Contribution of proteomics to understanding the role of tumor-derived exosomes in cancer progression: State of the art and new perspectives”, *Proteomics*, Vol. 13 No. 10–11, pp. 1581–1594.
- Francis, G.L. (2010), “Albumin and mammalian cell culture: Implications for biotechnology applications”, *Cytotechnology*.
- Ganguly, K.K., Pal, S., Moulik, S. and Chatterjee, A. (2013), “Integrins and metastasis”, *Cell Adhesion and Migration*.
- G Raposo, H W Nijman, W Stoorvogel, R Liejendekker, C V Harding, C J Melief, and H.J.G. (1996), “B Lymphocytes Secrete Antigen-presenting Vesicles”, *The Journal of Experimental Medicine*, Vol. 183 No. March, pp. 1161–1172.

- Garfield, D.H., Cadranel, J.L., Wislez, M., Franklin, W.A. and Hirsch, F.R. (2006), “The bronchioloalveolar carcinoma and peripheral adenocarcinoma spectrum of diseases”, *Journal of Thoracic Oncology*.
- Gassart, A. De, Ge, C. and Fe, B. (2003), “Lipid raft – associated protein sorting in exosomes”, *Proteins*, Vol. 102 No. December, pp. 4336–4344.
- Gay, L.J. and Felding-Habermann, B. (2011), “Contribution of platelets to tumour metastasis.”, *Nature Reviews. Cancer*, Nature Publishing Group, Vol. 11 No. FEBruAry, pp. 123–34.
- Geiger, T., Wehner, A., Schaab, C., Cox, J. and Mann, M. (2012), “Comparative Proteomic Analysis of Eleven Common Cell Lines Reveals Ubiquitous but Varying Expression of Most Proteins”, *Molecular & Cellular Proteomics*, Vol. 11 No. 3, p. M111.014050.
- Gesierich, S., Berezovskiy, I., Ryschich, E. and Zöller, M. (2006), “Systemic induction of the angiogenesis switch by the tetraspanin D6.1A/CO-029”, *Cancer Research*, Vol. 66 No. 14, pp. 7083–7094.
- Giehl, K. (2005), “Oncogenic Ras in tumour progression and metastasis”, *Biological Chemistry*.
- Global Burden of Disease Cancer Collaboration. (2017), “Global, Regional, and National Cancer Incidence, Mortality, Years of Life Lost, Years Lived With Disability, and Disability-Adjusted Life-years for 32 Cancer Groups, 1990 to 2015”, *JAMA Oncology*, Vol. 3 No. 4, p. 524.
- Gonzales, P.A., Pisitkun, T., Hoffert, J.D., Tchapyjnikov, D., Star, R.A., et al. (2009), “Large-Scale Proteomics and Phosphoproteomics of Urinary Exosomes”, *Journal of the American Society of Nephrology*, Vol. 20 No. 2, pp. 363–379.
- Gonzalez-Begne, M., Lu, B., Han, X., Hagen, F.K., Hand, A.R., et al. (2009), “Proteomic analysis of human parotid gland exosomes by multidimensional protein identification technology (MudPIT)”, *Journal of Proteome Research*, Vol. 8 No. 3, pp. 1304–1314.
- Good, D.M., Thongboonkerd, V., Novak, J., Bascands, J.L., Schanstra, J.P., et al. (2007), “Body fluid proteomics for biomarker discovery: Lessons from the past hold the key to success in the future”, *Journal of Proteome Research*, Vol. 6(12), pp. 4549-4555.
- Goodison, S., Rosser, C.J. and Urquidi, V. (2013), “Bladder cancer detection and monitoring:

- Assessment of urine- and blood-based marker tests”, *Molecular Diagnosis and Therapy*. Vol. 17(2), pp.71-84
- Goyal, A., Martin, T.A., Mansel, R.E. and Jiang, W.G. (2008), “Real time PCR analyses of expression of E-cadherin, alpha-, beta- and gamma-catenin in human breast cancer for predicting clinical outcome”, *World Journal of Surgical Oncology*, Vol. 6.
- Granvogl, B., Plösch, M. and Eichacker, L.A. (2007), “Sample preparation by in-gel digestion for mass spectrometry-based proteomics”, *Analytical and Bioanalytical Chemistry*, Vol. 389 No. 4, pp. 991–1002.
- Graves, P.R. and Haystead, T.A.J. (2002), “Molecular Biologist’s Guide to Proteomics”, *Microbiology and Molecular Biology Reviews*, Vol. 66 No. 1, pp. 39–63.
- Greening, D.W., Gopal, S.K., Xu, R., Simpson, R.J. and Chen, W. (2015), “Exosomes and their roles in immune regulation and cancer”, *Seminars in Cell and Developmental Biology*.
- Gupta, V.K., Steindorff, A.S., de Paula, R.G., Silva-Rocha, R., Mach-Aigner, A.R., et al. (2016), “The Post-genomic Era of *Trichoderma reesei*: What’s Next?”, *Trends in Biotechnology*.
- Ha, D., Yang, N. and Nadithe, V. (2016), “Exosomes as therapeutic drug carriers and delivery vehicles across biological membranes: current perspectives and future challenges”, *Acta Pharmaceutica Sinica B*. Vol. 6(4), pp. 287–296
- Halvaei, S., Daryani, S., Eslami-S, Z., Samadi, T., Jafarbeik-Iravani, N., et al. (2018), “Exosomes in Cancer Liquid Biopsy: A Focus on Breast Cancer”, *Molecular Therapy - Nucleic Acids*. Vol 10, pp. 131-141.
- Han, X., Wang, J. and Sun, Y. (2017), “Circulating Tumor DNA as Biomarkers for Cancer Detection”, *Genomics, Proteomics & Bioinformatics*, Vol. 15 No. 2, pp. 59–72.
- Hanahan, D. and Weinberg, R.A. (2000), “The hallmarks of cancer.”, *Cell*, Vol. 100 No. 1, pp. 57–70.
- Haney, M.J., Klyachko, N.L., Zhao, Y., Gupta, R., Plotnikova, E.G., et al. (2015), “Exosomes as drug delivery vehicles for Parkinson’s disease therapy”, *Journal of Controlled Release*, Vol. 207, pp. 18–30.

- Hansen, R.K. and Bissell, M.J. (2000), "Tissue architecture and breast cancer: The role of extracellular matrix and steroid hormones", *Endocrine-Related Cancer*, Vol. 7 No. 2, pp. 95–113.
- Harris, D.A., Patel, S.H., Gucek, M., Hendrix, A., Westbroek, W. and Taraska, J.W. (2015), "Exosomes released from breast cancer carcinomas stimulate cell movement", *PLoS ONE*, Vol. 10 No. 3.
- Harry, J.L., Wilkins, M.R., Herbert, B.R., Packer, N.H., Gooley, A.A. et al. (2000), "Proteomics: Capacity versus utility", *Electrophoresis*. Vol. 21(6), pp. 1071-1081.
- Hassanein, M., Callison, J.C., Callaway-Lane, C., Aldrich, M.C., Grogan, E.L. et al. (2012), "The state of molecular biomarkers for the early detection of lung cancer", *Cancer Prevention Research*. Vol. 5(8), pp. 992-1006.
- Hegmans, J.P.J.J., Bard, M.P.L., Hemmes, A., Luider, T.M., Kleijmeer, M.J., et al. (2004), "Proteomic analysis of exosomes secreted by human mesothelioma cells.", *The American Journal of Pathology*, Vol. 164 No. 5, pp. 1807–1815.
- Heijnen, H.F., Schiel, A.E., Fijnheer, R., Geuze, H.J. and Sixma, J.J. (1999), "Activated platelets release two types of membrane vesicles: microvesicles by surface shedding and exosomes derived from exocytosis of multivesicular bodies and alpha-granules", *Blood*, Vol. 94 No. 11, pp. 3791–3799.
- Helwa, I., Cai, J., Drewry, M.D., Zimmerman, A., Dinkins, M.B., et al. (2017), "A comparative study of serum exosome isolation using differential ultracentrifugation and three commercial reagents", *PLoS ONE*, Vol. 12 No. 1.
- Henderson, M.C. and Azorsa, D.O. (2012), "The Genomic and Proteomic Content of Cancer Cell-Derived Exosomes", *Frontiers in Oncology*, Vol. 2.
- Herold-Mende, C., Kartenbeck, J., Tomakidi, P. and Bosch, F.X. (2001), "Metastatic growth of squamous cell carcinomas is correlated with upregulation and redistribution of hemidesmosomal components", *Cell and Tissue Research*, Vol. 306 No. 3, pp. 399–408.
- Hiley, C., de Bruin, E.C., McGranahan, N. and Swanton, C. (2014), "Deciphering intratumor heterogeneity and temporal acquisition of driver events to refine precision medicine", *Genome Biology*. Vol. 15, pp. 454-463.
- Hoen, E.N.M.N. t, van der Vlist, E.J., Aalberts, M., Mertens, H.C.H., Bosch, B.J., Bartelink,

- W., et al. (2012), “Quantitative and qualitative flow cytometric analysis of nanosized cell-derived membrane vesicles”, *Nanomedicine: Nanotechnology, Biology, and Medicine*, Elsevier Inc., Vol. 8 No. 5, pp. 712–720.
- Hood, J.D. and Cheresh, D.A. (2002), “ROLE OF INTEGRINS IN CELL INVASION AND MIGRATION”, *Nature Reviews Cancer*, Vol. 2 No. 2, pp. 91–100.
- Hood, J.L., San, R.S., Wickline, S.A. and Roman, S.S. (2011), “Exosomes Released by Melanoma Cells Prepare Sentinel Lymph Nodes for Tumor Metastasis Exosomes Released by Melanoma Cells Prepare Sentinel Lymph Nodes for Tumor Metastasis”, *Cancer Research*, Vol. 71 No. 11, pp. 3792–3801.
- Hossain, M.M., Li, X., Evans, I.H. and Rahman, M.A. (2014), “A proteomic analysis of seed proteins expressed in a Brassica somatic hybrid and its two parental species”, *Plant Tissue Culture and Biotechnology*, Vol. 24 No. 1, pp. 11–26.
- Hotta, H., Ross, A.H., Huebner, K., Isobe, M., Wendeborn., et al. (1988), “Molecular Cloning and Characterization of an Antigen Associated with Early Stages of Melanoma Tumor Progression”, *Cancer Research*, Vol. 48 No. 11, pp. 2955–2962.
- Iero, M., Valenti, R., Huber, V., Filipazzi, P., Parmiani, G., Fais, S. and Rivoltini, L. (2008), “Tumour-released exosomes and their implications in cancer immunity.”, *Cell Death and Differentiation*, Vol. 15 No. 1, pp. 80–88.
- Ignatiadis, M., Lee, M. and Jeffrey, S.S. (2015), “Circulating tumor cells and circulating tumor DNA: Challenges and opportunities on the path to clinical utility”, *Clinical Cancer Research*.
- Inamdar, S., Nitiyanandan, R. and Rege, K. (2017), “Emerging applications of exosomes in cancer therapeutics and diagnostics”, *Bioengineering & Translational Medicine*, Vol. 2 No. 1, pp. 70–80.
- Iraci, N., Leonardi, T., Gessler, F., Vega, B. and Pluchino, S. (2016), “Focus on extracellular vesicles: Physiological role and signalling properties of extracellular membrane vesicles”, *International Journal of Molecular Sciences*, Vol. 17, pp. 171-203.
- Jang, H.-I. and Lee, H. (2003), “A decrease in the expression of CD63 tetraspanin protein elevates invasive potential of human melanoma cells.”, *Experimental & Molecular Medicine*, Vol. 35 No. 4, pp. 317–323.

- Janmaat, M.L. and Giaccone, G. (2003), “Small-Molecule Epidermal Growth Factor Receptor Tyrosine Kinase Inhibitors”, *The Oncologist*, Vol. 8, pp. 576–586.
- Jian, H., Yi, G., Jing, X., Wenjiong, S., Wei, Z., et al. (2015), “Overexpression of CD9 correlates with tumor stage and lymph node metastasis in esophageal squamous cell carcinoma”, *International Journal of Clinical and Experimental Pathology*, e-Century Publishing Corporation, Vol. 8 No. 3, pp. 3054–61.
- Jiang, S.-H., Wang, Y., Yang, J.-Y., Li, J., Feng, M.-X., Wang, Y.-H., et al. (2015), “Overexpressed EDIL3 predicts poor prognosis and promotes anchorage-independent tumor growth in human pancreatic cancer”, *Oncotarget*. Vol. 7(4), pp. 4226-4240.
- Jiang, W.G., Sanders, A.J., Katoh, M., Ungefroren, H., Gieseler, F., et al. (2015), “Tissue invasion and metastasis: Molecular, biological and clinical perspectives”, *Seminars in Cancer Biology*. Vol. 15, pp. 244-275.
- Jiang, X.C. and Gao, J.Q. (2017), “Exosomes as novel bio-carriers for gene and drug delivery”, *International Journal of Pharmaceutics*. Vol. 521 (1-2), pp. 167-175.
- Johnstone, R.M., Adam, M., Hammond, J.R., Orr, L. and Turbide, C. (1987), “Vesicle formation during reticulocyte maturation. Association of plasma membrane activities with released vesicles (exosomes).”, *Journal of Biological Chemistry*, Vol. 262 No. 19, pp. 9412–9420.
- Johnstone, R.M., Bianchini, A. and Teng, K. (1989), “Reticulocyte maturation and exosome release: transferrin receptor containing exosomes shows multiple plasma membrane functions.”, *Blood*, Vol. 74 No. 5, pp. 1844–51.
- Jones, M.B., Krutzsch, H., Shu, H., Zhao, Y., Liotta, L. et al. (2002), “Proteomic analysis and identification of new biomarkers and therapeutic targets for invasive ovarian cancer”, *Proteomics*, Vol. 2 No. 1, pp. 76–84.
- de Jong, O.G., Verhaar, M.C., Chen, Y., Vader, P., Gremmels, H., et al. (2012), “Cellular stress conditions are reflected in the protein and RNA content of endothelial cell-derived exosomes”, *Journal of Extracellular Vesicles*, Vol. 1 No. 4, pp. 1–12.
- Kahlert, C. and Kalluri, R. (2013), “Exosomes in tumor microenvironment influence cancer progression and metastasis”, *Journal of Molecular Medicine*, Vol. 91 No. 4, pp. 431–437.

- Kalani, A. and Tyagi, N. (2015), “Exosomes in neurological disease, neuroprotection, repair and therapeutics: Problems and perspectives”, *Neural Regeneration Research*, Vol. 10 No. 10, pp. 1565–1567.
- Kalia, M. (2015), “Biomarkers for personalized oncology: Recent advances and future challenges”, *Metabolism: Clinical and Experimental*, W.B. Saunders, Vol. 64 No. 3, pp. S16–S21.
- Kalluri, R. (2016), “The biology and function of exosomes in cancer”, *Journal of Clinical Investigation*. Vol. 126(4), pp. 1208-1215.
- Karachaliou, N., Mayo, C., Costa, C., Magrí, I., Gimenez-Capitan, A., et al. (2013), “KRAS mutations in lung cancer”, *Clinical Lung Cancer*. Vol. 14(3), pp. 205-214.
- Karlsson, M., Lundin, S., Dahlgren, U., Kahu, H., Pettersson, I. et al. (2001), “‘Tolerosomes’ are produced by intestinal epithelial cells”, *European Journal of Immunology*, Vol. 31 No. 10, pp. 2892–2900.
- Kayser, G., Csanadi, A., Otto, C., Plönes, T., Bittermann, N., et al. (2013), “Simultaneous Multi-Antibody Staining in Non-Small Cell Lung Cancer Strengthens Diagnostic Accuracy Especially in Small Tissue Samples”, *PLoS ONE*, Vol. 8 No. 2, pp. 1–10.
- Keller, E.T. (2002), “Overview of metastasis and metastases”, *Journal of Musculoskeletal Neuronal Interactions*, Vol. 2 No. 6, pp. 567–569.
- Keller, S., Ridinger, J., Rupp, A.-K., Janssen, J.W.G. and Altevogt, P. (2011), “Body fluid derived exosomes as a novel template for clinical diagnostics.”, *Journal of Translational Medicine*, BioMed Central Ltd, Vol. 9 No. 1, p. 86.
- Kesimer, M. and Gupta, R. (2015), “Physical characterization and profiling of airway epithelial derived exosomes using light scattering”, *Methods*, Elsevier Inc., Vol. 87, pp. 59–63.
- Khokhar, F.A., Muzzafar, T., Bueso-Ramos, C.E. and Medeiros, L.J. (2010), “Acute myeloid leukemia, not otherwise specified, with minimal differentiation: TDT+ and TDT-subsets have distinctive features.”, *Laboratory Investigation.Conference: United States and Canadian Academy of Pathology Annual Meeting Washington, DC United States.Conference Start: 20100320 Conference End: 20100326.Conference Publication: (Var.pagings)*, Vol. 90, p. 306A.

- Kim, S.H., Turnbull, J. and Guimond, S. (2011), “Extracellular matrix and cell signalling: The dynamic cooperation of integrin, proteoglycan and growth factor receptor”, *Journal of Endocrinology*.
- King, H.W., Michael, M.Z. and Gleadle, J.M. (2012), “Hypoxic enhancement of exosome release by breast cancer cells.”, *BMC Cancer*, Vol. 12 No. 1, p. 421.
- Ko, J., Carpenter, E. and Issadore, D. (2016), “Detection and isolation of circulating exosomes and microvesicles for cancer monitoring and diagnostics using micro-/nano-based devices”, *The Analyst*, Vol. 141 No. 2, pp. 450–460.
- Kollmannsberger, C., Beyer, J., Droz, J.P., Harstrick, A., Hartmann, J.T., et al. (1998), “Secondary leukemia following high cumulative doses of etoposide in patients treated for advanced germ cell tumors”, *Journal of Clinical Oncology*, Vol. 16 No. 10, pp. 3386–3391.
- Kooijmans, S.A.A., Vader, P., van Dommelen, S.M., van Solinge, W.W. and Schiffelers, R.M. (2012), “Exosome mimetics: A novel class of drug delivery systems”, *International Journal of Nanomedicine*.
- Korpal, M., Ell, B.J., Buffa, F.M., Ibrahim, T., Blanco, M.A., et al. (2011), “Direct targeting of Sec23a by miR-200s influences cancer cell secretome and promotes metastatic colonization”, *Nature Medicine*, Vol. 17 No. 9, pp. 1101–1109.
- Kösters, J.P. and Gøtzsche, P.C. (2003), “Regular self-examination or clinical examination for early detection of breast cancer.”, *The Cochrane Database of Systematic Reviews*, No. 2, p. CD003373.
- Koumangoye, R.B., Sakwe, A.M., Goodwin, J.S., Patel, T. and Ochieng, J. (2011), “Detachment of breast tumor cells induces rapid secretion of exosomes which subsequently mediate cellular adhesion and spreading”, *PLoS ONE*, Vol. 6 No. 9,
- Kräling, B.M., Wiederschain, D.G., Boehm, T., Rehn, M., Mulliken, J.B. et al. (1999), “The role of matrix metalloproteinase activity in the maturation of human capillary endothelial cells in vitro.”, *Journal of Cell Science*, Vol. 112 (Pt 1, pp. 1599–609.
- Kreuzer, M., Kreienbrock, L., Gerken, M., Heinrich, J., Bruske-Hohlfeld, I., et al. (1998), “Risk factors for lung cancer in young adults.”, *American Journal of Epidemiology*, Vol. 147 No. 11, pp. 1028–37.

- Kwon, H.J., Min, S.Y., Park, M.J., Lee, C., Park, J.H., et al. (2014), “Expression of CD9 and CD82 in clear cell renal cell carcinoma and its clinical significance”, *Pathology Research and Practice*, Urban und Fischer Verlag GmbH und Co. KG, Vol. 210 No. 5, pp. 285–290.
- Lakhal, S. and Wood, M.J.A. (2011), “Exosome nanotechnology: An emerging paradigm shift in drug delivery: Exploitation of exosome nanovesicles for systemic in vivo delivery of RNAi heralds new horizons for drug delivery across biological barriers”, *BioEssays*, Vol. 33 No. 10, pp. 737–741.
- Lamparski, H.G., Metha-Damani, A., Yao, J.Y., Patel, S., Hsu, D.H., et al. (2002), “Production and characterization of clinical grade exosomes derived from dendritic cells”, *Journal of Immunological Methods*, Vol. 270 No. 2, pp. 211–226.
- Lane, R.E., Korbie, D., Anderson, W., Vaidyanathan, R. and Trau, M. (2015), “Analysis of exosome purification methods using a model liposome system and tunable-resistive pulse sensing.”, *Scientific Reports*, Vol. 5, p. 7639.
- Lässer, C., Eldh, M. and Lötvall, J. (2012), “Isolation and Characterization of RNA-Containing Exosomes”, *Journal of Visualized Experiments*, No. 59, available at:<https://doi.org/10.3791/3037>.
- Laulagnier, K., Motta, C., Hamdi, S., Roy, S., Fauvelle, F., et al. (2004), “Mast cell- and dendritic cell-derived exosomes display a specific lipid composition and an unusual membrane organization.”, *The Biochemical Journal*, Vol. 380 No. Pt 1, pp. 161–71.
- Lee, A. V, Oesterreich, S. and Davidson, N.E. (2015), “MCF-7 cells--changing the course of breast cancer research and care for 45 years.”, *Journal of the National Cancer Institute*, Vol. 107 No. 7, p. djv073--djv073.
- Lee, Y.C., Wu, C.T., Chen, C.S., Hsu, H.H. and Chang, Y.L. (2002), “The significance of E-cadherin and alpha-, beta-, and gamma-catenin expression in surgically treated non-small cell lung cancers of 3 cm or less in size”, *J Thorac Cardiovasc Surg*, Vol. 123 No. 3, pp. 502–507.
- Levy, S., Todd, S.C. and Maecker, H.T. (1998), “CD81 (TAPA-1): a molecule involved in signal transduction and cell adhesion in the immune system.”, *Annual Review of Immunology*, Vol. 16, pp. 89–109.

- Li, D.Q., Wang, L., Fei, F., Hou, Y.F., Luo, J.M., et al. (2006), “Identification of breast cancer metastasis-associated proteins in an isogenic tumor metastasis model using two-dimensional gel electrophoresis and liquid chromatography-ion trap-mass spectrometry”, *Proteomics*, Vol. 6 No. 11, pp. 3352–3368.
- Li, M., Aliotta, J.M., Asara, J.M., Tucker, L., Quesenberry, P., et al. (2012), “Quantitative proteomic analysis of exosomes from HIV-1-infected lymphocytic cells”, *Proteomics*, Vol. 12 No. 13, pp. 2203–2211.
- Li, M., Zeringer, E., Barta, T., Schageman, J., Cheng, A. et al. (2014), “Analysis of the RNA content of the exosomes derived from blood serum and urine and its potential as biomarkers”, *Philosophical Transactions of the Royal Society B: Biological Sciences*, Vol. 369 No. 1652, pp. 20130502–20130502.
- Li, P., Kaslan, M., Lee, S.H., Yao, J. and Gao, Z. (2017), “Progress in exosome isolation techniques”, *Theranostics*. Vol. 7(3), pp. 789-804.
- Li, W., Li, C., Zhou, T., Liu, X., Liu, X., Li, X. and Chen, D. (2017), “Role of exosomal proteins in cancer diagnosis”, *Molecular Cancer*, Vol. 16 No. 1, p. 145.
- Lianos, G.D., Alexiou, G.A., Mangano, A., Mangano, A., Rausei, S., et al. (2015), “The role of heat shock proteins in cancer”, *Cancer Letters*.
- Liga, A., Vliegenthart, A.D.B., Oosthuyzen, W., Dear, J.W. and Kersaudy-Kerhoas, M. (2015), “Exosome isolation: a microfluidic road-map”, *Lab Chip*, Vol. 15 No. 11, pp. 2388–2394.
- Lin, J., Li, J., Huang, B., Liu, J., Chen, X., et al. (2015), “Exosomes: novel biomarkers for clinical diagnosis.”, *TheScientificWorldJournal*, Vol. 2015, p. 657086.
- Lin, R., Wang, S. and Zhao, R.C. (2013), “Exosomes from human adipose-derived mesenchymal stem cells promote migration through Wnt signaling pathway in a breast cancer cell model”, *Molecular and Cellular Biochemistry*, Vol. 383 No. 1–2, pp. 13–20.
- Link, A.J., Eng, J., Schieltz, D.M., Carmack, E., Mize, G.J., et al. (1999), “Direct analysis of protein complexes using mass spectrometry”, *Nature Biotechnology*, Vol. 17 No. 7, pp. 676–682.
- Lisacek, F.C., Traini, M.D., Sexton, D., Harry, J.L. and Wilkins, M.R. (2001), “Strategy for protein isoform identification from expressed sequence tags and its application to

- peptide mass fingerprinting”, *Proteomics*, Vol. 1 No. 2, pp. 186–193.
- Liu, E., Nisenblat, V., Farquhar, C., Fraser, I., Bossuyt, P.M.M., et al. (2015), “Urinary biomarkers for the non-invasive diagnosis of endometriosis”, *The Cochrane Database of Systematic Reviews*. Vol. 23(12).
- Liu, X. and Wang, H.-W. (2011), “Single Particle Electron Microscopy Reconstruction of the Exosome Complex Using the Random Conical Tilt Method”, *Journal of Visualized Experiments*, No. 49.
- Lobb, R.J., Becker, M., Wen, S.W., Wong, C.S.F., Wiegmans, A.P., Leimgruber, A. and Möller, A. (2015), “Optimized exosome isolation protocol for cell culture supernatant and human plasma”, *Journal of Extracellular Vesicles*, Vol. 4 No. 1.
- Logozzi, M., De Milito, A., Lugini, L., Borghi, M., Calabrò, L., et al. (2009), “High levels of exosomes expressing CD63 and caveolin-1 in plasma of melanoma patients”, *PLoS ONE*, Vol. 4 No. 4.
- Lötvall, J., Hill, A.F., Hochberg, F., Buzás, E.I., Vizio, D. Di, Gardiner, C., Gho, Y.S., et al. (2014), “Minimal experimental requirements for definition of extracellular vesicles and their functions: A position statement from the International Society for Extracellular Vesicles”, *Journal of Extracellular Vesicles*, Vol. 3 No. 1.
- Lou, X.-L., Sun, J., Gong, S.-Q., Yu, X.-F., Gong, R. and Deng, H. (2015), “Interaction between circulating cancer cells and platelets: clinical implication.”, *Chinese Journal of Cancer Research = Chung-Kuo Yen Cheng Yen Chiu*, Vol. 27 No. 5, pp. 450–60.
- Luchter-Wasylewska, E. and Wasylewski, M. (2007), “What are Prostasomes?”, *IUBMB Life*, Vol. 59 No. 12, pp. 791–792.
- Ludwig, A.K. and Giebel, B. (2012), “Exosomes: Small vesicles participating in intercellular communication”, *International Journal of Biochemistry and Cell Biology*, Elsevier Ltd, Vol. 44 No. 1, pp. 11–15.
- MacHnicka, B., Grochowalska, R., Bogusławska, D.M., Sikorski, A.F. and Lecomte, M.C. (2012), “Spectrin-based skeleton as an actor in cell signaling”, *Cellular and Molecular Life Sciences*.
- Mahul-Mellier, A.-L. (2006), “Alix, Making a Link between Apoptosis-Linked Gene-2, the Endosomal Sorting Complexes Required for Transport, and Neuronal Death In Vivo”,

Journal of Neuroscience, Vol. 26 No. 2, pp. 542–549.

- Maki, M., Kitaura, Y., Satoh, H., Ohkouchi, S. and Shibata, H. (2002), “Structures, functions and molecular evolution of the penta-EF-hand Ca²⁺-binding proteins.”, *Biochimica et Biophysica Acta*, Vol. 1600 No. 1–2, pp. 51–60.
- Mallegol, J., Van Niel, G., Lebreton, C., Lepelletier, Y., Candalh, C., et al. (2007), “T84-Intestinal Epithelial Exosomes Bear MHC Class II/Peptide Complexes Potentiating Antigen Presentation by Dendritic Cells”, *Gastroenterology*, Vol. 132 No. 5, pp. 1866–1876.
- Mariotto, A.B., Noone, A.M., Howlader, N., Cho, H., Keel, G.E., et al. (2014), “Cancer survival: An overview of measures, uses, and interpretation”, *Journal of the National Cancer Institute - Monographs*, Vol. 2014 No. 49, pp. 145–186.
- Martin, T.A., Ye, L., Sanders, A.J., Lane, J. and Jiang, W.G. (2000), “Cancer Invasion and Metastasis: Molecular and Cellular Perspective”, *Madame Curie Bioscience Database*, pp. 1–34.
- Massion, P.P. and Caprioli, R.M. (2006), “Proteomic strategies for the characterization and the early detection of lung cancer.”, *Journal of Thoracic Oncology : Official Publication of the International Association for the Study of Lung Cancer*, Vol. 1 No. 9, pp. 1027–39.
- Mathivanan, S., Ji, H. and Simpson, R.J. (2010), “Exosomes: Extracellular organelles important in intercellular communication”, *Journal of Proteomics*.
- Mathivanan, S. and Simpson, R.J. (2009), “ExoCarta: A compendium of exosomal proteins and RNA”, *Proteomics*, Vol. 9 No. 21, pp. 4997–5000.
- Mears, R., Craven, R.A., Hanrahan, S., Totty, N., Upton, C., et al. (2004), “Proteomic analysis of melanoma-derived exosomes by two-dimensional polyacrylamide gel electrophoresis and mass spectrometry”, *Proteomics*, Vol. 4 No. 12, pp. 4019–4031.
- Mehan, M.R., Ayers, D., Thirstrup, D., Xiong, W., et al. (2012), “Protein signature of lung cancer tissues”, *PLoS ONE*, Vol. 7 No. 4.
- Mehlen, P. and Puisieux, A. (2006), “Metastasis: A question of life or death”, *Nature Reviews Cancer*.

- Meldolesi, J. (2016), “Ectosomes and Exosomes-Two Extracellular Vesicles That Differ Only in Some Details”, *Biochemistry & Molecular Biology Journal*, Vol. 2 No. 1.
- Melo, S.A., Sugimoto, H., O’Connell, J.T., Kato, N., Villanueva, A., et al. (2014a), “Cancer Exosomes Perform Cell-Independent MicroRNA Biogenesis and Promote Tumorigenesis”, *Cancer Cell*, Elsevier Inc., Vol. 26 No. 5, pp. 707–721.
- Melo, S.A., Sugimoto, H., O’Connell, J.T., Kato, N., et al. (2014b), “Cancer Exosomes Perform Cell-Independent MicroRNA Biogenesis and Promote Tumorigenesis”, *Cancer Cell*, Vol. 26 No. 5, pp. 707–721.
- Miller, K.D., Siegel, R.L., Lin, C.C., Mariotto, A.B., Kramer, J.L., et al. (2016), “Cancer treatment and survivorship statistics, 2016”, *CA: A Cancer Journal for Clinicians*, Vol. 66 No. 4, pp. 271–289.
- Minciocchi, V.R., Freeman, M.R. and Di Vizio, D. (2015), “Extracellular Vesicles in Cancer: Exosomes, Microvesicles and the Emerging Role of Large Oncosomes”, *Seminars in Cell and Developmental Biology*.
- Miroshnikova, Y.A., Rozenberg, G.I., Cassereau, L., Pickup, M., Mouw, J.K., et al. (2017), “ $\alpha 5 \beta 1$ -Integrin promotes tension-dependent mammary epithelial cell invasion by engaging the fibronectin synergy site”, *Molecular Biology of the Cell*, Vol. 28 No. 22, pp. 2958–2977.
- Mitchell, M.J. and King, M.R. (2013), “Computational and Experimental Models of Cancer Cell Response to Fluid Shear Stress”, *Frontiers in Oncology*, Frontiers, Vol. 3, p. 44.
- Miyanishi, M., Tada, K., Koike, M., Uchiyama, Y., Kitamura, T. and Nagata, S. (2007), “Identification of Tim4 as a phosphatidylserine receptor.”, *Nature*, Vol. 450 No. 7168, pp. 435–439.
- Mizutani, K., Terazawa, R., Kameyama, K., Kato, T., Horie, K., et al. (2014), “Isolation of prostate cancer-related exosomes”, *Anticancer Research*, Vol. 34 No. 7, pp. 3419–3423.
- Morrissey, M.A., Hagedorn, E.J. and Sherwood, D.R. (2013), “Cell invasion through basement membrane”, *Worm*, Vol. 2 No. 3, p. e26169.
- Muller, L., Mitsuhashi, M., Simms, P., Gooding, W.E. and Whiteside, T.L. (2016), “Tumor-derived exosomes regulate expression of immune function-related genes in human T cell subsets.”, *Scientific Reports*, Nature Publishing Group, Vol. 6 No. April 2015, p. 20254.

- Munson, P. and Shukla, A. (2015), “Exosomes: Potential in Cancer Diagnosis and Therapy”, *Medicines*, Vol. 2 No. 4, pp. 310–327.
- Naidoo, N., Pawitan, Y., Soong, R., Cooper, D.N. and Ku, C.S. (2011), “Human genetics and genomics a decade after the release of the draft sequence of the human genome”, *Human Genomics*.
- Nambiar, M., Kari, V. and Raghavan, S.C. (2008), “Chromosomal translocations in cancer”, *Biochimica et Biophysica Acta - Reviews on Cancer*.
- Nardi, V. and Hasserjian, R.P. (2016), “Genetic Testing in Acute Myeloid Leukemia and Myelodysplastic Syndromes”, *Surgical Pathology Clinics*.
- Natasha G, Gundogan, B., Tan, A., Farhatnia, Y., Wu, W., Rajadas, J. and Seifalian, A.M. (2014), “Exosomes as immunotheranostic nanoparticles”, *Clinical Therapeutics*, Elsevier, Vol. 36 No. 6, pp. 820–829.
- Nesvizhskii, A.I., Keller, A., Kolker, E. and Aebersold, R. (2003), “A statistical model for identifying proteins by tandem mass spectrometry”, *Analytical Chemistry*, Vol. 75 No. 17, pp. 4646–4658.
- Neutzner, M., Lopez, T., Feng, X., Bergmann-Leitner, E.S., Leitner, W.W. et al. (2007), “MFG-E8/lactadherin promotes tumor growth in an angiogenesis-dependent transgenic mouse model of multistage carcinogenesis”, *Cancer Research*.
- Nguyen, D.H. and Hildreth, J.E. (2000), “Evidence for budding of human immunodeficiency virus type 1 selectively from glycolipid-enriched membrane lipid rafts.”, *Journal of Virology*, Vol. 74 No. 7, pp. 3264–72.
- Nguyen, D.X., Bos, P.D. and Massagué, J. (2009), “Metastasis: from dissemination to organ-specific colonization.”, *Nature Reviews. Cancer*, Vol. 9 No. 4, pp. 274–84.
- van Niel, G., Charrin, S., Simoes, S., Romao, M., Rochin, L., et al. (2011), “The Tetraspanin CD63 Regulates ESCRT-Independent and -Dependent Endosomal Sorting during Melanogenesis”, *Developmental Cell*, Vol. 21 No. 4, pp. 708–721.
- Nomura, S., Ozaki, Y. and Ikeda, Y. (2008), “Function and role of microparticles in various clinical settings”, *Thrombosis Research*, Elsevier Ltd, Vol. 123 No. 1, pp. 8–23.
- Ocaña, O.H., Córcoles, R., Fabra, Á., Moreno-Bueno, G., Acloque, H., Vega, S., et al.

- (2012), “Metastatic Colonization Requires the Repression of the Epithelial-Mesenchymal Transition Inducer Prrx1”, *Cancer Cell*, Vol. 22 No. 6, pp. 709–724.
- Odorizzi, G. (2006), “The multiple personalities of Alix.”, *Journal of Cell Science*, Vol. 119 No. Pt 15, pp. 3025–32.
- Oksvold, M.P., Kullmann, A., Forfang, L., Kierulf, B., Li, M., et al. (2014), “Expression of B-Cell surface antigens in subpopulations of exosomes released from B-cell lymphoma cells”, *Clinical Therapeutics*, Vol. 36 No. 6.
- Oshikawa, S., Sonoda, H. and Ikeda, M. (2016), “Aquaporins in urinary extracellular vesicles (Exosomes)”, *International Journal of Molecular Sciences*, Vol. 17 No. 6.
- Ostrowski, M., Carmo, N.B., Krumeich, S., Fanget, I., Raposo, G., et al. (2010), “Rab27a and Rab27b control different steps of the exosome secretion pathway.”, *Nature Cell Biology*, Nature Publishing Group, Vol. 12 No. 1, pp. 19-30–13.
- Palmieri, V., Lucchetti, D., Gatto, I., Maiorana, A., Marcantoni, M., et al. (2014), “Dynamic light scattering for the characterization and counting of extracellular vesicles: A powerful noninvasive tool”, *Journal of Nanoparticle Research*, Vol. 16 No. 9.
- Pan, B.T., Teng, K., Wu, C., Adam, M. and Johnstone, R.M. (1985), “Electron microscopic evidence for externalization of the transferrin receptor in vesicular form in sheep reticulocytes”, *Journal of Cell Biology*, Vol. 101 No. 3, pp. 942–948.
- Pan, J., Chen, H.-Q., Sun, Y.-H., Zhang, J.-H. and Luo, X.-Y. (2008), “Comparative proteomic analysis of non-small-cell lung cancer and normal controls using serum label-free quantitative shotgun technology.”, *Lung*, Vol. 186 No. 4, pp. 255–61.
- Pandey, a and Mann, M. (2000), “Proteomics to study genes and genomes.”, *Nature*, Vol. 405 No. 6788, pp. 837–846.
- Pant, S., Hilton, H. and Burczynski, M.E. (2012), “The multifaceted exosome: Biogenesis, role in normal and aberrant cellular function, and frontiers for pharmacological and biomarker opportunities”, *Biochemical Pharmacology*, Elsevier Inc., Vol. 83 No. 11, pp. 1484–1494.
- Pao, W. and Girard, N. (2011), “New driver mutations in non-small-cell lung cancer”, *Lancet Oncol*, Vol. 12 No. 2, pp. 175–180.

- Park, S.Y., Shin, J.-H. and Kee, S.-H. (2017), “E-cadherin expression increases cell proliferation by regulating energy metabolism through nuclear factor- κ B in AGS cells.”, *Cancer Science*, Vol. 108 No. 9, pp. 1769–1777.
- Parolini, I., Federici, C., Raggi, C., Lugini, L., Palleschi, S., et al. (2009), “Microenvironmental pH is a key factor for exosome traffic in tumor cells”, *Journal of Biological Chemistry*, Vol. 284 No. 49, pp. 34211–34222.
- Pascal, L.E., True, L.D., Campbell, D.S., Deutsch, E.W., Risk, M., et al. (2008), “Correlation of mRNA and protein levels: Cell type-specific gene expression of cluster designation antigens in the prostate”, *BMC Genomics*, Vol. 9.
- Peach, M., Marsh, N. and MacPhee, D.J. (2012), “Protein solubilization: Attend to the choice of lysis buffer”, *Methods in Molecular Biology*, Vol. 869, pp. 37–47.
- Pegtel, D.M., Cosmopoulos, K., Thorley-Lawson, D. a, van Eijndhoven, M. a J., Hopmans, E.S., et al. (2010), “Functional delivery of viral miRNAs via exosomes.”, *Proceedings of the National Academy of Sciences of the United States of America*, Vol. 107 No. 14, pp. 6328–33.
- Peinado, H., Alečković, M., Lavotshkin, S., Matei, I., Costa-Silva, B., et al. (2012), “Melanoma exosomes educate bone marrow progenitor cells toward a pro-metastatic phenotype through MET”, *Nature Medicine*, Vol. 18 No. 6, pp. 883–891.
- Petersen, C.M. (1994), “ α 2-Macroglobulin and pregnancy zone protein: Serum levels, α 2-macroglobulin receptors, cellular synthesis and aspects of function in relation to immunology”, *Acta Obstetrica et Gynecologica Scandinavica*, Vol. 73 No. 2, pp. 161–162.
- Peterson, M.F., Otoc, N., Sethi, J.K., Gupta, A. and Antes, T.J. (2015), “Integrated systems for exosome investigation”, *Methods*, Elsevier Inc., Vol. 87, pp. 31–45.
- Pierotti, M.A. (2017), “The molecular understanding of cancer: From the unspeakable illness to a curable disease”, *Ecancermedicalscience*, Vol. 11.
- Pisitkun, T., Shen, R.-F. and Knepper, M.A. (2004), “Identification and proteomic profiling of exosomes in human urine”, *Proc. Natl. Acad. Sci. USA*, Vol. 101 No. 36, pp. 13368–13373.
- Van Der Pol, E., Van Gemert, M.J.C., Sturk, A., Nieuwland, R. and Van Leeuwen, T.G.

- (2012), “Single vs. swarm detection of microparticles and exosomes by flow cytometry”, *Journal of Thrombosis and Haemostasis*, Vol. 10 No. 5, pp. 919–930.
- Van Der Pol, E., Hoekstra, A.G., Sturk, A., Otto, C., Van Leeuwen, T.G. et al. (2010), “Optical and non-optical methods for detection and characterization of microparticles and exosomes”, *Journal of Thrombosis and Haemostasis*, Vol. 8 No. 12, pp. 2596–2607.
- Pols, M.S. and Klumperman, J. (2009), “Trafficking and function of the tetraspanin CD63”, *Experimental Cell Research*, 15 May.
- Polyak, K. (2007), “Breast cancer: origins and evolution”, *J Clin Invest*, Vol. 117 No. 11, pp. 3155–3163.
- Pomplun, S. (2006), “Pathology of lung cancer”, *Lung Cancer*, pp. 12–26.
- Pospichalova, V., Svoboda, J., Dave, Z., Kotrbova, A., Kaiser, K., et al. (2015), “Simplified protocol for flow cytometry analysis of fluorescently labeled exosomes and microvesicles using dedicated flow cytometer.”, *Journal of Extracellular Vesicles*, Vol. 4, p. 25530.
- Qu, J.L., Qu, X.J., Zhao, M.F., Teng, Y.E., Zhang, Y., et al. (2009), “Gastric cancer exosomes promote tumour cell proliferation through PI3K/Akt and MAPK/ERK activation”, *Digestive and Liver Disease*, Vol. 41 No. 12, pp. 875–880.
- Quail, D.F. and Joyce, J.A. (2013), “Microenvironmental regulation of tumor progression and metastasis.”, *Nature Medicine*, Vol. 19 No. 11, pp. 1423–37.
- Quintana, J.F., Makepeace, B.L., Babayan, S.A., Ivens, A., Pfarr, K.M., Blaxter, M., Debrah, A., et al. (2015), “Extracellular Onchocerca-derived small RNAs in host nodules and blood”, *Parasites and Vectors*, Vol. 8 No. 1.
- Qureshi, A.H., Chaoji, V., Maignel, D., Faridi, M.H., Barth, C.J., et al. (2009), “Proteomic and phospho-proteomic profile of human platelets in basal, resting state: Insights into integrin signaling”, *PLoS ONE*, Vol. 4 No. 10.
- Rabilloud, T. (2009), “Solubilization of proteins in 2DE: an outline.”, *Methods in Molecular Biology (Clifton, N.J.)*, Vol. 519, pp. 19–30.
- Rabilloud, T. and Lelong, C. (2011), “Two-dimensional gel electrophoresis in proteomics: A tutorial”, *Journal of Proteomics*, 6 September.

- Rabinowits, G., Gerçel-Taylor, C., Day, J.M., Taylor, D.D. and Kloecker, G.H. (2009), “Exosomal microRNA: a diagnostic marker for lung cancer.”, *Clinical Lung Cancer*, Elsevier Inc., Vol. 10 No. 1, pp. 42–6.
- Ranza, E., Facchetti, A., Morbini, P., Benericetti, E. and Nano, R. (2007), “Exogenous Platelet-Derived Growth Factor (PDGF) induces human astrocytoma cell line proliferation”, *Anticancer Research*, Vol. 27 No. 4 B, pp. 2161–2166.
- Raposo, G., Nijman, H.W., Stoorvogel, willem, Liejendekker, R., Harding, C. V, et al. (1996), “B lymphocytes secrete antigen-presenting vesicles.”, *The Journal of Experimental Medicine*, Vol. 183 No. 3, pp. 1161–72.
- Raposo, G. and Stoorvogel, W. (2013), “Extracellular vesicles: Exosomes, microvesicles, and friends”, *Journal of Cell Biology*.
- Raz, D.J., He, B., Rosell, R. and Jablons, D.M. (2006), “Bronchioloalveolar carcinoma: A review”, *Clinical Lung Cancer*.
- Reclusa, P., Taverna, S., Pucci, M., Durendez, E., Calabuig, S., et al. (2017), “Exosomes as diagnostic and predictive biomarkers in lung cancer”, *Journal of Thoracic Disease*.
- Redzic, J.S., Kendrick, A.A., Bahmed, K., Dahl, K.D., Pearson, C.G., et al. (2013), “Extracellular Vesicles Secreted from Cancer Cell Lines Stimulate Secretion of MMP-9, IL-6, TGF- β 1 and EMMPRIN”, *PLoS ONE*, Vol. 8 No. 8.
- Rehman, A.A., Ahsan, H. and Khan, F.H. (2013), “Alpha-2-macroglobulin: A physiological guardian”, *Journal of Cellular Physiology*.
- Rekhtman, N. (2010), “Neuroendocrine Tumors of the Lung An Update”, *Arch Pathol Lab Med*, Vol. 134, pp. 1628–1638.
- Ribatti, D., Mangialardi, G. and Vacca, A. (2006), “Stephen Paget and the ‘seed and soil’ theory of metastatic dissemination”, *Clinical and Experimental Medicine*.
- Riches, A., Campbell, E., Borger, E. and Powis, S. (2014), “Regulation of exosome release from mammary epithelial and breast cancer cells-A new regulatory pathway”, *European Journal of Cancer*, Elsevier Ltd, Vol. 50 No. 5, pp. 1025–1034.
- Rider, M.A., Hurwitz, S.N. and Meckes, D.G. (2016), “ExtraPEG: A polyethylene glycol-based method for enrichment of extracellular vesicles”, *Scientific Reports*, Vol. 6.

- Ripperger, T., Gadzicki, D., Meindl, A. and Schlegelberger, B. (2009), “Breast cancer susceptibility: current knowledge and implications for genetic counselling.”, *European Journal of Human Genetics : EJHG*, Vol. 17 No. 6, pp. 722–731.
- Roberts, E., Cossigny, D. a F. and Quan, G.M.Y. (2013), “The Role of Vascular Endothelial Growth Factor in Metastatic Prostate Cancer to the Skeleton.”, *Prostate Cancer*, Vol. 2013 No. 418340, p. 418340.
- Rodrigues, C.A., Gonçalves, M.V., Ikoma, M.R.V., Lorand-Metze, I., Pereira, A.D., Farias, D.L.C. de, Chauffaille, M. de L.L.F., et al. (2016), “Diagnosis and treatment of chronic lymphocytic leukemia: recommendations from the Brazilian Group of Chronic Lymphocytic Leukemia”, *Revista Brasileira de Hematologia E Hemoterapia*, Vol. 38 No. 4, pp. 346–357.
- Ruoslahti, E. (1999), “Fibronectin and its integrin receptors in cancer.”, *Advances in Cancer Research*, Vol. 76, pp. 1–20.
- Saleem, S.N. and Abdel-Mageed, A.B. (2015), “Tumor-derived exosomes in oncogenic reprogramming and cancer progression”, *Cellular and Molecular Life Sciences*, Birkhauser Verlag AG.
- Salomon, C., Kobayashi, M., Ashman, K., Sobrevia, L., Mitchell, M.D. et al. (2013), “Hypoxia-induced changes in the bioactivity of cytotrophoblast-derived exosomes”, *PLoS ONE*, Vol. 8 No. 11.
- Samavarchi-Tehrani, P., Golipour, A., David, L., Sung, H.K., Beyer, T.A., Datti, et al. (2010), “Functional genomics reveals a BMP-Driven mesenchymal-to-Epithelial transition in the initiation of somatic cell reprogramming”, *Cell Stem Cell*, Vol. 7 No. 1, pp. 64–77.
- Sandfeld-Paulsen, B., Jakobsen, K.R., Bæk, R., Folkersen, B.H., Rasmussen, T.R., et al. (2016), “Exosomal Proteins as Diagnostic Biomarkers in Lung Cancer”, *Journal of Thoracic Oncology*, Vol. 0 No. 0, pp. 1462–1474.
- Saultz, J. and Garzon, R. (2016), “Acute Myeloid Leukemia: A Concise Review”, *Journal of Clinical Medicine*, Vol. 5 No. 3, p. 33.
- Sauter, W., Rosenberger, A., Beckmann, L., Kropp, S., Mittelstrass, K., et al. (2008), “Matrix metalloproteinase 1 (MMP1) is associated with early-onset lung cancer”, *Cancer*

Epidemiology Biomarkers and Prevention, Vol. 17 No. 5, pp. 1127–1135.

Van Schil, P.E., Asamura, H., Rusch, V.W., Mitsudomi, T., Tsuboi, M., Brambillae, E. and Travis, W.D. (2012), “Surgical implications of the new IASLC/ ATS/ERS adenocarcinoma classification”, *European Respiratory Journal*.

Schmittgen, T.D. and Livak, K.J. (2008), “Analyzing real-time PCR data by the comparative CT method”, *Nature Protocols*, Vol. 3 No. 6, pp. 1101–1108.

Schorey, J.S., Cheng, Y., Singh, P.P. and Smith, V.L. (2015), “Exosomes and other extracellular vesicles in host-pathogen interactions”, *EMBO Reports*, Vol. 16 No. 1, pp. 24–43.

Seiwert, T.Y., Tretiakova, M., Ma, P.C., Khaleque, M.A., Husain, A.N., et al. (2005), “Heat shock protein (HSP) overexpression in lung cancer and potential as a therapeutic target”, *Cancer Research*, Vol. 65 No. 9 Supplement, pp. 559–560.

Seo, J.S., Ju, Y.S., Lee, W.C., Shin, J.Y., Lee, J.K., et al. (2012), “The transcriptional landscape and mutational profile of lung adenocarcinoma”, *Genome Research*, Vol. 22 No. 11, pp. 2109–2119.

Sharma, S., Rasool, H.I., Palanisamy, V., Mathisen, C., Schmidt, M., et al. (2010), “Structural-mechanical characterization of nanoparticle exosomes in human saliva, using correlative AFM, FESEM, and force spectroscopy”, *ACS Nano*, Vol. 4 No. 4, pp. 1921–1926.

Sharma, S. V., Bell, D.W., Settleman, J. and Haber, D.A. (2007), “Epidermal growth factor receptor mutations in lung cancer”, *Nature Reviews Cancer*.

Sharma, S., Zuñiga, F., Rice, G.E., Perrin, L.C., Hooper, J.D. et al. (2017), “Tumor-derived exosomes in ovarian cancer – liquid biopsies for early detection and real-time monitoring of cancer progression”, *Oncotarget*, Vol. 8 No. 61, pp. 104687–104703.

Shelke, G.V., Lässer, C., Gho, Y.S. and Lötvall, J. (2014), “Importance of exosome depletion protocols to eliminate functional and RNA-containing extracellular vesicles from fetal bovine serum”, *Journal of Extracellular Vesicles*, Vol. 3 No. 1, available at:<https://doi.org/10.3402/jev.v3.24783>.

Shiwa, M., Nishimura, Y., Wakatabe, R., Fukawa, A., Arikuni, H., et al. (2003), “Rapid discovery and identification of a tissue-specific tumor biomarker from 39 human cancer

- cell lines using the SELDI ProteinChip platform”, *Biochemical and Biophysical Research Communications*, Vol. 309 No. 1, pp. 18–25.
- Sidoli, S., Lin, S., Karch, K.R. and Garcia, B.A. (2015), “Bottom-Up and Middle-Down Proteomics Have Comparable Accuracies in Defining Histone Post-Translational Modification Relative Abundance and Stoichiometry”, *Analytical Chemistry*, Vol. 87 No. 6, pp. 3129–3133.
- Siegel, R.L., Miller, K.D. and Jemal, A. (2016), “Cancer statistics, 2016.”, *CA: A Cancer Journal for Clinicians*, Vol. 66 No. 1, pp. 7–30.
- Siegel, R.L., Miller, K.D. and Jemal, A. (2018), “Cancer statistics, 2018”, *CA: A Cancer Journal for Clinicians*, Vol. 68 No. 1, pp. 7–30.
- Simons, M. and Raposo, G. (2009), “Exosomes--vesicular carriers for intercellular communication.”, *Current Opinion in Cell Biology*, Vol. 21, pp. 575–581.
- Simpson, R.J., Jensen, S.S. and Lim, J.W.E. (2008), “Proteomic profiling of exosomes: Current perspectives”, *Proteomics*, Vol. 8 No. 19, pp. 4083–4099.
- Simpson, R.J., Lim, J.W.E., Moritz, R.L. and Mathivanan, S. (2009), “Exosomes: Proteomic insights and diagnostic potential”, *Expert Review of Proteomics*.
- Skogberg, G., Lundberg, V., Berglund, M., Gudmundsdottir, J., Telemo, E., et al. (2015), “Human thymic epithelial primary cells produce exosomes carrying tissue-restricted antigens”, *Immunology and Cell Biology*, Vol. 93 No. 8, pp. 727–734.
- Skokos, D., Le Panse, S., Villa, I., Rousselle, J.-C., Peronet, R., et al. (2001), “Mast cell-dependent B and T lymphocyte activation is mediated by the secretion of immunologically active exosomes”, *The Journal of Immunology*, Vol. 166 No. 2, pp. 868–876.
- Smalheiser, N.R. (2007), “Exosomal transfer of proteins and RNAs at synapses in the nervous system.”, *Biology Direct*, Vol. 2, p. 35.
- Smalley, D.M., Sheman, N.E., Nelson, K. and Theodorescu, D. (2008), “Isolation and identification of potential urinary microparticle biomarkers of bladder cancer”, *Journal of Proteome Research*, Vol. 7 No. 5, pp. 2088–2096.
- Sokolova, V., Ludwig, A.-K., Hornung, S., Rotan, O., Horn, P.A., Epple, M. et al. (2011),

- “Characterisation of exosomes derived from human cells by nanoparticle tracking analysis and scanning electron microscopy”, *Colloids and Surfaces B: Biointerfaces*, Elsevier B.V., Vol. 87 No. 1, pp. 146–150.
- Sottrup-Jensen, L., Folkersen, J., Kristensen, T. and Tack, B.F. (1984), “Partial primary structure of human pregnancy zone protein: extensive sequence homology with human alpha 2-macroglobulin.”, *Proceedings of the National Academy of Sciences of the United States of America*, Vol. 81 No. 23, pp. 7353–7.
- Soung, Y.H., Nguyen, T., Cao, H., Lee, J. and Chung, J. (2015), “Emerging roles of exosomes in cancer invasion and metastasis.”, *BMB Reports*, Vol. 49 No. 1, pp. 18–25.
- Sparks, D.L. and Phillips, M.C. (1992), “Quantitative measurement of lipoprotein surface charge by agarose gel electrophoresis.”, *Journal of Lipid Research*, Vol. 33, pp. 123–130.
- Stellman, S.D., Muscat, J.E., Thompson, S., Hoffmann, D. and Wynder, E.L. (1997), “Risk of squamous cell carcinoma and adenocarcinoma of the lung in relation to lifetime filter cigarette smoking”, *Cancer*, Vol. 80 No. 3, pp. 382–388.
- Stewart, A.B., Anderson, W., Delves, G., Lwaleed, B.A., Birch, B. and Cooper, A. (2004), “Prostasomes: A role in prostatic disease?”, *BJU International*, Vol. 94 No. 7, pp. 985–989.
- Stuckey, A. (2011), “Breast cancer: Epidemiology and risk factors”, *Clinical Obstetrics and Gynecology*, Vol. 54 No. 1, pp. 96–102.
- Sun, D., Zhuang, X., Zhang, S., Deng, Z. Bin, Grizzle, W., et al. (2013), “Exosomes are endogenous nanoparticles that can deliver biological information between cells”, *Advanced Drug Delivery Reviews*, Elsevier B.V., Vol. 65 No. 3, pp. 342–347.
- Sun, S., Schiller, J.H. and Gazdar, A.F. (2007), “Lung cancer in never smokers — a different disease”, *Nature*, Vol. 7 No. october, pp. 778–790.
- Sunkara, V., Woo, H.-K. and Cho, Y.-K. (2016), “Emerging techniques in the isolation and characterization of extracellular vesicles and their roles in cancer diagnostics and prognostics”, *The Analyst*, Vol. 141 No. 2, pp. 371–381.
- Syn, N., Wang, L., Sethi, G., Thiery, J.P. and Goh, B.C. (2016), “Exosome-Mediated Metastasis: From Epithelial-Mesenchymal Transition to Escape from

- Immunosurveillance”, *Trends in Pharmacological Sciences*, Elsevier Ltd, 1 July.
- Takahashi, Y., Nishikawa, M., Shinotsuka, H., Matsui, Y., Ohara, S., et al. (2013), “Visualization and in vivo tracking of the exosomes of murine melanoma B16-BL6 cells in mice after intravenous injection”, *Journal of Biotechnology*, Vol. 165 No. 2, pp. 77–84.
- Talmadge, J.E. and Fidler, I.J. (2010), “AACR centennial series: The biology of cancer metastasis: Historical perspective”, *Cancer Research*, 15 July.
- Taylor, D.D. and Gerçel-Taylor, C. (2008), “MicroRNA signatures of tumor-derived exosomes as diagnostic biomarkers of ovarian cancer”, *Gynecologic Oncology*, Vol. 110 No. 1, pp. 13–21.
- Taylor, D.D., Lyons, K.S. and Gerçel-Taylor, Ç. (2002), “Shed membrane fragment-associated markers for endometrial and ovarian cancers”, *Gynecologic Oncology*, Vol. 84 No. 3, pp. 443–448.
- Taylor, D.D. and Shah, S. (2015a), “Methods of isolating extracellular vesicles impact downstream analyses of their cargoes”, *Methods*, Academic Press Inc., 1 October.
- Taylor, D.D., Zacharias, W. and Gerçel-Taylor, C. (2011), “Exosome isolation for proteomic analyses and RNA profiling”, *Methods in Molecular Biology*, Vol. 728, pp. 235–246.
- Théry, C., Amigorena, S., Raposo, G. and Clayton, A. (2006), “Isolation and characterization of exosomes from cell culture supernatants and biological fluids.”, *Current Protocols in Cell Biology / Editorial Board, Juan S. Bonifacino ... [et Al.]*, Vol. Chapter 3, p. Unit 3.22.
- Théry, C., Boussac, M., Veron, P., Ricciardi-Castagnoli, P., Raposo, G., et al. (2001), “Proteomic analysis of dendritic cell-derived exosomes: A secreted subcellular compartment distinct from apoptotic vesicles”, *The Journal of Immunology*, Vol. 166 No. 12, pp. 7309–7318.
- Théry, C., Duban, L., Segura, E., Véron, P., Lantz, O. et al., (2002), “Indirect activation of naïve CD4⁺ T cells by dendritic cell-derived exosomes”, *Nature Immunology*, Vol. 3 No. 12, pp. 1156–1162.
- Théry, C., Ostrowski, M. and Segura, E. (2009), “Membrane vesicles as conveyors of immune responses.”, *Nature Reviews. Immunology*, Vol. 9 No. 8, pp. 581–93.

- Théry, C., Regnault, A., Garin, J., Wolfers, J., Zitvogel, L., et al. (1999), “Molecular characterization of dendritic cell-derived exosomes: Selective accumulation of the heat shock protein hsc73”, *Journal of Cell Biology*, Vol. 147 No. 3, pp. 599–610.
- Théry, C., Zitvogel, L. and Amigorena, S. (2002), “Exosomes: composition, biogenesis and function.”, *Nature Reviews. Immunology*, Vol. 2 No. 8, pp. 569–579.
- Thind, A. and Wilson, C. (2016), “Exosomal miRNAs as cancer biomarkers and therapeutic targets”, *J Extracell Vesicles*, Vol. 5, p. 31292.
- Thomas, S.N., Liao, Z., Clark, D., Chen, Y., Samadani, R., et al. (2013), “Exosomal Proteome Profiling: A Potential Multi-Marker Cellular Phenotyping Tool to Characterize Hypoxia-Induced Radiation Resistance in Breast Cancer”, *Proteomes*, Vol. 1 No. 2, pp. 87–108.
- Thompson, W.H. (2004), “Bronchioloalveolar Carcinoma Masquerading as Pneumonia”, *Care*, Vol. 49 No. 11, p. 13491353.
- Tickner, J.A., Urquhart, A.J., Stephenson, S.-A., Richard, D.J. and O’Byrne, K.J. (2014), “Functions and therapeutic roles of exosomes in cancer.”, *Frontiers in Oncology*, Vol. 4 No. May, p. 127.
- Timofeeva, M., Kropp, S., Sauter, W., Beckmann, L., Rosenberger, A., et al. (2010), “Genetic polymorphisms of MPO, GSTT1, GSTM1, GSTP1, EPHX1 and NQO1 as risk factors of early-onset lung cancer”, *International Journal of Cancer*, Vol. 127 No. 7, pp. 1547–1561.
- Timofeeva, M.N., Kropp, S., Sauter, W., Beckmann, L., Rosenberger, A., et al. (2009), “CYP450 polymorphisms as risk factors for early-onset lung cancer: Gender-specific differences”, *Carcinogenesis*, Vol. 30 No. 7, pp. 1161–1169.
- Tkach, M. and Théry, C. (2016), “Communication by Extracellular Vesicles: Where We Are and Where We Need to Go”, *Cell*.
- De Toro, J., Herschlik, L., Waldner, C. and Mongini, C. (2015), “Emerging roles of exosomes in normal and pathological conditions: new insights for diagnosis and therapeutic applications.”, *Frontiers in Immunology*, Frontiers Media SA, Vol. 6, p. 203.
- Trajkovic, K., Hsu, C., Chiantia, S., Rajendran, L., Wenzel, D., et al. (2008), “Ceramide triggers budding of exosome vesicles into multivesicular endosomes.”, *Science (New*

- York, N.Y.), Vol. 319 No. April, pp. 1244–1247.
- Tran, J.C., Zamdborg, L., Ahlf, D.R., Lee, J.E., Catherman, A.D., et al. (2011), “Mapping intact protein isoforms in discovery mode using top-down proteomics”, *Nature*, Vol. 480 No. 7376, pp. 254–258.
- Trioulier, Y., Torch, S., Blot, B., Cristina, N., Chatellard-Causse, C., et al. (2004), “Alix, a Protein Regulating Endosomal Trafficking, Is Involved in Neuronal Death”, *Journal of Biological Chemistry*, Vol. 279 No. 3, pp. 2046–2052.
- Tsai, J.H., Donaher, J.L., Murphy, D.A., Chau, S. and Yang, J. (2012), “Spatiotemporal Regulation of Epithelial-Mesenchymal Transition Is Essential for Squamous Cell Carcinoma Metastasis”, *Cancer Cell*, Vol. 22 No. 6, pp. 725–736.
- Turay, D., Khan, S., Diaz Osterman, C.J., Curtis, M.P., Khaira, B., Neidigh, J.W., et al. (2016), “Proteomic Profiling of Serum-Derived Exosomes from Ethnically Diverse Prostate Cancer Patients.”, *Cancer Investigation*, Vol. 34 No. 1, pp. 1–11.
- Umezū, T., Tadokoro, H., Azuma, K., Yoshizawa, S., Ohyashiki, K. et al. (2014), “Exosomal miR-135b shed from hypoxic multiple myeloma cells enhances angiogenesis by targeting factor-inhibiting HIF-1”, *Blood*, Vol. 124 No. 25, pp. 3748–3757.
- Ummanni, R., Teller, S., Junker, H., Zimmermann, U., Venz, S., et al. (2008), “Altered expression of tumor protein D52 regulates apoptosis and migration of prostate cancer cells”, *FEBS Journal*, Vol. 275 No. 22, pp. 5703–5713.
- Urbanelli, L., Magini, A., Buratta, S., Brozzi, A., Sagini, K., et al. (2013), “Signaling pathways in exosomes biogenesis, secretion and fate”, *Genes*, Vol. 4 No. 2, pp. 152–170.
- Uzel, E.K. and Abacıoğlu, U. (2015), “Treatment of early stage non-small cell lung cancer: Surgery or stereotactic ablative radiotherapy?”, *Balkan Medical Journal*, Vol. 32 No. 1, pp. 8–16.
- Valadi, H., Ekström, K., Bossios, A., Sjöstrand, M., Lee, J.J. et al. (2007), “Exosome-mediated transfer of mRNAs and microRNAs is a novel mechanism of genetic exchange between cells”, *Nature Cell Biology*, Vol. 9 No. 6, pp. 654–659.
- Vences-Catalán, F., Rajapaksa, R., Srivastava, M.K., Marabelle, A., Kuo, C.C., et al. (2015), “Tetraspanin CD81 promotes tumor growth and metastasis by modulating the functions

- of T regulatory and myeloid-derived suppressor cells”, *Cancer Research*, American Association for Cancer Research Inc., Vol. 75 No. 21, pp. 4517–4526.
- Villarroya-Beltri, C., Baixauli, F., Gutiérrez-Vázquez, C., Sánchez-Madrid, F. and Mittelbrunn, M. (2014), “Sorting it out: Regulation of exosome loading”, *Seminars in Cancer Biology*, Vol. 28 No. 1, pp. 3–13.
- Vo, T.T., Ryan, J., Carrasco, R., Neuberg, D., Rossi, D.J., Stone, R.M., et al. (2012), “Relative mitochondrial priming of myeloblasts and normal HSCs determines chemotherapeutic success in AML”, *Cell*, Vol. 151 No. 2, pp. 344–355.
- Vogelstein, B., Papadopoulos, N., Velculescu, V.E., Zhou, S., Diaz, L., et al. (2013), “Cancer Genome Landscapes”, *Science*, Vol. 339 No. 6127, pp. 1546–1558.
- Wahlgren, J., Karlson, T.D.L., Brisslert, M., Vaziri Sani, F., Telemo, E., Sunnerhagen, P. and Valadi, H. (2012), “Plasma exosomes can deliver exogenous short interfering RNA to monocytes and lymphocytes”, *Nucleic Acids Research*, Vol. 40 No. 17.
- Wang, H.-X., Li, Q., Sharma, C., Knoblich, K. and Hemler, M.E. (2011), “Tetraspanin protein contributions to cancer.”, *Biochemical Society Transactions*, Vol. 39 No. 2, pp. 547–552.
- Wang, J., Sun, X., Zhao, J., Yang, Y., Cai, X., et al. (2017), “Exosomes: A novel strategy for treatment and prevention of diseases”, *Frontiers in Pharmacology*.
- Wang, J., Yao, Y., Wu, J. and Li, G. (2015), “Identification and analysis of exosomes secreted from macrophages extracted by different methods”, *International Journal of Clinical and Experimental Pathology*, Vol. 8 No. 6, pp. 6135–6142.
- Wasinger, V.C., Cordwell, S.J., Cerpa-Poljak, A., Yan, J.X., Gooley, A.A., et al. (1995), “Progress with gene-product mapping of the Mollicutes: *Mycoplasma genitalium*”, *Electrophoresis*, Vol. 16 No. 1, pp. 1090–1094.
- Webber, J., Steadman, R., Mason, M.D., Tabi, Z. and Clayton, A. (2010), “Cancer exosomes trigger fibroblast to myofibroblast differentiation”, *Cancer Research*, Vol. 70 No. 23, pp. 9621–9630.
- Webster, M., Witkin, K.L. and Cohen-Fix, O. (2009), “Sizing up the nucleus: nuclear shape, size and nuclear-envelope assembly”, *Journal of Cell Science*, Vol. 122 No. 10, pp. 1477–1486.

- Weng, Y., Sui, Z., Shan, Y., Hu, Y., Chen, Y., et al. (2016), “Effective isolation of exosomes with polyethylene glycol from cell culture supernatant for in-depth proteome profiling”, *The Analyst*, Vol. 141 No. 15, pp. 4640–4646.
- Whiteside, T. (2016), “Tumor-Derived Exosomes and Their Role in Tumor-Induced Immune Suppression”, *Vaccines*, Vol. 4 No. 4, p. 35.
- Willms, E., Johansson, H.J., Mäger, I., Lee, Y., Blomberg, K.E.M., et al. (2016), “Cells release subpopulations of exosomes with distinct molecular and biological properties.”, *Scientific Reports*, Nature Publishing Group, Vol. 6 No. February, p. 22519.
- Wirtz, D., Konstantopoulos, K. and Searson, P.C. (2011), “The physics of cancer: the role of physical interactions and mechanical forces in metastasis.”, *Nature Reviews. Cancer*, Nature Publishing Group, Vol. 11 No. 7, pp. 512–522.
- Witwer, K.W., Buzás, E.I., Bemis, L.T., Bora, A., Lässer, C., et al. (2013), “Standardization of sample collection, isolation and analysis methods in extracellular vesicle research”, *Journal of Extracellular Vesicles*, Vol. 2 No. 1.
- Wolters, D.A., Washburn, M.P. and Yates, J.R. (2001), “An automated multidimensional protein identification technology for shotgun proteomics”, *Analytical Chemistry*, Vol. 73 No. 23, pp. 5683–5690.
- Wu, J., Liu, T., Rios, Z., Mei, Q., Lin, X., et al. (2017), “Heat Shock Proteins and Cancer”, *Trends in Pharmacological Sciences*.
- Wu, W., Hu, W. and Kavanagh, J.J. (2002), “Proteomics in cancer research”, *International Journal of Gynecological Cancer*.
- Wubbolts, R., Leckie, R.S., Veenhuizen, P.T.M., Schwarzmann, G., Möbius, W., Hoernschemeyer, J., et al. (2003), “Proteomic and biochemical analyses of human B cell-derived exosomes: Potential implications for their function and multivesicular body formation”, *Journal of Biological Chemistry*, Vol. 278 No. 13, pp. 10963–10972.
- Xia, Y., Li, B., Gao, N., Xia, H., Men, Y., et al. (2014), “Expression of tumor-associated calcium signal transducer 2 in patients with salivary adenoid cystic carcinoma: Correlation with clinicopathological features and prognosis”, *Oncology Letters*, Vol. 8 No. 4, pp. 1670–1674.
- Xin, H., Li, Y., Buller, B., Katakowski, M., Zhang, Y., et al. (2012), “Exosome-mediated

- transfer of miR-133b from multipotent mesenchymal stromal cells to neural cells contributes to neurite outgrowth”, *Stem Cells*, Vol. 30 No. 7, pp. 1556–1564.
- YAMADA, T., INOSHIMA, Y., MATSUDA, T. and ISHIGURO, N. (2012), “Comparison of Methods for Isolating Exosomes from Bovine Milk”, *Journal of Veterinary Medical Science*, Vol. 74 No. 11, pp. 1523–1525.
- Yan, X.-J., Xu, J., Gu, Z.-H., Pan, C.-M., Lu, G., et al. (2011), “Exome sequencing identifies somatic mutations of DNA methyltransferase gene DNMT3A in acute monocytic leukemia”, *Nature Genetics*, Vol. 43 No. 4, pp. 309–315.
- Yáñez-Mó, M., Siljander, P.R.-M., Andreu, Z., Zavec, A.B., Borràs, F.E., et al. (2015), “Biological properties of extracellular vesicles and their physiological functions.”, *Journal of Extracellular Vesicles*, Vol. 4, p. 27066.
- Yang, C.-M., Ji, S., Li, Y., Fu, L.-Y., Jiang, T. and Meng, F. (2017), “ β -Catenin promotes cell proliferation, migration, and invasion but induces apoptosis in renal cell carcinoma”, *OncoTargets and Therapy*, Vol. 10, pp. 711–724.
- Yang, C. and Robbins, P.D. (2011), “The roles of tumor-derived exosomes in cancer pathogenesis”, *Clinical and Developmental Immunology*.
- Yang, T., Martin, P., Fogarty, B., Brown, A., Schurman, K., et al. (2015), “Exosome delivered anticancer drugs across the blood-brain barrier for brain cancer therapy in Danio Rerio”, *Pharmaceutical Research*, Vol. 32 No. 6, pp. 2003–2014.
- Yang, Y., Bucan, V., Baehre, H., Von Der Ohe, J., Otte, A., et al. (2015), “Acquisition of new tumor cell properties by MSC-derived exosomes”, *International Journal of Oncology*, Vol. 47 No. 1, pp. 244–252.
- Yates, J.R. (2004), “Mass Spectral Analysis in Proteomics”, *Annual Review of Biophysics and Biomolecular Structure*, Vol. 33 No. 1, pp. 297–316.
- Yellon, D.M. and Davidson, S.M. (2014), “Exosomes nanoparticles involved in cardioprotection?”, *Circulation Research*.
- Yoshioka, Y., Konishi, Y., Kosaka, N., Katsuda, T., Kato, T. and Ochiya, T. (2013), “Comparative marker analysis of extracellular vesicles in different human cancer types.”, *Journal of Extracellular Vesicles*, Vol. 2, pp. 1–9.

- You, S.-A. and Wang, Q.K. (2006), “Proteomics with two-dimensional gel electrophoresis and mass spectrometry analysis in cardiovascular research.”, *Methods in Molecular Medicine*, Vol. 129, pp. 15–26.
- Yousefpour, P. and Chilkoti, A. (2014), “Co-opting biology to deliver drugs”, *Biotechnology and Bioengineering*.
- Zaidel-Bar, R., Itzkovitz, S., Ma’ayan, A., Iyengar, R. and Geiger, B. (2007), “Functional atlas of the integrin adhesome”, *Nature Cell Biology*, Vol. 9 No. 8, pp. 858–867.
- Zeitouni, N.E., Chotikatum, S., von Köckritz-Blickwede, M. and Naim, H.Y. (2016), “The impact of hypoxia on intestinal epithelial cell functions: consequences for invasion by bacterial pathogens.”, *Molecular and Cellular Pediatrics*, Molecular and Cellular Pediatrics, Vol. 3 No. 1, p. 14.
- Zhang, B., Yin, Y., Lai, R.C. and Lim, S.K. (2014), “Immunotherapeutic potential of extracellular vesicles”, *Frontiers in Immunology*, Vol. 5 No. OCT.
- Zhang, J., Li, S., Li, L., Li, M., Guo, C., Yao, J. and Mi, S. (2015), “Exosome and exosomal microRNA: Trafficking, sorting, and function”, *Genomics, Proteomics and Bioinformatics*.
- Zhang, Y. and Wang, X.-F. (2015), “A niche role for cancer exosomes in metastasis”, *Nature Cell Biology*, Nature Publishing Group, Vol. 17 No. 6, pp. 709–711.
- Zhong, J., Eliceiri, B., Stupack, D., Penta, K., Sakamoto, G., et al. (2003), “Neovascularization of ischemic tissues by gene delivery of the extracellular matrix protein Del-1”, *Journal of Clinical Investigation*, Vol. 112 No. 1, pp. 30–41.
- Zhou, H., Yuen, P.S.T., Pisitkun, T., Gonzales, P.A., Yasuda, H., et al. (2006), “Collection, storage, preservation, and normalization of human urinary exosomes for biomarker discovery”, *Kidney International*, Vol. 69 No. 8, pp. 1471–1476.
- Zhou, L., Lv, T., Zhang, Q., Zhu, Q., Zhan, P., Zhu, S., et al. (2017), “The biology, function and clinical implications of exosomes in lung cancer”, *Cancer Letters*.
- Zitvogel, L., Regnault, a, Lozier, a, Wolfers, J., Flament, C., et al. (1998), “Eradication of established murine tumors using a novel cell-free vaccine: dendritic cell-derived exosomes.”, *Nature Medicine*, Vol. 4 No. 5, pp. 594-600.

Appendix

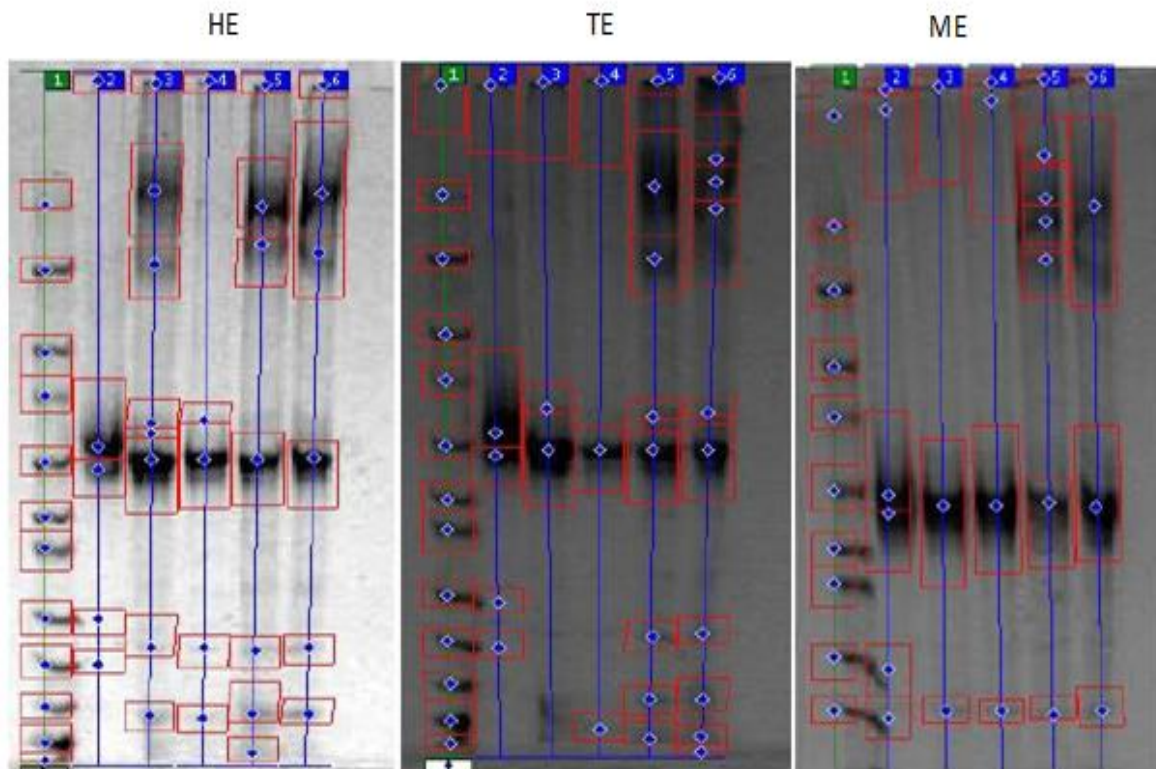


Figure 1: One dimensional gel electrophoresis of exosomes derived from H358 (HE), THP1 (TE) and MCF7 (ME). The gels are analysed by one dimensional gel electrophoresis software CLIQS.

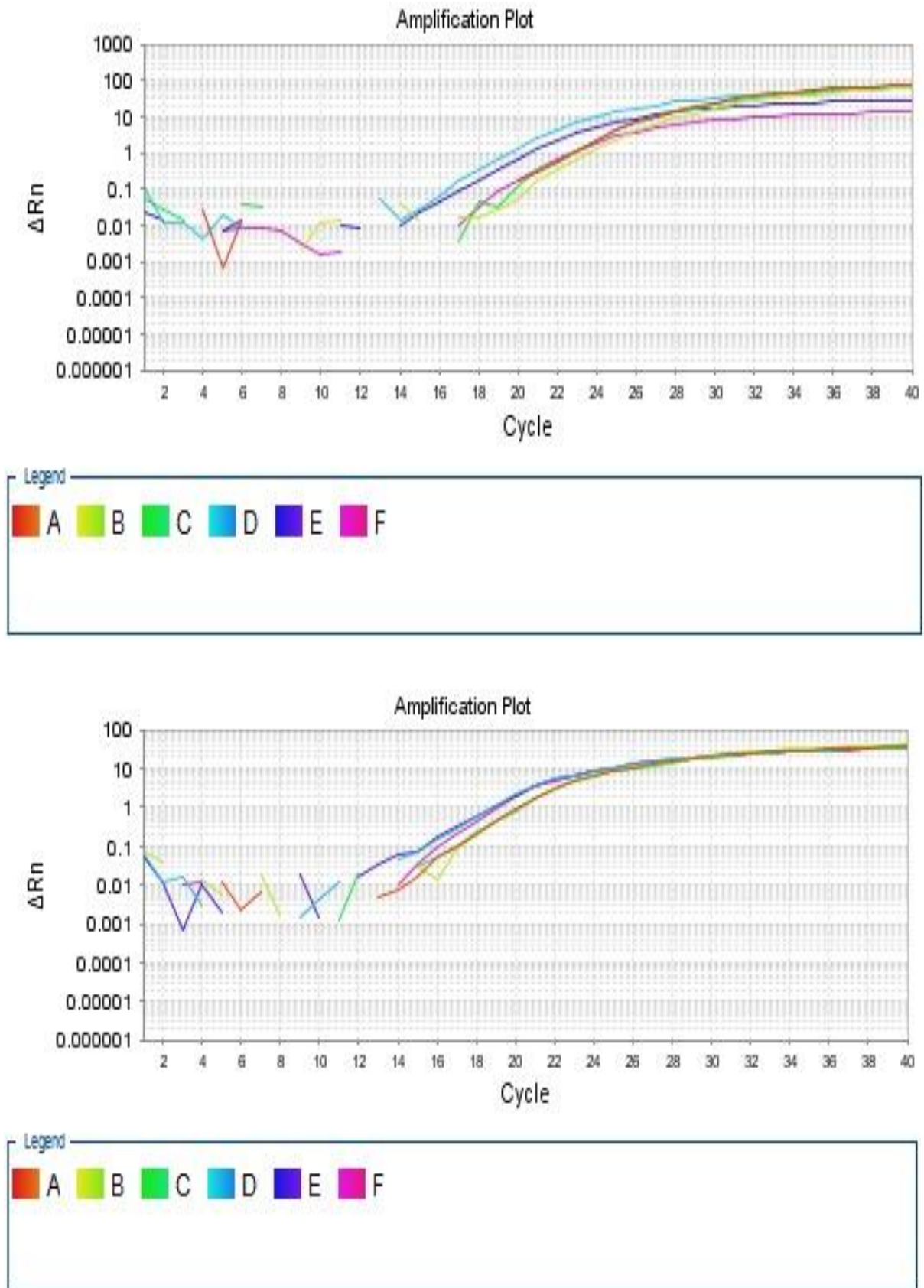


Figure 2: Amplification plot of Sample 1 & 2 of the biological triplicate Integrin alpha-3 (ITGA3). The color of the lines represents the technical replicates of each sample. A, B and C represents the technical samples from HBTE and E, F and G represents the technical replicates of cancer cell H358.

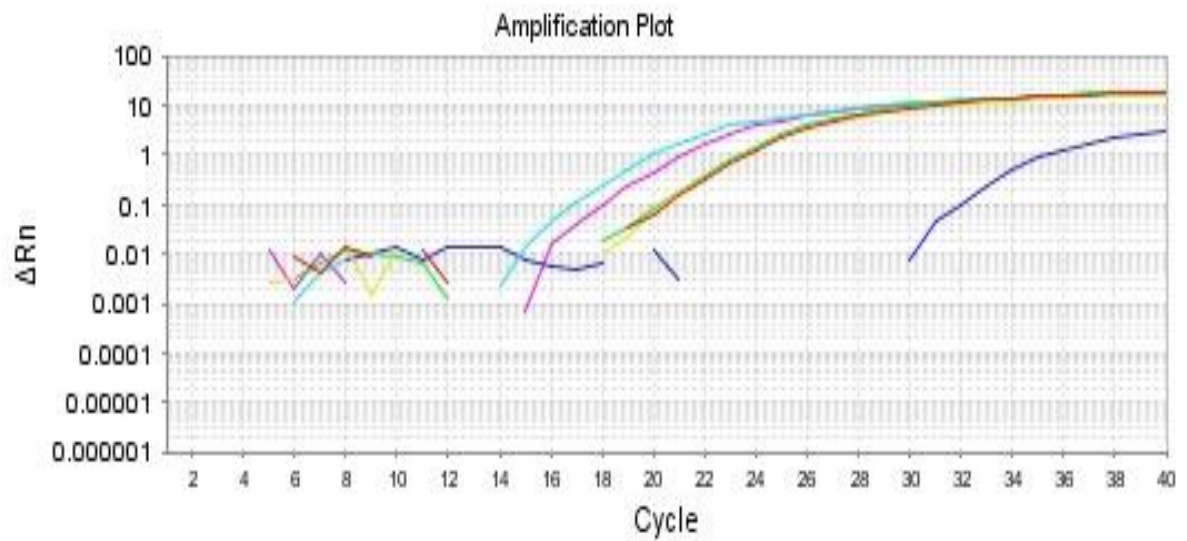
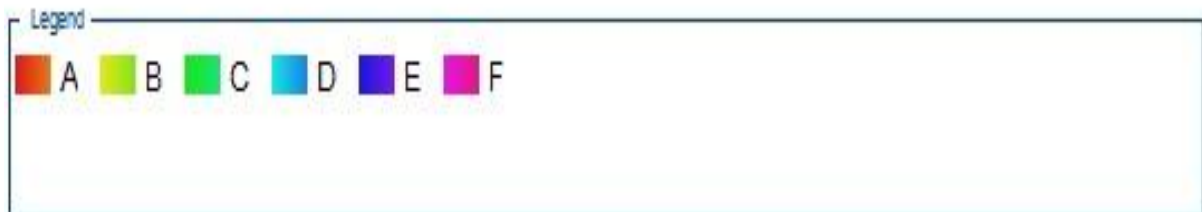
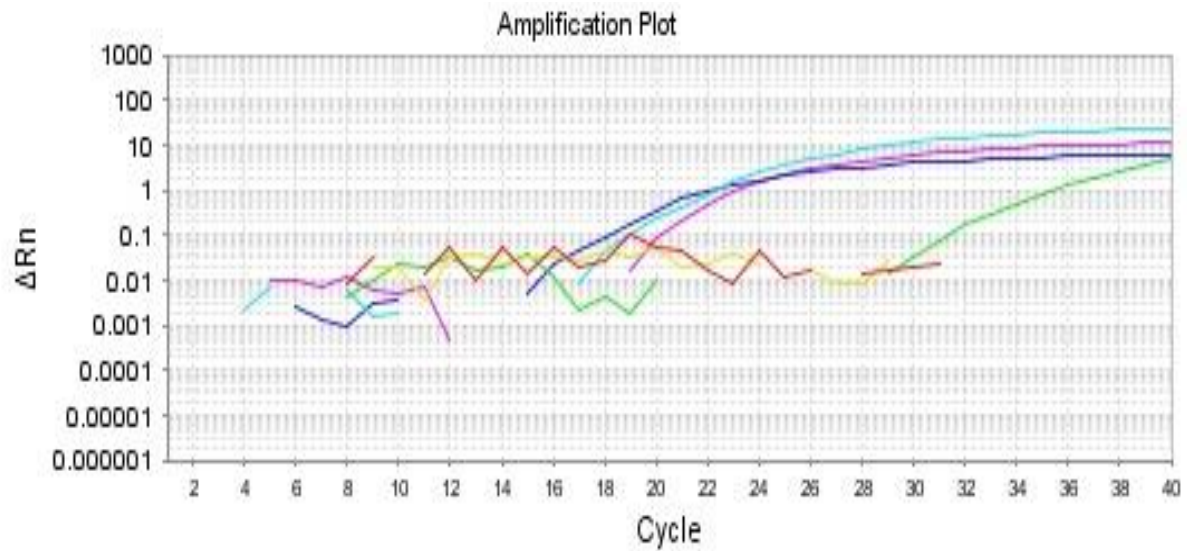


Figure 3: Amplification plot of Sample 1 & 2 of the biological triplicate Cadherin-1 (CDH1). The color of the lines represents the technical replicates of each sample. A, B and C represents the technical samples from HBTE and E, F and G represents the technical triplicates of cancer cell H358.

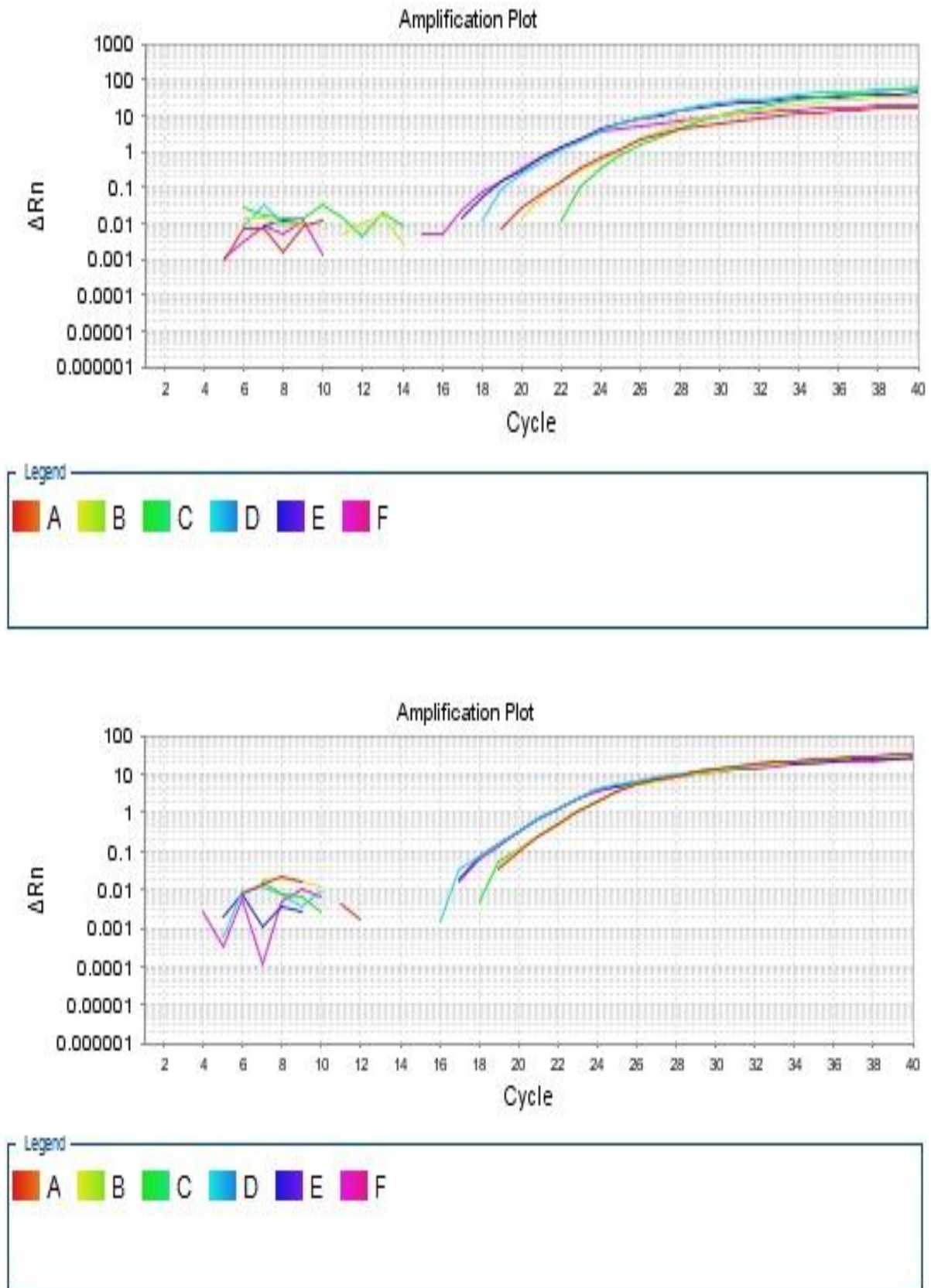


Figure 4: Amplification plot of Sample 1 & 2 of the biological triplicate Laminin gamma-1 (LAMC1). The color of the lines represents the technical replicates of each sample. A, B and C represents the technical samples from HBTE and E, F and G represents the technical replicates of cancer cell H358.

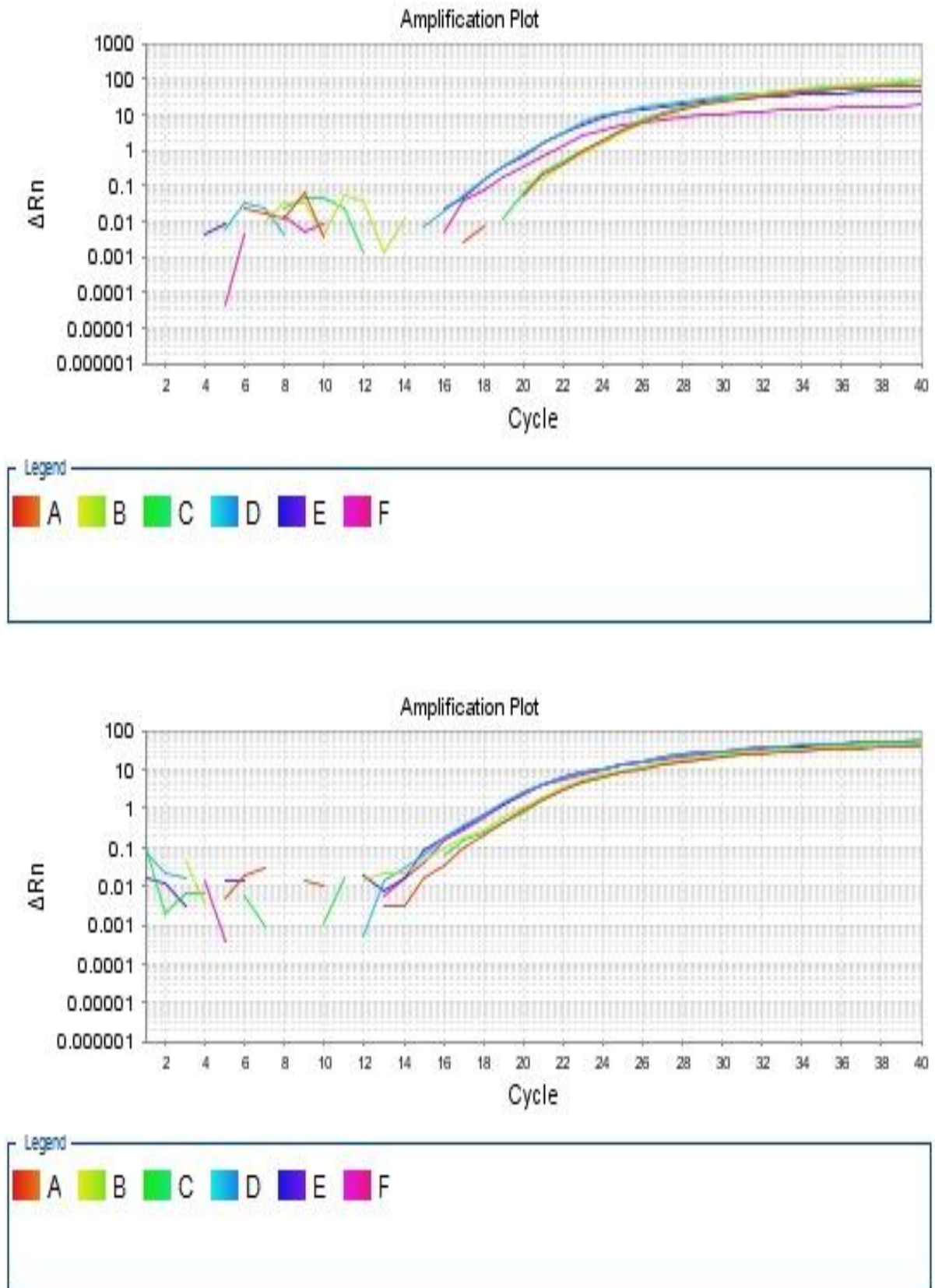


Figure 5: Amplification plot of Sample 1 & 2 of the biological triplicate Catenin beta-1 (CTNNB1). The color of the lines represents the technical replicates of each sample. A, B and C represents the technical samples from HBTE and E, F and G represents the technical triplicates of cancer cell H358.

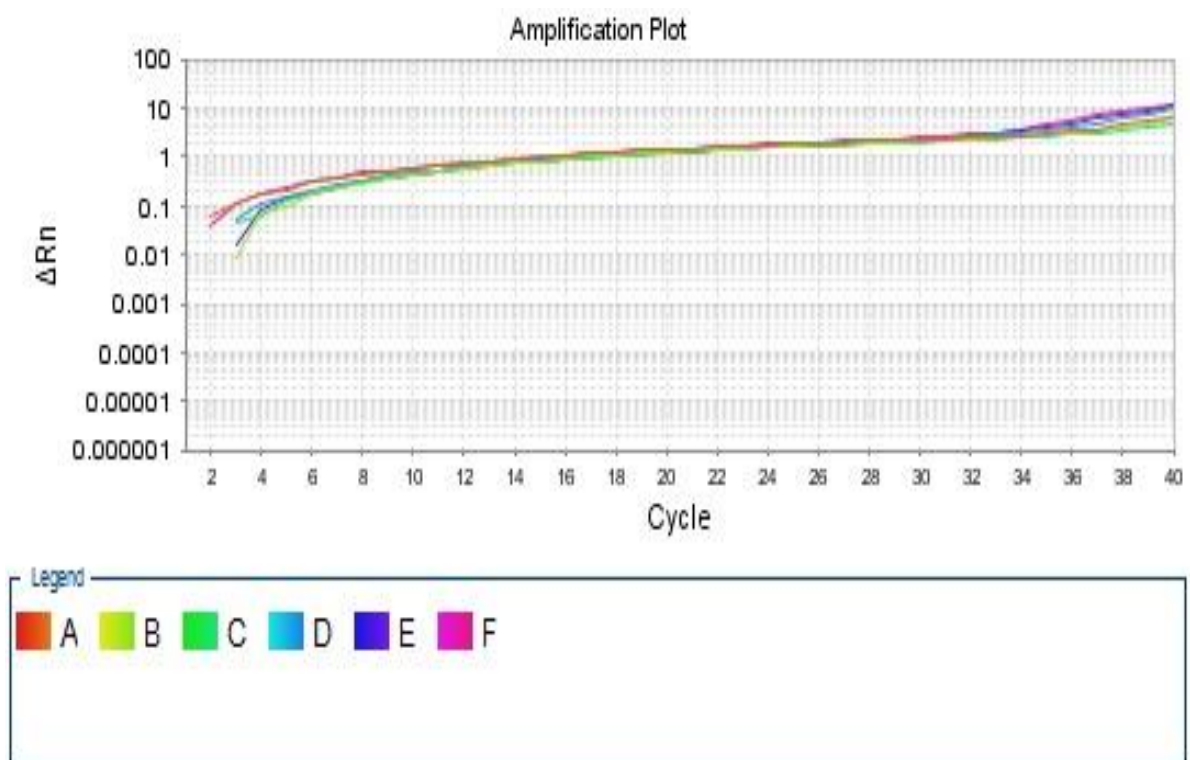
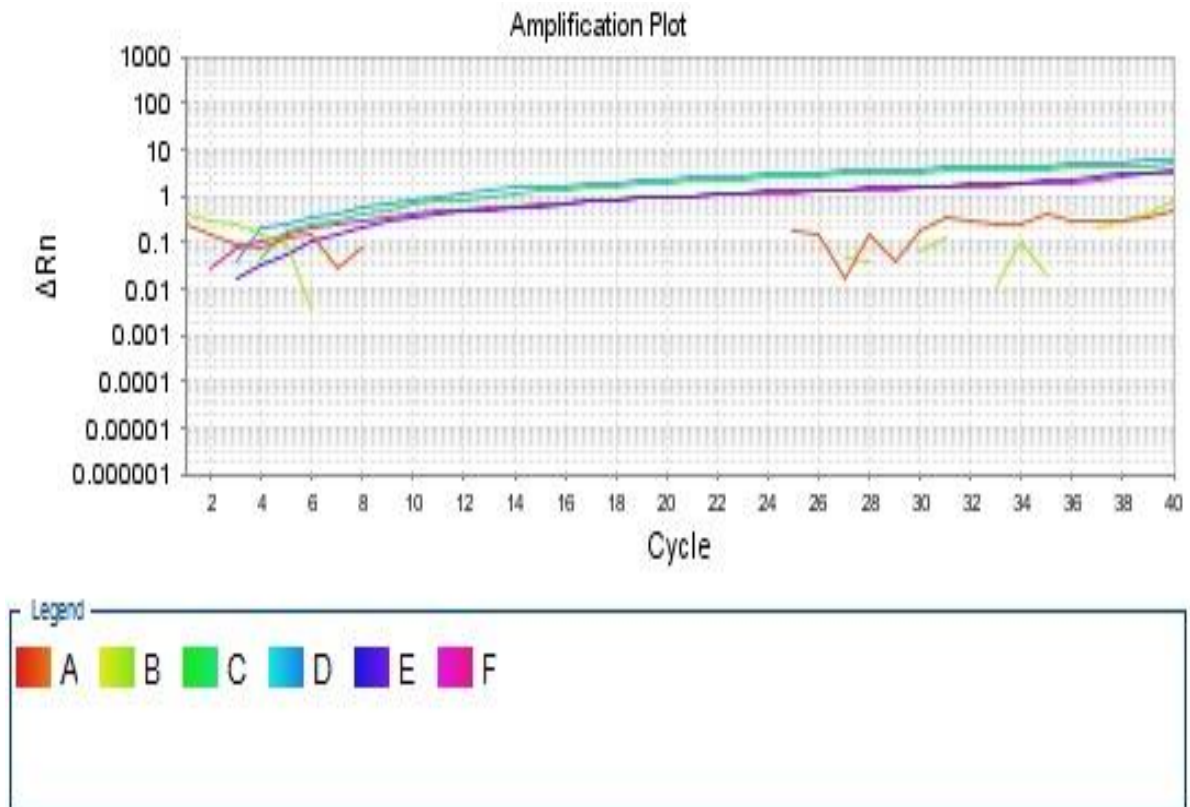


Figure 6: Amplification plot of Sample 1 & 2 of the biological triplicate Transforming growth factor beta-2 (TGFB2). The color of the lines represents the technical replicates of each sample. A, B and C represents the technical samples from HBTE and E, F and G represents the technical triplicates of cancer cell H358.

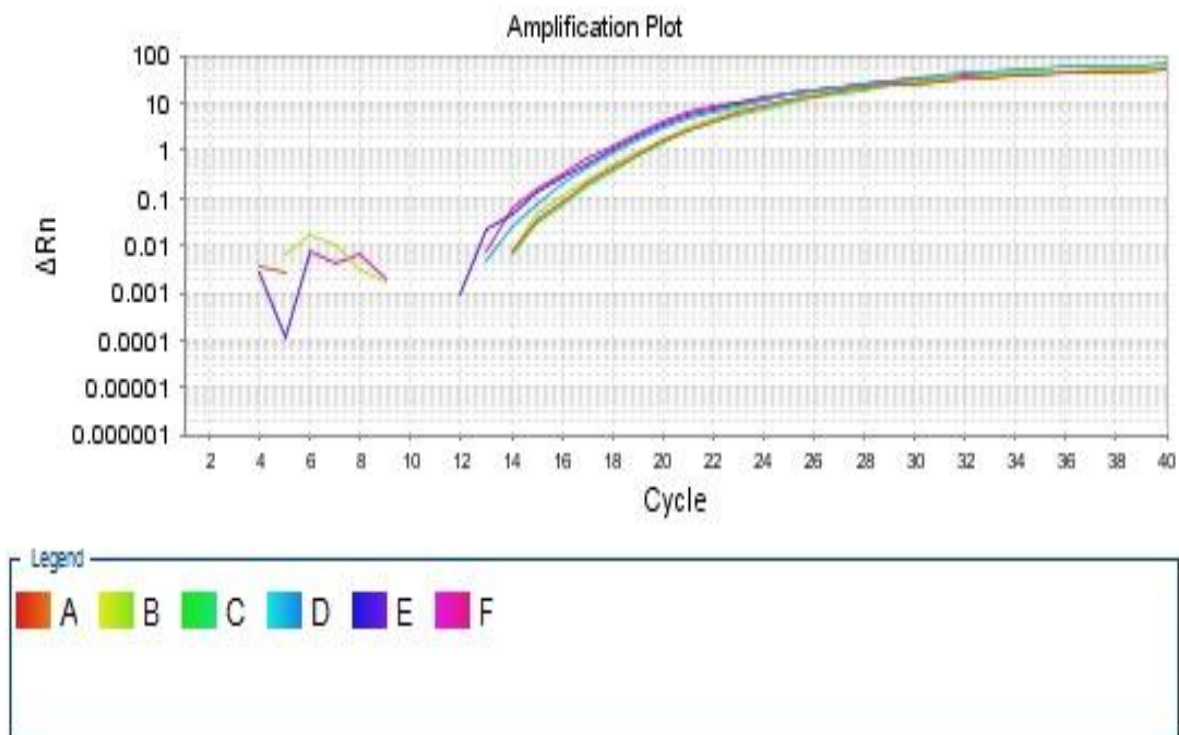
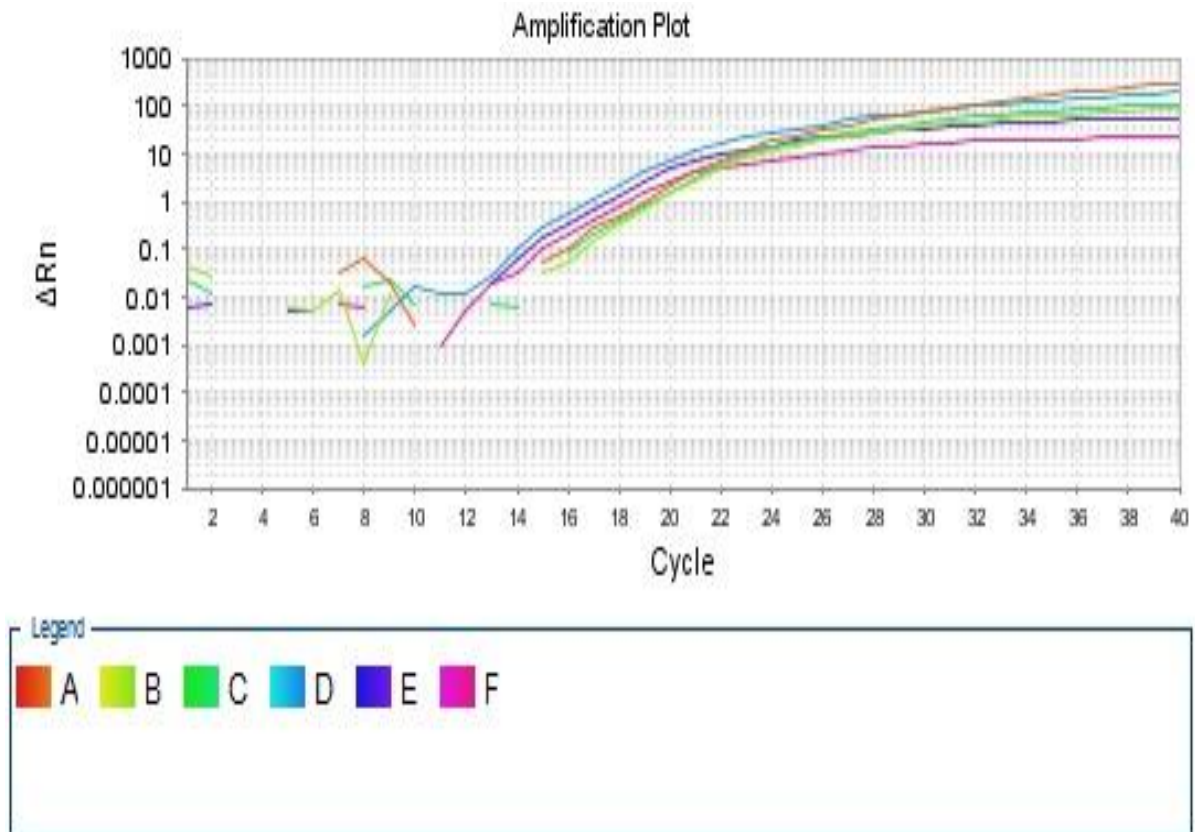


Figure 7: Amplification plot of Sample 1 & 2 of the biological triplicate Cathepsin D (CSTD). The color of the lines represents the technical replicates of each sample. A, B and C represents the technical samples from HBTE and E, F and G represents the technical triplicates of cancer cell H358.

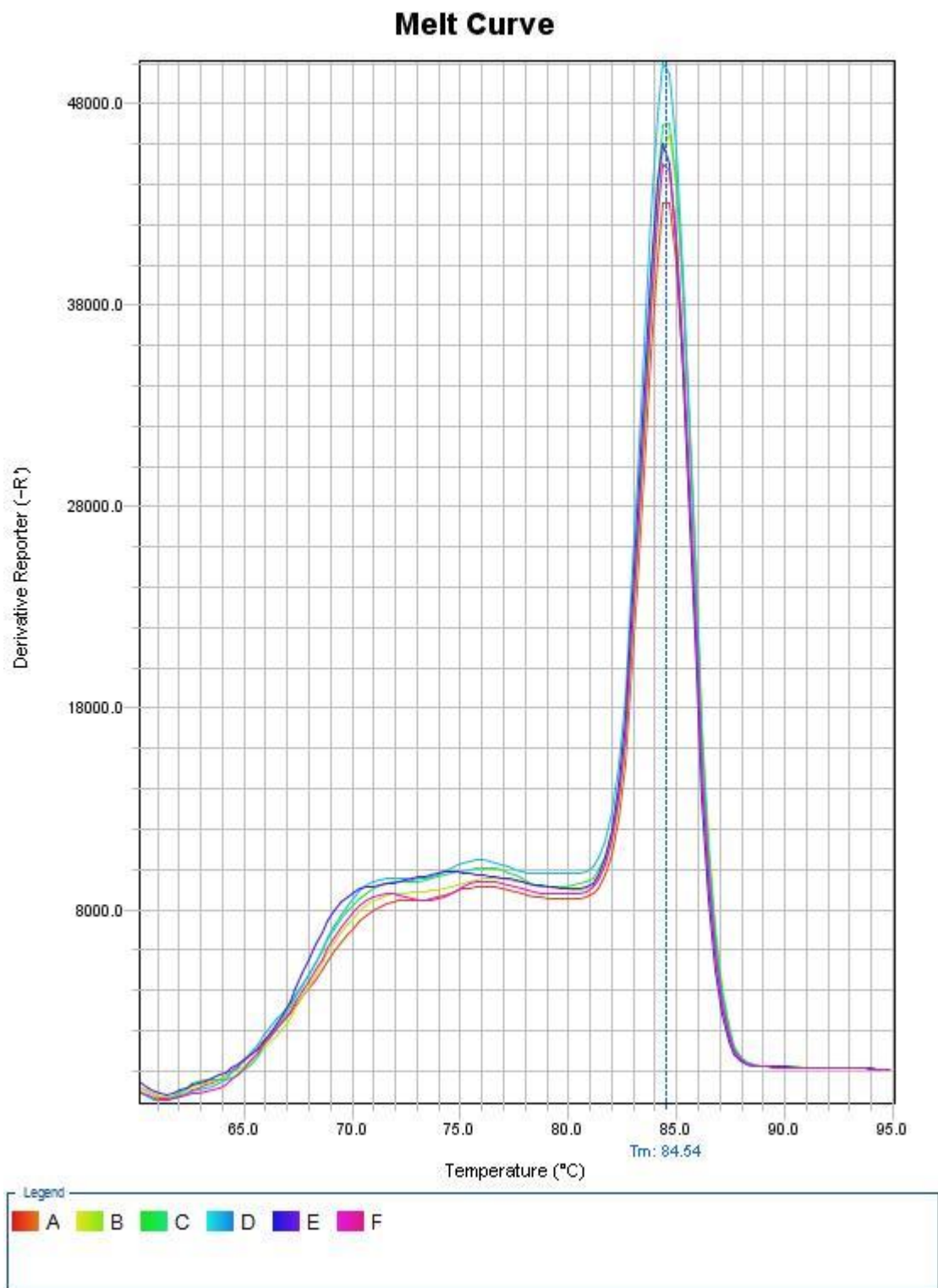


Figure 8: Melting curve of Sample 1 of the biological triplicate of Integrin alpha-3 (ITGA3). The color of the lines represents the technical replicates of each sample. A, B and C represents the technical samples from HBTE and E, F and G represents the technical replicates of cancer cell H358.

Melt Curve

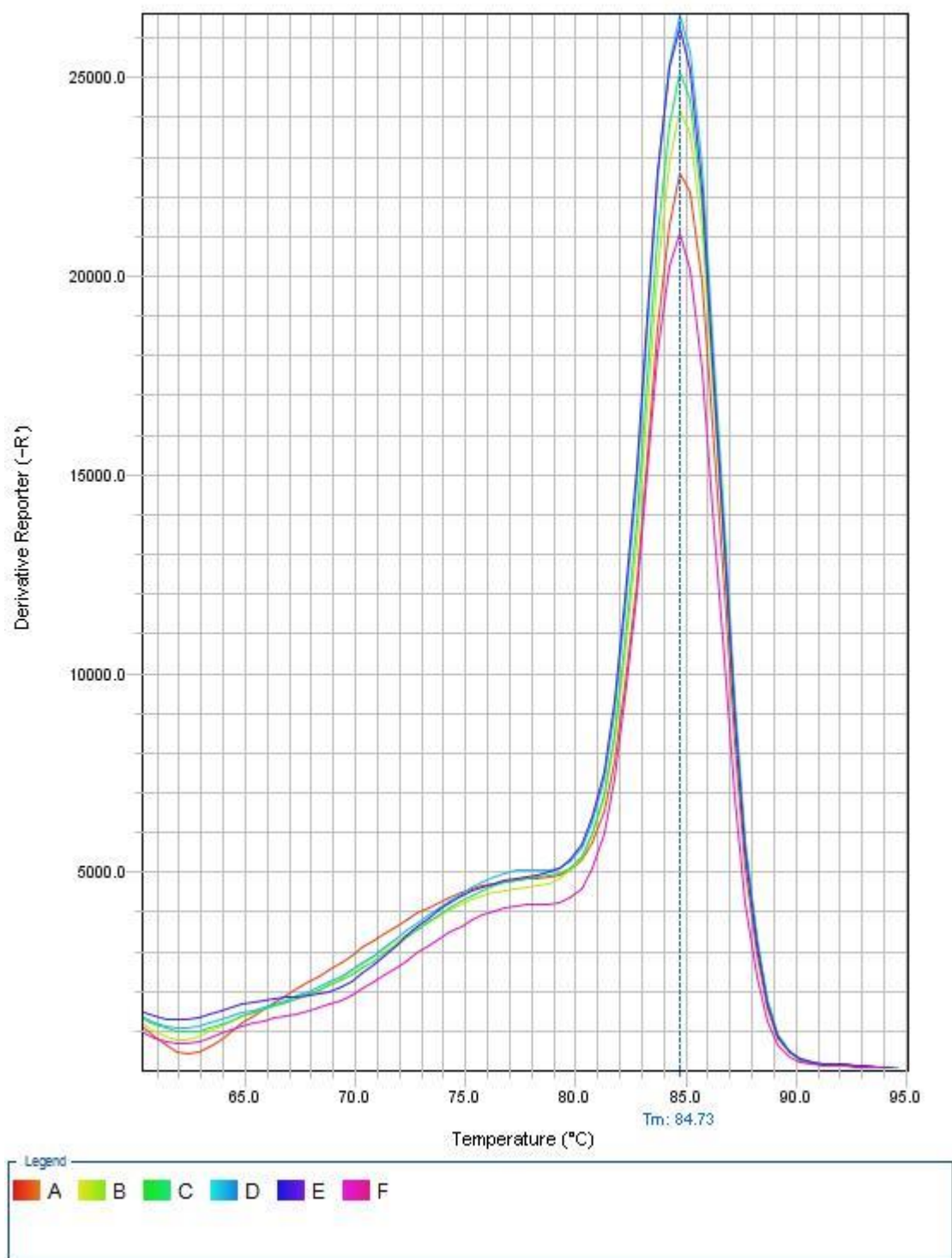


Figure 9: Melting curve of Sample 2 of the biological triplicate of Integrin alpha-3 (ITGA3). The color of the lines represents the technical replicates of each sample. A, B and C represents the technical samples from HBTE and E, F and G represents the technical replicates of cancer cell H358.

Melt Curve

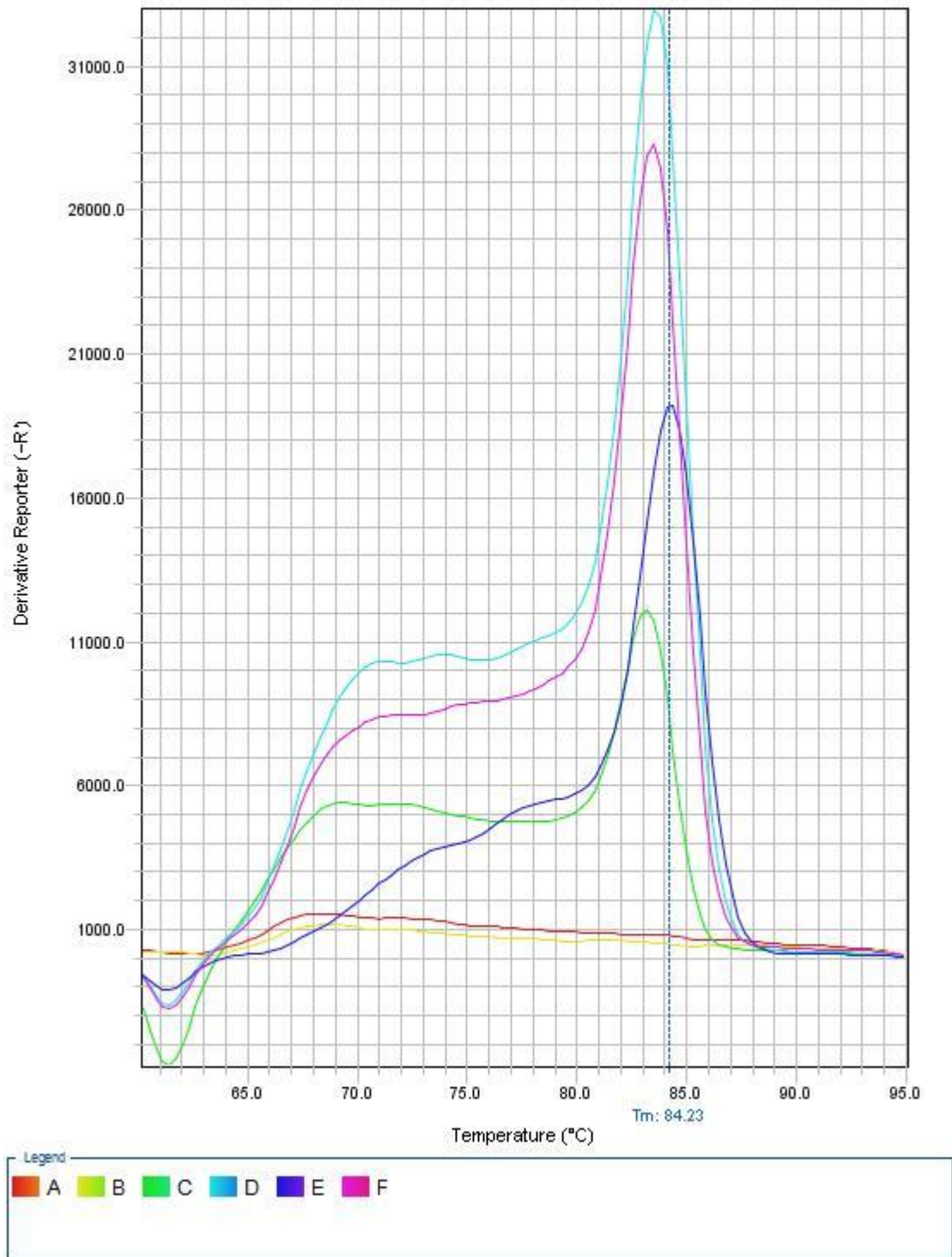


Figure 10: Melting curve of Sample 1 of the biological triplicate of Cadherin-1. The color of the lines represents the technical replicates of each sample. A, B and C represents the technical samples from HBTE and E, F and G represents the technical triplicates of cancer cell H358.

Melt Curve

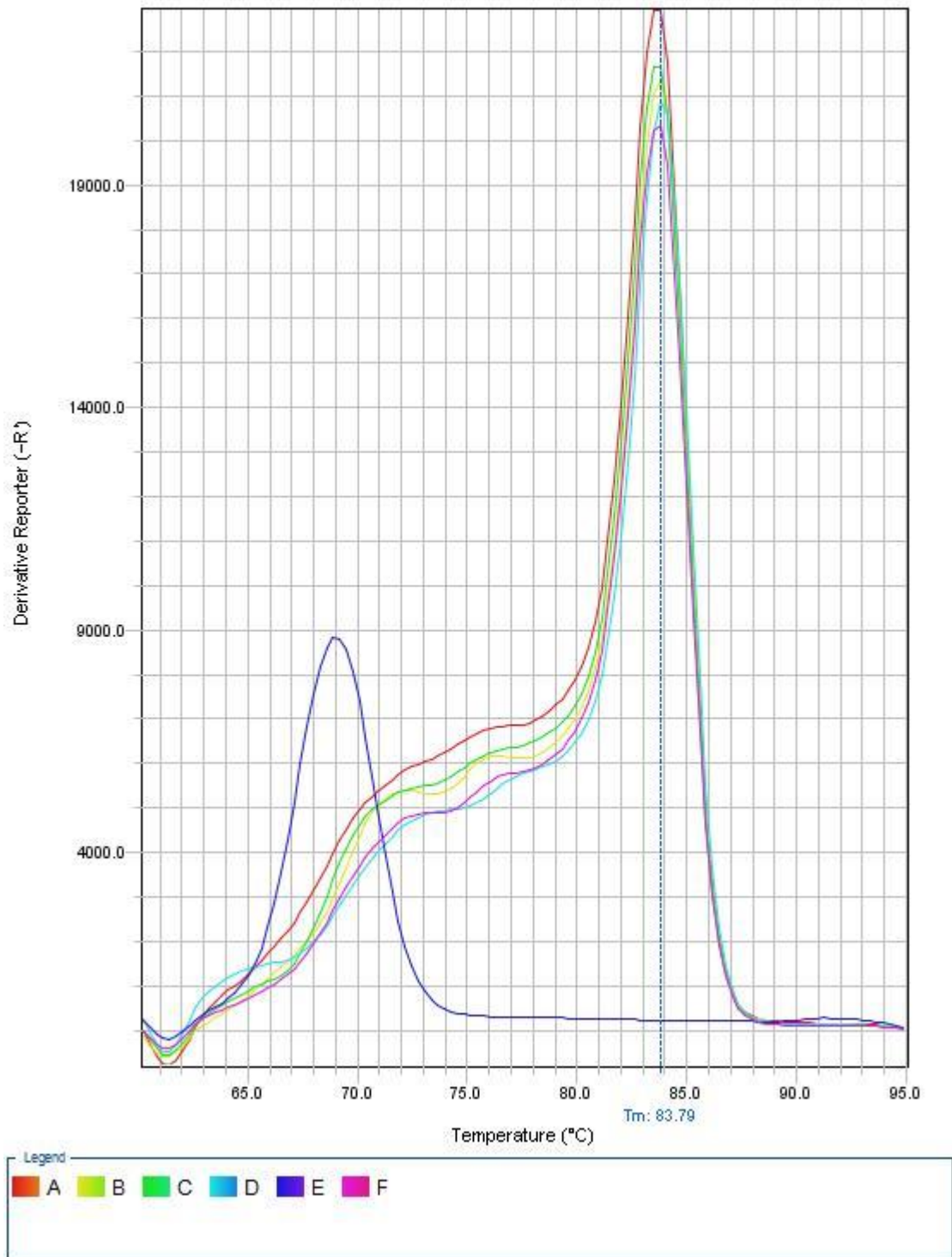


Figure 11: Melting curve of Sample 2 of the biological triplicate of Cadherin-1. The color of the lines represents the technical replicates of each sample. A, B and C represents the technical samples from HBTE and E, F and G represents the technical triplicates of cancer cell H358.

Melt Curve

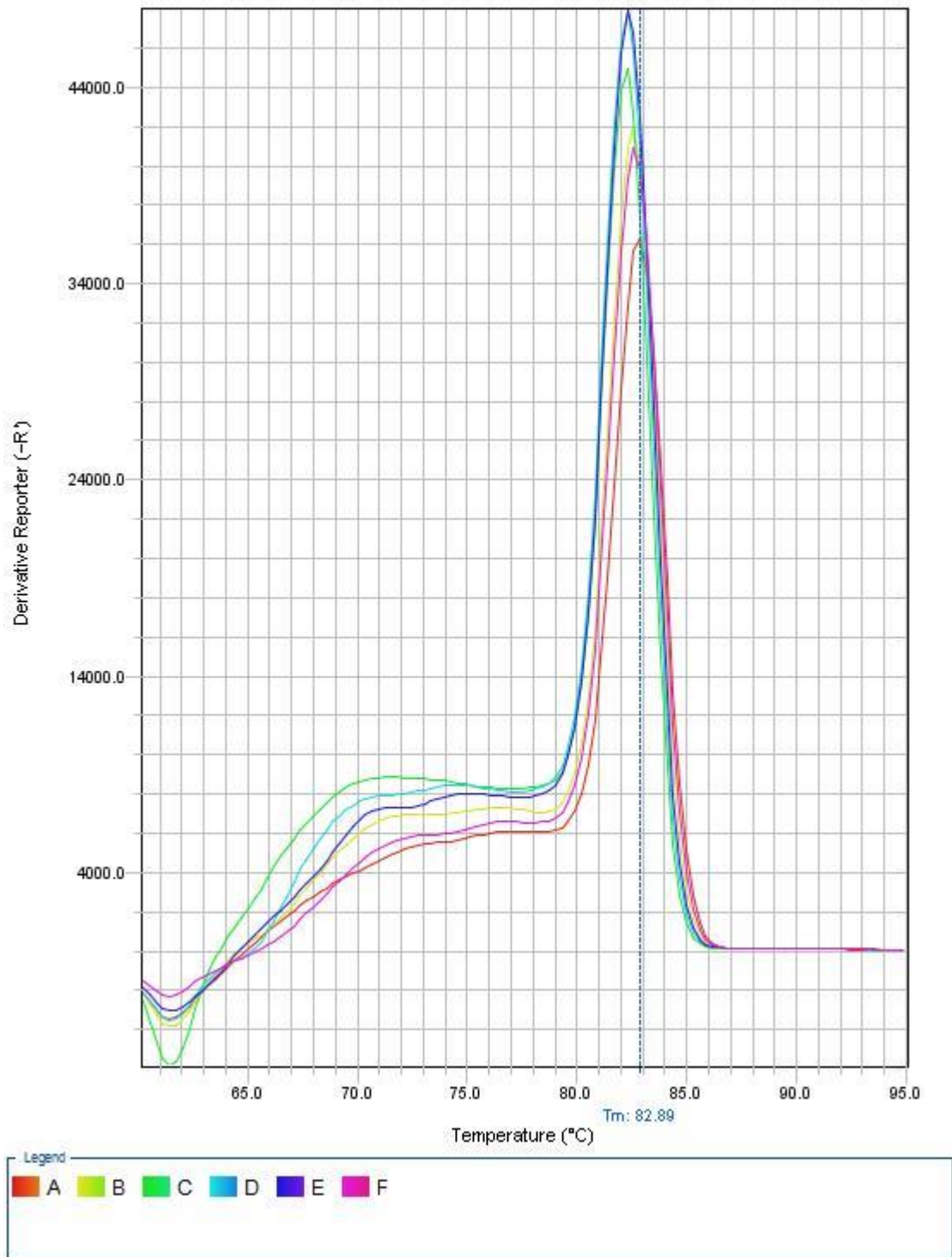


Figure 12: Melting curve of Sample 1 of the biological triplicate of Laminin gamma-1 (LAMC1). The color of the lines represents the technical replicates of each sample. A, B and C represents the technical samples from HBTE and E, F and G represents the technical triplicates of cancer cell H358.

Melt Curve

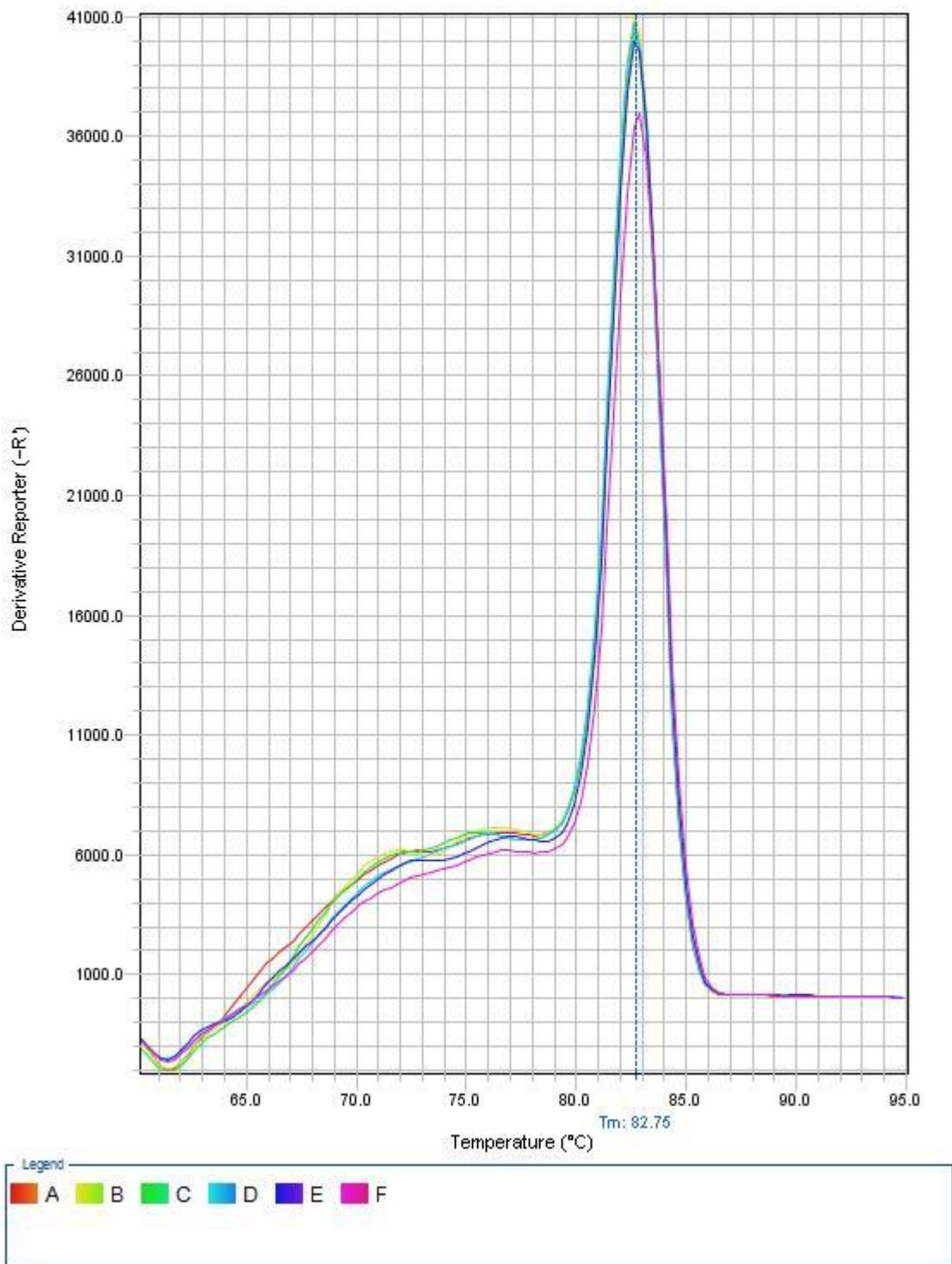


Figure 13: Melting curve of Sample 2 of the biological triplicate of Laminin gamma-1 (LAMC1). The color of the lines represents the technical replicates of each sample. A, B and C represents the technical samples from HBTE and E, F and G represents the technical replicates of cancer cell H358.

Melt Curve

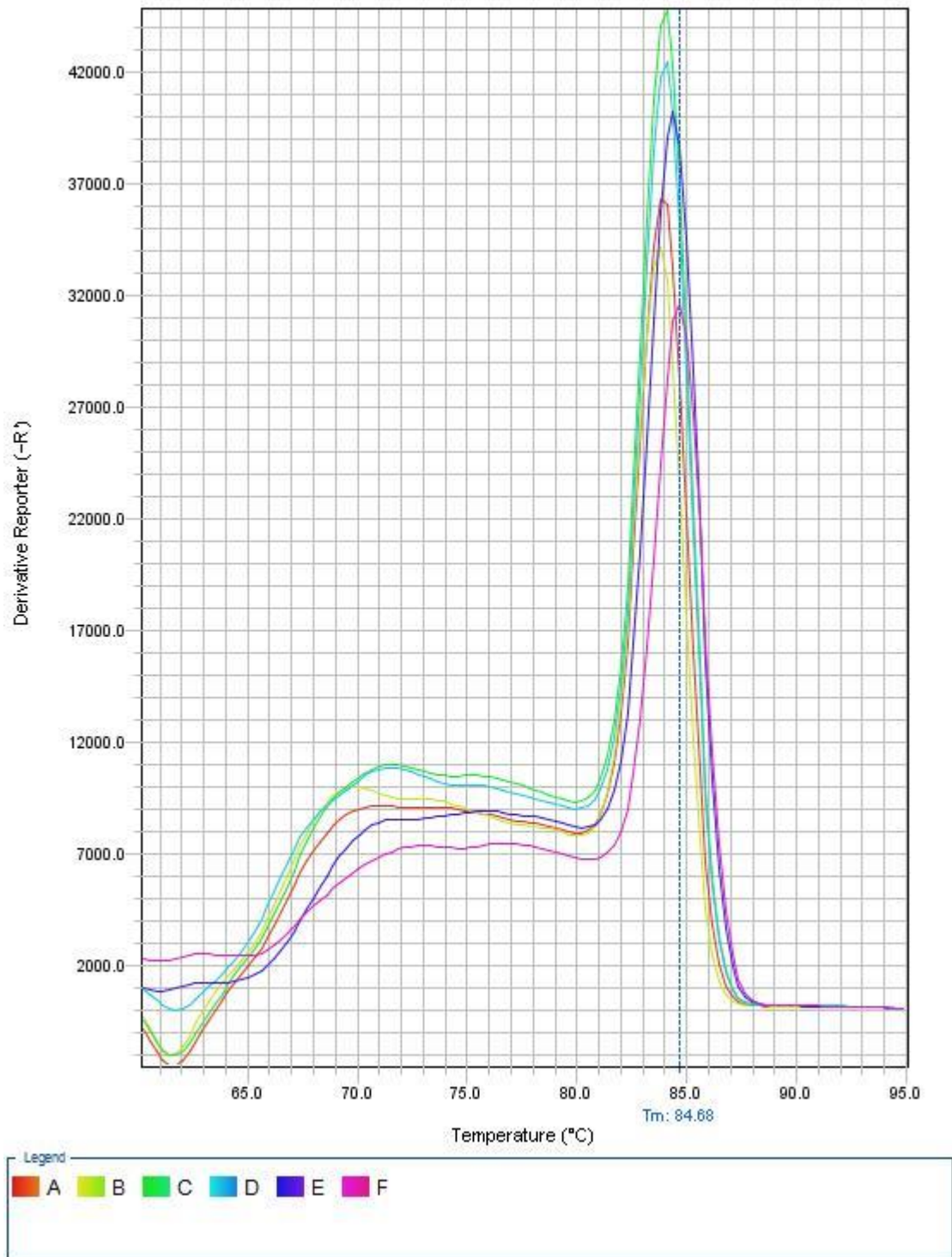


Figure 14: Melting curve of Sample 1 of the biological triplicate of Catenin beta-1 (CTNNB1). The color of the lines represents the technical replicates of each sample. A, B and C represents the technical samples from HBTE and E, F and G represents the technical triplicates of cancer cell H358.

Melt Curve

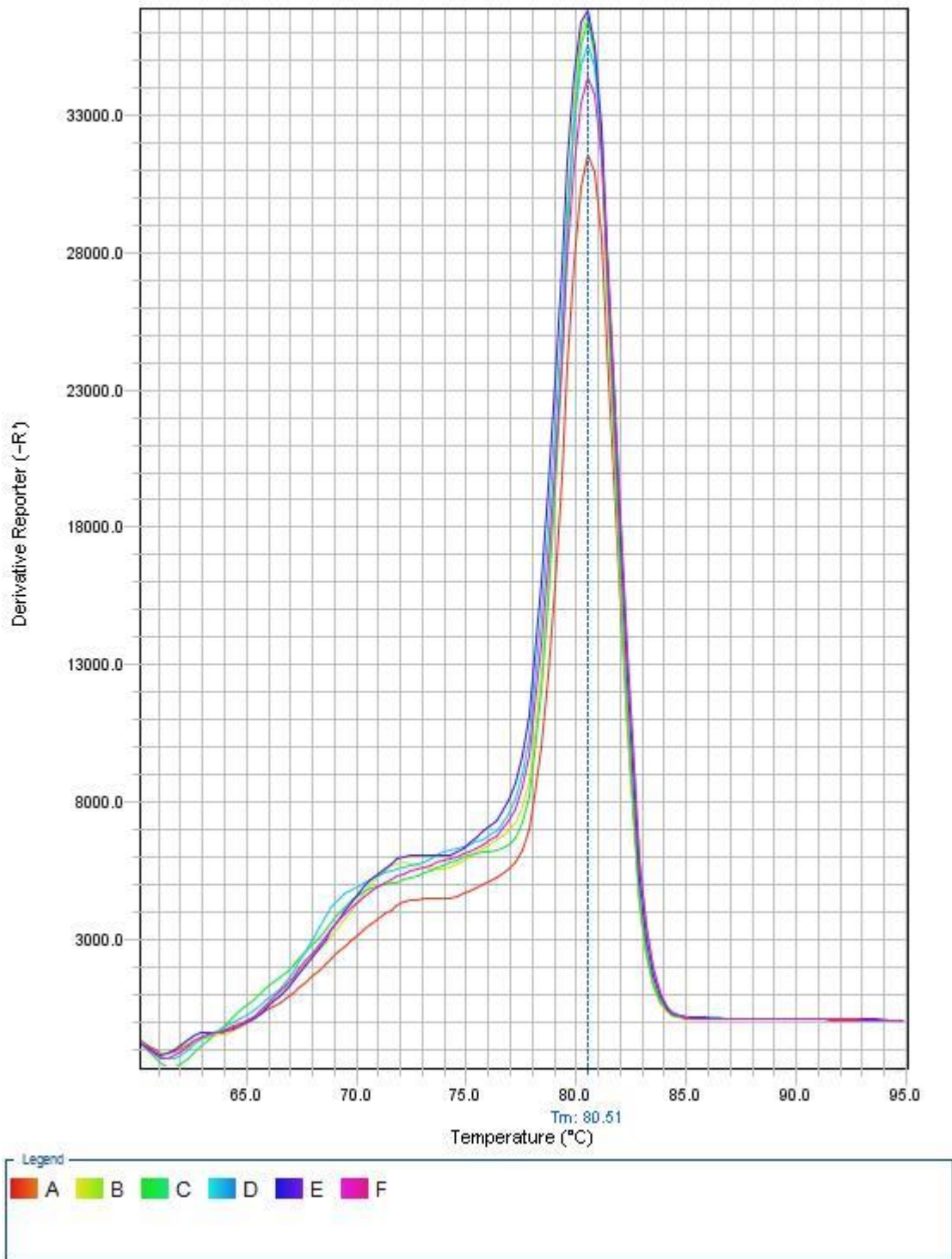


Figure 15: Melting curve of Sample 2 of the biological triplicate of Catenin beta-1 (CTNNB1). The color of the lines represents the technical replicates of each sample. A, B and C represents the technical samples from HBTE and E, F and G represents the technical triplicates of cancer cell H358.

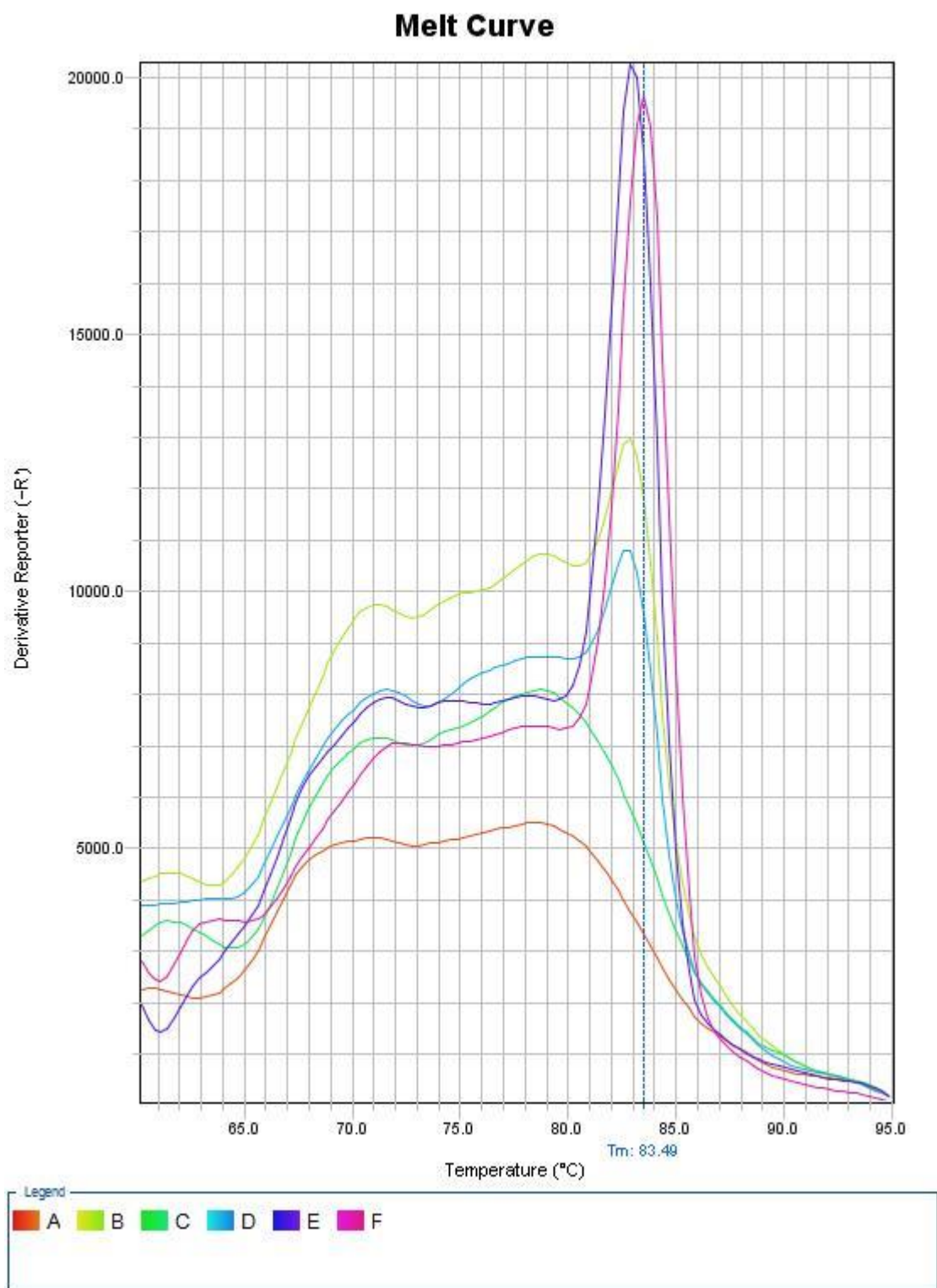


Figure 16: Melting curve of Sample 1 of the biological triplicate of Transforming growth factor beta-2 (TGFB2). The color of the lines represents the technical replicates of each sample. A, B and C represents the technical samples from HBTE and E, F and G represents the technical triplicates of cancer cell H358.

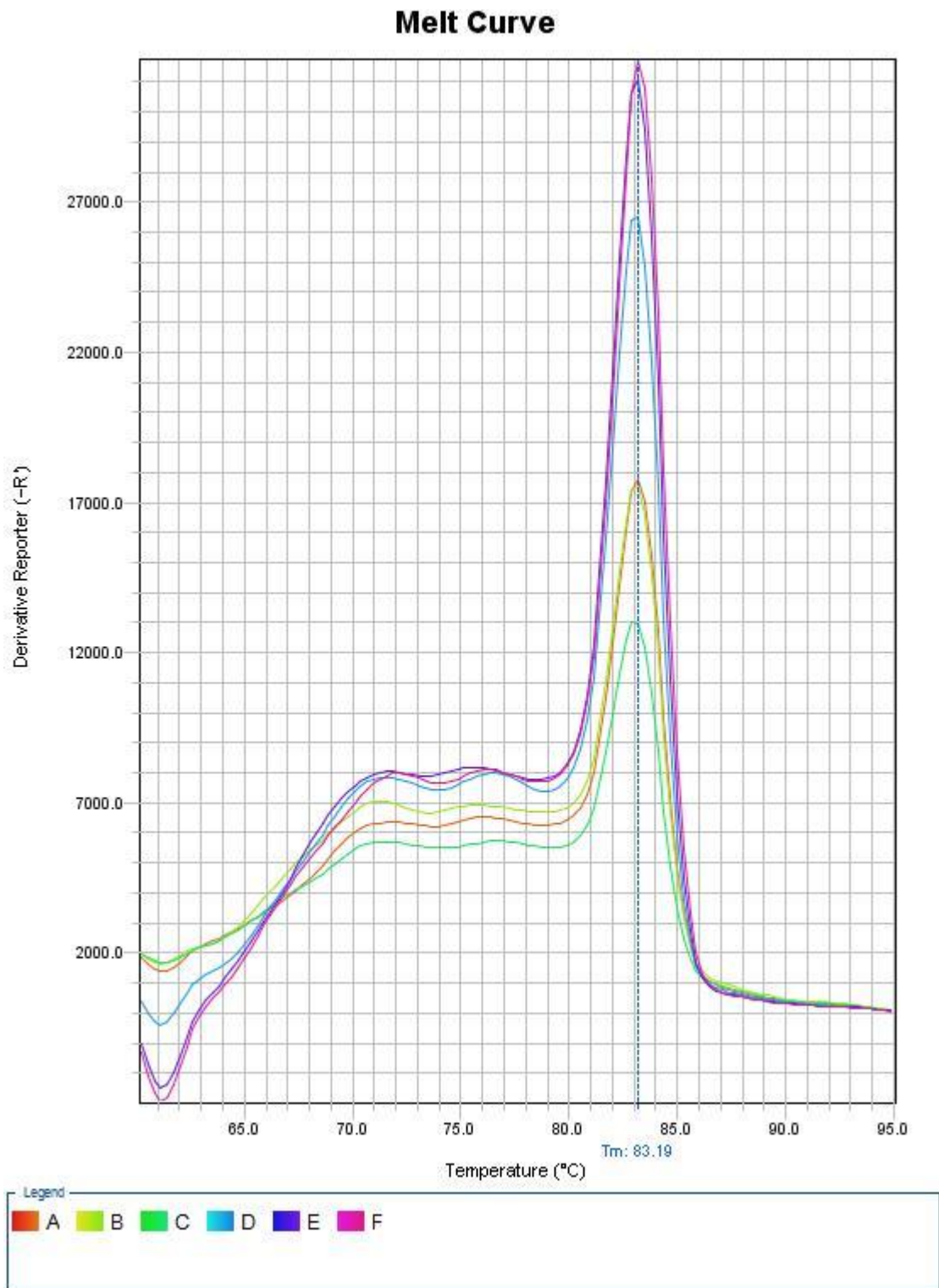


Figure 17: Melting curve of Sample 2 of the biological triplicate of Transforming growth factor beta-2 (TGFB2). The color of the lines represents the technical replicates of each sample. A, B and C represents the technical samples from HBTE and E, F and G represents the technical triplicates of cancer cell H358.

Melt Curve

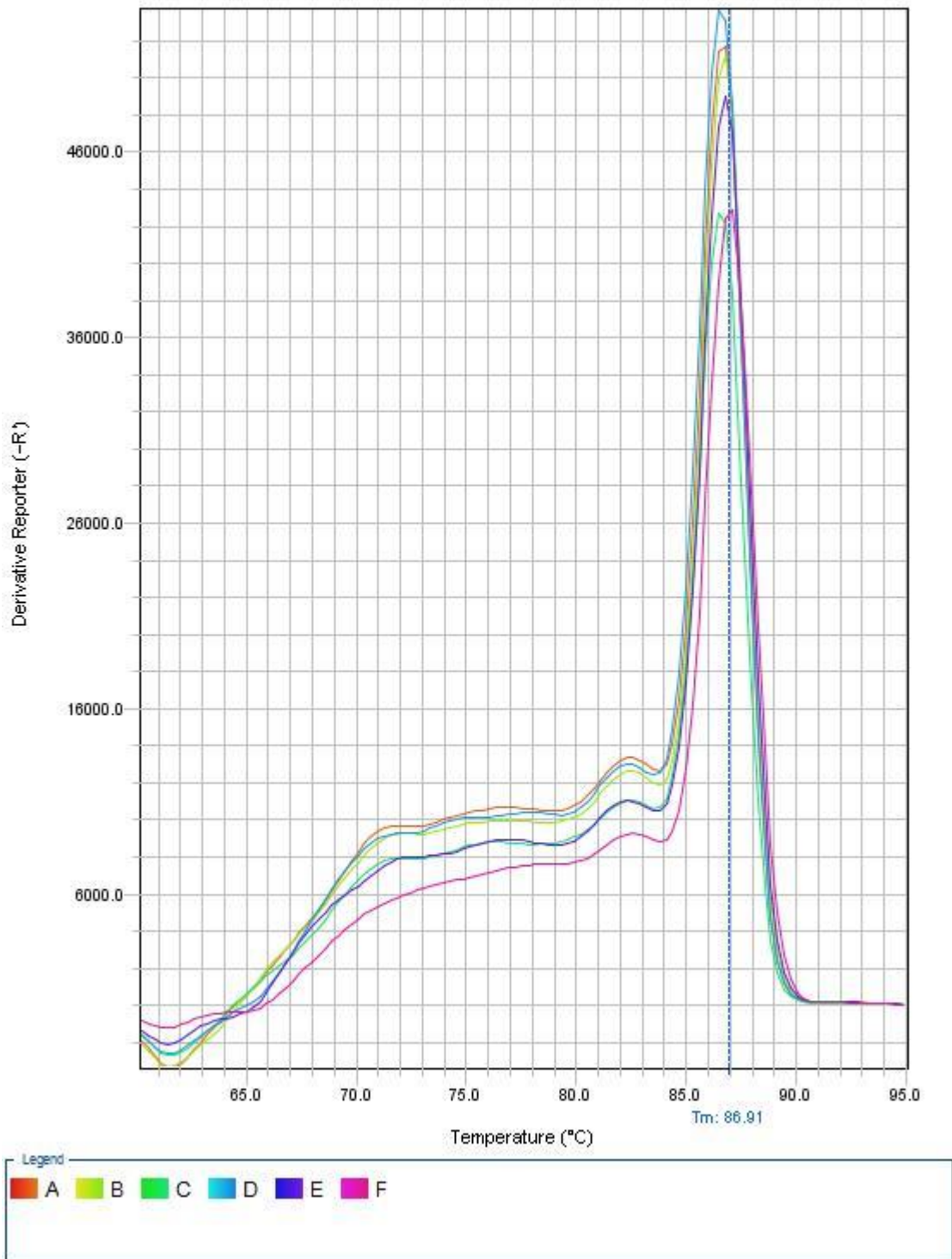


Figure 18: Melting curve of Sample 1 of the biological triplicate of Cathepsin D (CSTD). The color of the lines represents the technical replicates of each sample. A, B and C represents the technical samples from HBTE and E, F and G represents the technical replicates of cancer cell H358.

Melt Curve

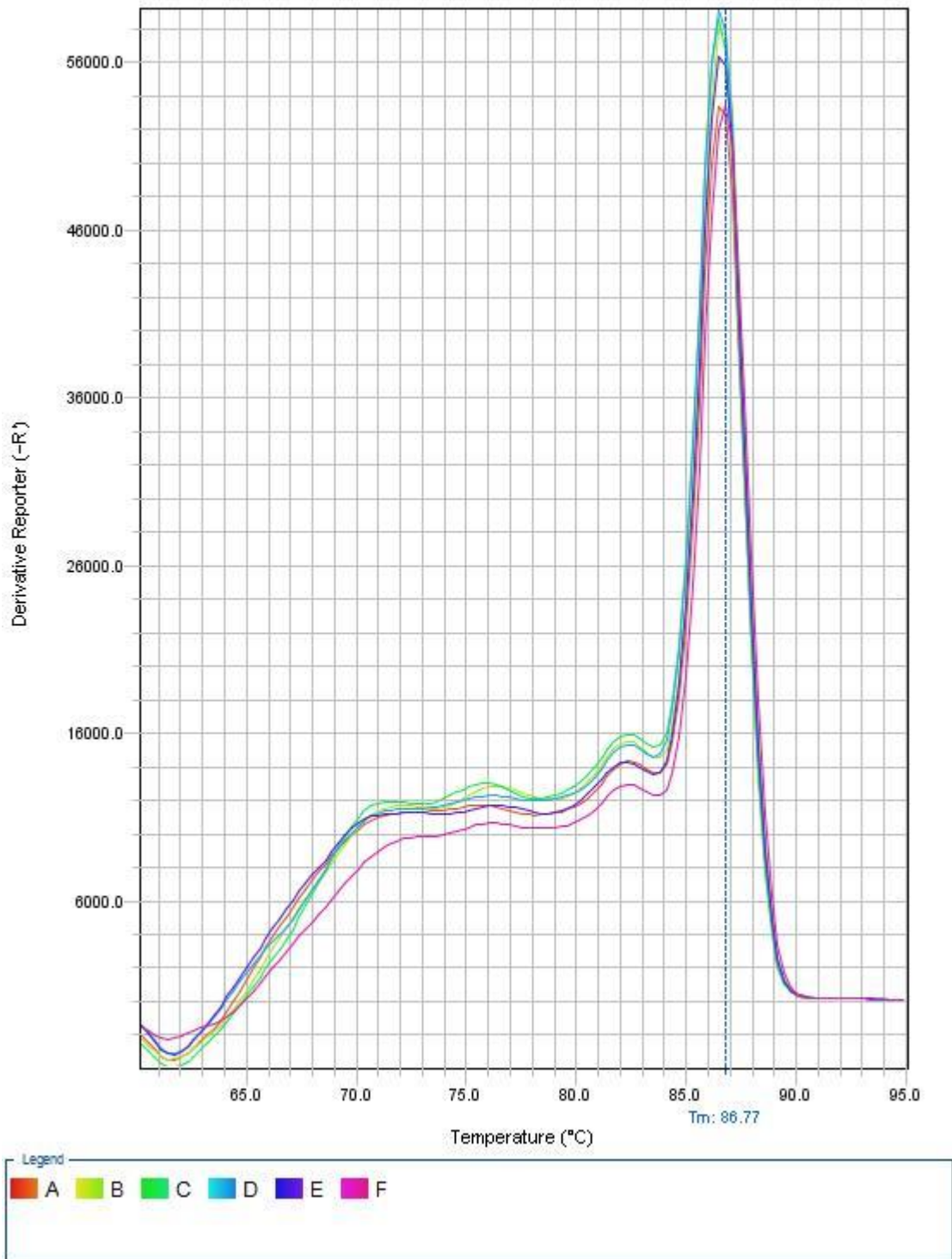


Figure 19: Melting curve of Sample 2 of the biological triplicate of Cathepsin D (CSTD). The color of the lines represents the technical replicates of each sample. A, B and C represents the technical samples from HBTE and E, F and G represents the technical triplicates of cancer cell H358.

Table 1: List of all proteins identified in these study from lung cancer cell line H358, leukaemia cell line THP1, breast cancer cell line MCF7. The p value represents the probability of the protein identification. The lower the p value the more the chance of any protein identification being false positive. The cut off for false positive here is $p \leq 0.05$ which means there is at 5% chance of a protein identification being false positive.

#	Protein	Accession Number	Alternate ID	Molecular Weight	ANOVA Test (p-value)
1	Adenylate kinase isoenzyme 1	KAD1_HUMAN	AK1	22 kDa	0.0001
2	Stromal cell-derived factor 1	SDF1_HUMAN	CXCL12	11 kDa	0.0001
3	Aconitate hydratase, mitochondrial	ACON_HUMAN	ACO2	85 kDa	0.0001
4	Dynactin subunit 2	DCTN2_HUMAN	DCTN2	44 kDa	0.0001
5	Parathyroid hormone-related protein	PTHHR_HUMAN	PTHLH	20 kDa	0.0001
6	Aldehyde dehydrogenase family 1 member A3	ALIA3_HUMAN	ALDH1A3	56 kDa	0.0001
7	Heterogeneous nuclear ribonucleoprotein F	HNRPF_HUMAN	HNRNPF	46 kDa	0.0001
8	Protein DEK	DEK_HUMAN	DEK	43 kDa	0.0001
9	ATPase ASNA1	ASNA_HUMAN	ASNA1	39 kDa	0.0001
10	G-protein coupled receptor 126	GPI26_HUMAN	GPR126	137 kDa	0.0001
11	Transgelin	TAGL_HUMAN	TAGLN	23 kDa	0.0001
12	Immunoglobulin superfamily member 1	IGSF1_HUMAN	IGSF1	149 kDa	0.0001
13	Syntaxin-binding protein 1	STXB1_HUMAN	STXBP1	68 kDa	0.0001
14	Alpha-1-antichymotrypsin	AACT_HUMAN	SERPINA3	48 kDa	0.0001
15	Tryptophan--tRNA ligase, cytoplasmic	SYWC_HUMAN	WARS	53 kDa	0.0001
16	DNA replication licensing factor MCM2	MCM2_HUMAN	MCM2	102 kDa	0.0001
17	General transcription factor IIF subunit 1	T2FA_HUMAN	GTF2F1	58 kDa	0.0001
18	Matrin-3	MATR3_HUMAN	MATR3	95 kDa	0.0001
19	Microtubule-associated protein tau	TAU_HUMAN	MAPT	79 kDa	0.0001
20	Splicing factor 3B subunit 4	SF3B4_HUMAN	SF3B4	44 kDa	0.0001
21	Protein S100-A13	S10AD_HUMAN	S100A13	11 kDa	0.0001
22	Nuclear valosin-containing protein-like	NVL_HUMAN	NVL	95 kDa	0.0001
23	Na(+)/H(+) exchange regulatory cofactor NHE-RF1	NHRF1_HUMAN	SLC9A3R1	39 kDa	0.0001
24	Ig kappa chain C region	IGKC_HUMAN	IGKC	12 kDa	0.0001
323	Cluster of High mobility group protein B1	HMGB1_HUMAN [3]	HMGB1	25 kDa	0.0041
26	Integrin alpha-3	ITA3_HUMAN	ITGA3	117 kDa	0.0001
27	Dihydropteridine reductase	DHPR_HUMAN	QDPR	26 kDa	0.0001
28	Tyrosine--tRNA ligase, cytoplasmic	SYYC_HUMAN	YARS	59 kDa	0.0001
29	Cluster of RNA-binding protein FUS	FUS_HUMAN [2]	FUS	53 kDa	0.0001
30	Asparagine--tRNA ligase, cytoplasmic	SYNC_HUMAN	NARS	63 kDa	0.0001
31	mRNA export factor	RAE1L_HUMAN	RAE1	41 kDa	0.0001
32	Cluster of Interleukin enhancer-binding factor 3	ILF3_HUMAN [2]	ILF3	95 kDa	0.0001
33	Myelin P2 protein	MYP2_HUMAN	PMP2	15 kDa	0.0001
34	Serpin B5	SPB5_HUMAN	SERPINB5	42 kDa	0.0001
35	Complement C1r subcomponent-like protein	C1RL_HUMAN	C1RL	53 kDa	0.0001
36	Serrate RNA effector molecule homolog	SRRT_HUMAN	SRRT	101 kDa	0.0001
37	Flap endonuclease 1	FEN1_HUMAN	FEN1	43 kDa	0.0001
38	Plasma protease C1 inhibitor	IC1_HUMAN	SERPING1	55 kDa	0.0001

39	Vasodilator-stimulated phosphoprotein	VASP_HUMAN	VASP	40 kDa	0.0001
40	Aldose reductase	ALDR_HUMAN	AKR1B1	36 kDa	0.0001
41	Chorionic somatomammotropin hormone	CSH_HUMAN	CSH1	25 kDa	0.0001
380	Catenin beta-1	CTNB1_HUMAN	CTNNB1	85 kDa	0.0075
586	Pregnancy zone protein	PZP_HUMAN	PZP	164 kDa	0.041
44	Luc7-like protein 3	LC7L3_HUMAN	LUC7L3	51 kDa	0.0001
45	Adenosine kinase	ADK_HUMAN	ADK	41 kDa	0.0001
46	Protein HID1	HID1_HUMAN	HID1	89 kDa	0.0001
47	Connective tissue growth factor	CTGF_HUMAN	CTGF	38 kDa	0.0001
48	Glutamine synthetase	GLNA_HUMAN	GLUL	42 kDa	0.0001
49	Cell cycle and apoptosis regulator protein 2	CCAR2_HUMAN	CCAR2	103 kDa	0.0001
50	F-actin-capping protein subunit beta	CAPZB_HUMAN	CAPZB	31 kDa	0.0001
51	Cluster of Transportin-1	TNPO1_HUMAN [2]	TNPO1	102 kDa	0.0001
52	Cluster of 26S proteasome non-ATPase regulatory subunit 4	PSMD4_HUMAN [2]	PSMD4	41 kDa	0.0001
53	Tight junction protein ZO-1	ZO1_HUMAN	TJP1	195 kDa	0.0001
54	Protein S100-A2	S10A2_HUMAN	S100A2	11 kDa	0.0001
55	Protein kinase C and casein kinase substrate in neurons protein 3	PACN3_HUMAN	PACSN3	48 kDa	0.0001
56	Nidogen-1	NID1_HUMAN	NID1	136 kDa	0.0001
57	Plakophilin-3	PKP3_HUMAN	PKP3	87 kDa	0.0001
58	Alpha-1-acid glycoprotein 1	A1AG1_HUMAN	ORM1	24 kDa	0.0001
59	F-actin-capping protein subunit alpha-1	CAZA1_HUMAN	CAPZA1	33 kDa	0.0001
60	Chromobox protein homolog 1	CBX1_HUMAN	CBX1	21 kDa	0.0001
61	Cluster of Vimentin	VIME_HUMAN [2]	VIM	54 kDa	0.0001
62	Insulin-like growth factor-binding protein 4	IBP4_HUMAN	IGFBP4	28 kDa	0.0001
63	Methylosome subunit pICln	ICLN_HUMAN	CLNS1A	26 kDa	0.0001
64	Calcyclin-binding protein	CYBP_HUMAN	CACYBP	26 kDa	0.0001
65	Importin-4	IPO4_HUMAN	IPO4	119 kDa	0.0001
66	Aflatoxin B1 aldehyde reductase member 2	ARK72_HUMAN	AKR7A2	40 kDa	0.0001
67	Coronin-1A	COR1A_HUMAN	CORO1A	51 kDa	0.0001
68	Programmed cell death protein 4	PDCD4_HUMAN	PDCD4	52 kDa	0.0001
69	72 kDa type IV collagenase	MMP2_HUMAN	MMP2	74 kDa	0.0001
70	Retinal dehydrogenase 1	AL1A1_HUMAN	ALDH1A1	55 kDa	0.0001
71	Leucine-rich alpha-2-glycoprotein	A2GL_HUMAN	LRG1	38 kDa	0.0001
72	Breast carcinoma-amplified sequence 1	BCAS1_HUMAN	BCAS1	62 kDa	0.0001
73	Serine protease HTRA1	HTRA1_HUMAN	HTRA1	51 kDa	0.0001
74	Synaptic vesicle membrane protein VAT-1 homolog-like	VAT1L_HUMAN	VAT1L	46 kDa	0.0001
75	Cluster of Eukaryotic translation initiation factor 4 gamma 1	IF4G1_HUMAN [2]	EIF4G1	175 kDa	0.0001
76	Histidine--tRNA ligase, cytoplasmic	SYHC_HUMAN	HARS	57 kDa	0.0001
77	Cluster of Haptoglobin	HPT_HUMAN [2]	HP	45 kDa	0.0001
78	GDNF family receptor alpha-1	GFRA1_HUMAN	GFRA1	51 kDa	0.0001
79	Clathrin light chain B	CLCB_HUMAN	CLTB	25 kDa	0.0001
80	Arfaptin-2	ARFP2_HUMAN	ARFIP2	38 kDa	0.0001
81	Pleckstrin homology domain-containing family F member 2	PKHF2_HUMAN	PLEKHF2	28 kDa	0.0001
82	Cathepsin S	CATS_HUMAN	CTSS	37 kDa	0.0001
83	Cleavage and polyadenylation specificity factor subunit 5	CPSF5_HUMAN	NUDT21	26 kDa	0.0001

84	Kininogen-1	KNG1_HUMAN	KNG1	72 kDa	0.0001
85	Splicing factor 3A subunit 1	SF3A1_HUMAN	SF3A1	89 kDa	0.0001
86	Negative elongation factor B	NELFB_HUMAN	NELFB	66 kDa	0.0001
87	Hyaluronidase-3	HYAL3_HUMAN	HYAL3	47 kDa	0.0001
88	Cluster of Testican-1	TICN1_HUMAN [2]	SPOCK1	49 kDa	0.00011
89	Eukaryotic translation initiation factor 4B	IF4B_HUMAN	EIF4B	69 kDa	0.00011
90	Clusterin	CLUS_HUMAN	CLU	52 kDa	0.00012
91	N-acetylmuramoyl-L-alanine amidase	PGRP2_HUMAN	PGLYRP2	62 kDa	0.00012
92	Dihydropyrimidinase-related protein 3	DPYL3_HUMAN	DPYSL3	62 kDa	0.00012
93	Extracellular matrix protein 1	ECM1_HUMAN	ECM1	61 kDa	0.00013
94	Cathepsin B	CATB_HUMAN	CTSB	38 kDa	0.00013
95	Mannose-1-phosphate guanylttransferase beta	GMPPB_HUMAN	GMPPB	40 kDa	0.00013
96	Cluster of Aldo-keto reductase family 1 member C1	AK1C1_HUMAN [2]	AKR1C1	37 kDa	0.00013
97	Apoptosis inhibitor 5	API5_HUMAN	API5	59 kDa	0.00014
98	Heterogeneous nuclear ribonucleoprotein R	HNRPR_HUMAN	HNRNPR	71 kDa	0.00014
99	Stress-induced-phosphoprotein 1	STIP1_HUMAN	STIP1	63 kDa	0.00014
100	Coiled-coil domain-containing protein 18	CCD18_HUMAN	CCDC18	169 kDa	0.00015
101	Proteasome activator complex subunit 2	PSME2_HUMAN	PSME2	27 kDa	0.00015
102	Ceruloplasmin	CERU_HUMAN	CP	122 kDa	0.00016
103	Afamin	AFAM_HUMAN	AFM	69 kDa	0.00017
104	Heterogeneous nuclear ribonucleoprotein M	HNRPM_HUMAN	HNRNPM	78 kDa	0.00017
105	Niban-like protein 1	NIBL1_HUMAN	FAM129B	84 kDa	0.00017
106	Serine/arginine-rich splicing factor 3	SRSF3_HUMAN	SRSF3	19 kDa	0.00018
107	Puromycin-sensitive aminopeptidase	PSA_HUMAN	NPEPPS	103 kDa	0.00019
108	Splicing factor 1	SF01_HUMAN	SF1	68 kDa	0.00019
109	DnaJ homolog subfamily C member 3	DNJC3_HUMAN	DNAJC3	58 kDa	0.0002
110	Pleckstrin	PLEK_HUMAN	PLEK	40 kDa	0.0002
596	Inter-alpha-trypsin inhibitor heavy chain H3	ITIH3_HUMAN	ITIH3	100 kDa	0.044
112	Mitochondrial import receptor subunit TOM70	TOM70_HUMAN	TOMM70A	67 kDa	0.0002
113	T-complex protein 1 subunit zeta	TCPZ_HUMAN	CCT6A	58 kDa	0.00021
114	Cluster of Ras GTPase-activating-like protein IQGAP1	IQGA1_HUMAN [3]	IQGAP1	189 kDa	0.00021
645	Cluster of Complement C4-A	CO4A_HUMAN [2]	C4A	193 kDa	0.056
116	Citrate synthase, mitochondrial	CISY_HUMAN	CS	52 kDa	0.00022
117	Far upstream element-binding protein 2	FUBP2_HUMAN	KHSRP	73 kDa	0.00022
118	L-lactate dehydrogenase B chain	LDHB_HUMAN	LDHB	37 kDa	0.00024
119	Signal recognition particle subunit SRP72	SRP72_HUMAN	SRP72	75 kDa	0.00024
120	Guanine nucleotide-binding protein subunit alpha-13	GNA13_HUMAN	GNA13	44 kDa	0.00024
121	CDK5 regulatory subunit-associated protein 3	CK5P3_HUMAN	CDK5RAP3	57 kDa	0.00024
122	Hypoxanthine-guanine phosphoribosyltransferase	HPRT_HUMAN	HPRT1	25 kDa	0.00025
123	High mobility group protein HMG-I/HMG-Y	HMGA1_HUMAN	HMGA1	12 kDa	0.00025
741	Putative histone H2B type 2-C	H2B2C_HUMAN (+1)	HIST2H2BC	21 kDa	0.08
125	UBX domain-containing protein 1	UBXN1_HUMAN	UBXN1	33 kDa	0.00027
126	Serine/threonine-protein phosphatase 2A 56 kDa regulatory subunit gamma isoform	2A5G_HUMAN	PPP2R5C	61 kDa	0.00027
127	D-3-phosphoglycerate dehydrogenase	SERA_HUMAN	PHGDH	57 kDa	0.00028
128	Protein S100-A4	S100A4_HUMAN	S100A4	12 kDa	0.00029

129	Secernin-1	SCRN1_HUMAN	SCRN1	46 kDa	0.00029
130	Cluster of Alpha-internexin	AIXN_HUMAN [3]	INA	55 kDa	0.00029
131	C-1-tetrahydrofolate synthase, cytoplasmic	C1TC_HUMAN	MTHFD1	102 kDa	0.0003
132	Serine/threonine-protein kinase VRK1	VRK1_HUMAN	VRK1	45 kDa	0.0003
798	Alpha-2-macroglobulin	A2MG_HUMAN	A2M	163 kDa	0.098
134	Acidic leucine-rich nuclear phosphoprotein 32 family member B	AN32B_HUMAN	ANP32B	29 kDa	0.00031
135	U2 small nuclear ribonucleoprotein A'	RU2A_HUMAN	SNRPA1	28 kDa	0.00031
136	Sorting nexin-1	SNX1_HUMAN	SNX1	59 kDa	0.00033
137	60S ribosomal protein L10a	RL10A_HUMAN	RPL10A	25 kDa	0.00033
138	Heterogeneous nuclear ribonucleoprotein H3	HNRH3_HUMAN	HNRNP3	37 kDa	0.00034
139	Cluster of Serine/threonine-protein kinase MST4	MST4_HUMAN [2]	MST4	47 kDa	0.00036
949	Histone H1.5	H15_HUMAN	HIST1H1B	23 kDa	0.16
141	Laminin subunit gamma-2	LAMC2_HUMAN	LAMC2	131 kDa	0.00038
142	26S proteasome non-ATPase regulatory subunit 8	PSMD8_HUMAN	PSMD8	40 kDa	0.0004
143	Leucine-rich repeat protein SHOC-2	SHOC2_HUMAN	SHOC2	65 kDa	0.0004
144	Cleavage stimulation factor subunit 2	CSTF2_HUMAN	CSTF2	61 kDa	0.0004
145	Cathepsin G	CATG_HUMAN	CTSG	29 kDa	0.0004
146	Nucleosome assembly protein 1-like 4	NP1L4_HUMAN	NAP1L4	43 kDa	0.00041
147	Insulin-like growth factor-binding protein 5	IBP5_HUMAN	IGFBP5	31 kDa	0.00041
148	Proliferating cell nuclear antigen	PCNA_HUMAN	PCNA	29 kDa	0.00041
149	Zyxin	ZYX_HUMAN	ZYX	61 kDa	0.00043
150	Synaptic vesicle membrane protein VAT-1 homolog	VAT1_HUMAN	VAT1	42 kDa	0.00043
151	Dihydrolypoyllysine-residue succinyltransferase component of 2-oxoglutarate dehydrogenase complex, mitochondrial	ODO2_HUMAN	DLST	49 kDa	0.00044
152	T-complex protein 1 subunit theta	TCPQ_HUMAN	CCT8	60 kDa	0.00045
153	Brain-specific angiogenesis inhibitor 1-associated protein 2-like protein 1	BI2L1_HUMAN	BAIAP2L1	57 kDa	0.00047
154	Transcription factor BTF3	BTF3_HUMAN	BTF3	22 kDa	0.00047
155	Stromelysin-2	MMP10_HUMAN	MMP10	54 kDa	0.00048
156	Fermitin family homolog 3	URP2_HUMAN	FERMT3	76 kDa	0.00048
157	Cluster of Histone-binding protein RBBP7	RBBP7_HUMAN [2]	RBBP7	48 kDa	0.00048
158	Poly [ADP-ribose] polymerase 1	PARP1_HUMAN	PARP1	113 kDa	0.0005
159	Nuclear ubiquitous casein and cyclin-dependent kinase substrate 1	NUCKS_HUMAN	NUCKS1	27 kDa	0.0005
160	Tumor necrosis factor receptor superfamily member 6B	TNF6B_HUMAN	TNFRSF6B	33 kDa	0.0005
161	Src substrate cortactin	SRC8_HUMAN	CTTN	62 kDa	0.00054
162	Microtubule-associated protein RP/EB family member 1	MARE1_HUMAN	MAPRE1	30 kDa	0.00055
163	Palmitoyl-protein thioesterase 1	PPT1_HUMAN	PPT1	34 kDa	0.00056
164	Dipeptidyl peptidase 2	DPP2_HUMAN	DPP7	54 kDa	0.00056
165	Serglycin	SRGN_HUMAN	SRGN	18 kDa	0.00056
166	Leucine zipper transcription factor-like protein 1	LZTL1_HUMAN	LZTFL1	35 kDa	0.00059
167	Ras GTPase-activating protein-binding protein 2	G3BP2_HUMAN	G3BP2	54 kDa	0.0006
168	Lysine--tRNA ligase	SYK_HUMAN	KARS	68 kDa	0.0006
169	Monocyte differentiation antigen CD14	CD14_HUMAN	CD14	40 kDa	0.00061
170	RNA-binding protein Raly	RALY_HUMAN	RALY	32 kDa	0.00061
171	Lamin-B1	LMNB1_HUMAN	LMNB1	66 kDa	0.00063
172	Aminoacyl tRNA synthase complex-interacting multifunctional protein 1	AIMP1_HUMAN	AIMP1	34 kDa	0.00066

173	Heterogeneous nuclear ribonucleoprotein Q	HNRPQ_HUMAN	SYNCRIP	70 kDa	0.00069
174	Density-regulated protein	DENR_HUMAN	DENR	22 kDa	0.00069
175	Alpha-aminoacidic semialdehyde dehydrogenase	AL7A1_HUMAN	ALDH7A1	58 kDa	0.00073
176	Cytosol aminopeptidase	AMPL_HUMAN	LAP3	56 kDa	0.00074
177	Lysozyme C	LYSC_HUMAN	LYZ	17 kDa	0.00076
178	Programmed cell death 6-interacting protein	PDC6L_HUMAN	PDCD6IP	96 kDa	0.00077
179	RNA-binding protein EWS	EWS_HUMAN	EWSR1	68 kDa	0.00077
180	Alanine--tRNA ligase, cytoplasmic	SYAC_HUMAN	AARS	107 kDa	0.00078
181	Caprin-1	CAPR1_HUMAN	CAPRIN1	78 kDa	0.00079
182	Hemopexin	HEMO_HUMAN	HPX	52 kDa	0.0008
183	Drebrin-like protein	DBNL_HUMAN	DBNL	48 kDa	0.0008
184	ATP synthase subunit beta, mitochondrial	ATPB_HUMAN	ATP5B	57 kDa	0.00081
124	Alpha-1B-glycoprotein	A1BG_HUMAN	A1BG	54 kDa	0.00025
236	Tumor-associated calcium signal transducer 2	TACD2_HUMAN	TACSTD2	36 kDa	0.0015
187	GRIP1-associated protein 1	GRAP1_HUMAN	GRIPAP1	96 kDa	0.00088
188	Cluster of Heterogeneous nuclear ribonucleoprotein H	HNRH1_HUMAN [2]	HNRNPH1	49 kDa	0.00089
189	Laminin subunit alpha-3	LAMA3_HUMAN	LAMA3	367 kDa	0.00089
190	Serine/threonine-protein phosphatase 2A 56 kDa regulatory subunit epsilon isoform	2A5E_HUMAN	PPP2R5E	55 kDa	0.0009
191	Spectrin alpha chain, non-erythrocytic 1	SPTN1_HUMAN	SPTAN1	285 kDa	0.0009
192	Receptor expression-enhancing protein 5	REEP5_HUMAN	REEP5	21 kDa	0.0009
193	Heterogeneous nuclear ribonucleoprotein A1	ROA1_HUMAN	HNRNPA1	39 kDa	0.00091
194	Cluster of Dual specificity mitogen-activated protein kinase kinase 1	MP2K1_HUMAN [2]	MAP2K1	43 kDa	0.00093
195	Ig alpha-1 chain C region	IGHA1_HUMAN	IGHA1	38 kDa	0.00099
196	Protein bicaudal D homolog 2	BICD2_HUMAN	BICD2	94 kDa	0.00099
197	V-type proton ATPase subunit E 1	VATE1_HUMAN	ATP6V1E1	26 kDa	0.00099
198	Glycine--tRNA ligase	SYG_HUMAN	GARS	83 kDa	0.001
199	Uncharacterized protein C19orf43	CS043_HUMAN	C19orf43	18 kDa	0.001
200	T-complex protein 1 subunit beta	TCPB_HUMAN	CCT2	57 kDa	0.001
201	T-complex protein 1 subunit delta	TCPD_HUMAN	CCT4	58 kDa	0.001
202	Elongation factor 1-beta	EF1B_HUMAN	EEF1B2	25 kDa	0.001
203	Cluster of AP-1 complex subunit beta-1	APIB1_HUMAN [2]	APIB1	105 kDa	0.0011
204	Chromodomain-helicase-DNA-binding protein 4	CHD4_HUMAN	CHD4	218 kDa	0.0011
205	Heterogeneous nuclear ribonucleoprotein L	HNRPL_HUMAN	HNRNPL	64 kDa	0.0011
1073	Growth/differentiation factor 15	GDF15_HUMAN	GDF15	34 kDa	0.23
207	Eukaryotic translation initiation factor 5	IF5_HUMAN	EIF5	49 kDa	0.0011
208	Transthyretin	TTHY_HUMAN	TTR	16 kDa	0.0011
209	Methionine aminopeptidase 1	MAP11_HUMAN	METAP1	43 kDa	0.0011
210	Importin subunit alpha-1	IMA1_HUMAN	KPNA2	58 kDa	0.0011
211	Chromobox protein homolog 5	CBX5_HUMAN	CBX5	22 kDa	0.0011
212	Eukaryotic translation initiation factor 5A-1	IF5A1_HUMAN (+1)	EIF5A	17 kDa	0.0011
213	EGF-containing fibulin-like extracellular matrix protein 1	FBLN3_HUMAN	EFEMP1	55 kDa	0.0012
214	Syntaxin-binding protein 2	STXB2_HUMAN	STXBP2	66 kDa	0.0012
215	Cluster of Serine/threonine-protein kinase PAK 2	PAK2_HUMAN [2]	PAK2	58 kDa	0.0012
216	Golgin subfamily A member 2	GOGA2_HUMAN	GOLGA2	113 kDa	0.0013
217	Chromobox protein homolog 3	CBX3_HUMAN	CBX3	21 kDa	0.0013

218	Heat shock 70 kDa protein 4	HSP74_HUMAN	HSPA4	94 kDa	0.0013
219	Coronin-1B	COR1B_HUMAN	CORO1B	54 kDa	0.0013
220	Cluster of Polyadenylate-binding protein 1	PABP1_HUMAN [4]	PABPC1	71 kDa	0.0013
221	Serotransferrin	TRFE_HUMAN	TF	77 kDa	0.0014
222	Cluster of Protein lin-7 homolog C	LIN7C_HUMAN [2]	LIN7C	22 kDa	0.0014
223	Thrombospondin type-1 domain-containing protein 4	THSD4_HUMAN	THSD4	112 kDa	0.0014
224	Programmed cell death protein 10	PDC10_HUMAN	PDCD10	25 kDa	0.0014
225	Large neutral amino acids transporter small subunit 1	LAT1_HUMAN	SLC7A5	55 kDa	0.0014
226	Protein S100-A16	S10AG_HUMAN	S100A16	12 kDa	0.0014
227	Disks large homolog 1	DLG1_HUMAN	DLG1	100 kDa	0.0014
228	Fibromodulin	FMOD_HUMAN	FMOD	43 kDa	0.0015
229	Inter-alpha-trypsin inhibitor heavy chain H1	ITIH1_HUMAN	ITIH1	101 kDa	0.0015
230	Cluster of Actin-related protein 3	ARP3_HUMAN [2]	ACTR3	47 kDa	0.0015
231	Eukaryotic translation initiation factor 3 subunit A	EIF3A_HUMAN	EIF3A	167 kDa	0.0015
232	Lysosomal alpha-mannosidase	MA2B1_HUMAN	MAN2B1	114 kDa	0.0015
233	NSFL1 cofactor p47	NSF1C_HUMAN	NSFL1C	41 kDa	0.0015
234	Interleukin enhancer-binding factor 2	ILF2_HUMAN	ILF2	43 kDa	0.0015
235	Far upstream element-binding protein 3	FUBP3_HUMAN	FUBP3	62 kDa	0.0015
489	Midkine	MK_HUMAN	MDK	16 kDa	0.019
237	Eukaryotic translation initiation factor 2 subunit 3	IF2G_HUMAN	EIF2S3	51 kDa	0.0015
238	Casein kinase II subunit beta	CSK2B_HUMAN	CSNK2B	25 kDa	0.0016
239	E3 ubiquitin-protein ligase TRIM33	TRIM33_HUMAN	TRIM33	123 kDa	0.0016
240	Telomeric repeat-binding factor 2-interacting protein 1	TE2IP_HUMAN	TERF2IP	44 kDa	0.0016
241	Bifunctional glutamate/proline--tRNA ligase	SYEP_HUMAN	EPRS	171 kDa	0.0016
421	Cadherin-1	CADH1_HUMAN	CDH1	97 kDa	0.011
243	Cullin-associated NEDD8-dissociated protein 1	CAND1_HUMAN	CAND1	136 kDa	0.0016
244	Epiplakin	EPIPL_HUMAN	EPPK1	556 kDa	0.0016
245	Alpha-1-acid glycoprotein 2	A1AG2_HUMAN	ORM2	24 kDa	0.0017
246	Guanine nucleotide-binding protein subunit beta-2-like 1	GBLP_HUMAN	GNB2L1	35 kDa	0.0017
247	Cluster of High mobility group protein B2	HMGB2_HUMAN [3]	HMGB2	24 kDa	0.0017
248	DNA topoisomerase 1	TOP1_HUMAN	TOP1	91 kDa	0.0018
249	Fibroblast growth factor-binding protein 1	FGFP1_HUMAN	FGFBP1	26 kDa	0.0019
250	Laminin subunit beta-3	LAMB3_HUMAN	LAMB3	130 kDa	0.0019
251	Fumarate hydratase, mitochondrial	FUMH_HUMAN	FH	55 kDa	0.0019
252	Sorting nexin-5	SNX5_HUMAN	SNX5	47 kDa	0.0019
253	Metalloproteinase inhibitor 3	TIMP3_HUMAN	TIMP3	24 kDa	0.0019
254	Transcription elongation regulator 1	TCRG1_HUMAN	TCERG1	124 kDa	0.0019
255	Quinone oxidoreductase	QOR_HUMAN	CRYZ	35 kDa	0.0019
256	Cluster of Serine/threonine-protein phosphatase 2A 65 kDa regulatory subunit A alpha isoform	2AAA_HUMAN [2]	PPP2R1A	65 kDa	0.0019
257	Obg-like ATPase 1	OLA1_HUMAN	OLA1	45 kDa	0.0019
258	T-complex protein 1 subunit epsilon	TCPE_HUMAN	CCT5	60 kDa	0.0019
259	Vacuolar protein sorting-associated protein 29	VPS29_HUMAN	VPS29	21 kDa	0.0021
260	Protein phosphatase 1G	PPM1G_HUMAN	PPM1G	59 kDa	0.0021
261	Olfactomedin-like protein 3	OLF3_HUMAN	OLFML3	46 kDa	0.0022
262	Testis-specific Y-encoded-like protein 5	TSYL5_HUMAN	TSPYL5	45 kDa	0.0022

263	Peptidyl-prolyl cis-trans isomerase C	PPIC_HUMAN	PPIC	23 kDa	0.0023
264	Plastin-1	PLSL_HUMAN	PLS1	70 kDa	0.0023
265	Urokinase-type plasminogen activator	UROK_HUMAN	PLAU	49 kDa	0.0023
266	E3 ubiquitin-protein ligase CHIP	CHIP_HUMAN	STUB1	35 kDa	0.0023
267	N(G),N(G)-dimethylarginine dimethylaminohydrolase 2	DDAH2_HUMAN	DDAH2	30 kDa	0.0023
268	Annexin A1	ANXA1_HUMAN	ANXA1	39 kDa	0.0023
269	Programmed cell death protein 6	PDCD6_HUMAN	PDCD6	22 kDa	0.0023
270	V-type proton ATPase catalytic subunit A	VATA_HUMAN	ATP6V1A	68 kDa	0.0024
271	Complement component C7	CO7_HUMAN	C7	94 kDa	0.0024
272	4-trimethylaminobutyraldehyde dehydrogenase	AL9A1_HUMAN	ALDH9A1	54 kDa	0.0024
273	T-complex protein 1 subunit eta	TCPH_HUMAN	CCT7	59 kDa	0.0024
274	Desmin	DESM_HUMAN	DES	54 kDa	0.0024
275	Choline-phosphate cytidyltransferase A	PCY1A_HUMAN	PCYT1A	42 kDa	0.0025
276	Apolipoprotein A-II	APOA2_HUMAN	APOA2	11 kDa	0.0026
277	Dihydropyrimidinase-related protein 2	DPYL2_HUMAN	DPYSL2	62 kDa	0.0026
278	Cluster of Non-histone chromosomal protein HMG-17	HMGN2_HUMAN [2]	HMGN2	9 kDa	0.0026
279	Heat shock 70 kDa protein 4L	HS74L_HUMAN	HSPA4L	95 kDa	0.0026
280	Transforming growth factor beta-2	TGFB2_HUMAN	TGFB2	48 kDa	0.0026
281	40S ribosomal protein S20	RS20_HUMAN	RPS20	13 kDa	0.0027
282	Sorting nexin-6	SNX6_HUMAN	SNX6	47 kDa	0.0027
283	Integrin alpha-5	ITA5_HUMAN	ITGA5	115 kDa	0.0027
284	Secretogranin-2	SCG2_HUMAN	SCG2	71 kDa	0.0028
285	COP9 signalosome complex subunit 7a	CSN7A_HUMAN	COP7A	30 kDa	0.0028
286	Cluster of Mitogen-activated protein kinase 1	MK01_HUMAN [2]	MAPK1	41 kDa	0.0028
287	RNA-binding motif protein, X chromosome	RBMX_HUMAN	RBMX	42 kDa	0.003
288	Cluster of DnaJ homolog subfamily B member 1	DNJB1_HUMAN [2]	DNAJB1	38 kDa	0.003
289	Endophilin-B2	SHLB2_HUMAN	SH3GLB2	44 kDa	0.003
290	LIM and SH3 domain protein 1	LASP1_HUMAN	LASP1	30 kDa	0.003
291	28 kDa heat- and acid-stable phosphoprotein	HAP28_HUMAN	PDAP1	21 kDa	0.003
292	Heat shock protein 105 kDa	HS105_HUMAN	HSPH1	97 kDa	0.0031
805	Prolactin-inducible protein	PIP_HUMAN	PIP	17 kDa	0.1
294	Aflatoxin B1 aldehyde reductase member 3	ARK73_HUMAN	AKR7A3	37 kDa	0.0031
295	Protein-L-isoaspartate(D-aspartate) O-methyltransferase	PIMT_HUMAN	PCMT1	25 kDa	0.0031
296	Cluster of Dynamin-2	DYN2_HUMAN [2]	DNM2	98 kDa	0.0032
297	Carbonic anhydrase 2	CAH2_HUMAN	CA2	29 kDa	0.0032
298	Splicing factor 3B subunit 2	SF3B2_HUMAN	SF3B2	100 kDa	0.0032
299	Neutrophil elastase	ELNE_HUMAN	ELANE	29 kDa	0.0033
300	Phosphoglucomutase-1	PGM1_HUMAN	PGM1	61 kDa	0.0033
313	Junction plakoglobin	PLAK_HUMAN	JUP	82 kDa	0.0037
302	Probable ATP-dependent RNA helicase DDX17	DDX17_HUMAN	DDX17	80 kDa	0.0034
303	Arfaptin-1	ARFP1_HUMAN	ARFIP1	42 kDa	0.0034
304	Bifunctional ATP-dependent dihydroxyacetone kinase/FAD-AMP lyase (cyclizing)	DHAK_HUMAN	DAK	59 kDa	0.0034
305	Eukaryotic translation initiation factor 3 subunit E	EIF3E_HUMAN	EIF3E	52 kDa	0.0034
306	TAR DNA-binding protein 43	TADBP_HUMAN	TARDBP	45 kDa	0.0035
307	Proteasome subunit beta type-7	PSB7_HUMAN	PSMB7	30 kDa	0.0035

308	Azurocidin	CAP7_HUMAN	AZU1	27 kDa	0.0036
309	Collagen alpha-1(XVII) chain	COHA1_HUMAN	COL17A1	150 kDa	0.0036
310	Nuclear mitotic apparatus protein 1	NUMA1_HUMAN	NUMA1	238 kDa	0.0036
311	Laminin subunit gamma-1	LAMC1_HUMAN	LAMC1	178 kDa	0.0036
312	C-type lectin domain family 11 member A	CLC11_HUMAN	CLEC11A	36 kDa	0.0037
669	Desmoplakin	DESP_HUMAN	DSP	332 kDa	0.061
314	Argininosuccinate synthase	ASSY_HUMAN	ASS1	47 kDa	0.0038
315	Cluster of Glutathione S-transferase Mu 3	GSTM3_HUMAN [3]	GSTM3	27 kDa	0.0038
316	EH domain-containing protein 4	EHD4_HUMAN	EHD4	61 kDa	0.0039
140	Cluster of Keratin, type I cytoskeletal 18	K1C18_HUMAN [2]	KRT18	48 kDa	0.00038
318	Cluster of Fructose-1,6-bisphosphatase 1	F16P1_HUMAN [2]	FBP1	37 kDa	0.004
319	Heterogeneous nuclear ribonucleoproteins A2/B1	ROA2_HUMAN	HNRNPA2B1	37 kDa	0.0041
320	T-complex protein 1 subunit gamma	TCPG_HUMAN	CCT3	61 kDa	0.0041
321	Chitinase-3-like protein 1	CH3L1_HUMAN	CHI3L1	43 kDa	0.0041
322	Perilipin-3	PLIN3_HUMAN	PLIN3	47 kDa	0.0041
293	Cluster of Catenin alpha-1	CTNA1_HUMAN [2]	CTNNA1	100 kDa	0.0031
324	Activated RNA polymerase II transcriptional coactivator p15	TCP4_HUMAN	SUB1	14 kDa	0.0041
325	Coatomer subunit zeta-1	COPZ1_HUMAN	COPZ1	20 kDa	0.0042
326	Collagen alpha-1(XIV) chain	COEA1_HUMAN	COL14A1	194 kDa	0.0042
327	Succinyl-CoA:3-ketoacid coenzyme A transferase 1, mitochondrial	SCOT1_HUMAN	OXCT1	56 kDa	0.0042
328	Tyrosine-protein phosphatase non-receptor type 6	PTN6_HUMAN	PTPN6	68 kDa	0.0043
329	Plasminogen activator inhibitor 1	PAI1_HUMAN	SERPINE1	45 kDa	0.0044
330	Protein TFG	TFG_HUMAN	TFG	43 kDa	0.0044
331	Far upstream element-binding protein 1	FUBP1_HUMAN	FUBP1	68 kDa	0.0045
332	Cluster of Gamma-enolase	ENOG_HUMAN [2]	ENO2	47 kDa	0.0045
333	Creatine kinase U-type, mitochondrial	KCRU_HUMAN	CKMT1A	47 kDa	0.0045
334	Dynamin-like 120 kDa protein, mitochondrial	OPA1_HUMAN	OPA1	112 kDa	0.0045
335	PDZ domain-containing protein GIPC1	GIPC1_HUMAN	GIPC1	36 kDa	0.0045
336	Leucine-rich repeat flightless-interacting protein 2	LRRF2_HUMAN	LRRFIP2	82 kDa	0.0045
337	Angiopoietin-related protein 4	ANGL4_HUMAN	ANGPTL4	45 kDa	0.0047
338	Pigment epithelium-derived factor	PEDF_HUMAN	SERPINF1	46 kDa	0.0047
339	Methionine aminopeptidase 2	MAP2_HUMAN	METAP2	53 kDa	0.0047
340	Eukaryotic translation initiation factor 3 subunit H	EIF3H_HUMAN	EIF3H	40 kDa	0.0047
341	Transmembrane protein C16orf54	CP054_HUMAN	C16orf54	24 kDa	0.0049
342	Antileukoproteinase	SLPI_HUMAN	SLPI	14 kDa	0.0049
343	Septin-9	SEPT9_HUMAN	Sep-09	65 kDa	0.0049
344	Protein AMBP	AMBP_HUMAN	AMBP	39 kDa	0.005
345	Transcription intermediary factor 1-beta	TIF1B_HUMAN	TRIM28	89 kDa	0.005
346	Catalase	CATA_HUMAN	CAT	60 kDa	0.005
347	ATP-dependent RNA helicase A	DHX9_HUMAN	DHX9	141 kDa	0.0053
960	Proteasome subunit beta type-6	PSB6_HUMAN	PSMB6	25 kDa	0.16
349	LINE-1 retrotransposable element ORF1 protein	LORF1_HUMAN	L1RE1	40 kDa	0.0053
350	Sialic acid synthase	SIAS_HUMAN	NANS	40 kDa	0.0054
351	Huntingtin-interacting protein 1-related protein	HIP1R_HUMAN	HIP1R	119 kDa	0.0054
352	Ran GTPase-activating protein 1	RAGP1_HUMAN	RANGAP1	64 kDa	0.0056

353	Transferrin receptor protein 1	TFRI_HUMAN	TFRC	85 kDa	0.0056
354	Aldehyde dehydrogenase, mitochondrial	ALDH2_HUMAN	ALDH2	56 kDa	0.0056
355	Deoxynucleoside triphosphate triphosphohydrolase SAMHD1	SAMH1_HUMAN	SAMHD1	72 kDa	0.0057
356	DNA replication licensing factor MCM6	MCM6_HUMAN	MCM6	93 kDa	0.0058
357	Peroxidase homolog	PXDN_HUMAN	PXDN	165 kDa	0.0059
358	N-terminal kinase-like protein	NTKL_HUMAN	SCYL1	90 kDa	0.0059
359	Signal transducer and activator of transcription 1-alpha/beta	STAT1_HUMAN	STAT1	87 kDa	0.006
360	Stress-70 protein, mitochondrial	GRP75_HUMAN	HSPA9	74 kDa	0.006
361	Ubiquitin carboxyl-terminal hydrolase isozyme L1	UCHL1_HUMAN	UCHL1	25 kDa	0.0061
362	Laminin subunit beta-2	LAMB2_HUMAN	LAMB2	196 kDa	0.0063
1018	Ribosome-binding protein 1	RRBP1_HUMAN	RRBP1	152 kDa	0.19
364	Granulins	GRN_HUMAN	GRN	64 kDa	0.0064
365	Basic leucine zipper and W2 domain-containing protein 1	BZW1_HUMAN	BZW1	48 kDa	0.0065
366	Septin-7	SEPT7_HUMAN	Sep-07	51 kDa	0.0066
367	X-ray repair cross-complementing protein 5	XRCC5_HUMAN	XRCC5	83 kDa	0.0066
368	Ubiquitin-like modifier-activating enzyme 1	UBA1_HUMAN	UBA1	118 kDa	0.0066
369	F-actin-capping protein subunit alpha-2	CAZA2_HUMAN	CAPZA2	33 kDa	0.0067
370	Paraspeckle component 1	PSPC1_HUMAN	PSPC1	59 kDa	0.0067
371	Cullin-4B	CUL4B_HUMAN	CUL4B	104 kDa	0.0067
372	Alpha-soluble NSF attachment protein	SNAAP_HUMAN	NAPA	33 kDa	0.0068
373	Plastin-2	PLSL_HUMAN	LCP1	70 kDa	0.0069
374	Angiotensinogen	ANGT_HUMAN	AGT	53 kDa	0.0069
375	Stanniocalcin-2	STC2_HUMAN	STC2	33 kDa	0.0069
376	Fermitin family homolog 2	FERM2_HUMAN	FERMT2	78 kDa	0.0071
377	Lactadherin	MFGM_HUMAN	MFGE8	43 kDa	0.0072
378	Proprotein convertase subtilisin/kexin type 9	PCSK9_HUMAN	PCSK9	74 kDa	0.0072
379	Protein diaphanous homolog 1	DIAP1_HUMAN	DIAPH1	141 kDa	0.0074
1061	Plectin	PLEC_HUMAN	PLEC	532 kDa	0.22
381	Cluster of Putative RNA-binding protein Luc7-like 2	LC7L2_HUMAN [2]	LUC7L2	47 kDa	0.0075
382	RuvB-like 1	RUVB1_HUMAN	RUVBL1	50 kDa	0.0076
383	Transcription elongation factor B polypeptide 2	ELOB_HUMAN	TCEB2	13 kDa	0.0077
384	Ubiquitin carboxyl-terminal hydrolase 14	UBP14_HUMAN	USP14	56 kDa	0.0077
385	Splicing factor 3A subunit 3	SF3A3_HUMAN	SF3A3	59 kDa	0.0078
386	Leucine--tRNA ligase, cytoplasmic	SYLC_HUMAN	LARS	134 kDa	0.0078
387	DnaJ homolog subfamily C member 7	DNJC7_HUMAN	DNAJC7	56 kDa	0.0079
388	Coatomer subunit delta	COPD_HUMAN	ARCN1	57 kDa	0.008
389	RNA-binding protein 8A	RBM8A_HUMAN	RBM8A	20 kDa	0.008
505	Cluster of Filamin-A	FLNA_HUMAN [3]	FLNA	281 kDa	0.021
391	Calcium-dependent secretion activator 1	CAPS1_HUMAN	CADPS	153 kDa	0.0081
392	Regulation of nuclear pre-mRNA domain-containing protein 1B	RPR1B_HUMAN	RPRD1B	37 kDa	0.0081
393	Scaffold attachment factor B1	SAFB1_HUMAN	SAFB	103 kDa	0.0081
394	COP9 signalosome complex subunit 7b	CSN7B_HUMAN	COPS7B	30 kDa	0.0081
396	Immunoglobulin lambda-like polypeptide 5	IGLL5_HUMAN	IGLL5	23 kDa	0.0081
766	Cluster of Ig lambda chain V-II region WIN (LV209_HUMAN)	LV209_HUMAN [2]		12 kDa	0.085
747	Adenosylhomocysteinase	SAHH_HUMAN	AHCY	48 kDa	0.082

398	THUMP domain-containing protein 1	THUM1_HUMAN	THUMPD1	39 kDa	0.0086
399	Heterogeneous nuclear ribonucleoprotein A3	ROA3_HUMAN	HNRNPA3	40 kDa	0.0087
400	Cluster of Hsc70-interacting protein	F10A1_HUMAN [2]	ST13	41 kDa	0.0088
401	Selenide, water dikinase 1	SPS1_HUMAN	SEPHS1	43 kDa	0.0088
402	Ribonucleoside-diphosphate reductase large subunit	RIR1_HUMAN	RRM1	90 kDa	0.009
403	Squamous cell carcinoma antigen recognized by T-cells 3	SART3_HUMAN	SART3	110 kDa	0.0092
404	Proliferation-associated protein 2G4	PA2G4_HUMAN	PA2G4	44 kDa	0.0092
405	Vacuolar protein sorting-associated protein 35	VPS35_HUMAN	VPS35	92 kDa	0.0093
406	Kallikrein-10	KLK10_HUMAN	KLK10	30 kDa	0.0094
407	Hypoxia up-regulated protein 1	HYOU1_HUMAN	HYOU1	111 kDa	0.0095
408	40S ribosomal protein S11	RS11_HUMAN	RPS11	18 kDa	0.0096
409	40S ribosomal protein S10	RS10_HUMAN	RPS10	19 kDa	0.0096
410	26S protease regulatory subunit 6A	PRS6A_HUMAN	PSMC3	49 kDa	0.01
411	ATP-citrate synthase	ACLY_HUMAN	ACLY	121 kDa	0.01
412	Adenine phosphoribosyltransferase	APT_HUMAN	APRT	20 kDa	0.01
413	BRISC and BRCA1-A complex member 1	BABA1_HUMAN	BABAM1	37 kDa	0.01
414	Ferritin light chain	FRIL_HUMAN	FTL	20 kDa	0.011
415	Proteasome activator complex subunit 1	PSME1_HUMAN	PSME1	29 kDa	0.011
416	Protein S100-A8	S10A8_HUMAN	S100A8	11 kDa	0.011
417	Latent-transforming growth factor beta-binding protein 2	LTBP2_HUMAN	LTBP2	195 kDa	0.011
418	Importin subunit alpha-5	IMAS_HUMAN	KPNA1	60 kDa	0.011
419	Tubulin gamma-1 chain	TBG1_HUMAN (+1)	TUBG1	51 kDa	0.011
420	Enhancer of rudimentary homolog	ERH_HUMAN	ERH	12 kDa	0.011
348	Proteasome subunit beta type-1	PSB1_HUMAN	PSMB1	26 kDa	0.0053
422	Small glutamine-rich tetratricopeptide repeat-containing protein alpha	SGTA_HUMAN	SGTA	34 kDa	0.012
423	Actin-related protein 2/3 complex subunit 4	ARPC4_HUMAN	ARPC4	20 kDa	0.012
424	Proteasome subunit beta type-4	PSB4_HUMAN	PSMB4	29 kDa	0.012
425	Splicing factor 3B subunit 1	SF3B1_HUMAN	SF3B1	146 kDa	0.012
426	Mitotic checkpoint protein BUB3	BUB3_HUMAN	BUB3	37 kDa	0.012
427	60S acidic ribosomal protein P1	RLA1_HUMAN	RPLP1	12 kDa	0.012
428	Cartilage oligomeric matrix protein	COMP_HUMAN	COMP	83 kDa	0.012
429	Mitochondrial fission 1 protein	FIS1_HUMAN	FIS1	17 kDa	0.012
430	Disco-interacting protein 2 homolog B	DIP2B_HUMAN	DIP2B	171 kDa	0.012
1214	Keratin, type II cuticular Hb2	KRT82_HUMAN	KRT82	57 kDa	0.4
432	Sorting nexin-2	SNX2_HUMAN	SNX2	58 kDa	0.013
433	Nuclear migration protein nudC	NUDC_HUMAN	NUDC	38 kDa	0.013
434	Hippocalcin-like protein 1	HPCL1_HUMAN	HPCAL1	22 kDa	0.013
435	ATP-dependent RNA helicase DDX1	DDX1_HUMAN	DDX1	82 kDa	0.013
436	Staphylococcal nuclease domain-containing protein 1	SND1_HUMAN	SND1	102 kDa	0.013
437	Phosphatidylcholine-sterol acyltransferase	LCAT_HUMAN	LCAT	50 kDa	0.013
438	Catenin delta-1	CTND1_HUMAN	CTNND1	108 kDa	0.013
439	X-ray repair cross-complementing protein 6	XRCC6_HUMAN	XRCC6	70 kDa	0.013
440	14-3-3 protein epsilon	1433E_HUMAN	YWHAE	29 kDa	0.014
441	Cluster of Nuclease-sensitive element-binding protein 1	YBOX1_HUMAN [3]	YBX1	36 kDa	0.014
442	Platelet-activating factor acetylhydrolase IB subunit beta	PA1B2_HUMAN	PAFAH1B2	26 kDa	0.014

443	V-type proton ATPase subunit B, brain isoform	VATB2_HUMAN	ATP6V1B2	57 kDa	0.014
444	Synaptogyrin-2	SNG2_HUMAN	SYNGR2	25 kDa	0.014
445	Carboxypeptidase E	CBPE_HUMAN	CPE	53 kDa	0.014
446	Proteasome activator complex subunit 3	PSME3_HUMAN	PSME3	30 kDa	0.014
447	PERQ amino acid-rich with GYF domain-containing protein 2	PERQ2_HUMAN	GIGYF2	150 kDa	0.014
448	Insulin-like growth factor-binding protein 6	IBP6_HUMAN	IGFBP6	25 kDa	0.014
449	Syntenin-1	SDCB1_HUMAN	SDCBP	32 kDa	0.014
450	Probable ATP-dependent RNA helicase DDX5	DDX5_HUMAN	DDX5	69 kDa	0.014
451	Nucleosome assembly protein 1-like 1	NPIL1_HUMAN	NAPIL1	45 kDa	0.014
452	Splicing factor, proline- and glutamine-rich	SFPQ_HUMAN	SFPQ	76 kDa	0.014
453	60S ribosomal protein L8	RL8_HUMAN	RPL8	28 kDa	0.014
1349	Protein S100-A11	S10AB_HUMAN	S100A11	12 kDa	0.47
455	Glia-derived nexin	GDN_HUMAN	SERPINE2	44 kDa	0.015
456	Polyadenylate-binding protein-interacting protein 1	PAIP1_HUMAN	PAIP1	54 kDa	0.015
457	CTP synthase 1	PYRG1_HUMAN	CTPS1	67 kDa	0.015
458	Insulin-like growth factor-binding protein 7	IBP7_HUMAN	IGFBP7	29 kDa	0.015
459	Neogenin	NEO1_HUMAN	NEO1	160 kDa	0.015
460	Myeloblastin	PRTN3_HUMAN	PRTN3	28 kDa	0.015
461	PHD finger-like domain-containing protein 5A	PHF5A_HUMAN	PHF5A	12 kDa	0.015
462	Cathepsin D	CATD_HUMAN	CTSD	45 kDa	0.015
463	Prefoldin subunit 2	PFD2_HUMAN	PFDN2	17 kDa	0.016
464	Methionine adenosyltransferase 2 subunit beta	MAT2B_HUMAN	MAT2B	38 kDa	0.016
465	Transcriptional activator protein Pur-alpha	PURA_HUMAN	PURA	35 kDa	0.016
466	3'(2'),5'-bisphosphate nucleotidase 1	BPNT1_HUMAN	BPNT1	33 kDa	0.016
467	Transcriptional activator protein Pur-beta	PURB_HUMAN	PURB	33 kDa	0.016
468	Collagen alpha-1(VII) chain	COT7A1_HUMAN	COL7A1	295 kDa	0.016
469	Importin-5	IPO5_HUMAN	IPO5	124 kDa	0.016
470	26S protease regulatory subunit 4	PRS4_HUMAN	PSMC1	49 kDa	0.016
1011	Protein S100-A6	S10A6_HUMAN	S100A6	10 kDa	0.19
472	Galectin-7	LEG7_HUMAN	LGALS7	15 kDa	0.016
473	Plasminogen activator inhibitor 1 RNA-binding protein	PAIRB_HUMAN	SERBP1	45 kDa	0.016
474	Kallikrein-6	KLK6_HUMAN	KLK6	27 kDa	0.017
475	Non-histone chromosomal protein HMG-14	HMGN1_HUMAN	HMGN1	11 kDa	0.017
476	3-hydroxyacyl-CoA dehydrogenase type-2	HCD2_HUMAN	HSD17B10	27 kDa	0.017
477	Proteasome subunit beta type-2	PSB2_HUMAN	PSMB2	23 kDa	0.017
478	Hsp90 co-chaperone Cdc37	CDC37_HUMAN	CDC37	44 kDa	0.017
479	DNA-(apurinic or apyrimidinic site) lyase	APEX1_HUMAN	APEX1	36 kDa	0.017
43	Annexin A2	ANXA2_HUMAN	ANXA2	39 kDa	0.0001
481	Apolipoprotein A-IV	APOA4_HUMAN	APOA4	45 kDa	0.017
482	Prefoldin subunit 5	PF5_HUMAN	PFDN5	17 kDa	0.017
483	Sorcin	SORCN_HUMAN	SRI	22 kDa	0.018
1108	Protein disulfide-isomerase A4	PDIA4_HUMAN	PDIA4	73 kDa	0.26
485	Cluster of Rab GDP dissociation inhibitor beta	GDIB_HUMAN [2]	GDI2	51 kDa	0.018
486	General vesicular transport factor p115	USO1_HUMAN	USO1	108 kDa	0.018
487	Cluster of Rootletin	CROCC_HUMAN [2]	CROCC	229 kDa	0.018

488	Non-POU domain-containing octamer-binding protein	NONO_HUMAN	NONO	54 kDa	0.018
568	Plasminogen	PLMN_HUMAN	PLG	91 kDa	0.035
490	40S ribosomal protein S16	RS16_HUMAN	RPS16	16 kDa	0.019
491	Interstitial collagenase	MMP1_HUMAN	MMP1	54 kDa	0.019
492	Glucose-6-phosphate 1-dehydrogenase	G6PD_HUMAN	G6PD	59 kDa	0.019
493	Laminin subunit alpha-5	LAMA5_HUMAN	LAMA5	400 kDa	0.019
494	Annexin A7	ANXA7_HUMAN	ANXA7	53 kDa	0.019
495	Fibronectin	FN1_HUMAN	FN1	263 kDa	0.019
496	Peptidyl-prolyl cis-trans isomerase FKBP4	FKBP4_HUMAN	FKBP4	52 kDa	0.02
497	Myosin-15	MYH15_HUMAN	MYH15	225 kDa	0.02
498	Cadherin EGF LAG seven-pass G-type receptor 2	CELR2_HUMAN	CELSR2	317 kDa	0.02
499	Procollagen-lysine,2-oxoglutarate 5-dioxygenase 2	PLOD2_HUMAN	PLOD2	85 kDa	0.02
500	Ribonuclease inhibitor	RINI_HUMAN	RNH1	50 kDa	0.02
501	Complement factor D	CFAD_HUMAN	CFD	27 kDa	0.02
502	Cleavage and polyadenylation specificity factor subunit 6	CPSF6_HUMAN	CPSF6	59 kDa	0.021
1338	Proteasome subunit alpha type-6	PSA6_HUMAN	PSMA6	27 kDa	0.45
504	Nuclear protein localization protein 4 homolog	NPL4_HUMAN	NPLOC4	68 kDa	0.021
480	Agrin	AGRIN_HUMAN	AGRN	217 kDa	0.017
506	Protein NDRG1	NDRG1_HUMAN	NDRG1	43 kDa	0.021
507	T-complex protein 1 subunit alpha	TCPA_HUMAN	TCPI	60 kDa	0.021
508	Lamin-B2	LMNB2_HUMAN	LMNB2	68 kDa	0.022
509	ELAV-like protein 1	ELAV1_HUMAN	ELAVL1	36 kDa	0.022
510	Mesothelin	MSLN_HUMAN	MSLN	69 kDa	0.022
511	Beta-2-glycoprotein 1	APOH_HUMAN	APOH	38 kDa	0.022
512	Formin-binding protein 1-like	FBP1L_HUMAN	FNBP1L	70 kDa	0.022
513	Cluster of KH domain-containing, RNA-binding, signal transduction-associated protein 1	KHDR1_HUMAN [2]	KHDRBS1	48 kDa	0.023
514	Beta-hexosaminidase subunit beta	HEXB_HUMAN	HEXB	63 kDa	0.023
515	Procollagen-lysine,2-oxoglutarate 5-dioxygenase 3	PLOD3_HUMAN	PLOD3	85 kDa	0.023
516	Cytoskeleton-associated protein 5	CKAP5_HUMAN	CKAP5	226 kDa	0.023
517	Metalloproteinase inhibitor 1	TIMP1_HUMAN	TIMP1	23 kDa	0.023
518	Eukaryotic translation initiation factor 3 subunit K	EIF3K_HUMAN	EIF3K	25 kDa	0.024
947	Cluster of Receptor-type tyrosine-protein phosphatase F	PTPRF_HUMAN [2]	PTPRF	213 kDa	0.16
612	Cluster of Thrombospondin-1	TSP1_HUMAN [2]	THBS1	129 kDa	0.05
521	Integrin alpha-6	ITA6_HUMAN	ITGA6	127 kDa	0.024
522	Macrophage-capping protein	CAPG_HUMAN	CAPG	38 kDa	0.024
1106	Fatty acid synthase	FAS_HUMAN	FASN	273 kDa	0.25
524	Tether containing UBX domain for GLUT4	ASPC1_HUMAN	ASPSR1	60 kDa	0.024
525	Proteasome subunit beta type-8	PSB8_HUMAN	PSMB8	30 kDa	0.025
526	Cluster of Protein SET	SET_HUMAN [2]	SET	33 kDa	0.025
527	Cluster of Lamina-associated polypeptide 2, isoform alpha	LAP2A_HUMAN [2]	TMPO	75 kDa	0.025
528	Heterogeneous nuclear ribonucleoprotein K	HNRPK_HUMAN	HNRNPK	51 kDa	0.025
529	Cluster of Hexokinase-1	HXK1_HUMAN [2]	HK1	102 kDa	0.025
530	COP9 signalosome complex subunit 2	CSN2_HUMAN	COPS2	52 kDa	0.025
531	DNA replication licensing factor MCM3	MCM3_HUMAN	MCM3	91 kDa	0.026
532	Signal recognition particle 9 kDa protein	SRP09_HUMAN	SRP9	10 kDa	0.026

533	Zinc finger RNA-binding protein	ZFR_HUMAN	ZFR	117 kDa	0.026
534	14-3-3 protein eta	1433F_HUMAN	YWHAH	28 kDa	0.027
535	Receptor-type tyrosine-protein phosphatase S	PTPRS_HUMAN	PTPRS	217 kDa	0.027
536	Bifunctional purine biosynthesis protein PURH	PUR9_HUMAN	ATIC	65 kDa	0.027
537	S-phase kinase-associated protein 1	SKP1_HUMAN	SKP1	19 kDa	0.027
538	Small nuclear ribonucleoprotein Sm D3	SMD3_HUMAN	SNRPD3	14 kDa	0.027
539	NADP-dependent malic enzyme	MAOX_HUMAN	ME1	64 kDa	0.028
540	RuvB-like 2	RUVB2_HUMAN	RUVBL2	51 kDa	0.028
883	Cluster of Myosin light polypeptide 6	MYL6_HUMAN [2]	MYL6	17 kDa	0.13
542	60S acidic ribosomal protein P0	RLA0_HUMAN	RPLP0	34 kDa	0.029
543	DnaJ homolog subfamily C member 8	DNJC8_HUMAN	DNAJC8	30 kDa	0.03
1164	Triosephosphate isomerase	TPIS_HUMAN	TPI1	31 kDa	0.32
545	Proteasome subunit beta type-5	PSB5_HUMAN	PSMB5	28 kDa	0.03
546	Transcription elongation factor B polypeptide 1	ELOC_HUMAN	TCEB1	12 kDa	0.031
547	Sortilin	SORT_HUMAN	SORT1	92 kDa	0.031
548	Eukaryotic translation initiation factor 4H	IF4H_HUMAN	EIF4H	27 kDa	0.032
549	E3 ubiquitin-protein ligase HUWE1	HUWE1_HUMAN	HUWE1	482 kDa	0.032
550	Epidermal growth factor receptor substrate 15-like 1	EP15R_HUMAN	EPS15L1	94 kDa	0.032
984	Protein piccolo	PCLO_HUMAN	PCLO	553 kDa	0.18
552	Golgi-associated plant pathogenesis-related protein 1	GAPR1_HUMAN	GLIPR2	17 kDa	0.032
553	Protein jagged-1	JAG1_HUMAN	JAG1	134 kDa	0.032
554	Nucleolar and coiled-body phosphoprotein 1	NOLC1_HUMAN	NOLC1	74 kDa	0.032
1049	Apolipoprotein M	APOM_HUMAN	APOM	21 kDa	0.21
556	Eukaryotic peptide chain release factor subunit 1	ERF1_HUMAN	ETF1	49 kDa	0.032
557	Tenascin	TENA_HUMAN	TNC	241 kDa	0.033
558	Eukaryotic translation initiation factor 3 subunit B	EIF3B_HUMAN	EIF3B	92 kDa	0.033
559	DNA-dependent protein kinase catalytic subunit	PRKDC_HUMAN	PRKDC	469 kDa	0.034
560	COP9 signalosome complex subunit 8	CSN8_HUMAN	COPS8	23 kDa	0.034
561	Cluster of Spectrin beta chain, non-erythrocytic 1	SPTB2_HUMAN [3]	SPTBN1	275 kDa	0.034
562	Lactotransferrin	TRFL_HUMAN	LTF	78 kDa	0.034
563	40S ribosomal protein S3	RS3_HUMAN	RPS3	27 kDa	0.034
564	Protein transport protein Sec31A	SC31A_HUMAN	SEC31A	133 kDa	0.034
565	THO complex subunit 4	THOC4_HUMAN	ALYREF	27 kDa	0.034
566	Protein FAM98B	FA98B_HUMAN	FAM98B	37 kDa	0.034
567	Nuclear transport factor 2	NTF2_HUMAN	NUTF2	14 kDa	0.035
185	Neutral alpha-glucosidase AB	GANAB_HUMAN	GANAB	107 kDa	0.00083
569	Glypican-1	GPC1_HUMAN	GPC1	62 kDa	0.035
570	40S ribosomal protein S5	RS5_HUMAN	RPS5	23 kDa	0.036
571	Laminin subunit beta-1	LAMB1_HUMAN	LAMB1	198 kDa	0.037
572	Ataxin-10	ATX10_HUMAN	ATXN10	53 kDa	0.037
573	Fascin	FSCN1_HUMAN	FSCN1	55 kDa	0.037
574	Apolipoprotein C-II	APOC2_HUMAN	APOC2	11 kDa	0.038
575	Ethylmalonyl-CoA decarboxylase	ECHD1_HUMAN	ECHDC1	34 kDa	0.038
576	Dystroglycan	DAG1_HUMAN	DAG1	97 kDa	0.038
577	60S ribosomal protein L22	RL22_HUMAN	RPL22	15 kDa	0.038

390	Galectin-3-binding protein	LG3BP_HUMAN	LGALS3BP	65 kDa	0.008
579	Lupus La protein	LA_HUMAN	SSB	47 kDa	0.039
580	Thyroxine-binding globulin	THBG_HUMAN	SERPINA7	46 kDa	0.039
581	40S ribosomal protein S15a	RS15A_HUMAN	RPS15A	15 kDa	0.039
582	Transforming growth factor-beta-induced protein ig-h3	BGH3_HUMAN	TGFBI	75 kDa	0.039
643	Histone H2A.V	H2AV_HUMAN (+1)	H2AFV	14 kDa	0.056
584	Semaphorin-3C	SEM3C_HUMAN	SEMA3C	85 kDa	0.041
585	Cluster of Acidic leucine-rich nuclear phosphoprotein 32 family member A	AN32A_HUMAN [2]	ANP32A	29 kDa	0.041
1014	Amyloid-like protein 2	APLP2_HUMAN	APLP2	87 kDa	0.19
587	40S ribosomal protein S8	RS8_HUMAN	RPS8	24 kDa	0.041
588	Serine/arginine-rich splicing factor 9	SRSF9_HUMAN	SRSF9	26 kDa	0.041
589	Growth arrest-specific protein 6	GAS6_HUMAN	GAS6	80 kDa	0.041
590	Renin receptor	RENH_HUMAN	ATP6AP2	39 kDa	0.041
591	Endoplasmic reticulum resident protein 44	ERP44_HUMAN	ERP44	47 kDa	0.041
662	14-3-3 protein gamma	1433G_HUMAN	YWHAG	28 kDa	0.059
1138	Cell division control protein 42 homolog	CDC42_HUMAN	CDC42	21 kDa	0.28
594	Cluster of Ras-related protein Rap-1b	RAP1B_HUMAN [2]	RAP1B	21 kDa	0.043
555	Alpha-fetoprotein	FETA_HUMAN	AFP	69 kDa	0.032
1171	14-3-3 protein zeta/delta	1433Z_HUMAN	YWHAZ	28 kDa	0.32
597	Malate dehydrogenase, cytoplasmic	MDHC_HUMAN	MDH1	36 kDa	0.046
25	Cluster of Hemoglobin subunit beta	HBB_HUMAN [5]	HBB	16 kDa	0.0001
599	Glyoxylate reductase/hydroxypyruvate reductase	GRHPR_HUMAN	GRHPR	36 kDa	0.046
600	Sushi repeat-containing protein SRPX2	SRPX2_HUMAN	SRPX2	53 kDa	0.047
601	Protein unc-45 homolog A	UN45A_HUMAN	UNC45A	103 kDa	0.047
602	Cytoplasmic dynein 1 intermediate chain 2	DC1I2_HUMAN	DYNC1I2	71 kDa	0.048
484	Cluster of Histone H3.2	H32_HUMAN [3]	HIST2H3A	15 kDa	0.018
604	Eukaryotic translation initiation factor 2A	EIF2A_HUMAN	EIF2A	65 kDa	0.048
520	Proteasome subunit alpha type-1	PSA1_HUMAN	PSMA1	30 kDa	0.024
606	Apolipoprotein D	APOD_HUMAN	APOD	21 kDa	0.049
607	Arginine--tRNA ligase, cytoplasmic	SYRC_HUMAN	RARS	75 kDa	0.049
608	Cluster of Serine/arginine-rich splicing factor 2	SRSF2_HUMAN [2]	SRSF2	25 kDa	0.049
609	Cluster of ATP-dependent RNA helicase DDX3X	DDX3X_HUMAN [2]	DDX3X	73 kDa	0.049
610	Cluster of Complement factor H	CFAH_HUMAN [2]	CFH	139 kDa	0.05
611	Carbohydrate sulfotransferase 14	CHST14_HUMAN	CHST14	43 kDa	0.05
846	Apolipoprotein E	APOE_HUMAN	APOE	36 kDa	0.11
613	Cluster of Ras-related C3 botulinum toxin substrate 1	RAC1_HUMAN [2]	RAC1	21 kDa	0.05
614	Eukaryotic translation initiation factor 3 subunit L	EIF3L_HUMAN	EIF3L	67 kDa	0.05
615	Collagen triple helix repeat-containing protein 1	CTHR1_HUMAN	CTHRC1	26 kDa	0.051
616	NAD(P)H dehydrogenase [quinone] 1	NQO1_HUMAN	NQO1	31 kDa	0.052
617	Claudin-3	CLDN3_HUMAN	CLDN3	23 kDa	0.052
878	Tetranectin	TETN_HUMAN	CLEC3B	23 kDa	0.12
619	Carbohydrate sulfotransferase 11	CHST11_HUMAN	CHST11	42 kDa	0.052
620	Biglycan	PGS1_HUMAN	BGN	42 kDa	0.052
621	PCTP-like protein	PCTL_HUMAN	STARD10	33 kDa	0.052
622	tRNA-splicing ligase RtcB homolog	RTCB_HUMAN	RTCB	55 kDa	0.052

623	Cluster of Phosphoglycerate mutase 1	PGAM1_HUMAN [2]	PGAM1	29 kDa	0.052
624	Isocitrate dehydrogenase [NADP] cytoplasmic	IDHC_HUMAN	IDH1	47 kDa	0.052
625	Prostaglandin F2 receptor negative regulator	FPRP_HUMAN	PTGFRN	99 kDa	0.052
626	Glutamine-dependent NAD(+) synthetase	NADE_HUMAN	NADSYN1	79 kDa	0.053
627	Importin subunit alpha-7	IMA7_HUMAN	KPNA6	60 kDa	0.053
628	Dynein light chain 1, cytoplasmic	DYL1_HUMAN	DYNLL1	10 kDa	0.053
629	Phosphatidylinositol 3,4,5-trisphosphate 5-phosphatase 1	SHIP1_HUMAN	INPP5D	133 kDa	0.053
630	Prothrombin	THRB_HUMAN	F2	70 kDa	0.053
631	Elongation factor 1-delta	EF1D_HUMAN	EEF1D	31 kDa	0.053
632	Annexin A3	ANXA3_HUMAN	ANXA3	36 kDa	0.053
633	Periostin	POSTN_HUMAN	POSTN	93 kDa	0.053
634	Integrin beta-6	ITB6_HUMAN	ITGB6	86 kDa	0.054
635	Phosphatidylinositol-glycan-specific phospholipase D	PHLD_HUMAN	GPLD1	92 kDa	0.054
636	Coagulation factor IX	FA9_HUMAN	F9	52 kDa	0.055
637	Glutathione peroxidase 1	GPX1_HUMAN	GPX1	22 kDa	0.055
638	Differentially expressed in FDCP 6 homolog	DEFI6_HUMAN	DEF6	74 kDa	0.055
639	Prolow-density lipoprotein receptor-related protein 1	LRP1_HUMAN	LRP1	505 kDa	0.055
640	Complement factor I	CFAI_HUMAN	CFI	66 kDa	0.055
641	Acidic mammalian chitinase	CHIA_HUMAN	CHIA	52 kDa	0.055
642	Cluster of Kinesin light chain 2	KLC2_HUMAN [2]	KLC2	69 kDa	0.055
317	Antithrombin-III	ANT3_HUMAN	SERPINC1	53 kDa	0.0039
644	Thioredoxin-like protein 1	TXNL1_HUMAN	TXNL1	32 kDa	0.056
654	Cluster of L-lactate dehydrogenase A chain	LDHA_HUMAN [2]	LDHA	37 kDa	0.057
646	Isoleucine--tRNA ligase, cytoplasmic	SYIC_HUMAN	IARS	145 kDa	0.056
647	Eukaryotic translation initiation factor 3 subunit F	EIF3F_HUMAN	EIF3F	38 kDa	0.056
648	Phospholipase A-2-activating protein	PLAP_HUMAN	PLAA	87 kDa	0.056
649	C-type mannose receptor 2	MRC2_HUMAN	MRC2	167 kDa	0.056
650	Integrin beta-2	ITB2_HUMAN	ITGB2	85 kDa	0.056
651	Eukaryotic translation initiation factor 2 subunit 1	IF2A_HUMAN	EIF2S1	36 kDa	0.057
652	Eukaryotic translation initiation factor 3 subunit D	EIF3D_HUMAN	EIF3D	64 kDa	0.057
653	Transcription factor TFIIIB component B'' homolog	BDP1_HUMAN	BDP1	294 kDa	0.057
206	Importin subunit beta-1	IMB1_HUMAN	KPNB1	97 kDa	0.0011
655	Collagen alpha-3(VI) chain	CO6A3_HUMAN	COL6A3	344 kDa	0.057
656	6-phosphogluconate dehydrogenase, decarboxylating	6PGD_HUMAN	PGD	53 kDa	0.058
657	Neuroendocrine convertase 2	NEC2_HUMAN	PCSK2	71 kDa	0.058
658	Proteasomal ubiquitin receptor ADRM1	ADRM1_HUMAN	ADRM1	42 kDa	0.058
659	SUMO-activating enzyme subunit 2	SAE2_HUMAN	UBA2	71 kDa	0.058
660	RNA-binding protein 10	RBM10_HUMAN	RBM10	104 kDa	0.058
661	Cluster of DCN1-like protein 1	DCNL1_HUMAN [2]	DCUN1D1	30 kDa	0.059
503	4F2 cell-surface antigen heavy chain	4F2_HUMAN	SLC3A2	68 kDa	0.021
663	Actin-related protein 2/3 complex subunit 3	ARPC3_HUMAN	ARPC3	21 kDa	0.059
664	40S ribosomal protein SA	RSSA_HUMAN	RPSA	33 kDa	0.059
665	Actin-related protein 2	ARP2_HUMAN	ACTR2	45 kDa	0.06
666	Histone-lysine N-methyltransferase setd3	SETD3_HUMAN	SETD3	67 kDa	0.06
667	Hepatoma-derived growth factor-related protein 2	HDGR2_HUMAN	HDGFRP2	74 kDa	0.06

668	EMILIN-2	EMIL2_HUMAN	EMILIN2	116 kDa	0.061
795	Integrin beta-1	ITB1_HUMAN	ITGB1	88 kDa	0.096
670	Prolyl 4-hydroxylase subunit alpha-1	P4HA1_HUMAN	P4HA1	61 kDa	0.061
671	Ig gamma-4 chain C region	IGHG4_HUMAN	IGHG4	36 kDa	0.061
672	Importin-7	IPO7_HUMAN	IPO7	120 kDa	0.062
673	PDZ and LIM domain protein 1	PDLI1_HUMAN	PDLIM1	36 kDa	0.062
674	182 kDa tankyrase-1-binding protein	TB182_HUMAN	TNKS1BP1	182 kDa	0.062
675	Microfibrillar-associated protein 1	MFAP1_HUMAN	MFAP1	52 kDa	0.062
676	Calcium-regulated heat stable protein 1	CHSP1_HUMAN	CARHSP1	16 kDa	0.062
677	Exportin-2	XPO2_HUMAN	CSEIL	110 kDa	0.062
678	Sorbitol dehydrogenase	DHSO_HUMAN	SORD	38 kDa	0.063
679	Na(+)/H(+) exchange regulatory cofactor NHE-RF2	NHRF2_HUMAN	SLC9A3R2	37 kDa	0.063
680	Glycogen phosphorylase, liver form	PYGL_HUMAN	PYGL	97 kDa	0.064
681	Profilin-1	PROF1_HUMAN	PFN1	15 kDa	0.064
592	Hemoglobin subunit alpha	HBA_HUMAN	HBA1	15 kDa	0.041
683	Probable E3 ubiquitin-protein ligase HECTD4	HECD4_HUMAN	HECTD4	439 kDa	0.064
684	Protein CYR61	CYR61_HUMAN	CYR61	42 kDa	0.064
685	Cluster of Heterogeneous nuclear ribonucleoproteins C1/C2	HNRPC_HUMAN [3]	HNRNPC	34 kDa	0.065
686	Tetratricopeptide repeat protein 1	TTC1_HUMAN	TTC1	34 kDa	0.065
687	Nck-associated protein 1	NCKP1_HUMAN	NCKAP1	129 kDa	0.065
688	Purine nucleoside phosphorylase	PNPH_HUMAN	PNP	32 kDa	0.066
689	SH3 domain-binding protein 1	3BP1_HUMAN	SH3BP1	76 kDa	0.066
690	FRAS1-related extracellular matrix protein 2	FREM2_HUMAN	FREM2	351 kDa	0.066
691	Polypeptide N-acetylgalactosaminyltransferase 2	GALT2_HUMAN	GALNT2	65 kDa	0.067
692	Heat shock protein beta-1	HSPB1_HUMAN	HSPB1	23 kDa	0.067
693	Ras GTPase-activating protein-binding protein 1	G3BP1_HUMAN	G3BP1	52 kDa	0.067
694	Kinectin	KTN1_HUMAN	KTN1	156 kDa	0.067
695	FACT complex subunit SSRP1	SSRP1_HUMAN	SSRP1	81 kDa	0.068
696	Receptor expression-enhancing protein 6	REEP6_HUMAN	REEP6	21 kDa	0.069
697	Tropomodulin-3	TMOD3_HUMAN	TMOD3	40 kDa	0.069
698	Ubiquitin carboxyl-terminal hydrolase 5	UBP5_HUMAN	USP5	96 kDa	0.069
699	5'-nucleotidase	5NTD_HUMAN	NT5E	63 kDa	0.069
700	Inhibin beta B chain	INHBB_HUMAN	INHBB	45 kDa	0.069
701	Platelet-derived growth factor C	PDGFC_HUMAN	PDGFC	39 kDa	0.069
702	Deoxyuridine 5'-triphosphate nucleotidohydrolase, mitochondrial	DUT_HUMAN	DUT	27 kDa	0.07
703	Protein-methionine sulfoxide oxidase MICAL1	MICA1_HUMAN	MICAL1	118 kDa	0.071
704	Nucleobindin-2	NUCB2_HUMAN	NUCB2	50 kDa	0.071
705	Glycogen phosphorylase, brain form	PYGB_HUMAN	PYGB	97 kDa	0.072
706	Creatine kinase B-type	KCRB_HUMAN	CKB	43 kDa	0.072
707	Desmocollin-1	DSC1_HUMAN	DSC1	100 kDa	0.072
708	Eukaryotic translation initiation factor 3 subunit C	EIF3C_HUMAN	EIF3C	105 kDa	0.072
709	Phenylalanine--tRNA ligase beta subunit	SYFB_HUMAN	FARSB	66 kDa	0.073
710	Treacle protein	TCOF_HUMAN	TCOF1	152 kDa	0.073
711	Interferon-induced 35 kDa protein	IN35_HUMAN	IFI35	32 kDa	0.073
712	26S proteasome non-ATPase regulatory subunit 2	PSMD2_HUMAN	PSMD2	100 kDa	0.073

713	Prefoldin subunit 6	PFD6_HUMAN	PFDN6	15 kDa	0.074
1498	Cluster of Nucleoside diphosphate kinase B	NDKB_HUMAN [2]	NME2	17 kDa	0.91
715	Cluster of Serine/arginine-rich splicing factor 6	SRSF6_HUMAN [2]	SRSF6	40 kDa	0.074
716	Beta-2-microglobulin	B2MG_HUMAN	B2M	14 kDa	0.074
717	Microtubule-associated protein 1B	MAP1B_HUMAN	MAP1B	271 kDa	0.074
718	Pyridoxal-dependent decarboxylase domain-containing protein 1	PDXD1_HUMAN	PDXDC1	87 kDa	0.074
719	YLP motif-containing protein 1	YLPM1_HUMAN	YLPM1	220 kDa	0.074
720	Proteasome subunit alpha type-2	PSA2_HUMAN	PSMA2	26 kDa	0.075
721	Basement membrane-specific heparan sulfate proteoglycan core protein	PGBM_HUMAN	HSPG2	469 kDa	0.075
722	Profilin-2	PROF2_HUMAN	PFN2	15 kDa	0.075
519	Fibulin-1	FBLN1_HUMAN	FBLN1	77 kDa	0.024
724	Coagulation factor V	FA5_HUMAN	F5	252 kDa	0.076
725	Annexin A11	ANX11_HUMAN	ANXA11	54 kDa	0.076
726	Cluster of 14-3-3 protein theta	1433T_HUMAN [2]	YWHAQ	28 kDa	0.077
727	Thrombospondin-4	TSP4_HUMAN	THBS4	106 kDa	0.077
728	Dynactin subunit 1	DCTN1_HUMAN	DCTN1	142 kDa	0.077
729	Integrin alpha-V	ITAV_HUMAN	ITGAV	116 kDa	0.077
730	Small nuclear ribonucleoprotein Sm D2	SMD2_HUMAN	SNRPD2	14 kDa	0.078
731	Fetuin-B	FETUB_HUMAN	FETUB	42 kDa	0.078
732	UDP-glucose 4-epimerase	GALE_HUMAN	GALE	38 kDa	0.078
733	von Willebrand factor A domain-containing protein 1	VWA1_HUMAN	VWA1	47 kDa	0.079
734	Cluster of Glutamine--fructose-6-phosphate aminotransferase [isomerizing] 1	GFPT1_HUMAN [2]	GFPT1	79 kDa	0.079
735	Proteasome subunit alpha type-5	PSA5_HUMAN	PSMA5	26 kDa	0.079
736	Isocitrate dehydrogenase [NAD] subunit alpha, mitochondrial	IDH3A_HUMAN	IDH3A	40 kDa	0.08
737	Heterogeneous nuclear ribonucleoprotein A/B	ROAA_HUMAN	HNRNPAB	36 kDa	0.08
738	Calsyntenin-3	CSTN3_HUMAN	CLSTN3	106 kDa	0.08
739	Tissue factor pathway inhibitor 2	TFPI2_HUMAN	TFPI2	27 kDa	0.08
740	Retinol-binding protein 4	RET4_HUMAN	RBP4	23 kDa	0.08
1208	Cluster of Histone H1.3	H13_HUMAN [4]	HIST1H1D	22 kDa	0.38
742	Protein FAM3C	FAM3C_HUMAN	FAM3C	25 kDa	0.081
743	Aspartyl/asparaginyl beta-hydroxylase	ASPH_HUMAN	ASPH	86 kDa	0.081
541	Cluster of Endoplasmic	ENPL_HUMAN [2]	HSP90B1	92 kDa	0.029
745	Signal recognition particle 14 kDa protein	SRP14_HUMAN	SRP14	15 kDa	0.082
746	HIV Tat-specific factor 1	HTSF1_HUMAN	HTATSF1	86 kDa	0.082
593	Cluster of Histone H2A type 2-A	H2A2A_HUMAN [4]	HIST2H2AA3	14 kDa	0.043
598	Histone H4	H4_HUMAN	HIST1H4A	11 kDa	0.046
749	Tripeptidyl-peptidase 2	TPP2_HUMAN	TPP2	138 kDa	0.083
750	Receptor-type tyrosine-protein phosphatase C	PTPRC_HUMAN	PTPRC	147 kDa	0.083
751	Microtubule-actin cross-linking factor 1, isoforms 1/2/3/5	MACF1_HUMAN	MACF1	838 kDa	0.083
752	EH domain-containing protein 1	EHD1_HUMAN	EHD1	61 kDa	0.083
753	Nucleophosmin	NPM_HUMAN	NPM1	33 kDa	0.084
754	Actin-related protein 2/3 complex subunit 5	ARPC5_HUMAN	ARPC5	16 kDa	0.084
755	Syntaxin-binding protein 3	STXB3_HUMAN	STXBP3	68 kDa	0.084
756	Nuclear cap-binding protein subunit 1	NCBP1_HUMAN	NCBP1	92 kDa	0.084
757	DnaJ homolog subfamily C member 17	DJC17_HUMAN	DNAJC17	35 kDa	0.084

758	Eukaryotic translation initiation factor 2 subunit 2	IF2B_HUMAN	EIF2S2	38 kDa	0.084
759	Serine hydroxymethyltransferase, cytosolic	GLYC_HUMAN	SHMT1	53 kDa	0.084
760	Wiskott-Aldrich syndrome protein family member 2	WASF2_HUMAN	WASF2	54 kDa	0.084
761	AH receptor-interacting protein	AIP_HUMAN	AIP	38 kDa	0.084
762	Grancalcin	GRAN_HUMAN	GCA	24 kDa	0.084
763	YTH domain-containing protein 1	YTDC1_HUMAN	YTHDC1	85 kDa	0.084
764	ATP-dependent RNA helicase DDX42	DDX42_HUMAN	DDX42	103 kDa	0.085
765	Signal transducer and activator of transcription 3	STAT3_HUMAN	STAT3	88 kDa	0.085
942	Complement C3	CO3_HUMAN	C3	187 kDa	0.15
767	Annexin A4	ANXA4_HUMAN	ANXA4	36 kDa	0.085
768	26S proteasome non-ATPase regulatory subunit 11	PSD11_HUMAN	PSMD11	47 kDa	0.085
769	Filaggrin-2	FILA2_HUMAN	FLG2	248 kDa	0.086
770	Serine/threonine-protein kinase 10	STK10_HUMAN	STK10	112 kDa	0.087
771	U6 snRNA-associated Sm-like protein LSM6	LSM6_HUMAN	LSM6	9 kDa	0.088
772	Eukaryotic translation initiation factor 3 subunit J	EIF3J_HUMAN	EIF3J	29 kDa	0.089
773	Actin-like protein 6A	ACL6A_HUMAN	ACTL6A	47 kDa	0.089
774	Eukaryotic translation initiation factor 3 subunit I	EIF3I_HUMAN	EIF3I	37 kDa	0.089
775	Proteasome subunit alpha type-4	PSA4_HUMAN	PSMA4	29 kDa	0.089
523	Cluster of Heat shock 70 kDa protein 1A/1B	HSP71_HUMAN [3]	HSPA1A	70 kDa	0.024
777	60S ribosomal protein L13	RL13_HUMAN	RPL13	24 kDa	0.09
778	MARCKS-related protein	MRP_HUMAN	MARCKSL1	20 kDa	0.091
779	Exportin-1	XPO1_HUMAN	XPO1	123 kDa	0.092
780	Proteasome-associated protein ECM29 homolog	ECM29_HUMAN	ECM29	204 kDa	0.092
781	Splicing factor U2AF 35 kDa subunit	U2AF1_HUMAN	U2AF1	28 kDa	0.092
782	Delta-aminolevulinic acid dehydratase	HEM2_HUMAN	ALAD	36 kDa	0.093
783	Ferritin heavy chain	FRIH_HUMAN	FTH1	21 kDa	0.093
784	FK506-binding protein 15	FKB15_HUMAN	FKBP15	134 kDa	0.093
785	Proteasome subunit beta type-9	PSB9_HUMAN	PSMB9	23 kDa	0.093
786	40S ribosomal protein S14	RS14_HUMAN	RPS14	16 kDa	0.093
787	Dihydropyrimidinase-related protein 1	DPYL1_HUMAN	CRMP1	62 kDa	0.093
788	Tubulointerstitial nephritis antigen-like	TINAL_HUMAN	TINAGL1	52 kDa	0.094
789	Eukaryotic translation initiation factor 4 gamma 2	IF4G2_HUMAN	EIF4G2	102 kDa	0.094
790	Rab3 GTPase-activating protein non-catalytic subunit	RBGPR_HUMAN	RAB3GAP2	156 kDa	0.094
791	Vacuolar protein sorting-associated protein 26A	VP26A_HUMAN	VPS26A	38 kDa	0.094
792	Metastasis-associated protein MTA2	MTA2_HUMAN	MTA2	75 kDa	0.094
793	Very low-density lipoprotein receptor	VLDLR_HUMAN	VLDLR	96 kDa	0.095
794	Collagen alpha-1(XVIII) chain	COIA1_HUMAN	COL18A1	178 kDa	0.096
968	Elongation factor 1-gamma	EF1G_HUMAN	EEF1G	50 kDa	0.17
796	Brain acid soluble protein 1	BASP1_HUMAN	BASP1	23 kDa	0.097
797	Fibrinogen gamma chain	FIBG_HUMAN	FGG	52 kDa	0.097
744	Amyloid beta A4 protein	A4_HUMAN	APP	87 kDa	0.081
799	40S ribosomal protein S7	RS7_HUMAN	RPS7	22 kDa	0.098
800	Phosphatidylethanolamine-binding protein 1	PEBP1_HUMAN	PEBP1	21 kDa	0.099
801	Tumor susceptibility gene 101 protein	TS101_HUMAN	TSG101	44 kDa	0.099

802	AP-1 complex subunit gamma-1	APIG1_HUMAN	APIG1	91 kDa	0.099
803	Alpha-1-antitrypsin	A1AT_HUMAN	SERPINA1	47 kDa	0.099
804	Eukaryotic initiation factor 4A-III	IF4A3_HUMAN	EIF4A3	47 kDa	0.099
776	Ubiquitin-40S ribosomal protein S27a	RS27A_HUMAN	RPS27A	18 kDa	0.089
806	m7GpppX diphosphatase	DCPS_HUMAN	DCPS	39 kDa	0.1
807	Actin-related protein 2/3 complex subunit 1B	ARC1B_HUMAN	ARPC1B	41 kDa	0.1
808	Heterogeneous nuclear ribonucleoprotein U-like protein 2	HNRL2_HUMAN	HNRNPUL2	85 kDa	0.1
809	Nicotinamide phosphoribosyltransferase	NAMPT_HUMAN	NAMPT	56 kDa	0.1
810	Electron transfer flavoprotein subunit beta	ETFB_HUMAN	ETFB	28 kDa	0.1
811	Dynactin subunit 3	DCTN3_HUMAN	DCTN3	21 kDa	0.1
812	Protein enabled homolog	ENAH_HUMAN	ENAH	67 kDa	0.1
813	ATP-dependent RNA helicase DHX29	DHX29_HUMAN	DHX29	155 kDa	0.1
814	Serine protease 23	PRSS23_HUMAN	PRSS23	43 kDa	0.1
1126	Peroxiredoxin-1	PRDX1_HUMAN	PRDX1	22 kDa	0.27
816	40S ribosomal protein S27	RS27_HUMAN	RPS27	9 kDa	0.1
817	40S ribosomal protein S15	RS15_HUMAN	RPS15	17 kDa	0.1
818	Ribonuclease H2 subunit A	RNH2A_HUMAN	RNASEH2A	33 kDa	0.1
819	Histone acetyltransferase type B catalytic subunit	HAT1_HUMAN	HAT1	50 kDa	0.1
820	Protein-glutamine gamma-glutamyltransferase 2	TGM2_HUMAN	TGM2	77 kDa	0.11
1173	Cluster of Myosin-9	MYH9_HUMAN [4]	MYH9	227 kDa	0.32
822	CD81 antigen	CD81_HUMAN	CD81	26 kDa	0.11
823	45 kDa calcium-binding protein	CAB45_HUMAN	SDF4	42 kDa	0.11
824	U2 small nuclear ribonucleoprotein B''	RU2B_HUMAN	SNRNPB2	25 kDa	0.11
825	Aspartate-tRNA ligase, cytoplasmic	SYDC_HUMAN	DARS	57 kDa	0.11
826	Abl interactor 1	ABII_HUMAN	ABII	55 kDa	0.11
827	Cell division cycle and apoptosis regulator protein 1	CCAR1_HUMAN	CCAR1	133 kDa	0.11
828	Shootin-1	SHOT1_HUMAN	KIAA1598	72 kDa	0.11
829	Regulation of nuclear pre-mRNA domain-containing protein 1A	RPR1A_HUMAN	RPRD1A	36 kDa	0.11
830	Abl interactor 2	ABI2_HUMAN	ABI2	56 kDa	0.11
831	Biliverdin reductase A	BIEA_HUMAN	BLVRA	33 kDa	0.11
832	Cleavage stimulation factor subunit 3	CSTF3_HUMAN	CSTF3	83 kDa	0.11
833	U4/U6 small nuclear ribonucleoprotein Prp31	PRP31_HUMAN	PRPF31	55 kDa	0.11
834	Kelch domain-containing protein 4	KLDC4_HUMAN	KLHDC4	58 kDa	0.11
835	Sec1 family domain-containing protein 1	SCFD1_HUMAN	SCFD1	72 kDa	0.11
397	Fructose-bisphosphate aldolase C	ALDOC_HUMAN	ALDOC	39 kDa	0.0081
837	Calpain-1 catalytic subunit	CAN1_HUMAN	CAPN1	82 kDa	0.11
838	GMP synthase [glutamine-hydrolyzing]	GUAA_HUMAN	GMPS	77 kDa	0.11
839	60S ribosomal protein L30	RL30_HUMAN	RPL30	13 kDa	0.11
840	Aspartyl aminopeptidase	DNPEP_HUMAN	DNPEP	52 kDa	0.11
841	Endophilin-B1	SHLB1_HUMAN	SH3GLB1	41 kDa	0.11
842	Cullin-3	CUL3_HUMAN	CUL3	89 kDa	0.11
843	UDP-glucose 6-dehydrogenase	UGDH_HUMAN	UGDH	55 kDa	0.11
844	DAZ-associated protein 1	DAZP1_HUMAN	DAZAP1	43 kDa	0.11
845	Cluster of Eukaryotic initiation factor 4A-I	IF4A1_HUMAN [2]	EIF4A1	46 kDa	0.11
723	Cluster of HLA class I histocompatibility antigen, A-2 alpha chain	1A02_HUMAN [7]	HLA-A	41 kDa	0.075

847	Latent-transforming growth factor beta-binding protein 3	LTBP3_HUMAN	LTBP3	139 kDa	0.12
848	Protein disulfide-isomerase A6	PDIA6_HUMAN	PDIA6	48 kDa	0.12
849	Growth-regulated alpha protein	GROA_HUMAN	CXCL1	11 kDa	0.12
850	Septin-2	SEPT2_HUMAN	Sep-02	41 kDa	0.12
851	Protein RCC2	RCC2_HUMAN	RCC2	56 kDa	0.12
852	Nucleobindin-1	NUCB1_HUMAN	NUCB1	54 kDa	0.12
853	Protein SEC13 homolog	SEC13_HUMAN	SEC13	36 kDa	0.12
854	Clathrin light chain A	CLCA_HUMAN	CLTA	27 kDa	0.12
855	Large proline-rich protein BAG6	BAG6_HUMAN	BAG6	119 kDa	0.12
856	Ubiquitin fusion degradation protein 1 homolog	UFD1_HUMAN	UFD1L	35 kDa	0.12
857	Cluster of Coatamer subunit gamma-1	COPG1_HUMAN [2]	COPG1	98 kDa	0.12
858	Small nuclear ribonucleoprotein Sm D1	SMD1_HUMAN	SNRPD1	13 kDa	0.12
859	Cullin-1	CUL1_HUMAN	CUL1	90 kDa	0.12
860	Carboxypeptidase M	CBPM_HUMAN	CPM	51 kDa	0.12
861	Spliceosome RNA helicase DDX39B	DX39B_HUMAN	DDX39B	49 kDa	0.12
862	Inter-alpha-trypsin inhibitor heavy chain H4	ITIH4_HUMAN	ITIH4	103 kDa	0.12
863	Rho-related GTP-binding protein RhoG	RHOG_HUMAN	RHOG	21 kDa	0.12
864	Protein tweety homolog 3	TTYH3_HUMAN	TTYH3	58 kDa	0.12
865	Amyloid beta A4 precursor protein-binding family B member 1-interacting protein	AB1IP_HUMAN	APBB1IP	73 kDa	0.12
866	Coronin-7	CORO7_HUMAN	CORO7	101 kDa	0.12
867	Alpha-galactosidase A	AGAL_HUMAN	GLA	49 kDa	0.12
868	Complement C1q tumor necrosis factor-related protein 3	C1QT3_HUMAN	C1QTNF3	27 kDa	0.12
869	V-type proton ATPase subunit H	VATH_HUMAN	ATP6V1H	56 kDa	0.12
870	Ectonucleotide pyrophosphatase/phosphodiesterase family member 2	ENPP2_HUMAN	ENPP2	99 kDa	0.12
871	Cysteine and glycine-rich protein 1	CSRP1_HUMAN	CSRP1	21 kDa	0.12
872	Apolipoprotein A-I	APOA1_HUMAN	APOA1	31 kDa	0.12
873	Platelet-activating factor acetylhydrolase IB subunit gamma	PAIB3_HUMAN	PAFAH1B3	26 kDa	0.12
874	Regulator of chromosome condensation	RCC1_HUMAN	RCC1	45 kDa	0.12
875	U1 small nuclear ribonucleoprotein A	SNRPA_HUMAN	SNRPA	31 kDa	0.12
876	60S ribosomal protein L18a	RL18A_HUMAN	RPL18A	21 kDa	0.12
877	Follistatin	FST_HUMAN	FST	38 kDa	0.12
186	Alpha-2-HS-glycoprotein	FETUA_HUMAN	AHSG	39 kDa	0.00085
879	Peptidyl-prolyl cis-trans isomerase FKBP5	FKBP5_HUMAN	FKBP5	51 kDa	0.12
880	Serpin H1	SERPH_HUMAN	SERPINH1	46 kDa	0.12
881	AP-1 complex subunit mu-2	AP1M2_HUMAN	AP1M2	48 kDa	0.12
882	Prefoldin subunit 4	PFD4_HUMAN	PFDN4	15 kDa	0.12
544	Cluster of Phosphoglycerate kinase 1	PGK1_HUMAN [2]	PGK1	45 kDa	0.03
884	Switch-associated protein 70	SWP70_HUMAN	SWAP70	69 kDa	0.13
885	26S proteasome non-ATPase regulatory subunit 14	PSDE_HUMAN	PSMD14	35 kDa	0.13
886	DnaJ homolog subfamily B member 11	DJB11_HUMAN	DNAJB11	41 kDa	0.13
887	Dermcidin	DCD_HUMAN	DCD	11 kDa	0.13
888	Interleukin-6 receptor subunit alpha	IL6RA_HUMAN	IL6R	52 kDa	0.13
889	Proteasome subunit beta type-10	PSB10_HUMAN	PSMB10	29 kDa	0.13
890	Histone deacetylase 2	HDAC2_HUMAN	HDAC2	55 kDa	0.13
891	60S ribosomal protein L12	RL12_HUMAN	RPL12	18 kDa	0.13

892	Lactoylglutathione lyase	LGUL_HUMAN	GLO1	21 kDa	0.13
893	1-phosphatidylinositol 4,5-bisphosphate phosphodiesterase gamma-2	PLCG2_HUMAN	PLCG2	148 kDa	0.13
894	Leucine-rich repeat flightless-interacting protein 1	LRRF1_HUMAN	LRRFIP1	89 kDa	0.13
895	60S ribosomal protein L3	RL3_HUMAN	RPL3	46 kDa	0.13
896	Proteasome subunit beta type-3	PSB3_HUMAN	PSMB3	23 kDa	0.13
897	CD9 antigen	CD9_HUMAN	CD9	25 kDa	0.13
898	Alcohol dehydrogenase [NADP(+)]	AK1A1_HUMAN	AKR1A1	37 kDa	0.13
899	Protein S100-A14	S10AE_HUMAN	S100A14	12 kDa	0.13
900	Alpha-crystallin B chain	CRYAB_HUMAN	CRYAB	20 kDa	0.13
901	Collagenase 3	MMP13_HUMAN	MMP13	54 kDa	0.13
578	Cluster of Histone H2B type 1-D	H2B1D_HUMAN [2]	HIST1H2BD	14 kDa	0.038
903	26S proteasome non-ATPase regulatory subunit 7	PSMD7_HUMAN	PSMD7	37 kDa	0.13
904	60S ribosomal protein L15	RL15_HUMAN	RPL15	24 kDa	0.13
905	Splicing factor 3B subunit 3	SF3B3_HUMAN	SF3B3	136 kDa	0.13
906	PRKC apoptosis WT1 regulator protein	PAWR_HUMAN	PAWR	37 kDa	0.13
907	60S ribosomal protein L6	RL6_HUMAN	RPL6	33 kDa	0.13
908	Acidic leucine-rich nuclear phosphoprotein 32 family member E	AN32E_HUMAN	ANP32E	31 kDa	0.13
909	Cluster of Ras-related protein Rab-14	RAB14_HUMAN [12]	RAB14	24 kDa	0.13
910	Phenylalanine--tRNA ligase alpha subunit	SYFA_HUMAN	FARSA	58 kDa	0.13
911	Protein FAM49B	FA49B_HUMAN	FAM49B	37 kDa	0.13
912	La-related protein 1	LARP1_HUMAN	LARP1	124 kDa	0.14
913	SAP domain-containing ribonucleoprotein	SARNP_HUMAN	SARNP	24 kDa	0.14
914	Neutral amino acid transporter B(0)	AAAT_HUMAN	SLC1A5	57 kDa	0.14
915	Glutamate dehydrogenase 1, mitochondrial	DHE3_HUMAN	GLUD1	61 kDa	0.14
916	Microtubule-associated protein 4	MAP4_HUMAN	MAP4	121 kDa	0.14
917	PC4 and SFRS1-interacting protein	PSIP1_HUMAN	PSIP1	60 kDa	0.14
918	Latent-transforming growth factor beta-binding protein 1	LTBP1_HUMAN	LTBP1	187 kDa	0.14
919	Cytoplasmic dynein 1 light intermediate chain 2	DCIL2_HUMAN	DYNCIL2	54 kDa	0.14
920	26S proteasome non-ATPase regulatory subunit 10	PSD10_HUMAN	PSMD10	24 kDa	0.14
921	Zinc finger CCCH domain-containing protein 4	ZC3H4_HUMAN	ZC3H4	140 kDa	0.14
922	SWI/SNF complex subunit SMARCC2	SMRC2_HUMAN	SMARCC2	133 kDa	0.14
923	Proteasome subunit alpha type-3	PSA3_HUMAN	PSMA3	28 kDa	0.14
924	Threonine--tRNA ligase, cytoplasmic	SYTC_HUMAN	TARS	83 kDa	0.14
925	Cleavage and polyadenylation specificity factor subunit 1	CPSF1_HUMAN	CPSF1	161 kDa	0.14
926	DnaJ homolog subfamily A member 1	DNJA1_HUMAN	DNAJA1	45 kDa	0.14
927	Tumor protein D52	TPD52_HUMAN	TPD52	24 kDa	0.14
928	Coronin-1C	COR1C_HUMAN	CORO1C	53 kDa	0.14
929	Syndecan-2	SDC2_HUMAN	SDC2	22 kDa	0.15
930	Cluster of Cytoplasmic FMRI-interacting protein 1	CYFP1_HUMAN [2]	CYFIP1	145 kDa	0.15
931	SNW domain-containing protein 1	SNW1_HUMAN	SNW1	61 kDa	0.15
932	Septin-8	SEPT8_HUMAN	Sep-08	56 kDa	0.15
933	40S ribosomal protein S13	RS13_HUMAN	RPS13	17 kDa	0.15
934	Charged multivesicular body protein 2b	CHM2B_HUMAN	CHMP2B	24 kDa	0.15
935	Cluster of Transcription elongation factor A protein 1	TCEA1_HUMAN [2]	TCEA1	34 kDa	0.15
936	AP-2 complex subunit alpha-1	AP2A1_HUMAN	AP2A1	108 kDa	0.15

363	Inter-alpha-trypsin inhibitor heavy chain H2	ITIH2_HUMAN	ITIH2	106 kDa	0.0063
938	Aldehyde dehydrogenase family 16 member A1	A16A1_HUMAN	ALDH16A1	85 kDa	0.15
939	Isocitrate dehydrogenase [NADP], mitochondrial	IDHP_HUMAN	IDH2	51 kDa	0.15
940	Glutathione S-transferase P	GSTP1_HUMAN	GSTP1	23 kDa	0.15
941	Cluster of Polypyrimidine tract-binding protein 1	PTBP1_HUMAN [2]	PTBP1	57 kDa	0.15
1405	Transketolase	TKT_HUMAN	TKT	68 kDa	0.56
943	COP9 signalosome complex subunit 3	CSN3_HUMAN	COPS3	48 kDa	0.15
944	B-cell receptor-associated protein 31	BAP31_HUMAN	BCAP31	28 kDa	0.16
945	Ras-related protein Rab-11B	RB11B_HUMAN	RAB11B	24 kDa	0.16
946	UMP-CMP kinase	KCY_HUMAN	CMPK1	22 kDa	0.16
115	Vinculin	VINC_HUMAN	VCL	124 kDa	0.00021
948	EGF-like repeat and discoidin I-like domain-containing protein 3	EDIL3_HUMAN	EDIL3	54 kDa	0.16
1453	Peptidyl-prolyl cis-trans isomerase A	PPIA_HUMAN	PPIA	18 kDa	0.62
950	Signal recognition particle 19 kDa protein	SRP19_HUMAN	SRP19	16 kDa	0.16
951	Mesencephalic astrocyte-derived neurotrophic factor	MANF_HUMAN	MANF	21 kDa	0.16
952	STE20-like serine/threonine-protein kinase	SLK_HUMAN	SLK	143 kDa	0.16
953	Phosphatidylinositol 3,4,5-trisphosphate-dependent Rac exchanger 1 protein	PREX1_HUMAN	PREX1	186 kDa	0.16
954	Ig lambda-2 chain C regions	LAC2_HUMAN (+1)	IGLC2	11 kDa	0.16
955	Plasma kallikrein	KLKB1_HUMAN	KLKB1	71 kDa	0.16
956	Exportin-7	XPO7_HUMAN	XPO7	124 kDa	0.16
957	Leucine-rich repeat-containing protein 47	LRC47_HUMAN	LRRRC47	63 kDa	0.16
958	Ubiquilin-2	UBQL2_HUMAN	UBQLN2	66 kDa	0.16
959	Syntaxin-4	STX4_HUMAN	STX4	34 kDa	0.16
986	Hornerin	HORN_HUMAN	HRNR	282 kDa	0.18
961	Cluster of Retinal dehydrogenase 2	AL1A2_HUMAN [2]	ALDH1A2	57 kDa	0.16
962	Replication protein A 70 kDa DNA-binding subunit	RFA1_HUMAN	RPA1	68 kDa	0.16
963	Tyrosine-protein kinase CSK	CSK_HUMAN	CSK	51 kDa	0.16
964	Signal recognition particle subunit SRP68	SRP68_HUMAN	SRP68	71 kDa	0.16
965	60S ribosomal protein L17	RL17_HUMAN	RPL17	21 kDa	0.17
966	Phosphoribosyl pyrophosphate synthase-associated protein 1	KPRA_HUMAN	PRPSAP1	39 kDa	0.17
967	Low-density lipoprotein receptor	LDLR_HUMAN	LDLR	95 kDa	0.17
1489	60 kDa heat shock protein, mitochondrial	CH60_HUMAN	HSPD1	61 kDa	0.82
969	Fibrinogen beta chain	FIBB_HUMAN	FGB	56 kDa	0.17
970	Probable aminopeptidase NPEPL1	PEPL1_HUMAN	NPEPL1	56 kDa	0.17
971	Insulin-like growth factor-binding protein 2	IBP2_HUMAN	IGFBP2	35 kDa	0.17
972	Heterogeneous nuclear ribonucleoprotein D0	HNRPD_HUMAN	HNRNPD	38 kDa	0.17
973	Monocarboxylate transporter 4	MOT4_HUMAN	SLC16A3	49 kDa	0.17
974	Cytoplasmic aconitate hydratase	ACOC_HUMAN	ACO1	98 kDa	0.17
975	DNA repair protein complementing XP-C cells	XPC_HUMAN	XPC	106 kDa	0.17
976	Apoptotic chromatin condensation inducer in the nucleus	ACINU_HUMAN	ACIN1	152 kDa	0.17
977	40S ribosomal protein S19	RS19_HUMAN	RPS19	16 kDa	0.17
978	Early endosome antigen 1	EEA1_HUMAN	EEA1	162 kDa	0.17
979	NHP2-like protein 1	NHP2L1_HUMAN	NHP2L1	14 kDa	0.17
980	Eukaryotic translation initiation factor 5B	IF2P_HUMAN	EIF5B	139 kDa	0.17
981	60S ribosomal protein L11	RL11_HUMAN	RPL11	20 kDa	0.17

982	Ubiquitin-conjugating enzyme E2 O	UBE2O_HUMAN	UBE2O	141 kDa	0.17
983	Actin-related protein 2/3 complex subunit 2	ARPC2_HUMAN	ARPC2	34 kDa	0.17
1472	Cluster of Tubulin alpha-4A chain	TBA4A_HUMAN [4]	TUBA4A	50 kDa	0.73
985	60S ribosomal protein L28	RL28_HUMAN	RPL28	16 kDa	0.18
937	Glyceraldehyde-3-phosphate dehydrogenase	G3P_HUMAN	GAPDH	36 kDa	0.15
987	Procollagen-lysine,2-oxoglutarate 5-dioxygenase 1	PLOD1_HUMAN	PLOD1	84 kDa	0.18
988	Apolipoprotein B-100	APOB_HUMAN	APOB	516 kDa	0.18
989	Beta-1,4-galactosyltransferase 4	B4GT4_HUMAN	B4GALT4	40 kDa	0.18
990	Stanniocalcin-1	STC1_HUMAN	STC1	28 kDa	0.18
991	Ornithine aminotransferase, mitochondrial	OAT_HUMAN	OAT	49 kDa	0.18
992	Delta(3,5)-Delta(2,4)-dienoyl-CoA isomerase, mitochondrial	ECH1_HUMAN	ECH1	36 kDa	0.18
993	Collagen alpha-1(XII) chain	COCA1_HUMAN	COL12A1	333 kDa	0.18
994	Complement decay-accelerating factor	DAF_HUMAN	CD55	41 kDa	0.18
995	Transmembrane protein 43	TMM43_HUMAN	TMEM43	45 kDa	0.18
996	Nuclear pore complex protein Nup88	NUP88_HUMAN	NUP88	84 kDa	0.18
997	Basigin	BASI_HUMAN	BSG	42 kDa	0.18
998	CD44 antigen	CD44_HUMAN	CD44	82 kDa	0.19
999	BRC1A1-A complex subunit BRE	BRE_HUMAN	BRE	44 kDa	0.19
1000	Sodium/potassium-transporting ATPase subunit beta-1	AT1B1_HUMAN	ATP1B1	35 kDa	0.19
1001	Bone morphogenetic protein 1	BMP1_HUMAN	BMP1	111 kDa	0.19
1002	Translin	TSN_HUMAN	TSN	26 kDa	0.19
1003	mRNA turnover protein 4 homolog	MRT4_HUMAN	MRTO4	28 kDa	0.19
1004	Phosphatidylinositol-binding clathrin assembly protein	PICAL_HUMAN	PICALM	71 kDa	0.19
1045	Cluster of Elongation factor 1-alpha 1	EF1A1_HUMAN [2]	EEF1A1	50 kDa	0.21
1006	Platelet-activating factor acetylhydrolase IB subunit alpha	LIS1_HUMAN	PAFAH1B1	47 kDa	0.19
1007	Transaldolase	TALDO_HUMAN	TALDO1	38 kDa	0.19
1008	Collagen alpha-2(I) chain	CO1A2_HUMAN	COL1A2	129 kDa	0.19
603	Calsyntenin-1	CSTN1_HUMAN	CLSTN1	110 kDa	0.048
1010	Peptidyl-prolyl cis-trans isomerase FKBP3	FKBP3_HUMAN	FKBP3	25 kDa	0.19
1419	Cluster of Pyruvate kinase PKM	KPYM_HUMAN [2]	PKM	58 kDa	0.57
1012	GTP-binding nuclear protein Ran	RAN_HUMAN	RAN	24 kDa	0.19
1013	Galectin-3	LEG3_HUMAN	LGALS3	26 kDa	0.19
1110	Elongation factor 2	EF2_HUMAN	EEF2	95 kDa	0.26
1015	Gamma-glutamyl hydrolase	GGH_HUMAN	GGH	36 kDa	0.19
1016	GTPase NRas	RASN_HUMAN	NRAS	21 kDa	0.19
1017	60S ribosomal protein L5	RL5_HUMAN	RPL5	34 kDa	0.19
836	Transitional endoplasmic reticulum ATPase	TERA_HUMAN	VCP	89 kDa	0.11
1019	Rho GDP-dissociation inhibitor 2	GDIR2_HUMAN	ARHGDIB	23 kDa	0.2
1020	YTH domain-containing family protein 3	YTH3_HUMAN	YTHDF3	64 kDa	0.2
1021	Junctional adhesion molecule A	JAM1_HUMAN	F11R	33 kDa	0.2
1022	Cysteine--tRNA ligase, cytoplasmic	SYCC_HUMAN	CARS	85 kDa	0.2
1023	Prominin-2	PROM2_HUMAN	PROM2	92 kDa	0.2
1024	Transmembrane protein 132A	T132A_HUMAN	TMEM132A	110 kDa	0.2
1025	Dickkopf-related protein 1	DKK1_HUMAN	DKK1	29 kDa	0.2
1026	Coatomer subunit beta	COPB_HUMAN	COPB1	107 kDa	0.2

1027	Epididymal secretory protein E1	NPC2_HUMAN	NPC2	17 kDa	0.2
1028	Nucleoporin p54	NUP54_HUMAN	NUP54	55 kDa	0.2
1029	Cluster of ADP-ribosylation factor 3	ARF3_HUMAN [2]	ARF3	21 kDa	0.2
1030	40S ribosomal protein S3a	RS3A_HUMAN	RPS3A	30 kDa	0.2
1031	Myristoylated alanine-rich C-kinase substrate	MARCS_HUMAN	MARCKS	32 kDa	0.2
1032	Pancreatic alpha-amylase	AMYP_HUMAN	AMY2A	58 kDa	0.2
1033	Lysosomal protective protein	PPGB_HUMAN	CTSA	54 kDa	0.2
1034	Metastasis-associated protein MTA1	MTA1_HUMAN	MTA1	81 kDa	0.2
1035	40S ribosomal protein S4, X isoform	RS4X_HUMAN	RPS4X	30 kDa	0.2
1036	Inorganic pyrophosphatase	IPYR_HUMAN	PPA1	33 kDa	0.2
1037	Disintegrin and metalloproteinase domain-containing protein 10	ADA10_HUMAN	ADAM10	84 kDa	0.2
1038	E3 UFM1-protein ligase 1	UFL1_HUMAN	UFL1	90 kDa	0.21
1039	Eukaryotic translation initiation factor 3 subunit M	EIF3M_HUMAN	EIF3M	43 kDa	0.21
1040	SWI/SNF-related matrix-associated actin-dependent regulator of chromatin subfamily E member 1	SMCE1_HUMAN	SMARCE1	47 kDa	0.21
1041	Annexin A6	ANXA6_HUMAN	ANXA6	76 kDa	0.21
1042	Valine--tRNA ligase	SYVC_HUMAN	VARS	140 kDa	0.21
1043	Neurofibromin	NF1_HUMAN	NF1	319 kDa	0.21
1044	Epidermal growth factor receptor kinase substrate 8-like protein 2	ESSL2_HUMAN	EPS8L2	81 kDa	0.21
714	Peptidyl-prolyl cis-trans isomerase B	PPIB_HUMAN	PPIB	24 kDa	0.074
1046	60S ribosomal protein L7	RL7_HUMAN	RPL7	29 kDa	0.21
1047	Serine/arginine-rich splicing factor 1	SRSF1_HUMAN	SRSF1	28 kDa	0.21
1048	Protein scribble homolog	SCRIB_HUMAN	SCRIB	175 kDa	0.21
471	78 kDa glucose-regulated protein	GRP78_HUMAN	HSPA5	72 kDa	0.016
1050	DNA repair protein XRCC1	XRCC1_HUMAN	XRCC1	69 kDa	0.22
1051	Cluster of E3 ubiquitin-protein ligase CBL	CBL_HUMAN [2]	CBL	100 kDa	0.22
1052	Fibulin-2	FBLN2_HUMAN	FBLN2	127 kDa	0.22
1053	Calpain small subunit 1	CPNS1_HUMAN	CAPNS1	28 kDa	0.22
1054	Small nuclear ribonucleoprotein-associated proteins B and B'	RSMB_HUMAN (+1)	SNRPB	25 kDa	0.22
1055	Peroxiredoxin-6	PRDX6_HUMAN	PRDX6	25 kDa	0.22
1056	Basal cell adhesion molecule	BCAM_HUMAN	BCAM	67 kDa	0.22
1057	Thioredoxin domain-containing protein 5	TXND5_HUMAN	TXNDC5	48 kDa	0.22
1058	Collagen alpha-1(I) chain	CO1A1_HUMAN	COL1A1	139 kDa	0.22
1059	N-acetylserotonin O-methyltransferase-like protein	ASML_HUMAN	ASMTL	69 kDa	0.22
1060	Nucleoprotein TPR	TPR_HUMAN	TPR	267 kDa	0.22
111	Cluster of Tropomyosin alpha-4 chain	TPM4_HUMAN [5]	TPM4	29 kDa	0.0002
1062	26S protease regulatory subunit 8	PRS8_HUMAN	PSMC5	46 kDa	0.22
1063	Complement C5	CO5_HUMAN	C5	188 kDa	0.22
1064	E3 ubiquitin-protein ligase UBR4	UBR4_HUMAN	UBR4	574 kDa	0.22
1065	N-acylneuraminate cytidyltransferase	NEUA_HUMAN	CMAS	48 kDa	0.22
1066	Serine hydroxymethyltransferase, mitochondrial	GLYM_HUMAN	SHMT2	56 kDa	0.22
1067	N-alpha-acetyltransferase 10	NAA10_HUMAN	NAA10	26 kDa	0.22
1068	Ubiquilin-1	UBQL1_HUMAN	UBQLN1	63 kDa	0.22
1069	Exocyst complex component 4	EXOC4_HUMAN	EXOC4	111 kDa	0.23
1070	Alpha-taxilin	TXLNA_HUMAN	TXLNA	62 kDa	0.23
1071	C-Jun-amino-terminal kinase-interacting protein 4	JIP4_HUMAN	SPAG9	146 kDa	0.23

1072	40S ribosomal protein S18	RS18_HUMAN	RPS18	18 kDa	0.23
1005	Protein disulfide-isomerase A3	PDIA3_HUMAN	PDIA3	57 kDa	0.19
1074	40S ribosomal protein S9	RS9_HUMAN	RPS9	23 kDa	0.23
1075	D-tyrosyl-tRNA(Tyr) deacylase 1	DTD1_HUMAN	DTD1	23 kDa	0.23
1076	Alcohol dehydrogenase class-3	ADHX_HUMAN	ADH5	40 kDa	0.23
1077	Complement component C8 beta chain	CO8B_HUMAN	C8B	67 kDa	0.23
1078	Nucleolin	NUCL_HUMAN	NCL	77 kDa	0.23
1079	UTP--glucose-1-phosphate uridylyltransferase	UGPA_HUMAN	UGP2	57 kDa	0.23
1080	Neuroblast differentiation-associated protein AHNAK	AHNAK_HUMAN	AHNAK	629 kDa	0.24
1081	Coactosin-like protein	COTL1_HUMAN	COTL1	16 kDa	0.24
1082	Cysteine-rich protein 2	CRIP2_HUMAN	CRIP2	22 kDa	0.24
1083	Protein phosphatase 1 regulatory subunit 12A	MYPT1_HUMAN	PPP1R12A	115 kDa	0.24
1084	Protein LYRIC	LYRIC_HUMAN	MTDH	64 kDa	0.24
1085	Protein phosphatase methylesterase 1	PPME1_HUMAN	PPME1	42 kDa	0.24
1086	Calpain-2 catalytic subunit	CAN2_HUMAN	CAPN2	80 kDa	0.24
1087	14-3-3 protein sigma	1433S_HUMAN	SFN	28 kDa	0.24
1088	Minor histocompatibility protein HA-1	HMHA1_HUMAN	HMHA1	125 kDa	0.24
1089	Putative 40S ribosomal protein S26-like 1	RS26L_HUMAN (+1)	RPS26P11	13 kDa	0.24
1090	Glutathione S-transferase omega-1	GSTO1_HUMAN	GSTO1	28 kDa	0.24
1091	60S ribosomal protein L23a	RL23A_HUMAN	RPL23A	18 kDa	0.24
1092	Vitamin D-binding protein	VTDB_HUMAN	GC	53 kDa	0.24
1093	Peptide-N(4)-(N-acetyl-beta-glucosaminyl)asparagine amidase	NGLY1_HUMAN	NGLY1	74 kDa	0.24
1094	Fibrillin-2	FBN2_HUMAN	FBN2	315 kDa	0.24
1095	Destrin	DEST_HUMAN	DSTN	19 kDa	0.24
1096	Tyrosine-protein kinase receptor UFO	UFO_HUMAN	AXL	98 kDa	0.24
1097	Exostosin-1	EXT1_HUMAN	EXT1	86 kDa	0.25
1098	Nicotinate phosphoribosyltransferase	PNCB_HUMAN	NAPRT1	58 kDa	0.25
1099	Dynamin-1-like protein	DNM1L_HUMAN	DNM1L	82 kDa	0.25
1100	60S ribosomal protein L4	RL4_HUMAN	RPL4	48 kDa	0.25
1101	Cluster of Core histone macro-H2A.1	H2AY_HUMAN [2]	H2AFY	40 kDa	0.25
1102	Prefoldin subunit 3	PFD3_HUMAN	VBP1	23 kDa	0.25
1103	Cluster of S-adenosylmethionine synthase isoform type-2	METK2_HUMAN [2]	MAT2A	44 kDa	0.25
1104	COP9 signalosome complex subunit 6	CSN6_HUMAN	COPS6	36 kDa	0.25
1105	Pre-mRNA-processing factor 19	PRP19_HUMAN	PRPF19	55 kDa	0.25
682	Alpha-enolase	ENOA_HUMAN	ENO1	47 kDa	0.064
1107	S-formylglutathione hydrolase	ESTD_HUMAN	ESD	31 kDa	0.25
815	Annexin A5	ANXA5_HUMAN	ANXA5	36 kDa	0.1
1109	Cytosolic non-specific dipeptidase	CNDP2_HUMAN	CNDP2	53 kDa	0.26
454	Cluster of Tubulin beta chain	TBB5_HUMAN [9]	TUBB	50 kDa	0.014
1111	Inactive tyrosine-protein kinase 7	PTK7_HUMAN	PTK7	118 kDa	0.26
1112	26S proteasome non-ATPase regulatory subunit 12	PSD12_HUMAN	PSMD12	53 kDa	0.26
1113	Serine/threonine-protein phosphatase 5	PPP5_HUMAN	PPP5C	57 kDa	0.26
1114	Oxysterol-binding protein 1	OSBP1_HUMAN	OSBP	89 kDa	0.26
1115	Cluster of Poly(rC)-binding protein 1	PCBP1_HUMAN [3]	PCBP1	37 kDa	0.26
1116	WD repeat-containing protein 1	WDR1_HUMAN	WDR1	66 kDa	0.26

1117	Lysyl oxidase homolog 2	LOXL2_HUMAN	LOXL2	87 kDa	0.26
1118	Negative elongation factor E	NELFE_HUMAN	NELFE	43 kDa	0.26
1119	Epidermal growth factor receptor kinase substrate 8	EPS8_HUMAN	EPS8	92 kDa	0.26
1120	Coatomer subunit epsilon	COPE_HUMAN	COPE	34 kDa	0.26
1121	Protein S100-A10	S100A_HUMAN	S100A10	11 kDa	0.26
1122	L-xylulose reductase	DCXR_HUMAN	DCXR	26 kDa	0.27
1123	Protein transport protein Sec24C	SC24C_HUMAN	SEC24C	118 kDa	0.27
1124	Cluster of BTB/POZ domain-containing protein KCTD12	KCD12_HUMAN [2]	KCTD12	36 kDa	0.27
1125	Vitamin K-dependent protein S	PROS_HUMAN	PROS1	75 kDa	0.27
242	Cluster of Ezrin	EZRI_HUMAN [3]	EZR	69 kDa	0.0016
1127	Small proline-rich protein 2A	SPR2A_HUMAN (+4)	SPRR2A	8 kDa	0.27
1128	Dickkopf-related protein 2	DKK2_HUMAN	DKK2	28 kDa	0.27
1129	ERO1-like protein alpha	ERO1A_HUMAN	ERO1L	54 kDa	0.27
1130	40S ribosomal protein S6	RS6_HUMAN	RPS6	29 kDa	0.28
1131	Glutathione reductase, mitochondrial	GSHR_HUMAN	GSR	56 kDa	0.28
1132	Titin	TITIN_HUMAN	TTN	3816 kDa	0.28
1133	Tyrosine-protein phosphatase non-receptor type 11	PTN11_HUMAN	PTPN11	68 kDa	0.28
1134	General transcription factor II-I	GTF2I_HUMAN	GTF2I	112 kDa	0.28
1135	Actin-related protein 2/3 complex subunit 5-like protein	ARP5L_HUMAN	ARPC5L	17 kDa	0.28
1136	26S proteasome non-ATPase regulatory subunit 13	PSD13_HUMAN	PSMD13	43 kDa	0.28
1137	Voltage-dependent anion-selective channel protein 1	VDAC1_HUMAN	VDAC1	31 kDa	0.28
1009	Cluster of Heat shock cognate 71 kDa protein	HSP7C_HUMAN [2]	HSPA8	71 kDa	0.19
1139	40S ribosomal protein S17-like	RS17L_HUMAN (+1)	RPS17L	16 kDa	0.28
1140	Histone H1.0	H10_HUMAN	H1F0	21 kDa	0.29
1141	116 kDa U5 small nuclear ribonucleoprotein component	U5S1_HUMAN	EFTUD2	109 kDa	0.29
1142	Cystatin-C	CYTC_HUMAN	CST3	16 kDa	0.29
1143	Activator of 90 kDa heat shock protein ATPase homolog 1	AHSA1_HUMAN	AHSA1	38 kDa	0.29
1144	Clathrin interactor 1	EPN4_HUMAN	CLINT1	68 kDa	0.29
1145	Tight junction protein ZO-3	ZO3_HUMAN	TJP3	101 kDa	0.3
1146	Epithelial cell adhesion molecule	EPCAM_HUMAN	EPCAM	35 kDa	0.3
1147	Serine/arginine-rich splicing factor 7	SRSF7_HUMAN	SRSF7	27 kDa	0.3
1148	Ubiquitin carboxyl-terminal hydrolase 7	UBP7_HUMAN	USP7	128 kDa	0.3
1149	COP9 signalosome complex subunit 4	CSN4_HUMAN	COPS4	46 kDa	0.3
1150	60S acidic ribosomal protein P2	RLA2_HUMAN	RPLP2	12 kDa	0.3
1151	40S ribosomal protein S12	RS12_HUMAN	RPS12	15 kDa	0.3
1152	Apolipoprotein C-III	APOC3_HUMAN	APOC3	11 kDa	0.3
1153	Tissue-type plasminogen activator	TPA_HUMAN	PLAT	63 kDa	0.3
1154	Eukaryotic translation initiation factor 3 subunit G	EIF3G_HUMAN	EIF3G	36 kDa	0.3
1155	Cluster of Transgelin-2	TAGL2_HUMAN [2]	TAGLN2	22 kDa	0.3
1156	Calponin-1	CNN1_HUMAN	CNN1	33 kDa	0.31
1157	Serine/threonine-protein phosphatase 2A catalytic subunit beta isoform	PP2AB_HUMAN	PPP2CB	36 kDa	0.31
1158	Cluster of Importin subunit alpha-3	IMA3_HUMAN [2]	KPNA4	58 kDa	0.31
1159	Acetyl-CoA acetyltransferase, cytosolic	THIC_HUMAN	ACAT2	41 kDa	0.31
1160	Host cell factor 1	HCFC1_HUMAN	HCFC1	209 kDa	0.31
1161	HLA class I histocompatibility antigen, B-7 alpha chain	1B07_HUMAN	HLA-B	40 kDa	0.31

1162	Complement component C9	CO9_HUMAN	C9	63 kDa	0.31
1163	AP-3 complex subunit beta-1	AP3B1_HUMAN	AP3B1	121 kDa	0.31
431	Sulfhydryl oxidase 1	QSOX1_HUMAN	QSOX1	83 kDa	0.013
1165	Transforming protein RhoA	RHOA_HUMAN	RHOA	22 kDa	0.32
1166	Phospholipase D3	PLD3_HUMAN	PLD3	55 kDa	0.32
1167	Dehydrogenase/reductase SDR family member 2, mitochondrial	DHRS2_HUMAN	DHRS2	30 kDa	0.32
1168	Caldesmon	CALD1_HUMAN	CALD1	93 kDa	0.32
1169	Dystonin	DYST_HUMAN	DST	861 kDa	0.32
1170	26S proteasome non-ATPase regulatory subunit 1	PSMD1_HUMAN	PSMD1	106 kDa	0.32
748	Fructose-bisphosphate aldolase A	ALDOA_HUMAN	ALDOA	39 kDa	0.082
1172	SUMO-activating enzyme subunit 1	SAE1_HUMAN	SAE1	38 kDa	0.32
618	Prelamin-A/C	LMNA_HUMAN	LMNA	74 kDa	0.052
1174	Putative pre-mRNA-splicing factor ATP-dependent RNA helicase DHX15	DHX15_HUMAN	DHX15	91 kDa	0.33
1175	60S ribosomal protein L18	RL18_HUMAN	RPL18	22 kDa	0.33
1176	Vitronectin	VTNC_HUMAN	VTN	54 kDa	0.33
1177	Vesicle-fusing ATPase	NSF_HUMAN	NSF	83 kDa	0.33
1178	Protein transport protein Sec23A	SC23A_HUMAN	SEC23A	86 kDa	0.33
1179	Cathepsin L2	CATL2_HUMAN	CTSV	37 kDa	0.33
1180	Extracellular sulfatase Sulf-2	SULF2_HUMAN	SULF2	100 kDa	0.33
1181	Cluster of Ribose-phosphate pyrophosphokinase 1	PRPS1_HUMAN [2]	PRPS1	35 kDa	0.33
1182	Histone deacetylase complex subunit SAP18	SAP18_HUMAN	SAP18	18 kDa	0.33
1183	Kallikrein-7	KLK7_HUMAN	KLK7	28 kDa	0.33
1184	Galectin-1	LEG1_HUMAN	LGALS1	15 kDa	0.33
1185	Coiled-coil domain-containing protein 6	CCDC6_HUMAN	CCDC6	53 kDa	0.34
1186	Cellular retinoic acid-binding protein 2	RABP2_HUMAN	CRABP2	16 kDa	0.34
1187	Eukaryotic translation initiation factor 4E	IF4E_HUMAN	EIF4E	25 kDa	0.34
1188	Chloride intracellular channel protein 1	CLIC1_HUMAN	CLIC1	27 kDa	0.35
1189	Cofilin-1	COF1_HUMAN	CFL1	19 kDa	0.35
1190	Cluster of Eukaryotic peptide chain release factor GTP-binding subunit ERF3A	ERF3A_HUMAN [2]	GSPT1	56 kDa	0.35
1191	Insulin-like growth factor 2 mRNA-binding protein 2	IF2B2_HUMAN	IGF2BP2	66 kDa	0.35
1192	Serine/threonine-protein kinase N1	PKN1_HUMAN	PKN1	104 kDa	0.35
1193	Prosaposin	SAP_HUMAN	PSAP	58 kDa	0.35
1194	Vacuolar protein-sorting-associated protein 25	VPS25_HUMAN	VPS25	21 kDa	0.35
1195	Zinc finger protein 638	ZN638_HUMAN	ZNF638	221 kDa	0.35
1196	ATP synthase subunit alpha, mitochondrial	ATPA_HUMAN	ATP5A1	60 kDa	0.36
1197	DCC-interacting protein 13-alpha	DP13A_HUMAN	APPL1	80 kDa	0.36
1198	Major prion protein	PRIO_HUMAN	PRNP	28 kDa	0.36
1199	Coatomer subunit beta'	COPB2_HUMAN	COPB2	102 kDa	0.36
1200	Eukaryotic translation initiation factor 1A, X-chromosomal	IF1AX_HUMAN (+1)	EIF1AX	16 kDa	0.36
1201	BRISC complex subunit Abro1	F175B_HUMAN	FAM175B	47 kDa	0.36
1202	Desmoglein-1	DSG1_HUMAN	DSG1	114 kDa	0.37
1203	Protein RTF2 homolog	RTF2_HUMAN	RTFDC1	34 kDa	0.37
1204	Cystatin-A	CYTA_HUMAN	CSTA	11 kDa	0.37
1205	Protein kinase C and casein kinase substrate in neurons protein 2	PACN2_HUMAN	PACSIN2	56 kDa	0.38
1206	U4/U6 small nuclear ribonucleoprotein Prp4	PRP4_HUMAN	PRPF4	58 kDa	0.38

1207	60S ribosomal protein L19	RL19_HUMAN	RPL19	23 kDa	0.38
42	Serum albumin	ALBU_HUMAN	ALB	69 kDa	0.0001
1209	Testis-specific serine kinase substrate	TSKS_HUMAN	TSKS	65 kDa	0.38
1210	Kinesin-like protein KIF23	KIF23_HUMAN	KIF23	110 kDa	0.39
1211	Malate dehydrogenase, mitochondrial	MDHM_HUMAN	MDH2	36 kDa	0.39
1212	DNA damage-binding protein 1	DDB1_HUMAN	DDB1	127 kDa	0.39
1213	U1 small nuclear ribonucleoprotein 70 kDa	RU17_HUMAN	SNRNP70	52 kDa	0.4
605	Gelsolin	GELS_HUMAN	GSN	86 kDa	0.048
1215	RNA-binding protein 25	RBM25_HUMAN	RBM25	100 kDa	0.4
1216	Golgi reassembly-stacking protein 2	GORS2_HUMAN	GORASP2	47 kDa	0.4
1217	40S ribosomal protein S25	RS25_HUMAN	RPS25	14 kDa	0.4
1218	Cellular nucleic acid-binding protein	CNBP_HUMAN	CNBP	19 kDa	0.4
1219	Cluster of UDP-glucose:glycoprotein glucosyltransferase 1	UGGG1_HUMAN [2]	UGGT1	177 kDa	0.4
1220	Catechol O-methyltransferase	COMT_HUMAN	COMT	30 kDa	0.41
1221	Brain-specific angiogenesis inhibitor 1-associated protein 2	BAIP2_HUMAN	BAIAP2	61 kDa	0.41
1222	Vascular endothelial growth factor C	VEGFC_HUMAN	VEGFC	47 kDa	0.41
1223	Vigilin	VIGLN_HUMAN	HDLBP	141 kDa	0.42
1224	Histidine triad nucleotide-binding protein 1	HINT1_HUMAN	HINT1	14 kDa	0.42
1225	ATP-binding cassette sub-family E member 1	ABCE1_HUMAN	ABCE1	67 kDa	0.42
1226	Syndecan-4	SDC4_HUMAN	SDC4	22 kDa	0.42
1227	Thrombospondin type-1 domain-containing protein 7A	THS7A_HUMAN	THSD7A	185 kDa	0.42
1228	Inosine-5'-monophosphate dehydrogenase 2	IMDH2_HUMAN	IMPDH2	56 kDa	0.42
1229	Probable ATP-dependent RNA helicase DDX23	DDX23_HUMAN	DDX23	96 kDa	0.42
1230	V-type proton ATPase subunit C 1	VATC1_HUMAN	ATP6V1C1	44 kDa	0.43
1231	Cluster of Mucin-5B	MUC5B_HUMAN [2]	MUC5B	596 kDa	0.43
1232	Alpha-centractin	ACTZ_HUMAN	ACTR1A	43 kDa	0.43
1233	60S ribosomal protein L10-like	RL10L_HUMAN (+1)	RPL10L	25 kDa	0.44
1234	Chloride intracellular channel protein 4	CLIC4_HUMAN	CLIC4	29 kDa	0.44
1235	Heterogeneous nuclear ribonucleoprotein D-like	HNRDL_HUMAN	HNRNPDL	46 kDa	0.44
1236	Gamma-glutamyltranspeptidase 1	GGT1_HUMAN	GGT1	61 kDa	0.44
1237	MAGUK p55 subfamily member 7	MPP7_HUMAN	MPP7	66 kDa	0.44
1238	Peripheral plasma membrane protein CASK	CSKP_HUMAN	CASK	105 kDa	0.44
1239	Desmoglein-2	DSG2_HUMAN	DSG2	122 kDa	0.44
1240	Amphiregulin	AREG_HUMAN	AREG	28 kDa	0.44
1241	Sodium- and chloride-dependent taurine transporter	SC6A6_HUMAN	SLC6A6	70 kDa	0.44
1242	Inverted formin-2	INF2_HUMAN	INF2	136 kDa	0.44
1243	Melanoma-associated antigen D2	MAGD2_HUMAN	MAGED2	65 kDa	0.44
1244	Membrane-associated progesterone receptor component 1	PGRC1_HUMAN	PGRMC1	22 kDa	0.44
1245	Neurogenic locus notch homolog protein 2	NOTC2_HUMAN	NOTCH2	265 kDa	0.44
1246	Neural cell adhesion molecule L1	L1CAM_HUMAN	L1CAM	140 kDa	0.44
1247	BAH and coiled-coil domain-containing protein 1	BAHC1_HUMAN	BAHCC1	277 kDa	0.44
1248	Clathrin coat assembly protein AP180	AP180_HUMAN	SNAP91	93 kDa	0.44
1249	Probable ATP-dependent RNA helicase DDX6	DDX6_HUMAN	DDX6	54 kDa	0.44
1250	Calcyphosin	CAYP1_HUMAN	CAPS	21 kDa	0.44
1251	Caspase-14	CASPE_HUMAN	CASP14	28 kDa	0.44

1252	Procollagen C-endopeptidase enhancer 1	PCOC1_HUMAN	PCOLCE	48 kDa	0.44
1253	Aminopeptidase N	AMPN_HUMAN	ANPEP	110 kDa	0.44
1254	TBC1 domain family member 5	TBCD5_HUMAN	TBC1D5	89 kDa	0.44
1255	Voltage-dependent calcium channel subunit alpha-2/delta-1	CA2D1_HUMAN	CACNA2D1	125 kDa	0.44
1256	High affinity immunoglobulin epsilon receptor subunit gamma	FCERG_HUMAN	FCER1G	10 kDa	0.44
1257	Tyrosine-protein kinase HCK	HCK_HUMAN	HCK	60 kDa	0.44
1258	Secretory carrier-associated membrane protein 2	SCAM2_HUMAN	SCAMP2	37 kDa	0.44
1259	Chromatin assembly factor 1 subunit B	CAF1B_HUMAN	CHAF1B	61 kDa	0.44
1260	A disintegrin and metalloproteinase with thrombospondin motifs 17	ATS17_HUMAN	ADAMTS17	121 kDa	0.44
1261	Heat shock protein 75 kDa, mitochondrial	TRAP1_HUMAN	TRAP1	80 kDa	0.44
1262	Bone morphogenetic protein 3	BMP3_HUMAN	BMP3	53 kDa	0.44
1263	Netrin-4	NET4_HUMAN	NTN4	70 kDa	0.44
1264	Semaphorin-3A	SEM3A_HUMAN	SEMA3A	89 kDa	0.44
1265	Enoyl-CoA hydratase, mitochondrial	ECHM_HUMAN	ECHS1	31 kDa	0.44
1266	Protein IWS1 homolog	IWS1_HUMAN	IWS1	92 kDa	0.44
1267	Endophilin-A2	SH3G1_HUMAN (+1)	SH3GL1	41 kDa	0.44
1268	A disintegrin and metalloproteinase with thrombospondin motifs 1	ATS1_HUMAN	ADAMTS1	105 kDa	0.44
1269	SEC23-interacting protein	S23IP_HUMAN	SEC23IP	111 kDa	0.44
1270	Importin-9	IPO9_HUMAN	IPO9	116 kDa	0.44
1271	Platelet endothelial cell adhesion molecule	PECA1_HUMAN	PECAM1	83 kDa	0.44
1272	Lysine-specific demethylase 2B	KDM2B_HUMAN	KDM2B	153 kDa	0.44
1273	Villin-1	VIL1_HUMAN	VIL1	93 kDa	0.44
1274	Plexin-B2	PLXB2_HUMAN	PLXNB2	205 kDa	0.44
1275	Protein tyrosine phosphatase type IVA 2	TP4A2_HUMAN	PTP4A2	19 kDa	0.44
1276	Heparan sulfate glucosamine 3-O-sulfotransferase 1	HS3S1_HUMAN	HS3ST1	36 kDa	0.44
1277	Heparan-sulfate 6-O-sulfotransferase 2	H6S2_HUMAN	HS6ST2	69 kDa	0.44
1278	E3 ubiquitin-protein ligase ARIH1	ARI1_HUMAN	ARIH1	64 kDa	0.44
1279	Neuroplastin	NPTN_HUMAN	NPTN	44 kDa	0.44
1280	Tubulin-specific chaperone D	TBCD_HUMAN	TBCD	133 kDa	0.44
1281	Protocadherin Fat 1	FAT1_HUMAN	FAT1	506 kDa	0.44
1282	Anosmin-1	KALM_HUMAN	KAL1	76 kDa	0.44
1283	Alpha-2-macroglobulin-like protein 1	A2ML1_HUMAN	A2ML1	161 kDa	0.44
1284	6-phosphogluconolactonase	6PGL_HUMAN	PGLS	28 kDa	0.44
1285	Succinate-semialdehyde dehydrogenase, mitochondrial	SSDH_HUMAN	ALDH5A1	57 kDa	0.44
1286	Matrix metalloproteinase-9	MMP9_HUMAN	MMP9	78 kDa	0.44
1287	60S ribosomal protein L23	RL23_HUMAN	RPL23	15 kDa	0.44
1288	V-type proton ATPase subunit d 1	VA0D1_HUMAN	ATP6V0D1	40 kDa	0.44
1289	Serine/threonine-protein kinase WNK1	WNK1_HUMAN	WNK1	251 kDa	0.44
1290	CUGBP Elav-like family member 2	CELF2_HUMAN	CELF2	54 kDa	0.44
1291	Myosin light chain kinase, smooth muscle	MYLK_HUMAN	MYLK	211 kDa	0.44
1292	Arginine and glutamate-rich protein 1	ARGL1_HUMAN	ARGLU1	33 kDa	0.44
1293	NEDD8-conjugating enzyme Ubc12	UBC12_HUMAN	UBE2M	21 kDa	0.44
1294	LIM domain and actin-binding protein 1	LIMA1_HUMAN	LIMA1	85 kDa	0.44
1295	Carboxypeptidase N subunit 2	CPN2_HUMAN	CPN2	61 kDa	0.44
1296	Protein Hook homolog 3	HOOK3_HUMAN	HOOK3	83 kDa	0.44

1297	Dihydropolyllysine-residue acetyltransferase component of pyruvate dehydrogenase complex, mitochondrial	ODP2_HUMAN	DLAT	69 kDa	0.44
1298	Cytoskeleton-associated protein 4	CKAP4_HUMAN	CKAP4	66 kDa	0.44
1299	Glutathione peroxidase 3	GPX3_HUMAN	GPX3	26 kDa	0.44
1300	Exportin-5	XPO5_HUMAN	XPO5	136 kDa	0.44
1301	Arf-GAP with coiled-coil, ANK repeat and PH domain-containing protein 2	ACAP2_HUMAN	ACAP2	88 kDa	0.44
1302	Epidermal growth factor receptor substrate 15	EPS15_HUMAN	EPS15	99 kDa	0.44
1303	Dehydrogenase/reductase SDR family member 11	DHR11_HUMAN	DHRS11	28 kDa	0.44
1304	Epidermal growth factor receptor kinase substrate 8-like protein 1	ESL1_HUMAN	EPS8L1	80 kDa	0.44
1305	Hyaluronan mediated motility receptor	HMMR_HUMAN	HMMR	84 kDa	0.44
1306	Gamma-soluble NSF attachment protein	SNAG_HUMAN	NAPG	35 kDa	0.44
1307	Cold shock domain-containing protein E1	CSDE1_HUMAN	CSDE1	89 kDa	0.44
1308	Vasopressin-neurophysin 2-copeptin	NEU2_HUMAN	AVP	17 kDa	0.44
1309	Platelet glycoprotein 4	CD36_HUMAN	CD36	53 kDa	0.44
1310	Splicing factor U2AF 65 kDa subunit	U2AF2_HUMAN	U2AF2	54 kDa	0.44
1311	Protein ITFG3	ITFG3_HUMAN	ITFG3	60 kDa	0.44
1312	Tubulin--tyrosine ligase-like protein 12	TTL12_HUMAN	TLL12	74 kDa	0.44
1313	Fragile X mental retardation syndrome-related protein 1	FXR1_HUMAN	FXR1	70 kDa	0.44
1314	Protein FAM98A	FA98A_HUMAN	FAM98A	55 kDa	0.44
1315	Ephrin type-B receptor 4	EPHB4_HUMAN	EPHB4	108 kDa	0.44
1316	Flavin reductase (NADPH)	BLVRB_HUMAN	BLVRB	22 kDa	0.44
1317	Trefoil factor 1	TFF1_HUMAN	TFF1	9 kDa	0.44
1318	Translation initiation factor eIF-2B subunit delta	EI2BD_HUMAN	EIF2B4	58 kDa	0.44
1319	DNA damage-binding protein 2	DDB2_HUMAN	DDB2	48 kDa	0.44
1320	Immunoglobulin superfamily member 3	IGSF3_HUMAN	IGSF3	135 kDa	0.44
1321	Chromogranin-A	CMGA_HUMAN	CHGA	51 kDa	0.44
1322	ADP-ribosylation factor 6	ARF6_HUMAN	ARF6	20 kDa	0.44
1323	Envoplakin	EVPL_HUMAN	EVPL	232 kDa	0.44
1324	Coiled-coil-helix-coiled-coil-helix domain-containing protein 3, mitochondrial	CHCH3_HUMAN	CHCHD3	26 kDa	0.44
1325	Malectin	MLEC_HUMAN	MLEC	32 kDa	0.44
1326	Semaphorin-3G	SEM3G_HUMAN	SEMA3G	87 kDa	0.44
1327	Cytochrome c1, heme protein, mitochondrial	CY1_HUMAN	CYC1	35 kDa	0.44
1328	Kunitz-type protease inhibitor 1	SPIT1_HUMAN	SPINT1	58 kDa	0.44
1329	Thioredoxin-dependent peroxide reductase, mitochondrial	PRDX3_HUMAN	PRDX3	28 kDa	0.44
1330	Prohibitin	PHB_HUMAN	PHB	30 kDa	0.44
1331	Reticulon-3	RTN3_HUMAN	RTN3	113 kDa	0.44
1332	Peptidyl-prolyl cis-trans isomerase FKBP1A	FKB1A_HUMAN	FKBP1A	12 kDa	0.44
1333	Voltage-dependent anion-selective channel protein 3	VDAC3_HUMAN	VDAC3	31 kDa	0.44
1334	Aspartate aminotransferase, mitochondrial	AATM_HUMAN	GOT2	48 kDa	0.44
1335	Dynein light chain 2, cytoplasmic	DYL2_HUMAN	DYNLL2	10 kDa	0.44
1336	Protein S100-P	S100P_HUMAN	S100P	10 kDa	0.45
1337	Peroxisredoxin-4	PRDX4_HUMAN	PRDX4	31 kDa	0.45
301	Cluster of Talin-1	TLN1_HUMAN [2]	TLN1	270 kDa	0.0033
1339	60S ribosomal protein L36	RL36_HUMAN	RPL36	12 kDa	0.45
1340	Methylcytosine dioxygenase TET3	TET3_HUMAN	TET3	179 kDa	0.45
1341	Nascent polypeptide-associated complex subunit alpha, muscle-specific form	NACAM_HUMAN	NACA	205 kDa	0.45

1342	Collagen alpha-1(II) chain	CO2A1_HUMAN	COL2A1	142 kDa	0.45
1343	Serine-threonine kinase receptor-associated protein	STRAP_HUMAN	STRAP	38 kDa	0.46
1344	Cluster of Guanine nucleotide-binding protein G(I)/G(S)/G(T) subunit beta-2	GNAS1_HUMAN [6]	GNAS	111 kDa	0.46
1345	Protein DJ-1	PARK7_HUMAN	PARK7	20 kDa	0.46
1346	Peptidyl-prolyl cis-trans isomerase H	PPIH_HUMAN	PPIH	19 kDa	0.46
1347	OCIA domain-containing protein 2	OCAD2_HUMAN	OCIAD2	17 kDa	0.46
1348	Cluster of Guanine nucleotide-binding protein G(s) subunit alpha isoforms XLas	GNAS1_HUMAN [6]	GNAS	111 kDa	0.46
595	Keratin, type I cytoskeletal 9	K1C9_HUMAN	KRT9	62 kDa	0.044
1350	Hepatoma-derived growth factor	HDGF_HUMAN	HDGF	27 kDa	0.47
1351	Cluster of E3 SUMO-protein ligase RanBP2	RBP2_HUMAN [2]	RANBP2	358 kDa	0.47
1352	DnaJ homolog subfamily C member 10	DJC10_HUMAN	DNAJC10	91 kDa	0.47
1353	FACT complex subunit SPT16	SP16H_HUMAN	SUPT16H	120 kDa	0.47
1354	Anterior gradient protein 2 homolog	AGR2_HUMAN	AGR2	20 kDa	0.47
1355	Thioredoxin	THIO_HUMAN	TXN	12 kDa	0.47
1356	Charged multivesicular body protein 4b	CHM4B_HUMAN	CHMP4B	25 kDa	0.48
1357	COP9 signalosome complex subunit 5	CSN5_HUMAN	COP55	38 kDa	0.48
1358	Dihydropyridyl dehydrogenase, mitochondrial	DLDH_HUMAN	DLD	54 kDa	0.48
1359	COP9 signalosome complex subunit 1	CSN1_HUMAN	GPS1	56 kDa	0.48
1360	Ubiquitin-protein ligase E3A	UBE3A_HUMAN	UBE3A	101 kDa	0.49
1361	CD276 antigen	CD276_HUMAN	CD276	57 kDa	0.49
1362	Adenylate kinase 2, mitochondrial	KAD2_HUMAN	AK2	26 kDa	0.49
1363	Glucosamine 6-phosphate N-acetyltransferase	GNA1_HUMAN	GNPNAT1	21 kDa	0.49
1364	Integrin beta-4	ITB4_HUMAN	ITGB4	202 kDa	0.49
1365	Insulin-like growth factor II	IGF2_HUMAN	IGF2	20 kDa	0.49
1366	Complement component 1 Q subcomponent-binding protein, mitochondrial	C1QBP_HUMAN	C1QBP	31 kDa	0.49
1367	Vesicle-associated membrane protein-associated protein A	VAPA_HUMAN	VAPA	28 kDa	0.49
1368	Claudin-4	CLD4_HUMAN	CLDN4	22 kDa	0.5
1369	Glutathione synthetase	GSHB_HUMAN	GSS	52 kDa	0.5
1370	Leukotriene A-4 hydrolase	LKHA4_HUMAN	LTA4H	69 kDa	0.5
1371	Sodium/potassium-transporting ATPase subunit beta-3	AT1B3_HUMAN	ATP1B3	32 kDa	0.5
1372	Calpastatin	ICAL_HUMAN	CAST	77 kDa	0.5
1373	Alpha-2-antiplasmin	A2AP_HUMAN	SERPINF2	55 kDa	0.5
1374	Structural maintenance of chromosomes protein 3	SMC3_HUMAN	SMC3	142 kDa	0.5
1375	Lysine-specific histone demethylase 1A	KDM1A_HUMAN	KDM1A	93 kDa	0.5
1376	Proteasome subunit alpha type-7	PSA7_HUMAN	PSMA7	28 kDa	0.5
1377	5'-3' exoribonuclease 2	XRN2_HUMAN	XRN2	109 kDa	0.5
1378	N-acetyllactosaminide beta-1,3-N-acetylglucosaminyltransferase	B3GN1_HUMAN	B3GNT1	47 kDa	0.5
1379	Protein S100-A9	S10A9_HUMAN	S100A9	13 kDa	0.51
1380	Heterogeneous nuclear ribonucleoprotein U-like protein 1	HNRL1_HUMAN	HNRNPUL1	96 kDa	0.51
1381	Attractin	ATRN_HUMAN	ATRN	159 kDa	0.51
1382	Ras-related protein Rab-7a	RAB7A_HUMAN	RAB7A	23 kDa	0.51
1383	Latent-transforming growth factor beta-binding protein 4	LTBP4_HUMAN	LTBP4	173 kDa	0.51
1384	10 kDa heat shock protein, mitochondrial	CH10_HUMAN	HSPE1	11 kDa	0.52
1385	Fibronectin type III domain-containing protein 1	FNDC1_HUMAN	FNDC1	206 kDa	0.52
1386	Beta-catenin-like protein 1	CTBL1_HUMAN	CTNBL1	65 kDa	0.52

1387	Pro-cathepsin H	CATH_HUMAN	CTSH	37 kDa	0.52
1388	Tissue factor pathway inhibitor	TFPI1_HUMAN	TFPI	35 kDa	0.52
1389	Calmodulin	CALM_HUMAN	CALM1	17 kDa	0.53
1390	Farnesyl pyrophosphate synthase	FPPS_HUMAN	FDPS	48 kDa	0.53
1391	High mobility group nucleosome-binding domain-containing protein 3	HMG3_HUMAN	HMG3	11 kDa	0.53
1392	Peripheral-type benzodiazepine receptor-associated protein 1	RIMB1_HUMAN	BZRAP1	200 kDa	0.53
1393	Protein arginine N-methyltransferase 5	ANM5_HUMAN	PRMT5	73 kDa	0.53
1394	Single-stranded DNA-binding protein, mitochondrial	SSBP_HUMAN	SSBP1	17 kDa	0.54
1395	3-ketoacyl-CoA thiolase, mitochondrial	THIM_HUMAN	ACAA2	42 kDa	0.54
1396	Striatin	STRN_HUMAN	STRN	86 kDa	0.55
1397	Omega-amidase NIT2	NIT2_HUMAN	NIT2	31 kDa	0.55
1398	Small subunit processome component 20 homolog	UTP20_HUMAN	UTP20	318 kDa	0.55
1399	Cystathionine beta-synthase	CBS_HUMAN	CBS	61 kDa	0.55
1400	Endothelial differentiation-related factor 1	EDF1_HUMAN	EDF1	16 kDa	0.55
1401	Erythrocyte band 7 integral membrane protein	STOM_HUMAN	STOM	32 kDa	0.55
1402	60S ribosomal protein L35	RL35_HUMAN	RPL35	15 kDa	0.55
1403	Leucine-rich repeat-containing protein 59	LRC59_HUMAN	LRRC59	35 kDa	0.55
1404	Choline transporter-like protein 1	CTL1_HUMAN	SLC44A1	73 kDa	0.56
583	Cluster of Actin, cytoplasmic 1	ACTB_HUMAN [7]	ACTB	42 kDa	0.04
1406	Fibrinogen alpha chain	FIBA_HUMAN	FGA	95 kDa	0.56
1407	Protein transport protein Sec16A	SCI16A_HUMAN	SEC16A	234 kDa	0.56
1408	ADP-ribosylation factor-like protein 3	ARL3_HUMAN	ARL3	20 kDa	0.56
1409	Myosin regulatory light chain 12A	ML12A_HUMAN (+1)	MYL12A	20 kDa	0.56
1410	Probable G-protein coupled receptor 125	GP125_HUMAN	GPR125	146 kDa	0.56
1411	60S ribosomal protein L7a	RL7A_HUMAN	RPL7A	30 kDa	0.56
1412	Cytoplasmic dynein 1 heavy chain 1	DYHC1_HUMAN	DYNC1H1	532 kDa	0.56
1413	Putative tripartite motif-containing protein 64B	TR64B_HUMAN (+1)	TRIM64B	52 kDa	0.56
1414	Septin-6	SEPT6_HUMAN	Sep-06	50 kDa	0.56
1415	Hepatocyte growth factor-regulated tyrosine kinase substrate	HGS_HUMAN	HGS	86 kDa	0.57
1416	Vesicle-associated membrane protein 2	VAMP2_HUMAN	VAMP2	13 kDa	0.57
1417	Prothymosin alpha	PTMA_HUMAN	PTMA	12 kDa	0.57
1418	SCY1-like protein 2	SCYL2_HUMAN	SCYL2	104 kDa	0.57
551	Cluster of Heat shock protein HSP 90-alpha	HS90A_HUMAN [6]	HSP90AA1	85 kDa	0.032
1420	Calreticulin	CALR_HUMAN	CALR	48 kDa	0.57
1421	Calnexin	CALX_HUMAN	CANX	68 kDa	0.57
1422	Cysteine and histidine-rich domain-containing protein 1	CHRDI_HUMAN	CHORDC1	37 kDa	0.57
1423	Endoplasmic reticulum resident protein 29	ERP29_HUMAN	ERP29	29 kDa	0.58
1424	REST corepressor 1	RCOR1_HUMAN	RCOR1	53 kDa	0.58
1425	Tsukushin	TSK_HUMAN	TSKU	38 kDa	0.58
1426	26S protease regulatory subunit 6B	PRS6B_HUMAN	PSMC4	47 kDa	0.58
1427	Transcription elongation factor SPT6	SPT6H_HUMAN	SUPT6H	199 kDa	0.58
1428	CAP-Gly domain-containing linker protein 1	CLIP1_HUMAN	CLIP1	162 kDa	0.58
1429	E3 ubiquitin-protein ligase MYCBP2	MYCB2_HUMAN	MYCBP2	510 kDa	0.58
1430	Keratinocyte proline-rich protein	KPRP_HUMAN	KPRP	64 kDa	0.58
1431	Carbonyl reductase [NADPH] 1	CBR1_HUMAN	CBR1	30 kDa	0.58

1432	Plastin-3	PLST_HUMAN	PLS3	71 kDa	0.58
1433	Synaptotagmin-1	SYTL_HUMAN	SYT1	48 kDa	0.59
1434	Heparin cofactor 2	HEP2_HUMAN	SERPIND1	57 kDa	0.59
1435	Serine/threonine-protein phosphatase 1 regulatory subunit 10	PP1RA_HUMAN	PPP1R10	99 kDa	0.59
1436	Ubiquitin carboxyl-terminal hydrolase isozyme L5	UCHL5_HUMAN	UCHL5	38 kDa	0.59
1437	Partner of Y14 and mago	WIBG_HUMAN	WIBG	23 kDa	0.59
1438	Lipolysis-stimulated lipoprotein receptor	LSR_HUMAN	LSR	71 kDa	0.59
1439	Tenascin-X	TENX_HUMAN	TNXB	464 kDa	0.59
1440	DNA replication licensing factor MCM4	MCM4_HUMAN	MCM4	97 kDa	0.59
1441	Vasorin	VASN_HUMAN	VASN	72 kDa	0.59
1442	Solute carrier family 2, facilitated glucose transporter member 1	GTR1_HUMAN	SLC2A1	54 kDa	0.59
1443	RUN and FYVE domain-containing protein 1	RUFY1_HUMAN	RUFY1	80 kDa	0.6
1444	Protein transport protein Sec23B	SC23B_HUMAN	SEC23B	86 kDa	0.6
1445	Cluster of Sodium/potassium-transporting ATPase subunit alpha-1	AT1A1_HUMAN [2]	ATP1A1	113 kDa	0.6
1446	Protein disulfide-isomerase	PDIA1_HUMAN	P4HB	57 kDa	0.6
1447	Metalloproteinase inhibitor 2	TIMP2_HUMAN	TIMP2	24 kDa	0.61
1448	Histone H1x	H1X_HUMAN	H1FX	22 kDa	0.61
1449	Heterogeneous nuclear ribonucleoprotein U	HNRPU_HUMAN	HNRNPU	91 kDa	0.61
1450	Cluster of Serine/threonine-protein phosphatase PP1-alpha catalytic subunit	PP1A_HUMAN [3]	PPP1CA	38 kDa	0.61
1451	Aldo-keto reductase family 1 member B10	AK1BA_HUMAN	AKR1B10	36 kDa	0.61
1452	Suppressor of tumorigenicity 14 protein	ST14_HUMAN	ST14	95 kDa	0.62
133	Cluster of Adenylyl cyclase-associated protein 1	CAP1_HUMAN [2]	CAP1	52 kDa	0.00031
1454	Protein furry homolog	FRY_HUMAN	FRY	339 kDa	0.62
1455	Tumor protein D54	TPD54_HUMAN	TPD52L2	22 kDa	0.62
1456	Cornifin-A	SPR1A_HUMAN (+1)	SPRR1A	10 kDa	0.63
1457	Glucosidase 2 subunit beta	GLU2B_HUMAN	PRKCSH	59 kDa	0.64
1458	Serine--tRNA ligase, cytoplasmic	SYSC_HUMAN	SARS	59 kDa	0.64
1459	Collagen alpha-1(VI) chain	CO6A1_HUMAN	COL6A1	109 kDa	0.65
1460	Glucose-6-phosphate isomerase	G6PI_HUMAN	GPI	63 kDa	0.65
1461	Coatomer subunit alpha	COPA_HUMAN	COPA	138 kDa	0.66
1462	Reticulon-4	RTN4_HUMAN	RTN4	130 kDa	0.66
1463	Major vault protein	MVP_HUMAN	MVP	99 kDa	0.67
1464	Multifunctional protein ADE2	PUR6_HUMAN	PAICS	47 kDa	0.68
1465	Superoxide dismutase [Cu-Zn]	SODC_HUMAN	SOD1	16 kDa	0.68
1466	Transportin-3	TNPO3_HUMAN	TNPO3	104 kDa	0.69
1467	Cullin-4A	CUL4A_HUMAN	CUL4A	88 kDa	0.69
1468	Cluster of Kinesin-1 heavy chain	KINH_HUMAN [2]	KIF5B	110 kDa	0.71
1469	Adenylosuccinate lyase	PUR8_HUMAN	ADSL	55 kDa	0.72
1470	Neurogenic locus notch homolog protein 3	NOTC3_HUMAN	NOTCH3	244 kDa	0.73
1471	Cystatin-B	CYTB_HUMAN	CSTB	11 kDa	0.73
395	Cluster of Alpha-actinin-4	ACTN4_HUMAN [4]	ACTN4	105 kDa	0.0081
1473	26S proteasome non-ATPase regulatory subunit 3	PSMD3_HUMAN	PSMD3	61 kDa	0.74
1474	Dystrophin	DMD_HUMAN	DMD	427 kDa	0.74
1475	Prostaglandin E synthase 3	TEBP_HUMAN	PTGES3	19 kDa	0.74
1476	Lumican	LUM_HUMAN	LUM	38 kDa	0.76

1477	Septin-11	SEP11_HUMAN	Sep-11	49 kDa	0.77
1478	1-phosphatidylinositol 4,5-bisphosphate phosphodiesterase beta-3	PLCB3_HUMAN	PLCB3	139 kDa	0.77
1479	Lysosomal alpha-glucosidase	LYAG_HUMAN	GAA	105 kDa	0.78
1480	Protein Hook homolog 1	HOOK1_HUMAN	HOOK1	85 kDa	0.79
1481	Dr1-associated corepressor	NC2A_HUMAN	DRAP1	22 kDa	0.79
1482	GMP reductase 2	GMPR2_HUMAN	GMPR2	38 kDa	0.8
1483	Peroxisredoxin-2	PRDX2_HUMAN	PRDX2	22 kDa	0.81
1484	Golgi apparatus protein 1	GSLG1_HUMAN	GLG1	135 kDa	0.81
1485	N-acetyl-D-glucosamine kinase	NAGK_HUMAN	NAGK	37 kDa	0.81
1486	Proteolipid protein 2	PLP2_HUMAN	PLP2	17 kDa	0.81
1487	Cluster of 6-phosphofructokinase type C	K6PP_HUMAN [2]	PFKP	86 kDa	0.82
1488	CD166 antigen	CD166_HUMAN	ALCAM	65 kDa	0.82
902	Cluster of Keratin, type I cytoskeletal 10	K1C10_HUMAN [15]	KRT10	59 kDa	0.13
1490	26S protease regulatory subunit 10B	PRS10_HUMAN	PSMC6	44 kDa	0.84
1491	Cluster of Serine/threonine-protein phosphatase 2B catalytic subunit alpha isoform	PP2BA_HUMAN [2]	PPP3CA	59 kDa	0.86
1492	40S ribosomal protein S2	RS2_HUMAN	RPS2	31 kDa	0.87
1493	26S proteasome non-ATPase regulatory subunit 6	PSMD6_HUMAN	PSMD6	46 kDa	0.88
1494	26S protease regulatory subunit 7	PRS7_HUMAN	PSMC2	49 kDa	0.88
1495	Cluster of Clathrin heavy chain 1	CLH1_HUMAN [2]	CLTC	192 kDa	0.88
1496	DnaJ homolog subfamily A member 2	DNJA2_HUMAN	DNAJA2	46 kDa	0.89
1497	Cluster of Ras-related protein Rab-5C	RAB5C_HUMAN [3]	RAB5C	23 kDa	0.91
821	Cluster of Keratin, type II cytoskeletal 8	K2C8_HUMAN [19]	KRT8	54 kDa	0.11
1499	Deleted in malignant brain tumors 1 protein	DMBT1_HUMAN	DMBT1	261 kDa	0.91
1500	60S ribosomal protein L27	RL27_HUMAN	RPL27	16 kDa	0.92
1501	Ubiquitin-conjugating enzyme E2 N	UBE2N_HUMAN (+1)	UBE2N	17 kDa	0.99

Table 2: List of proteins indentified only form lung cancer cell line H358

Proteins	Accession Number	Alternate ID	Molecular Weight	ANOVA Test (p-value)
Keratin, type II cytoskeletal 8	K2C8_HUMAN	KRT8	54 kDa	0.11
Chitinase-3-like protein 1	CH3L1_HUMAN	CHI3L1	43 kDa	0.0041
Cathepsin G	CATG_HUMAN	CTSG	29 kDa	0.0004
C-type lectin domain family 11 member A	CLC11_HUMAN	CLEC11A	36 kDa	0.0037
Histone H2A type 2-A	H2A2A_HUMAN	HIST2H2AA3	14 kDa	0.043
Nidogen-1	NID1_HUMAN	NID1	136 kDa	< 0.00010
Nuclear mitotic apparatus protein 1	NUMA1_HUMAN	NUMA1	238 kDa	0.0036
Lysozyme C	LYSC_HUMAN	LYZ	17 kDa	0.00076
DNA-(apurinic or apyrimidinic site) lyase	APEX1_HUMAN	APEX1	36 kDa	0.017
Activated RNA polymerase II transcriptional coactivator p15	TCP4_HUMAN	SUB1	14 kDa	0.0041
Histone H1.3	H13_HUMAN	HIST1H1D	22 kDa	0.38
HLA class I histocompatibility antigen, A-2 alpha chain	1A02_HUMAN	HLA-A	41 kDa	0.075
Neutrophil elastase	ELNE_HUMAN	ELANE	29 kDa	0.0033
Inter-alpha-trypsin inhibitor heavy chain H3	ITI3_HUMAN	ITI3	100 kDa	0.044
Ras-related protein Rab-14	RAB14_HUMAN	RAB14	24 kDa	0.13
T-complex protein 1 subunit alpha	TCPA_HUMAN	TCP1	60 kDa	0.021
ATP-dependent RNA helicase A	DHX9_HUMAN	DHX9	141 kDa	0.0053
Na(+)/H(+) exchange regulatory cofactor NHE-RF1	NHRF1_HUMAN	SLC9A3R1	39 kDa	< 0.00010
Protein diaphanous homolog 1	DIAP1_HUMAN	DIAPH1	141 kDa	0.0074
DNA topoisomerase 1	TOP1_HUMAN	TOP1	91 kDa	0.0018
Histone H1.5	H15_HUMAN	HIST1H1B	23 kDa	0.16
Epithelial cell adhesion molecule	EPCAM_HUMAN	EPCAM	35 kDa	0.3
Proteasome activator complex subunit 2	PSME2_HUMAN	PSME2	27 kDa	0.00015
Cell cycle and apoptosis regulator protein 2	CCAR2_HUMAN	CCAR2	103 kDa	< 0.00010
Disks large homolog 1	DLG1_HUMAN	DLG1	100 kDa	0.0014
Mitochondrial import receptor subunit TOM70	TOM70_HUMAN	TOMM70A	67 kDa	0.0002
Nucleolar and coiled-body phosphoprotein 1	NOLC1_HUMAN	NOLC1	74 kDa	0.032
Prothrombin	THRB_HUMAN	F2	70 kDa	0.053
Importin subunit alpha-1	IMA1_HUMAN	KPNA2	58 kDa	0.0011
Nucleosome assembly protein 1-like 1	NP1L1_HUMAN	NAP1L1	45 kDa	0.014
Serine/arginine-rich splicing factor 3	SRSF3_HUMAN	SRSF3	19 kDa	0.00018
Catenin delta-1	CTND1_HUMAN	CTNND1	108 kDa	0.013
Protein RCC2	RCC2_HUMAN	RCC2	56 kDa	0.12
Cysteine-rich protein 2	CRIP2_HUMAN	CRIP2	22 kDa	0.24
Core histone macro-H2A.1	H2AY_HUMAN	H2AFY	40 kDa	0.25
Proteasome activator complex subunit 3	PSME3_HUMAN	PSME3	30 kDa	0.014
Paraspeckle component 1	PSPC1_HUMAN	PSPC1	59 kDa	0.0067

Enhancer of rudimentary homolog	ERH_HUMAN	ERH	12 kDa	0.011
Eukaryotic translation initiation factor 2A	EIF2A_HUMAN	EIF2A	65 kDa	0.048
Large neutral amino acids transporter small subunit 1	LAT1_HUMAN	SLC7A5	55 kDa	0.0014
Sorting nexin-6	SNX6_HUMAN	SNX6	47 kDa	0.0027
Serine/arginine-rich splicing factor 2	SRSF2_HUMAN	SRSF2	25 kDa	0.049
Eukaryotic translation initiation factor 5	IF5_HUMAN	EIF5	49 kDa	0.0011
Tumor protein D52	TPD52_HUMAN	TPD52	24 kDa	0.14
Catenin beta-1	CTNB1_HUMAN	CTNNB1	85 kDa	0.0075
Leucine-rich repeat-containing protein 47	LRC47_HUMAN	LRRC47	63 kDa	0.16
Asparagine--tRNA ligase, cytoplasmic	SYNC_HUMAN	NARS	63 kDa	< 0.00010
Inter-alpha-trypsin inhibitor heavy chain H4	ITI4_HUMAN	ITI4	103 kDa	0.12
Chromobox protein homolog 3	CBX3_HUMAN	CBX3	21 kDa	0.0013
Mitotic checkpoint protein BUB3	BUB3_HUMAN	BUB3	37 kDa	0.012
NAD(P)H dehydrogenase [quinone] 1	NQO1_HUMAN	NQO1	31 kDa	0.052
Proliferating cell nuclear antigen	PCNA_HUMAN	PCNA	29 kDa	0.00041
Glutathione reductase, mitochondrial	GSHR_HUMAN	GSR	56 kDa	0.28
Cartilage oligomeric matrix protein	COMP_HUMAN	COMP	83 kDa	0.012
MARCKS-related protein	MRP_HUMAN	MARCKSL1	20 kDa	0.091
60S ribosomal protein L23a	RL23A_HUMAN	RPL23A	18 kDa	0.24
UDP-glucose 6-dehydrogenase	UGDH_HUMAN	UGDH	55 kDa	0.11
5'-3' exoribonuclease 2	XRN2_HUMAN	XRN2	109 kDa	0.5
Leucine-rich repeat-containing protein 59	LRC59_HUMAN	LRRC59	35 kDa	0.55
Splicing factor 3B subunit 1	SF3B1_HUMAN	SF3B1	146 kDa	0.012
Ras GTPase-activating protein-binding protein 1	G3BP1_HUMAN	G3BP1	52 kDa	0.067
Purine nucleoside phosphorylase	PNPH_HUMAN	PNP	32 kDa	0.066
SAP domain-containing ribonucleoprotein	SARNP_HUMAN	SARNP	24 kDa	0.14
Importin-7	IPO7_HUMAN	IPO7	120 kDa	0.062
40S ribosomal protein S13	RS13_HUMAN	RPS13	17 kDa	0.15
Endoplasmic reticulum resident protein 29	ERP29_HUMAN	ERP29	29 kDa	0.58
Complement C5	CO5_HUMAN	C5	188 kDa	0.22
Cytoplasmic FMR1-interacting protein 1	CYFIP1_HUMAN	CYFIP1	145 kDa	0.15
EGF-like repeat and discoidin I-like domain-containing protein 3	EDIL3_HUMAN	EDIL3	54 kDa	0.16
Inter-alpha-trypsin inhibitor heavy chain H1	ITI1_HUMAN	ITI1	101 kDa	0.0015
Prefoldin subunit 2	PFD2_HUMAN	PFDN2	17 kDa	0.016
Receptor-type tyrosine-protein phosphatase S	PTPRS_HUMAN	PTPRS	217 kDa	0.027
Thrombospondin-4	TSP4_HUMAN	THBS4	106 kDa	0.077
Coagulation factor V	FA5_HUMAN	F5	252 kDa	0.076
60S ribosomal protein L13	RL13_HUMAN	RPL13	24 kDa	0.09
Vitronectin	VTNC_HUMAN	VTN	54 kDa	0.33
U1 small nuclear ribonucleoprotein 70 kDa	RUI7_HUMAN	SNRNP70	52 kDa	0.4
60S ribosomal protein L22	RL22_HUMAN	RPL22	15 kDa	0.038
Dehydrogenase/reductase SDR family member 2, mitochondrial	DHRS2_HUMAN	DHRS2	30 kDa	0.32
Keratinocyte proline-rich protein	KPRP_HUMAN	KPRP	64 kDa	0.58

Pregnancy zone protein	PZP_HUMAN	PZP	164 kDa	0.041
Acidic mammalian chitinase	CHIA_HUMAN	CHIA	52 kDa	0.055
Protein scribble homolog	SCRIB_HUMAN	SCRIB	175 kDa	0.21
Pancreatic alpha-amylase	AMYP_HUMAN	AMY2A	58 kDa	0.2
Collagen triple helix repeat-containing protein 1	CTHR1_HUMAN	CTHRC1	26 kDa	0.051
Histone H1.0	H10_HUMAN	H1F0	21 kDa	0.29
Junctional adhesion molecule A	JAM1_HUMAN	F11R	33 kDa	0.2
Claudin-3	CLD3_HUMAN	CLDN3	23 kDa	0.052
Syntaxin-4	STX4_HUMAN	STX4	34 kDa	0.16
Desmocollin-1	DSC1_HUMAN	DSC1	100 kDa	0.072
Brain-specific angiogenesis inhibitor 1-associated protein 2	BAIP2_HUMAN	BAIAP2	61 kDa	0.41
CD276 antigen	CD276_HUMAN	CD276	57 kDa	0.49
CD81 antigen	CD81_HUMAN	CD81	26 kDa	0.11
Basal cell adhesion molecule	BCAM_HUMAN	BCAM	67 kDa	0.22
Complement decay-accelerating factor	DAF_HUMAN	CD55	41 kDa	0.18
Prominin-2	PROM2_HUMAN	PROM2	92 kDa	0.2
Voltage-dependent anion-selective channel protein 1	VDAC1_HUMAN	VDAC1	31 kDa	0.28
Small nuclear ribonucleoprotein Sm D1	SMD1_HUMAN	SNRPD1	13 kDa	0.12
Golgin subfamily A member 2	GOGA2_HUMAN	GOLGA2	113 kDa	0.0013
Annexin A3	ANXA3_HUMAN	ANXA3	36 kDa	0.053
Fibulin-2	FBLN2_HUMAN	FBLN2	127 kDa	0.22
Histone H1x	H1X_HUMAN	H1FX	22 kDa	0.61
Integrin alpha-V	ITAV_HUMAN	ITGAV	116 kDa	0.077
Monocarboxylate transporter 4	MOT4_HUMAN	SLC16A3	49 kDa	0.17
Delta(3,5)-Delta(2,4)-dienoyl-CoA isomerase, mitochondrial	ECH1_HUMAN	ECH1	36 kDa	0.18
N-acetyllactosaminide beta-1,3-N-acetylglucosaminyltransferase	B3GN1_HUMAN	B3GNT1	47 kDa	0.5
Heparin cofactor 2	HEP2_HUMAN	SERPIND1	57 kDa	0.59
Putative tripartite motif-containing protein 64B	TR64B_HUMAN (+1)	TRIM64B	52 kDa	0.56
Latent-transforming growth factor beta-binding protein 3	LTBP3_HUMAN	LTBP3	139 kDa	0.12
Dickkopf-related protein 2	DKK2_HUMAN	DKK2	28 kDa	0.27
Ubiquitin-protein ligase E3A	UBE3A_HUMAN	UBE3A	101 kDa	0.49
Endothelial differentiation-related factor 1	EDF1_HUMAN	EDF1	16 kDa	0.55
Membrane-associated progesterone receptor component 1	PGRC1_HUMAN	PGRMC1	22 kDa	0.44
Sortilin	SORT_HUMAN	SORT1	92 kDa	0.031
Protein FAM3C	FAM3C_HUMAN	FAM3C	25 kDa	0.081
Collagenase 3	MMP13_HUMAN	MMP13	54 kDa	0.13
Nicotinate phosphoribosyltransferase	PNCB_HUMAN	NAPRT1	58 kDa	0.25
Pro-cathepsin H	CATH_HUMAN	CTSH	37 kDa	0.52
Charged multivesicular body protein 4b	CHM4B_HUMAN	CHMP4B	25 kDa	0.48
Vacuolar protein-sorting-associated protein 25	VPS25_HUMAN	VPS25	21 kDa	0.35
E3 ubiquitin-protein ligase MYCBP2	MYCB2_HUMAN	MYCBP2	510 kDa	0.58
SWI/SNF-related matrix-associated actin-dependent regulator of chromatin subfamily E member 1	SMCE1_HUMAN	SMARCE1	47 kDa	0.21
D-tyrosyl-tRNA(Tyr) deacylase 1	DTD1_HUMAN	DTD1	23 kDa	0.23

5'-nucleotidase	SNTD_HUMAN	NTSE	63 kDa	0.069
Integrin beta-6	ITB6_HUMAN	ITGB6	86 kDa	0.054
Inhibin beta B chain	INHBB_HUMAN	INHBB	45 kDa	0.069
Adenylate kinase 2, mitochondrial	KAD2_HUMAN	AK2	26 kDa	0.49
Platelet-derived growth factor C	PDGFC_HUMAN	PDGFC	39 kDa	0.069
Hepatoma-derived growth factor	HDGF_HUMAN	HDGF	27 kDa	0.47
Serine/arginine-rich splicing factor 7	SRSF7_HUMAN	SRSF7	27 kDa	0.3
von Willebrand factor A domain-containing protein 1	VWA1_HUMAN	VWA1	47 kDa	0.079
Peroxiredoxin-4	PRDX4_HUMAN	PRDX4	31 kDa	0.45
Coactosin-like protein	COTL1_HUMAN	COTL1	16 kDa	0.24
Small proline-rich protein 2A	SPR2A_HUMAN	SPRR2A	8 kDa	0.27
Putative pre-mRNA-splicing factor ATP-dependent RNA helicase DHX15	DHX15_HUMAN	DHX15	91 kDa	0.33
SH3 domain-binding protein 1	3BP1_HUMAN	SH3BP1	76 kDa	0.066
Serine/threonine-protein kinase N1	PKN1_HUMAN	PKN1	104 kDa	0.35
Envoplakin	EVPL_HUMAN	EVPL	232 kDa	0.44
Dr1-associated corepressor	NC2A_HUMAN	DRAP1	22 kDa	0.79
Fibronectin type III domain-containing protein 1	FNDC1_HUMAN	FNDC1	206 kDa	0.52
1-phosphatidylinositol 4,5-bisphosphate phosphodiesterase beta-3	PLCB3_HUMAN	PLCB3	139 kDa	0.77
Collagen alpha-1(II) chain	CO2A1_HUMAN	COL2A1	142 kDa	0.45
Anterior gradient protein 2 homolog	AGR2_HUMAN	AGR2	20 kDa	0.47
Bone morphogenetic protein 3	BMP3_HUMAN	BMP3	53 kDa	0.44
Netrin-4	NET4_HUMAN	NTN4	70 kDa	0.44
60S ribosomal protein L15	RL15_HUMAN	RPL15	24 kDa	0.13
Epidermal growth factor receptor kinase substrate 8-like protein 2	ES8L2_HUMAN	EPS8L2	81 kDa	0.21
HLA class I histocompatibility antigen, B-7 alpha chain	1B07_HUMAN	HLA-B	40 kDa	0.31
Semaphorin-3A	SEM3A_HUMAN	SEMA3A	89 kDa	0.44
Inactive tyrosine-protein kinase 7	PTK7_HUMAN	PTK7	118 kDa	0.26
Protein LYRIC	LYRIC_HUMAN	MTDH	64 kDa	0.24
Thioredoxin domain-containing protein 5	TXND5_HUMAN	TXNDC5	48 kDa	0.22
Tissue-type plasminogen activator	TPA_HUMAN	PLAT	63 kDa	0.3
Catechol O-methyltransferase	COMT_HUMAN	COMT	30 kDa	0.41
Heterogeneous nuclear ribonucleoprotein U-like protein 1	HNRL1_HUMAN	HNRNPUL1	96 kDa	0.51
Tissue factor pathway inhibitor	TFPI1_HUMAN	TFPI	35 kDa	0.52
Synaptotagmin-1	SYT1_HUMAN	SYT1	48 kDa	0.59
Calcyphosin	CAYP1_HUMAN	CAPS	21 kDa	0.44
Exostosin-1	EXT1_HUMAN	EXT1	86 kDa	0.25
Transmembrane protein 43	TMM43_HUMAN	TMEM43	45 kDa	0.18
Caspase-14	CASPE_HUMAN	CASP14	28 kDa	0.44
Calpastatin	ICAL_HUMAN	CAST	77 kDa	0.5
Coiled-coil-helix-coiled-coil-helix domain-containing protein 3, mitochondrial	CHCH3_HUMAN	CHCHD3	26 kDa	0.44
A disintegrin and metalloproteinase with thrombospondin motifs 1	ATS1_HUMAN	ADAMTS1	105 kDa	0.44

Complement component 1 Q subcomponent-binding protein, mitochondrial	C1QBP_HUMAN	C1QBP	31 kDa	0.49
Vesicle-associated membrane protein-associated protein A	VAPA_HUMAN	VAPA	28 kDa	0.49
Asparlyl/asparaginyl beta-hydroxylase	ASPH_HUMAN	ASPH	86 kDa	0.081
Malectin	MLEC_HUMAN	MLEC	32 kDa	0.44
Lysine-specific demethylase 2B	KDM2B_HUMAN	KDM2B	153 kDa	0.44
Semaphorin-3G	SEM3G_HUMAN	SEMA3G	87 kDa	0.44
Cytochrome c1, heme protein, mitochondrial	CY1_HUMAN	CYC1	35 kDa	0.44
Kunitz-type protease inhibitor 1	SPIT1_HUMAN	SPINT1	58 kDa	0.44
Plexin-B2	PLXB2_HUMAN	PLXNB2	205 kDa	0.44
Heparan sulfate glucosamine 3-O-sulfotransferase 1	HS3S1_HUMAN	HS3ST1	36 kDa	0.44
Heparan-sulfate 6-O-sulfotransferase 2	H6ST2_HUMAN	HS6ST2	69 kDa	0.44
Neuropilin	NPTN_HUMAN	NPTN	44 kDa	0.44
Thioredoxin-dependent peroxide reductase, mitochondrial	PRDX3_HUMAN	PRDX3	28 kDa	0.44
Prohibitin	PHB_HUMAN	PHB	30 kDa	0.44
Reticulon-3	RTN3_HUMAN	RTN3	113 kDa	0.44
Peptidyl-prolyl cis-trans isomerase FKBP1A	FKBP1A_HUMAN	FKBP1A	12 kDa	0.44
Voltage-dependent anion-selective channel protein 3	VDAC3_HUMAN	VDAC3	31 kDa	0.44

Table 3: List of proteins identified only in leukaemia cell line THP1

Proteins	Accession Number	Alternate ID	Molecular Weight	ANOVA Test (p-value)
Keratin, type I cytoskeletal 10	K1C10_HUMAN	KRT10	59 kDa	0.13
Keratin, type I cytoskeletal 10	K1C10_HUMAN	KRT10	59 kDa	0.053
Keratin, type I cytoskeletal 19	K1C19_HUMAN	KRT19	44 kDa	0.0036
Keratin, type I cytoskeletal 14	K1C14_HUMAN	KRT14	52 kDa	0.19
Keratin, type I cytoskeletal 17	K1C17_HUMAN	KRT17	48 kDa	0.17
Keratin, type I cytoskeletal 16	K1C16_HUMAN	KRT16	51 kDa	0.3
Keratin, type I cytoskeletal 13	K1C13_HUMAN	KRT13	50 kDa	0.087
Keratin, type I cytoskeletal 24	K1C24_HUMAN	KRT24	55 kDa	0.0061
Keratin, type I cytoskeletal 20	K1C20_HUMAN	KRT20	48 kDa	0.6
Keratin, type I cytoskeletal 12	K1C12_HUMAN	KRT12	54 kDa	1
Keratin, type I cytoskeletal 27	K1C27_HUMAN	KRT27	50 kDa	0.44
Keratin, type I cytoskeletal 25	K1C25_HUMAN	KRT25	49 kDa	1
Keratin, type I cuticular Ha3-II	KT33B_HUMAN	KRT33B	46 kDa	1
Keratin, type I cytoskeletal 15	K1C15_HUMAN	KRT15	49 kDa	0.44
Keratin, type I cytoskeletal 26	K1C26_HUMAN	KRT26	52 kDa	1
Keratin-like protein KRT222	KT222_HUMAN	KRT222	34 kDa	1
Endoplasmic	ENPL_HUMAN	HSP90B1	92 kDa	0.043
Putative endoplasmic-like protein	ENPLL_HUMAN	HSP90B2P	46 kDa	0.00015
Complement factor D	CFAD_HUMAN	CFD	27 kDa	0.02

Macrophage-capping protein	CAPG_HUMAN	CAPG	38 kDa	0.024
Carbonic anhydrase 2	CAH2_HUMAN	CA2	29 kDa	0.0032
Azurocidin	CAP7_HUMAN	AZU1	27 kDa	0.0036
Metalloproteinase inhibitor 3	TIMP3_HUMAN	TIMP3	24 kDa	0.0019
Lysosomal alpha-mannosidase	MA2B1_HUMAN	MAN2B1	114 kDa	0.0015
Fermitin family homolog 3	URP2_HUMAN	FERMT3	76 kDa	0.00048
Very low-density lipoprotein receptor	VLDLR_HUMAN	VLDLR	96 kDa	0.095
Carbohydrate sulfotransferase 11	CHSTB_HUMAN	CHST11	42 kDa	0.052
Tyrosine-protein phosphatase non-receptor type 6	PTN6_HUMAN	PTPN6	68 kDa	0.0043
Collagen alpha-3(VI) chain	CO6A3_HUMAN	COL6A3	344 kDa	0.057
Dual specificity mitogen-activated protein kinase kinase 1	MP2K1_HUMAN [2]	MAP2K1	43 kDa	0.00093
Dual specificity mitogen-activated protein kinase kinase 1	MP2K1_HUMAN	MAP2K1	43 kDa	0.0027
Dual specificity mitogen-activated protein kinase kinase 2	MP2K2_HUMAN	MAP2K2	44 kDa	0.00013
Complement component C7	CO7_HUMAN	C7	94 kDa	0.0024
Apolipoprotein A-I	APOA1_HUMAN	APOA1	31 kDa	0.12
E3 ubiquitin-protein ligase CBL	CBL_HUMAN [2]	CBL	100 kDa	0.22
E3 ubiquitin-protein ligase CBL	CBL_HUMAN	CBL	100 kDa	0.15
E3 ubiquitin-protein ligase CBL-B	CBLB_HUMAN	CBLB	109 kDa	0.75
Proteasome subunit beta type-8	PSB8_HUMAN	PSMB8	30 kDa	0.025
Tripeptidyl-peptidase 2	TPP2_HUMAN	TPP2	138 kDa	0.083
60S ribosomal protein L3	RL3_HUMAN	RPL3	46 kDa	0.13
Fibromodulin	FMOD_HUMAN	FMOD	43 kDa	0.0015
Integrin alpha-5	ITA5_HUMAN	ITGA5	115 kDa	0.0027
Pleckstrin	PLEK_HUMAN	PLEK	40 kDa	0.0002
60S ribosomal protein L7	RL7_HUMAN	RPL7	29 kDa	0.21
Gamma-glutamyl hydrolase	GGH_HUMAN	GGH	36 kDa	0.19
Mitogen-activated protein kinase 1	MK01_HUMAN [2]	MAPK1	41 kDa	0.0028
Mitogen-activated protein kinase 1	MK01_HUMAN	MAPK1	41 kDa	0.0021
Mitogen-activated protein kinase 3	MK03_HUMAN	MAPK3	43 kDa	0.44
Growth arrest-specific protein 6	GAS6_HUMAN	GAS6	80 kDa	0.041
Plasma kallikrein	KLKB1_HUMAN	KLKB1	71 kDa	0.16
UDP-glucose:glycoprotein glucosyltransferase 1	UGGG1_HUMAN [2]	UGGT1	177 kDa	0.4
UDP-glucose:glycoprotein glucosyltransferase 1	UGGG1_HUMAN	UGGT1	177 kDa	0.33
UDP-glucose:glycoprotein glucosyltransferase 2	UGGG2_HUMAN	UGGT2	175 kDa	1
Phosphatidylinositol 3,4,5-trisphosphate 5-phosphatase 1	SHIP1_HUMAN	INPP5D	133 kDa	0.053
Cathepsin S	CATS_HUMAN	CTSS	37 kDa	< 0.00010
Acetyl-CoA acetyltransferase, cytosolic	THIC_HUMAN	ACAT2	41 kDa	0.31
Fibrinogen gamma chain	FIBG_HUMAN	FGG	52 kDa	0.097
Hyaluronidase-3	HYAL3_HUMAN	HYAL3	47 kDa	< 0.00010
UMP-CMP kinase	KCY_HUMAN	CMPK1	22 kDa	0.16
Complement component C8 beta chain	CO8B_HUMAN	C8B	67 kDa	0.23
Vitamin K-dependent protein S	PROS_HUMAN	PROS1	75 kDa	0.27

Ethylmalonyl-CoA decarboxylase	ECHD1_HUMAN	ECHDC1	34 kDa	0.038
Transmembrane protein C16orf54	CP054_HUMAN	C16orf54	24 kDa	0.0049
Apolipoprotein C-II	APOC2_HUMAN	APOC2	11 kDa	0.038
60S ribosomal protein L18a	RL18A_HUMAN	RPL18A	21 kDa	0.12
Polypeptide N-acetylgalactosaminyltransferase 2	GALT2_HUMAN	GALNT2	65 kDa	0.067
Phospholipase A-2-activating protein	PLAP_HUMAN	PLAA	87 kDa	0.056
N(G),N(G)-dimethylarginine dimethylaminohydrolase 2	DDAH2_HUMAN	DDAH2	30 kDa	0.0023
Peptidyl-prolyl cis-trans isomerase C	PPIC_HUMAN	PPIC	23 kDa	0.0023
Gamma-glutamyltranspeptidase 1	GGT1_HUMAN	GGT1	61 kDa	0.44
C-type mannose receptor 2	MRC2_HUMAN	MRC2	167 kDa	0.056
Integrin beta-2	ITB2_HUMAN	ITGB2	85 kDa	0.056
Receptor-type tyrosine-protein phosphatase C	PTPRC_HUMAN	PTPRC	147 kDa	0.083
Carboxypeptidase M	CBPM_HUMAN	CPM	51 kDa	0.12
Coagulation factor IX	FA9_HUMAN	F9	52 kDa	0.055
40S ribosomal protein S27	RS27_HUMAN	RPS27	9 kDa	0.1
Deoxynucleoside triphosphate triphosphohydrolase SAMHD1	SAMH1_HUMAN	SAMHD1	72 kDa	0.0057
Dihydrolipoyl dehydrogenase, mitochondrial	DLDH_HUMAN	DLD	54 kDa	0.48
Insulin-like growth factor 2 mRNA-binding protein 2	IF2B2_HUMAN	IGF2BP2	66 kDa	0.35
Testis-specific serine kinase substrate	TSKS_HUMAN	TSKS	65 kDa	0.38
Casein kinase II subunit beta	CSK2B_HUMAN	CSNK2B	25 kDa	0.0016
Protein-methionine sulfoxide oxidase MICAL1	MICA1_HUMAN	MICAL1	118 kDa	0.071
Rho-related GTP-binding protein RhoG	RHOG_HUMAN	RHOG	21 kDa	0.12
Protein tweety homolog 3	TTYH3_HUMAN	TTYH3	58 kDa	0.12
Dipeptidyl peptidase 2	DPP2_HUMAN	DPP7	54 kDa	0.00056
Glutathione peroxidase 1	GPX1_HUMAN	GPX1	22 kDa	0.055
Mesencephalic astrocyte-derived neurotrophic factor	MANF_HUMAN	MANF	21 kDa	0.16
Differentially expressed in FDCP 6 homolog	DEFI6_HUMAN	DEF6	74 kDa	0.055
BAH and coiled-coil domain-containing protein 1	BAHC1_HUMAN	BAHCC1	277 kDa	0.44
Interleukin-6 receptor subunit alpha	IL6RA_HUMAN	IL6R	52 kDa	0.13
Proteasome subunit beta type-10	PSB10_HUMAN	PSMB10	29 kDa	0.13
Nucleobindin-2	NUCB2_HUMAN	NUCB2	50 kDa	0.071
1-phosphatidylinositol 4,5-bisphosphate phosphodiesterase gamma-2	PLCG2_HUMAN	PLCG2	148 kDa	0.13
Golgi-associated plant pathogenesis-related protein 1	GAPR1_HUMAN	GLIPR2	17 kDa	0.032
Prolow-density lipoprotein receptor-related protein 1	LRP1_HUMAN	LRP1	505 kDa	0.055
60S ribosomal protein L18	RL18_HUMAN	RPL18	22 kDa	0.33
Serglycin	SRGN_HUMAN	SRGN	18 kDa	0.00056
Fibrinogen alpha chain	FIBA_HUMAN	FGA	95 kDa	0.56
Probable ATP-dependent RNA helicase DDX6	DDX6_HUMAN	DDX6	54 kDa	0.44
Amyloid beta A4 precursor protein-binding family B member 1-interacting protein	AB1IP_HUMAN	APBB1IP	73 kDa	0.12
Coronin-7	CORO7_HUMAN	CORO7	101 kDa	0.12
Alpha-galactosidase A	AGAL_HUMAN	GLA	49 kDa	0.12

Rho GDP-dissociation inhibitor 2	GDIR2_HUMAN	ARHGDIB	23 kDa	0.2
Complement C1q tumor necrosis factor-related protein 3	C1QT3_HUMAN	C1QTNF3	27 kDa	0.12
Anosmin-1	KALM_HUMAN	KAL1	76 kDa	0.44
3-ketoacyl-CoA thiolase, mitochondrial	THIM_HUMAN	ACAA2	42 kDa	0.54
Procollagen C-endopeptidase enhancer 1	PCOC1_HUMAN	PCOLCE	48 kDa	0.44
Histone deacetylase 2	HDAC2_HUMAN	HDAC2	55 kDa	0.13
Aminopeptidase N	AMPN_HUMAN	ANPEP	110 kDa	0.44
Platelet endothelial cell adhesion molecule	PECA1_HUMAN	PECAM1	83 kDa	0.44
V-type proton ATPase subunit H	VATH_HUMAN	ATP6V1H	56 kDa	0.12
Annexin A11	ANX11_HUMAN	ANXA11	54 kDa	0.076
Serine/threonine-protein phosphatase 1 regulatory subunit 10	PP1RA_HUMAN	PPP1R10	99 kDa	0.59
TBC1 domain family member 5	TBCD5_HUMAN	TBC1D5	89 kDa	0.44
Transcription factor TFIIIB component B'' homolog	BDP1_HUMAN	BDP1	294 kDa	0.057
Ectonucleotide pyrophosphatase/phosphodiesterase family member 2	ENPP2_HUMAN	ENPP2	99 kDa	0.12
Voltage-dependent calcium channel subunit alpha-2/delta-1	CA2D1_HUMAN	CACNA2D1	125 kDa	0.44
Serine/threonine-protein kinase WNK1	WNK1_HUMAN	WNK1	251 kDa	0.44
High affinity immunoglobulin epsilon receptor subunit gamma	FCERG_HUMAN	FCER1G	10 kDa	0.44
Tyrosine-protein kinase HCK	HCK_HUMAN	HCK	60 kDa	0.44
Secretory carrier-associated membrane protein 2	SCAM2_HUMAN	SCAMP2	37 kDa	0.44
Chromatin assembly factor 1 subunit B	CAF1B_HUMAN	CHAF1B	61 kDa	0.44
CUGBP Elav-like family member 2	CELF2_HUMAN	CELF2	54 kDa	0.44
A disintegrin and metalloproteinase with thrombospondin motifs 17	ATS17_HUMAN	ADAMTS17	121 kDa	0.44

Table 4: List of proteins only identified from breast cancer cell line MCF7

Proteins	Accession Number	Alternate ID	Molecular Weight	ANOVA Test (p-value)
Keratin, type II cytoskeletal 8	K2C8_HUMAN	KRT8	54 kDa	0.0002
Keratin, type II cytoskeletal 1	K2C1_HUMAN	KRT1	66 kDa	0.059
Keratin, type II cytoskeletal 2 epidermal	K22E_HUMAN	KRT2	65 kDa	0.07
Keratin, type II cytoskeletal 5	K2C5_HUMAN	KRT5	62 kDa	0.075
Keratin, type II cytoskeletal 7	K2C7_HUMAN	KRT7	51 kDa	0.13
Glial fibrillary acidic protein	GFAP_HUMAN	GFAP	50 kDa	0.025
Keratin, type II cytoskeletal 6A	K2C6A_HUMAN	KRT6A	60 kDa	0.22
Keratin, type II cytoskeletal 6B	K2C6B_HUMAN	KRT6B	60 kDa	0.22
Keratin, type II cytoskeletal 1b	K2C1B_HUMAN	KRT77	62 kDa	0.043
Keratin, type II cytoskeletal 4	K2C4_HUMAN	KRT4	57 kDa	0.22
Keratin, type II cytoskeletal 3	K2C3_HUMAN	KRT3	64 kDa	0.36
Keratin, type II cytoskeletal 75	K2C75_HUMAN	KRT75	60 kDa	0.052
Keratin, type II cytoskeletal 73	K2C73_HUMAN	KRT73	59 kDa	0.59

Keratin, type II cytoskeletal 80	K2C80_HUMAN	KRT80	51 kDa	0.59
Keratin, type II cytoskeletal 78	K2C78_HUMAN	KRT78	57 kDa	0.44
Neurofilament heavy polypeptide	NFH_HUMAN	NEFH	112 kDa	1
Keratin, type II cuticular Hb4	KRT84_HUMAN	KRT84	65 kDa	0.44
Keratin, type II cytoskeletal 74	K2C74_HUMAN	KRT74	58 kDa	0.41
Keratin, type II cytoskeletal 2 oral	K22O_HUMAN	KRT76	66 kDa	0.44
Nuclease-sensitive element-binding protein 1	YBOX1_HUMAN	YBX1	36 kDa	0.0086
Y-box-binding protein 2	YBOX2_HUMAN	YBX2	39 kDa	0.44
Y-box-binding protein 3	YBOX3_HUMAN	YBX3	40 kDa	1
Transportin-1	TNPO1_HUMAN	TNPO1	102 kDa	< 0.00010
Transportin-2	TNPO2_HUMAN	TNPO2	101 kDa	0.074
Latent-transforming growth factor beta-binding protein 1	LTBP1_HUMAN	LTBP1	187 kDa	0.14
Fructose-1,6-bisphosphatase 1	F16P1_HUMAN	FBP1	37 kDa	0.0045
Fructose-1,6-bisphosphatase isozyme 2	F16P2_HUMAN	FBP2	37 kDa	0.067
Dynactin subunit 2	DCTN2_HUMAN	DCTN2	44 kDa	< 0.00010
Glutamine--fructose-6-phosphate aminotransferase [isomerizing] 1	GFPT1_HUMAN	GFPT1	79 kDa	0.37
Glutamine--fructose-6-phosphate aminotransferase [isomerizing] 2	GFPT2_HUMAN	GFPT2	77 kDa	< 0.00010
Creatine kinase U-type, mitochondrial	KCRU_HUMAN	CKMT1A	47 kDa	0.0045
Semaphorin-3C	SEM3C_HUMAN	SEMA3C	85 kDa	0.041
Treacle protein	TCOF_HUMAN	TCOF1	152 kDa	0.073
Transcription elongation factor A protein 1	TCEA1_HUMAN	TCEA1	34 kDa	0.17
Transcription elongation factor A protein 2	TCEA2_HUMAN	TCEA2	34 kDa	0.44
Protein lin-7 homolog C	LIN7C_HUMAN	LIN7C	22 kDa	0.00023
Protein lin-7 homolog A	LIN7A_HUMAN	LIN7A	26 kDa	0.44
Dystroglycan	DAG1_HUMAN	DAG1	97 kDa	0.038
Huntingtin-interacting protein 1-related protein	HIP1R_HUMAN	HIP1R	119 kDa	0.0054
Breast carcinoma-amplified sequence 1	BCAS1_HUMAN	BCAS1	62 kDa	< 0.00010
Neogenin	NEO1_HUMAN	NEO1	160 kDa	0.015
Serine/threonine-protein kinase MST4	MST4_HUMAN [2]	MST4	47 kDa	0.00036
Serine/threonine-protein kinase MST4	MST4_HUMAN	MST4	47 kDa	0.0052
Serine/threonine-protein kinase 24	STK24_HUMAN	STK24	49 kDa	0.084
Clathrin light chain B	CLCB_HUMAN	CLTB	25 kDa	< 0.00010
Microtubule-associated protein tau	TAU_HUMAN	MAPT	79 kDa	< 0.00010
Protein S100-A13	S10AD_HUMAN	S100A13	11 kDa	< 0.00010
LINE-1 retrotransposable element ORF1 protein	LORF1_HUMAN	L1RE1	40 kDa	0.0053
Protein kinase C and casein kinase substrate in neurons protein 3	PACN3_HUMAN	PACSIN3	48 kDa	< 0.00010
Plakophilin-3	PKP3_HUMAN	PKP3	87 kDa	< 0.00010
Squamous cell carcinoma antigen recognized by T-cells 3	SART3_HUMAN	SART3	110 kDa	0.0092
28 kDa heat- and acid-stable phosphoprotein	HAP28_HUMAN	PDAP1	21 kDa	0.003
Protein unc-45 homolog A	UN45A_HUMAN	UNC45A	103 kDa	0.047

26S protease regulatory subunit 6A	PRS6A_HUMAN	PSMC3	49 kDa	0.01
Bifunctional ATP-dependent dihydroxyacetone kinase/FAD-AMP lyase (cyclizing)	DHAK_HUMAN	DAK	59 kDa	0.0034
Na(+)/H(+) exchange regulatory cofactor NHE-RF2	NHRF2_HUMAN	SLC9A3R2	37 kDa	0.063
Dynamin-like 120 kDa protein, mitochondrial	OPA1_HUMAN	OPA1	112 kDa	0.0045
Transmembrane protein 132A	T132A_HUMAN	TMEM132A	110 kDa	0.2
UBX domain-containing protein 1	UBXN1_HUMAN	UBXN1	33 kDa	0.00027
Uncharacterized protein C19orf43	CS043_HUMAN	C19orf43	18 kDa	0.001
26S proteasome non-ATPase regulatory subunit 8	PSMD8_HUMAN	PSMD8	40 kDa	0.0004
Thrombospondin type-1 domain-containing protein 4	THSD4_HUMAN	THSD4	112 kDa	0.0014
Stromal cell-derived factor 1	SDF1_HUMAN	CXCL12	11 kDa	< 0.00010
Leucine-rich repeat protein SHOC-2	SHOC2_HUMAN	SHOC2	65 kDa	0.0004
26S proteasome non-ATPase regulatory subunit 14	PSDE_HUMAN	PSMD14	35 kDa	0.13
Leucine--tRNA ligase, cytoplasmic	SYLC_HUMAN	LARS	134 kDa	0.0078
Arfaptin-2	ARFP2_HUMAN	ARFIP2	38 kDa	< 0.00010
Protein enabled homolog	ENAH_HUMAN	ENAH	67 kDa	0.1
Phenylalanine--tRNA ligase beta subunit	SYFB_HUMAN	FARSB	66 kDa	0.073
Heat shock protein 75 kDa, mitochondrial	TRAP1_HUMAN	TRAP1	80 kDa	0.44
EH domain-containing protein 1	EHD1_HUMAN	EHD1	61 kDa	0.083
General transcription factor IIF subunit 1	T2FA_HUMAN	GTF2F1	58 kDa	< 0.00010
Sorcin	SORCN_HUMAN	SRI	22 kDa	0.018
Dynactin subunit 3	DCTN3_HUMAN	DCTN3	21 kDa	0.1
COP9 signalosome complex subunit 6	CSN6_HUMAN	COPS6	36 kDa	0.25
Cleavage stimulation factor subunit 2	CSTF2_HUMAN	CSTF2	61 kDa	0.0004
Serine/threonine-protein phosphatase 2A 56 kDa regulatory subunit epsilon isoform	2A5E_HUMAN	PPP2R5E	55 kDa	0.0009
ATPase ASNA1	ASNA_HUMAN	ASNA1	39 kDa	< 0.00010
Calsyntenin-3	CSTN3_HUMAN	CLSTN3	106 kDa	0.08
Luc7-like protein 3	LC7L3_HUMAN	LUC7L3	51 kDa	< 0.00010
Tetratricopeptide repeat protein 1	TTC1_HUMAN	TTC1	34 kDa	0.065
Coiled-coil domain-containing protein 6	CCDC6_HUMAN	CCDC6	53 kDa	0.34
G-protein coupled receptor 126	GP126_HUMAN	GPR126	137 kDa	< 0.00010
Prefoldin subunit 6	PFD6_HUMAN	PFDN6	15 kDa	0.074
Cell division cycle and apoptosis regulator protein 1	CCAR1_HUMAN	CCAR1	133 kDa	0.11
Nck-associated protein 1	NCKP1_HUMAN	NCKAP1	129 kDa	0.065
Brain-specific angiogenesis inhibitor 1-associated protein 2-like protein 1	BI2L1_HUMAN	BAIAP2L1	57 kDa	0.00047
Electron transfer flavoprotein subunit beta	ETFB_HUMAN	ETFB	28 kDa	0.1
Transcription factor BTF3	BTF3_HUMAN	BTF3	22 kDa	0.00047
Kinesin light chain 2	KLC2_HUMAN [2]	KLC2	69 kDa	0.055
Kinesin light chain 2	KLC2_HUMAN	KLC2	69 kDa	0.055
Kinesin light chain 1	KLC1_HUMAN	KLC1	65 kDa	1
SWI/SNF complex subunit SMARCC2	SMRC2_HUMAN	SMARCC2	133 kDa	0.14

Protein phosphatase methylesterase 1	PPME1_HUMAN	PPME1	42 kDa	0.24
182 kDa tankyrase-1-binding protein	TB182_HUMAN	TNKS1BP1	182 kDa	0.062
Signal recognition particle subunit SRP72	SRP72_HUMAN	SRP72	75 kDa	0.00024
Syntaxin-binding protein 3	STXB3_HUMAN	STXBP3	68 kDa	0.084
Formin-binding protein 1-like	FBP1L_HUMAN	FNBP1L	70 kDa	0.022
Arfaptin-1	ARFP1_HUMAN	ARFIP1	42 kDa	0.0034
E3 ubiquitin-protein ligase TRIM33	TRI33_HUMAN	TRIM33	123 kDa	0.0016
Vasorin	VASN_HUMAN	VASN	72 kDa	0.59
GRIP1-associated protein 1	GRAP1_HUMAN	GRIPAP1	96 kDa	0.00088
Caldesmon	CALD1_HUMAN	CALD1	93 kDa	0.32
Oxysterol-binding protein 1	OSBP1_HUMAN	OSBP	89 kDa	0.26
Neurogenic locus notch homolog protein 2	NOTC2_HUMAN	NOTCH2	265 kDa	0.44
PCTP-like protein	PCTL_HUMAN	STARD10	33 kDa	0.052
Tubulin gamma-1 chain	TBG1_HUMAN (+1)	TUBG1	51 kDa	0.011
N-acetylserotonin O-methyltransferase-like protein	ASML_HUMAN	ASMTL	69 kDa	0.22
Neural cell adhesion molecule L1	L1CAM_HUMAN	L1CAM	140 kDa	0.44
Tyrosine-protein kinase receptor UFO	UFO_HUMAN	AXL	98 kDa	0.24
Negative elongation factor E	NELFE_HUMAN	NELFE	43 kDa	0.26
PDZ domain-containing protein GIPC1	GIPC1_HUMAN	GIPC1	36 kDa	0.0045
General transcription factor II-I	GTF2I_HUMAN	GTF2I	112 kDa	0.28
Guanine nucleotide-binding protein subunit alpha-13	GNA13_HUMAN	GNA13	44 kDa	0.00024
Telomeric repeat-binding factor 2-interacting protein 1	TE2IP_HUMAN	TERF2IP	44 kDa	0.0016
mRNA export factor	RAE1L_HUMAN	RAE1	41 kDa	< 0.00010
S-phase kinase-associated protein 1	SKP1_HUMAN	SKP1	19 kDa	0.027
Pyridoxal-dependent decarboxylase domain-containing protein 1	PDXD1_HUMAN	PDXDC1	87 kDa	0.074
Methionine aminopeptidase 1	MAP11_HUMAN	METAP1	43 kDa	0.0011
CDK5 regulatory subunit-associated protein 3	CK5P3_HUMAN	CDK5RAP3	57 kDa	0.00024
YLP motif-containing protein 1	YLPM1_HUMAN	YLPM1	220 kDa	0.074
ATP-dependent RNA helicase DHX29	DHX29_HUMAN	DHX29	155 kDa	0.1
Epidermal growth factor receptor kinase substrate 8	EPS8_HUMAN	EPS8	92 kDa	0.26
Charged multivesicular body protein 2b	CHM2B_HUMAN	CHMP2B	24 kDa	0.15
Leucine-rich repeat flightless-interacting protein 2	LRRF2_HUMAN	LRRFIP2	82 kDa	0.0045
Protein TFG	TFG_HUMAN	TFG	43 kDa	0.0044
Alpha-taxilin	TXLNA_HUMAN	TXLNA	62 kDa	0.23
Transcription elongation factor B polypeptide 2	ELOB_HUMAN	TCEB2	13 kDa	0.0077
Extracellular sulfatase Sulf-2	SULF2_HUMAN	SULF2	100 kDa	0.33
Attractin	ATRN_HUMAN	ATRN	159 kDa	0.51
Cytoplasmic dynein 1 light intermediate chain 2	DC1L2_HUMAN	DYNC1LI2	54 kDa	0.14
MAGUK p55 subfamily member 7	MPP7_HUMAN	MPP7	66 kDa	0.44
Phosphoribosyl pyrophosphate synthase-associated protein 1	KPRA_HUMAN	PRPSAP1	39 kDa	0.17
RNA-binding protein 10	RBM10_HUMAN	RBM10	104 kDa	0.058

Serpin H1	SERPH_HUMAN	SERPINH1	46 kDa	0.12
Ras-related protein Rab-7a	RAB7A_HUMAN	RAB7A	23 kDa	0.51
Shootin-1	SHOT1_HUMAN	KIAA1598	72 kDa	0.11
Coatomer subunit epsilon	COPE_HUMAN	COPE	34 kDa	0.26
Pleckstrin homology domain-containing family F member 2	PKHF2_HUMAN	PLEKHF2	28 kDa	< 0.00010
Nuclear cap-binding protein subunit 1	NCBP1_HUMAN	NCBP1	92 kDa	0.084
Glutamine-dependent NAD(+) synthetase	NADE_HUMAN	NADSYN1	79 kDa	0.053
Nuclear valosin-containing protein-like	NVL_HUMAN	NVL	95 kDa	< 0.00010
Peripheral plasma membrane protein CASK	CSKP_HUMAN	CASK	105 kDa	0.44
Protein transport protein Sec16A	SC16A_HUMAN	SEC16A	234 kDa	0.56
DNA repair protein XRCC1	XRCC1_HUMAN	XRCC1	69 kDa	0.22
Desmoglein-2	DSG2_HUMAN	DSG2	122 kDa	0.44
Proteasome-associated protein ECM29 homolog	ECM29_HUMAN	ECM29	204 kDa	0.092
DNA repair protein complementing XP-C cells	XPC_HUMAN	XPC	106 kDa	0.17
26S proteasome non-ATPase regulatory subunit 10	PSD10_HUMAN	PSMD10	24 kDa	0.14
60S acidic ribosomal protein P1	RLA1_HUMAN	RPLP1	12 kDa	0.012
DnaJ homolog subfamily C member 17	DJC17_HUMAN	DNAJC17	35 kDa	0.084
Dihydropyrimidinase-related protein 1	DPYL1_HUMAN	CRMP1	62 kDa	0.093
AP-1 complex subunit mu-2	AP1M2_HUMAN	AP1M2	48 kDa	0.12
SNW domain-containing protein 1	SNW1_HUMAN	SNW1	61 kDa	0.15
Translin	TSN_HUMAN	TSN	26 kDa	0.19
Eukaryotic translation initiation factor 2 subunit 2	IF2B_HUMAN	EIF2S2	38 kDa	0.084
Low-density lipoprotein receptor	LDLR_HUMAN	LDLR	95 kDa	0.17
Methylcytosine dioxygenase TET3	TET3_HUMAN	TET3	179 kDa	0.45
Amphiregulin	AREG_HUMAN	AREG	28 kDa	0.44
Sodium- and chloride-dependent taurine transporter	SC6A6_HUMAN	SLC6A6	70 kDa	0.44
Serine hydroxymethyltransferase, cytosolic	GLYC_HUMAN	SHMT1	53 kDa	0.084
Regulation of nuclear pre-mRNA domain-containing protein 1A	RPR1A_HUMAN	RPRD1A	36 kDa	0.11
Abl interactor 2	ABI2_HUMAN	ABI2	56 kDa	0.11
REST corepressor 1	RCOR1_HUMAN	RCOR1	53 kDa	0.58
Enoyl-CoA hydratase, mitochondrial	ECHM_HUMAN	ECHS1	31 kDa	0.44
Wiskott-Aldrich syndrome protein family member 2	WASF2_HUMAN	WASF2	54 kDa	0.084
Receptor expression-enhancing protein 6	REEP6_HUMAN	REEP6	21 kDa	0.069
PRKC apoptosis WT1 regulator protein	PAWR_HUMAN	PAWR	37 kDa	0.13
Biliverdin reductase A	BIEA_HUMAN	BLVRA	33 kDa	0.11
Cleavage stimulation factor subunit 3	CSTF3_HUMAN	CSTF3	83 kDa	0.11
Protein IWS1 homolog	IWS1_HUMAN	IWS1	92 kDa	0.44
Inverted formin-2	INF2_HUMAN	INF2	136 kDa	0.44
Importin subunit alpha-7	IMA7_HUMAN	KPNA6	60 kDa	0.053
Zinc finger CCCH domain-containing protein 4	ZC3H4_HUMAN	ZC3H4	140 kDa	0.14
Endophilin-A2	SH3G1_HUMAN (+1)	SH3GL1	41 kDa	0.44
Tsukushin	TSK_HUMAN	TSKU	38 kDa	0.58

ADP-ribosylation factor-like protein 3	ARL3_HUMAN	ARL3	20 kDa	0.56
Microfibrillar-associated protein 1	MFAP1_HUMAN	MFAP1	52 kDa	0.062
AH receptor-interacting protein	AIP_HUMAN	AIP	38 kDa	0.084
U4/U6 small nuclear ribonucleoprotein Prp31	PRP31_HUMAN	PRPF31	55 kDa	0.11
Melanoma-associated antigen D2	MAGD2_HUMAN	MAGED2	65 kDa	0.44
Proteins	Accession Number	Alternate ID	Molecular Weight	ANOVA Test (p-value)
Calcium-regulated heat stable protein 1	CHSP1_HUMAN	CARHSP1	16 kDa	0.062
Apoptotic chromatin condensation inducer in the nucleus	ACINU_HUMAN	ACIN1	152 kDa	0.17
Grancalcin	GRAN_HUMAN	GCA	24 kDa	0.084
SEC23-interacting protein	S23IP_HUMAN	SEC23IP	111 kDa	0.44
Kelch domain-containing protein 4	KLDC4_HUMAN	KLHDC4	58 kDa	0.11
Exportin-5	XPO5_HUMAN	XPO5	136 kDa	0.44
YTH domain-containing protein 1	YTDC1_HUMAN	YTHDC1	85 kDa	0.084
Arf-GAP with coiled-coil, ANK repeat and PH domain-containing protein 2	ACAP2_HUMAN	ACAP2	88 kDa	0.44
Importin-9	IPO9_HUMAN	IPO9	116 kDa	0.44
Epidermal growth factor receptor substrate 15	EPS15_HUMAN	EPS15	99 kDa	0.44
Epidermal growth factor receptor kinase substrate 8-like protein 1	ES8L1_HUMAN	EPS8L1	80 kDa	0.44
PERQ amino acid-rich with GYF domain-containing protein 2	PERQ2_HUMAN	GIGYF2	150 kDa	0.014
Hyaluronan mediated motility receptor	HMMR_HUMAN	HMMR	84 kDa	0.44
Villin-1	VILI_HUMAN	VIL1	93 kDa	0.44
Septin-8	SEPT8_HUMAN	Sep-08	56 kDa	0.15
Gamma-soluble NSF attachment protein	SNAG_HUMAN	NAPG	35 kDa	0.44
Cold shock domain-containing protein E1	CSDE1_HUMAN	CSDE1	89 kDa	0.44
Platelet glycoprotein 4	CD36_HUMAN	CD36	53 kDa	0.44
Splicing factor U2AF 65 kDa subunit	U2AF2_HUMAN	U2AF2	54 kDa	0.44
Protein ITFG3	ITFG3_HUMAN	ITFG3	60 kDa	0.44
Protein tyrosine phosphatase type IVA 2	TP4A2_HUMAN	PTP4A2	19 kDa	0.44
Fragile X mental retardation syndrome-related protein 1	FXR1_HUMAN	FXR1	70 kDa	0.44
E3 ubiquitin-protein ligase ARIH1	ARI1_HUMAN	ARIH1	64 kDa	0.44
Dynein light chain 1, cytoplasmic	DYL1_HUMAN	DYNLL1	10 kDa	0.053
Protein FAM98A	FA98A_HUMAN	FAM98A	55 kDa	0.44
Ephrin type-B receptor 4	EPHB4_HUMAN	EPHB4	108 kDa	0.44
Flavin reductase (NADPH)	BLVRB_HUMAN	BLVRB	22 kDa	0.44
Trefoil factor 1	TFF1_HUMAN	TFF1	9 kDa	0.44
Translation initiation factor eIF-2B subunit delta	EI2BD_HUMAN	EIF2B4	58 kDa	0.44
DNA damage-binding protein 2	DDB2_HUMAN	DDB2	48 kDa	0.44
Immunoglobulin superfamily member 3	IGSF3_HUMAN	IGSF3	135 kDa	0.44
ADP-ribosylation factor 6	ARF6_HUMAN	ARF6	20 kDa	0.44
Tubulin-specific chaperone D	TBCD_HUMAN	TBCD	133 kDa	0.44

Table 5: List of proteins identified only from primary lung cell HBTE

Myosin-9	MYH9_HUMAN	MYH9	227 kDa	0.32
Endoplasmic	ENPL_HUMAN	HSP90B1	92 kDa	0.029
Spectrin beta chain, non-erythrocytic 1	SPTB2_HUMAN	SPTBN1	275 kDa	0.034
Eukaryotic translation initiation factor 4 gamma 1	IF4G1_HUMAN	EIF4G1	175 kDa	< 0.00010
Poly [ADP-ribose] polymerase 1	PARP1_HUMAN	PARP1	113 kDa	0.0005
Phosphoglycerate mutase 1	PGAM1_HUMAN	PGAM1	29 kDa	0.052
Argininosuccinate synthase	ASSY_HUMAN	ASS1	47 kDa	0.0038
RNA-binding protein FUS	FUS_HUMAN	FUS	53 kDa	< 0.00010
Eukaryotic translation initiation factor 3 subunit A	EIF3A_HUMAN	EIF3A	167 kDa	0.0015
Tryptophan--tRNA ligase, cytoplasmic	SYWC_HUMAN	WARS	53 kDa	< 0.00010
Tyrosine--tRNA ligase, cytoplasmic	SYYC_HUMAN	YARS	59 kDa	< 0.00010
Transportin-1	TNPO1_HUMAN	TNPO1	102 kDa	< 0.00010
Lysine--tRNA ligase	SYK_HUMAN	KARS	68 kDa	0.0006
Vasodilator-stimulated phosphoprotein	VASP_HUMAN	VASP	40 kDa	< 0.00010
Heterogeneous nuclear ribonucleoprotein H	HNRH1_HUMAN	HNRNPH1	49 kDa	0.00089
Macrophage-capping protein	CAPG_HUMAN	CAPG	38 kDa	0.024
Latent-transforming growth factor beta-binding protein 1	LTBP1_HUMAN	LTBP1	187 kDa	0.14
Ras-related protein Rab-14	RAB14_HUMAN	RAB14	24 kDa	0.13
Splicing factor 3A subunit 1	SF3A1_HUMAN	SF3A1	89 kDa	< 0.00010
Calcyclin-binding protein	CYBP_HUMAN	CACYBP	26 kDa	< 0.00010
Programmed cell death protein 4	PDCD4_HUMAN	PDCD4	52 kDa	< 0.00010
Protein phosphatase 1G	PPM1G_HUMAN	PPM1G	59 kDa	0.0021
Heterogeneous nuclear ribonucleoprotein A3	ROA3_HUMAN	HNRNPA3	40 kDa	0.0087
KH domain-containing, RNA-binding, signal transduction-associated protein 1	KHDR1_HUMAN	KHDRBS1	48 kDa	0.023
Dynactin subunit 2	DCTN2_HUMAN	DCTN2	44 kDa	< 0.00010
Epiplakin	EPIPL_HUMAN	EPPK1	556 kDa	0.0016
Heterogeneous nuclear ribonucleoprotein M	HNRPM_HUMAN	HNRNPM	78 kDa	0.00017
Actin-related protein 2/3 complex subunit 5	ARPC5_HUMAN	ARPC5	16 kDa	0.084
Heat shock protein 105 kDa	HS105_HUMAN	HSPH1	97 kDa	0.0031
Zyxin	ZYX_HUMAN	ZYX	61 kDa	0.00043
Carbonic anhydrase 2	CAH2_HUMAN	CA2	29 kDa	0.0032
E3 ubiquitin-protein ligase HUWE1	HUWE1_HUMAN	HUWE1	482 kDa	0.032
Actin-related protein 2/3 complex subunit 3	ARPC3_HUMAN	ARPC3	21 kDa	0.059
Exportin-1	XPO1_HUMAN	XPO1	123 kDa	0.092
Basic leucine zipper and W2 domain-containing protein 1	BZW1_HUMAN	BZW1	48 kDa	0.0065
Histone-binding protein RBBP7	RBBP7_HUMAN	RBBP7	48 kDa	0.00048
Septin-7	SEPT7_HUMAN	Sep-07	51 kDa	0.0066

Hexokinase-1	HXK1_HUMAN	HK1	102 kDa	0.025
40S ribosomal protein S4, X isoform	RS4X_HUMAN	RPS4X	30 kDa	0.2
Glutathione S-transferase Mu 3	GSTM3_HUMAN	GSTM3	27 kDa	0.0038
Microtubule-associated protein RP/EB family member 1	MARE1_HUMAN	MAPRE1	30 kDa	0.00055
Receptor expression-enhancing protein 5	REEP5_HUMAN	REEP5	21 kDa	0.0009
Protein S100-A4	S10A4_HUMAN	S100A4	12 kDa	0.00029
Splicing factor 1	SF01_HUMAN	SF1	68 kDa	0.00019
Drebrin-like protein	DBNL_HUMAN	DBNL	48 kDa	0.0008
Coatomer subunit beta	COPB_HUMAN	COPB1	107 kDa	0.2
Sorting nexin-1	SNX1_HUMAN	SNX1	59 kDa	0.00033
26S proteasome non-ATPase regulatory subunit 7	PSMD7_HUMAN	PSMD7	37 kDa	0.13
Putative RNA-binding protein Luc7-like 2	LC7L2_HUMAN	LUC7L2	47 kDa	0.0075
DnaJ homolog subfamily B member 1	DNJB1_HUMAN	DNAJB1	38 kDa	0.003
COP9 signalosome complex subunit 2	CSN2_HUMAN	COPS2	52 kDa	0.025
NADP-dependent malic enzyme	MAOX_HUMAN	ME1	64 kDa	0.028
Src substrate cortactin	SRC8_HUMAN	CTTN	62 kDa	0.00054
Microtubule-actin cross-linking factor 1, isoforms 1/2/3/5	MACF1_HUMAN	MACF1	838 kDa	0.083
Aconitate hydratase, mitochondrial	ACON_HUMAN	ACO2	85 kDa	< 0.00010
Coronin-1C	COR1C_HUMAN	CORO1C	53 kDa	0.14
Creatine kinase U-type, mitochondrial	KCRU_HUMAN	CKMT1A	47 kDa	0.0045
60S ribosomal protein L5	RL5_HUMAN	RPL5	34 kDa	0.19
Dynamin-1-like protein	DNM1L_HUMAN	DNM1L	82 kDa	0.25
Eukaryotic translation initiation factor 5A-1	IF5A1_HUMAN	EIF5A	17 kDa	0.0011
Proprotein convertase subtilisin/kexin type 9	PCSK9_HUMAN	PCSK9	74 kDa	0.0072
Cullin-4B	CUL4B_HUMAN	CUL4B	104 kDa	0.0067
Fermitin family homolog 3	URP2_HUMAN	FERMT3	76 kDa	0.00048
ATP-dependent RNA helicase DDX3X	DDX3X_HUMAN	DDX3X	73 kDa	0.049
Transcription elongation factor A protein 1	TCEA1_HUMAN	TCEA1	34 kDa	0.15
L-xylulose reductase	DCXR_HUMAN	DCXR	26 kDa	0.27
Puromycin-sensitive aminopeptidase	PSA_HUMAN	NPEPPS	103 kDa	0.00019
Ras-related protein Rab-5C	RAB5C_HUMAN	RAB5C	23 kDa	0.91
Protein lin-7 homolog C	LIN7C_HUMAN	LIN7C	22 kDa	0.0014
Ataxin-10	ATX10_HUMAN	ATXN10	53 kDa	0.037
Glyoxylate reductase/hydroxypyruvate reductase	GRHPR_HUMAN	GRHPR	36 kDa	0.046
Eukaryotic translation initiation factor 5B	IF2P_HUMAN	EIF5B	139 kDa	0.17
Microtubule-associated protein 4	MAP4_HUMAN	MAP4	121 kDa	0.14
40S ribosomal protein S14	RS14_HUMAN	RPS14	16 kDa	0.093
Small glutamine-rich tetratricopeptide repeat-containing protein alpha	SGTA_HUMAN	SGTA	34 kDa	0.012

Serine/threonine-protein phosphatase 5	PPP5_HUMAN	PPP5C	57 kDa	0.26
Testican-1	TICN1_HUMAN	SPOCK1	49 kDa	0.00011
Prostaglandin F2 receptor negative regulator	FPRP_HUMAN	PTGFRN	99 kDa	0.052
Importin-5	IPO5_HUMAN	IPO5	124 kDa	0.016
Aspartate--tRNA ligase, cytoplasmic	SYDC_HUMAN	DARS	57 kDa	0.11
Renin receptor	RENH_HUMAN	ATP6AP2	39 kDa	0.041
40S ribosomal protein S10	RS10_HUMAN	RPS10	19 kDa	0.0096
Alpha-internexin	AINX_HUMAN	INA	55 kDa	0.00029
Complement C1r subcomponent-like protein	C1RL_HUMAN	C1RL	53 kDa	< 0.00010
Transcription elongation factor B polypeptide 1	ELOC_HUMAN	TCEB1	12 kDa	0.031
Aminoacyl tRNA synthase complex-interacting multifunctional protein 1	AIMP1_HUMAN	AIMP1	34 kDa	0.00066
Isocitrate dehydrogenase [NADP], mitochondrial	IDHP_HUMAN	IDH2	51 kDa	0.15
Epidermal growth factor receptor substrate 15-like 1	EP15R_HUMAN	EPS15L1	94 kDa	0.032
Small nuclear ribonucleoprotein-associated proteins B and B'	RSMB_HUMAN	SNRPB	25 kDa	0.22
Dystroglycan	DAG1_HUMAN	DAG1	97 kDa	0.038
Dextrin	DEST_HUMAN	DSTN	19 kDa	0.24
Huntingtin-interacting protein 1-related protein	HIP1R_HUMAN	HIP1R	119 kDa	0.0054
Adenylate kinase isoenzyme 1	KAD1_HUMAN	AK1	22 kDa	< 0.00010
Arginine--tRNA ligase, cytoplasmic	SYRC_HUMAN	RARS	75 kDa	0.049
Eukaryotic translation initiation factor 4 gamma 2	IF4G2_HUMAN	EIF4G2	102 kDa	0.094
Nucleobindin-1	NUCB1_HUMAN	NUCB1	54 kDa	0.12
Programmed cell death protein 6	PDCD6_HUMAN	PDCD6	22 kDa	0.0023
Polyadenylate-binding protein-interacting protein 1	PAIP1_HUMAN	PAIP1	54 kDa	0.015
Secretogranin-2	SCG2_HUMAN	SCG2	71 kDa	0.0028
Ubiquitin carboxyl-terminal hydrolase 5	UBP5_HUMAN	USP5	96 kDa	0.069
Nuclear protein localization protein 4 homolog	NPL4_HUMAN	NPLOC4	68 kDa	0.021
Signal recognition particle subunit SRP68	SRP68_HUMAN	SRP68	71 kDa	0.16
Programmed cell death protein 10	PDC10_HUMAN	PDCD10	25 kDa	0.0014
ADP-ribosylation factor 3	ARF3_HUMAN	ARF3	21 kDa	0.2
Ribose-phosphate pyrophosphokinase 1	PRPS1_HUMAN	PRPS1	35 kDa	0.33
Early endosome antigen 1	EEA1_HUMAN	EEA1	162 kDa	0.17
Hepatoma-derived growth factor-related protein 2	HDGR2_HUMAN	HDGFRP2	74 kDa	0.06
Ig kappa chain C region	IGKC_HUMAN	IGKC	12 kDa	< 0.00010
40S ribosomal protein S8	RS8_HUMAN	RPS8	24 kDa	0.041
Collagen alpha-3(VI) chain	CO6A3_HUMAN	COL6A3	344 kDa	0.057
Peptidyl-prolyl cis-trans isomerase FKBP5	FKBP5_HUMAN	FKBP5	51 kDa	0.12

Eukaryotic translation initiation factor 4H	IF4H_HUMAN	EIF4H	27 kDa	0.032
Dual specificity mitogen-activated protein kinase kinase 1	MP2K1_HUMAN	MAP2K1	43 kDa	0.00093
Angiotensinogen	ANGT_HUMAN	AGT	53 kDa	0.0069
Heterogeneous nuclear ribonucleoprotein U-like protein 2	HNRL2_HUMAN	HNRNPUL2	85 kDa	0.1
Endophilin-B2	SHLB2_HUMAN	SH3GLB2	44 kDa	0.003
Leucine zipper transcription factor-like protein 1	LZTL1_HUMAN	LZTFL1	35 kDa	0.00059
Cystathionine beta-synthase	CBS_HUMAN	CBS	61 kDa	0.55
Ferritin light chain	FRIL_HUMAN	FTL	20 kDa	0.011
SUMO-activating enzyme subunit 2	SAE2_HUMAN	UBA2	71 kDa	0.058
Protein phosphatase 1 regulatory subunit 12A	MYPT1_HUMAN	PPP1R12A	115 kDa	0.24
40S ribosomal protein S11	RS11_HUMAN	RPS11	18 kDa	0.0096
Adenosine kinase	ADK_HUMAN	ADK	41 kDa	< 0.00010
Cullin-3	CUL3_HUMAN	CUL3	89 kDa	0.11
Myelin P2 protein	MYP2_HUMAN	PMP2	15 kDa	< 0.00010
40S ribosomal protein S6	RS6_HUMAN	RPS6	29 kDa	0.28
Squamous cell carcinoma antigen recognized by T-cells 3	SART3_HUMAN	SART3	110 kDa	0.0092
Prefoldin subunit 5	PFD5_HUMAN	PFDN5	17 kDa	0.017
Apolipoprotein A-I	APOA1_HUMAN	APOA1	31 kDa	0.12
Prefoldin subunit 3	PFD3_HUMAN	VBP1	23 kDa	0.25
DnaJ homolog subfamily A member 1	DNJA1_HUMAN	DNJA1	45 kDa	0.14
40S ribosomal protein S9	RS9_HUMAN	RPS9	23 kDa	0.23
Ran GTPase-activating protein 1	RAGP1_HUMAN	RANGAP1	64 kDa	0.0056
NSFL1 cofactor p47	NSFL1C_HUMAN	NSFL1C	41 kDa	0.0015
26S protease regulatory subunit 4	PRS4_HUMAN	PSMC1	49 kDa	0.016
Cytoplasmic dynein 1 intermediate chain 2	DC1I2_HUMAN	DYNC1I2	71 kDa	0.048
Kininogen-1	KNG1_HUMAN	KNG1	72 kDa	< 0.00010
60S ribosomal protein L3	RL3_HUMAN	RPL3	46 kDa	0.13
Fibromodulin	FMOD_HUMAN	FMOD	43 kDa	0.0015
26S protease regulatory subunit 6A	PRS6A_HUMAN	PSMC3	49 kDa	0.01
Bifunctional ATP-dependent dihydroxyacetone kinase/FAD-AMP lyase (cyclizing)	DHAK_HUMAN	DAK	59 kDa	0.0034
Monocyte differentiation antigen CD14	CD14_HUMAN	CD14	40 kDa	0.00061
U6 snRNA-associated Sm-like protein LSM6	LSM6_HUMAN	LSM6	9 kDa	0.088
Transmembrane protein 132A	T132A_HUMAN	TMEM132A	110 kDa	0.2
Synaptic vesicle membrane protein VAT-1 homolog-like	VAT1L_HUMAN	VAT1L	46 kDa	< 0.00010
Probable aminopeptidase NPEPL1	PEPL1_HUMAN	NPEPL1	56 kDa	0.17
Splicing factor U2AF 35 kDa subunit	U2AF1_HUMAN	U2AF1	28 kDa	0.092
60S ribosomal protein L7	RL7_HUMAN	RPL7	29 kDa	0.21

Angiopoietin-related protein 4	ANGL4_HUMAN	ANGPTL4	45 kDa	0.0047
Transgelin	TAGL_HUMAN	TAGLN	23 kDa	< 0.00010
60S ribosomal protein L28	RL28_HUMAN	RPL28	16 kDa	0.18
Gamma-glutamyl hydrolase	GGH_HUMAN	GGH	36 kDa	0.19
Vigilin	VIGLN_HUMAN	HDLBP	141 kDa	0.42
Disintegrin and metalloproteinase domain-containing protein 10	ADA10_HUMAN	ADAM10	84 kDa	0.2
SUMO-activating enzyme subunit 1	SAE1_HUMAN	SAE1	38 kDa	0.32
S-formylglutathione hydrolase	ESTD_HUMAN	ESD	31 kDa	0.25
Endophilin-B1	SHLB1_HUMAN	SH3GLB1	41 kDa	0.11
26S proteasome non-ATPase regulatory subunit 14	PSDE_HUMAN	PSMD14	35 kDa	0.13
60S ribosomal protein L10-like	RL10L_HUMAN	RPL10L	25 kDa	0.44
Leucine--tRNA ligase, cytoplasmic	SYLC_HUMAN	LARS	134 kDa	0.0078
COP9 signalosome complex subunit 7b	CSN7B_HUMAN	COPS7B	30 kDa	0.0081
Importin subunit alpha-3	IMA3_HUMAN	KPNA4	58 kDa	0.31
E3 SUMO-protein ligase RanBP2	RBP2_HUMAN	RANBP2	358 kDa	0.47
Mitogen-activated protein kinase 1	MK01_HUMAN	MAPK1	41 kDa	0.0028
Fibrillin-2	FBN2_HUMAN	FBN2	315 kDa	0.24
Phenylalanine--tRNA ligase beta subunit	SYFB_HUMAN	FARSB	66 kDa	0.073
EH domain-containing protein 1	EHD1_HUMAN	EHD1	61 kDa	0.083
Growth arrest-specific protein 6	GAS6_HUMAN	GAS6	80 kDa	0.041
Glutathione S-transferase omega-1	GSTO1_HUMAN	GSTO1	28 kDa	0.24
Sorcini	SORCN_HUMAN	SRI	22 kDa	0.018
Calcium-dependent secretion activator 1	CAPS1_HUMAN	CADPS	153 kDa	0.0081
Dynactin subunit 3	DCTN3_HUMAN	DCTN3	21 kDa	0.1
COP9 signalosome complex subunit 6	CSN6_HUMAN	COPS6	36 kDa	0.25
Adenylosuccinate lyase	PUR8_HUMAN	ADSL	55 kDa	0.72
Plasma kallikrein	KLKB1_HUMAN	KLKB1	71 kDa	0.16
26S proteasome non-ATPase regulatory subunit 12	PSD12_HUMAN	PSMD12	53 kDa	0.26
Apolipoprotein B-100	APOB_HUMAN	APOB	516 kDa	0.18
DAZ-associated protein 1	DAZP1_HUMAN	DAZAP1	43 kDa	0.11
Putative 40S ribosomal protein S26-like 1	RS26L_HUMAN	RPS26P11	13 kDa	0.24
UDP-glucose:glycoprotein glucosyltransferase 1	UGGG1_HUMAN	UGGT1	177 kDa	0.4
Serine/threonine-protein phosphatase 2A 56 kDa regulatory subunit epsilon isoform	2A5E_HUMAN	PPP2R5E	55 kDa	0.0009
Alpha-1-acid glycoprotein 2	A1AG2_HUMAN	ORM2	24 kDa	0.0017
Coiled-coil domain-containing protein 6	CCDC6_HUMAN	CCDC6	53 kDa	0.34
Eukaryotic translation initiation factor 3 subunit G	EIF3G_HUMAN	EIF3G	36 kDa	0.3
Nck-associated protein 1	NCKP1_HUMAN	NCKAP1	129 kDa	0.065
Electron transfer flavoprotein subunit beta	ETFB_HUMAN	ETFB	28 kDa	0.1

Acetyl-CoA acetyltransferase, cytosolic	THIC_HUMAN	ACAT2	41 kDa	0.31
Fibrinogen gamma chain	FIBG_HUMAN	FGG	52 kDa	0.097
Immunoglobulin superfamily member 1	IGSF1_HUMAN	IGSF1	149 kDa	< 0.00010
Parathyroid hormone-related protein	PTHHR_HUMAN	PTHHR	20 kDa	< 0.00010
60S ribosomal protein L17	RL17_HUMAN	RPL17	21 kDa	0.17
Aflatoxin B1 aldehyde reductase member 3	ARK73_HUMAN	AKR7A3	37 kDa	0.0031
Isoleucine--tRNA ligase, cytoplasmic	SYIC_HUMAN	IARS	145 kDa	0.056
Peptidyl-prolyl cis-trans isomerase H	PPIH_HUMAN	PPIH	19 kDa	0.46
Q4ADV7-DECOY	Q4ADV7-DECOY		?	0.033
UMP-CMP kinase	KCY_HUMAN	CMPK1	22 kDa	0.16
Annexin A7	ANXA7_HUMAN	ANXA7	53 kDa	0.019
Biglycan	PGS1_HUMAN	BGN	42 kDa	0.052
Fetuin-B	FETUB_HUMAN	FETUB	42 kDa	0.078
Protein phosphatase methylesterase 1	PPME1_HUMAN	PPME1	42 kDa	0.24
Eukaryotic translation initiation factor 1A, X-chromosomal	IF1AX_HUMAN (+1)	EIF1AX	16 kDa	0.36
Apolipoprotein C-II	APOC2_HUMAN	APOC2	11 kDa	0.038
Arfaptin-1	ARFP1_HUMAN	ARFIP1	42 kDa	0.0034
Histidine triad nucleotide-binding protein 1	HINT1_HUMAN	HINT1	14 kDa	0.42
60S ribosomal protein L36	RL36_HUMAN	RPL36	12 kDa	0.45
Syntaxin-binding protein 1	STXB1_HUMAN	STXBP1	68 kDa	< 0.00010
Ubiquitin carboxyl-terminal hydrolase isozyme L5	UCHL5_HUMAN	UCHL5	38 kDa	0.59
Vesicle-fusing ATPase	NSF_HUMAN	NSF	83 kDa	0.33
Alpha-1-antichymotrypsin	AACT_HUMAN	SERPINA3	48 kDa	< 0.00010
60S ribosomal protein L18a	RL18A_HUMAN	RPL18A	21 kDa	0.12
Polypeptide N-acetylgalactosaminyltransferase 2	GALT2_HUMAN	GALNT2	65 kDa	0.067
Nuclear transport factor 2	NTF2_HUMAN	NUTF2	14 kDa	0.035
Coatamer subunit beta'	COPB2_HUMAN	COPB2	102 kDa	0.36
BRISC complex subunit Abro1	F175B_HUMAN	FAM175B	47 kDa	0.36
AP-3 complex subunit beta-1	AP3B1_HUMAN	AP3B1	121 kDa	0.31
Vasorin	VASN_HUMAN	VASN	72 kDa	0.59
Caldesmon	CALD1_HUMAN	CALD1	93 kDa	0.32
ATP-binding cassette sub-family E member 1	ABCE1_HUMAN	ABCE1	67 kDa	0.42
N(G),N(G)-dimethylarginine dimethylaminohydrolase 2	DDAH2_HUMAN	DDAH2	30 kDa	0.0023
Oxysterol-binding protein 1	OSBP1_HUMAN	OSBP	89 kDa	0.26
Neuroendocrine convertase 2	NEC2_HUMAN	PCSK2	71 kDa	0.058
Tyrosine-protein kinase receptor UFO	UFO_HUMAN	AXL	98 kDa	0.24
Collagen alpha-1(XIV) chain	COEA1_HUMAN	COL14A1	194 kDa	0.0042
3'(2'),5'-bisphosphate nucleotidase 1	BPNT1_HUMAN	BPNT1	33 kDa	0.016
S-phase kinase-associated protein 1	SKP1_HUMAN	SKP1	19 kDa	0.027

Alpha-1-antitrypsin	A1AT_HUMAN	SERPINA1	47 kDa	0.099
Cullin-4A	CUL4A_HUMAN	CUL4A	88 kDa	0.69
Isocitrate dehydrogenase [NAD] subunit alpha, mitochondrial	IDH3A_HUMAN	IDH3A	40 kDa	0.08
Tyrosine-protein kinase CSK	CSK_HUMAN	CSK	51 kDa	0.16
40S ribosomal protein S27	RS27_HUMAN	RPS27	9 kDa	0.1
Connective tissue growth factor	CTGF_HUMAN	CTGF	38 kDa	< 0.00010
Transportin-3	TNPO3_HUMAN	TNPO3	104 kDa	0.69
Succinyl-CoA:3-ketoacid coenzyme A transferase 1, mitochondrial	SCOT1_HUMAN	OXCT1	56 kDa	0.0042
Charged multivesicular body protein 2b	CHM2B_HUMAN	CHMP2B	24 kDa	0.15
40S ribosomal protein S17-like	RS17L_HUMAN (+1)	RPS17L	16 kDa	0.28
Protein TFG	TFG_HUMAN	TFG	43 kDa	0.0044
Alpha-taxilin	TXLNA_HUMAN	TXLNA	62 kDa	0.23
Transcription elongation factor B polypeptide 2	ELOB_HUMAN	TCEB2	13 kDa	0.0077
Dihydrolipoyl dehydrogenase, mitochondrial	DLDH_HUMAN	DLD	54 kDa	0.48
Insulin-like growth factor 2 mRNA-binding protein 2	IF2B2_HUMAN	IGF2BP2	66 kDa	0.35
Arginine and glutamate-rich protein 1	ARGL1_HUMAN	ARGLU1	33 kDa	0.44
Glutamine synthetase	GLNA_HUMAN	GLUL	42 kDa	< 0.00010
Testis-specific serine kinase substrate	TSKS_HUMAN	TSKS	65 kDa	0.38
Casein kinase II subunit beta	CSK2B_HUMAN	CSNK2B	25 kDa	0.0016
Secernin-1	SCRN1_HUMAN	SCRN1	46 kDa	0.00029
Thrombospondin type-1 domain-containing protein 7A	THS7A_HUMAN	THSD7A	185 kDa	0.42
Extracellular sulfatase Sulf-2	SULF2_HUMAN	SULF2	100 kDa	0.33
Attractin	ATRN_HUMAN	ATRN	159 kDa	0.51
Stanniocalcin-1	STC1_HUMAN	STC1	28 kDa	0.18
Alpha-crystallin B chain	CRYAB_HUMAN	CRYAB	20 kDa	0.13
Alpha-1-acid glycoprotein 1	A1AG1_HUMAN	ORM1	24 kDa	< 0.00010
Phosphoribosyl pyrophosphate synthase-associated protein 1	KPRA_HUMAN	PRPSAP1	39 kDa	0.17
Serpin H1	SERPH_HUMAN	SERPINH1	46 kDa	0.12
Ras-related protein Rab-7a	RAB7A_HUMAN	RAB7A	23 kDa	0.51
Coatomer subunit epsilon	COPE_HUMAN	COPE	34 kDa	0.26
NEDD8-conjugating enzyme Ubc12	UBC12_HUMAN	UBE2M	21 kDa	0.44
LIM domain and actin-binding protein 1	LIMA1_HUMAN	LIMA1	85 kDa	0.44
Aldehyde dehydrogenase family 1 member A3	AL1A3_HUMAN	ALDH1A3	56 kDa	< 0.00010
Prolyl 4-hydroxylase subunit alpha-1	P4HA1_HUMAN	P4HA1	61 kDa	0.061
Mesencephalic astrocyte-derived neurotrophic factor	MANF_HUMAN	MANF	21 kDa	0.16
45 kDa calcium-binding protein	CAB45_HUMAN	SDF4	42 kDa	0.11
Ig alpha-1 chain C region	IGHA1_HUMAN	IGHA1	38 kDa	0.00099
Protein transport protein Sec16A	SC16A_HUMAN	SEC16A	234 kDa	0.56

Protein bicaudal D homolog 2	BICD2_HUMAN	BICD2	94 kDa	0.00099
60S acidic ribosomal protein P1	RLA1_HUMAN	RPLP1	12 kDa	0.012
Phosphatidylinositol-glycan-specific phospholipase D	PHLD_HUMAN	GPLD1	92 kDa	0.054
Clathrin coat assembly protein AP180	AP180_HUMAN	SNAP91	93 kDa	0.44
Dihydropyrimidinase-related protein 1	DPYL1_HUMAN	CRMP1	62 kDa	0.093
AP-1 complex subunit mu-2	AP1M2_HUMAN	AP1M2	48 kDa	0.12
Fermitin family homolog 2	FERM2_HUMAN	FERMT2	78 kDa	0.0071
Translin	TSN_HUMAN	TSN	26 kDa	0.19
V-type proton ATPase subunit E 1	VATE1_HUMAN	ATP6V1E1	26 kDa	0.00099
60S ribosomal protein L18	RL18_HUMAN	RPL18	22 kDa	0.33
Low-density lipoprotein receptor	LDLR_HUMAN	LDLR	95 kDa	0.17
Fibrinogen alpha chain	FIBA_HUMAN	FGA	95 kDa	0.56
Protein Hook homolog 1	HOOK1_HUMAN	HOOK1	85 kDa	0.79
Methylcytosine dioxygenase TET3	TET3_HUMAN	TET3	179 kDa	0.45
Q5VZ66-DECOY	Q5VZ66-DECOY		?	0.17
Dynein light chain 2, cytoplasmic	DYL2_HUMAN	DYNLL2	10 kDa	0.44
Carboxypeptidase N subunit 2	CPN2_HUMAN	CPN2	61 kDa	0.44
UDP-glucose 4-epimerase	GALE_HUMAN	GALE	38 kDa	0.078
Protein Hook homolog 3	HOOK3_HUMAN	HOOK3	83 kDa	0.44
REST corepressor 1	RCOR1_HUMAN	RCOR1	53 kDa	0.58
Dihydropyridyllysine-residue acetyltransferase component of pyruvate dehydrogenase complex, mitochondrial	ODP2_HUMAN	DLAT	69 kDa	0.44
Cytoskeleton-associated protein 4	CKAP4_HUMAN	CKAP4	66 kDa	0.44
Protocadherin Fat 1	FAT1_HUMAN	FAT1	506 kDa	0.44
Tsukushin	TSK_HUMAN	TSKU	38 kDa	0.58
Growth-regulated alpha protein	GROA_HUMAN	CXCL1	11 kDa	0.12
ADP-ribosylation factor-like protein 3	ARL3_HUMAN	ARL3	20 kDa	0.56
3-ketoacyl-CoA thiolase, mitochondrial	THIM_HUMAN	ACAA2	42 kDa	0.54
Glutathione peroxidase 3	GPX3_HUMAN	GPX3	26 kDa	0.44
Dehydrogenase/reductase SDR family member 11	DHR11_HUMAN	DHRS11	28 kDa	0.44
Probable E3 ubiquitin-protein ligase HECTD4	HECD4_HUMAN	HECTD4	439 kDa	0.064
Protein CYR61	CYR61_HUMAN	CYR61	42 kDa	0.064
Serine/threonine-protein phosphatase 1 regulatory subunit 10	PP1RA_HUMAN	PPP1R10	99 kDa	0.59
Alpha-2-macroglobulin-like protein 1	A2ML1_HUMAN	A2ML1	161 kDa	0.44
Ornithine aminotransferase, mitochondrial	OAT_HUMAN	OAT	49 kDa	0.18
6-phosphogluconolactonase	6PGL_HUMAN	PGLS	28 kDa	0.44
Succinate-semialdehyde dehydrogenase, mitochondrial	SSDH_HUMAN	ALDH5A1	57 kDa	0.44
Vasopressin-neurophysin 2-copeptin	NEU2_HUMAN	AVP	17 kDa	0.44
Tubulin--tyrosine ligase-like protein 12	TTL12_HUMAN	TTL12	74 kDa	0.44

Matrix metalloproteinase-9	MMP9_HUMAN	MMP9	78 kDa	0.44
60S ribosomal protein L23	RL23_HUMAN	RPL23	15 kDa	0.44
V-type proton ATPase subunit d 1	VA0D1_HUMAN	ATP6V0D1	40 kDa	0.44
Ig gamma-4 chain C region	IGHG4_HUMAN	IGHG4	36 kDa	0.061
Chromogranin-A	CMGA_HUMAN	CHGA	51 kDa	0.44
Myosin light chain kinase, smooth muscle	MYLK_HUMAN	MYLK	211 kDa	0.44

Chapter 9:

Poster Presentations

9.1 Poster presented on 28th April 2016:

**Presented at the University of Greenwich in the 4th Faculty
Research Day Poster Presentation**

Introduction

Cancer is the leading cause of death worldwide according to WHO (1). In recent years several studies suggested that exosomes signal or influence the major cancer related pathways such as angiogenesis and metastasis. Further evidences also revealed that exosomal proteins can accelerate the fibroblast growth which makes a major barrier for effective drug delivery in cancer treatment (2). Exosomes are round-cup shaped vesicles, 30-150nm in size released by almost all cancer and normal cells and contain a vast range of nucleic acids, mRNA, lipids, and a wide array of proteins (3). In this study, both cellular and exosomal proteomic profiles will be compared by 1D and 2D gel electrophoresis and differential protein spots will be identified using MS from three cancer cells: H358 (Bronchi alveolar Carcinoma); THP1 (acute monocytic leukemia) and MCF7 (Breast Cancer) and counterpart normal cells.

Methods

- **Cell culture:** Both H358 and THP1 was cultured in RPMI-1640 and MCF7 was cultured in DEMEM using 10% DFBS and 1% antibiotic (Penicillin-Streptomycin). All three cells were maintained in a humidified atmosphere, 95% air, 5.0% CO₂ at 37°C.
- **Protein Extraction and concentration determination:** When the cell reached 80%-90% confluency, medium was removed and kept separately for exosome isolation and the cells were trypsinized and washed with PBS twice and subjected to RIPA buffer protein extraction. Protein concentration was determined by Bradford assay.
- **Isolation and characterization of exosomes:** Exosomes were isolated by using Invitrogen total exosomes isolation kit from cell culture medium. Purified exosomes were analysed by SEM/TEM, and Dynamic light scattering method. Exosomes were quantified by using system bioscience ExoElisa Kit following the manufacturer protocol.
- **Gel Electrophoresis:** Both 1D and 2D gel electrophoreses were performed using cellular and exosomal protein samples.

Results

- In figure 1, exosomes were analysed by both TEM and SEM which showed large numbers of membrane bound cup-shaped vesicles within the mentioned size limit.

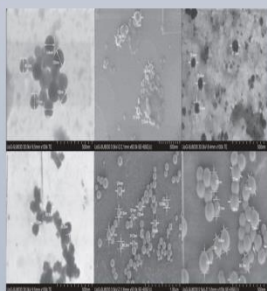


Figure 1: Electron microscopic images of exosomes isolated from the three cell lines

- On 1D PAGE around 20 protein bands were detected on the cell lysates, compared to exosome samples protein bands were less. Apart from some common bands there were some protein bands of the cellular samples were absent or present in very low level while the intensity of some bands are much clearer in the exosome sample.

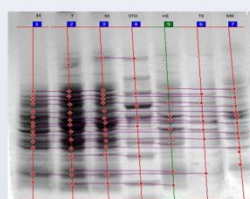


Figure 2: 1D Gel Analysis of Cell lysate and Exosomal Protein.

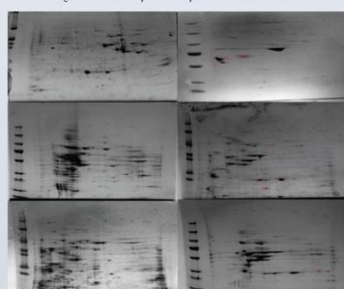


Figure 3: 2D Gel Analysis of Cellular Protein and Exosomal Protein

- The spot patterns in figure 3 of exosomes of all three cells were less complex compared to the cellular protein spots and the different protein spots were marked red in exosome sample.
- The number of exosomes increases with increase of cell number and in case of MCF7 the number of exosomes keeps increasing when the cell is in decline phase.



Figure 4: Cellular Growth Curve VS Number of Exosomes Per Day

- The size distribution is shown in figure five, where the average size is around 200nm which is due to the aggregation of particles together which is also seen in the TEM/SEM images.

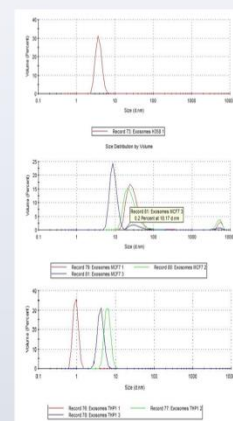


Figure 5: Size Distribution of Exosome by DLS

Conclusion

This study reports the isolation and characterization of exosomes from three cancer cell lines, H358, THP1, and MCF7. The different protein spots in 2D gel will be analysed by 2D gel analysis software and will be identified by mass spectrometry. The result of this study may be important because of the biological significance of the onco-protein released from exosomes which can easily enter the blood circulation and may affect the non-malignant cells.

References

1. Stewart, B.W. & Wild, C.P., 2014. *World Cancer Report 2014*.
2. Azmi, A.S., Bao, B. & Sarkar, F.H., 2013. Exosomes in cancer development, metastasis, and drug resistance: A comprehensive review. *Cancer and Metastasis Reviews*, 32(3-4), p.623-642.
3. Yu, X., Harris, S.L. & Levine, A.J., 2006. The regulation of exosome secretion: A novel function of the p53 protein. *Cancer Research*, 66(9), p.4795-4801.

Acknowledgement

Special thanks to all the technicians of school of science, University of Greenwich, specially Dr. Ian Slipper from the SEM Lab.

Contact

MD Faruk Abdullah Saurav

PhD Student

G138

School of Science University of Greenwich

Mob: 07429822559

9.2 Poster presented on 23th January 2017:

Presented at the Royal Society in a seminar on Extracellular vesicles and Tumour microenvironment

Aims

- Identification and characterisation of exosomes from Lung cancer cell line H358, Leukemia cell line THP1 and Breast cancer cell line MCF7.
- Dynamics of exosome secretion in different cellular growth phases.
- Comparative proteomic analysis of exosomes derived from the mentioned cell lines.

Introduction

- Exosomes are a distinct type of extracellular vesicles enclosed by a lipid bilayer, released by almost all cells including normal and cancer cells which have a round-cup shaped morphology with a size range of 30-150nm¹.
- They are enriched in proteins, lipids, nucleic acid and RNAs².
- Exosomes are formed by the inward budding of the late endosomes with the plasma membrane and represents a fraction of the cellular proteome.
- They play vital role in tumorigenesis, apoptosis, and chemotherapeutic resistance.
- Exosomes are useful tool for biomarkers in cancer therapeutics and also in drug delivery³.

Methods

> **Identification and characterisation:**

- Exosomes were isolated by using Invitrogen total exosomes isolation kit (Fisher Scientific) from cell culture supernatant and analysed by scanning electron microscopy (SEM) and Dynamic light scattering (DLS) method and they are confirmed by western blot analysis using CD63 antibody.

> **Protein extraction and 1D gel analysis:**

- Proteins were extracted from exosomes by RIPA buffer and subjected to 1D gel analysis.

> **Quantification of exosomes:**

- Exosomes were counted using ExoElisa Kit from System Bioscience with exosomal antibody CD63, CD9, CD81 and Hsp70 following the manufacturer protocol.

> **Proteomic analysis:**

- Proteomic analysis was performed by LC-MS

Results

- In figure 1, exosomes were analysed by SEM which showed large numbers of membrane bound cup-shaped vesicles within the mentioned size limit and western blot analysis with CD63 antibody confirms the presence of exosomes (Figure 2)

- The size distribution showed the exosomes were between 35-155nm with in three exosomes, the highest being H358 (Avg 117nm) and lowest was MCF7 (75nm). The average exosome size of THP1 was found 93nm

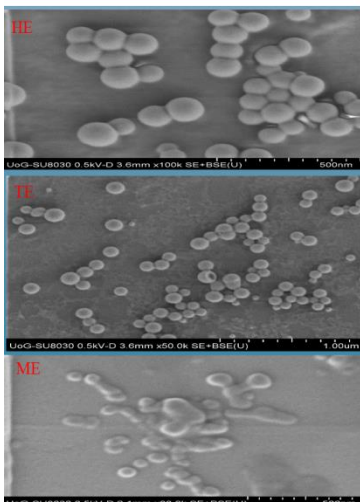


Figure 1: Electron microscopic images of exosomes isolated from H358 (HE), THP1 (TE) and MCF7 (ME)

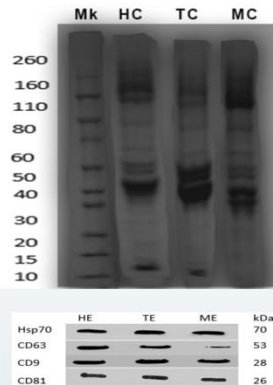


Figure 2: 1D gel analysis and western blot analysis using CD63, CD81, CD9 and Hsp70 antibody

- The dark band around 60Kda to 70Kda was identified as BSA by LC-MS (Figure 4)
- The bands in the red circles which appeared in stress conditioned has yet to be identified (Figure 4).

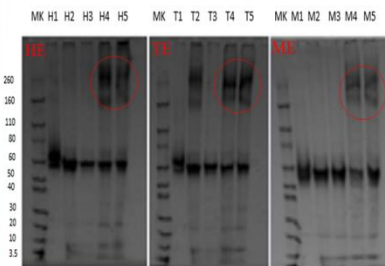


Figure 4: 1D gel analysis of exosomal proteins collected from different growth phases.

- Proteomic analysis resulted a total of 919 proteins were identified by LC-MS analysis with minimum 2 peptide match and less than 1.0 FDR for both proteins and peptide (Figure 5)
- 238 number of proteins were shared by all three exosomes which includes some tumour proteins along with some exosomal marker proteins (Figure 5).

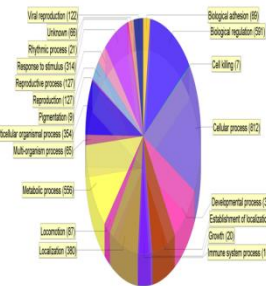


Figure 6: Biological function determined by GO terms.

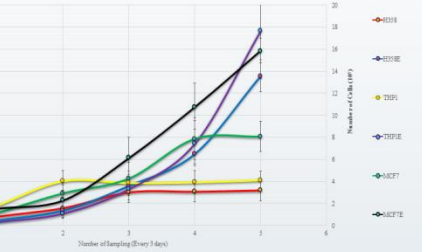


Figure 3: Number of exosomes in different cellular growth phases.

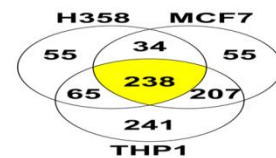


Figure 5: Number of shared and individual proteins identified from exosomes

- A total of 751 proteins were identified from THP1 cell line, 337 from H358 and 534 from MCF7 (Figure 5).
- Comparative proteomics was done which resulted:
 - ~ Some house keeping common proteins e.g. keratin, actin.
 - ~ Exosomal Marker Proteins: CD63, CD9, CD82, Hsp, Annexin A1, A5 etc
 - ~ Cellular Signalling Proteins: Sideroflexin 1, Spectrin
 - ~ Tumour Associated Proteins: Fibronectin, Tumour associated calcium transducer and Tumour protein D54.

Discussion

- Exosomes were successfully isolated from the three cancer cells, identified and characterised.
- The size distribution of exosomes were within the limit of published papers.
- The presence of CD63 confirms the presence of exosomes in all three cells.
- The number of exosomes were found similar in previous published work for both normal and stressed condition⁴
- Number of exosomes increased at stationary phase or stress condition (possible hypoxia) compared to log phase of cellular growth⁵.
- The number of proteins identified from three different exosomes resembles previously published results.
- 89 proteins were found to be involved in cellular adhesion which assists in tumour metastasis.
- Some individual tumour marker proteins were also identified such as Beta-2-microglobulin, for non-small cell lung cancer, Immunoglobulins related to leukemia and plasminogen activator inhibitor 1 for breast cancer.

Bibliography

1. Yellon DM and Davidson SM., 2014. Exosomes: nanoparticles involved in cardioprotection?. *Circ Res* 14(2), 325-332.
2. Kalani, A. & Tyagi, N., 2015. Exosomes in neurological disease, neuroprotection, repair and therapeutics: Problems and perspectives. *Neural Regeneration Research*, 10(10), p.1565-1567.
3. Minciacchi VR et al., 2015. Extracellular vesicles in cancer: exosomes, microvesicles and the emerging role of large oncosomes. *Semin Cell Dev Bio*, 40, 41-45.
4. Agarwal, K et al., 2015. Analysis of exosome release as a cellular response to MAPK pathway inhibition. *Langmuir*, 31(19), 5440-5448.
5. Rehman, A.A., Ahsan, H. & Khan, F.H., 2013. Alpha-2-macroglobulin: A physiological guardian. *Journal of Cellular Physiology*, 228(8), p.1665-1675.

Contact

MD Faruk A Saurav
University of Greenwich
email:
sm42@greenwich.ac.uk
Mob: 07429822559

THANK YOU